NON-EQUILIBRIUM STATISTICAL PHYSICS TODAY

Proceedings of the 11th Granada Seminar on Computational and Statistical Physics

La Herradura, Spain 13 – 17 September 2010

EDITORS

Pedro L. Garrido
Joaquín Marro
Francisco de los Santos

AIP
American Institute
of Physics

AIP | CONFERENCE PROCEEDINGS ■ 1332

Garrido
Marro
Santos

NON-EQUILIBRIUM STATISTICAL PHYSICS TODAY

1332

AIP

ISBN 978-0-7354-0887-6
ISSN 0094-243X

NON-EQUILIBRIUM STATISTICAL PHYSICS TODAY

NON-EQUILIBRIUM STATISTICAL PHYSICS TODAY

Proceedings of the 11th Granada Seminar on Computational and Statistical Physics

La Herradura, Spain 13 – 17 September 2010

EDITORS
Pedro L. Garrido
Joaquín Marro
Francisco de los Santos

SPONSORING ORGANIZATIONS
Spanish Minister for Science and Technology
Regional Administration "Junta de Andalucía"
European Physical Society
Institute "Carlos I" for Theoretical and Computational Physics
University of Granada

All papers have been peer reviewed

AIP
American Institute of Physics

Melville, New York, 2011
AIP CONFERENCE PROCEEDINGS ■ 1332

Editors

Pedro L. Garrido
Joaquín Marro
Francisco de los Santos

Institute "Carlos I" for Theoretical and Computational Physics
University of Granada
18071 – Granada, Spain

E-mail: garrido@onsager.ugr.es

Authorization to photocopy items for internal or personal use, beyond the free copying permitted under the 1978 U.S. Copyright Law (see statement below), is granted by the American Institute of Physics for users registered with the Copyright Clearance Center (CCC) Transactional Reporting Service, provided that the base fee of $30.00 per copy is paid directly to CCC, 222 Rosewood Drive, Danvers, MA 01923, USA. For those organizations that have been granted a photocopy license by CCC, a separate system of payment has been arranged. The fee code for users of the Transactional Reporting Services is: 978-0-7354-0887-6/11/$30.00

© 2011 American Institute of Physics

Permission is granted to quote from the AIP Conference Proceedings with the customary acknowledgment of the source. Republication of an article or portions thereof (e.g., extensive excerpts, figures, tables, etc.) in original form or in translation, as well as other types of reuse (e.g., in course packs) require formal permission from AIP and may be subject to fees. As a courtesy, the author of the original proceedings article should be informed of any request for republication/reuse. Permission may be obtained online using Rightslink. Locate the article online at http://proceedings.aip.org, then simply click on the Rightslink icon/"Permission for Reuse" link found in the article abstract. You may also address requests to: AIP Office of Rights and Permissions, Suite 1NO1, 2 Huntington Quadrangle, Melville, NY 11747-4502, USA; Fax: 516-576-2450; Tel.: 516-576-2268; E-mail: rights@aip.org.

L.C. Catalog Card No. 2010943018
ISBN 978-0-7354-0887-6
ISSN 0094-243X
Printed in the United States of America

AIP Conference Proceedings, Volume 1332
Non-equilibrium Statistical Physics Today
Proceedings of the 11th Granada Seminar on Computational and Statistical Physics

Table of Contents

Preface
J. Marro 1

Nonequilibrium statistical physics today. Where shall we go from here?
Pedro L. Garrido, Joaquín Marro, Francisco de los Santos, and Joel L. Lebowitz 3

Three lectures: NEMD, SPAM, and shockwaves
Wm. G. Hoover and Carol G. Hoover 23

Stochastic thermodynamics: An introduction
Udo Seifert 56

Hydrodynamics from dynamical non-equilibrium MD
Sergio Orlandini, Simone Meloni, and Giovanni Ciccotti 77

Recent progress in fluctuation theorems and free energy recovery
A. Alemany, M. Ribezzi, and F. Ritort 96

Universality in equilibrium and away from it: A personal perspective
Miguel A. Muñoz 111

Fourier law, phase transitions, and the Stefan problem
Errico Presutti 123

Bringing thermodynamics to non-equilibrium microscopic processes
J. M. Rubí 134

Noise-induced transitions *vs.* noise-induced phase transitions
Raúl Toral 145

On the approach to thermal equilibrium of macroscopic quantum systems
Sheldon Goldstein and Roderich Tumulka 155

Temperature, entropy and second law beyond local equilibrium: An illustration
David Jou 164

Griffiths phases in the contact process on complex networks
Géza Ódor, Róbert Juhász, Claudio Castellano, and Miguel A. Muñoz 172

Stationary points approach to thermodynamic phase transitions
Michael Kastner 179

Energy bursts in vibrated shallow granular systems
N. Rivas, D. Risso, R. Soto, and P. Cordero 184

Layering and wetting transitions for an interface model
Salvador M. Solé 190

On the role of Galilean invariance in KPZ
H. S. Wio, J. A. Revelli, C. Escudero, R. R. Deza, and M. S. de La Lama 195

Anomalous diffusion and basic theorems of statistical mechanics
Luciano C. Lapas, J. M. Rubí, and Fernando A. Oliveira 200

Large deviations of the current in a two-dimensional diffusive system
C. Pérez-Espigares, J.J. del Pozo, P.L. Garrido, and P.I. Hurtado 204

Stochastic resonance between propagating extended attractors
M. G. dell'Erba, G. G. Izús, R. R. Deza, and H. S. Wio 214

Heat and chaotic velocity in special relativity
A. L. Garcia-Perciante 216

Computing free energy differences using conditioned diffusions
Carsten Hartmann and Juan Latorre 218

Dynamical behavior of heat conduction in solid Argon
Hideo Kaburaki, Ju Li, Sidney Yip, and Hajime Kimizuka 221

Fast transients in mesoscopic systems
A. Kalvová, V. Špička, and B. Velický 223

Dynamical aspect of group chase and escape
Shigenori Matsumoto, Tomoaki Nogawa, Atsushi Kamimura, Nobuyasu Ito, and Toru Ohira 226

Onset of thermal rectification in graded mass systems: Analysis of the classic and quantum self-consistent harmonic chain of oscillators
Emmanuel Pereira, Humberto C. Lemos, and Ricardo R. Ávila 228

Covariant Lyapunov vectors and local exponents
Harald A. Posch and Hadrien Bosetti 230

Statics and dynamics of a harmonic oscillator coupled to a one-dimensional Ising system
A. Prados, L. L. Bonilla, and A. Carpio 232

Strong ratchet effects for heterogeneous granular particles in the Brownian limit
Pascal Viot, Alexis Burdeau, and Julian Talbot 235

Stochastic protein production and time-dependent current fluctuations
Mieke Gorissen and Carlo Vanderzande 237

Creating the conditions of anomalous self-diffusion in a liquid with molecular dynamics
J. Ryckebusch, S. Standaert, and L. De Cruz 239

Cluster size distribution in Gaussian glasses
S.V. Novikov 241

A non-equilibrium potential function to study competition in neural systems
Jorge F. Mejías 243

Quasi-stationary states and a classification of the range of pair interactions
A. Gabrielli, M. Joyce, and B. Marcos 245

Fluctuation relations and fluctuation-response relations for molecular motors
G. Verley and D. Lacoste 247

Why are so many networks disassortative?
Samuel Johnson, Joaquín J. Torres, J. Marro, and Miguel A. Muñoz 249

Analytical study of hysteresis in the *T* = 0 random field Ising model
T. P. Handford, F-J Perez-Reche, and S N Taraskin 251

Queues on narrow roads and in airplanes
Vidar Frette and Per C. Hemmer 253

Fluctuations out of equilibrium
V. V. Belyi 255

Long-range interacting systems and dynamical phase transitions
Fulvio Baldovin, Enzo Orlandini, and Pierre-Henri Chavanis 257

Irreversibility of the renormalization group flow and information theory
S. M. Apenko 259

Classical systems: Moments, continued fractions, long-time approximations and irreversibility
R. F. Álvarez-Estrada 261

ABSTRACTS OF SELECTED CONTRIBUTIONS

Reentrant behavior of effective attraction between like-charged macroions immersed in electrolyte solution
Ryo Akiyama, Ryo Sakata, and Yuji Ide 265

Nonlinear Boltzmann equation for the homogeneous isotropic case: Some improvements to deterministic methods and applications to relaxation towards local equilibrium
P. Asinari 266

Effective dimension in flocking mechanisms
Gabriel Baglietto and Ezequiel V. Albano 267

The Liouville equation and BBGKY hierarchy for a stochastic particle system
M. Baryło 268

To model kinetic description
V.V. Belyi 269

Experimental densities of binary mixtures: Acetic acid with benzene at several temperatures
Georgiana Bolat, Daniel Sutiman, and Gabriela Lisa 270

Enhanced memory performance thanks to neural network assortativity
S. de Franciscis, S. Johnson, and J. J. Torres 271

New insights in a 2-D hard disk system under a temperature gradient
J. J. del Pozo, C. Pérez-Espigares, P.I. Hurtado, and P.L. Garrido 272

Automatic optimization of experiments with coupled stochastic resonators
Mauro F. Calabria and Roberto R. Deza 273

Velocity-velocity correlation function for anomalous diffusion
Rogelma M. Ferreira and Fernando A. Oliveira 274

Excess of low frequency vibrational modes, glass transition and inherent structures
Hugo M. Flores-Ruiz and Gerardo G. Naumis 275

Analysis of ship maneuvering data from simulators
Vidar Frette, G. Kleppe, and K. Christensen 276

Unfying approach for fluctuation theorems from joint probability distributions
Reinaldo García-García, D. Domínguez, Vivien Lecomte, and A.B. Kolton 277

Thermally activated escape far from equilibrium: A unified path-integral approach
S. Getfert and P. Reimann 278

The crystal nucleation theory revisited: The case of 2D colloidal crystals
A.E. González and L. Ixtlilco-Cortés 279

Space-time phase transitions in the totally asymmetric simple exclusion process
M. Gorissen and C. Vanderzande 280

Modeling of early stages of island growth during pulsed deposition: Role of closed compact islands
M. Kotrla and M. Masin 281

Fluctuations of the dissipated energy in a granular system
Antonio Lasanta, Pablo I. Hurtado, Pedro L. Garrido, and J. J. Brey 282

Study of the dynamic behavior of quantum cellular automata in graphane nanoclusters
A. León and M. Pacheco 283

Breeding gravitational lenses
J. Liesenborgs, S. De Rijcke, H. Dejonghe, and P. Bekaert 284

Improved macroscopic traffic flow model for aggresive drivers
A. R. Méndez and R. M. Velasco 285

A formula on the pressure for a set of generic points
A.M. Meson and F. Vericat 286

Statistical thermodynamics of a relativistic gas
Afshin Montakhab and Malihe Ghodrat 287

Noninteracting classical spins in a rotating magnetic field: Exact results
Suhk K. Oh and Seong-Cho Yu 288

Optimal mutation rates in dynamic environments: The Eigen model
Mark Ancliff and Jeong-Man Park 289

Current fluctuations in a two dimensional model of heat conduction
Carlos Pérez-Espigares, Pedro L. Garrido, and Pablo I. Hurtado 290

Quasistatic heat processes in mesoscopic non-equilibrium systems
J. Pešek and K. Netočný 291

Violation of fluctuation-dissipation theorem in the off-equilibrium dynamics of a system with nonadditive interactions
O. A. Pinto, F. Romá, A.J. Ramirez-Pastor, and F. Nieto 292

Geometric aspects of Schnakenberg's network theory of macroscopic nonequilibrium observables
M. Polettini 293

Nonequilibrium thermodynamics of single DNA hairpins in a dual-trap optical tweezers setup
M. R. Crivellari, J. M. Huguet, and F. Ritort 294

Quantum revivals and Zitterwebegung in monolayer graphene
Elvira Romera and Francisco de los Santos 295

The non-equilibrium and energetic cost of sensory adaptation
G. Lan, Pablo Sartori, and Y. Tu 296

Negative specific heat in the canonical statistical ensemble
F. Staniscia, A. Turchi, D. Fanelli, P.H. Chavanis, and G. De Ninno 297

Dynamical systems approach to the study of a sociophysics agent-based model
Andrá M. Timpanaro and Carmen P. Prado 298

Conversion process of chemical reaction into mechanical work through solvation change
Ken Tokunaga, Takuya Furumi, and Ryo Akiyama 299

Participants List 301

Author Index 303

EDITORS' PREFACE

This volume originated at the 11th Granada Seminar organized by the University of Granada, Spain, and contains the main lectures, a transcription of the discussions in an open round table (of which the book takes its title), and a selection of contributed papers in that conference. This is the eleventh of a series of Granada Lectures previously published by:

- World Scientific (Singapore 1993),
- Springer Verlag (*Lecture Notes in Physics* volumes 448 and 493),
- Elsevier (*Computer Physics Communications* volume 121-122), and
- American Institute of Physics (*Conference Proceedings Series*, volumes 574, 661, 779, 887 and 1091).

These books and the successive editions of the Seminar since 1990 are described in detail at http://ergodic.ugr.es/cp/. This *web* also contains updated information on the next edition.

The Granada Seminar is defined as a small topical conference whose pedagogical effort is especially aimed at young researchers. In fact, one interesting aspect of this meeting is the opportunity given to the youngest to present their results and to discuss their problems with leading specialists. There were in this edition a total of 60 lectures and 42 poster contributions. More than one hundred participants came from nearly thirty countries (Spain contributed with 21%, the rest of Europe including Russia with 48%, North America with 7%, Central and South America with 15%, Asia with 7%, and Africa with 2%); most of the participants received partial support from the organization.

The 11th Granada Seminar was organized by the Institute *Carlos I* for Theoretical and Computational Physics of the University of Granada, sponsored by the European Physical Society, endorsed by The American Physical Society, and financed by the Spanish Minister for Science, project MICINN FIS2009-08191E, by the regional administration *Junta de* Andalucía, and by the University of Granada. We also wish to express gratitude to all those who have collaborated in making this event a success. In particular, we mention the remarkably high quality and friendly cooperation of invited speakers, among which we should distinguish Joel Lebowitz whose (80+⅓)th anniversary we celebrated during the meeting, and other participants, whose personal effort enabled us to accomplish the goals of the Seminar, the Steering Committee's help in designing format and contents, and further *in situ* collaboration from colleagues and students. This edition of the Seminar was held from 13 to 17 of September 2010 in the charming village of La Herradura, a remarkable spot of the *Tropical Coast* of Granada, where the participants enjoyed a paradisiacal setting with excellent hotels and restaurants.

Finally, let us notice that an effort has been made by authors and editors to offer pedagogical notes here; in particular, each topic is comprehensively described within its scientific context. We try to mold the *Granada Lectures* into a series of books that help introduce the beginner to novel advances in statistical physics and to the creative use of computers in scientific research, as well as to serve as a work of reference for teachers, students and researchers.

Granada, 18 November 2010

GRANADA SEMINAR
STEERING COMMITTEE

- K. Binder, Institute of Physics of Condensed Matter, University of Mainz
- H. J. Herrmann, ICA1, University of Stuttgart
- J. L. Lebowitz, Department of Mathematics, Rutgers University, New Jersey
- R. de la Llave, Department of Mathematics, University of Texas, Austin
- M. Mareschal, Faculté des Sciences, Université Libre de Bruxelles
- J. F. Fernández, Institute for Materials Science, C.S.I.C. and University of Zaragoza
- P. L. Garrido, Institute "Carlos I" for Theoretical and Computational Physics, University of Granada
- H. J. Kappen, Department of Biophysics, University of Nijmegen
  J. Marro, Departamento de E. y Física de la Materia, University of Granada

Nonequilibrium Statistical Physics today.
Where shall we go from here?

This is an edited transcription, by Pedro L. Garrido, Joaquín Marro, and Francisco de los Santos, of the directly recorded sound during an open round table, the third day of the Seminar, which was chaired by Prof. Joel L. Lebowitz.[1]

• **Joel L. Lebowitz (JLL)**: This was supposed to be the last slide of my talk on Monday... It will serve here to say what I consider important open problems in understanding nonequilibrium phenomena. These, I think, are very central issues... though not the only ones.

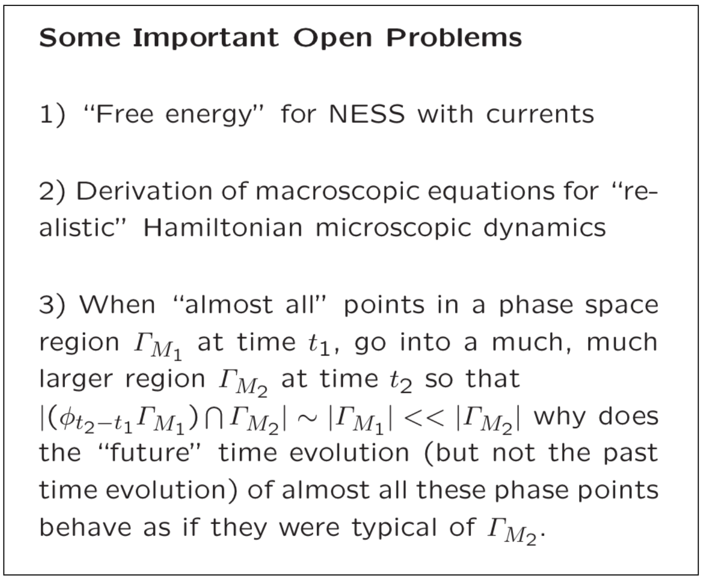

Some Important Open Problems

1) "Free energy" for NESS with currents

2) Derivation of macroscopic equations for "realistic" Hamiltonian microscopic dynamics

3) When "almost all" points in a phase space region Γ_{M_1} at time t_1, go into a much, much larger region Γ_{M_2} at time t_2 so that $|(\phi_{t_2-t_1}\Gamma_{M_1})\bigcap\Gamma_{M_2}| \sim |\Gamma_{M_1}| << |\Gamma_{M_2}|$ why does the "future" time evolution (but not the past time evolution) of almost all these phase points behave as if they were typical of Γ_{M_2}.

FIGURE 1. The slide from Lebowitz's talk (not included in the book) which is often referred to within the discussions. (NESS stands for Nonequilibrium Steady States.)

The first thing is the free energy for a nonequilibrium stationary state. Consider a system in contact with two reservoirs, one temperature on the left, and one temperature on the right, in a stationary state. Question: *is there a reasonable definition of free energy for such an open nonequilibrium system?* In my talk I was saying that if you start a state,

---

[1] The speakers had a chance to swiftly revise the text. The fresh, informal way of talking during the discussions, and some eventual references made to the blackboard there have been kept whenever the meaning is still reasonably evident. A few indecipherable sentences have been replaced by [...].

say a temperature profile, then the large deviation function will decrease to the stationary one in a monotone way. In other words, the log of the probability of having such a profile in the stationary state [which is not typical], will as the time evolves (assuming Fourier's law is satisfied; we are not talking about anomalous systems here) increase, with the system eventually coming to the stationary state. I argue that this is analogous to what you find if you have an isolated macroscopic system with fixed total energy in a nontypical initial state, then it will eventually come to something that is uniform. So the final state will be an equilibrium state which, as I argued several times already, is essentially something which occupies the whole energy surface, but not really the total full energy surface. There are going to be some regions, more unlikely the larger the system, this will be exponential with the size of the system. By the way, I'm very much an individualist that will later ask for someone to defend the ensemblist point of view that Shelly was saying over there. The microcanonical ensemble gives you a certain probability, a large deviation, and then the second law says that this large deviation function which is the difference between the entropy of the actual macroscopic state, and the equilibrium entropy, (which is equivalent to the Gibbs entropy of a uniform distribution over the energy surface when the system is large), is going to be monotone.

If you have the same temperature on the two sides, the stationary state will correspond to a canonical distribution with this temperature. The energy will no longer be constant but the system will go to a state with a uniform temperature.

What about a nonequilibrium stationary state, when you actually have transport of energy along the system? Then, I argue again, the large deviation function will be monotone. This depends on the log of the ratio of the probability of the typical state to the one you started out with, which is not typical.

In equilibrium, entropy plays more than one role: it is the large deviation function but in addition if you take the derivative of the entropy with respect to the energy you get one over the temperature, you can get the pressure by taking the derivative of the entropy with respect to the volume for a given energy, etc. People have tried for many, many years to find an equivalent thing for this nonequilibrium stationary ensemble. I have certainly been trying since when I did my thesis, it was before any of you here were born probably. In 1956 I was trying to find what the analogous thing to the thermodynamic free energy is in a nonequilibrium stationary state. That problem has not been solved. In fact I don't think much progress has been made on that for the last 60 years. In particular, Tasaki and his coworkers have tried to develop something, I don't think very successfully, maybe there simply isn't anything like that. It's an open question.

The second open question is even simpler: it is just to derive macroscopic equations for realistic Hamiltonian microscopic dynamics. As Roberto [Livi] was saying, let's say that equations like Fourier's law don't necessarily always hold when you are in low dimensions (and other things we know don't hold). But experimentally it seems to be very, very good for most systems. When you have a metal bar between two temperatures, or just a metal bar by itself and you start with a nonuniform temperature, Fourier's law holds. It would be very, very nice if one could derive that from microscopic dynamics, classical or quantum mechanical, I mean, quantum mechanical would be even better, even though I don't agree at all with Sandu [Popescu] that there is any problem with the classical understanding. In fact I think there are some problems with the quantum thing, but I'll come to that later.

The third issue is really, if you wish, a subset of the first one. This is supposed to be the energy surface... This is what I call Γ_1. It's a region on the energy surface, which corresponds to some particular macrostate at time t_1. I'm thinking again of an isolated system having an energy density profile corresponding to a macrostate but which has a very small volume, it's very unlikely with respect to the microcanonical ensemble. Then at time t_2 you will get a new macrostate, Γ_2, which is going to be, let's say much more uniform, and will have a much larger region in the phase space. Now you want to predict what is going to happen next time, let's say at time t_3. Γ_2 will very likely go to a state M_3 of much larger region Γ_3.

The point is, let me say it again: To have a deterministic macroscopic equation, I mean that almost all the phase points in the region Γ_1 go into Γ_2 and the values of the macrovariables associated to Γ_2 are a solution of the deterministic equations like the Fourier Law. You know, the derivative of the energy density with respect to time is given by the divergence of some energy flux, and this energy flux is given by minus the gradient of temperature. So, if I say I have deterministic equations which lead me from a profile at time t_1 to a profile at time t_2, according to the solution of the heat equation for isolated systems, I mean that almost all of the phase points initially in Γ_1 end up in Γ_2. By the Liouville theorem, the volume of Γ_1 is preserved so the intersection of the evolved Γ_1 and Γ_2 will have the same volume, or maybe slightly smaller because some of the phase points in Γ_1 have "leaked out". So it's a very, very sparse set. In a certain respect it's a very atypical set because if I reverse all the velocities I'll be going exactly back over there [Γ_1], which is very atypical. Almost any point in Γ_2, reversing the velocities, will go to the bigger set Γ_3. Nevertheless, if you are going to have a deterministic time evolution, it must mean that this set over here $[U(t_2,t_1)\Gamma_1]$, which is clearly atypical as far as the past time evolution, behaves typically as far as the future time evolution goes. And this is really the crux of the mathematical problem of deriving deterministic macroscopic equations from microscopic dynamics. To show, that the set $[U(t_2,t_1)\Gamma_1]$ behaves typically as far as the future goes with respect to all the points in Γ_2.

So, those are the issues I was going to write down at the end of my talk on Monday which I consider some of the important problems in nonequilibrium statistical mechanics from a foundational point of view. Let me stop now and start having some comments from you.

• **Giovanni Ciccotti (GC)**: I understand what you say. However, as you know, the hydrodynamic equations are closed, because we add to the conservation law the phenomenological relations that are given by the constitutive equations i.e. empirical relationships. Therefore, although we can trust them practically, they are not completely founded, being phenomenological equations. Correct? Instead, If I can compute this property by numerical molecular dynamics, by atomistic dynamics, I can check your ansatz. It seems to me that what one should do is to find the way in which, without assuming anything for the continuum representation, one computes directly the behavior of the fields involved by microscopic dynamics, and then one can check your hypothesis. I think this is possible. There are people doing this and, indeed, they find correspondence. I don't see, instead, your mathematical problem because you want to give a theoretical foundation to equations which are intrinsically only phenomenological.

• **JLL**: Equations that are phenomenological presumably are used because they actually work. So real systems do behave according to those phenomenological equations. We also believe that liquids are made up of molecules. These molecules undergo microscopic dynamics, so a given microstate of the liquid which is basically under classical mechanics would be a state where you have positions and velocities.
• **GC**: On that we agree completely. Let me try restate my question. I still would like to understand what your mathematical problem is because if you start from phenomenological equations I think is very difficult to give to them a deep justification because they are phenomenological, so sometime they are valid and some other time not…
• **JLL**: I'm totally on your side. I do want to understand the origin of these phenomenological equations. And I think that to understand the origin I have to go to the microscopic dynamics.
• **GC**: Absolutely.
• **JLL**: That's what I'm saying. Going back to your simulations, suppose you start from a non-uniform macrostate, so you pick a random point in this region of the phase space. You would see it evolving, let's say to the more uniform. Now you start with something which is more distorted; you see after a while it goes to the previous initial macrostate. Assuming you do your molecular dynamics perfectly exact, so you have now a new point in the phase space which has the property, if you reverse all the velocities it will go backwards, as compared as if you pick simply a point at random here. You will find that the reverse of the velocities will still make it go over here. It will not change at all.
• **GC**: OK.
• **JLL**: So the point in Γ_2 that you get from coming from Γ_1 is very different with respect to velocity reversal from a point you pick at random in Γ_2. Nevertheless the system behaves macroscopically in a similar way in the future, as you can predict phenomenologically or see in your computer, and that's what I think to prove mathematically or to understand mathematically is an essential problem.
• **GC**: Then I totally agree. Your problem is strictly macroscopic. You start from the phenomenological equations when you find that they are satisfied. Why is this, it is not your problem. Fine.
• **Lev Shchur (LS)**: I don't completely agree with you that it is possible to check in molecular dynamics with any precision. Typically, in the picture you showed us, you have some typical time scale, and Lyapunov exponents. Suppose you can make several mappings of such a kind but at some point you really forgot the initial one because you need some exponential precision for that. You know, your derivatives should be exponentially fine in a way.
• **JLL**: I don't think Giovanni says that you can do it experimentally, with infinite precision. But at least in some simulations we have done on integer arithmetic we did not have that problem, and still have the same answer. And, after all, the real system, presumably, to the extent that you can make it isolated, which again is not perfect, you cannot make it isolated, but I don't think anyone here doubts that if you make a truly isolated system and you did truly infinitely precise molecular dynamics, that you would get any different answer.
• **LS**: Yes, because in your picture you have Lyapunov exponent which is somehow connected with the Kolmogorov-Sinai entropy, which is a different entropy which characterizes the topology of your domains. What is not understandable also from your lecture,

is which domain you keep in your mind. Maybe you speak about some special domain on which you define your system.

- **JLL:** Let's say for the simplest case I would think of a hard sphere system, one with a Lennard-Jones potential in a given box, conceptually totally isolated, with reflecting boundary conditions. That's what I have in mind. As far as one understands, at least in certain regimes, the phenomenological equations would be just absolutely well.
- **Miguel Rubí (MR)**: I want to make a comment on the first point. The question you raised is very important, to know under what conditions concepts introduced for systems in equilibrium such as entropy, free energy or temperature, can also be used in systems away from equilibrium. I think that this is a crucial point. In my opinion, this question is very much related to the nature of the noise present in the system. The nature of the noise may sometimes justify or invalidate the use of equilibrium concepts in non-equilibrium situations. So, for the particular case of a Gaussian noise, which is common to many physical systems, one can extend the use of some of these concepts. When the noise is Gaussian, the stochastic variables vary in a small amount for short time intervals, so the process is very slow and the probability distribution undergoes a diffusion processes governed by a Fokker-Planck equation which is simply a diffusion equation, linear in the probability. In these cases you can establish a connection with the second law and use the concept of entropy. However, if the noise is not Gaussian one has to use other kinetic equations the form of which is different from a diffusion equation. In these cases there is not a clear connection between the dynamics and the second law. To obtain an entropy functional compatible with these kinetic equations is not obvious. An example is the case of a multiplicative noise or other noises such as Poisson or Shot noises. When the distribution function is non-Gaussian, we do not know how to define the temperature. Sometimes, one may define effective temperatures but these quantities are not robust, they depend on the particular situation you are considering, on the observables and the initial conditions. These temperatures are not temperatures in a thermodynamic sense. When the noise is Gaussian the temperature inferred from the variance of the distribution coincides with the thermodynamic temperature and everything fits perfectly well. I want to make a comment on the distinction between the Gaussian nature of the noise and the Gaussian form of the probability distribution function. In the example I discussed in my talk on the Brownian motion in a shear-flow, in a stationary flow, the noise is Gaussian because the particle is immersed in a heat bath. But if you solve the Smoluchowski equation for a nonlinear velocity profile, for example a Poiseuille flow, you don't get a Gaussian form. A Gaussian noise for which the kinetic equation is of the Fokker-Planck type does not necessarily imply that the probability distribution be a Gaussian. In the case of a gentle Poisseuille flow in which the system is not far from equilibrium this distribution function is non-Gaussian. Since the noise is Gaussian you can establish a connection with the second law and use the concept of entropy. So I insist in the fact that the nature of the noise is a crucial point in establishing the link between thermodynamics and stochasticity.
- **JLL**: You are talking about noise. Presumably, this noise you expect is really internal. I mean, you don't think the system would behave differently if it was truly isolated and followed the laws of the dynamics of classical mechanics. Whatever noise comes out, I mean, from the dynamics. Of course you don't want to follow the molecules, you substitute, you replace it by some kind of noise. But I'm asking the questions at a more

conceptual level. There still will be, I expect, a stationary state but you have the two different temperatures, inside I take it to be just real dynamics. I'm not pretending I can solve it, but there is going to be, you know, such a state and I ask, yes it's a question and I don't know the answer. In some cases one can approximate it well enough by means of some kind of Gaussian distribution and have a kind of thermodynamic local thermal equilibrium. In other cases you may not, and I think that's quite likely to be the right answer.

- **MR**: The theory of stochastic processes is very useful because if you know the form of the kinetic equations you can determine the stochastic dynamics of the system, you can calculate the correlation functions which are related to physical quantities one can measure. Then you can establish the link between the second law and the stochastic behavior of the system. In my opinion this is an important point.
- **JLL**: I am not really worried about the second law. I think the second law can take care of itself. It is going to do all right. What these people are saying they would like to have a formalism which is analogous in some sense to the equilibrium formalism and have some function, in particular Tasaki and his group they say, even if you are in local equilibrium of course you still have a current flowing so they want to add to the thermodynamic variables, a local energy density, local particle density, local velocity, ... They want to add a current as a hydrodynamic, as a macroscopic thermodynamic variable, to find a function of these, including the current as a parameter which would somehow play a role like free energy in equilibrium. If you differentiate it, you get the specific heat or you get some other things. I mean, that sort of conceptual question... I think it's important but probably doesn't have a unique answer. Equilibrium is probably, really a special case, it's a very unique case. When you are not in equilibrium you don't have any such universal type of things.
- **Sandu Popescu (SP)**: So, coming to your first thing, to the point with all the molecules starting in a corner, then they expand through the box and you reach a point that is not critical towards the future, it behaves as any other typical point. I just want to mention that, just a comment, that in fact any initial condition is not typical if you define it in a precise way. So suppose you have a situation in which the molecules are uniformly distributed, but you say, well, this is a particular one in which molecule number one is here, molecule number two is there, so it is very non-typical. Let it evolve and you say if I would reverse all the velocities will come back to precisely this point. Most of the others will not do that, but towards the future they all behave the same. So every single initial condition gives rise to a non-typical case.
- **JLL**: Yes, sure. What I'm saying here is on the macroscopic level. [...] I get back maybe to typicality, what do you mean by typical, Shelly [Goldstein]? I think we give it in our paper. Or not? Take the unit interval, from zero to one. Everyone knows that if you take Lebesgue measure all the rational points have measure zero. So every rational point is atypical. Nevertheless, there are certain theorems about typical points. Almost all points with respect to Lebesgue measure are so called normal. This means that in any expansion –decimal expansion or binary expansion– the fraction of times I see in decimal expansions a seven to occur is exactly one tenth of the time, so fraction of times that 693 appears is exactly one thousand of the times. That's normal, that's a theorem. For almost all numbers, "almost all" meaning with respect to Lebesgue measure,... almost all numbers are normal. Obviously, no rational number satisfies that.

Still, if I give you a number, pick 677000 at random, random in the usual sense, for the numerator and a similar type of number for the denominator, and I ask you if I make an expansion, and go up to 500000 decimal places, am I likely to find equal number of sevens and equal number of eights? You would say, unless you really pick your number very specially, “I expect that”. So in that sense I think of typical over here. [somebody interrupts, almost inaudible] Shelly was saying that… almost all the energy, here is your whole energy surface and almost all of it, I mean, really almost all of it, except up to a tenth to the minus 20 corresponds to equilibrium. No, he doesn’t disagree with that, I don’t think at all.

• **SP**: I would actually disagree with you. From your point of view, you see, there is a conflict in what you say because, on one hand, you would like to define a point of being typical just by [. . .] looking at macroscopic conditions. But if you would be able to view with infinite precision, then every point would be atypical in some sense towards the past. But they are all typical towards the future.

• **JLL**: I don’t think so. I think that in Classical Mechanics and in Quantum Mechanics, whatever you said for the fraction of time, going from zero to infinity, in an isolated system I could just as well go from zero to minus infinity and arrive exactly at the same theorem. As long as the system stays isolated, of course. Why then do we see this irreversibility in life, in nature? I think that really goes back, you have to go back to initial conditions. Feynman emphasizes it, and Boltzmann already said it. I forgot now the exact phrasing of Boltzmann but something when he answers Zermelo. When Zermelo said, you know, that you have eventually Poincare recurrence, and things like that. Boltzmann said that what is important to realize is that the behavior of systems is not determined by dynamics alone. It also involves initial conditions. That’s very crucial. The dynamics are time symmetric. It’s initial conditions which are not time symmetric. But if you simply look at the dynamics and pick a point, it is going to be time symmetric. Is what Shelly was saying, and von Neumann. [. . .] In reality we don’t see that because of the initial conditions. Sometimes I have this picture from Roger Penrose where there is the good lord creating the universe and pointing to some very, very little macrostate over there. Again, I point to Boltzmann saying in a different way the important part: you do not have to take a particular microscopic state.

• **Roberto Livi (RL)**: I want to add some comment about what Joel was discussing before. Well, on the concept of reversibility and trajectories and so on. These are quite troublesome arguments, but let me give you a piece of information that I know for sure because I published a paper on this fact. [laughs] These are not just conjectures, these are results. Take that stuff and put it in contact with two heat baths. With two heat baths, I mean, the chain I was showing you before. And take it a harmonic chain. Joel solved that problem many years ago with Rieder and Lieb, and you can work out an analytical collection, and you know everything about that. In that case you are in a very anomalous situation. Everybody knows that, you know it follows that [. . .] there is no Fourier law, there is nothing about that. But now suppose that you add, and this comes again as an example of a special kind of noise, a martingale process, which amounts to add randomly collisions that preserve energy and momentum. So you have the dynamics but sometimes a couple of particles collide. This can be worked out very easily. [. . .] The very important point is that you can compute analytically everything of this problem and you can compute the nonequilibrium invariant measure. Compute means with analytic formula, without any approximation or integration scheme. And then you find a very nice expression, and you find everything that you need to know about this state. The correlations, spatial correlations appear, you have local thermal equilibrium with the exception that the tails of these Gaussian distributions certainly have to feel the effect that you are not in an equilibrium state, so that these tails maintain this memory effect. So everything here is analytical. Now you take any other model, for instance the FPU model or any other kind of nonlinear chain, and then in that case your covariance matrix can be solved numerically, obviously. And then you apply standard molecular dynamics method. What do you find? Something which in practice is completely in agreement with the previous analytical solution, concerning the main ingredients. I'm not saying the same model but the ingredients. The description of this out of equilibrium stationary measure obtained by the eigenvalues and eigenvectors of this covariance matrix behave very gently and very close to what you have observed in the analytic solution of that problem. So it seems that, for any practical purpose, you obtain what you expect to obtain despite you have a finite system, despite you have round off errors in your computation and so on and so forth. And even if you have a small system, this works perfectly. Obviously, as I was saying before in my talk, you must take care if you want to exploit numerical simulations to integrate things you don't know how to integrate in any other way, you must be very careful in order to control any finite size effect, any time length effect and so on and so forth in measuring this covariance matrix elements. But once you have done that, I mean, you will know also when this will be violated. You can really predict it on the basis of analytic argument that if you go too far away in computing these correlations, you lose the information that you want. And in some sense this goes back to the fact that if you look at these things in a finite time, there is a typical finite time which is related to the finite length of the system, but once you have taken that into account the thermodynamic limit problem does not enter the game. Now, in any numerical simulation, on the other hand, you know that you have round off errors. And this will affect how the information propagates. There is no way out of that. Irreversibility in this kind of simulations doesn't exist because if you reverse your process you don't go back to the initial state.

• **JLL**: You mean of integer matrix?

• **RL**: In the case of integer matrix I agree, you can do it. But in that case there are other technical problems that you have to take into account in order to say over which time scale you can trust what you observe. [somebody intervenes. Inaudible]

• **RL**: Yes, I agree. Absolutely if you control and you increase your numerical precision register to 256 or 512 bits. This is your job at the very end. So, I mean, you make it correctly. I don't know if this is sort of miracle, but things work. That's what I can say, no more.

• **William G. Hoover (WGH)**: [Going back to Joel's statements at the beginning] Number three of your statements looks to me very difficult indeed, but I have a few remarks on the first two. It seems to me that Helmholtz' free energy and entropy are not interesting variables away from equilibrium. Certainly they are in the equilibrium case. But it seems to me from our experience in simulations that kinetic temperature is a perfectly good variable away from equilibrium. And it seems to me that if you are interested in constitutive relations you could start out by thinking of the energy and the kinetic temperature rather than free energy and entropy. Similarly, there are perfectly good expressions from kinetic theory, even at high density, for the heat flux vector and the pressure tensor. So, as long as you are not too fussy about where these quantities are localized, everybody agrees on how to calculate the momentum flux and the energy flux. Now, if you would like to define those things at points, and in particular if you would like to define them at points in such a way that you have spatial derivatives that are continuous everywhere, you can do this by introducing Lucy's or Monaghan's smooth-particle weight functions, which describe the contributions of each particle in space. And if you do that, which Carol [Hoover] will be talking about tomorrow, you will find that the pressure tensor at a point and the heat flux vector at a point depend on the details of the weight function. To me, instead of looking at this as disastrous, it's actually an opportunity, in the sense that you can ask yourself which weight function gives the simplest macroscopic description.

• **JLL**: When you say wave function, you mean you are talking Quantum Mechanics or not?

• **WGH**: *Weight* function, not wave *function*! It's simply the idea that the influence of each particle on the nearby density is not represented by a delta function but instead by something like a Gaussian, but compact, with a range of perhaps two or three particle diameters. Then the fluctuations in the macroscopic description are small with respect to one percent in a homogeneous fluid. That's a very easy thing to do. Carol [Hoover] will be talking about this tomorrow.

• **JLL**: May I just summarize what you said? You are saying that even if you don't have a free energy or a distribution function like a Gibbs distribution for the stationary state, things are not so bad. You can get along with that. Go ahead. I just wanted to summarize what you have said.

• **WGH**: You are right, and I just wanted to say one other thing regarding numerical simulations of a stationary state. There is always some kind of thermostat, so we would have a cold one at the left hand side and a hot one at the right hand side, for instance. You can calculate, as long as the thermostats are deterministic, the Lyapunov spectrum, so you can see what happens to Gibbs' entropy as time goes on. After a while, when one achieves a nonequilibrium steady state, one finds the interesting news that Gibbs' entropy is diverging to minus infinity, because the system is collapsing onto a [multi] fractal attractor. In an example that I'll show tomorrow, the change in the dimensionality of the steady state with 32 particles is about ten percent. So, instead of having a 192-dimensional distribution like Gibbs', the distribution is somewhere between 170 and 180 dimensional. So, if you try to take the logarithm of that fractal distribution, it will diverge. So that is the physical-conceptual basis of my talk, that the kinetic temperature tensor is a better thing to look at than entropy.

• **JLL**: We will wait for your talk tomorrow but another discussion, you know, I mean, if you use different reservoirs like the one that Roberto was talking about, Langevin type of thing, then you don't get any such collapse. But again, as you are saying, the properties of the system that you are interested in are exactly the same more or less, because we believe, I think it's correct, I think that Giovanni [Gallavotti] quoted it from 1959, that the boundary conditions really should not affect what happens.

• **GC**: Joel, I'd like to add something to this point, and is that to do statistical mechanics you need an invariant measure, an invariant measure with time, and you find that this problem of the degrees in dimension, if you use the Lebesgue measurement, but the Lebesgue measurement with the dynamics associated to something like the Nosé-Hoover thermostat, is no more invariant. So I think this is a question really to be clarified, it is not at all evident that the statistical measurement that you use when you use non Hamiltonian dynamics is a Lebesgue one. I would take this as possible…

- **JLL**: I agree with that. Maybe let's hear from some other people.
- **Vaclav Spicka (VS)**: I would like to comment on Joel's first statements. So, maybe this derivation of macroscopic equations, I would say that this is the general problem of correlations between particles, I mean, a many body problem because I'm starting from some many body problem, I'm writing microscopic equations and then, as everybody knows, you must do approximations to come out with some macroscopic equation. So, I'm leaving out some interactions and so on. I'm emerging with irreversible macroscopic equations. Another addition is that I must define some initial conditions for this. This is another tricky point because when I'm defining initial conditions I must somehow know the history of the system. Because then I don't know how from scratch what means initial condition and how I neglect or not neglect correlations. So, basically this is tricky and as soon as I will derive so-called such equations I must compare this with experiment because I have no other chance basically. So, I must do this because every time I'm forced to do approximations and irreversibility is emerging as like something like effect of approximations, in fact.
- **JLL**: Maybe you do approximations. I do not know that a metal bar does any approximations. I know perfectly well what I mean when I start with a metal bar with some temperature profile and it evolves according to the heat equation. I do not think the metal bar knows about your approximations.
- **VS**: But the problem is a realistic Hamiltonian. Because realistic Hamiltonian includes all these interactions and so on.
- **JLL**: Of course.
- **VS**: Then I am in trouble with these things and, moreover, I would say that when I derive some kind of equations from ideal density matrix or Green functions or, there are many methods, then in fact I have some clue how to calculate observables. And then I basically don't care about any free energy or entropy. So basically, I'm in complete nonequilibrium state, maybe, it depends basically on time scales and interactions in the system. If some steady state emerges or not, if free energy is good description or not, it depends… Basically, this is question of how far I want to generalize thermodynamics and if it is reasonable to generalize it…
- **JLL**: I think… You talked both about my first and second points. […] What I wrote down was just the heat equation. I give you an energy profile, say for a metal bar, a copper bar, and I look how it changes with time, and I find very accurately, maybe not absolutely perfectly, that it satisfies the Fourier's law, its equation. And that's what I would like to derive, if it is possible to do it, I mean, mathematically, we certainly have not succeeded so far. So it's an open problem. We have not succeeded but we tried.
- **JLL**: Younger people should speak up. Where are the young people?
- **Afshin Montakhab (AM)**: I'm not sure that I qualify as a young person but at the risk of not being invited here again I would do the following comment from the information theoretic point of view. I hold the view that if we had as human beings devices that actually measured with infinite precision the positions of the particles, or the initial state of constituents of macroscopic systems with infinite precision, that we measured

the forces between them, then we would never need thermodynamics. We would not be talking about things like entropy or anything. So, since uncertainty is a part of our existence, then there is such a thing called entropy, which is the Shannon entropy. And from the uncertainty or the measure of which is entropy you can actually calculate quantities that an observer would make, a macroscopic observer with a thermometer, a barometer and these kind of devices that we normally have in our laboratory, would make. So I can hold the view that perhaps trying to derive thermodynamics from Newtonian dynamics is a bit misguided either you have to make approximations, like Boltzmann made, and you don't really know where the irreversibility comes from. So I think these two points are divorced from each other. Either you have precision, exact precision, in which you can actually answer all kinds of questions you ask, or you don't. And the fact is we don't have those precisions. Therefore we have to deal with thermodynamics. And that's all I want to say. Just as a comment.

- **JLL**: I would say I would strongly disagree philosophically and conceptually with that point of view. I mean, do you think if I knew exactly the positions and velocities of all the molecules in the water, and I put in this thermometer I would get a different answer than what I get when I don't know?
- **AM**: Thermometer is a macroscopic...
- **JLL**: Yes, so supposing I know all the atoms and molecules of the water and of the thermometer, would I get a different reading than I get...?
- **AM**: No, no; you wouldn't, but the point is you don't have that. That's impossible.
- **JLL**: Who cares? I mean, I think it's a conceptual thing. I never know, nobody knows, what π is exactly, the number π. You can approximate it up to decimals; does that mean that π does not exist as a number?
- **AM**: Yeah, but that's mathematics, it's a little bit different from physical reality.
- **JLL**: I think we have a disagreement there. Many people take the point of view... like Roberto... I have written an article too with Christian Maes. It's about this man who is a very good man, who dies and goes up to heaven and he meets an angel there, and the angel has a big bowl filled with hard spheres. And the guy asks: Do you know every position and velocity? The angel says yes. Then the guy asks, what is the entropy of this system, the thermodynamic entropy?
- **AM**: It's zero.
- **JLL**: Our answer is that it is exactly the same for the angel and us. Does it make any difference at all as whether you know them or not? The behavior that we have discussed is the same. So, my own feeling is that information theory is very, very useful but I don't think it really should be part of the foundations or of these questions, where it is irrelevant.
- **AM**: I would just say the angel would say entropy is zero. Entropy is zero, you have everything you need to have, therefore you can answer all kind of questions. Once you have the dynamic questions you can answer any question.
- **JLL**: Sure, you can answer any questions but that doesn't mean entropy is zero because you can answer all the questions. It is still true that if you start with one part hot and the other part cold, heat will go from the hot to the cold, and as you know, entropy describes that evolution of going from hot to cold but it doesn't change at all that angel knows everything.
- **AM**: OK. Don't use this against me and invite me again [laughs].

- **Matteo Polettini (MP)**: I do qualify as a young one, but I'm not really expert on the arguments… I do like the point of view of the information theoretic, but I think that there's a little bit problem, is entropic, it's an anthropic reasoning. It puts man on a special footing and you say, of course, thermalization occurs in any case but [âĂę] in any case we are always talking about a piece of the universe, a system, which will never be isolated from the rest of the universe. So, when we reason about reversible, Newtonian equations what we are really talking about is the universe itself. It's a sort of cosmological problem. And my question is, does it make sense to derive macroscopic thermodynamics from microscopic dynamics without worrying about the universe on the whole? The universe has a peculiar behavior, for example, it's expanding so things in the universe are diluting and this might be one of the mechanisms for equilibration.
- **JLL**: I agree totally with you about non-isolation in practice, but do you think really the Navier-Stokes equations depend on having non-isolation? I don't think so. I think it is true that you don't have isolation but I think the behavior of diffusion equation will not be affected if you really had the isolated system. That's what I would think. That's my answer.
- **AM**: I wanted to make a comment about the comment you made about the observer. That's the same question Joel responded when I asked the question about the observer the other day and is that, is the observer a Ph.D. student? The answer to the question is we have observers in most physics theories; we have an observer in Quantum Mechanics; we have an observer in special relativity; we have observers in thermodynamics. An observer in thermodynamics is a device that has a thermometer, a barometer or whatever, you know, can just do the experiments and measure quantities that are relevant. So that's the observer, it's not me or you, or a given person's uncertainty.
- **JLL**: I believe that there is an objective world which behaves totally the same whether anybody has precise knowledge of it or not. The universe does not depend on observations. The laws of motion were always there, we don't know them exactly, they were there before there were thermometers, before there were dinosaurs…
- **AM**: What about Quantum Mechanics?
- **JLL**: Just the same. I think we should go, maybe let Shelly answer that.
- **AM**: Special relativity? I mean, physical theories always have observables.
- **JLL**: No, no. I totally disagree with you.
- **AM**: Maybe we should shut up this.
- **André Timpanaro (AT)**: I would like to just make a comment on this discussion about what I understand as Shannon entropy and what I understand as thermodynamic entropy. Thermodynamic entropy is a kind of Shannon entropy when your only information are the thermodynamic variables. Suppose you have a gas. The entropy depends on the temperature, the pressure and the volume. So the thermodynamic entropy of that gas is the Shannon entropy that you would have if you only had those three informations. Suppose then you expand your gas, you make a free expansion, the thermodynamic entropy would increase but the Shannon entropy remains the same. The previous temperature, pressure and volume are still the same. Now, if you had a new box with the same macroscopic variables than the expanded box, then you can't say about it the same things you could about the first box, because its Shannon entropy is bigger, it is the new thermodynamic entropy.

- **JLL**: I think in general… What I call the Boltzmann entropy, logarithm of the macroscopic phase coincides with your Shannon entropy when your system is in equilibrium. If it is in equilibrium it coincides. It does not coincide, as you pointed out, when you go out of equilibrium because the Shannon entropy will not change with time, well the thermodynamic entropy and the Boltzmann entropy will. I don't think there is any contradiction there.
- **AT**: But suppose I got the expanded box and showed it to you. If I ask you what the Shannon entropy is, you'll tell me it's the thermodynamic entropy. You don't know what the three macroscopic variables were before expanding the box, so you can't say the same things I can say about it.
- **JLL**: No, for me thermodynamic entropy is what the thermodynamic entropy is. And if it happens to coincide with the Shannon's, fine.
- **SP**: If you allow me to just to make one more comment regarding to this discussion. I think that the main point is the following. Obviously if you know the position and velocity of every single molecule in the gas, or in your cup of coffee, will not change the fact that if you put a thermometer will show the same thing. And that heat goes from the cold to the hot and so on, well the other way around. So, from that point of view is good to still continue and have the same notion of entropy because that allows you to answer all these questions. But the point is that if you actually know the positions and the velocities, there are new things that you can do. So, for the old thing of putting the thermometer is the same. But now, if you know…, now you can actually extract work of that thing because you can put mirrors… So, it is this difference, that now you can do other things, that previously you couldn't do. And for this is good to have a different notion of entropy that will reflect that.
- **JLL**: I think I would not disagree that you can do more things if you know more. I think I would not disagree with that. You can have many, many notions of entropy. As I mentioned, the Shannon entropy was called entropy, at least according to legend, because von Neumann said to Shannon "if you call it entropy then it has a resonance, and then since nobody knows what entropy is nobody can argue with you". I should mention just one relevant fact. I showed in my talk on Monday a quotation from Thomson which I think was the first to clearly raise the question that, if you reverse all the velocities, everything would go in the other way. Then you go down to say that, an actual fact, because our sensitivity to initial conditions or perturbations… if you really try to … you can make any error, any even slight error in reversing the velocities, you will find that it behaves just as you expected to behave before. Because any imprecision will lead you again to, say, the bigger region of the phase space. In order to get into a very small region you have to be infinitely or very, very precise. The more chaotic the dynamics and the larger the number of particles, the more precise. To get out from the small region into the big region you don't have to be very precise. That answers also the question: why doesn't the noise make a big difference? Because if you are going in the direction of the expanding phase space volume, we would expect if you make a small perturbation it is not going to change that. However if you are going into something very, very small, any small perturbation is going to make an effect. It's like, you know, the situation if you try to park a car in a very tight space or get out from a very tight space. It is not at all the same effort. I mean, it is much easier to get out because there is much, much more space there, so a small error doesn't matter but getting in you are going to scrape your car on

your neighbor's car if you are not infinitely precise.

- **Harald Posch (HP)**: I think one can view these things by looking at the blackboard. The picture you draw there is a bit misleading. You start out with a little blob in phase space, which presumes that you have a partition in phase space. Then take a little volume. If we evolve this little blob forward in time, then we know what will happen: the system, let's assume it is isolated, will change such that the volume is conserved, and we'll get a very fine filament all over the whole phase space. What counts is what Kolmogorov called mixing in phase space. That's the key quantity. And this is measured by the Kolmogorov-Sinai entropy. So the Kolmogorov-Sinai entropy is the key question. If we compare now the original blob with the filamented situation at a later time, most of the measure will be spread out over the whole phase space, and only a small part of it will have remained in the volume of our original blob. When we do a measurement we are necessarily forced to project down onto such a partition. So, if you put your thermometer in, it will not be infinitely thin. The projection introduces irreversibility into this problem.
- **JLL**: So you think an isolated system following Newtonian laws will not behave in the way I said?
- **HP**: No, no. I just wanted to build the bridge between these various view points.
- **JLL**: Oh, yeah, I think I understand what you are saying and think that it is absolutely correct, I would agree. That is,... things are really much more mixed up over there and, therefore, despite the fact that they are very atypical, this is a very specific thing [...]. I agree with that. That's really a mathematical question, to be able to show, to prove that is central. I mean, I think we agree entirely. The reason is indeed conceptual; this is very, very mixed up over there. Yeah.
- **HP**: If one takes this into account, I mean, then all these different view points can be seen on the same level, and we do not have difficulties, going from one picture to the other.
- **JLL**: I agree. There is only one true picture for a system evolving in time.
- **Errico Presutti (EP)**: It's a very short comment. I want to say that von Neumann was terribly wrong, because we don't know anything about it, but we have been arguing a lot.
- **JLL**: So, why was he wrong, in what way?
- **EP**: Because he says nobody cannot argue.
- **JLL**: Oh, about the entropy thing! Yes, he was very wrong over there.
- **Francisco Pérez-Reche (FPR)**: This is just in case I qualify as a young person. Well just to tell my opinion about the second item, derivation of macroscopic equations for realistic Hamiltonian microscopic dynamics. So, well, based on my experience in working on complex systems, I would say that it all depends on what you want to reproduce at the macroscale. I mean, you have to start at the right microscale in order to reproduce what you want to reproduce at the macroscale. For me is already challenging to obtain realistic Hamiltonians. It looks to me close to impossible in some cases, but I think there is some hope if we are able for instance to find the right scale of description and then we can from this right scale to reproduce the big picture at the macroscale. So, for instance, there are phase transitions for which you wouldn't be able to explain everything at the macroscale if you would be starting with molecular dynamics, because, first, is a technical problem and, second, maybe you are missing

something some interactions that appear at larger scales. So, I think the challenge is to start at the right microscale and then, if you are at the right microscale, then hopefully you can derive something that makes sense at the macroscale. And then (it links to the first of Joel's questions), having said that, probably yeah it would be very nice to have something similar to the free energy for nonequilibrium steady states, but I think that it looks a bit hopeless. Well, it's perhaps hopeless in the sense that perhaps it's not going to be useful because it will depend on each particular system and probably on the scale you choose at the microscale to describe it. So, maybe we have to think in a different way, because we were very lucky that thermodynamics exists. But this is a very particular situation and maybe life is much more than that and then we shouldn't try to stand beyond the limits. Obviously, this is just my opinion.

• **JLL**: What you are saying is correct and reasonable. Certainly, yes I agree. I think it's nice that there's some universality… Almost every substance we know has a liquid, a gas, and a solid phase, with many other phases also. Almost every substance, I mean, we don't go to one-dimensional, pathological systems of something, seems to satisfy a kind of diffusion equation for the heat conduction. So there's a very nice universality, and so what I mean, by realistic, so I mean realistic just in the sense of Lennard-Jones hard spheres, which are not truly realistic, but sufficiently so that they seem to behave the way actual systems do behave. We always have to make idealizations and simplifications and, surprisingly, you can get away with it. Why should we be able to use classical mechanics at all? I do not know really an answer to that. The world is truly quantum mechanical and it's not clear at all why classical mechanics gives not only qualitative, but even quantitative things in many cases. There is a certain universality which transcends even the quantum-classical thing. Of course, we do not get superconductivity classically, and many things are not the same obviously, but still trying to focus on things that are the same, which are universal.

• **Pablo Sartori**: I was wondering whether instead of using the free energy as something to characterize nonequilibrium steady states, it would also be a good choice to use other quantities such as the entropy production rate. I mean, I know people use that and I don't know if it's more useful or more…, yeah using the entropy production rate instead of the free energy.

• **JLL**: That's certainly something which seems to be a useful thing to do. I guess, I don't see Gallavotti here but he would argue that probably you should not define any entropy for such a system for the reason that Bill [Hoover] was saying before that, you really would get minus infinity or something if you do that. But you can well define entropy production anyway. I mean, energy production is useful and probably much more useful than free energy, especially since we don't have any free energy. So certainly it could be more useful.

• **Marco Ribezzi**: I would like to ask a question about the first of Joel's points; maybe it is completely nonsense. If I got it right from your lecture you say that a possible candidate for free energy in nonequilibrium steady states is the large deviation functional. Well, this is the case in some systems that have been studied. I know just two examples in this field which are stochastic differential equations and then the macroscopic fluctuation theorem for lattice gases, and in both of these cases the differences in this free energy, in the large deviation functional, can be obtained from a variational problem on a functional on trajectories. Am I clear? I mean, you have a large deviation functional for trajectories and from that you can derive this free energy. In these two cases, the large deviation functional for trajectories has, according to me, a very similar form, which is something like an Ohm's law, because it is resistance times a current squared integrated in time, so this is something like a dissipated work along the trajectory. My question is, if this has any chance to be something more general or if this rests on some specific features of the system.

- **JLL**: I think it is general, but it only gives you differences. The large deviation functional vanishes for the typical state. So it gives you the difference, and the question is then what happens with the typical state itself? Just like in equilibrium for the typical state you have an entropy which has properties as a function of energy you can differentiate, and that's what the question is here. So that the large deviation functional is the difference between the typical and the untypical. I think in that case, I believe that, yes, it does play the same role, but entropy plays a special role even in equilibrium, and that's what we are looking in the nonequilibrium stationary state. Is it clear what I mean?
- **Giovanni Gallavotti (GG)**: Since you just mentioned what I would say about entropy...
- **JLL**: Oh, I didn't know you were here.
- **GG**: Where could I be? So, I agree that I would say that entropy does not make sense for nonequilibrium systems, but I also said and wrote in some papers that, even though entropy probably does not make much sense, I think you still can define for every system which is evolving a Lyapunov function which will indicate that you are approaching the equilibrium and will come with zero derivative at that limit. Exactly this function does not have the characteristics of entropy, of being a function of the state of the system. It is a function which depends on the parameters, and on the precision you use to describe your system itself. That's what I have said and written.
- **JLL**: So, I did not totally misquote you. Giovanni says, this is his point of view, he would not call what I call the Boltzmann entropy for a macrostate which is not in equilibrium, he does not want to call that an entropy. But he does agree that if we take the difference between that function and the equilibrium entropy then, it shows that the logarithm of it shows up as a Lyapunov functional for time evolution of a macroscopic system, an isolated microscopic system. Is that correct?
- **GG**: I just wanted to make a comment.
- **Carol Hoover (CH)**: Since we are talking about entropy production, let me remind you that [in 1984] Nosé introduced temperature into a Hamiltonian, and in mid-July of 1996, at CECAM/Lyon, Carl Dettmann generated a Hamiltonian similar to, but better than, Nosé's, that included the temperature and gave directly the Nosé-Hoover equations of motion. So I think there is some work done on Joel's second point because Nosé did show that you could get Gibbs' ensembles for equilibrium. And so I thought that was a very nice piece of work done in 1984, by Nosé. For the nonequilibrium steady state you really do have the option of computing thermodynamic and hydrodynamic variables except for the entropy and free energies. You get entropy production instead. So, to me, this is a real step forward for nonequilibrium steady states.
- **JLL**: Did you say Dettmann?
- **CH**: Well, [Shuichi] Nosé was the first to put temperature in. Bill [Hoover] and I met up with [Carl] Dettmann in July 1996 and wanted to generate a Hamiltonian that would give us Nosé's feedback equations that are used for the thermostats and the proper

equations of motion. Working just over one night –Dettmann was then an astrophysicist– he came up with his new Hamiltonian the very next day. He does have a publication on it with Gary Morriss. So, I mean, at least for the nonequilibrium steady states you do have some connection between macroscopic variables and the variables you would measure in the steady state with molecular dynamics. And Bill [Hoover] mentioned that to get a point function for the pressure tensor you do have to use some smooth-particle averaging technique and the one I'll describe tomorrow [Lucy's] is reasonably good, as I'll show in our calculations.

• **JLL**: Thank you. I'm not familiar with the theory of that paper. Seems interesting, certainly.

• **Félix Ritort (FR)**: I want to make a comment about the first question, this free energy in steady states. Actually, there are many nonequilibrium steady states and it is always difficult to know what you really mean by a free energy in a nonequilibrium steady state. Then, as far as I know, I mean, there are some reasonable results, always on some phenomenological models, based on some approximations like Gaussian noise, where you can prove that there is a fluctuation-dissipation theorem in the steady state. I think there is a recent paper by Prost, Johanny and Parrondo, I think it's a nice paper.

• **JLL**: Say the names again.

• **FR**: Jacques Prost, Jean François Johanny, and Juan Parrondo. They prove that by defining some kind of observables it's possible to prove the validity of a fluctuation-dissipation theorem in a steady state. Related results, I think, have also been produced by Udo Seifert, maybe he would talk in these days, and this proves that you don't have a free energy, but you have something that resembles what you expect an equilibrium state-like should have. And, well, we have been working in these experiments pulling molecules, in which you move an optical trap and you have a bit and you make transitions between steady states. In an optical trap experiment, a transition between steady states means that you have your trap moving at a velocity, and you accelerate the trap and you change the velocity. We have a paper published a few years ago in PNAS where we test one equality derived by Hatano and Sasha which of course it is also based on approximations and so on, and it tells you that there is a *W* function that always increases between transitions between nonequilibrium steady states. So, if you accelerate very fast, the average *W* is big. But if the transition is very slow, if you don't accelerate, the transition between the two speeds of the trap, so you do a quasistatic transition between the steady states, then this *W* is zero. And then it turns out that you can define in this simple case a state function. The equivalent of a free energy, the equivalent of a reversible work, the equivalent of basically, well, you can define the state function of this transition. The caveat is that in this formulation of Hatano and Sasha, which is also related to the result by Prost, Johanny, and Parrondo, the caveat is that you need to know for constructing this *W* function, you need to know the steady state solution for all intermediate states through this transition, in these experiments. So if you change from one speed to another speed you need to know the steady state distribution for all intermediate, let's say, conditions, OK? So, it's not practical because either you have to measure experimentally before the steady state and then you can evaluate the *W* function. But still, if you have an experiment, you can do that. Of course, we cannot do that from calculations because we should solve the equations exactly, but there is a procedure to measure this thing. And this has not been done in other nonequilibrium steady states, but I think it would be very nice to do experiments because it's very clear this W function what it means, and I think it would be nice to see more experiments on measuring these state functions [...] experimentally.

• **JLL**: I guess that's a joint work with Tasaki also.

• **FR**: Yes, well this Tasaki you mention, I think is slightly bit different, because I'm not sure they are the same people. I think they are Japanese but not the same. It's a different work.

• **JLL**: I think it is certainly a very interesting work.

• **SP**: It is just my ignorance. What do you define to be a steady state? Because, obviously, may have a bit of fluctuations. How big the fluctuations do you allow?

• **JLL**: It's like in an equilibrium state. I mean, in the region which Shelly [Goldstein] showed, or I showed also, we do include fluctuations of square root of N type of thing. In the steady state they might be different, but normal fluctuations I would include in.

• **SP**: So, for example, if instead of the metal bar you just have a cube with water and a bit of carbon and hydrogen, eventually you will get a fish. So, if instead of being a metal bar you have a cube that is filled with a homogeneous solution of water, and carbon and hydrogen, after a long time you will get a fish swimming. That is a too big fluctuation.

• **JLL**: I think so. I think that is a too big fluctuation. I would consider that as different macrostates.

• **SP**: So although are on average, say, a thousand fish swimming, that would not be a steady state.

• **JLL**: Yes, I mean, let's stick to the metal bar. Or let's take still water where there is not going to be any fish swimming over there. I you have got a fish swimming, presumably you have put in something besides just water. [...]

• **SP**: Some Carbon, some Hydrogen, and it's homogeneous but eventually there will be a fluctuation that will lead you to...

• **JLL**: Wouldn't that be true in equilibrium also? You also have a fluctuation that will lead you to something like that?

• **SP**: Suppose that this will be maintained for a long time. Suppose this situation will be... Well, the other interesting question is obviously whether there is a limit to the complexity that may arise in such a system.

• **JLL**: I don't know the answer to that. But I think somebody asked me again in connection with your question on Monday. What is the steady... ? Who is that? Julio [Fernández]? was asking me the question: what is the steady state of us on Earth assuming that the sun doesn't give out on us, or other thing. What's going to happen? My private opinion maybe I don't want to tell you [laughs]. But, I don't know. I mean, things can be very, very complex as you say, and specially in nonequilibrium situations. It's a good point.

• **Anonymous**: You can find it through the hydrodynamic equations. So you start with the hydrodynamic equations, and you set the time derivative equal to zero. This is the way, one of the ways, in which you can identify these states.

• **JLL**: Macroscopic, but still it doesn't include everything. Anybody else?

• **Sergey Apenko**: I have a kind of a technical question because I'm not an expert in the field. I feel that the whole discussion is somehow predetermined by these three questions put forward. They are certainly very fundamental and very difficult to solve. But it's written here that these are only some of important open problems. I have a question: do you have some other open problems which are more easy to solve, probably?

• **JLL**: Well, one problem I would like to understand, maybe Roberto [Livi] can say, in one dimensional systems you get this anomalous heat conduction, apparently as long as you have momentum conservation. Even if you have nonlinear harmonic things, as long as you have momentum conservation you simply get anomalous things. If you don't have momentum conservation, then if you also have nonlinearities and typical things, you seem to get Fourier's law, so ordinary conduction. Now, there is a claim of a theorem to that effect, that for systems with momentum conservation you have infinite heat conductivity. But it is not really a theorem because the proof is not correct. I mean, the theorem may be correct, but the proof is not correct at all. So one question is really: are there any systems which do conserve momentum in one dimension which might still have normal heat conductivity?

• **RL**: The answer is yes, I know perfectly the model, One example, there are many class of models, is the rotator model.

• **JLL**: You are conserving some quantity. I'm thinking of real linear momentum.

• **RL**: Ah, linear momentum! No, the answer is no. In that case you have a special situation.

• **JLL**: Are there any special situation even with conservation of linear momentum?

• **RL**: No. The general outcome is the one that you know.

• **JLL**: There is no real proof for that and I think that is an interesting open question both in one and two dimensions. Well, it sort of included on derivation of macroscopic equations. Somebody wants to say something?

• **MP**: I think one interesting question would be to find variational principles for nonequilibrium steady states. We have maximum entropy at equilibrium. Jaynes talked about a minimum entropy production out of equilibrium or near equilibrium, and in great generality, I think variational principles would be interesting to learn.

• **JLL**: Very, very much so. I guess for diffusive systems, stochastic diffusive systems, macroscopic diffusive systems, the work of Bertini et al. is relevant. Well, there are large deviation functions which can be seen in some way as a sort of variational thing. But certainly I would like to have a more general thing. Absolutely, very much so.

• **CH**: We've done a Rayleigh-Bénard calculation which is, you know, conduction rolls, and we actually did not find an entropy production minimization principle or an entropy maximization. So there are problems for which, at least we haven't found any kind of optimization principle.

• **JLL**: Yeah, I guess there are no reasons why there should be one, I mean, you are not very close to equilibrium.

• **CH**: I should add the point that we can have multiple solutions for the same boundary conditions. That is certainly one difference.

• **JLL**: [. . .] That's exactly what we would like to have, such a free energy functional. To be able to derive these different possible steady states for the Rayleigh-Bénard problem. I mean, that's a very specific case where it would be nice to have. . . , but it might not exist. Yeah, but you could have multiple things even with free energy functional. Of course, there are many, multiple equilibrium states.

• **Reinaldo García**: I refer to the first point. I think that the recent developments or approaches related to fluctuation theorems and thermodynamics are, in a certain way, as you have already said here, just trying to fill this gap between equilibrium and nonequilibrium steady states. But there is a wide class of nonequilibrium systems that cannot be included in this effort trying to fill this gap. It seems to me that all these theoretical approaches to fluctuation theorems and entropy production and so on demand, at least in the examples I've seen in the literature, a sort of Markovianity in the dynamics. So, all these fluctuation theorems have been proved mainly in Markovian systems. But there is a class of systems related to, for example, systems undergoing a glass transition, systems with quenched disorder or even selfgenerated disorder, where these theorems are difficult to prove because of the lack of Markovianity, I mean, the gap in this kind of systems is even broader. So I think that, for example, it is known that if you have in a random landscape a set of particles, in the vicinity of certain depinning transition you can measure a fluctuation theorem. But these kinds of things are not understood well. So I think that it is an important or open question to try to fill this other gap because there is a wide class of systems which fall out of Markovian systems.

• **JLL**: I agree fully. Certain glassy systems are very much an open problem which we don't understand.

• **JLL**: I think it is time for us to go to lunch. So, thank you all very, very much for your contribution.

Three lectures: NEMD, SPAM, and shockwaves

Wm. G. Hoover and Carol G. Hoover

Ruby Valley Research Institute, Highway Contract 60, Box 601, Ruby Valley, Nevada 89833

Abstract. We discuss three related subjects well suited to graduate research. The first, Nonequilibrium molecular dynamics or "NEMD", makes possible the simulation of atomistic systems driven by external fields, subject to dynamic constraints, and thermostated so as to yield stationary nonequilibrium states. The second subject, Smooth Particle Applied Mechanics or "SPAM", provides a particle method, resembling molecular dynamics, but designed to solve continuum problems. The numerical work is simplified because the SPAM particles obey ordinary, rather than partial, differential equations. The interpolation method used with SPAM is a powerful interpretive tool converting point particle variables to twice-differentiable field variables. This interpolation method is vital to the study and understanding of the third research topic we discuss, strong shockwaves in dense fluids. Such shockwaves exhibit stationary far-from-equilibrium states obtained with purely reversible Hamiltonian mechanics. The SPAM interpolation method, applied to this molecular dynamics problem, clearly demonstrates both the tensor character of kinetic temperature and the time-delayed response of stress and heat flux to the strain rate and temperature gradients. The dynamic Lyapunov instability of the shockwave problem can be analyzed in a variety of ways, both with and without symmetry in time. These three subjects suggest many topics suitable for graduate research in nonlinear nonequilibrium problems.

Keywords: Temperature, Thermometry, Thermostats, Fractals
PACS: 05.20.-y, 05.45.-a,05.70.Ln, 07.05.Tp, 44.10.+i

THERMODYNAMICS, STATISTICAL MECHANICS, AND NEMD

Introduction and Goals

Most interesting systems are *nonequilibrium* ones, with gradients in velocity, pressure, and temperature causing flows of mass, momentum, and energy. Systems with *large* gradients, so that *nonlinear* transport is involved, are the most challenging. The fundamental method for simulating such systems at the particle level is nonequilibrium molecular dynamics (NEMD) [1, 2, 3]. Nonequilibrium molecular dynamics couples together Newtonian, Hamiltonian, and Nosé-Hoover mechanics with thermodynamics and continuum mechanics, with the help of Gibbs' statistical mechanics, and Maxwell and Boltzmann's kinetic theory. Impulsive hard-sphere collisions or continuous interactions can both be treated.

NEMD necessarily includes microscopic representations of the macroscopic thermodynamic energy E, pressure and temperature tensors P and T, and heat-flux vector Q. The underlying microscopic-to-macroscopic connection is made by applying Boltzmann and Gibbs' statistical phase-space theories, generalized to include Green and Kubo's approach to the evaluation of transport coefficients, together with Nosé's approach to introducing thermostats, ergostats, and barostats into particle motion equations.

These temperature, energy, and pressure controls make it possible to simulate the behavior of a wide variety of nonequilibrium flows with generalized mechanics. The nonequilibrium phase-space distributions which result are typically multifractal, as is illustrated here with a few examples taken from our website, [http://williamhoover.info]. These ideas are summarized in more detail in the books "Molecular Dynamics", "Computational Statistical Mechanics" and "Time Reversibility, Computer Simulation, and Chaos". The one-particle "Galton Board" (with impulsive forces) and the "thermostated nonequilibrium oscillator" problem (with continuous forces) are simple enough for thorough phase-space analyses. Macroscopic problems, like the steady shockwave and Rayleigh-Bénard flow, can be analyzed locally in phase space by computing local growth rates and nonlocal Lyapunov exponents.

The main goal of all this computational work is "understanding", developing simplifying pictures of manybody systems. The manybody systems themselves are primarily computational entities, solutions of ordinary or partial differential equations for model systems. Quantum mechanics and manybody forces are typically omitted, mostly for lack of compelling and realistic computer algorithms. There is an enduring gap between microscopic simulations and realworld engineering. The uncertainties in methods for predicting catastrophic failures will continue to surprise us, no matter the complexity of the computer models we use to "understand" systems of interest.

Number-dependence in atomistic simulations is typically small: $1/N$ for the thermodynamic properties of periodic N-body systems, perhaps $1/\sqrt{N}$ or even $1/\ln N$ in problems better treated with continuum mechanics. So far we have come to understand the equilibrium equation of state, the linear transport coefficients, the Lyapunov instability of manybody trajectories, and the irreversibility underlying the Second Law. Improved understanding of relatively-simple hydrodynamic flows, like the Rayleigh-Bénard flow treated here, will follow from the special computational techniques developed to connect different length scales. Smooth Particle Applied Mechanics, "SPAM" [4, 5, 6], has proved itself as not only a useful simulation technique for continuum systems, but also as a powerful interpolation tool for all point-particle systems, as is illustrated here for the shockwave problem [7, 8, 9].

Development of Molecular Dynamics at and Away from Equilibrium

In the early days of expensive vacuum-tube computing the hardware and software were largely controlled by the Federal Government and located at the various weapons and energy laboratories at Argonne, Brookhaven, Livermore, Los Alamos and Oak Ridge. Fermi developed molecular dynamics at the Los Alamos Laboratory in the summers of 1952-1953, discovering many of the interesting nonergodic recurrence features characterizing the low-energy behavior of one-dimensional anharmonic "Fermi-Pasta-Ulam chains". The Los Alamos Report summarizing his work was prepared a few months after his death [10, 11, 12]. At sufficiently low energies the anharmonic chains showed no tendency toward equilibration while (it was discovered much later that) at higher energies they did. Figure 1 shows time-averaged "mode energies" for a six-particle chain with two different initial conditions. In both cases the nearest-neighbor

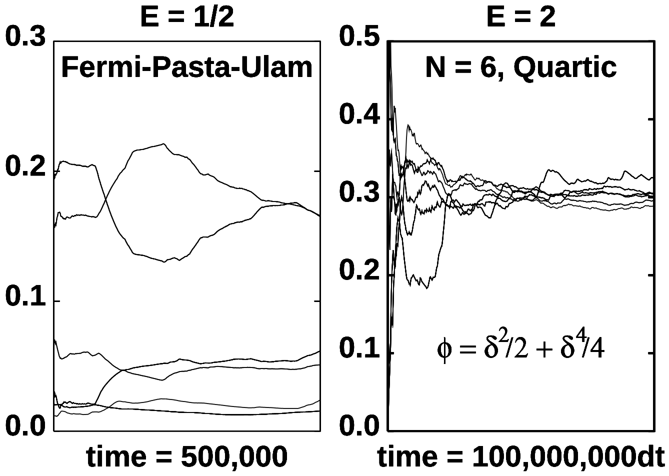

FIGURE 1. The time averages of the six harmonic mode energies (calculated just as was done by Benettin [12]) are shown as functions of time for two different initial conditions, with total energies of 0.5 and 2.0. The six-particle chain of unit mass particles with least-energy coordinates of $\pm 0.5, \pm 1.5,$ and ± 2.5 is bounded by two additional fixed particles at ± 3.5.

potential generates both linear and cubic forces:

$$\phi(r) = (1/2)(r-1)^2 + (1/4)(r-1)^4 \, .$$

Initially we choose the particles equally spaced and give all the energy to Particle 1, $E = p_1^2/2$. The left side of the Figure corresponds to an initial momentum of 1 while the right side follows a similarly long trajectory (100 million Runge-Kutta timesteps) starting with the initial momentum $p_1 = 2$. Fermi was surprised to find that at moderate energies there was no real tendency toward equilibration despite the anharmonic forces. Thus the averaging techniques of statistical mechanics can't usefully be applied to such oversimplified systems.

Fermi also carried out some groundbreaking two-dimensional work. He solved Newton's equations of motion,

$$\{ \, m\ddot{r} = F(r) \, \} \, ,$$

and didn't bother to describe the integration algorithm. A likely choice would be the time-reversible centered second-difference "Leapfrog" algorithm,

$$\{ \, r_{t+dt} = 2r_t - r_{t-dt} + (F/m)_t (dt)^2 \, \} \, ,$$

where the timestep dt is a few percent of a typical vibrational period. The dominant error in this method is a "phase error", with the orbit completing prematurely. A harmonic oscillator with unit mass and force constant has a vibrational period of 2π. The second-difference Leapfrog algorithm's period is 6, rather than 6.2832, for a relatively large timestep, $dt = 1$. A typical set of six (repeating) coordinate values for this timestep choice is:

$$\{ \, +2, +1, -1, -2, -1, +1, \, \ldots \, \}$$

The Leapfrog algorithm diverges, with a period of $2\sqrt{2}$, as dt approaches $\sqrt{2}$.

Vineyard used the Leapfrog algorithm at the Brookhaven Laboratory, including irreversible viscous quiet-boundary forces designed to minimize the effect of surface reflections on his simulations of radiation damage [13]. Alder and Wainwright, at the Livermore Laboratory, studied hard disks and spheres in parallel with Wood and Jacobsen's Monte Carlo work at the Los Alamos laboratory, finding a melting/freezing transition for spheres [14, 15]. The disks and spheres required different techniques, with impulsive instantaneous momentum changes at discrete collision times. All these early simulations gave rise to a new discipline, "molecular dynamics", which could be used to solve a wide variety of dynamical problems for gases, liquids, and solids, either at, or away from, equilibrium. By the late 1960s the results of computer simulation supported a successful semiquantitative approach to the equilibrium thermodynamics of simple fluids [16].

In the 1970s Ashurst [17] (United States), Dremin [18] (Union of Soviet Socialist Republics), Verlet [19] (France), and Woodcock [20] (United Kingdom), were among those adapting molecular dynamics to the solution of nonequilibrium problems. Shockwaves, the subject of our third lecture, were among the first phenomena treated in the effort to understand the challenging problems of far-from-equilibrium many-body systems.

Temperature Control à la Nosé

Shuichi Nosé made a major advance in 1984 [21, 22], developing a dynamics, "Nosé-Hoover dynamics", which provides sample isothermal configurations from Gibbs' and Boltzmann's canonical distribution,

$$f(q,p) \propto e^{-\mathscr{H}(q,p)/kT} \ ; \ \mathscr{H}(q,p) = \Phi(q) + K(p) \ .$$

The motion equations contain one or more friction coefficients $\{\zeta\}$ which influence the motion, forcing the longtime average of one or more of the p_i^2 to be mkT_i:

$$\{ \ m\ddot{r}_i = F_i - \zeta_i p_i \ ; \ \dot{\zeta}_i = [(p_i^2/mkT_i) - 1]/\tau_i^2 \ \} \ .$$

The thermostat variable ζ can introduce or extract heat. The adjustable parameter τ is the characteristic time governing the response of the thermostat variable ζ. A useful special case that follows from Nosé's work in the limit $\tau \to 0$ is "Gaussian" isokinetic dynamics, a dynamics with fixed, rather than fluctuating, kinetic energy $K(p) = K_0$,

In 1996 Dettmann showed that the Nosé-Hoover equations of motion follow generally from a special Hamiltonian, without the need for the time scaling Nosé used in his original work:

$$\mathscr{H}_{\rm Dettmann} = s[\Phi(q) + K(p/s) + \#kT \ln s + \#kT(p_s\tau)^2/2] \equiv 0 \ .$$

Here the friction coefficient is $\zeta \equiv \#kT\tau^2 p_s$, where p_s is the Hamiltonian momentum conjugate to s. The trick of setting the Hamiltonian equal to a special value, 0, is essential to Dettmann's derivation [23].

Consider the simplest interesting case, a harmonic oscillator with unit mass, force constant, temperature, and relaxation time:

$$\mathscr{H} = s[q^2 + (p/s)^2 + \ln s^2 + p_s^2]/2 = 0 \rightarrow$$

$$\dot{q} = (p/s)\ ;\ \dot{p} = -sq\ ;\ \dot{s} = sp_s\ ;\ \dot{p}_s = -[0] + (p/s)^2 - 1\ \rightarrow$$

$$\ddot{q} = (1/s)\dot{p} - (p/s)(\dot{s}/s) = -q - \zeta\dot{q}\ ;\ \dot{p}_s \equiv \dot{\zeta} = \dot{q}^2 - 1\ .$$

The time average of the $\dot{\zeta}$ equation shows that the longtime average of $\dot{q}^2$ is unity. In particular applications τ should be chosen to maximize the efficiency of the simulation by minimizing the necessary computer time.

Runge-Kutta integration is a particularly convenient method for solving such sets of coupled first-order differential equations. The fourth-order method is the most useful. The time derivative is an average from four evaluations, $\{\ \dot{y}_0, \dot{y}_1, \dot{y}_2, \dot{y}_3\ \}$, of the righthand sides of all the differential equations, here collected in the form of a single differential equation for the vector y:

$$y_1 = y_0 + (dt/2)\dot{y}_0\ ;\ y_2 = y_0 + (dt/2)\dot{y}_1\ ;\ y_3 = y_0 + dt\dot{y}_2\ ;$$

$$y_{dt} = y_0 + (dt/6)[\dot{y}_0 + 2\dot{y}_1 + 2\dot{y}_2 + \dot{y}_3]\ .$$

The Runge-Kutta energy decays with time as dt^5 at a fixed time for a chosen timestep dt. Here the vector y is (q,p) so that

$$\dot{y} \equiv (\dot{q}, \dot{p}) \equiv (+p, -q)\ .$$

For small dt the Runge-Kutta trajectory for a harmonic oscillator with the exact trajectory $q = \cos(t)$ has an error $\delta q = +dt^4 t\sin(t)/120$. The corresponding Leapfrog error is $\delta q = -dt^2 t\sin(t)/24$. The two methods should give equally good solutions (where the two curves in the Figure cross) when

$$dt_{\mathrm{LF}} \simeq dt_{\mathrm{RK}}/4 = \sqrt{5/256} \simeq 0.14\ ,$$

corresponding to about 45 force evaluations per oscillator period [24].

For a 14-digit-accurate trajectory calculation, with $dt_{RK} = 0.001$ and $dt_{LF} = 0.00025$, the Runge-Kutta error would be smaller than the Leapfrog error by seven orders of magnitude. At the cost of additional programming complexity choosing one of the fourth-order Gear integrators can reduce the integration error by an additional factor of $\simeq 60$ [25].

Connecting Microscopic Dynamics to Macroscopic Physics

To connect the microscopic dynamics to macroscopic thermodynamics and continuum mechanics is quite easy for a homogeneous system confined to the volume V. A numerical solution of the equations of motion for the coordinates and momenta, $\{\ q, p\ \}$,

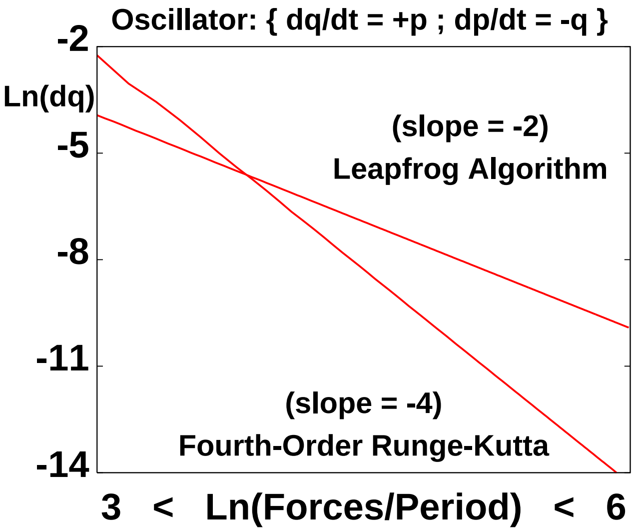

FIGURE 2. Comparison of the maximum error (which occurs near a time of $3\pi/2$), in a harmonic oscillator coordinate for the Leapfrog and Fourth-Order-Runge-Kutta integrators. The abscissa shows the logarithm of the number of force evaluations (which varies from about 20 to about 400) used during a full vibrational period, 2π. The oscillator equations of motion are $\dot{q} = p$; $\ddot{q} = \dot{p} = -q$.

makes it possible to compute the energy E, the temperature tensor T, the pressure tensor P, and the heat-flux vector Q:

$$E = \Phi(q) + K(p) = \sum_{i<j} \phi_{ij} + \sum_i p_i^2/(2m) \ ;$$

$$T_{xx} = \langle p_x^2/mk \rangle = \sum_i (p_x^2/mk)_i/N \ ; \ T_{yy} = \langle p_y^2/mk \rangle \ ;$$

$$PV = \sum_{i<j} F_{ij} r_{ij} + \sum_i (pp/m)_i \ ;$$

$$QV = \sum_{i<j} F_{ij} \cdot p_{ij} r_{ij} + \sum_i (ep/m)_i \ .$$

These expressions can be derived directly from the dynamics, by computing the mean momentum and energy fluxes (flows per unit area and time) in the volume V. Alternatively they can be derived by multiplying the Newtonian equations of motion by (p/m) (giving the “Virial Theorem”) or by e (giving the “Heat Theorem”) and time averaging [1]. We will see that local versions of these definitions lead to practical implementations of numerical hydrodynamics at atomistic length and time scales.

The thermomechanical bases of these relations are statistical mechanics and kinetic theory. Hamilton’s mechanics yields Liouville’s theorem for the time derivative of the many-body phase-space probability density following the motion:

$$\dot{f}/f = d\ln f/dt = 0 \text{ [Hamiltonian Mechanics] } ;$$

Nosé-Hoover mechanics opens up the possibility for f to change:

$$\dot{f}/f = d\ln f/dt = \zeta = -\dot{E}/kT = \dot{S}_{\rm ext}/k \ [\text{Nosé} - \text{Hoover Mechanics}]\ .$$

The primary distinction between nonequilibrium and equilibrium systems lies in the friction coefficients $\{\ \zeta\ \}$. At equilibrium (ordinary Newtonian or Hamiltonian dynamics) the average friction vanishes while in *nonequilibrium* steady states $\langle \sum k\zeta \rangle = \dot{S}_{\rm ext} > 0$ it is equal to the time-averaged entropy production rate.

In any stationary nonequilibrium state the sum of the friction coefficients is necessarily positive – a negative sum would correspond to phase-space instability incompatible with a steady state. An important consequence of the positive friction is that the probability density for these states diverges as time goes on, indicating the collapse of the probability density onto a fractal strange attractor. Fractals differ from Gibbs' smooth distributions in that the density is singular, and varies as a fractional power of the coordinates and momenta in phase space [2, 26, 27, 28, 29].

Fractal Phase-Space Distributions

The harmonic oscillator problem is not ergodic with Nosé-Hoover dynamics. One way to make it so is to fix the fourth moment of the velocity distribution as well as the second. This improvement also makes it possible to study interesting nonequilibrium oscillator-based problems, such as the conduction of energy from hot to cold through the oscillator motion. Figure 3 shows the time development of (the two-dimensional projection of) such a problem. The isothermal oscillator, along with two friction coefficients, $\{\zeta,\xi\}$, fixing the second and fourth moments, $\langle (p^2,p^4) \rangle$ has a Gaussian distribution in its four-dimensional phase space. A special *nonisothermal* case, with a coordinate-dependent temperature leading to heat flow, generates a 2.56-dimensional fractal in the four-dimensional $\{q,p,\zeta,\xi\}$ phase space. The dynamics governing this continuous nonequilibrium motion is as follows:

$$\dot{q} = p\ ;\ \dot{p} = -q - \zeta p - \xi p^3\ ;$$

$$\dot{\zeta} = [p^2 - T]\ ;\ \dot{\xi} = [p^4 - 3p^2T]\ ;\ T = T(q) = 1 + \tanh(q)\ .$$

Here time averages of the control-variable equations show that the second and fourth moments satisfy the usual thermometric definitions:

$$\langle p^2 \rangle = \langle T \rangle\ ;\ \langle p^4 \rangle = 3\langle p^2 T \rangle\ .$$

The phase-space distribution for this oscillator has an interesting fractal nature [26, 27]. Figure 3 shows how the continuous trajectory comes to give a fractal distribution, as is typical of thermostated nonequilibrium problems. Besides the æsthetic interest that this model provides, it illustrates the possibilities for controlling moments of the velocity distribution beyond the first and second, as well as the possibility of introducing a coordinate-dependent temperature directly into the motion equations.

Figure 4 shows a more typical textbook fractal, the Sierpinski sponge, in which the probability density is concentrated on a set of dimension 2.727. In almost all of the

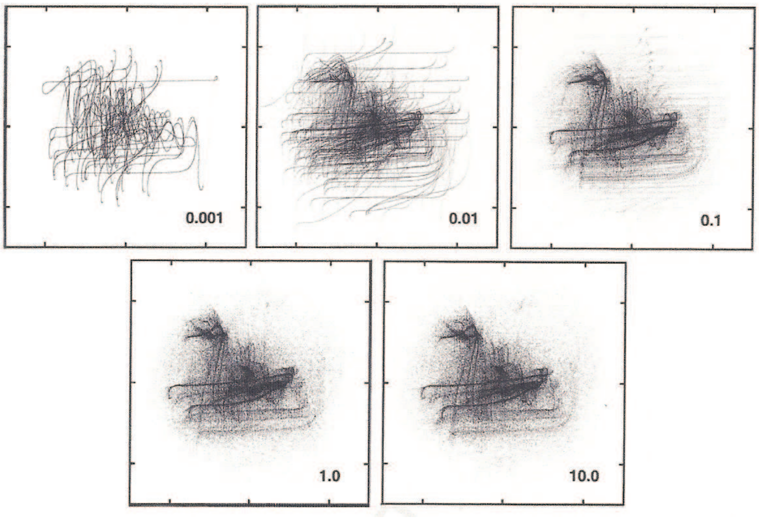

FIGURE 3. This (ζ, ξ) projection of the doubly-thermostated oscillator fractal is shown at five successive stages of temporal resolution. The time intervals between successive points range from 0.001, the Runge-Kutta timestep, to 10.0, showing how a continuous trajectory can lead to a fractal object.

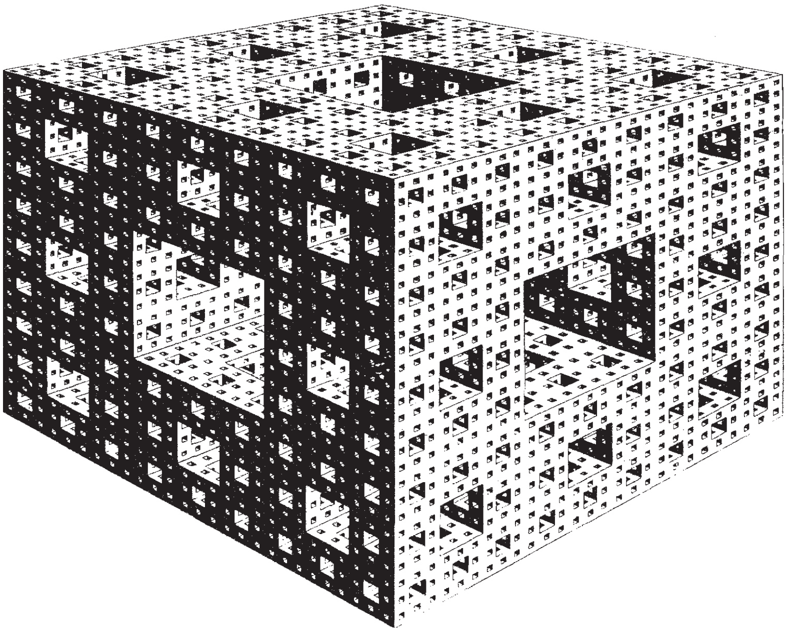

FIGURE 4. Sierpinski Sponge, constructed by removing 7 of the 27 equal cubes contained in the unit cube, leaving 20 smaller cubes, and then iterating this process *ad infinitum* leaving a 2.727-dimensional fractal of zero volume.

largest cube the density vanishes. Unlike the multifractal of Figure 3, the Sierpinski sponge is homogeneous, so that an n-fold enlarged view of a small part of the sponge, with an overall volume $1/27^n$ of the total, looks precisely like the entire object.

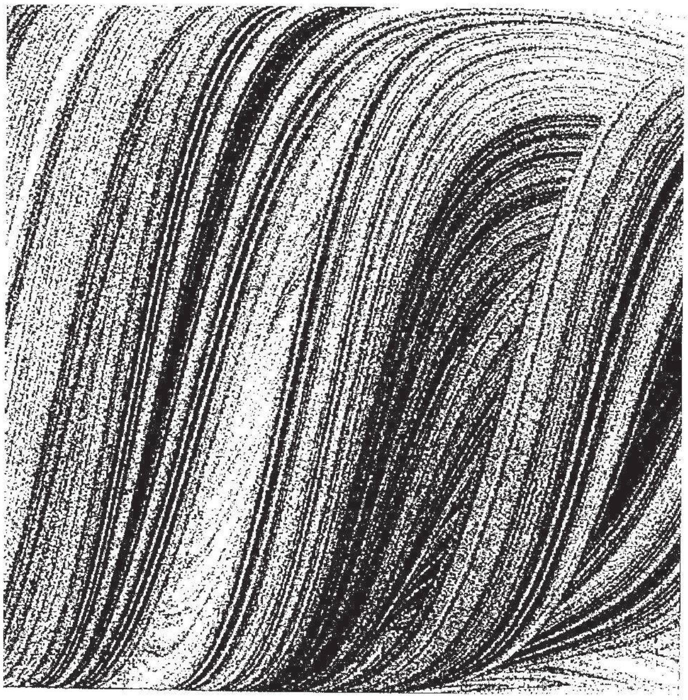

FIGURE 5. A series of 200,000 Galton Board collisions are plotted as separate points, with ordinate $-1 < \sin(\beta) < 1$ and abscissa $0 < \alpha < \pi$, where α is measured relative to the field direction, as shown in Figure 6.

The Galton Board

The situation with impulsive forces is quite different. Whenever impulsive collisions occur the phase-space trajectory makes a jump in momentum space, from one phase point to another. Consider the simplest interesting case: a single point mass, passing through a triangular lattice of hard scatterers [2, 30, 31]. That model generates exactly the same ergodic dynamics as does a periodic two-hard-disk system with no center-of-mass motion:

$$r_1 + r_2 = 0 \; ; \; v_1 + v_2 = 0 \; .$$

By adding a constant field and an isokinetic thermostat to the field-dependent motion, the trajectory tends smoothly toward the field direction until a collisional jump occurs. Over long times (Figure 5 is based on 200,000 collisions) an extremely interesting nonequilibrium stationary state results, with a fractal phase-space distribution. The example shown in the Figure has an information dimension of 1.832. As a consequence, the coarse-grained entropy, $-k\langle f \ln f \rangle$, when evaluated with phase-space cells of size δ, diverges as $\delta^{-0.168}$, approaching minus infinity as a limiting case.

The probability densities for nonequilibrium steady states, such as the Galton Board, shown in Figure 5, are qualitatively different to the sponge, where the probability density

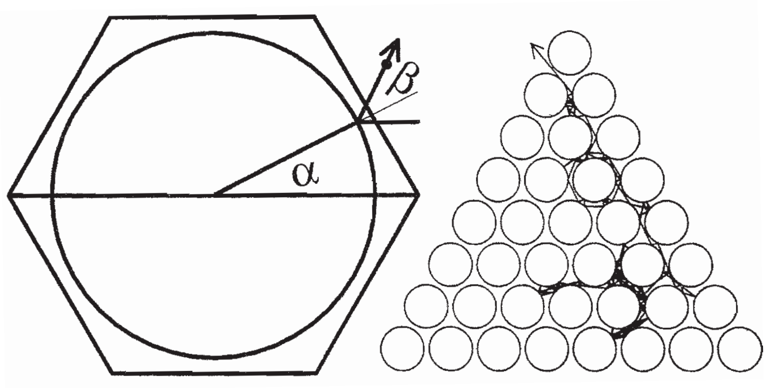

FIGURE 6. The Galton Board geometry is shown, defining the angles α and β identifying each collision. The unit cell shown here, extended periodically, is sufficient to describe the problem of a moving particle in an infinite lattice of scatterers.

is equally singular wherever it is nonzero. The Galton Board's nonequilibrium probability density is nonzero for *any* configuration consistent with the initial conditions on the dynamics. Further, the (multi)fractal dimension of these inhomogeneous distributions varies throughout the phase space.

The concentrated nature of the nonequilibrium probability density shows first of all that nonequilibrium states are very rare in phase space. Finding one by accident has probability zero. The time reversibility of the equations of motion additionally shows that the probability density going forward in time contracts (onto a strange attractor), and so is necessarily stable relative to a hypothetical reversed trajectory going backward in time, which would expand in an unstable way. This symmetry breaking is a microscopic equivalent of the Second Law of Thermodynamics, a topic to which we'll return. It is evidently closely related to the many "fluctuation theorems" [32, 33] which seek to give the relative probabilities of forward and backward nonequilibrium trajectories as calculated from Liouville's Theorem.

Determination of Transport Coefficients *via* NEMD

With measurement comes the possibility of control. Feedback forces, based on the results of measurement, can be used to increase or decrease a "control variable" (such as the friction coefficient ζ which controls the kinetic temperature through a "thermostating" force). Equations of motion controlling the energy, or the temperature, or the pressure, or the heat flux, can all be developed in such a way that they are exactly consistent with Green and Kubo's perturbation-theory of transport [2, 3]. That theory is a first-order perturbation theory of Gibbs' statistical mechanics. It expresses linear-response transport coefficients in terms of the decay of equilibrium correlation functions. For instance, the shear viscosity η can be computed from the decay of the stress

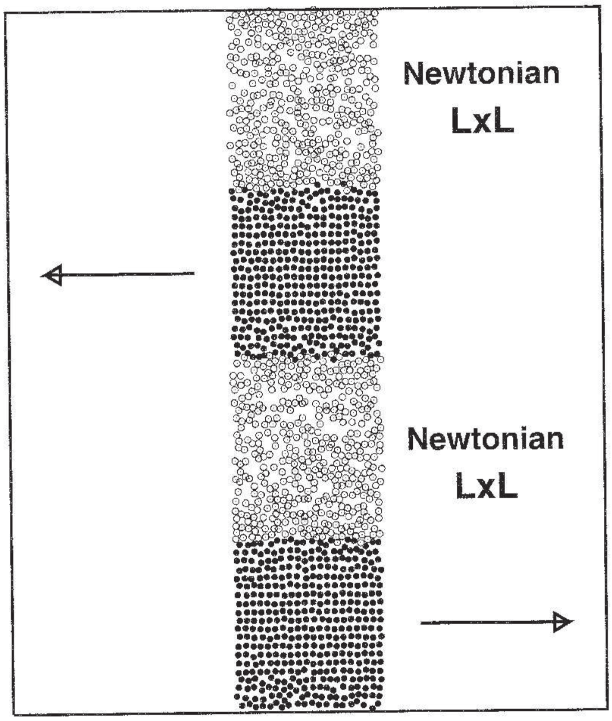

FIGURE 7. A Four Chamber viscous flow. Solid blocks (filled circles), move antisymmetrically to the left and right, so as to shear the two chambers containing Newtonian fluid (open circles). This geometry makes it possible to characterize the nonlinear differences among the diagonal components of the pressure and temperature tensors.

autocorrelation function:

$$\eta = (V/kT)\int_0^\infty \langle P_{xy}(0)P_{xy}(t)\rangle_{\rm eq} dt \ ,$$

and the heat conductivity κ can be computed from the decay of the heat flux autocorrelation function:

$$\kappa = (V/kT^2)\int_0^\infty \langle Q_x(0)Q_x(t)\rangle_{\rm eq} dt \ .$$

Nosé's ideas have made it possible to simulate and interpret a host of controlled nonequilibrium situations. A Google search for "Nosé-Hoover" in midJuly of 2010 produced over eight million separate hits.

Figure 7 shows a relatively-simple way to obtain transport coefficients using nonequilibrium molecular dynamics. Ashurst [17], in his thesis work at the University of California, "Dense Fluid Shear Viscosity and Thermal Conductivity *via* Molecular Dynamics", introduced two "fluid walls", with different specified velocities and/or temperatures, in order to simulate Newtonian viscosity and Fourier heat flow. Figure 7, a fully periodic variation of Ashurst's idea, shows two "reservoir" regions, actually "solid walls", separating two Newtonian regions. In both the Newtonian regions momentum and energy fluxes react to the different velocities and temperatures imposed in the "wall" reservoirs. This four-chamber technique produces two separate nonequilibrium profiles [34, 35, 36].

In the Newtonian chambers, where no thermostat forces are exerted, the velocity or temperature gradients are nearly constant, so that accurate values of the viscosity and heat conductivity can be determined by measuring the (necessarily constant) shear stress or the heat flux:

$$\eta = -P_{xy}/[(dv_y/dx) + (dv_x/dy)] \; ; \; \kappa = -Q_x/(dT/dx) \; .$$

Nonlinear Transport

This same "solid-wall" or "four-chamber" method has been used to study a more complicated aspect of nonequilibrium systems, the nonlinear contributions to the fluxes. Because the underlying phase-space distributions are necessarily fractal it is to be expected that there is no analytic expansion of the transport properties analogous to the virial (powers of the density) expansion of the equilibrium pressure. Periodic shear flows, with the mean x velocity increasing linearly with y,

$$\{ \, \dot{x} = (p_x/m) + \dot{\epsilon}y \; ; \; \dot{y} = (p_y/m) \, \} \; ;$$

can be generated with any one member of the family of motion equations:

$$\{ \, \dot{p}_x = F_x - \dot{\epsilon}\alpha_x p_y - \zeta p_x \; ; \; \dot{p}_y = F_y - \dot{\epsilon}\alpha_y p_x - \zeta p_y \, \} \; ,$$

so long as the sum $\alpha_x + \alpha_y$ is unity and ζ is chosen to control the overall energy or temperature. Careful comparisons of the two limiting approaches,

$$\alpha_x = 0 \; ; \; \alpha_y = 1 \text{ [Doll's]} \; ;$$

$$\alpha_x = 1 \; ; \; \alpha_y = 0 \text{ [s'lloD]} \; ,$$

with corresponding boundary-driven four-chamber flows show that though both of the algorithms satisfy the nonequilibrium energy requirement:

$$\dot{E} \equiv -\dot{\epsilon}P_{xy}V \; ,$$

exactly, neither of them provides the correct "normal stress" difference, $P_{xx} - P_{yy}$.

This same problem highlights another interesting parallel feature of nonequilibrium systems, the *tensor* nature of temperature [7, 8, 9, 37, 38, 39, 40]. In a boundary-driven shearflow with the repulsive pair potential,

$$\phi(r < 1) = 100(1 - r^2)^4 \; ,$$

the temperature tensors in the Newtonian regions show the orderings

$$\langle p_x^2 \rangle > \langle p_z^2 \rangle > \langle p_y^2 \rangle \; \longleftrightarrow \; T_{xx} > T_{zz} > T_{yy} \text{ [Boundary Driven]} \; .$$

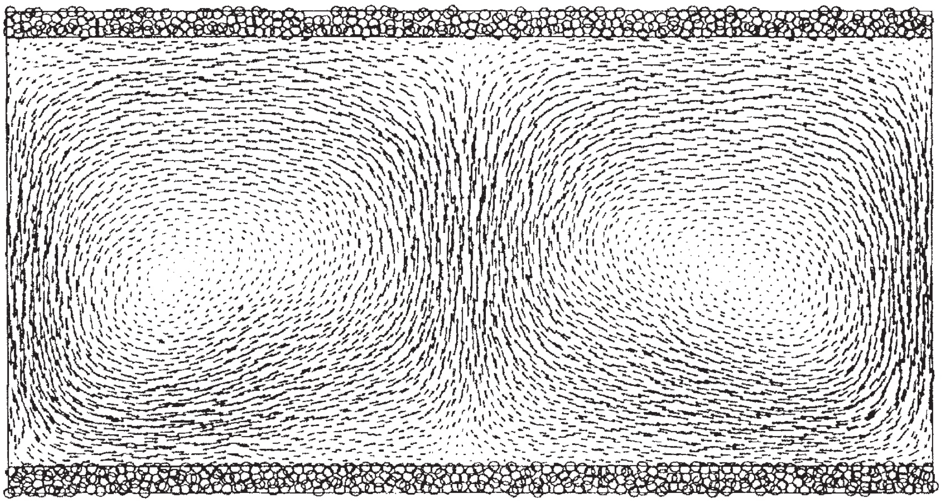

FIGURE 8. Rayleigh-Bénard problem, simulated with 5000 particles. The fluid-wall image particles which enforce the thermal and velocity boundary conditions are shown as circles above and below the main flow.

The homogeneous periodic shear flows generated with the Doll's and s'llоD algorithms show instead two other orderings:

$$T_{xx} > T_{yy} > T_{zz}\ [\mathrm{s'lloD}] \ \ \text{and} \ \ T_{yy} > T_{xx} > T_{zz}\ [\mathrm{Doll's}]\ ,$$

so that neither the Doll's nor the s'lloD algorithm correctly accounts for the *nonlinear* properties of stationary shear flows [35]. Nonequilibrium molecular dynamics provides an extremely versatile tool for determining nonlinear as will as linear transport. We will come back to tensor temperature in the third lecture, on shockwaves. Nonlinear transport problems can require the definition of local hydrodynamic variables whenever the system is inhomogeneous, as it is in boundary-driven shear and heat flows.

Thermostats, ergostats, barostats, and many other kinds of constraints and controls simplify the treatment of complex failure problems with molecular dynamics. Using the Doll's and s'lloD ideas it is quite feasible to study the stationary nonequilibrium flow of solids, "plastic flow", in order to interpret nonsteady failure problems like fracture and indentation. Nonequilibrium molecular dynamics makes it possible to remove the irreversible heat generated by strongly nonequilibrium processes such as the machining of metals. The basic idea of control can be implemented from the standpoint of Gauss' Principle, which states that the smallest possible constraint force should be used to accomplish control [41]. Near equilibrium a more reliable basis is Green and Kubo's linear-response theory. This can be used to formulate controls consistent with exact statistical mechanics in the linear regime, just as was done in deriving the Doll's and s'lloD approaches to simulating shear flow.

A slightly more complex problem is illustrated in Figure 8. A nonequilibrium system with fixed mass is contained within two thermal "fluid wall" boundaries, hot on the bottom and cold on the top, with a gravitational field acting downward. If the gradients are small the fluid is stationary, and conducts heat according to Fourier's Law. When the Rayleigh Number,

$$R = gL^4(d\ln T/dy)/(\nu\kappa) \ ; \ \nu \equiv \eta/\rho \ ,$$

exceeds a critical value (which can be approximated by carrying out a linear stability analysis of the hydrodynamic equations) two rolls, one clockwise and the other counterclockwise provide another, faster, mode of heat transfer. At higher values of R the rolls oscillate vertically; at higher values still the rolls are replaced by chaotic heat plumes, which move horizontally. With several thousand particles molecular dynamics provides solutions in good agreement with the predictions of the Navier-Stokes-Fourier equations.

This problem [42, 43, 44] is specially interesting in that several topologically different solutions can exist for exactly the same applied boundary conditions. Carol will talk more about this problem in her exposition of Smooth Particle Applied Mechanics, "SPAM". SPAM provides a useful numerical technique for interpolating the particle properties of nonequilibrium molecular dynamics onto convenient spatial grids.

PARTICLE-BASED CONTINUUM MECHANICS & SPAM

Introduction and Goals

Smooth Particle Applied Mechanics, "SPAM", was invented at Cambridge, somewhat independently, by Lucy and by Monaghan in 1977 [4, 5, 6]. The particles both men considered were astrophysical in size as their method was designed to treat clusters of stars. SPAM can be used on smaller scales too. SPAM provides a simple and versatile particle method for solving the continuum equations numerically with a twice-differentiable interpolation method for the various space-and-time-dependent field variables (density, velocity, energy, ...) . SPAM looks very much like "Dissipative Particle Dynamics" [45], though, unlike DPD, it is typically fully deterministic, with no stochastic ingredients. Three pedagogical problems are discussed here using SPAM: the free expansion of a compressed fluid; the collapse of a water column under the influence of gravity; and thermally driven convection, the Rayleigh-Bénard problem. Research areas well-suited to graduate research (tensile instability, angular momentum conservation, phase separation, and surface tension) are also described.

SPAM provides an extremely simple particle-based solution method for solving the conservation equations of continuum mechanics. For a system without external fields the basic partial differential equations we aim to solve are:

$$\dot\rho = -\rho\nabla\cdot v \ ;$$

$$\rho\dot v = -\nabla\cdot P \ ;$$

$$\rho\dot e = -\nabla v : P - \nabla\cdot Q \ .$$

SPAM solves the equations by providing a particle interpretation for each of the continuum variables occurring in these conservation laws. The main difficulty in applying the method involves the choice and implementation of boundary conditions, which vary from problem to problem.

SPAM Algorithms and the Continuity Equation

The fluid dynamics notation here, $\{\rho, v, e, P, Q\}$, with each of these variables dependent on location r and time t, is standard but the SPAM particle interpretation of them is novel. The density ρ and momentum density (ρv) at any location r are local sums of nearby individual particle contributions,

$$\rho(r) \equiv \sum_j m_j w(r - r_j) \ ; \ \rho(r_i) = \sum_j m_j w(r_i - r_j) \ ; \ \rho(r)v(r) \equiv \sum_j m_j v_j w(r - r_j) \ ,$$

where particles have an extent h, the "range" of the weight function w, so that only those particles within h of the location r contribute to the averages there.

In the second expression (for the density *at* the particle location r_i) the "self" term $(r_i = r_j)$ is included so that the two definitions coincide at the particle locations. The weight function w, which describes the spatial distribution of particle mass, or region of influence for particle j, is normalized, has a smooth maximum at the origin, and a finite range h, at which both w' and w'' vanish. The simplest polynomial filling all these needs is Lucy's [4, 6], here normalized for two-dimensional calculations:

$$w_{2D}(r < h) = (5/\pi h^2)[1 - 6x^2 + 8x^3 - 3x^4] \ ; \ x \equiv r/h \ .$$

Monaghan's weight function, shown for comparison in the Figure, uses two different polynomials in the region where w is nonzero. The range h of $w(r < h)$ is typically a scalar, chosen so that a few dozen smooth particles contribute to the various field-point averages at a point. As shown in Figure 9 Lucy's function looks much like a Gaussian, but vanishes very smoothly as $r \to h$. By systematically introducing the weight function into expressions for the instantaneous spatial averages of the density, velocity, energy, pressure, and heat flux, the continuum equations at the particle locations become ordinary differential equations much like those of molecular dynamics. The method has the desirable characteristic that the continuum variables have continuous first and second spatial derivatives.

The continuity equation (conservation of mass) is satisfied automatically. At a fixed point r in space, the time derivative of the density depends upon the velocities of all those particles within the range h of r:

$$(\partial \rho / \partial t)_r \equiv \sum_j m_j v_j \cdot \nabla_j w_{rj} \equiv -\sum_j m_j v_j \cdot \nabla_r w_{rj} \ ,$$

where v_j is the velocity of particle j. On the other hand, the divergence of the quantity (ρv) at r is:

$$\nabla_r \cdot (\rho v_r) = \nabla_r \cdot \sum_j m_j w_{rj} v_j \ ,$$

establishing the Eulerian and Lagrangian forms of the continuity equation:

$$(\partial \rho / \partial t)_r \equiv -\nabla_r \cdot (\rho v) \ \longleftrightarrow \ \dot{\rho} = -\rho \nabla \cdot v \ .$$

These fundamental identities linking the density and velocity definitions establish the smooth-particle method as the most "natural" for expressing continuous field variables in terms of particle properties.

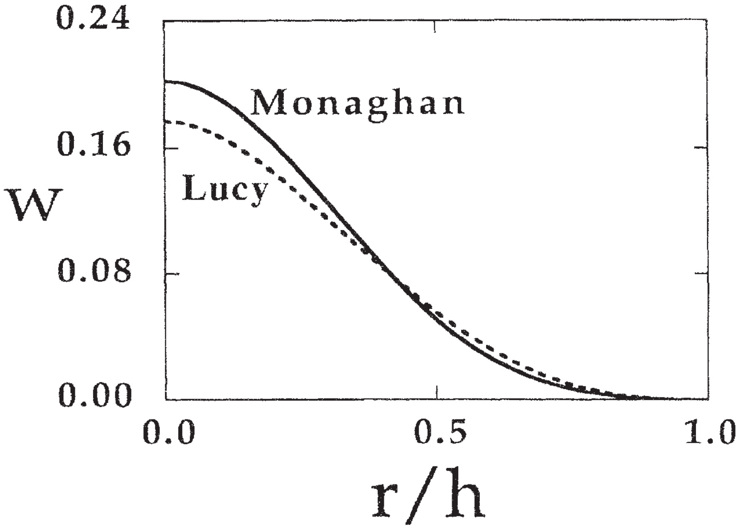

FIGURE 9. Lucy's and Monaghan's weight functions. Both functions are normalized for two space dimensions and $h = 3$. The weight function $w(r < h)$ describes the spatial influence of particles to properties in their neighborhood, as explained in the text.

The smooth-particle equations of motion have a form closely resembling the equations of motion for classical molecular dynamics:

$$\{ m_j \dot{v}_j = -\sum_k m_j m_k [(P/\rho^2)_j + (P/\rho^2)_k] \cdot \nabla_j w_{jk} \} .$$

It is noteworthy that the field velocity at the location of particle i

$$v(r = r_i) = \sum_j v_j w_{ij} / \sum_j w_{ij} = \sum_j m_j v_j w_{ij} / \rho(r = r_i) ,$$

(where the "self" term is again included) is usually different to the particle velocity v_i, opening up the possibility for computing velocity fluctuations *at* a point, as we do in the next Section.

Notice that the simple adiabatic equation of state $P \propto \rho^2/2$ gives exactly the same motion equations for SPAM as does molecular dynamics. That isomorphism pictures the weight function $w(r)$ as the equivalent of a short-ranged purely-repulsive pair potential. Thus the continuum dynamics of a special two-dimensional fluid become identical to the molecular dynamics of a dense fluid with smooth short-ranged repulsive forces [6]. We consider this case further in applying SPAM to the free expansion problem in the next Section.

Free Expansion Problem

Figure 10 shows snapshots from a free expansion problem in which 16,384 particles, obeying the adiabatic equation of state $P \propto (\rho^2/2)$, expand to fill a space four times that

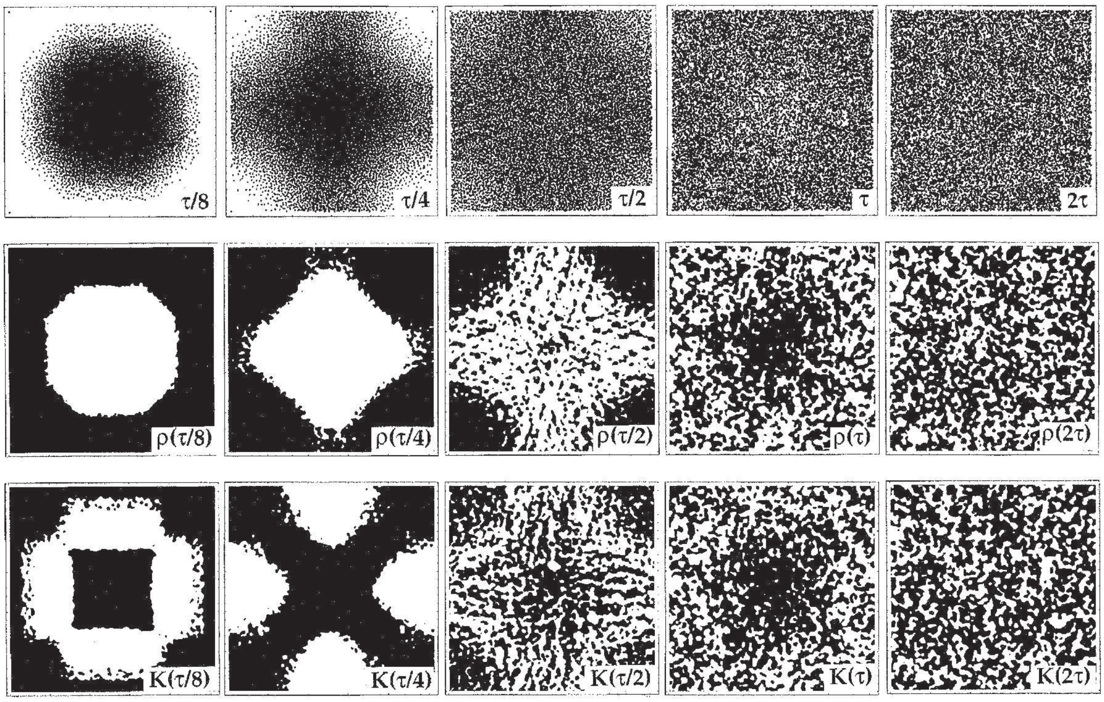

FIGURE 10. Contours of average density (middle row) and average temperature (bottom row) calculated from the instantaneous 16,384-particle snapshots (top row) taken during a free expansion simulation. The last picture in each row corresponds to two sound traversal times.

of the initial compressed gas. This problem provides a resolution of Gibbs' Paradox (that the entropy increases by $Nk\ln 4$ while Gibbs' Liouville-based entropy, $-k\langle \ln f \rangle$, remains unchanged) [46, 47]. Detailed calculations show that the missing Liouville entropy is embodied in the kinetic-energy fluctuations. When these fluctuations are computed in a frame moving at the local average velocity,

$$v(r) = \sum_j w_{rj} v_j / \sum_j w_{rj} \ ,$$

the corresponding velocity fluctuations, $(\langle v^2 \rangle - \langle v \rangle^2)$ are just large enough to reproduce the thermal entropy. Most of the spatial equilibration occurs very quickly, in just a few sound traversal times. The contours of average density and average kinetic energy shown here illustrate another advantage of the SPAM averaging algorithm. The field variables are defined *everywhere* in the system, so that evaluating them on a regular grid, for plotting or analyses, is easy to do.

These local velocity fluctuations begin to be important only when the adiabatic expansion stretches all the way across the periodic confining box so that rightward-moving fluid collides with its leftward-moving periodic image and *vice versa*. The thermodynamic irreversibility of that collision process, reproduced in the thermal entropy, is just sufficient for the reversible dynamics to reflect the irreversible entropy increase, $Nk\ln 4$.

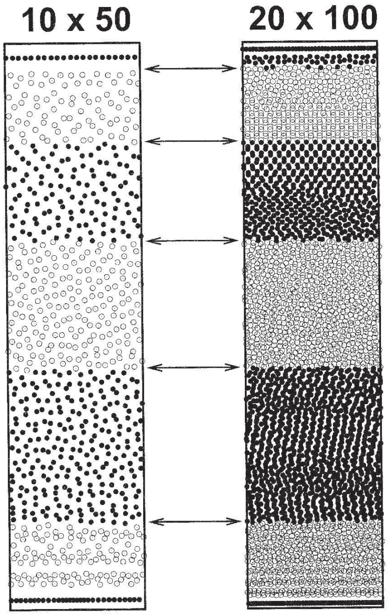

FIGURE 11. Equilibrated column for two system sizes. Five density contours are indicated by changes in plotting symbols. The arrows corresponding to the contours were calculated analytically from the continuum force-balance equation, $dP/dy = -\rho g$.

A dense-fluid version of this dilute-gas free expansion problem appears in Bill's lecture on shockwaves.

Collapse of a Fluid Column

Figure 11 shows the distribution of smooth particles in an equilibrated periodic water column in a gravitational field [6]. Figure 12 shows snapshots from the subsequent collapse of the water column when the vertical periodic boundaries are released. Both the equilibration shown in Figure 11 and the collapse shown in Figure 12 use the simple equation of state $P = \rho^3 - \rho^2$, chosen to give zero pressure at unit density. Here the gravitational field strength has been chosen to give a maximum density of 2 at the reflecting lower boundary. Initially, the vertical boundaries are periodic, preventing horizontal motion. After a brief equilibration period, the SPAM density profile can be compared to its analytic analog, derived by integrating the static version of the equation of motion:

$$dP/dy = -\rho g \ .$$

The arrows in Figure 11, computed from the analytic static density profile, show excellent agreement with the numerical SPAM simulation.

In smooth particle applied mechanics (SPAM) the boundary conditions are invariably the most difficult aspect of carrying out a simulation [6, 48]. Here we have used a simple mirror boundary condition at the bottom of the column and a periodic boundary at

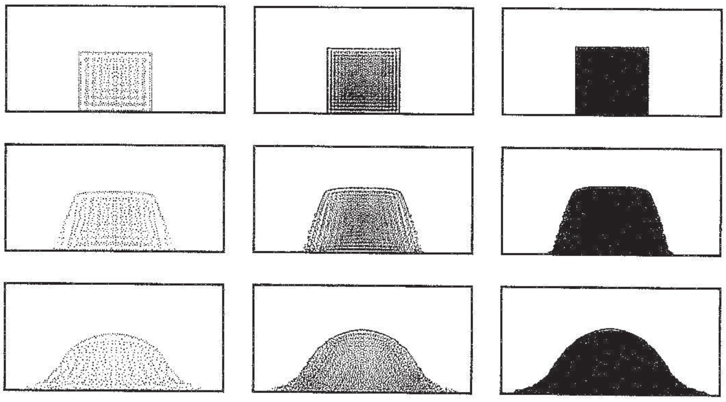

FIGURE 12. Water Column collapse for three system sizes, with 640, 2560, and 10,240 particles. The computational time for this two-dimensional problem varies as the three-halves power of the number of particles used because corresponding times increase as $\sqrt{N}$ while the number of interactions varies as N.

the sides, in the vertical direction. When the vertical periodic boundary constraint is released, rarefaction waves create a tensile region inside the falling column. By varying the size of the smooth particles the resolution of the motion can be enhanced, as Figure 12 shows. With "mirror boundaries", elaborated in the next Section, more complicated situations can be treated. With mirrors there is an image particle across the boundary, opposite to each SPAM particle, with the mirror particle's velocity and temperature both chosen to satisfy the corresponding boundary conditions.

Rayleigh-Bénard Convection

Figure 13 shows a typical snapshot for a slightly more complicated problem, the Rayleigh-Bénard problem, the convective flow of a compressible fluid in a gravitational field with the temperature specified at both the bottom (hot) and top (cold) boundaries. The velocities at both these boundaries must vanish, and can be imposed by using mirror particles resembling the image charges of electricity and magnetism. A particularly interesting aspect of the Rayleigh-Bénard problem is that multiple solutions of the continuum equations can coexist, for instance two rolls or four, with exactly the same boundary conditions [42, 43, 44, 49]. Such work has been used to show that neither the entropy nor the entropy production rate allows one to choose "the solution". Which solution is observed in practice can depend sensitively on the initial conditions. The Rayleigh-Bénard problem illustrates the need for *local* hydrodynamic averages describing the anisotropies of two- and three-dimensional flows.

SPAM provides an extremely useful interpolation method for generating twice-differentiable averages from particle data. In the following lecture this method will be used to analyze a dense-fluid molecular dynamics shockwave problem, where all of

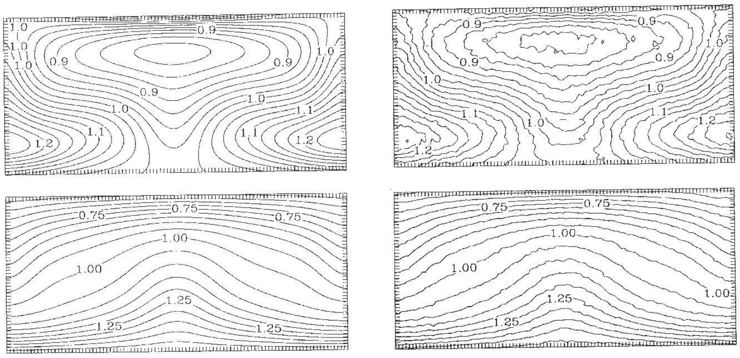

FIGURE 13. Instantaneous temperature (below) and density (above) contours for the two-roll Rayleigh-Bénard problem. The stationary continuum solution (left) is compared to a SPAM snapshot with 5000 particles (right).

the thermomechanical variables make near-discontinuous changes linking an incoming cold state to an outgoing hot one. The continuous differentiable field variables provided by SPAM make it possible to analyze the relatively subtle nonlinear properties of such strongly nonequilibrium flow fields.

SPAM is a particularly promising field for graduate research. In addition to the many possible treatments of boundaries (including boundaries between different phases), the conservation of angular momentum (when shear stresses are present) and the tensile instability (where w acts as an attractive rather than repulsive force) and the treatment of surface tension all merit more investigation. For a summary of the current State of the Art see our recent book [6].

TENSOR-TEMPERATURE SHOCKWAVES *VIA* MOLECULAR DYNAMICS

Introduction and Goals

Shockwaves are an ideal nonlinear nonequilibrium application of molecular dynamics. The boundary conditions are purely equilibrium and the gradients are quite large. The shockwave process is a practical method for obtaining high-pressure thermodynamic data. There are some paradoxical aspects too. Just as in the free expansion problem, time-reversible motion, with constant Gibbs' entropy, describes a macroscopically irreversible process in which entropy increases. The increase is third-order in the compression, for weak shocks [50]. The shockwave problem is a compelling example of Loschmidt's reversibility paradox.

We touch on all these aspects of the shockwave problem here. We generate and analyze the pair of shockwaves which results from the collision of two stress-free blocks [8, 9]. The blocks are given initial velocities just sufficient to compress the two cold blocks to a hot one, at twice the initial density. Further evolution of this

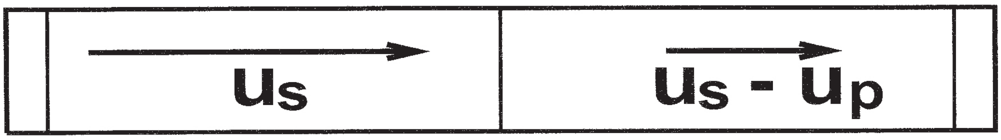

FIGURE 14. Stationary shockwave in the comoving frame. Cold material enters at the left, with velocity $+u_s$, and is decelerated by the denser hotter material which exits at the right, with velocity $u_s - u_p$. It is in this coordinate frame that the fluxes given in the text are constant.

atomistic system, with the initial kinetic energy of the blocks converted to internal energy, leads to a dense-fluid version of the free expansion problem discussed earlier for an adiabatic gas. Here we emphasize the dynamical reversibility and mechanical instability of this system, show the shortcomings of the usual Navier-Stokes-Fourier description of shockwaves, and introduce a two-temperature continuum model which describes the strong shockwave process quite well.

Shockwave Geometry

There is an excellent treatment of shockwaves in Chapter IX of Landau and Lifshitz' "Fluid Mechanics" text [50]. A stationary shockwave, with steady flow in the x direction, obeys three equations for the fluxes of mass, momentum, and energy derived from the three continuum equations expressing the conservation of mass, momentum, and energy:

$$\rho v = \rho_C u_s = \rho_H(u_s - u_p) \ ;$$

$$P_{xx} + \rho v^2 = P_C + \rho_C u_s^2 = P_H + \rho_H(u_s - u_p)^2 \ ;$$

$$\rho v[e + (P_{xx}/\rho) + (v^2/2)] + Q_x =$$

$$[e + (P_{xx}/\rho)]_C + (u_s^2/2) = [e + (P_{xx}/\rho)]_H + (u_s - u_p)^2/2 \ .$$

Figure 14 illustrates the shockwave geometry in a special coordinate frame. In this frame the shockwave is stationary. Cold material enters from the left at the "shock speed" u_s and hot material exits at the right, at speed $u_s - u_p$, where u_p is the "particle" or "piston" velocity. The terminology comes from an alternative coordinate system, in which motionless cold material is compressed by a piston (moving at u_p), launching a shockwave (moving at u_s).

Eliminating the two speeds from the three conservation equations gives the Hugoniot equation,

$$e_H - e_C = (P_H + P_C)(V_C - V_H)/2 \ ,$$

which relates the equilibrium pressures, volumes, and energies of the cold and hot states. Evidently purely equilibrium thermodynamic equation of state information can be obtained by applying the conservations laws to optical or electrical velocity measurements in the highly-nonequilibrium shockwave compression process. Ragan described

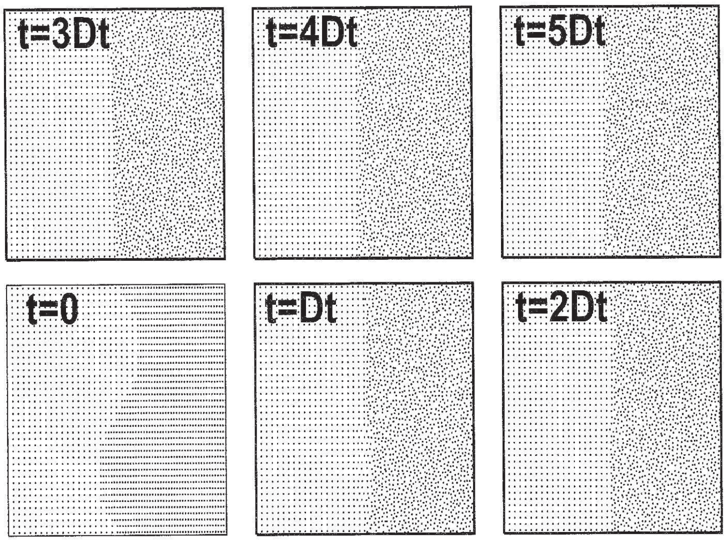

FIGURE 15. A series of snapshots showing the stability of a planar shockwave. Note that the decay of the initial sinewave profile is slightly underdamped. Here $Dt = 2000dt$ is the time required for a shockwave to traverse the width shown here, 2000 Runge-Kutta timesteps with $dt = 0.02/u_s \simeq 0.01$.

the threefold compression of a variety of materials (using an atomic bomb explosion to provide the pressure) at pressures up to 60 Megabars, about 15 times the pressure at the center of the earth [51].

Hoover carried out simulations of the shockwave compression process for a repulsive potential, $\phi(r) = r^{-12}$, in 1967 [52], but put off completing the project for several years, until computer storage capacity and execution speeds allowed for more accurate work [53]. Comparison of Klimenko and Dremin's computer simulations [18] using the Lennard-Jones potential, $\phi(r) = r^{-12} - 2r^{-6}$, showed that relatively weak shockwaves (30 kilobars for argon, 1.5-fold compression) could be described quite well [53, 54] with the three-dimensional Navier-Stokes equations, using Newtonian viscosity and Fourier heat conduction:

$$P = P_{eq} - \lambda \nabla \cdot v - \eta [\nabla v + \nabla v^t] \; ;$$

$$\lambda_{2D} = \eta_v - \eta \; ; \; \lambda_{3D} = \eta_V - (2/3)\eta \; ;$$

$$Q = -\kappa \nabla T \; .$$

Here λ is the "second viscosity", defined in such a way that the excess hydrostatic pressure due to a finite strain rate is $-\eta_V \nabla \cdot v$. The shear viscosity η and heat conductivity κ were determined independently using molecular dynamics simulations. The small scale of the waves [54], just a few atomic diameters, was welcomed by high-pressure experimentalists weary of arguing that their explosively-generated shockwaves measured equilibrium properties.

It is necessary to verify the one-dimensional nature of the waves too. It turns out that shockwaves *do* become planar very rapidly, at nearly the sound velocity. The rate at

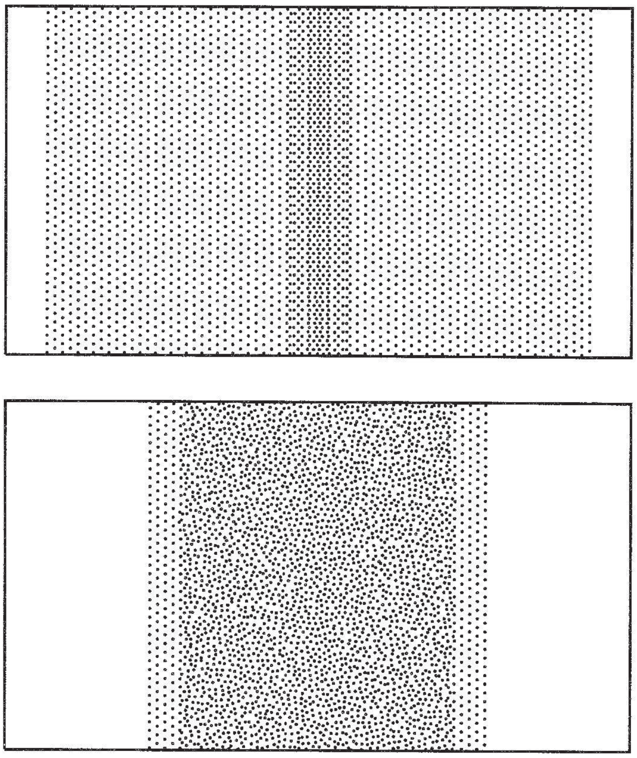

FIGURE 16. Snapshots near the beginning (upper) and end (lower) of an inelastic collision between two 1600-particle blocks. The initial velocities, ± 0.965, are just sufficient for a twofold compression of the cold material. The unit-mass particles interact with a short-ranged potential $(10/\pi)(1-r)^3$ and have an initial density $\sqrt{4/3}$.

which sinusoidal perturbations are damped out has been used to determine the plastic viscosity of a variety of metals at high pressure [55]. Figure 15 shows the rapid approach to planarity of a dense-fluid shockwave [9].

Stronger shockwaves, where the bulk viscosity is more important (400 kilobars for argon, twofold compression), showed that the Navier-Stokes description needs improvement at higher pressures. In particular, within strong shockwaves temperature becomes a symmetric tensor, with $T_{xx} >> T_{yy}$, where x is again the propagation direction. In addition, the Navier-Stokes-Fourier shockwidth, using linear transport coefficients, is too narrow. The tensor character of temperature in dilute-gas shockwaves had been carefully discussed in the 1950s by Mott-Smith [37].

Analysis of Instantaneous Shockwave Profiles using SPAM Averaging

Data for systems with impulsive forces, like hard spheres, require both time and space averaging for a comparison with traditional continuum mechanics. Analyses of molecular dynamics data with continuous potentials need no time averaging, but still require a spatial smoothing operation to convert instantaneous particle data, $\{x, y, p_x, p_y\}_i$, including $\{P, Q, T, e\}_i$, to equivalent continuous continuum profiles, $\{\rho(r,t), v(r,t), e(r,t), P(r,t), T(r,t), Q(r,t)\}$.

The potential parts of the virial-theorem and heat-theorem expressions for the pressure tensor P and the heat-flux vector Q,

$$PV = \sum_{i<j} F_{ij} r_{ij} + \sum_i (pp/m)_i \ ;$$

$$QV = \sum_{i<j} F_{ij} \cdot p_{ij} r_{ij} + \sum_i (ep/m)_i \ ,$$

can be apportioned in at least three "natural" ways between pairs of interacting particles [7, 56].

Consider the potential energy of two particles, $\phi(|r_{12}|)$. This contribution to the system's energy can be split equally between the two particle locations, r_1 and r_2, or located at the midpoint between them, $(r_1 + r_2)/2$, or distributed uniformly [56] along the line $r_1 - r_2$ joining them. These three possibilities can be augmented considerably in systems with manybody forces between particles of different masses. It is fortunate that for the short-ranged forces we study here the differences among the three simpler approaches are numerically insignificant. Once a choice has been made, so as to define *particle* pressures and heat fluxes, these can in turn be used to define the corresponding continuum field variables at any location r by using the weight-function approach of smooth particle applied mechanics:

$$P(r) \equiv \sum_j P_j w_{rj} / \sum_j w_{rj} \ ; \ Q(r) \equiv \sum_j Q_j w_{rj} / \sum_j w_{rj} \ .$$

By using this approach our own simulations have characterized another constitutive complication of dense-fluid shockwaves – the time delays between [1] the maximum shear stress and the maximum strainrate and [2] the maximum heat flux and and the maxima of the two temperature gradients (dT_{xx}/dx) and (dT_{yy}/dx) [8, 57]. The study of such delays goes back to Maxwell. The "Maxwell relaxation" of a viscoelastic fluid can be described by the model [7, 8, 57]:

$$\sigma + \tau \dot{\sigma} = \eta \dot{\varepsilon} \ .$$

so that stress reacts to a changing strainrate after a time of order τ. Cattaneo considered the same effect for the propagation of heat. The phenomenological delays, found in the dynamical results, are a reminder that the irreversible nature of fluid mechanics is fundamentally different to the purely-reversible dynamics underlying it.

The irreversible shock process is particularly interesting from the pedagogical standpoint. The increase in entropy stems from the conversion of the fluid's kinetic energy density, $\rho v^2/2$ to heat. To avoid the need for discussing the work done by the moving pistons of Figure 14, we choose here to investigate shockwaves generated by symmetric collisions of two stressfree blocks, periodic in the direction parallel to the shockfront. The entropy increase is *large* here (a zero-temperature classical system has an entropy of minus infinity). Figure 16 shows two snapshots for a strong shockwave yielding twofold

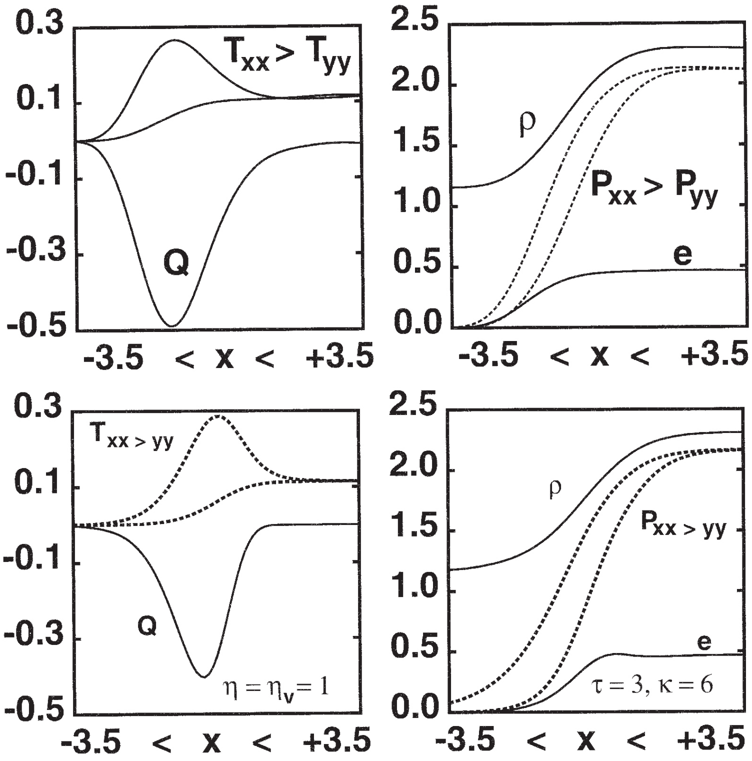

FIGURE 17. Shock Thermal and Mechanical Profiles from molecular dynamics are shown at the top. Corresponding numerical solutions of the generalized continuum equations are shown at the bottom. This rough comparison suggests that the generalized equations can be fitted to particle simulations. The generalized equations use tensor temperature and apportion heat and work between the two temperatures T_{xx} and T_{yy}. They also include delay times for shear stress, for heat flux, and for thermal equilibration.

compression of the initial cold zero-pressure lattice. The mechanical and thermal variables in a strong dense-fluid shockwave are shown in Figure 17. In order to model these results two generalizations of traditional hydrodynamics need to be made: the tensor nature of temperature and the delayed response of stress and heat flux both need to be treated. A successful approach is described next.

Macroscopic Generalizations of the Navier-Stokes-Fourier Approach

By generalizing continuum mechanics to include tensor temperature and the time delays for stress and heat flux,

$$\sigma + \tau\dot{\sigma} = \eta\dot{\epsilon} \; ; \; Q + \tau\dot{Q} = -\kappa\nabla T \; ,$$

with an additional relaxation time describing the joint thermal equilibration of T_{xx} and T_{yy} to a common temperature T_H the continuum and dynamical results can be made consistent [7, 8, 9, 37, 38, 40]. In doing this we partition the work done and the heat

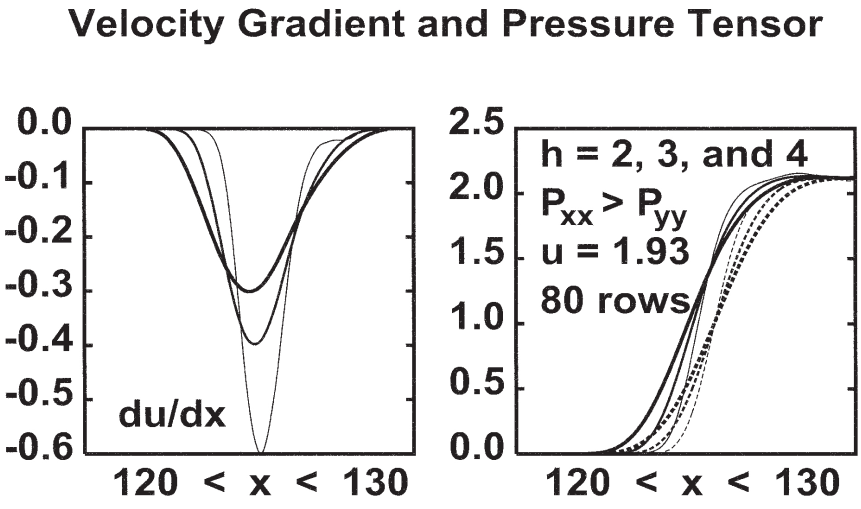

FIGURE 18. Shear Stress lags behind the strainrate. The molecular dynamics gradients, using smooth-particle interpolation, are much more sensitive to the range of the weighting function than are the fluxes. The results here are shown for $h = 2, 3, 4$, with line widths corresponding to h.

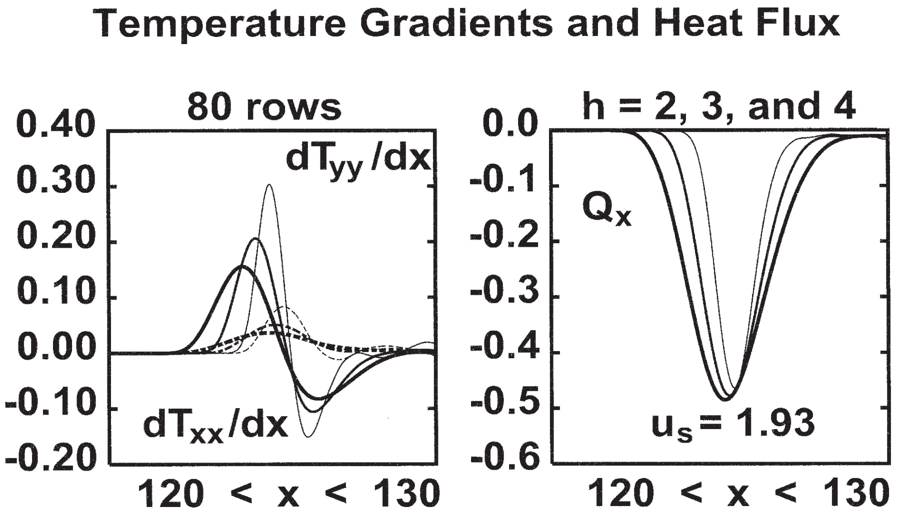

FIGURE 19. Heat Flux lags behind the temperature gradients. The molecular dynamics gradients, using smooth-particle interpolation, are much more sensitive to the range of the weighting function than are the fluxes. The results here are shown for $h = 2, 3, 4$, with line widths corresponding to h.

gained into separate longitudinal (x) and transverse (y) parts:

$$\rho \dot{T}_{xx} \propto -\alpha \nabla v : P - \beta \nabla \cdot Q + \rho (T_{yy} - T_{xx})/\tau \ ;$$

$$\rho \dot{T}_{yy} \propto -(1-\alpha) \nabla v : P - (1-\beta) \nabla \cdot Q + \rho (T_{xx} - T_{yy})/\tau \ .$$

Solving the time-dependent continuum equations for such shockwave problems is not difficult [9, 42]. If all the spatial derivatives in the continuum equations are expressed as centered differences, with density defined in the center of a grid of cells, and all the other variables (velocity, energy, stress, heat flux, ...) at the nodes defining the cell vertices, fourth-order Runge-Kutta integration converges nicely to solutions of the kind shown in Figure 17.

Shockwaves from Two Colliding Blocks are Nearly Reversible

To highlight the reversibility of the irreversible shockwave process let us consider the collision of two blocks of two-dimensional zero-pressure material, at a density of $\sqrt{4/3}$ (nearest-neighbor distance is unity, as is also the particle mass). Measurement of the equation of state with ordinary Newtonian mechanics, using the pair potential,

$$\phi(r<1) = (10/\pi)(1-r)^3 \ ,$$

indicates (and simulation confirms) that the two velocities u_s and u_p,

$$u_s = 2u_p = 1.930 \ ,$$

correspond to twofold compression with a density change $\sqrt{4/3} \rightarrow 2\sqrt{4/3}$. To introduce a little chaos into the initial conditions random initial velocities, corresponding to a temperature 10^{-10} were chosen. Because the initial pressure is zero the conservation relations are as follows:

$$\rho v = \sqrt{4/3} \times 1.930 = 2.229 \ ;$$

$$P_{xx} + \rho v^2 = \sqrt{4/3} \times 1.930^2 = 4.301 \ ;$$

$$\rho v[e + (P_{xx}/\rho) + \rho v^2/2)] + Q_x = \sqrt{4/3} \times 1.930^3/2 = 4.151 \ .$$

Although the reversibility of the dynamics cannot be perfect, the shockwave propagates so rapidly that a visual inspection of the reversed dynamics shows no discrepancies over thousands of Runge-Kutta timesteps. To assess the mechanical instability of the shock compression process we explore the effects of small perturbations to the reversible dynamics in the following Sections. We begin by illustrating phase-space instability [26, 58] for a simpler problem, the harmonic chain.

Linear Growth Rates for a Harmonic Chain

Even the one-dimensional harmonic chain, though not chaotic, exhibits linear phase-volume growth in certain phase-space directions. Consider the equations of motion for a periodic chain incorporating an arbitrary scalefactor s^{+2}:

$$\{ \ \dot{q} = ps^{+2} \ ; \ \dot{p} = (q_+ - 2q + q_-)s^{-2} \ \} \ ;$$

the subscripts indicate nearest-neighbor particles to the left and right. The motion equations for a $2N$-dimensional perturbation vector $\delta = (\delta q, \delta p)$ follow by differentiation:

$$\{ \ \delta \dot{q} = \delta p s^{+2} \ ; \ \delta \dot{p} = (\delta q_+ - 2\delta q + \delta q_-) s^{-2} \ \} \ .$$

If we choose the length of the perturbation vector equal to unity, the logarithmic growth rate, $\Lambda = (d \ln \delta / dt)_{q,p}$, is a sum of the individual particle contributions:

$$\Lambda(\delta) = \sum [\delta q \delta p (s^{+2} - 2s^{-2}) + \delta p (\delta q_+ + \delta q_-) s^{-2}] \ .$$

For a *large* scale factor s^{+2} it is evident that choosing equal components of the vector provides the maximum growth rate,

$$\{\delta q = \delta p = \sqrt{1/2N}\} \ \rightarrow \ \Lambda_{\text{max}} = 2^{-1} s^{+2} \ .$$

For s^2 small, rather than large, alternating signs give the largest growth rate, with

$$\{ \ +\delta q_{\text{even}} = +\delta p_{\text{odd}} = -\delta q_{\text{odd}} = -\delta p_{\text{even}} \ \} \ ,$$

the growth rate is

$$\Lambda_{\text{max}} = 2^{+1} s^{-2} - 2^{-1} s^{+2} \ .$$

The growth rate is $2^{-1/2}$ at the transition between the two regions, where $s^2 \lessgtr 2^{1/2}$.

These same growth-rate results can be found numerically by applying "singular value decomposition" to the dynamical matrix D [26, 58]. This analysis details the deformation of an infinitesimal phase-space hypersphere for a short time dt. During this time the hypersphere has its components $\delta q, \delta p$ changed by the equations of motion:

$$\delta \xrightarrow{dt} (I + Ddt) \cdot \delta \ ,$$

so that the growth and decay rates can be found from the diagonal elements of the singular value decomposition

$$I + Ddt = U \cdot W \cdot V^t \rightarrow \{\Lambda = (1/dt) \ln W\} \ .$$

Numerical evaluation gives the complete spectrum of the growth and decay rates. The maximum matches the analytic results given above. Although locally the growth rates $\{\Lambda(r,t)\}$ are nonzero, the harmonic chain is not at all chaotic and the long-time-averaged Lyapunov exponents $\{\lambda = \langle \lambda(r,t) \rangle\}$, all vanish. Let us now apply the concepts of phase-space growth rates $\{\Lambda\}$ and the Lyapunov exponents $\{\lambda\}$ to the shockwave problem.

Linear Instability in Many Body Systems, Λ for Shockwaves

The time reversibility of the Hamiltonian equations of motion guarantees that any stationary situation shows both a long-time-averaged and a local symmetry between the

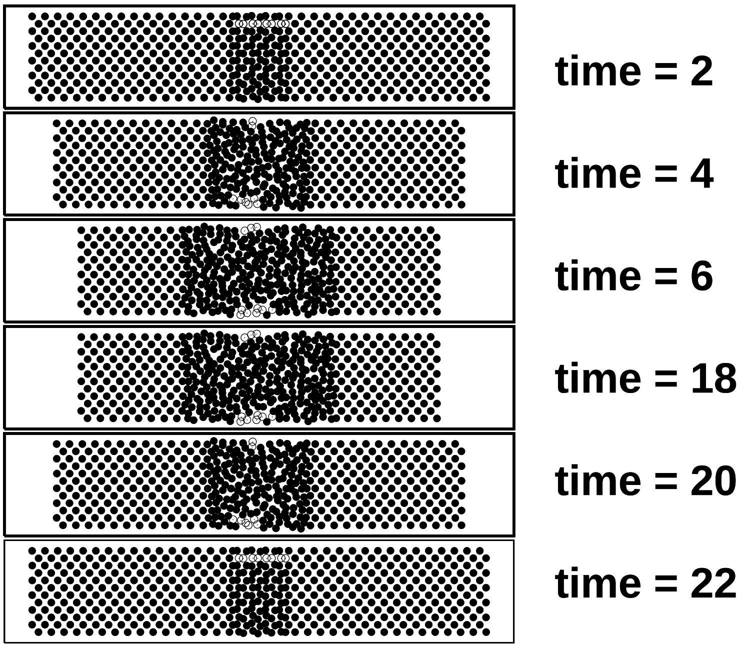

FIGURE 20. Phase-space Growth Rates $\{\Lambda\}$ during the collision of two 240-particle blocks of length 20. The collision leads to twofold compression of the original cold material at a time of order $20/1.93 \simeq 10.4$. At time = 12 the velocities were reversed, so that the configurations at times 2, 4, and 6 correspond closely to those at 22, 20, and 18 respectively. Those particles making above average contributions to the largest phase-space growth direction are indicated with open circles. The fourth-order Runge-Kutta timestep is $dt = 0.002$.

forward and reversed directions of time. In such a case the N nonzero time-averaged Lyapunov exponents as well as the local growth rates, obey the relations

$$\{\ \lambda_{N+1-k} + \lambda_k\} = 0\ ;\ \{\ \Lambda_{N+1-k} + \Lambda_k\} = 0\ .$$

The instantaneous Lyapunov exponents $\{\lambda(t)\}$ depend on the dynamical history, while the instantaneous diagonalized phase-space growth rates, which we indicate with $\Lambda(t)$ rather than $\lambda(t)$, do not.

The rates $\{\Lambda(t)\}$ for different directions in phase space can be calculated efficiently from the dynamical matrix D, by using singular value decomposition, just as we did for the harmonic chain:

$$D = \begin{pmatrix} \partial\dot{q}/\partial q & \partial\dot{q}/\partial p \\ \partial\dot{p}/\partial q & \partial\dot{p}/\partial p \end{pmatrix} = \begin{pmatrix} 0 & 1/m \\ \partial F/\partial q & 0 \end{pmatrix} .$$

Here we analyze a 480-particle shockwave problem, the collision of two blocks with x velocity components ± 0.965. Figure 20 shows those particles making above-average contributions to the maximum phase-space growth rate at times 2, 4, and 6. At time 12 the particle velocities are all reversed, so that the configurations at times 22, 20 and 18 closely match those at times 2, 4, and 6. Generally there is six-figure agreement between the coordinates going forward in time and those in the reversed trajectory at corresponding times. Note this symmetry in Figure 20, where the most sensitive particles going forward and backward are exactly the same at corresponding times. The forward-backward agreement could be made perfect by following Levesque and Verlet's suggestion [59] to use *integer* arithmetic in evaluating a time-reversible (even *bit-reversible*!) algorithm such as

$$\mathrm{Int}[q_{t+dt} - 2q_t + q_{t-dt}] = \mathrm{Int}[F_t dt^2/m] \text{ or}$$

$$\mathrm{Int}[q_{t+2dt} - q_{t+dt} - q_{t-dt} + q_{t-2dt}] = \mathrm{Int}[(dt^2/4m)(5F_{t+dt} + 2F_t + 5F_{t-dt})] \ .$$

Evidently, as would be expected, from their definition, the point-function growth rates $\{\Lambda(r(t))\}$ can show no "arrow of time" distinguishing the backward trajectory from the forward one. We turn next to the Lyapunov exponents, which *can* and *do* show such an arrow.

Lyapunov Spectrum in a Strong Shockwave

Most manybody dynamics is Lyapunov unstable, in the sense that the length of the phase-space vector joining two nearby trajectories has a tendency to grow at a (time-dependent) rate $\lambda_1(t)$ (with the time-averaged result $\lambda_1 \equiv \langle \lambda_1(t) \rangle > 0$). Likewise, the area of a moving phase-space triangle, with its vertices at three nearby trajectories, grows at $\lambda_1(t) + \lambda_2(t)$, with a time-averaged rate $\lambda_1 + \lambda_2$. The volume of a tetrahedron defined by four trajectories grows as $\lambda_1(t) + \lambda_2(t) + \lambda_3(t)$, and so on. By changing the scale factor linking coordinates to momenta – the s^{+2} of the last Section – these exponents can be determined separately in either coordinate or momentum space.

Posch and Hoover, and independently Goldhirsch, Sulem, and Orszag, discovered a thought-provoking representation of local Lyapunov exponents [60, 61]. If an array of Lagrange multipliers is chosen to propagate a comoving corotating orthonormal set of basis vectors centered on a phase space trajectory, the diagonal elements express *local* growth and decay rates. These are typically quite different (and unrelated) in the forward and backward directions of time.

Let us apply the Lyapunov spectrum [59, 60, 61] to the phase-space instability of a strong shockwave. Because the Lyapunov exponents, $\{\lambda(t)\}$, are evaluated so as to reflect only the past, times less than t, we expect to find that the Lyapunov vector corresponding to maximum growth soon becomes localized near the shock front. Starting out with randomly oriented vectors the time required for this localization is about 1/2. The time-linked disparities between the forward and backward motions suggest that the Lyapunov exponents *can* provide an "Arrow of Time" because the stability properties forward in time differ from those in the backward (reversed) direction of time [62].

Figure 21 shows the particles making above-average contributions to the largest of the local Lyapunov exponents, $\lambda_1(t)$. There are many more of these particles than the few

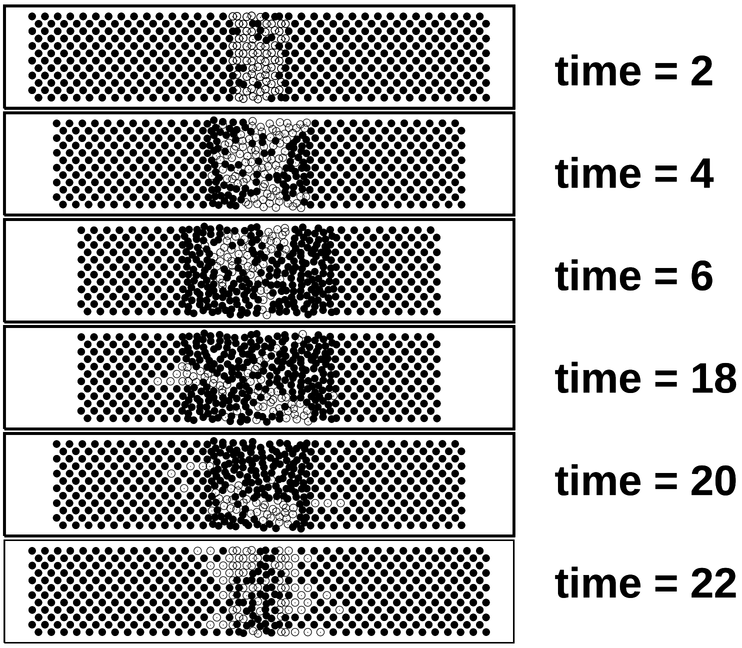

FIGURE 21. Phase-space Growth Rates $\{\lambda\}$ during the collision of two similar blocks which lead to the twofold compression of the original cold material. At time = 12 the velocities were reversed, so that the configurations at times 2 and 4 correspond to those at 22 and 20, respectively. The particles making above average contributions to the largest Lyapunov exponent are indicated with open circles.

which contribute to the largest of the phase-space growth rates, $\Lambda_1(t)$. The shockwave simulation was run forward in time for 6000 timesteps, after which the velocities were reversed. The phase-space offset vectors, chosen randomly at time 0 and again at time 12, became localized near the shockfront at a time of order 0.5. The particles to which the motion is most sensitive, as described by the Lyapunov exponent $\lambda_1(t)$ are more localized in space in the forward direction of time than in the backward direction. Evidently the Lyapunov vectors are more useful than the vectors corresponding to local growth rates in describing the irreversibility of Hamiltonian systems.

CONCLUSION

Particle dynamics, both NEMD and SPAM, provides a flexible approach to the simulation, representation, and analysis of nonequilibrium problems. The two particle methods are closely related, making it possible to infer constitutive relations directly from atomistic simulations. These useful tools provide opportunities for steady progress in understanding far-from-equilibrium states. It is our hope that these tools will become widely adopted.

ACKNOWLEDGMENTS

We thank Vitaly Kuzkin for encouraging our work on this review. Francisco de los Santos, Pedro Garrido, and Joaquin Marro kindly facilitated our presentations and the preparation of this manuscript. We thank Harald Posch for his careful reading of the manuscript.

REFERENCES

1. Wm. G. Hoover, *Molecular Dynamics*, Springer-Verlag, Berlin, 1986, available at the homepage http://williamhoover.info/MD.pdf.
2. Wm. G. Hoover, *Computational Statistical Mechanics*, Elsevier, Amsterdam, 1991, available at the homepage http://williamhoover.info/book.pdf.
3. D. J. Evans, and G. P. Morriss, *Statistical Mechanics of NonEquilibrium Liquids*, Academic Press, London, 1990.
4. L. B. Lucy, *The Astronomical Journal* **82**, 1013–1024 (1977).
5. R. A. Gingold, and J. J. Monaghan, *Monthly Notices of the Royal Astronomical Society* **181**, 375-389 (1977).
6. Wm. G. Hoover, *Smooth Particle Applied Mechanics — The State of the Art*, World Scientific Publishers, Singapore, 2006.
7. Wm. G. Hoover, and C. G. Hoover, “Shockwaves and Local Hydrodynamics; Failure of the Navier-Stokes Equations" in *New Trends in Statistical Physics, Festschrift in Honor of Leopoldo García-Colín’s 80th Birthday*, edited by Alfredo Macias and Leonardo Dagdug, World Scientific, Singapore, 2010.
8. Wm. G. Hoover, and C. G. Hoover, *Phys. Rev. E* **81**, 046302 (2010).
9. Wm. G. Hoover, C. G. Hoover, and F. J. Uribe, “Flexible Macroscopic Models for Dense-Fluid Shockwaves: Partitioning Heat and Work; Delaying Stress and Heat Flux; Two-Temperature Thermal Relaxation”, in *Proceedings of Advanced Problems in Mechanics*, Saint Petersburg, July 2010, (available in arXiv 1005.1525 (2010)).
10. E. Fermi, J. Pasta, and S. Ulam, Los Alamos report LA-1940 (1955), in *Collected Papers of Enrico Fermi*, edited by E. Segré, University of Chicago Press, 1965.
11. J. L. Tuck, and M. T. Menzel, *Advances in Mathematics* **9**, 399-407 (1972).
12. G. Benettin, “Ordered and Chaotic Motions in Dynamical Systems with Many Degrees of Freedom”, in *Molecular Dynamics Simulation of Statistical Mechanical Systems; Proceedings of the International School of Physics Enrico Fermi, Course XCVII*, edited by G. Ciccotti and W. G. Hoover, North-Holland, Amsterdam, 1986, pp. 15-40.
13. J. B. Gibson, A. N. Goland, M. Milgram, and G. H. Vineyard, *Phys. Rev.* **120**, 1229-1253 (1960).
14. W. W. Wood, and J. D. Jacobson, *J. Chem. Phys.* **27**, 1207-1208 (1957).
15. B. J. Alder, and T. E. Wainwright, *J. Chem. Phys.* **27**, 1208-1209 (1957).
16. J. A. Barker, and D. Henderson, *Rev. Mod. Phys.* **48**, 587-671 (1976).
17. W. T. Ashurst, and W. G. Hoover, *Phys. Rev. Lett.* **31**, 206-208 (1973).
18. V. Y. Klimenko, and A. N. Dremin, “Structure of a Shockwave Front in a Liquid”, in *Detonatsiya, Chernokolovka*, edited by G. N. Breusov *et alii*, Akademia Nauk, Moscow, 1978, pp. 79–83.
19. D. Levesque, L. Verlet, and J. Kürkijarvi, *Phys. Rev. A* **7**, 1690-1700 (1973).
20. L. V. Woodcock, *Chem. Phys. Lett.* **10**, 257-261 (1971).
21. S. Nosé, *Progress of Theoretical Physics Supplement* **103** (*Molecular Dynamics Simulations*, S. Nosé, Editor), 1-46 (1991).
22. W. G. Hoover, *Phys. Rev. A* **31**, 1695-1697 (1985).
23. W. G. Hoover, *Physica A* **240**, 1-11 (1997).
24. G. D. Venneri, and W. G. Hoover, *J.Computational Phys.* **73**, 468-475 (1987).
25. H. J. C. Berendsen and W. G. van Gunsteren, “Practical Algorithms for Dynamics Simulations”, in *Molecular Dynamics Simulation of Statistical Mechanical Systems; Proceedings of the International School of Physics Enrico Fermi, Course XCVII*, edited by G. Ciccotti and W. G. Hoover, North-

Holland, Amsterdam, 1986, pp. 43–65.
26. W. G. Hoover, C. G. Hoover, and F. Grond, *Communications in Nonlinear Science and Numerical Simulation* **13**, 1180-1193 (2008).
27. W. G. Hoover, C. G. Hoover, H. A. Posch, and J. A. Codelli, *Communications in Nonlinear Science and Numerical Simulation* **12**, 214-231 (2007).
28. B. L. Holian, W. G. Hoover, and H. A. Posch, *Phys. Rev. Lett.* **59**, 10-13 (1987).
29. J. D. Farmer, E. Ott, and J. A. Yorke, *Physica D* **7**, 153-180 (1983).
30. B. Moran, W. G. Hoover, and S. Bestiale, *J. Stat. Phys.* **48**, 709-726 (1987).
31. C. Dellago, and W. G. Hoover, *Phys. Rev. E* **62**, 6275-6281 (2000).
32. D. J. Evans, E. G. D. Cohen, and G. P. Morriss, *Phys. Rev. Lett.* **71**, 2401-2404, and 3616 (1993).
33. C. Jarzynski, *Euro. Phys. J. B* **64**, 331-340 (2008).
34. W. G. Hoover, H. A. Posch, and C. G. Hoover, *Chaos* **2**, 245-252 (1992).
35. W. G. Hoover, C. G. Hoover, and J. Petravic, *Phys. Rev. E* **78**, 046701 (2008).
36. Wm. G. Hoover, and H. A. Posch, *Phys. Rev. E* **54**, 5142-5145 (1996).
37. H. M. Mott-Smith, *Phys. Rev.* **82**, 885-892 (1951).
38. K. Xu, and E. Josyula, *Phys. Rev. E* **71**, 056308 (2005).
39. O. Kum, Wm. G. Hoover, and C. G. Hoover, *Phys. Rev. E* **56**, 462-465 (1997).
40. B. L. Holian, and M. Mareschal, *Phys. Rev. E* **82**, 026707 (2010).
41. D. J. Evans, W. G. Hoover, B. H. Failor, B. Moran, and A. J. C. Ladd, *Phys. Rev. A* **28**, 1016-1021 (1983).
42. A. Puhl, M. M. Mansour, and M. Mareschal, *Phys. Rev. A* **40**, 1999-2012 (1989).
43. V. M. Castillo, Wm. G. Hoover, and C. G. Hoover, *Phys. Rev. E* **55**, 5546-5550 (1997).
44. C. Normand, Y. Pomeau, and M. G. Velarde, *Rev. Mod. Phys.* **49**, 581-624 (1977).
45. P. Español, and P. Warren, *Europhys. Lett.* **30**, 191-196 (1995).
46. Wm. G. Hoover, H. A. Posch, V. M. Castillo, and C. G. Hoover, *J. Stat. Phys.* **100**, 313-326 (2000).
47. Wm. G. Hoover, and C. G. Hoover, *Computing in Science and Engineering* **3**, 78-85 (2001).
48. O. Kum, Wm. G. Hoover, and C. G. Hoover, *Phys. Rev. E* **68**, 017701 (2003).
49. V. M. Castillo, and Wm. G. Hoover, *Phys. Rev. E* **58**, 7350-7354 (1998).
50. L. D. Landau, and E. M. Lifshitz, *Fluid Mechanics*, Reed Elsevier, Oxford, 2000.
51. C. E. Ragan, III, *Phys. Rev. A* **29**, 1391-1402 (1984).
52. R. E. Duff, W. H. Gust, E. B. Royce, M. Ross, A. C. Mitchell, R. N. Keeler, and W. G. Hoover, "Shockwave Studies in Condensed Media", in the *Proceedings of the 1967 Paris Symposium Behaviour of Dense Media Under High Dynamic Pressures*, Gordon and Breach, New York, 1968.
53. B. L. Holian, W. G. Hoover, B. Moran, and G. K. Straub, *Phys. Rev. A* **22**, 2798-2808 (1980).
54. W. G. Hoover, *Phys. Rev. Lett.* **42**, 1531-1542 (1979).
55. V. N. Mineev, and A. V. Mineev, *Supplement to Journal de Physique III* C3-583-585 (1997).
56. R. J. Hardy, *J. Chem. Phys.* **76**, 622-628 (1982).
57. D. D. Joseph, and L. Preziosi, *Rev. Mod. Phys.* **61**, 41-73 (1989).
58. F. Grond, H. H. Diebner, S. Sahle, S. Fischer, and O. E. Rossler, "A Robust, Locally Interpretable Algorithm for Lyapunov Exponents", *Chaos, Solitons, and Fractals* **16**, 841-852 (2003).
59. Wm. G. Hoover, *Time Reversibility, Computer Simulation, and Chaos*, World Scientific, Singapore, 1999 and 2001.
60. W. G. Hoover, and H. A. Posch, *Phys. Lett. A* **123**, 227-230 (1987).
61. I. Goldhirsch, P.-L. Sulem, and S. A. Orszag, *Physica D* **27**, 311-337 (1987).
62. Wm. G. Hoover, C. G. Hoover, and H. A. Posch, *Computational Methods in Science and Technology* **7**, 55-65 (2001).

Stochastic thermodynamics: An introduction

Udo Seifert

II. Institut für Theoretische Physik, Universität Stuttgart

Abstract. These seminar notes contain a brief introduction into the principles of stochastic thermodynamics and some of its recent ramifications from a personal perspective. Thermodynamic concepts like work, exchanged heat and entropy production can consistently be defined on the level of individual fluctuating trajectories taken from either a time-dependent or a non-equilibrium steady state ensemble. Fluctuation theorems constrain the probability distributions for these thermodynamic quantities. For systems containing fast internal degrees of freedom the crucial distinction between internal and free energy for a correct identification of both dissipated heat and system entropy is emphasized. For non-equilibrium steady states, a generalized fluctuation-dissipation theorem relates the response to a small perturbation to correlation functions in the steady state involving observables expressing the various contributions to entropy production along the trajectory.

Keywords: thermodynamics, first law, entropy production, fluctuation-dissipation-theorem
PACS: 05.40.-a, 05.70.-a, 82.70.-y

CLASSICAL VS. STOCHASTIC THERMODYNAMICS

Stochastic thermodynamics provides a conceptual framework for describing a large class of soft and bio matter systems under well specified but still fairly general non-equilibrium conditions [1, 2, 3]. Typical examples comprise colloidal particles driven by time-dependent laser traps and polymers or biomolecules like RNA, DNA or proteins manipulated by optical tweezers, micropipets or AFM tips [4]. Three features are characteristic for such systems: (i) the source of non-equilibrium are external mechanical forces or unbalanced chemical potentials; (ii) these small systems are inevitably embedded in an aqueous solution which serves as a heat bath of well defined temperature T; (iii) fluctuations play a prominent role.

As the main idea behind stochastic thermodynamics, notions like applied work, exchanged heat and entropy developed in classical thermodynamics about 200 years ago are adapted to this micro- or nano-world. Specifically, the stochastic energetics approach introduced a decade ago by Sekimoto [5] is combined with the observation that entropy can consistently be assigned to an individual fluctuating trajectory [6].

For a juxtaposition of classical and stochastic thermodynamics we consider for each a paradigmatic experiment. For the classical compression of a gas or fluid in contact with a heat reservoir of temperature T (see Fig. 1), the first law

$$W = \Delta E + Q \tag{1}$$

expresses energy conservation. The work W applied to the system either increases the internal energy E of the system or is dissipated as heat $Q = T\Delta S_{\mathrm{m}}$ in the surrounding

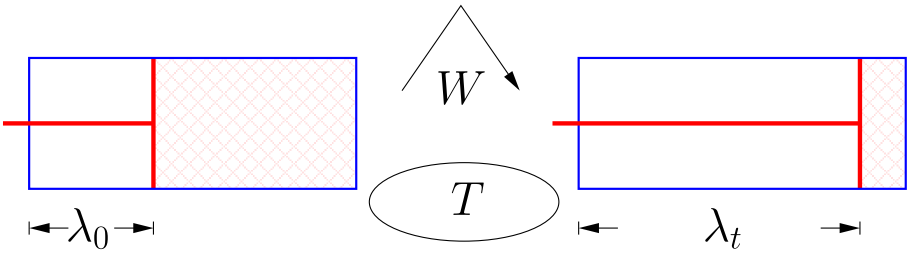

FIGURE 1. Typical experiment in classical thermodynamics: Starting from an initial position at λ_0, an external control parameter is changed according to a protocol $\lambda(\tau)$ during time $0 \leq \tau \leq t$ to a final position λ_t. This process requires work W while the system remains in contact with a heat bath at temperature T.

medium, where ΔS_m is the entropy change of the medium. The second law

$$\Delta S_\mathrm{tot} \equiv \Delta S + \Delta S_\mathrm{m} \geq 0 \tag{2}$$

combined with the first law leads to an inequality

$$W_\mathrm{diss} \equiv W - \Delta\mathscr{F} \geq 0 \tag{3}$$

expressing the fact that the work put in is never smaller than the free energy difference $\Delta\mathscr{F}$ between final and initial state. Their difference, the dissipated work W_diss, is zero only if the process takes place quasistatically.

A similar experiment on a nano-scale, the stretching of RNA, is shown in Fig. 2. Two conceptual issues must be faced if one wants to use the same macroscopic notions to describe such an experiment. First, how should work, exchanged heat and internal energy be defined on this scale. Second, these quantities do not acquire sharp values but rather lead to distributions, as shown in Fig. 3.

The occurrence of negative values of the dissipated work W_diss in such distributions seems to be in conflict with too narrow an interpretation of the second law. Two originally independent discoveries have led to profound statements not only constraining such distributions but also requiring such negative values. First, the (detailed) fluctuation theorem dealing with non-equilibrium steady states provides a symmetry between the probability for observing asymptotically a certain entropy production and the probability for the corresponding entropy annihilation [8, 9, 10, 11]. Second, the Jarzynski relation expresses the free energy difference between two equilibrium states as a nonlinear average over the non-equilibrium work required to drive the system from one state to the other in a finite time [12, 13]. Similarly, the Crooks relation compares the distributions for this work for forward and backward processes [14, 15]. The Hatano-Sasa relation constrains the "excess heat" associated with driving one non-equilibrium steady state to another [16].

The purpose of these seminar notes is to introduce the principles of stochastic thermodynamics from a personal perspective using first a driven colloidal particle as paradigm and later generalizing to systems with interacting degrees of freedom obeying coupled Langevin equations. For lack of space, the easily possible generalization of these concepts to Markovian dynamics on a set of discrete states as applicable to many biophysical and biochemical systems like molecular motors must be left out. Neither has any

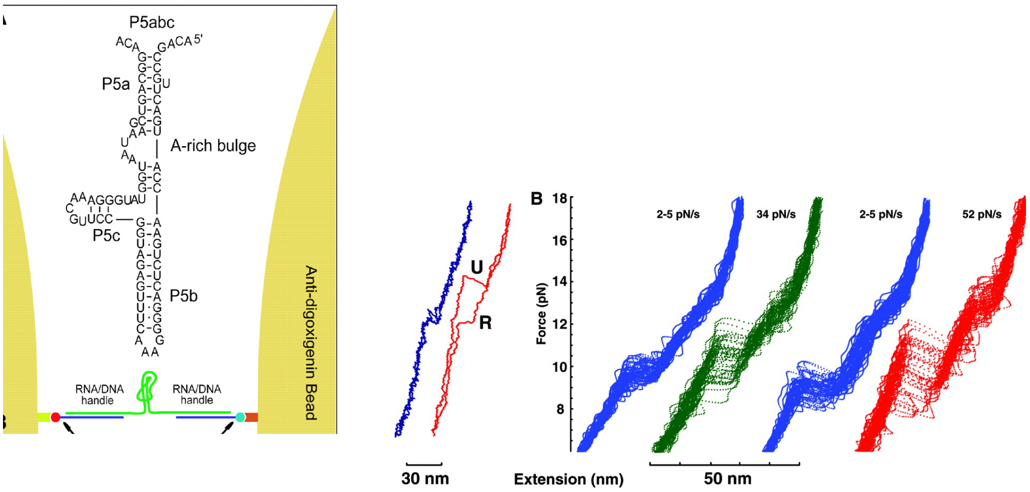

FIGURE 2. Typical experiment in stochastic thermodynamics: The two ends of an RNA molecule are attached to two beads which can be manipulated by micropipets. By pulling these beads, the hairpin structure of the RNA can be unfolded leading to force extension curves. For slow pulling (middle panel: left trace) these curves are almost reversible whereas for large pulling speed the curves show pronounced hysteresis (U, R) which is a signature of non-equilibrium. For all pulling speeds, the overlay of several traces shows the role of fluctuation; adapted from [7].

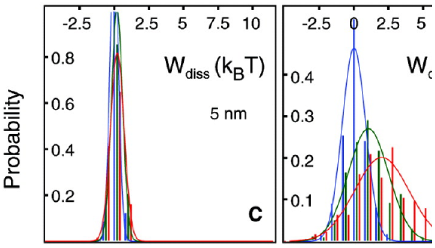

FIGURE 3. Measured distributions for dissipative work W_{diss} for the experiment shown Fig 2. The three panels correspond to different extensions. In each, the three distributions refer to different pulling speeds; adapted from [7].

attempt been made to achieve a comprehensive historical presentation. The monograph [3] and several (mostly) review articles can provide such complementary and occasionally broader perspectives [1, 2, 4, 17, 18, 19, 20, 21, 22, 23, 24, 25, 26, 27].

THERMODYNAMICS ALONG AN INDIVIDUAL TRAJECTORY

Stochastic dynamics

In this section, three equivalent but complementary descriptions of stochastic dynamics, the Langevin equation, the Fokker-Planck equation, and the path integral, are recalled [28, 29, 30] using a driven colloidal particle as paradigm.

The Langevin equation for the overdamped motion $x(\tau)$ in one dimension reads

$$\dot{x} = \mu F(x,\lambda) + \zeta = \mu(-\partial_x V(x,\lambda) + f(x,\lambda)) + \zeta. \tag{4}$$

The systematic force $F(x,\lambda)$ can arise from a conservative potential $V(x,\lambda)$ and/or be applied to the particle directly as $f(x,\lambda)$. Both sources may be time-dependent through an external control parameter $\lambda(\tau)$ varied from $\lambda(0) \equiv \lambda_0$ to $\lambda(t) \equiv \lambda_t$ according to some prescribed experimental protocol. The thermal noise has correlations

$$\langle \zeta(\tau)\zeta(\tau') \rangle = 2D\delta(\tau - \tau') \tag{5}$$

where D is the diffusion constant. In equilibrium, D and the mobility μ are related by the Einstein relation

$$D = T\mu \tag{6}$$

where T is the temperature of the surrounding medium with Boltzmann's constant k_B set to unity throughout the paper to make entropy dimensionless. In stochastic thermodynamics, one assumes that the strength of the noise is not affected by the presence of a time-dependent force. The range of validity of this crucial assumption can be tested experimentally or in simulations by comparing with theoretical results derived on the basis of this assumption.

The Fokker-Planck equation equivalent to the Langevin equation for the probability $p(x,\tau)$ to find the particle at x at time τ is

$$\begin{aligned} \partial_\tau p(x,\tau) &= -\partial_x j(x,\tau) \\ &= -\partial_x \left(\mu F(x,\lambda)p(x,\tau) - D\partial_x p(x,\tau)\right) \end{aligned} \tag{7}$$

where $j(x,\tau)$ is the probability current. This partial differential equation must be augmented by a normalized initial distribution $p(x,0) \equiv p_0(x)$. It will become crucial to distinguish the dynamical solution $p(x,\tau)$ of this Fokker-Planck equation, which depends on this given initial condition, from the solution $p^s(x,\lambda)$ for which the right hand side of (7) vanishes at any fixed λ. The latter corresponds either to a steady state for a non-vanishing non-conservative force or to equilibrium for $f \neq 0$ and $f = 0$, respectively.

A third equivalent description of the dynamics is given by assigning a weight

$$p[x(\tau)|x_0] = \mathcal{N} \exp\left[-\int_0^t d\tau[(\dot{x} - \mu F)^2/4D + \mu\partial_x F/2]\right] \tag{8}$$

to each path or trajectory where the last term arises from the Stratonovich convention for the discretization. Path dependent observables can then be averaged using this weight in a path integral which requires a path-independent normalization $\mathcal{N}$ such that summing the weight (8) over all paths is 1.

More technical background concerning these three equivalent descriptions is provided in the monographs [28, 29, 30].

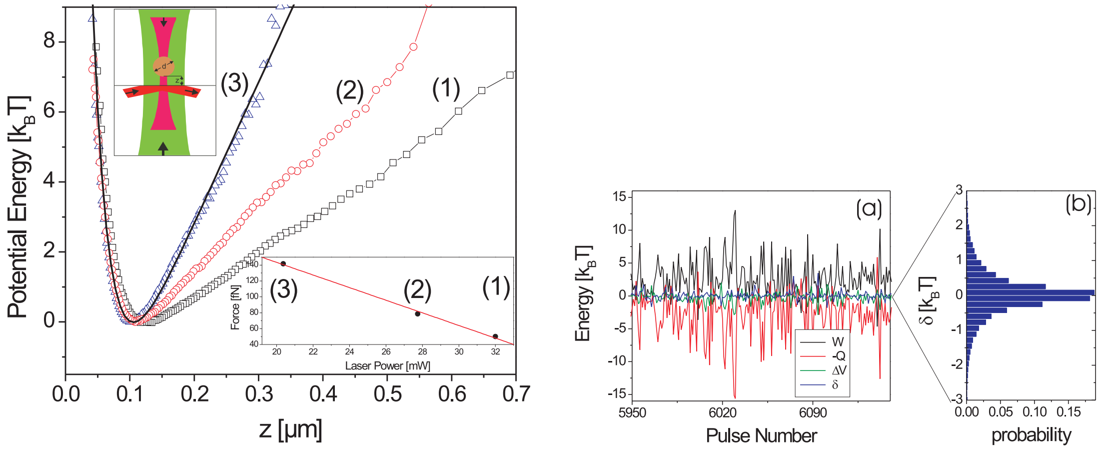

FIGURE 4. Experimental illustration of the first law. A colloidal particle is pushed by a laser towards a repulsive substrate. The (almost) linear attractive part of the potential depends linearly (see insert) on the laser intensity. For fixed laser intensity, the potential can be extracted by inverting the Boltzmann factor. If the laser intensity is modulated periodically, the potential becomes time-dependent. For each period (or pulse) the work W, heat Q and change in internal energy ΔV can be inferred from the trajectory using (10-11). Ideally, these quantities should add up to zero for each pulse, while the histogram shows the small ($\delta \lesssim 1k_{\mathrm{B}}T$) experimental error; adapted from [31].

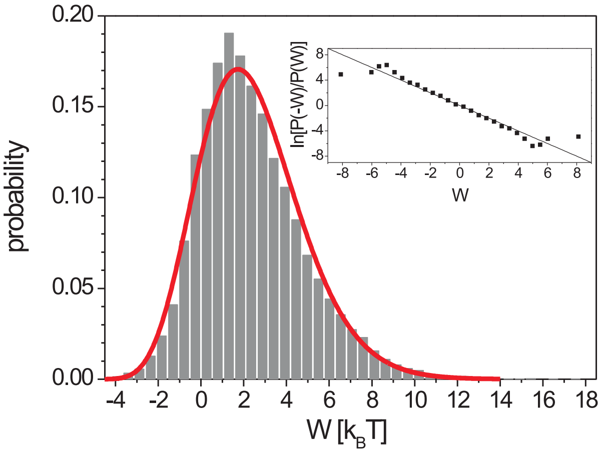

FIGURE 5. Work distribution for a fixed trajectory length for the experiment shown in Fig. 4. The histogram are experimental data, the full curve shows the theoretical prediction with no free fit parameters. The non-Gaussian shape proves that the experimental conditions probe the regime beyond linear response. The insert shows that the work distribution obeys the detailed fluctuation theorem; adapted from [31].

First law

Following Sekimoto who introduced the stochastic energetics approach [3], we first identify the first-law-like energy balance

$$dw = dE + dq \tag{9}$$

for the Langevin equation (4). The increment in work applied to the system, i.e., here the colloidal particle,

$$dw = (\partial V/\partial \lambda)\ \dot{\lambda}\ d\tau + f\ dx \tag{10}$$

consists of two contributions. The first term arises from changing the potential (at fixed particle position) and the second from applying a non-conservative force to the particle directly. The internal energy for a simple colloidal particle can be identified with the potential, i.e. $dE \equiv dV$.

If one accepts these quite natural definitions, for the first law to hold along a trajectory, the heat dissipated into the medium must be identified with

$$dq = F dx. \tag{11}$$

This relation is quite physical since in an overdamped system the total force times the displacement corresponds to dissipation. Integrated over a time interval t one obtains the expressions

$$w[x(\tau)] = \int_0^t [(\partial V/\partial \lambda)\dot{\lambda} + f\dot{x}]\, d\tau \quad \text{and} \quad q[x(\tau)] = \int_0^t F\dot{x}\, d\tau \tag{12}$$

and the first law

$$w[x(\tau)] = q[x(\tau)] + \Delta V = q[x(\tau)] + V(x_t, \lambda_t) - V(x_0, \lambda_0) \tag{13}$$

on the level of an individual trajectory.

In the experiment [31], the three quantities applied work, exchanged heat and internal energy were inferred from the trajectory of a colloidal particle pushed periodically by a laser trap against a repulsive substrate, see Fig. 4.

The measured non-Gaussian distribution for the applied work shown in Fig. 5 indicates that this system is driven beyond the linear response regime since it has been proven that within the linear response regime the work distribution is always Gaussian [32]. Moreover, the good agreement between the experimentally measured distribution and the theoretically calculated one indicates that the assumption of noise correlations being unaffected by the driving is still valid in this regime beyond linear response.

Stochastic Entropy

For a refinement of the second law on the level of individual trajectories, we need to define the corresponding entropy as well which, for this simple colloid, turns out to have two contributions. First, the heat dissipated into the environment should be identified with an increase in entropy of the medium

$$\Delta s_m[x(\tau)] \equiv q[x(\tau)]/T. \tag{14}$$

Second, one defines as a stochastic or trajectory dependent entropy of the system the quantity [6]

$$s(\tau) \equiv -\ln p(x(\tau), \tau) \tag{15}$$

where the probability $p(x,\tau)$ obtained by first solving the Fokker-Planck equation is evaluated along the stochastic trajectory $x(\tau)$. This stochastic entropy has the following properties.

- **Dependence on the ensemble**
  The stochastic entropy depends not only on the individual trajectory but also on the ensemble. If the same trajectory $x(\tau)$ is taken from an ensemble generated by another initial condition $p(x,0)$, it will lead to a different value for $s(\tau)$.
- **Relation to non-equilibrium ensemble entropy**
  Upon averaging with the given ensemble $p(x,\tau)$, this trajectory-dependent entropy becomes the usual ensemble entropy

$$S(\tau) \equiv -\int dx\, p(x,\tau) \ln p(x,\tau) = \langle s(\tau) \rangle. \tag{16}$$

  Here and throughout these notes the brackets $\langle ... \rangle$ denote the non-equilibrium average generated by the Langevin dynamics from some given initial distribution $p(x,0) = p_0(x)$.
- **Relation to thermodynamics in equilibrium**
  It is interesting to note that in equilibrium, i.e. for $f \equiv 0$ and constant λ, the stochastic entropy $s(\tau)$ obeys the well-known thermodynamic relation between entropy, internal energy and free energy

$$s(\tau) = (V(x(\tau),\lambda) - \mathscr{F}(\lambda))/T, \tag{17}$$

  along the fluctuating trajectory at any time with the free energy

$$\mathscr{F}(\lambda) \equiv -T \ln \int dx\, \exp[-V(x,\lambda)/T]. \tag{18}$$

- **Equations of motion**
  The rate of change of the entropy of the system (15) is given by [6]

$$\begin{aligned} \dot{s}(\tau) &= -\left.\frac{\partial_\tau p(x,\tau)}{p(x,\tau)}\right|_{x(\tau)} - \left.\frac{\partial_x p(x,\tau)}{p(x,\tau)}\right|_{x(\tau)} \dot{x} \\ &= -\left.\frac{\partial_\tau p(x,\tau)}{p(x,\tau)}\right|_{x(\tau)} + \left.\frac{j(x,\tau)}{Dp(x,\tau)}\right|_{x(\tau)} \dot{x} - \left.\frac{\mu F(x,\lambda)}{D}\right|_{x(\tau)} \dot{x}. \end{aligned} \tag{19}$$

  The first equality identifies the explicit and the implicit time-dependence. The second one uses the Fokker-Planck equation (7) for the current. The third term in the second line can be related to the rate of heat dissipation in the medium (14)

$$\dot{q}(\tau) = F(x,\lambda)\dot{x} = T\dot{s}_{\mathrm{m}}(\tau) \tag{20}$$

  using the Einstein relation $D = T\mu$. Then (19) can be written as a balance equation for the trajectory-dependent total entropy production

$$\dot{s}_{\mathrm{tot}}(\tau) \equiv \dot{s}_{\mathrm{m}}(\tau) + \dot{s}(\tau) = -\left.\frac{\partial_\tau p(x,\tau)}{p(x,\tau)}\right|_{x(\tau)} + \left.\frac{j(x,\tau)}{Dp(x,\tau)}\right|_{x(\tau)} \dot{x}. \tag{21}$$

The first term on the right hand side signifies a change in $p(x,\tau)$ which can be due to a time-dependent $\lambda(\tau)$ or, even at fixed λ, due to relaxation from a non-stationary initial state $p_0(x) \neq p^s(x,\lambda_0)$.
Upon averaging, the total entropy production rate $\dot{s}_{\rm tot}(\tau)$ has to become positive as required by the second law. This ensemble average proceeds in two steps. First, we conditionally average over all trajectories which are at time τ at a given x leading to

$$\langle \dot{x}|x,\tau\rangle = j(x,\tau)/p(x,\tau). \tag{22}$$

Second, with $\int dx \partial_\tau p(x,\tau) = 0$ due to probability conservation, averaging over all x with $p(x,\tau)$ leads to

$$\dot{S}_{\rm tot}(\tau) \equiv \langle \dot{s}_{\rm tot}(\tau)\rangle = \int dx \frac{j(x,\tau)^2}{Dp(x,\tau)} \geq 0, \tag{23}$$

where equality holds in equilibrium only. Averaging the increase in entropy of the medium along similar lines leads to

$$\begin{aligned} \dot{S}_{\rm m}(\tau) &\equiv \langle \dot{s}_{\rm m}(\tau)\rangle = \langle F(x,\tau)\dot{x}\rangle/T & (24)\\ &= \int dx F(x,\tau) j(x,\tau)/T. & (25) \end{aligned}$$

Hence upon averaging, the increase in entropy of the system itself becomes $\dot{S}(\tau) \equiv \langle \dot{s}(\tau)\rangle = \dot{S}_{\rm tot}(\tau) - \dot{S}_{\rm m}(\tau)$. On the ensemble level, this balance equation for the averaged quantities can also be derived directly from the ensemble definition (16) [33].

- **Integral fluctuation theorem (IFT)**
  The total entropy change along a trajectory follows from (14) and (15)

$$\Delta s_{\rm tot} \equiv \Delta s_{\rm m} + \Delta s \tag{26}$$

with

$$\Delta s \equiv -\ln p(x_t,\lambda_t) + \ln p(x_0,\lambda_0). \tag{27}$$

It obeys a remarkable integral fluctuation theorem (IFT) [6]

$$\langle e^{-\Delta s_{\rm tot}}\rangle = 1 \tag{28}$$

which can be interpreted as a refinement of the second law $\langle \Delta s_{\rm tot}\rangle \geq 0$. The latter follows from (28) by Jensen's inequality $\langle \exp x\rangle \geq \exp\langle x\rangle$. This integral fluctuation theorem for $\Delta s_{\rm tot}$ is quite universal since it holds for any kind of initial condition (not only for $p_0(x_0) = p^s(x_0,\lambda_0)$), any time-dependence of force and potential, with (for $f = 0$) and without (for $f \neq 0$) detailed balance at fixed λ, and any length of trajectory t.

INTEGRAL FLUCTUATION AND WORK THEOREMS

A general IFT

The IFT for entropy production (28) follows from a more general fluctuation theorem which unifies several relations previously derived independently. Based on the concept of time-reversed trajectories and time-reversed protocol [10, 15, 20], it is easy to prove the relation [6]

$$\langle \exp[-\Delta s_{\mathrm{m}}]\; p_1(x_t)/p_0(x_0)\rangle = 1 \tag{29}$$

for any function $p_1(x)$ with normalization $\int dx\; p_1(x) = 1$. Here, the initial distribution $p_0(x)$ is arbitrary. This relation can also be written in the form

$$\langle \exp[-(w-\Delta V)/T]\; p_1(x_t)/p_0(x_0)\rangle = 1 \tag{30}$$

with no reference to an entropy change.

The arguably most natural choice for the function $p_1(x)$ is to take the solution $p(x,\tau)$ of the Fokker-Planck equation at time t which leads to the IFT (28) for the total entropy production. Other choices lead to similar relations originally derived differently among which the Jarzynski relation is the most prominent one. Further relations that can be obtained from the IFT (29) can be found in Ref. [2].

Jarzynski relation

The Jarzynski relation (JR) originally derived using Hamiltonian dynamics [12]

$$\langle \exp[-w/T]\rangle = \exp[-\Delta\mathscr{F}/T] \tag{31}$$

expresses the free energy difference $\Delta\mathscr{F} \equiv \mathscr{F}(\lambda_t) - \mathscr{F}(\lambda_0)$ between two equilibrium states characterized by the initial value λ_0 and the final value λ_t of the control parameter, respectively, as a non-linear average over the work required to drive the system from one equilibrium state to another. At first sight, this is a surprising relation since on the left hand side there is a non-equilibrium average which should in principle depend on the protocol $\lambda(\tau)$, whereas the free energy difference on the right hand side is a pure equilibrium quantity.

Within stochastic thermodynamics the JR follows, a posteriori, from the more general relation (30), by specializing to the following conditions: (i) There is only a time-dependent potential $V(x,\lambda(\tau))$ and no non-conservative force ($f\equiv 0$), (ii) initially the system is in thermal equilibrium with the distribution

$$p_0(x) = \exp[-(V(x,\lambda_0) - \mathscr{F}(\lambda_0))/T]. \tag{32}$$

Plugging this expression with the free choice $p_1(x) = \exp[-(V(x,\lambda_t) - \mathscr{F}(\lambda_t))/T]$ into (30), the JR indeed follows within two lines. It is crucial to note that its validity does not require that the system has relaxed at time t into the new equilibrium. In fact, the actual distribution at the end will be $p(x,t)$.

As an important application, based on a slight generalization discussed below [34], the Jarzynski relation can be used to reconstruct the free energy landscape of a biomolecule $G(x)$ where x denotes a "reaction coordinate" like the end-to-end distance in forced protein folding as reviewed in [4].

Bochkov-Kuzolev relation

The Jarzynski relation should be distinguished from an earlier relation derived by Bochkov and Kuzolev [35, 36]. For a system initially in equilibrium in a time-independent potential $V_0(x)$ and for $0 \leq \tau \leq t$ subject to an additional space and time-dependent force $f(x,\tau)$, one obtains from (30) the Bochkov-Kuzolev relation (BKR)

$$\langle \exp[-\tilde{w}/T] \rangle = 1 \tag{33}$$

with

$$\tilde{w} \equiv \int_{x_0}^{x_t} f(x,\lambda(\tau))dx \tag{34}$$

by choosing $p_1(x) = p_0(x) = \exp[-(V_0(x) - \mathscr{F}_0)/T]$. Under these conditions, $\tilde{w}$ is the work performed at the system. Since this relation looks almost like the Jarzynski relation there have been both claims that the two are the same and some confusion around the apparent contradiction that $\langle \exp[-w/T] \rangle$ seems to be both $\exp[-\Delta\mathscr{F}/T]$ or 1. The present derivation shows that the two relations are different since they apply a priori to somewhat different situations. The JR as discussed above applies to processes in a time-dependent potential, whereas the BKR as discussed here applies to a process in a constant potential with some additional force. If, however, in the latter case, this explicit force arises from a potential as well, $f(x,\tau) = -V_1'(x,\tau)$, there still seems to be an ambiguity. It can be resolved by recognizing that in this case the work entering the BKR (33)

$$\tilde{w} = \int dx f = -\int dx V_1'(x,\tau) = -\Delta V_1 + w \tag{35}$$

differs by a boundary term from the definition of work w given in eq. (10) and used throughout this paper. Thus, if the force arises from a time-dependent but conservative potential both the BKR in the form $\langle \exp[-\tilde{w}/T] \rangle = 1$ and the JR (31) hold. The connection between the two relations can also be discussed within a Hamiltonian dynamics approach [37].

BEYOND THE COLLOIDAL PARADIGM

Heat and system entropy

The theory developed so far has been described using a single driven colloidal particle. The general concepts, however, are applicable to a much wider class of systems. An obvious generalization is to a system with several or many slow degrees of freedom $\{x\}$ obeying coupled Langevin equations or the corresponding Fokker-Planck equation or path integral. Formally, if one keeps the definitions as introduced so far, the general relations, being based on mathematical identities, remain true apart from the trivial change of notation replacing some of the scalar quantities for a colloidal particle with vectors (like, e.g., for the force and the current) or tensors (for mobility and diffusion constants).To keep the notation simple, we will stick to the scalar notation even for this more general case understood to be discussed from now on in these notes.

Such a simple extension, while mathematically correct, however, would miss one physically essential point which has to do with the proper identification of heat as pointed out by Sekimoto [38]. In consequence, the identification of a physically meaningful entropy for the system requires a slight modification as well. Its origin lies in the crucial difference between internal energy and free energy. The former should show up in the first law, whereas the latter belongs to the realm of the second law.

Consider a system like a polymer or protein with a few slow degrees of freedom $\{x_i\}$ collectively labeled by x which obey a Langevin equation (4) in a time-dependent potential $V(x,\lambda)$ where λ refers to an external control parameter like the position of a laser trap or of the base of an AFM cantilever [4], see Fig. 6. If there are no non-conservative forces f, the system is in equilibrium for any fixed λ. Then the probability to find the system at positions x is given by $p(x,\lambda) = \exp[-(V(x,\lambda) - \mathscr{F}(\lambda))/T]$. The crucial point is that $V(x,\lambda)$ now corresponds to an effective *free* energy (constrained to the slow variables x). This constrained free energy is temperature dependent since it is obtained by integrating out in a microscopic Hamiltonian both the fast degrees of freedom of the biopolymer and the degrees of freedom of the solutes and solvent molecules interacting with the slow degrees of freedom x. Hence, a state characterized by only the slow variable x carries some intrinsic entropy $s_{\text{int}}(x,\lambda)$ and also some internal energy $E(x,\lambda)$. These three quantities are related via the usual relation for a free energy as

$$V(x,\lambda) = E(x,\lambda) - Ts_{\text{int}}(x,\lambda) = E(x,\lambda) + T\partial_T V(x,\lambda). \tag{36}$$

This distinction between free energy and internal energy implies a modification of the heat compared to the case without internal degrees of freedom discussed above. While the work showing up in the first law is still given by (10), the increment in internal energy is given by

$$dE = dV + Tds_{\text{int}}. \tag{37}$$

Consequently, the correct identification of the heat follows as

$$dq = Tds_{\text{m}} = dw - dE = [f - \partial_x V(x,\lambda)]dx - Tds_{\text{int}}, \tag{38}$$

where we allow for full generality for non-conservative forces f as well. Thus, in contrast to the simpler colloidal case, the expression for heat now acquires a contribution from the intrinsic entropy.

Likewise, to characterize the full entropy s_{sys} of the system along an individual trajectory $x(\tau)$, we have to add this intrinsic entropy to the stochastic one (introduced in (15)) leading to

$$s_{\text{sys}}(\tau) \equiv s(\tau) + s_{\text{int}}(x(\tau)). \tag{39}$$

In the total entropy balance,

$$\dot{s}_{\text{tot}} = \dot{s}_{\text{sys}} + \dot{q}/T = \dot{s} + [f - \partial_x V]\dot{x}/T, \tag{40}$$

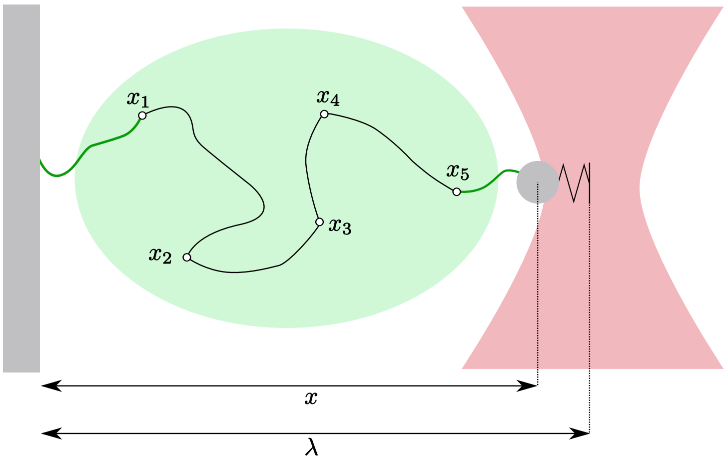

FIGURE 6. Sketch of protein unfolding experiment. The $\{x_i\}$ denote the position of selected slow degrees of freedom of the protein attached on one end to a bead subject to an optical trap. For a simple description, one considers only the (projected) end-to-end distance x. The time-dependent position λ of the center of the trap can be controlled externally.

the contributions of the intrinsic entropy cancel. Therefore, the expression for the total entropy change as given by the right-hand side of (21) remains unchanged.

Energy and entropy landscape of a protein

For an example illustrating this subtlety, consider the forced unfolding of a protein for which x now labels the end to end distance, considered to be the only slow variable, as sketched in Fig. 6. For simplicity we ignore the linkers between the polymer and the bead in the trap and rather assume one end of the protein being directly joined with the bead. The total potential then reads

$$V(x,\lambda) = G(x) + k(\lambda - x)^2/2 \tag{41}$$

with the first term being the free energy landscape of the protein and the second one the elastic energy associated with the trap of stiffness k centered at $\lambda(\tau)$.

The increment in work reads

$$dw = \partial_\lambda V(x,\lambda)d\lambda = k(\lambda - x)d\lambda \tag{42}$$

which corresponds to force times displacement of the center of trap. Clearly, if that position is not moved there is no external work applied to the total system comprising the protein and the bead. The increment in heat (38) becomes

$$dq = dw - dV(x,\lambda) - T ds_{\text{int}}(x) = [-\partial_x G(x) + k(\lambda - x)]dx - T ds_{\text{int}}(x) \tag{43}$$

where we exploit the fact that the intrinsic entropy is independent of the position λ of the center of the trap. The dissipated heat not only comprises the force appearing in the Langevin equation times displacement but in addition acquires a contribution from the "intrinsic entropy landscape" $s_{\text{int}}(x)$. The latter is in general not known. It could, however, be obtained by measuring the temperature dependence of the free energy landscape $s_{\text{int}}(x) = -\partial_T G(x)$. If such data became accessible, one could still infer the exchanged heat from measuring the trajectory $x(\tau)$ just as in the colloidal case.

The free energy landscape $G(z)$ can be reconstructed using

$$e^{-G(z)/T} = \langle \delta[z - x(t)] e^{-w(t)/T} \rangle e^{(k/2)(z-\lambda_t)^2/T} e^{-\mathscr{F}(\lambda_0)/T} \tag{44}$$

This expression follows from the general IFT (30) by plugging the initial distribution $p_0(x) = \exp[-(V(x,\lambda_0) - \mathscr{F}(\lambda_0))/T]$ and the choice $p_1(x) = \delta(x-z)$ into it [2]. It has first been derived by Hummer and Szabo [34] using a Feynman-Kac approach. Thus to get the potential $G(z)$ it is sufficient to select those trajectories that have reached z after time t and record the corresponding work $w(t) = k\int_0^t d\tau(\lambda(\tau) - x(\tau))\dot{\lambda}$ accumulated up to time t . The experiment on unfolding RNA mentioned in the Introduction has been one of the first real-world tests of this z-resolved Jarzynski relation [7].

NON-EQUILIBRIUM STEADY STATES

Characterization

Non-equilibrium does not necessarily require that the system is driven by time-dependent potentials or forces as discussed so far. A non-equilibrium steady state (NESS) is generated if time-independent but non-conservative forces $f(x)$ act on the system. Such systems are characterized by a time-independent or stationary distribution

$$p^s(x) \equiv \exp[-\phi(x)]. \tag{45}$$

As a fundamental difficulty, there is no simple way to calculate $p^s(x)$ or, equivalently, as it is sometimes called the "non-equilibrium potential" $\phi(x)$. In one dimension, it follows from quadratures [30] but for more degrees of freedom, setting the right hand side of the Fokker-Plank equation (7) to zero represents a formidable partial differential equation. Physically, the complexity arises from the fact that detailed balance is broken. Then a non-zero stationary current arises given by

$$j^s(x) = \mu F(x) p^s(x) - D\partial_x p^s(x) = v^s(x) p^s(x) \tag{46}$$

with the mean local velocity [6]

$$v^s(x) \equiv \langle \dot{x} | x \rangle. \tag{47}$$

This local mean velocity $v_s(x)$ is the average of the stochastic velocity $\dot{x}$ over the subset of trajectories passing through x. This current leads to a mean entropy production rate (23)

$$\sigma \equiv \langle \Delta s_{\text{tot}} \rangle / t = \int dx j^s(x) D^{-1} j^s(x) / p^s(x). \tag{48}$$

Even though the stationary distribution and current can not be calculated in general, an exact relation concerning entropy production can be derived for any NESS.

Detailed fluctuation theorem

In a NESS, the (detailed) fluctuation theorem

$$p(-\Delta s_{\text{tot}})/p(\Delta s_{\text{tot}}) = \exp[-\Delta s_{\text{tot}}] \tag{49}$$

expresses a symmetry of the probability distribution $p(\Delta s_{\text{tot}})$ for the total entropy production accumulated after time t in the steady state. This relation has first been found in simulations of two-dimensional sheared fluids [8] and then been proven by Gallavotti and Cohen [9] using assumptions about chaotic dynamics. For a stochastic dynamics, it has been proven by Kurchan [10] and Lebowitz and Spohn [11]. Strictly speaking, in all these works the relation holds only asymptotically in the long-time limit since entropy production had been associated with what in our approach is called entropy production in the medium. If one includes the entropy change of the system (27), the DFT holds even for finite times in the steady state [6]. This fact shows another benefit of defining an entropy along an individual trajectory.

For an experimental test including the system entropy, a colloidal particle has been driven by a constant force along a periodic potential, see Fig. 7 [39]. This experimental set-up constitutes the simplest realization of a genuine NESS. The same set-up has been used to test other recent aspects of stochastic thermodynamics like the possibility to infer the potential $V(x)$ from the measured stationary distribution and current [40] or a generalization of the Einstein relation beyond the linear response regime [41, 42] discussed below. For experimental illustration of the DFT using Brownian particles in a harmonic trap, electric circuits and a torsion pendulum, see [43, 44, 45].

The DFT for total entropy production holds even under the more general situation of periodic driving $F(x,\tau) = F(x,\tau+\tau_p)$, where τ_p is the period, if (i) the system has settled into a periodic distribution $p(x,\tau) = p(x,\tau+\tau_p)$, and (ii) the trajectory length t is an integer multiple of τ_p. For the distribution of work $p(W)$, a similar DFT can be proven provided the protocol is symmetric $\lambda(\tau) = \lambda(t-\tau)$, the non-conservative force zero, and the systems starts in equilibrium initially. For such conditions, the DFT for work was tested experimentally using a colloidal particle pushed periodically by a laser trap against a repulsive substrate [31], as shown in the insert of Fig. 5 above.

Generalized Einstein relation

In a NESS, the relation between fluctuation, response to an external perturbation and dissipation is more involved than in equilibrium. The well-known Einstein relation can here serve as a paradigm. First, for a free particle in a thermal environment, the diffusion constant D_0 and the mobility μ_0 are related by

$$D_0 = T\mu_0\,. \tag{50}$$

If this diffusion is modelled by a Langevin equation the strength of the noise becomes also D_0 as introduced above. For notational simplicity, we have ignored the subscript “0” in all but the present section of these notes. Second, if the particle is not free but

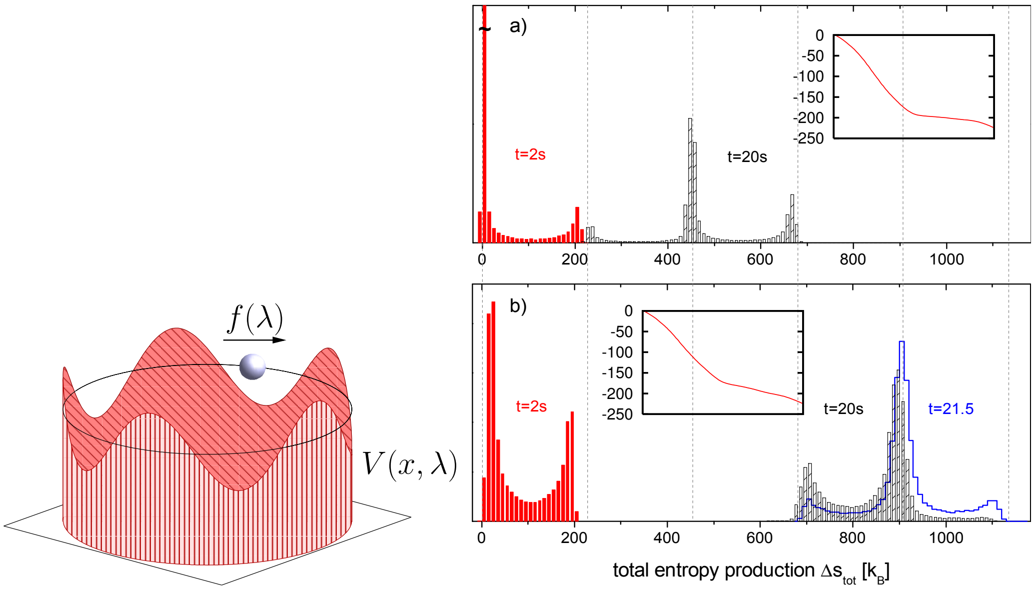

FIGURE 7. Left: Colloidal particle driven by a non-conservative force $f(\lambda)$ along a potential $V(x,\lambda)$ to generate a NESS. Right: Corresponding histograms of the total entropy production $p(\Delta s_{\text{tot}})$ for different lengths of trajectories and two different strengths of the applied force f. The inserts show the total potential $V(x) - fx$ in the two cases; adapted from [39].

rather diffuses in a potential $V(x)$, the diffusion coefficient

$$D \equiv \lim_{t\to\infty} [\langle x^2(t)\rangle - \langle x(t)\rangle^2]/2t, \tag{51}$$

and the effective mobility

$$\mu \equiv \frac{\partial\langle\dot{x}\rangle}{\partial f} \tag{52}$$

which quantifies the response of the mean velocity $\langle\dot{x}\rangle$ to a small external force f still obey $D = T\mu$ for any potential $V(x)$. Note that with this notation $D < D_0$ for any non-zero potential, since it is more difficult to surmount barriers by thermal excitation. Third, one can ask how the relation between the diffusion coefficient and mobility changes in a genuine NESS as shown in the set-up of Fig. 7. The definitions (51) and (52) are then still applicable if in the latter the derivative is taken at non-zero force. Using path-integral techniques, one can derive a generalized Einstein relation of the form [41]

$$D = T\mu + \int_0^\infty d\tau\, I(\tau), \tag{53}$$

with

$$I(\tau) \equiv \langle[\dot{x}(t+\tau) - \langle\dot{x}\rangle][v_{\text{s}}(x(t)) - \langle\dot{x}\rangle]\rangle. \tag{54}$$

The "violation" function $I(\tau)$ correlates the *actual* velocity $\dot{x}(t+\tau)$ with the *local* mean velocity $v_{\text{s}}(x)$ introduced in (47) after subtracting from both the *global* mean velocity $\langle\dot{x}\rangle = \int v_{\text{s}}(x)p^{\text{s}}(x) = 2\pi R j_{\text{s}}$ that is given by the net particle flux j_{s} along the ring of radius

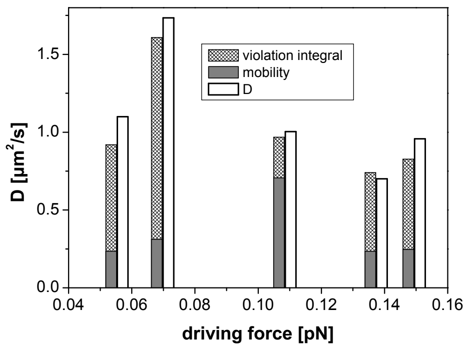

FIGURE 8. Experimental test of the generalized Einstein relation (53) for different driving forces f, using the set up shown in Fig. 7. The open bars show the measured diffusion coefficients D. The stacked bars are mobility μ (grey bar) and integrated violation I (hatched bar); adapted from [42].

R. In one dimension for a steady state, the current must be the same everywhere and hence j_s is a constant. The offset t is arbitrary because of time-translational invariance in a steady state. In equilibrium, detailed balance holds and therefore $v_s(x) = \langle \dot{x} \rangle = 0$. Then, the violation (54) vanishes and (53) reduces to the equilibrium relation (50).

For an experimental test of the non-equilibrium Einstein relation (53), trajectories of a single colloidal particle for different driving forces f were measured and evaluated [42]. Fig. 8 shows the three terms appearing in (53) for five different values of the driving force in the set-up shown in Fig. 7. Their sum is in good agreement with the independently measured diffusion coefficient directly obtained from the particles trajectory using (51). For very small driving forces, the bead is close to equilibrium and its motion can be described using linear response theory. As a result, the violation integral is negligible. Experimentally, this regime is difficult to access since D and μ become exponentially small and cannot be measured at reasonable time scales for small forces and potentials as deep as 40 T. For very large driving forces, the relative magnitude of the violation term becomes smaller as well. In this limit, the imposed potential becomes irrelevant and the spatial dependence of the local mean velocity, which is the source of the violation term, vanishes. The fact that the violation term is about four times larger than the mobility proves that this experiment indeed probes the regime beyond linear response. Still, the description of the colloidal motion by a Markovian (memory-less) Brownian motion with drift as implicit in the analysis remains obviously a faithful representation since the theoretical results are derived from such a framework.

Generalized FDT for a driven particle

The generalized Einstein relation just discussed is in fact the time-integrated version of a generalized fluctuation-dissipation-theorem (FDT) of the form [41]

$$T\frac{\partial\langle\dot{x}(\tau_2)\rangle}{\partial f(\tau_1)} = \langle\dot{x}(\tau_2)\dot{x}(\tau_1)\rangle - \langle\dot{x}(\tau_2)v_{\mathrm{s}}(x(\tau_1))\rangle. \qquad (55)$$

The left hand side quantifies the response of the mean velocity at time τ_2 to an additional force pulse at the earlier time τ_1. In equilibrium, i.e., more strictly speaking in the linear response regime, this response function is given by the velocity-velocity correlation function which is the first term on the right hand side. In non-equilibrium, an additive second term on the right hand side contributes which involves again the crucial mean velocity v_{s}. Both correlation functions on the right-hand side are taken in the NESS.

The equilibrium form of the FDT can be restored by referring the velocity to the local mean velocity according to

$$v(\tau_2) \equiv \dot{x}(\tau_2) - v_s(x(\tau_2)) \qquad (56)$$

for which the form

$$T\frac{\partial\langle v(\tau_2)\rangle}{\partial f(\tau_1)} = \langle v(\tau_2)\,v(\tau_1)\rangle \qquad (57)$$

holds even in non-equilibrium [41].

This form can be interpreted physically as an extension of the Onsager regression principle to NESSs. Observed in the locally comoving frame, the decay of a spontaneous fluctuation can not be distinguished from the decay of an externally generated one. A comprehensive mathematical formulation of this concept has been given in [46, 47].

Generalized FDT for an arbitrary NESS

These results for the response of the velocity to a force can in fact be generalized to the response of any observable to any perturbation in an arbitrary NESS. Remarkably, in such a generalized FDT, the stochastic entropy and its splitting into two contributions plays a prominent role.

For the general setting, consider a set of coupled Langevin equations (4) (with vector indices suppressed). The non-conservative forces f allow for a genuine NESS. If this NESS is perturbed by some small “field” h in a delta-like fashion at time τ_1, one can ask for the effect of this perturbation on a measurement of an observable $A(x)$ at the later time τ_2. The field h can enter the potential, the non-conservative force f or even the mobility μ. In any case, the response can be expressed by a correlation function in the unperturbed NESS according to

$$\frac{\delta\langle A(\tau_2)\rangle}{\delta h(\tau_1)} = \langle A(\tau_2)B(\tau_1)\rangle. \qquad (58)$$

At first sight, one might not have expected that the response can be expressed by such a correlation function let alone that the "conjugate" observable $B(x)$ depends only on the perturbation and is the same for all observables $A(x)$ and time-differences $\tau_2 - \tau_1$. In fact, a general expression for $B(x)$ follows from naive perturbation theory for the Fokker-Planck equation corresponding to (7) as shown in [30], for a comprehensive review see also [48].

It is instructive first to recall the familiar linear response result around genuine equilibrium ($f \equiv 0$) in this setting. Suppose that the perturbation h affects the potential according to $V(x) \to V(x,h)$. In this case, B is given by

$$TB(x) = -\partial_\tau \partial_h V(x,h)_{|h=0}. \tag{59}$$

If, e.g., the perturbation h is a genuine force, $h = f$, then the potential becomes $V(x,f) = V(x) - fx$ leading to the conjugate variable $B = \dot{x}$ as discussed above.

In a NESS, the conjugate variable can be expressed as [49]

$$B(x) = -\partial_\tau \partial_h s(x,h)|_{h=0} \tag{60}$$

where $s(x,h) = \phi(x) = -\ln p^s(x,h)$ is given by the non-equilibrium potential (45), which, in a time-independent NESS, is identical to the observable yielding the stochastic entropy along the trajectory. Note that this expression covers the equilibrium FDT as well, since with $p^{\mathrm{eq}}(x,h) = \exp[-(V(x,h) - \mathscr{F}(h))/T]$ we have $s(x,h) = (V(x,h) - \mathscr{F}(h))/T$. Since the free energy $\mathscr{F}(h)$ is time-independent, (59) and (60) lead to the same observable.

In a NESS, by expressing the stochastic entropy through medium, intrinsic (as introduced in (36)) and total entropy, we can split $B(x)$ into two contributions

$$B(x) = -\partial_\tau \partial_h s(x,f) = \partial_h [\dot{s}_m(x,h) + \dot{s}_{\mathrm{int}}(x,h)] - \partial_h \dot{s}_{\mathrm{tot}}(x,h). \tag{61}$$

If the NESS has been generated by applying a finite perturbation h_0 to an equilibrium state and is now further perturbed by a small perturbation δh in the same "direction", one can show that the first term in (61) corresponds to the conjugate observable in the corresponding equilibrium FDT for a small perturbation applied in h direction. Thus, in this situation, the FDT for a NESS is obtained by taking the equilibrium FDT, evaluating the right hand side under NESS conditions, and then subtracting a term which involves a variable associated with total entropy production. Such an additive structure is physically more transparent than the often used phenomenological description of a FDT in a NESS using an effective temperature [50].

Finally, it is interesting to observe that the conjugate variable $B(x)$ is not unique, i.e., there exists an equivalence class (denoted by $\cong$) of such variables which can be used as equivalent observables when appearing at the earlier time in a correlation function in a NESS [49]. For the paradigmatic case of the colloidal particle driven along the ring and perturbed by an additional small force, e. g., it turns out that $B(x) = \dot{x} - v_s(x) \cong v_s(x) - \mu F(x)$. Both expressions are thus equivalent when used in a correlation function in a NESS at the earlier time τ_1, i.e.

$$\langle A(x(\tau_2))[\dot{x}(\tau_1) - v_s(x(\tau_1))]\rangle = \langle A(x(\tau_2))[v_s(x(\tau_1)) - \mu F(x(\tau_1))]\rangle \tag{62}$$

holds for any observable $A(x)$ in this NESS. The conjugate variable becomes unique only by imposing additional conditions like that it should not contain a time-derivative as it holds for the second choice. Whether there is some deeper significance hidden behind this non-uniqueness remains to be explored.

In two recent experiments, this generalized FDT has been tested for a driven colloidal particle [51, 52]. In the second experiment, the non-uniqueness of the conjugate observable has been exploited to choose the observable leading to the best statistics for the corresponding correlation function.

For related interpretation of the generalized FDT, compare also [53, 54, 55] and for applications to interacting many body systems like sheared suspensions, see [56, 57].

CONCLUDING PERSPECTIVE

Within the last decade, stochastic thermodynamics has developed into a comprehensive framework for describing systems which, despite being embedded in an aqueous solution of well-defined temperature, are still in non-equilibrium due to external forces or fields. This theory can best be introduced using a driven colloidal particle as paradigm. The generalization to many interacting degrees of freedom is then straightforward if the crucial distinction between internal and free energy is kept in mind. The exact relations derived within stochastic thermodynamics quantify what previously has sometimes been called events “violating the second law”. Apart from serving as consistency checks, being so universal, the genuine fluctuation theorems – whether integral or detailed – are unlikely to reveal peculiarities of any specific system. From a more practical perspective, the Jarzynski relation might be the most useful one since it provides access to free energy differences from non-equilibrium measurements. Likewise, with the generalized FDTs it becomes possible to predict the response of a NESS to a perturbation by just monitoring an appropriate correlation function.

For a perspective, we close with three research problems drawn again from a personal point of view with selected references that could serve as guide to earlier and related work.

The detailed fluctuation theorem expresses a universal symmetry of the distribution of entropy production valid for any NESS. A classification of NESSs, however, may arise from investigating this distribution in the long-term limit where it obeys a large deviation principle [58]. Are there “universality classes” based on the behavior of the corresponding rate function? What is the origin of the almost singular behavior of the rate function at zero entropy production even for very simple systems [59, 60]? Why does a system even deep in a NESS seem to “remember” where equilibrium was?

Thermodynamics has originally been developed for understanding the rules of how to convert heat into work. With stochastic thermodynamics providing the same concepts for micro and nano scales, it should help finding the optimal design of such machines in these ranges. Establishing and controlling temperature differences on these scales remains a challenge. Chemical gradients, in contrast, can easily be maintained as the ubiquitous molecular motors in cell biology prove. Calculating the efficiency of biological motors and optimizing the one of artificial machines becomes possible if the framework described here for Langevin dynamics is generalized to a Markovian dynamics on a set of internal states of the machine or motor [61, 62, 63, 64, 65, 66, 67, 68]. The first experimental studies of a rotary enzyme, the F1-ATPase, using the concept of stochastic thermodynamics for data analysis have just appeared [69, 70].

Finally, in a sense coming back to the origins, the so far unmentioned zeroth law of thermodynamics states the transitivity of the concept of two states being in equilibrium. One could wonder whether a similar relation holds for NESS in contact. In general, certainly not. Quite surprisingly, however, a numerical study of driven lattice gases weakly coupled to another to allow for particle exchange has shown that for these systems an effective zeroth law almost holds [71]. The challenge to quantitatively understand the coupling between NESS in general still remains a significant one [72, 73].

ACKNOWLEDGMENTS

An enjoyable and fruitful collaboration with T. Speck on many aspects of the theory described here and with V. Blickle, J. Mehl and C. Bechinger on its experimental realization is gratefully acknowledged as is financial support from both DFG and ESF (through the EPSD network). I thank B. Lander and E. Zimmermann for a critical reading of these notes.

REFERENCES

1. C. Bustamante, J. Liphardt, and F. Ritort, *Physics Today* **58(7)**, 43 (2005).
2. U. Seifert, *Eur. Phys. J. B* **64**, 423–431 (2008).
3. K. Sekimoto, *Stochastic Energetics*, Springer-Verlag, 2010.
4. F. Ritort, *Adv. Chem. Phys.* **137**, 31–123 (2008).
5. K. Sekimoto, *Prog. Theor. Phys. Supp.* **130**, 17 (1998).
6. U. Seifert, *Phys. Rev. Lett.* **95**, 040602 (2005).
7. J. Liphardt, S. Dumont, S. B. Smith, I. Tinoco Jr, and C. Bustamante, *Science* **296**, 1832 (2002).
8. D. J. Evans, E. G. D. Cohen, and G. P. Morriss, *Phys. Rev. Lett.* **71**, 2401 (1993).
9. G. Gallavotti, and E. G. D. Cohen, *Phys. Rev. Lett.* **74**, 2694 (1995).
10. J. Kurchan, *J. Phys. A: Math. Gen.* **31**, 3719 (1998).
11. J. L. Lebowitz, and H. Spohn, *J. Stat. Phys.* **95**, 333 (1999).
12. C. Jarzynski, *Phys. Rev. Lett.* **78**, 2690 (1997).
13. C. Jarzynski, *Phys. Rev. E* **56**, 5018 (1997).
14. G. E. Crooks, *Phys. Rev. E* **60**, 2721 (1999).
15. G. E. Crooks, *Phys. Rev. E* **61**, 2361 (2000).
16. T. Hatano, and S. Sasa, *Phys. Rev. Lett.* **86**, 3463 (2001).
17. D. J. Evans, and D. J. Searles, *Adv. Phys.* **51**, 1529 – 1585 (2002).
18. R. D. Astumian, and P. Hänggi, *Physics Today* **55(11)**, 33 (2002).
19. J. M. R. Parrondo, and B. J. D. Cisneros, *Applied Physics A* **75**, 179 (2002).
20. C. Maes, *Sém. Poincaré* **2**, 29 (2003).
21. D. Andrieux, and P. Gaspard, *J. Chem. Phys.* **121**, 6167 (2004).
22. H. Qian, *J. Phys. Chem. B* **110**, 15063–15074 (2006).
23. A. Imparato, and L. Peliti, *C. R. Physique* **8**, 556–566 (2007).
24. R. J. Harris, and G. M. Schütz, *J. Stat. Mech.: Theor. Exp.* p. P07020 (2007).
25. R. Kawai, J. M. R. Parrondo, and C. van den Broeck, *Phys. Rev. Lett.* **98**, 080602 (2007).
26. C. Jarzynski, *Eur. Phys. J. B* **64**, 331–340 (2008).
27. M. Esposito, and C. van den Broeck, *Phys. Rev. Lett.* **104**, 090601 (2010).
28. C. W. Gardiner, *Handbook of Stochastic Methods*, Springer-Verlag, Berlin, 2004, 3rd edn.

29. N. G. van Kampen, *Stochastic Processes in Physics and Chemistry*, North-Holland, Amsterdam, 1981.
30. H. Risken, *The Fokker-Planck Equation*, Springer-Verlag, Berlin, 1989, 2nd edn.
31. V. Blickle, T. Speck, L. Helden, U. Seifert, and C. Bechinger, *Phys. Rev. Lett.* **96**, 070603 (2006).
32. T. Speck, and U. Seifert, *Phys. Rev. E* **70**, 066112 (2004).
33. H. Qian, *Phys. Rev. E* **64**, 022101 (2001).
34. G. Hummer, and A. Szabo, *Proc. Natl. Acad. Sci. U.S.A.* **98**, 3658 (2001).
35. G. N. Bochkov, and Y. E. Kuzovlev, *Physica A* **106**, 443–479 (1981).
36. G. N. Bochkov, and Y. E. Kuzovlev, *Physica A* **106**, 480–520 (1981).
37. C. Jarzynski, *C. R. Physique* **8**, 495–506 (2007).
38. K. Sekimoto, *Phys. Rev. E* **76**, 060103(R) (2007).
39. T. Speck, V. Blickle, C. Bechinger, and U. Seifert, *Europhys. Lett.* **79**, 30002 (2007).
40. V. Blickle, T. Speck, U. Seifert, and C. Bechinger, *Phys. Rev. E* **75**, 060101 (2007).
41. T. Speck, and U. Seifert, *Europhys. Lett.* **74**, 391 (2006).
42. V. Blickle, T. Speck, C. Lutz, U. Seifert, and C. Bechinger, *Phys. Rev. Lett.* **98**, 210601 (2007).
43. G. M. Wang, J. C. Reid, D. M. Carberry, D. R. M. Williams, E. M. Sevick, and D. J. Evans, *Phys. Rev. E* **71**, 046142 (2005).
44. D. Andrieux, P. Gaspard, S. Ciliberto, N. Garnier, S. Joubaud, and A. Petrosyan, *Phys. Rev. Lett.* **98**, 150601 (2007).
45. S. Joubaud, N. B. Garnier, and S. Ciliberto, *Europhys. Lett.* **82**, 30007 (2008).
46. R. Chetrite, G. Falkovich, and K. Gawedzki, *J. Stat. Mech.: Theor. Exp.* **8**, P08005 (2008).
47. R. Chetrite, and K. Gawedzki, *J. Stat. Phys.* **137**, 890–916 (2009).
48. U. Marconi, A. Puglisi, L. Rondoni, and A. Vulpiani, *Phys. Rep.* **461**, 111–195 (2008).
49. U. Seifert, and T. Speck, *Europhys. Lett.* **89**, 10007 (2010).
50. L. F. Cugliandolo, J. Kurchan, and L. Peliti, *Phys. Rev. E* **55**, 3898 (1997).
51. J. R. Gomez-Solano, A. Petrosyan, S. Ciliberto, and R. Chetrite, *Phys. Rev. Lett.* **103**, 040601 (2009).
52. J. Mehl, V. Blickle, U. Seifert, and C. Bechinger, *Phys. Rev. E* **82**, 032401 (2010).
53. T. Harada, and S. Sasa, *Phys. Rev. Lett.* **95**, 130602 (2005).
54. J. Prost, J.-F. Joanny, and J. M. R. Parrondo, *Phys. Rev. Lett.* **103**, 090601 (2009).
55. M. Baiesi, C. Maes, and B. Wynants, *Phys. Rev. Lett.* **103**, 010602 (2009).
56. T. Speck, and U. Seifert, *Phys. Rev. E* **79** (2009).
57. M. Krüger, and M. Fuchs, *Phys. Rev. Lett.* **102**, 135701 (2009).
58. H. Touchette, *Phys. Rep.* **478**, 1–69 (2009).
59. J. Mehl, T. Speck, and U. Seifert, *Phys. Rev. E* **78**, 011123 (2008).
60. T. Speck, J. Mehl, and U. Seifert, *Phys. Rev. Lett.* **100**, 178302 (2008).
61. A. Kolomeisky, and M. Fischer, *Annu. Rev. Phys. Chem.* **58**, 675–695 (2007).
62. A. W. C. Lau, D. Lacoste, and K. Mallick, *Phys. Rev. Lett.* **99**, 158102 (2007).
63. P. Gaspard, and E. Gerritsma, *J. Theor. Biol.* **247**, 672–686 (2007).
64. R. D. Astumian, *Proc. Natl. Acad. Sci. U.S.A.* **104**, 19715–19718 (2007).
65. T. Schmiedl, and U. Seifert, *Europhys. Lett.* **83**, 30005 (2008).
66. Z. C. Tu, *J. Phys. A: Math. Gen.* **41**, 312003 (2008).
67. M. Esposito, K. Lindenberg, and C. van den Broeck, *Phys. Rev. Lett.* **102**, 130602 (2009).
68. R. Lipowsky, and S. Liepelt, *J. Stat. Phys.* **135**, 777–778 (2009).
69. S. Toyabe, T. Okamoto, T. Watanabe-Nakayama, H. Taketani, S. Kudo, and E. Muneyuki, *Phys. Rev. Lett.* **104**, 198103 (2010).
70. K. Hayashi, H. Ueno, R. Iino, and H. Noji, *Phys. Rev. Lett.* **104**, 218103 (2010).
71. P. Pradhan, C. P. Amann, and U. Seifert, *Phys. Rev. Lett.* **105**, 150601 (2010).
72. S. I. Sasa, and H. Tasaki, *J. Stat. Phys.* **125**, 125–224 (2006).
73. E. Bertin, K. Martens, O. Dauchot, and M. Droz, *Phys. Rev. E* **75**, 031120 (2007).

Hydrodynamics from dynamical non-equilibrium MD

Sergio Orlandini[*,†], Simone Meloni[1, **,†] and Giovanni Ciccotti[‡,§]

[*]*Dipartimento di Chimica, Università "Sapienza", P.le A. Moro 5, 00185 Roma, Italy*
[†]*Consorzio Interuniversitario per le Applicazioni di Supercalcolo Per Università e Ricerca (CASPUR), Via dei Tizii 6, 00185 Roma, Italy*
[**]*School of Physics, Room 302 UCD-EMSC, University College Dublin, Belfield, Dublin 4, Ireland*
[‡]*School of Physics, Room 302B UCD-EMSC, University College Dublin, Belfield, Dublin 4, Ireland*
[§]*Dipartimento di Fisica, Università "La Sapienza" and CNISM, Piazzale Aldo Moro 5, 00185 Roma, Italy*

Abstract. We review a dynamical approach to non-equilibrium MD (D-NEMD). We show how, using a proper simulation setup, is possible to treat interesting cases in which the initial condition is a stationary non-equilibrium state produced by a suitable dynamical system. We then extend the class of non-equilibrium phenomena that can be studied by atomistic simulations to the case of complex initial conditions consisting in assigning a macroscopic value of a scalar or vector observable or a field. We illustrate the functioning of this method by applying it to the relaxation of an interface between two immiscible liquids. We have shown that our method generate unbiased results while this might not be the case for the often used short time average approach.

Keywords: D-NEMD, restrained MD, hydrodynamics
PACS: 83.10.Rs, 68.05.-n

INTRODUCTION

By time averages, the macroscopic properties, that are the object of equilibrium statistical mechanics, emerge from the microscopic interactions among the elementary constituents of a macroscopic body in a natural way. This is the Boltzmann point of view put in practice by molecular dynamics (MD) simulations. The situation is much less settled in the case of non-equilibrium statistical mechanics, except for the linear response to an external field [1, 2] and for stationary non-equilibrium situations [3, 4, 5, 6] (where the use of time averages is still justified). In the first case, the Kubo formula reduces the determination of the linear response to the calculation of equilibrium time correlation functions, which are easy to sample accurately by MD simulations; in the second case, time averages can still be used to replace ensemble averages over the unknown ensemble corresponding to the steady state (provide the system remains ergodic). Thus, for both cases, with a proper setup the physical properties of the system can be computed.

A MD method to compute the statistical properties of a non-equilibrium non-stationary systems has been proposed quite some time ago [7]. with this method

---

[1] To whom correspondence should be addressed: s.meloni@caspur.it

rigorous ensemble averages can be obtained by following the so called *dynamical approach* to non-equilibrium molecular dynamics (D-NEMD) [7, 8, 9]. This method, which is just the generalization and the numerical implementation of the Onsager principle of regressive fluctuations [10, 11], tells that the time dependent statistical average of a microscopic observable is computed by taking an average over the initial ensemble of the observable evolved in time under a perturbed dynamics. When the initial ensemble corresponds either to a system in equilibrium or to the stationary non-equilibrium state of a given perturbation, it can be easily sampled by MD. The Onsager-Kubo relation (see below) is thus exploited to perform non-equilibrium MD ensemble averages. That involves choosing independent configurations of the system in a steady state, performing the perturbed time evolution of every independent initial configuration and computing averages over the set of these different trajectories [7, 8, 9]. However, when the initial distribution corresponds to the equilibrium distribution of a system submitted to a macroscopic constraint, the prescription above must be complemented by a method which allows to sample the conditional Probability Density Function (PDF) associated with this condition. In this paper we shall illustrate how to deal with both cases: i) initial conditions corresponding to a stationary non-equilibrium distribution [12], and ii) initial conditions corresponding to the conditional equilibrium distribution of a system subject to an external macroscopic constraint, be it of scalar, vectorial or field nature [13]. This latter method allows to treat constraint of both scalar or field nature. We will achieve this objective by combining D-NEMD with restrained MD. The latter is used to perform the conditional average satisfying the macroscopic constraint mentioned above then, like in standard D-NEMD, the Onsager-Kubo relation is used to compute time-dependent statistical average of the relaxation from this state. It is worth to mention that the scalar and vectorial cases have been already implicitly solved by the Blue Moon approach in Ref. [14]. However, using the Blue Moon approach for vector or, even worse, field-like constraints, especially in molecular systems in which constraints are also used for imposing the molecular geometry, might result inconvenient in practice.

As an illustration of the case of stationary non-equilibrium initial conditions we will study the transient hydrodynamical behavior in the formation of convective cells within a two-dimensional fluid system subject to orthogonal thermal gradient and gravity field. We follow the time-dependence of the density $\rho(x;t)$, velocity $\mathbf{v}(x;t)$ and temperature $T(x;t)$ fields induced adding a gravity to a system in stationary conditions under the thermal gradient.

To illustrate our method to sample from a microscopic system under macroscopic constraints, we study the hydrodynamic relaxation to the equilibrium of the interface between two immiscible liquids. We compute the time evolution of the difference of density fields of the species A and B ($\Delta\rho(x;t) = \rho^A(x;t) - \rho^B(x;t)$) and the associated velocity field ($v^A(x;t)$) and show the usefulness of our approach that does not rely on the separation of timescale of atomistic and hydrodynamical processes, as it is the case for the often used method of local time average.

The paper is organized as follows. In Sec. we describe the theoretical background of D-NEMD and our method for sampling complex initial conditions. In Sec. we present an application of D-NEMD to the study of the formation of convective cells in a system subject to thermal gradient and gravity field. In Sec. we discuss an application of our combined restrained MD + D-NEMD method. Finally, in Sec. we draw some conclusions.

THEORETICAL BACKGROUND

In D-NEMD we consider a classical system with N particles in d spatial dimensions. Let $\mathbf{r}_i$ and $\mathbf{p}_i$ be the position and the momentum of the i-th particle, respectively, and $\Gamma = \{\mathbf{r}_i, \mathbf{p}_i\}$ be a point in phase space. The Hamiltonian governing the system is $H(\Gamma,t)$, which we assume to be explicitly time dependent (the generalization to non-Hamiltonian systems could be easily worked out [16, 17, 18]).

In statistical mechanics an observable, including a macroscopic field (see below for its definition), is obtained as an ensemble average in phase space of the corresponding microscopic observable:

$$O(t) = \int d\Gamma \hat{O}(\Gamma) w(\Gamma,t) \equiv \left\langle \hat{O}(\Gamma) w(\Gamma,t) \right\rangle \tag{1}$$

where $O(t)$ is the macroscopic observable and $\hat{O}(\Gamma)$ is the corresponding microscopic observable. $w(\Gamma,t)$ is the (time dependent) phase-space PDF. As a consequence of the conservation of probability, $w(\Gamma,t)$ obeys the Liouville equation:

$$\begin{aligned} \frac{\partial w(\Gamma,t)}{\partial t} &= -\nabla_\Gamma[\dot{\Gamma} w(\Gamma,t)] \\ & \quad \{w(\Gamma,t), H(\Gamma,t)\} = -iL(t) w(\Gamma,t) \end{aligned} \tag{2}$$

where $\{\cdot,\cdot\}$ is the Poisson bracket and $L(t)$ is the Liouville operator. A formal solution of Eq.(2) is:

$$w(\Gamma,t) = S^\dagger(t) w(\Gamma,0) \tag{3}$$

where $S^\dagger(t)$ is the adjoint time evolution operator of the dynamical system.

We now consider the time-evolution of a non-time-dependent phase-space observable:

$$\frac{d\hat{O}(\Gamma)}{dt} = \{\hat{O}(\Gamma), H(\Gamma,t)\} = iL(t)\hat{O}(\Gamma) \tag{4}$$

which has the following formal solution

$$\hat{O}(\Gamma(t)) = S(t)\hat{O}(\Gamma(0)) \tag{5}$$

where $S(t)$ is the time-evolution operator.

By combining Eq.(1) with Eq. (3) and (5) we get the Onsager-Kubo relation:

$$
\begin{aligned}
O(t) \quad &= \quad < \hat{O}(\Gamma)S^{\dagger}(t)w(\Gamma,0) > \\
& \qquad < S(t)\hat{O}(\Gamma)w(\Gamma,0) >
\end{aligned} \tag{6}
$$

The meaning of the above equation is that the ensemble average of the microscopic observable $\hat{O}(\Gamma)$ over the time-dependent PDF $w(\Gamma,t)$ at time t is the same as the ensemble average of the microscopic observable at the point $\Gamma(t)$, corresponding to the evolution in time of the initial phase-space point $\Gamma(0)$, averaged over the PDF at time $t=0$ ($w(\Gamma,0)$).

In the standard D-NEMD approach we assume that $w(\Gamma,0)$ corresponds to a stationary condition, then can be sampled via an MD simulation possibly governed by the Hamiltonian $H_0(\Gamma)$ (more general stationary conditions can be constructed, see below and in Ref. [12]). Then we can evolve initial configurations taken from that trajectory with the dynamics generated by $H(\Gamma,t)$. Along these paths we compute the microscopic observable $\hat{O}(\Gamma(t))$. The time-dependent behavior of the macroscopic observable $O(t)$ is the ensemble average of $\hat{O}(\Gamma(t))$ over all the trajectories originated from each of the initial states (see Eq. (6)). An example of how to generate stationary non-equilibrium conditions might be by putting the sample in contact with two thermal reservoirs at different temperature at the border of the simulation box. Using this setup it is possible by MD to sample an initial stationary PDF corresponding to a system under thermal gradient.

We will now generalize the standard D-NEMD approach to the case of an initial PDF associated with a macroscopic constraint, i.e. the conditional PDF to find the system at the point Γ in phase space given that a microscopic field $\hat{F}(\mathbf{x}|\mathbf{r})$, function of the atomic position only, at the time $t=0$ is equal to $F^*(\mathbf{x})$ ($\hat{F}(\mathbf{x}|\mathbf{r}) = F^*(\mathbf{x})$). Our method a fortiori applies to the case in which the observable F is a scalar. For sake of clarity we first introduce our method assuming that F is scalar and then explain how to extend it to the case of space-dependent fields. Let us start recalling that the conditional PDF mentioned above reads:

$$
w(\Gamma|F=F^*) = \frac{w(\Gamma)\delta(\hat{F}(\mathbf{r})-F^*)}{\mathscr{Z}P_F(F^*)} \tag{7}
$$

where $\hat{F}(\mathbf{r})$ is the microscopic observable associated with the macroscopic observable F, $\mathscr{Z}$ is the partition function associated with $w(\Gamma)$ and $P_F(F^*) = \int d\Gamma w(\Gamma)\delta(\hat{F}(\mathbf{r}) - F^*)/\mathscr{Z}$ is the PDF to find the system in the state $F=F^*$.

We propose to sample this conditional PDF by the biased MD simulation governed by the following Hamiltonian:

$$
\tilde{H}(\Gamma) = H_0(\Gamma) + \frac{k}{2}(\hat{F}(\mathbf{r}) - F^*)^2 \tag{8}
$$

where k is a tunable parameter. The PDF sampled by this biased MD is:

$$
w_k(\Gamma) \quad = \quad \frac{\exp[-\beta\tilde{H}(\Gamma)]}{\int d\Gamma \exp[-\beta\tilde{H}(\Gamma)]} \tag{9}
$$

$$= \frac{\exp[-\beta(H_0(\Gamma)+\frac{k}{2}(\hat{F}(\mathbf{r})-F^*)^2)]}{\int d\Gamma \exp[-\beta(H(\Gamma,0)+\frac{k}{2}(\hat{F}(\mathbf{r})-F^*)^2)]}$$

By recalling that $\exp(-(y-\mu)^2/2\sigma^2)/\sqrt{2\pi}\sigma \to \delta(y-\mu)$, in the limit of $k\to\infty$, we see that Eq. (9) goes to

$$w_k(\Gamma) \to \frac{\exp[-\beta(H_0(\Gamma)]\delta(\hat{F}(\mathbf{r})-F^*)}{\int d\Gamma \exp[-\beta(H_0(\Gamma)]\delta(\hat{F}(\mathbf{r})-F^*)} \tag{10}$$

Multiplying and dividing by $\mathscr{Z}$ it is apparent that $w_k(\Gamma) \to w(\Gamma|F=F^*)$.

We now extend our discussion to the case in which the condition (and the observables of interest) is with respect to a macroscopic field, rather than to a scalar. Generally speaking, in statistical mechanics the microscopic observable associated to a macroscopic field is defined as [21]:

$$\hat{F}(\mathbf{x},\Gamma) = \sum_{i=1}^{N} \mathscr{F}_i(\Gamma)\delta(\mathbf{x}-\mathbf{r}_i) \tag{11}$$

where $\mathscr{F}_i(\Gamma)$ is the microscopic property under consideration relative to the particle i and $\mathbf{x}$ is a point in the ordinary $\Re^3$ space. Eq. (11) means that only atoms at the point $\mathbf{r}_i = \mathbf{x}$ contribute to the field at that point. Examples of fields of interest for the problem presented in Sec. and are the fields density ($\rho(\mathbf{x},t)$), velocity ($\mathbf{v}(\mathbf{x},t)$) and temperature ($T(\mathbf{x},t)$). These fields at time t are given by:

$$\rho(\mathbf{x},t) =< \sum_{i=1}^{N} \mu_i \delta(\mathbf{x}-\mathbf{r}_i) w(\Gamma,t) > \tag{12}$$

$$\mathbf{v}(\mathbf{x},t) = \frac{< \sum_{i=1}^{N} \mathbf{p}_i \delta(\mathbf{x}-\mathbf{r}_i) w(\Gamma,t) >}{\rho(\mathbf{x},t)} \tag{13}$$

$$T(\mathbf{x},t) = \frac{1}{3k_B} \frac{< \sum_{i=1}^{N} \delta(\mathbf{x}-\mathbf{r}_i)[\mathbf{p}_i - \mu_i \mathbf{v}(\mathbf{x},t)]^2 w(\Gamma,t) >}{\rho(\mathbf{x},t)} \tag{14}$$

where μ_i is the mass of the i-th atom.

Eq. (7) can be easily extended to the case in which the condition is a field:

$$w[\Gamma|\hat{F}(\mathbf{x},\Gamma) = F^*(\mathbf{x})] = \frac{w(\Gamma)\delta(\hat{F}(\mathbf{x},\Gamma)-F^*(\mathbf{x}))}{\mathscr{Z} P_F[F^*(\mathbf{x})]} \tag{15}$$

Now $w[\Gamma|\hat{F}(\mathbf{x})]$ is functional of the field $F(\mathbf{x})$ and the notation $\delta(\hat{F}(\mathbf{x}|\Gamma)-F^*(\mathbf{x})) \equiv \prod_{\mathbf{x}\in\Re^3} \delta(\hat{F}(\mathbf{x},\Gamma)-F^*(\mathbf{x}))$ indicates that the delta function is considered acting all over the $\mathbf{x}$ space. Of course, this definition of the conditional probability density functional is of no practical use in simulations. We overcome this problem by introducing a discretization $\{\mathbf{x}_\alpha\}_{\alpha=1,m}$ of the $\Re^3$ space, where m is the number of points over which the space is discretized. Consistently with this discretization the microscopic observable fields is defined as the average over the cells around around each point $\mathbf{x}_\alpha$:

$$\hat{F}(\mathbf{x}_\alpha,\Gamma) \;=\; \frac{1}{\Omega_\alpha}\int_{\Omega_\alpha} d\mathbf{x}\sum_{i=1}^{N}\mathscr{F}_i(\Gamma)\delta(\mathbf{x}-\mathbf{r}_i) = \frac{1}{\Omega_\alpha}\sum_{l=1}^{N_\alpha}\mathscr{F}_l(\Gamma) \tag{16}$$

where the sum in the r.h.s. runs over the atoms belonging to the cell around the point $\mathbf{x}_\alpha$. However, this definition is not suitable for our restrained MD method as it might produce impulsive forces on the atoms moving from one cell to another (see below). Therefore we smooth the central term of Eq. (16) by replacing $\delta(\mathbf{x}-\mathbf{r}_i)$ with the (normalized) Gaussian $g(\mathbf{x};\mathbf{r}_i,\sigma) = \exp[-(\mathbf{x}-\mathbf{r}_i)^2/2\sigma^2]/\sqrt{2\pi}\sigma$. With this approximation, Eq. (16) becomes:

$$\begin{aligned}\hat{F}(\mathbf{x}_\alpha,\Gamma) \;&=\; \\ \frac{1}{\Omega_\alpha}\;\; \textstyle\sum_{i=1}^{N} \;\;& \mathscr{F}_i(\Gamma)\Pi_{\chi=1}^{3}\left[erf(\bar{x}_{\alpha,\chi}-r_{i,\chi},\sigma) - erf(\underline{x}_{\alpha,\chi}-r_{i,\chi},\sigma)\right]\end{aligned} \tag{17}$$

where $erf(c,\sigma) = \int_{-\infty}^{c} dx\ g(x;0,\sigma)$ is the error function, and $\bar{x}_{\alpha,\chi}$ and $\underline{x}_{\alpha,\chi}$ is the χ component of the upper and lower limit of the orthorhombic cell around the point $\mathbf{x}_\alpha$.

The conditional PDF associated to the field $F(\mathbf{x})$ on the discrete representation of the $\Re^3$ space is:

$$w\left(\Gamma|\{\hat{F}(\mathbf{x}_\alpha,\Gamma) = F^*(\mathbf{x}_\alpha)\}_{\alpha=1,m}\right) = \frac{w(\Gamma)\Pi_{\alpha=1}^{m}\delta(\hat{F}(\mathbf{x}_\alpha,\Gamma)-F^*(\mathbf{x}_\alpha))}{\mathscr{L}P_F(\{F^*(\mathbf{x}_\alpha)\}_{\alpha=1,m})} \tag{18}$$

where $P_F(\{F^*(\mathbf{x}_\alpha)\}_{\alpha=1,m})$ is the joint probability that $\hat{F}(\mathbf{x}_1,\Gamma) = F^*(\mathbf{x}_1),\ldots,\hat{F}(\mathbf{x}_m,\Gamma) = F^*(\mathbf{x}_m)$. This conditional PDF can be sampled by a MD governed by the following Hamiltonian

$$\tilde{H}(\Gamma) = H_0(\Gamma) + \sum_{\alpha=1}^{m}\frac{k}{2}(\hat{F}(\mathbf{x}_\alpha,\mathbf{r}) - F^*(\mathbf{x}_\alpha))^2 \tag{19}$$

which is the straightforward extension of the Hamiltonian of Eq. (19) to the case of a macroscopic field in the discrete space approximation. Then, as in standard D-NEMD approach, we evolve a set of initial configurations taken from the trajectory above with the dynamics generated by $H(\Gamma,t)$. Along these paths we can compute the microscopic observables and calculate the ensemble average over all the trajectories originated from each initial state (Eq. (6)).

Before closing this section it is worth to mention that the problem of sampling initial conditions consistent with a macroscopic constraint was already implicitly solved by the Blue Moon ensemble (see Refs. [14] and [15]). Blue Moon does not sample directly the conditional PDF $w(\Gamma|F=F^*)$ (or $w\left(\Gamma|\{\hat{F}(\mathbf{x}_\alpha,\Gamma)=F^*(\mathbf{x}_\alpha)\}_{\alpha=1,m}\right)$ for the vectorial case) but rather it samples the constrained PDF in configurational space $w_{F^*}(\mathbf{r})$. The relation between the Blue Moon ensemble average and conditional average in the configurational space is given by (see Ref. [15]):

$$< \hat{O}(\mathbf{r}) >_{F=F^*} = \frac{< \hat{O}(\mathbf{r}) 1/\sqrt{|\det[C(\mathbf{r})]|} >_{BM}}{< 1/\sqrt{|\det[C(\mathbf{r})]|} >_{BM}} \tag{20}$$

where $\hat{O}(\mathbf{r})$ is a microscopic observable and $C_{ij}(\mathbf{r}) = \nabla\sigma_i(\mathbf{r}) M^{-1} \nabla\sigma_j(\mathbf{r})$, being $\sigma_i(\mathbf{r})$ the (vectorial) condition $\hat{F}(\mathbf{r}) = F^*$ or any other constraint imposed on the system, in particular constraints imposed for modeling (partly) rigid molecules [19], and M the mass matrix ($M_{ij} = \mu_i \delta_{ij}$). The $F = F^*$ and BM indexes denote that the ensemble averages are taken according to the conditional or constrained (Blue Moon) PDF, respectively. If the observable of interest depends on the phase space ($\hat{O}(\Gamma)$) rather than on the configurational space it is possible to extend the validity of Eq. 20 by generating the momentum component of the PDF from a suitable Maxwellian distribution.

Two comments are in order concerning the restraint method for sampling the complex initial condition described in this paper versus the approach based on the Blue Moon ensemble. First of all, depending on the macroscopic condition and the molecular constraints, calculating the unbiasing term $1/\sqrt{|\det[C(\mathbf{r})]|}/ < 1/\sqrt{|\det[C(\mathbf{r})]|} >_{BM}$ might be complex. Moreover, while the restraint approach can be combined with Monte Carlo simulation when the microscopic observable connected to the macroscopic condition is not analytical (see Ref. [20] for a detailed description of this approach), the same cannot be done with the Blue Moon approach.

In the following two sections we show two applications of the D-NEMD described above. We first present the case of an initial condition corresponding to a stationary non-equilibrium system. In particular we study the transient state of formation of convection cells when a gravity force is added to a system subject to a thermal gradient (Sec.). Then we illustrate an application of the restrained method to sample initial conditions corresponding to a system subject to macroscopic constraints by studying the relaxation to the equilibrium of the interface between two immiscible liquids (Sec.).

FORMATION OF CONVECTIVE CELLS

Computational Model and Setup.

A fluid system consisting of $N = 5041$ particles is contained in a two- dimensional box in the $\{xz\}$ plane, with the gravity force directed along the negative verse of the z axis. The particles interact via a WCA (Weeks-Chandler-Andersen) potential

$$u(r) = \begin{cases} 4\varepsilon\left[(\sigma/r)^{12} - (\sigma/r)^6\right], \forall\, r \leq 2^{1/6}\sigma \\ 0, \forall\, r \geq 2^{1/6}\sigma \end{cases} \tag{21}$$

where ε and σ are the usual Lennard-Jones parameters. This potential is a purely repulsive potential obtained from the Lennard-Jones 12-6 potential, truncated in its minimum (so that the force is continuous), and shifted (so that the potential is continuous). Each particle has mass μ. Hereafter, we will use reduced units putting the typical scale of energy, mass, and length equal to unity, i.e., $\varepsilon = 1$, $\mu = 1$, and $\sigma = 1$. Times are then measured in units of $\sqrt{\mu\sigma^2/\varepsilon}$.

We want to study the system in physical conditions that allow the formation of a convective cell, i.e., when gravity and a thermal gradient are present. Moreover, we want to analyze the transient evolution to the formation of the steady-state roll. For this we can take as initial condition of the system the steady state under the effect of a thermal gradient and then study the dynamical response of the system to the ignition of gravity. As far as the physical setting is concerned, we take the thermal gradient orthogonal to the gravity force. This allows a straightforward application of the D-NEMD technique. At the top and at the bottom of the box there are repulsive walls to avoid particles from drifting downwards under the effect of the gravity force. The thermal reservoirs which produce the thermal gradient are realized as two stripes such that the components of the velocity of each particle located in one of these stripes are sampled from a Maxwellian distribution at the temperature of the wall. We assume periodic boundary conditions at the thermal walls located at the two lateral sides of the box, i.e., a particle can move from the hotter to the colder reservoir. To avoid that particles near a thermal reservoir interact simultaneously with both reservoirs, we chose the thickness of the reservoir $x_T = 1.68$, larger than the cutoff of the WCA interaction. When the system is in equilibrium, each reservoir contains roughly 100 particles on average. We chose the temperature of the colder reservoir as $T_1 = 1.5$ and a theoretical thermal gradient $|\nabla T| = 0.1$, so that the hotter reservoir has a temperature $T_2 = |\nabla T|L + T_1 = 9.9$. The gravity force used is $g = 0.1$ in Lennard-Jones units. In SI units, taking Ar as a reference fluid, we have $g = 7 \times 10^{12}$ m/s^2, $T_2 = 1196$ K, and $T_1 = 179.7$ K. The box length is $L = 2.89 \times 10^{-8}$ m, so that the thermal gradient is $|\nabla T| = (T_2 - T_1)/L = 3.52 \times 10^{10}$ K/m. External fields of this strength are necessary to reach a sufficient signal to noise ratio in a small system. The density, velocity and temperature fields are computed on a 15×15 discretization of the $\Re^2$ space. Finally, The averages for these simulations are performed over an ensemble made of 1000 copies of the system

Results and discussion.

We follow the evolution of the system after the ignition of the gravity field by monitoring the time evolution of the temperature and density fields in some characteristic cells (see Fig. 1). These fields become stationary at $t = 250$. During the transient, both temperature and density oscillate with nearly the same period $\tau = 18$ in all cells. The phase of these oscillation is constant in all cells at the bottom of the box, and it is the same for ρ and T. The same feature holds for the phase in the cells at the top of the box, which is, however, opposite to the phase in the cells at the bottom. During the transient, an increase (decrease) in T corresponds to an increase (decrease) in ρ in the same cell, while, in the stationary state at large time, a temperature lower (higher) than the initial value is associated with a density higher (lower) than the initial value, as expected.

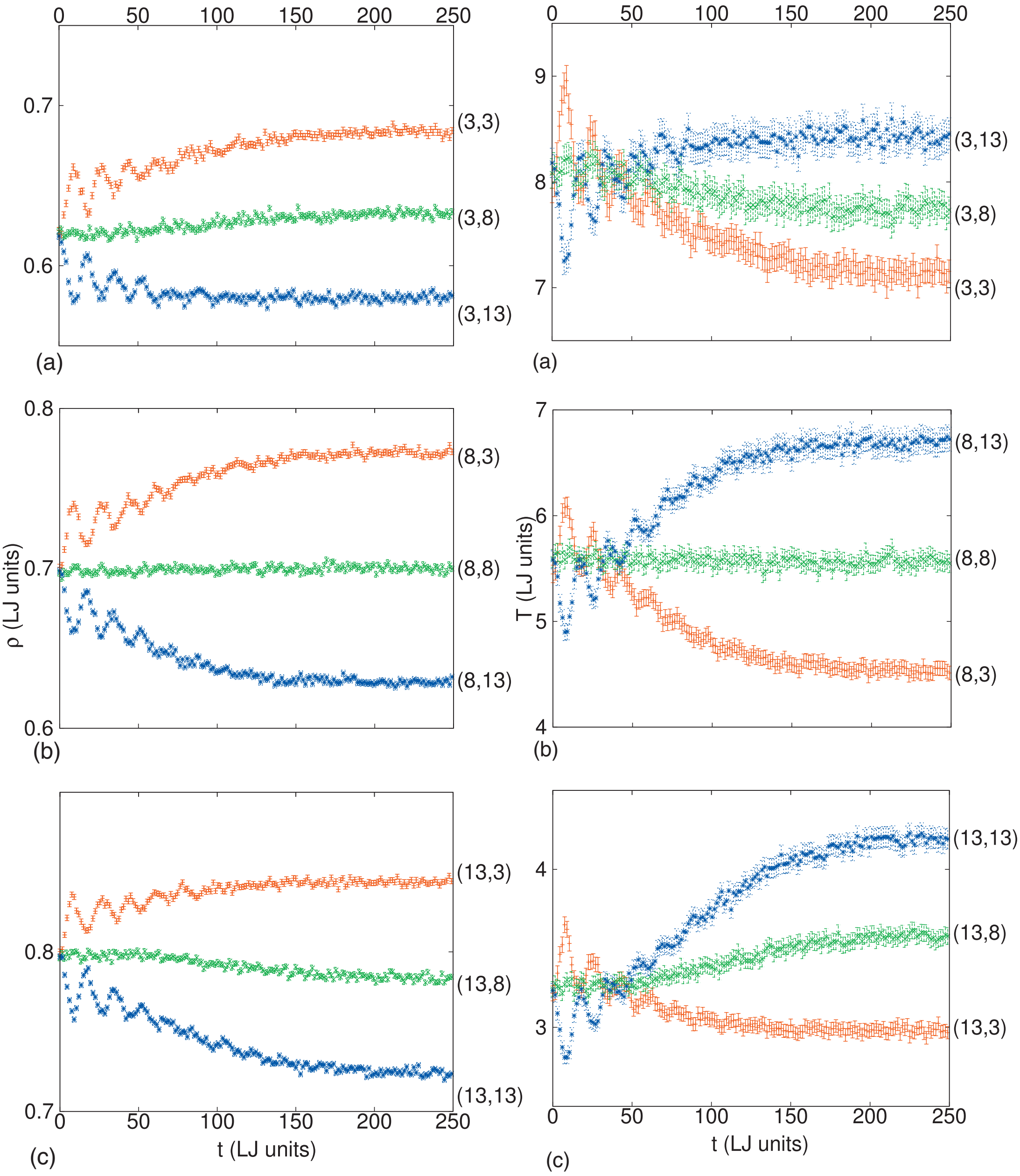

FIGURE 1. Density (left) and temperature (right) fields as a function of time in selected cells near the hot reservoir (top panel), in the middle (middle panel) and near the cold reservoir (bottom panel). For a given distance from the reservoirs, three cells at different height are shown.

This behavior can be followed by plotting the transient velocity field at every quarter period of the density and temperature oscillations (Fig. 2). At $t = \tau/4$ (Fig. 2/a) the velocity field points downwards as a consequence of the ignition of gravity at $t = 0$. At $t = \tau/2$ (Fig. 2/b), the velocity field is almost null, and the fluid is almost at rest on average. At $t = 3\tau/4$ (Fig. 2/c) the fluid is expanding against the gravity force and the velocity field is directed upward, as a reaction to compression. Once again, in correspondence to the subsequent relative maxima or minima (Fig. 2/d) the fluid is nearly at rest. During the following compressions and expansions the flux becomes localized, respectively, near the cold the hot reservoirs (see Fig. 3). In correspondence of the next relative maxima and minima the fluid is no longer at rest, and instead it begins to support a convective flow. The sequence of compressions and expansions strengthens the flux, which becomes stable at $t = 250$. The final shape of the convective pattern is symmetric (see Fig. 4).

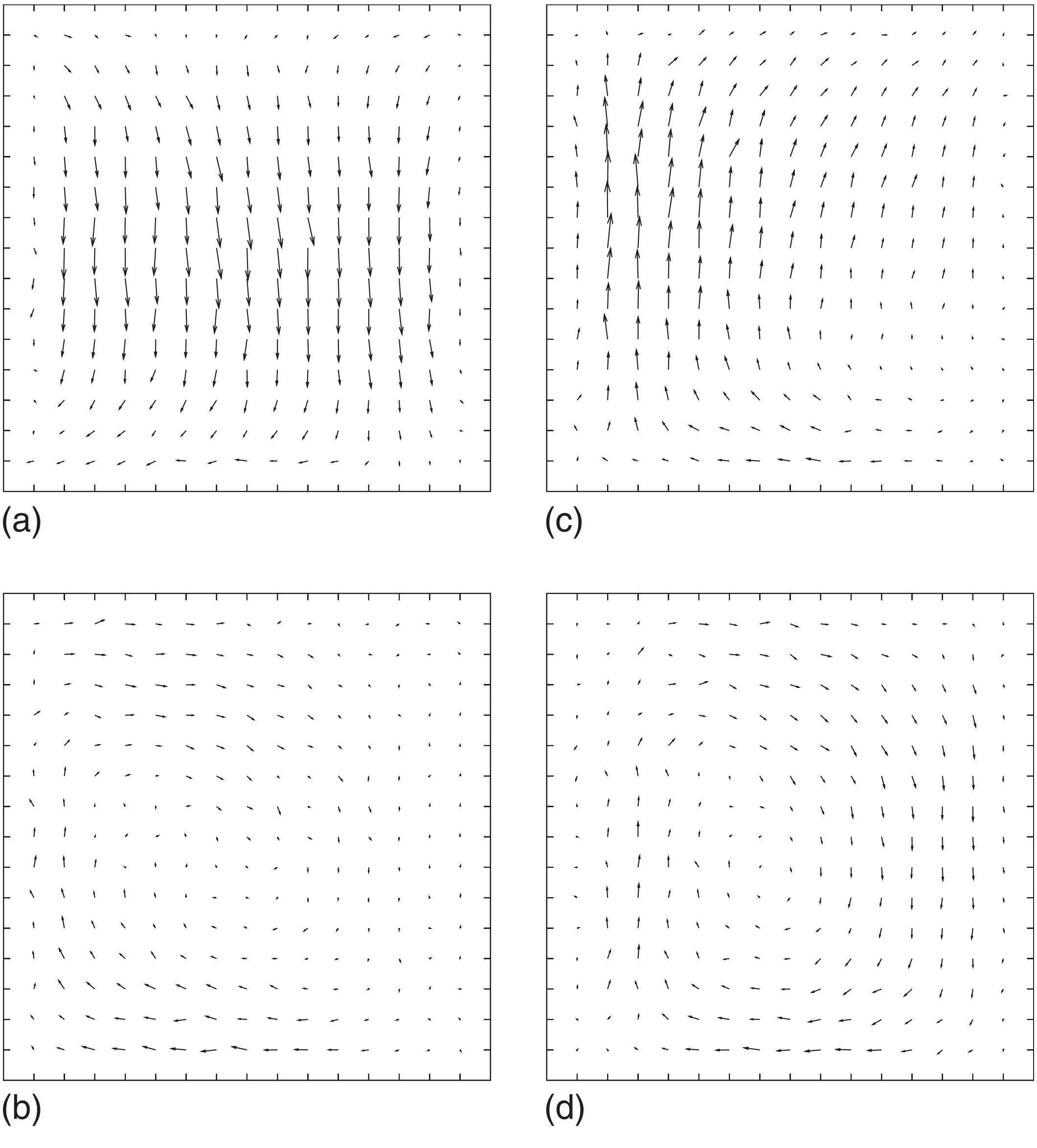

FIGURE 2. Local velocity field averaged over 1000 independent initial configurations during the first oscillation of temperature and density fields, i.e., at (a) $t = 4.5 \sim \tau/4$, (b) $t = 9 \sim \tau/2$, (c) $t = 13 \sim 3\tau/4$, and (d) $t = 18 \sim \tau$. Hot reservoir on the left side of the box, cold reservoir on the right side of the box.

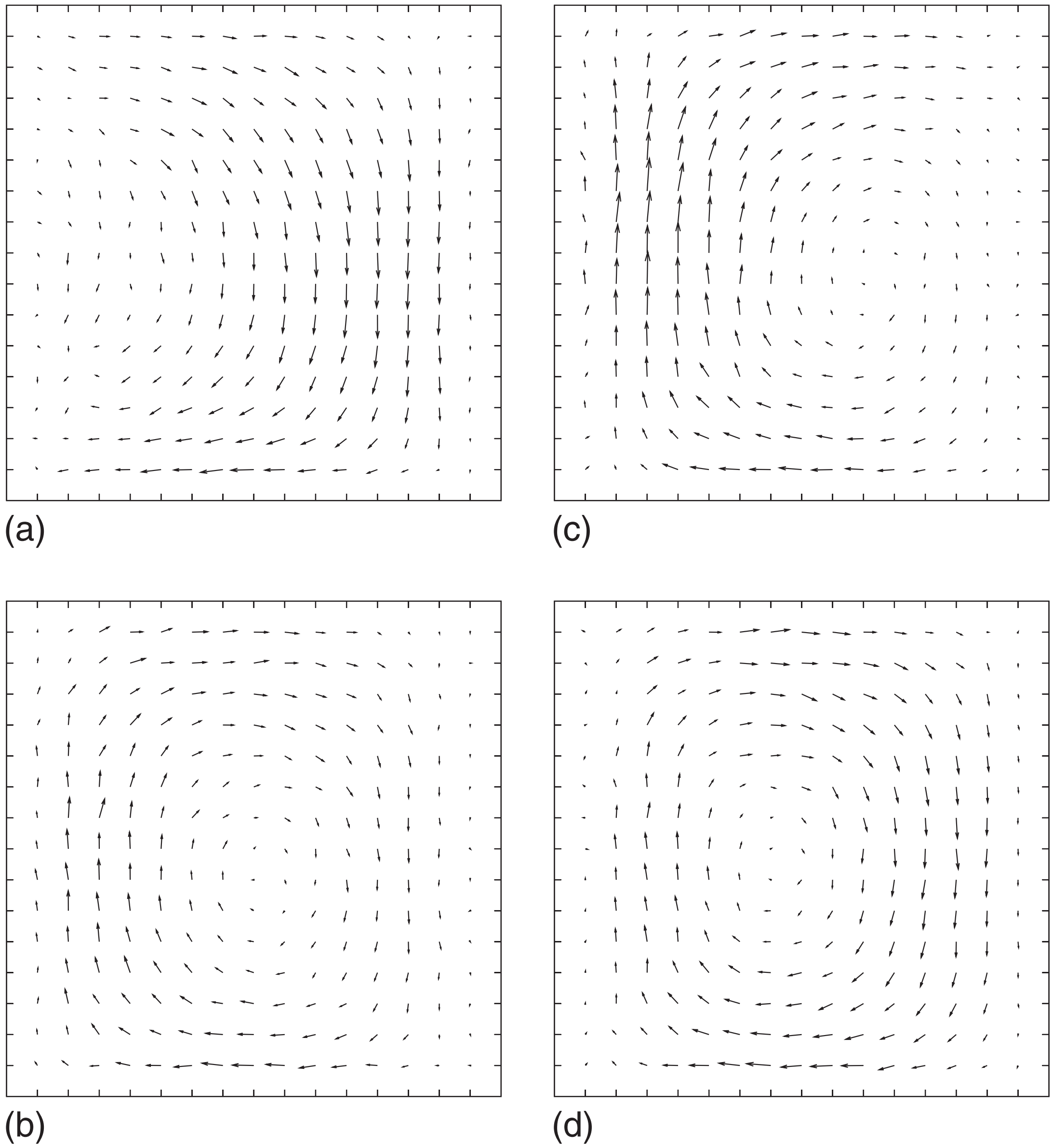

FIGURE 3. Local velocity field averaged over 1000 independent initial configurations during the first oscillation of temperature and density fields, i.e., at (a) $t = 22.5 \sim 5\tau/4$, (b) $t = 27 \sim 3\tau/2$, (c) $t = 31.5 \sim 7\tau/4$, and (d) $t = 36 \sim 2\tau$. Same conditions as in Fig. 2

RELAXATION OF THE INTERFACE BETWEEN TWO IMMISCIBLE LIQUIDS

Computational Model and Setup.

We now illustrate the method described in Sec. for sampling complex initial conditions by studying the relaxation to equilibrium of the interface between two immis-

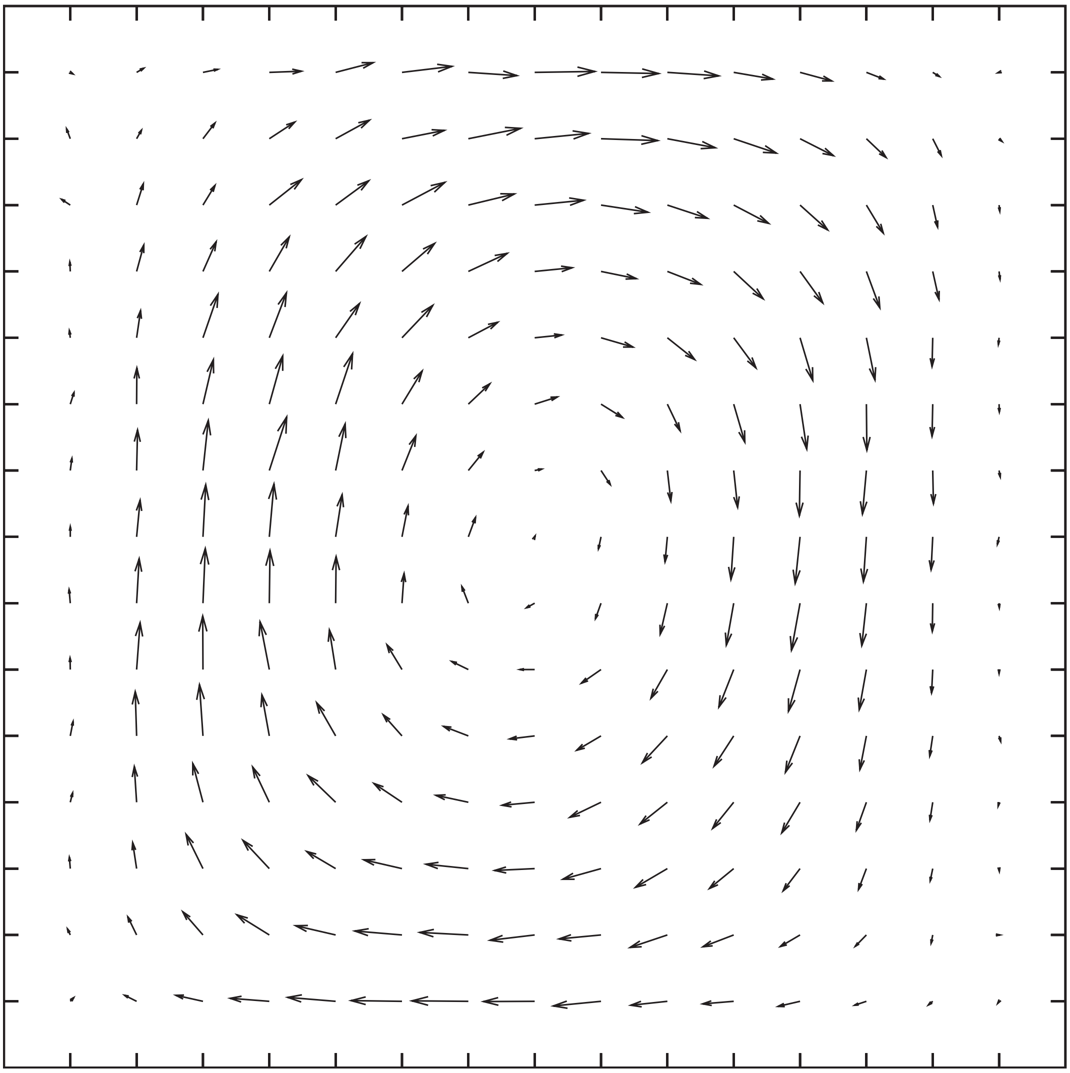

FIGURE 4. Local velocity field averaged over 1000 independent initial configurations at $t = 250$, i. e. at the end of simulation. Same conditions as in Fig. 2

cible liquids. We define the interface between the two liquids as the surface at which $\Delta\rho(\mathbf{x}) = \rho^A(\mathbf{x}) - \rho^B(\mathbf{x}) = 0$, where $\rho^A(\mathbf{x})$ and $\rho^B(\mathbf{x})$ are the densities of the liquids A and B (see Eq. (12)), respectively. We start from the interface defined below and follow the isosurface $S(t) = \{\mathbf{x} : \Delta\rho(\mathbf{x},t) = 0\}$ of the fields $\Delta\rho(\mathbf{x},t)$ and $\mathbf{v}^A(\mathbf{x},t)$ till equilibrium. The initial conditional PDF is sampled using the method described in Sec. with the restraint that $\Delta\rho(\mathbf{x}_\alpha) = 0$ in the cells, centered around the points $\mathbf{x}_\alpha$, through which passes the following surface:

$$S = \left\{ \mathbf{x} : x_3 = \mathscr{A} \sin\left(\frac{\pi x_1}{L_1}\right) + \frac{L_3}{2} - \frac{A}{2} \right\} \tag{22}$$

where $\mathscr{A}$ is the amplitude of the curved surface and $\{L_\chi\}_{\chi=1,3}$ is the length of the simulation box along the χ-th Cartesian direction. The terms $\frac{L_3}{2}$ and $-\frac{\mathscr{A}}{2}$ are added to place the interface at the centre of the simulation box. The condition above is the discrete counterpart of the continuous condition $\Delta\rho(\mathbf{x}) = 0, \forall\, \mathbf{x} \in S$. We do not impose any other condition on the density. However, we prepare the system such that all the particles on one side of the interface are of one kind, say A, and of the other kind on the other side, say B. Since we apply periodic boundary conditions along all the Cartesian directions, we have a second flat interface at the beginning/end of the simulation box.

The sample used in our simulation consists of 171,500 particles: 88,889 of type A and 82,611 of type B. Two particles of the same type interact via Lennard-Jones potential $u^{AA}(r) \equiv u^{BB}(r) = 4\varepsilon\left[(\sigma/r)^{12} - (\sigma/r)^{6}\right]$, while two particles of different type interact via the repulsive potential $u^{AB}(r) = 4\varepsilon\left[(\sigma/r)^{12}\right]$, where ε and σ are the usual Lennard-Jones parameters. The simulation box is a parallelepiped of size $\sim 45 \times 45 \times 90$ in reduced units (average density $\rho = 1.024 particles/\sigma^3$). In the restrained MD the temperature of the sample is kept fixed at $1.5\varepsilon/k_B$ (k_B Boltzmann constant). This density and temperature are in the fluid domain of a pure Lennard-Jones system. The ordinary space is discretized in 5488 points (a $14 \times 14 \times 28$ grid) and each cell contains, on average, ~ 30 particles.

The system is prepared by thermalizing a sample of pure type A Lennard-Jones particles at the target temperature and density, and then transforming those particles belonging to the cells on one side of the interface in type B particles (see Fig. (5)). In the cells belonging to the interface $S(\mathbf{x})$ only half of the particles are transformed from A to B, so as to have $\Delta\rho(\mathbf{x}) = 0$ in these cells. The system is then thermalized with the restraint on the $\Delta\rho(\mathbf{x})$ for 1.6×10^6 timesteps. Such a very long run is needed to relax the gradient of temperature formed when the nature of particles on one side of the interface is changed from A to B (immediately after the A-to-B transformation the interfaces - the curved one and the flat one due to the periodic boundary conditions - due to the strong repulsive forces among particles of different type, are warmer than the bulk). The timestep used in this and the next phase (restrained MD runs) is 4.56×10^{-4} LJ time units, which is one order of magnitude smaller than the typical timestep for simulation of Lennard-Jones systems. This very short timestep is required by the stiff force associated to the restraint. After this relaxation, a 10^6 timestep long restrained MD is performed along which, at regular intervals of 25,000 timesteps, we collect 40 initial positions and velocities for the second step of the D-NEMD procedure. The atomic configuration corresponding to one snapshot of this trajectory is shown in Fig. (5).

In Fig. (6) is reported the $\Delta\rho(\mathbf{x},t)$ field on the points $\{\mathbf{x}_\alpha\}_{\alpha=1,m}$ together with the isosurface $\Delta\rho(\mathbf{x}) = 0$ obtained as a linear interpolation of the value of the field on the grid points. This figure shows that the interface is rather sharp, involving typically one or two shells along the direction orthogonal to it.

From each of these initial conditions we start 25,000 timestep long unrestrained MD simulations along which we compute the microscopic observables of interest. By averaging over the (40) initial conditions we get $\rho^A(\mathbf{x},t)$ and $\mathbf{v}^A(\mathbf{x},t)$.

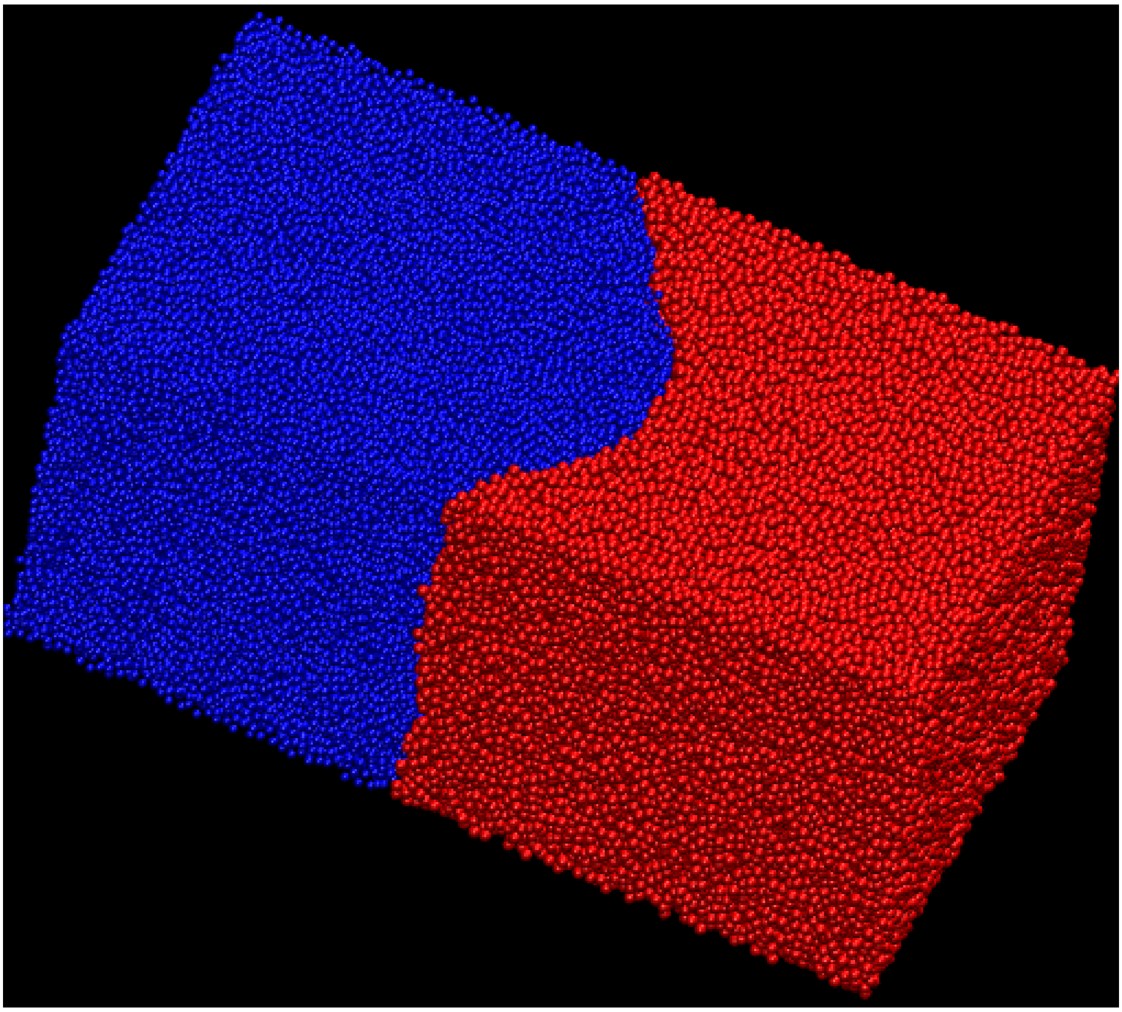

FIGURE 5. One atomic configuration extracted from the restrained MD used for sampling the initial conditional PDF. In blue particles of type A, in red particles of type B.

Results and discussion.

In this section we present our results obtained with the restrained MD method and compare them with those obtained by computing the relevant fields along one unrestrained trajectory started from a configuration sampled from the restrained dynamics. This second type of simulation, often combined with a "local time average" (i.e. averaging over a small time-window centered at the current time), are used to study hydrodynamical phenomena by atomistic simulation. We show that the fields obtained from this latter type of simulation violate some of the properties of the hydrodynamical fields associated to the process under investigation while our D-NEMD approach does not.

Let us start by analyzing the surface $S(t) = \{\mathbf{x} : \Delta\rho(\mathbf{x},t) = 0\}$. In Fig. (7) it is shown a series of snapshots of the $S(t)$ surface. First of all we remark that all along its evolution the surface satisfies the symmetry of the problem, i.e. it is symmetric with respect the

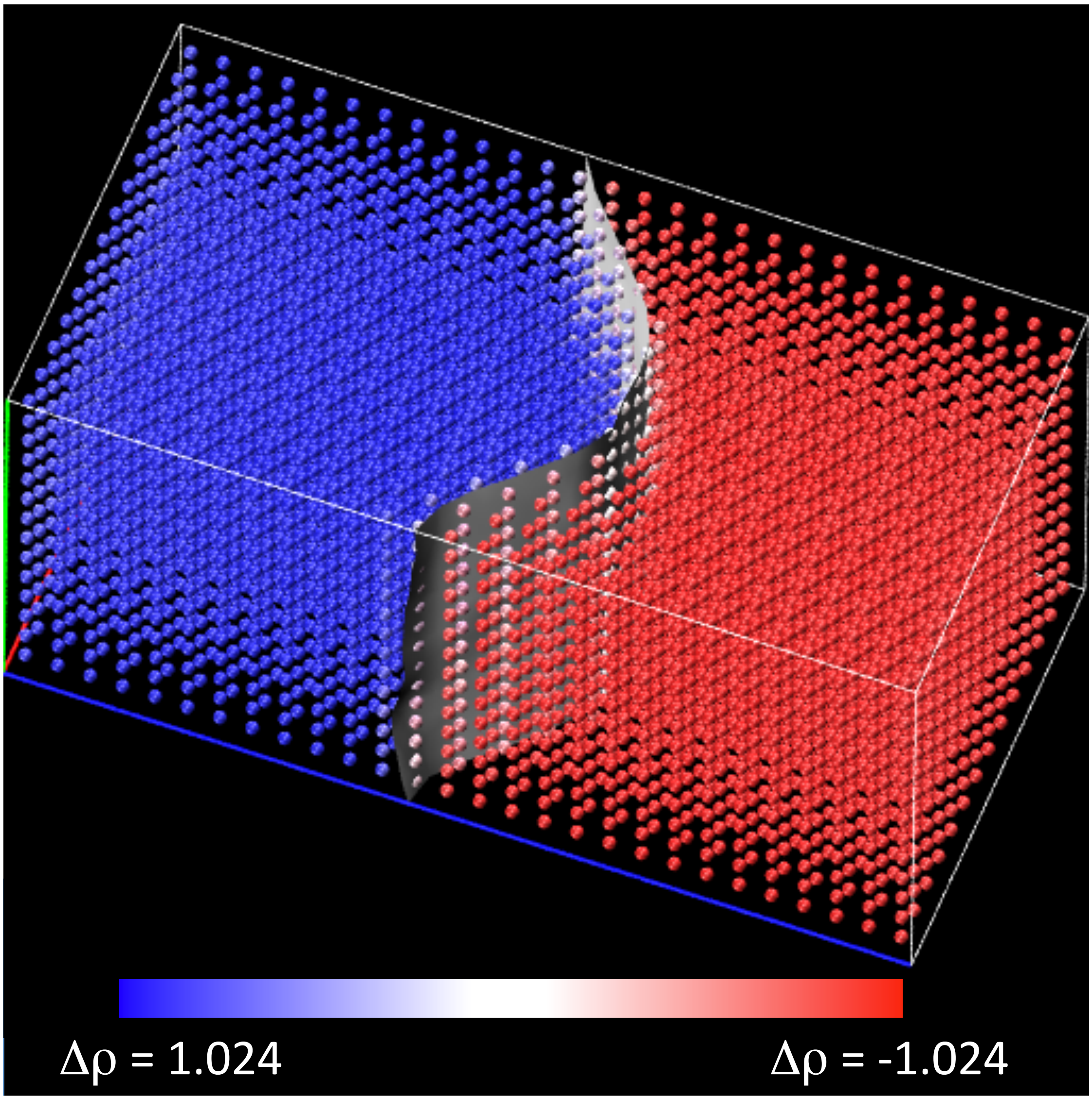

FIGURE 6. $\Delta\rho(\mathbf{x})$ field over the grid points $\{\mathbf{x}_\alpha\}_{\alpha=1,m}$. The color of each point depends on the $\Delta\rho(\mathbf{x})$ on that point. Intense red means that all the particles in the cell are of type A and intense blue means that they are all of type B. Intermediate colors indicate that the cell contains both types of particles (white correspond to 50% of each type of particle). The curved interface represent the isosurface $\Delta\rho(\mathbf{x}) = 0$ as obtained from the linear interpolation of the density on the grid points. The second interface due to the periodic boundary conditions on the long edge of the simulation box is not shown.

$\{yz\}$ reflection plane passing by the middle of the simulation box and it is translationally invariant along the y direction. The tiny bumps on the $S(t)$ surface are due to the limited number of initial conditions (40) used for computing $\Delta\rho(\mathbf{x},t)$. In the limit of an infinite number of such initial conditions the surface would be completely smooth, as expected and predicted by classical hydrodynamics. The relaxation from the initial curved surface to the final flat surface takes approximately 20,000 timesteps which, if we chose for the Lennard-Jones parameters the values $\sigma = 3.405$ Å and $\varepsilon = 0.01032\ eV$ (suitable for modeling Ar) and an amplitude of the initial interface $\mathscr{A} = 50$ Å, corresponds to a maximum value of the field $\mathbf{v}(\mathbf{x})$ of $\sim 80\ m/s$.

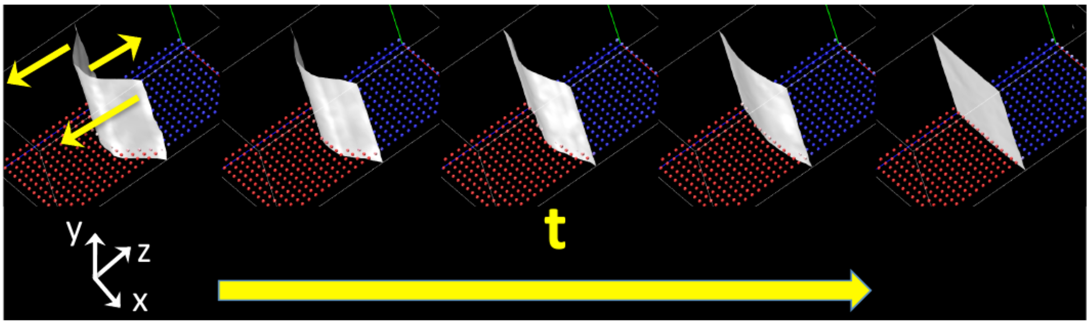

FIGURE 7. Snapshots of the interface $S(t)$. The arrows on the first snapshot show the direction of evolution of the interface: the center and the extreme of the interface move in opposite directions. The field $\Delta\rho(\mathbf{x},t)$ is also shown on one $\{xz\}$ plane by adopting the same colorcoding of Fig. 7

We now move to the analysis of the velocity field, focusing on the velocity field of only the chemical species A:

$$\mathbf{v}^A(\mathbf{x},t) = \frac{\sum_{\Gamma_0}\sum_{i=1}^{N_A}\mathbf{p}_i(\Gamma_0)\Pi_{\chi=1}^3\left[erf(\overline{x}_{\alpha,\chi}-r_{i,\chi}(\Gamma_0),\sigma)-erf(\underline{x}_{\alpha,\chi}-r_{i,\chi}(\Gamma_0),\sigma)\right]}{\sum_{\Gamma_0}\sum_{i=1}^{N_A}\Pi_{\chi=1}^3\mu_i\left[erf(\overline{x}_{\alpha,\chi}-r_{i,\chi}(\Gamma_0),\sigma)-erf(\underline{x}_{\alpha,\chi}-r_{i,\chi}(\Gamma_0),\sigma)\right]} \tag{23}$$

where the sum $\sum_{i=1}^{N_A}$ runs only over the atoms of type A, and it is implicitly assumed that $\mathbf{p}_i$ and $\mathbf{r}_i$ are taken at the time t starting from the initial condition Γ_0 (see Eqs. (17) and (13)). The sum $\sum_{\Gamma_0}$ run over the initial conditions along the restrained MD. We consider the field $\mathbf{v}^A(\mathbf{x},t)$ as, due to the conservation of the total momentum and the fact that the initial total momentum was set to zero, the total field, i.e. those including A and B specie, is, on average, zero. In the left column of Fig. 8 is shown the velocity field $\mathbf{v}^A(\mathbf{x},t)$ at various times. This field is computed only on the grid points corresponding to cells that contains at least one particle of type A. This fact makes the field "noisy" (large values of the field rapidly changing orientation) close to the A/B interface, where the cells contain less A particles, and therefore the average of the atomic velocities over the particles in the cell (see Eqs. (16) and (17)) is less effective in smoothing the field. This effect is reduced by making larger the number of initial configurations used to perform the ensemble average over the initial conditional PDF. As a first remark, it is worth to mention that relatively few cell layers nearby the interface are involved in the relaxation process. In fact, already $5-10$ cells far from the interface the velocity field is essentially zero at any time during the relaxation. Coming to the hydrodynamical process producing the relaxation of the interface, we notice that initially (see panel 1 of Fig. 8) the velocity field at the top of the interface is pointing downward while at bottom it is pointing upward. After some time this field stabilizes into a double symmetric roll, one rotating clockwise and the other one rotating counter clockwise, both starting at the top of the interface and ending at its bottom (see panel 2 of Fig. 8). Overall, this velocity field produce the phenomenon of pushing up the side of the interface and pulling down the center as shown in Fig. 7. The relaxation of the interface follows this mechanism almost till the end of the process. In fact, in panel 3 of Fig. 8 we see that still after 45.6 LJ time units (10^4 timesteps), when the interface is almost flat, the double roll is still present. Eventually, after 114 units of time (2.5×10^5 timesteps) the interface is completely flat and the field is null everywhere (panel 4).

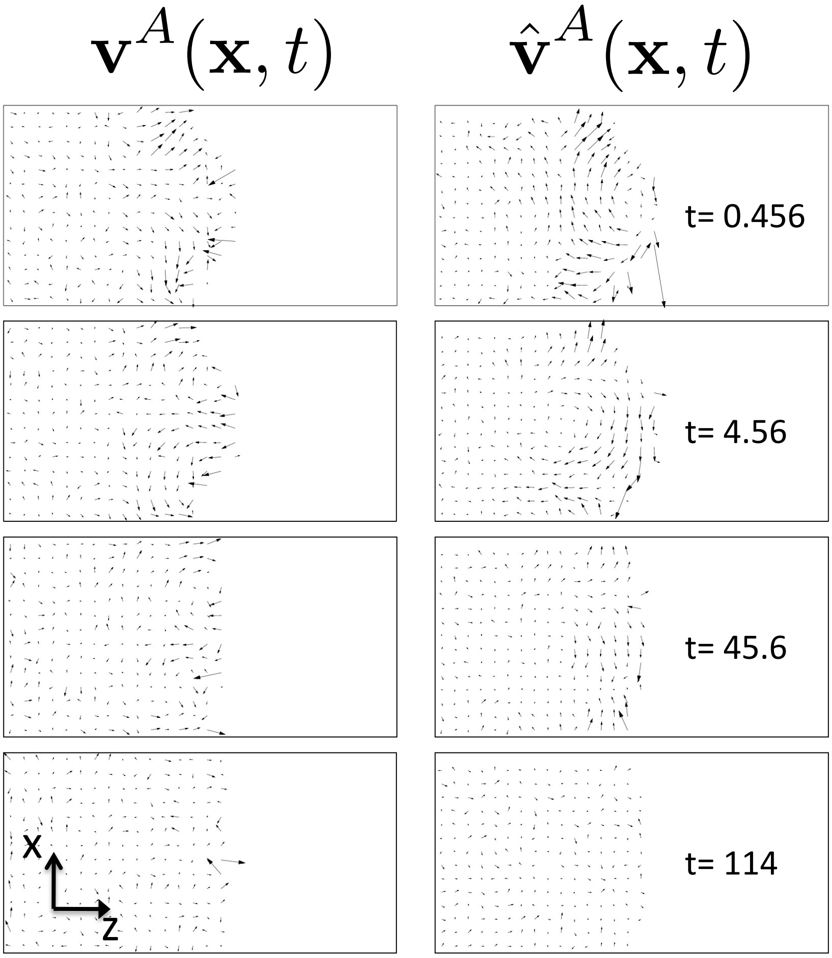

FIGURE 8. Snapshots of the $\mathbf{v}^A(\mathbf{x},t)$ (left, see Eq. (13)) and $\hat{\mathbf{v}}^A(\mathbf{x},t)$ (right, see Eq. (24)) fields on the grid points belonging to one $\{xz\}$ plane at various times.

It is very interesting to compare the $\mathbf{v}^A(\mathbf{x},t)$ field as obtained from the D-NEMD simulation with the instantaneous field $\hat{\mathbf{v}}^A(\mathbf{x},t)$ defined as

$$\hat{\mathbf{v}}^A(\mathbf{x},t) = \frac{\sum_{i=1}^{N_A} \mathbf{p}_i \Pi_{\chi=1}^{3} \left[erf(\overline{x}_{\alpha,\chi} - r_{i,\chi}, \sigma) - erf(\underline{x}_{\alpha,\chi} - r_{i,\chi}, \sigma) \right]}{\sum_{i=1}^{N_A} \Pi_{\chi=1}^{3} \mu_i \left[erf(\overline{x}_{\alpha,\chi} - r_{i,\chi}, \sigma) - erf(\underline{x}_{\alpha,\chi} - r_{i,\chi}, \sigma) \right]} \tag{24}$$

Few snapshots of this field are shown in Fig. 8. First of all we notice that the interface relaxation process occurs via the formation of a clockwise roll, which is initially at the top of the interface (panel 1 of Fig. 8) and then move toward the bulk (panel 2 of the same figure). This roll is stable all over the duration of the simulation (see panel 3) and eventually disappear when the equilibrium is reached (panel 4). The shape of the field $\mathbf{v}^A(\mathbf{x},t)$ contrasts with the symmetry imposed on the problem, which implies a $\{yz\}$ mirror plane passing through the middle of the simulation box. This problem cannot be solved by the "local time average" that is often used in simulation of hydrodynamical processes by atomistic simulations. In fact, as mentioned above, the clockwise vortex is very stable and a local time average will not restore the proper symmetry expected for this field. This problem illustrates that a proper statistical average is needed in order to compute by atomistic simulation hydrodynamic fields as otherwise a unlucky choice of the initial conditions can produce unphysical results.

CONCLUSIONS.

In this paper we have reviewed the dynamical approach to non-equilibrium MD. We have shown that using a proper simulation setup it is possible to treat interesting cases in which the initial condition is either a stationary non-equilibrium condition or a constrained equilibrium consistent with the value of a macroscopic scalar or field-like observable. We illustrated the functioning of the method by applying it to two cases: the establishing of convective cells and the relaxation of an interface between two immiscible liquids. We have shown that our method generates rigorous time-dependent non-equilibrium averages, while the method of local time average, often used to simulate hydrodynamical processes from atomistic simulation, can, sometimes, fail.

Our conclusion is that the method is ready for challenging applications. Work is in progress in this direction.

ACKNOWLEDGMENTS

S. M. and G. C. acknowledge SFI Grant 08-IN.1-I1869 for the financial support. S.O. acknowledges SimBioMa for the financial support. Finally, the authors wish to acknowledge the SFI/HEA Irish Centre for High-End Computing (ICHEC) for the provision of computational facilities.

REFERENCES

1. B. J. Alder, and T. E. Wainwright, *Phys. Rev. A* **1**, 18 (1970).
2. T. Wainwright, B. Alder, and D. Gass, *Phys. Rev. A* **4**, 233 (1971).
3. A. W. Less, and S. F. Edwards, *J. Phys. C* **5**, 1921 (1972).
4. E. Gosling, I. McDonald, and K. Singer, *Mol. Phys.* **26**, 1475 (1973).
5. W. Ashurst, and W. Hoover, *Phys. Rev. Lett.* **31**, 206 (1973).
6. W. G. Hoover, and W. T. Ashurst, *Adv. Theor. Chem.* **1**, 1 (1973).
7. G. Ciccotti, and G. Jacucci, *Phys. Rev. Lett.* **35**, 789 (1975).
8. G. Ciccotti, G. Jacucci, and I. R. McDonald, *J. Stat. Phys.* **21**, 1 (1979).
9. G. Ciccotti, C. Pierleoni, and J. P. Ryckaert, in *Microscopic Simulations of Complex Hydrodynamic Phenomena*, Plenum, New York, 1992.
10. L. Onsager, *Phys. Rev.* **37**, 405 (1931).

11. R. Kubo, *J. Phys. Soc. Jpn.* **12**, 570 (1957).
12. M. L. Mugnai, S. Caprara, G. Ciccotti, C. Pierleoni, and M. Mareschal, *J. Chem. Phys.* **131**, 064106 (2009).
13. S. Orlandini, S. Meloni, and G. Ciccotti, in preparation.
14. E. A. Carter, G. Ciccotti, J. T. Hynes, and R. Kapral, *Chem. Phys. Lett.* **156**, 472 (1989).
15. G. Ciccotti, R. Kapral, and E. Vanden-Eijnden, *Chem. Phys. Chem.* **6**, 1809 (2005).
16. M. E. Tuckerman, C. J. Mundy, and G. J. Martyna, *Europhys. Lett.* **45**, 149 (1999).
17. M. E. Tuckerman, Y. Liu, G. Ciccotti, and G. J. Martyna, *J. Chem. Phys.* **115**, 1678 (2001).
18. C. Hartmann, C. Schütte, and G. Ciccotti, *J. Chem. Phys.* **132**, 111103 (2010).
19. G. Ciccotti, and J. P. Ryckaert, *Comp. Phys. Rep.* **4**, 347 (1986).
20. G. Ciccotti, and S. Meloni, submitted to *Phys. Chem. Chem. Phys.*
21. J. H. Irving, and J. G. Kirkwood, *J. Chem. Phys.* **18**, 817 (1950).

Recent progress in fluctuation theorems and free energy recovery

A. Alemany*, M. Ribezzi* and F. Ritort*,†

*Small Biosystems Lab, Departament de Fisica Fonamental, Facultat de Fisica, Universitat de Barcelona, Diagonal 647, 08028 Barcelona, Spain
†CIBER-BBN, Networking Center of Bioengineering, Biomaterials and Nanomedicine, ISCIII, Madrid, Spain

Abstract. In this note we review recent progress about fluctuation relations and their applicability to free energy recovery in single molecule experiments. We underline the importance of the operational definition for the mechanical work and the non-invariance of fluctuation relations under Galilean transformations, both aspects currently amenable to experimental test. Finally we describe a generalization of the Crooks fluctuation relation useful to recover free energies of partially equilibrated states and thermodynamic branches.

Keywords: Nonequilibrium systems, fluctuation theorems,single-molecule experiments, optical tweezers
PACS: 87.14.Ee,82.20.Db,87.15.Cc

NONEQUILIBRIUM SMALL SYSTEMS

In 1944 Erwin Schrödinger published the classic monograph *What is life?* where he pointed out the importance of physical and chemistry laws to understand living systems [1]. The notion that genetic information should be encoded in an “aperiodic crystal” seeded the subsequent discovery of the double helix structure of DNA. Chapter 7 of Schrödinger’s monograph contains an interesting discussion about the similarities and differences between a clockwork motion and the functioning of an organism. According to Schrödinger the regular motion of a clock must be secured by a weak spring. Yet, whatever the weakness of the spring is, it will produce frictional effects that do compensate for the external driving of the clock (e.g. the battery) in order to secure its regular motion. Being friction a statistical phenomenon he concludes that the regular motion of the clock cannot be understood without statistical mechanics. Then he further states: *For it must not believed that the driving mechanism really does away with the statistical nature of the process. The true physical picture includes the possibility that even a regularly going clock should all at once invert its motion and, working backward, rewind its own spring -at the expense of the heat of the environment. The event is just ’still a little less likely’ than a ’Brownian fit’ of a clock without driving mechanism.*

Recent advances in microfabrication techniques, detection systems and instrumentation have made possible the measurement of such ’inverted motions’ referred by Schrödinger. The controlled manipulation and detection of very small objects makes possible to exert and measure tiny forces applied on them and follow their trajectories in space-time with resolution of piconewtons, nanometers and microseconds respectively.

According to the equipartition law, systems with a low number of degrees of freedom embedded in a thermal environment exhibit energy fluctuations that are a few times k_BT (k_B being the Boltzmann constant and T the environmental temperature). Techniques such as atomic force microscopy (AFM), optical tweezers (OT) and magnetic tweezers (MT) allow for the controlled manipulation of individual molecules such as nucleic acid structures and proteins [2], the measurement of very small energies (within the k_BT scale) [23] and the observation of 'inverted motion' in translocating enzymes [3]. These developments during the past years have been accompanied by a concomitant progress of theoretical results in the domain of nonequilibrium physics [4]. This contribution reviews some of the most basic concepts around fluctuation theorems and their experimental verification.

Control parameters, configurational variables and the definition of work

In small systems it is crucial to make a distinction between controlled parameters and non-controlled or fluctuating variables. Controlled parameters are those macroscopic variables that are imposed on the system by the external sources (e.g. the thermal environment) and do not fluctuate with time. In contrast, non-controlled variables are microscopic quantities describing the internal configuration of the system and do fluctuate in time because they are subject to Brownian forces. Let us consider a typical single molecule experiment where a protein is pulled by an AFM. In this case the control parameter is given by the position of the cantilever that determines the degree of stretching and the average tension applied to the ends of the protein. Also the temperature and the pressure inside the fluidic chamber are controlled parameters. However, the height of the tip respect to the substrate or the force acting on the protein are fluctuating variables describing the molecular extension of the protein tethered between tip and substrate. Also the position of each of the residues along the polypeptide chain are fluctuating variables. Both molecular extension or force and the residues positions define different types of configurational variables. However only the former are subject to experimental measurement and therefore we will restrict our discussion throughout this paper to such kind of experimentally accessible configurational variables. Figure 1 illustrates other examples of control parameters and configurational variables. In what follows we will denote by λ the set of controlled (i.e. non-fluctuating) parameters and x the set of configurational (i.e. fluctuating) variables. The definition of what are controlled parameters or configurational variables is broad. For example, a force can be a configurational variable and a molecular extension can be a controlled parameter, or vice versa, depending on the experimental setup (see Figure 1, right example).

The energy of a system acted by external sources can be generally described by a Hamiltonian or energy function, $U(x,\lambda)$. The net variation of U is given by the conservation law,

$$dU = \left(\frac{\partial U}{\partial x}\right) dx + \left(\frac{\partial U}{\partial \lambda}\right) d\lambda = \text{đ}Q + \text{đ}W \tag{1}$$

where $\text{đ}Q, \text{đ}W$ stand for the infinitesimal heat and work transferred to the system. The previous mathematical relation has simple physical interpretation. Heat accounts for the energy transferred to the system when the configurational variables change at fixed value of the control parameter. Work is the energy delivered to the system by the external sources upon changing the control parameter for a given configuration. The total work performed by the sources on the system when the control parameter is varied from λ_i to λ_f is given by,

$$W = \int_{\lambda_i}^{\lambda_f} đW = \int_{\lambda_i}^{\lambda_f} \left(\frac{\partial U}{\partial \lambda}\right) d\lambda = \int_{\lambda_i}^{\lambda_f} F(x,\lambda) d\lambda \tag{2}$$

where $F(x,\lambda)$ is a generalized force defined as,

$$F(x,\lambda) = \left(\frac{\partial U}{\partial \lambda}\right) \quad . \tag{3}$$

It is important to stress that the generalized force is not necessarily equal to the mechanical force acting on the system. In other words, $F(x,\lambda)$ is a configurational dependent variable conjugated to the control parameter λ and has dimensions of [energy]/[λ] which are not necessarily Newtons. In the example shown in the right of Figure 1 the control parameter is the magnetic force $\lambda \equiv f$ and the configurational variable x is the molecular extension of the polymer. The total Hamiltonian of the system is then given by $U(x,f) = U_0(x) - fx$ where $U_0(x)$ is the energy of the system at $\lambda = f = 0$. In other words, the external force f shifts all energy levels (defined by x) of the original system by the amount -fx. The generalized force is then given by $F(x,f) = -x$ (i.e. it has the dimensions of a length) and$đW = -xdf$. The fact that$đW$ is equal to $-xdf$ and not equal to fdx has generated some controversy [5]. Below we show how this distinction is already important for the simplest case of a bead in the optical trap. In Section we also show how the physically sound definition of mechanical work is amenable to experimental test.

A classical experiment: the bead in the optical trap

In 2002 Dennis Evans and coworkers in Canberra (Australia) performed the first experiment where the 'inverted motions' could be observed [6]. The experiment is shown in Figure 2a. A micron-sized spherical bead made of silica or polystyrene is immersed in water inside a fluidic chamber and captured in an optical trap of infrared light generated by a high numerical aperture objective. Initially the trap is at a rest position and the bead is in thermal equilibrium and fluctuating around the center trap position. Suddenly the trap is set into motion at a constant speed v and the bead is dragged through the water. After a transient time $\tau = \gamma/k$ the bead reaches a steady state where the Stokes frictional force is counter balanced by the optical trapping force. The average bead position lags behind the center of the trap by a distance $\overline{y} = \gamma v/k$ where $\gamma = 6\pi\eta R$ is the friction coefficient (η is the water viscosity and R is the bead radius) and k is the stiffness of the trap. In the laboratory frame (see Figure 2a) the bead and trap center have coordinates $x(t)$ and $x^*(t) = vt$ (we take $x = x^* = 0$ at $t = 0$ when the trap is set in motion). The distance between the center of the trap and the bead is $y = x^* - x$

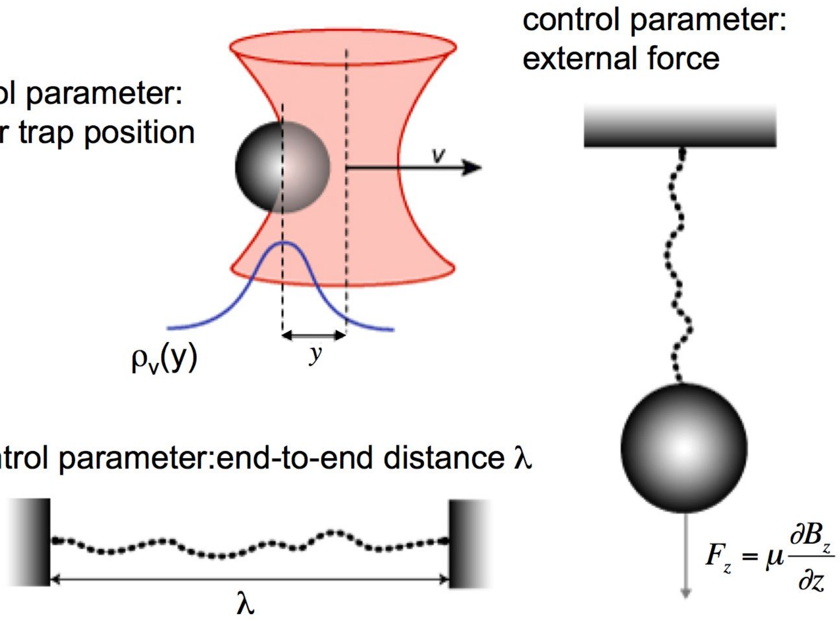

FIGURE 1. Control parameter and configurational variables. Different experimental setups corresponding to different types of control parameters (denoted as λ) or configurational variables (denoted as x). (Top left) A micron-sized bead dragged through water. λ could be the center of the trap measured in the lab (i.e. fixed to the water) frame whereas x is the displacement of the bead, indicated as y, respect to the center of the trap. (Bottom left) A polymer tethered between two surfaces. λ is the distance between the surfaces and x the force acting on the polymer. (Right) A polymer stretched with magnetic tweezers. λ is the force acting on the magnetic bead and x is the molecular extension of the tether. Figure taken from [3].

and the restoring force acting on the bead is given by $F(y) = ky$. In this example the control parameter is given by the trap center $\lambda = x^*$ whereas x is the configurational variable. The trapping energy of the bead is given by $U(x,\lambda) = (1/2)k(x-\lambda)^2$ and the generalized force $F = k(\lambda - x) = ky$ (cf. Eq.(3)). The work exerted by the trap on the bead is then equal to $W = \int_0^t F(y)dx^* = vk\int_0^t y(s)ds$. The first remarkable fact in this expression is that the work W is neither equal to $W' = \int_0^t F(y)dx$ nor $W'' = \int_0^t F(y)dy$. These three quantities have different physical meaning. In fact, by exactly integrating the force, W'' becomes equal to the energy difference between the initial and final configurations. Whereas W' is equal to minus the heat, $-Q$. Since $dy = dx^* - dx$ what we are now facing is again the mathematical statement of energy conservation. Note also that the work definition is non-invariant under Galilean transformations. In fact, the work definition requires that x, as measured in the lab frame, is the proper configurational variable. If we choose y rather than x (y is now measured in the trap-moving frame) then $U(y,\lambda) = (1/2)ky^2$ is independent of λ and the work would be identically zero which makes no sense.

By repeating the moving trap experiment an infinite number of times a work distribution will be produced. The shape of the work distribution must be Gaussian because the stochastic variable y follows an Ornstein-Uhlenbeck process that can be described by a linear Langevin equation. Consequently, only the first and second cumulants of the work distribution are non-zero. Let us note in passing that the Gaussian property is not fulfilled by the heat and the energy difference, which are known to exhibit exponential tails [8, 9]. The mean work $\overline{W}$ and variance $\sigma_W^2 = \overline{W^2} - \overline{W}^2$ can be easily worked out in the asymptotic regime for times t that are longer than the relaxation time of the bead, $t >> \gamma/k$. In this limit,

$$\overline{W} = vk \int_0^t \overline{y(s)} ds \to vk\overline{y}t = \gamma v^2 t \tag{4}$$

$$\begin{aligned} \sigma_W^2 = \overline{W^2} - \overline{W}^2 = v^2k^2 \int_0^t \int_0^t \overline{y(s_1)y(s_2)} ds_1 ds_2 \to 2v^2k^2 t \int_0^t \overline{y(0)y(s)} ds = \\ = 2v^2k^2 t \overline{y^2} \tau = 2v^2k^2 t \frac{k_BT}{k} \frac{\gamma}{k} = 2k_BT\gamma v^2 t \end{aligned} \tag{5}$$

where $\overline{...}$ stands for an average over trajectories. In deriving Eq.(5) we used time-translational invariance in the steady state and the result $\overline{y(0)y(s)} = \overline{y(0)^2} \exp(-s\tau)$ in the steady state ($\tau = \gamma/k$ being the bead relaxation time) with $\overline{y(0)^2} = k_BT/k$ due to the equipartition law. The work probability distribution is finally given by,

$$P(W) = \frac{1}{\sqrt{2\pi\sigma_W^2}} \exp\Big(-\frac{(W - \overline{W})^2}{2\sigma_W^2} \Big) \quad . \tag{6}$$

These relations teach us various things:

1. **Second law.** The mean work $\overline{W}$ is always positive (second law) and only vanishes at all times for $v \to 0$, i.e. when the trap is moved in a quasistatic way.
2. **Observation of 'Inverted motions'.** Although $\overline{W} > 0$ there are always trajectories for which $W < 0$. These are the 'inverted motions' refereed to by Schrödinger and recently renamed as 'transient violations of the second law'. Along these 'inverted motion' trajectories the bead extracts energy from heat fluctuations to overcome the frictional forces and to move ahead of the center of the trap.
3. **'Inverted motions' as rare events.** Both the mean work and the standard deviation of the work increase with time and trap speed. However the standard deviation σ_W increases as $\sqrt{t}$ whereas $\overline{W}$ increases faster (linearly with t). Therefore, although it is possible to find trajectories where $W < 0$, these are rare events because their relative fraction decreases exponentially fast with time. $W < 0$ trajectories become more probable (i.e. less rare) at short times. In the limit $t \to 0$ they reach the 50% of all events.
4. **Fluctuation relation.** The work probability density function shown in Eq.(6) satisfies a fluctuation relation. From Eqs.(4,5) we find $\sigma_W^2 = 2k_BT\overline{W}$. It is straightforward to check that the following relation holds,

   $$\frac{P(W)}{P(-W)} = \exp\Big(\frac{W}{k_BT} \Big) \quad . \tag{7}$$

   Eq.(7) receives the name of a fluctuation relation because it is an exact mathematical relation describing arbitrarily large work fluctuations. Eq.(7) was derived

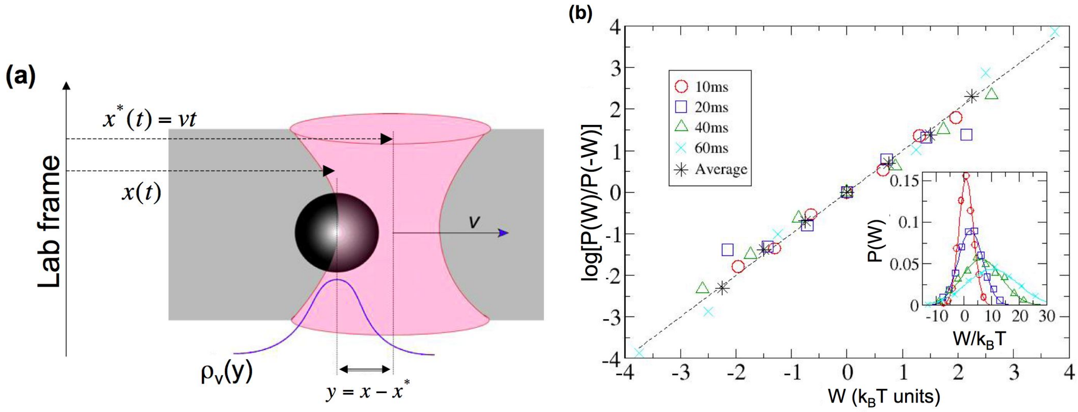

FIGURE 2. The bead in the optical trap dragged through water. (a) Variables defining the experiment. (b) Work distribution measurements corresponding to different elapsed times. The mean work $\overline{W}$ and variance σ_W^2 increase with time (Inset). The main panel shows the experimental test of the fluctuation relation Eq.(7) for all experimental data put together.

from Eq.(6) which was obtained in the limit of long enough times. More elaborate calculations show that this relation is exact for arbitrary times [7, 8].

In Figure 2b we show an experimental test of these results. The fluctuation relation in Eq.(7) corresponds to a special case of what is known as transient fluctuation theorem (TFT) [10]. The system is initially in equilibrium and transiently driven out of equilibrium by external forces. The generalization of such relation to include arbitrary nonequilibrium transient states gives the fluctuation relation by Crooks described in the next section.

THE CROOKS FLUCTUATION RELATION AND FREE ENERGY RECOVERY.

Let us consider a generic system in thermal equilibrium that is transiently driven out of equilibrium during the time interval $[0, t_f]$ by varying λ according to a protocol $\lambda(t)$ from an initial value $\lambda(0) = \lambda_i$ to a final value $\lambda(t_f) = \lambda_f$. We refer to this as the forward (F) process. By repeating this process an infinite number of times we generate the work distribution $P_F(W)$. Let us consider now the reverse process where the system starts in equilibrium at λ_f and λ is varied according to the time reversal protocol, $\lambda(t_f - t)$, until reaching the final value λ_i (see Figure 3). The reverse (R) process can be repeated an infinite number of times to produce the work distribution $P_R(W)$. The Crooks fluctuation relation (CFR) reads [11],

$$\frac{P_F(W)}{P_R(-W)} = \exp\left(\frac{W - \Delta G}{k_B T}\right) \tag{8}$$

where $\Delta G = G(\lambda_f) - G(\lambda_i)$ is equal to the free energy difference between the equilibrium states at λ_f and λ_i. Eq.(7) is a particular case of the CFR where $P_F(W) = P_R(W)$

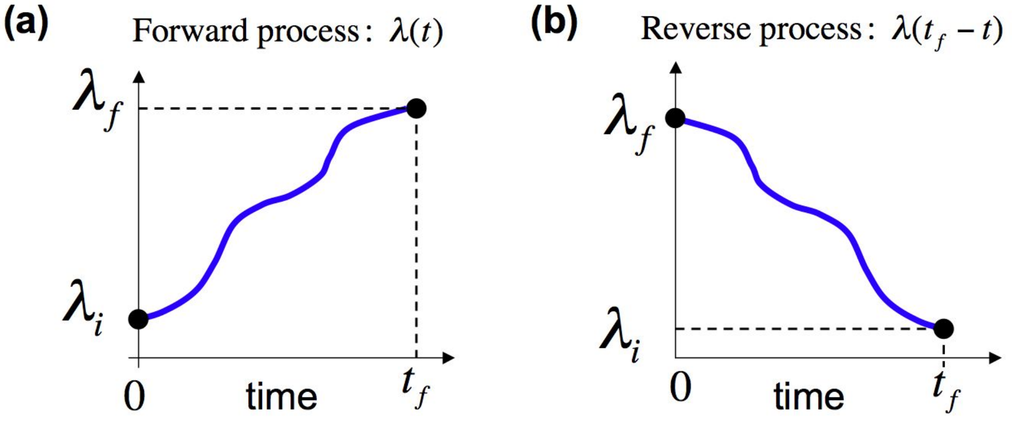

FIGURE 3. Forward and reverse paths. (a) An arbitrary forward protocol. The system starts in equilibrium at λ_i and is transiently driven out of equilibrium until λ_f. At λ_f the system may be or not in equilibrium. (b) The reverse protocol of (a). The system starts in equilibrium at λ_f and is transiently driven out of equilibrium until λ_i. At λ_i the system may be or not in equilibrium.

(the trapping potential is symmetric $V(y) = V(-y)$) and $\Delta G = 0$ (the free energy of the bead in the trap does not depend on the position of the trap, x^*). A particular result of the CFR is the well-known Jarzynski equality [12], $\overline{\exp(-W/k_BT)} = \exp(-\Delta G/k_BT)$, that has been used for free energy recovery [13, 14] by inverting the mathematical identity, $\Delta G = -k_BT \log(\overline{\exp(-W/k_BT)})$. However this expression is strongly biased for a finite number of measurements [15, 16]. Bidirectional methods that combine information from the forward and reverse processes and use the CFR have proven more predictive [17, 18, 19]. In particular the CFR immediately implies that $P_F(W) = P_R(-W)$ for $W = \Delta G$ showing that it is possible to measure ΔG in irreversible processes by measuring the forward and reverse irreversible work distributions and looking for the value of W where they cross each other. The CFR was experimentally tested in 2005 in RNA pulling experiments with laser tweezers [20] showing this to be a reliable and useful methodology to extract free energy differences between states that could not be measured with bulk methods.

In Figure 4 we summarize recent results obtained in the Small Biosystems lab in Barcelona for the mechanical unfolding/refolding of DNA hairpins [21, 22] using a dual-beam miniaturized optical tweezers [23]. DNA hairpins are versatile structures formed by a stem of a few tens of base pairs that end in loop. They have some advantages as compared to RNA structures such as the easier synthesis and larger chemical stability. DNA hairpins can be easily synthesized and ligated to dsDNA handles to produce a construct ready to be pulled with the tweezers [24]. By chemically labeling the ends of the dsDNA handles it is possible to tether a DNA construct (formed by the DNA hairpin inserted between the two flanking handles) between two micron sized beads. One bead is immobilized in the tip of a pipette. The other bead is captured in the optical trap. The deflected light by the trapped bead provides a direct measurement of the force applied on the molecule. By repeatedly steering the optical trap back and forth it is possible to unfold and refold the hairpin structure many times until the tether breaks.

The unfolding of the hairpin is revealed by a sudden drop in the force due to the increase in molecular extension from the released single-stranded DNA of the hairpin. Such increase causes a retraction in the position of the bead in the trap and a force drop. Analogously, when the hairpin refolds a sudden increase in force is observed. One of the most successful constructs we have designed in our lab consists of DNA hairpins linked to two beads via extremely short (29bp) dsDNA handles [25]. These constructs are found to moderately increase the signal-to-noise ratio of the measurements allowing for precise work measurements. In a pulling experiment the force versus the relative trap-pipette distance is recorded and the area below that curve provides a direct measurement of the work. Repeated measurements of the work make possible an experimental verification of the CFR (see figure 5).

About the right definition of work: accumulated versus transferred work

In a pulling experiment there are two possible representations of the pulling curves (Figure 6b). In one representation the force is plotted versus the relative trap-pipette distance (λ), the so-called force-distance curve (hereafter referred as FDC). In the other representation the force is plotted versus the relative molecular extension (x), the so-called force-extension curve (hereafter referred as FEC). In the optical tweezers setup $\lambda = x + y$ where y is the distance between the bead and the center of the trap. The measured force is given by $F = ky$ where k is the stiffness of the trap. The areas below the FDC and the FEC define two possible work quantities, $W = \int_{\lambda_i}^{\lambda_f} F d\lambda$ and $W' = \int_{x_i}^{x_f} F dx$. From the relation $d\lambda = dx + dy$ we get,

$$W = W' + W_b = W' + \frac{F_f^2 - F_i^2}{2k} \tag{9}$$

where F_i, F_f are the initial and final forces along a given trajectory. W is often called the total accumulated work and contains the work exerted to displace the bead in the trap, W_b, and the work transferred to the molecular system, W' (therefore receiving the name of transferred work) [26, 27]. The term W_b appearing in Eq.(9) implies that W, W' cannot simultaneously satisfy the CFR. What is the right definition of the mechanical work? In other words, which work definition satisfies the CFR? The problem we are facing now is identical to the one we previously encountered in section where we had to distinguish between work and heat. The answer to our question is straightforward if we correctly identify which are the control parameters and which are the configurational variables. In the lab frame defined by the pipette (or by the fluidic chamber to which the pipette is glued) the control parameter λ is given by the relative trap-pipette distance, whereas the molecular extension x stands for the configurational variable. Note that, due to the non-invariance property of the CFR under Galilean transformations, y cannot be used as configurational variable because it is defined respect to the co-moving frame defined by the trap. The same problem was found in section when comparing the distances x and y for the bead in the trap. The total energy of the molecular system is then given by

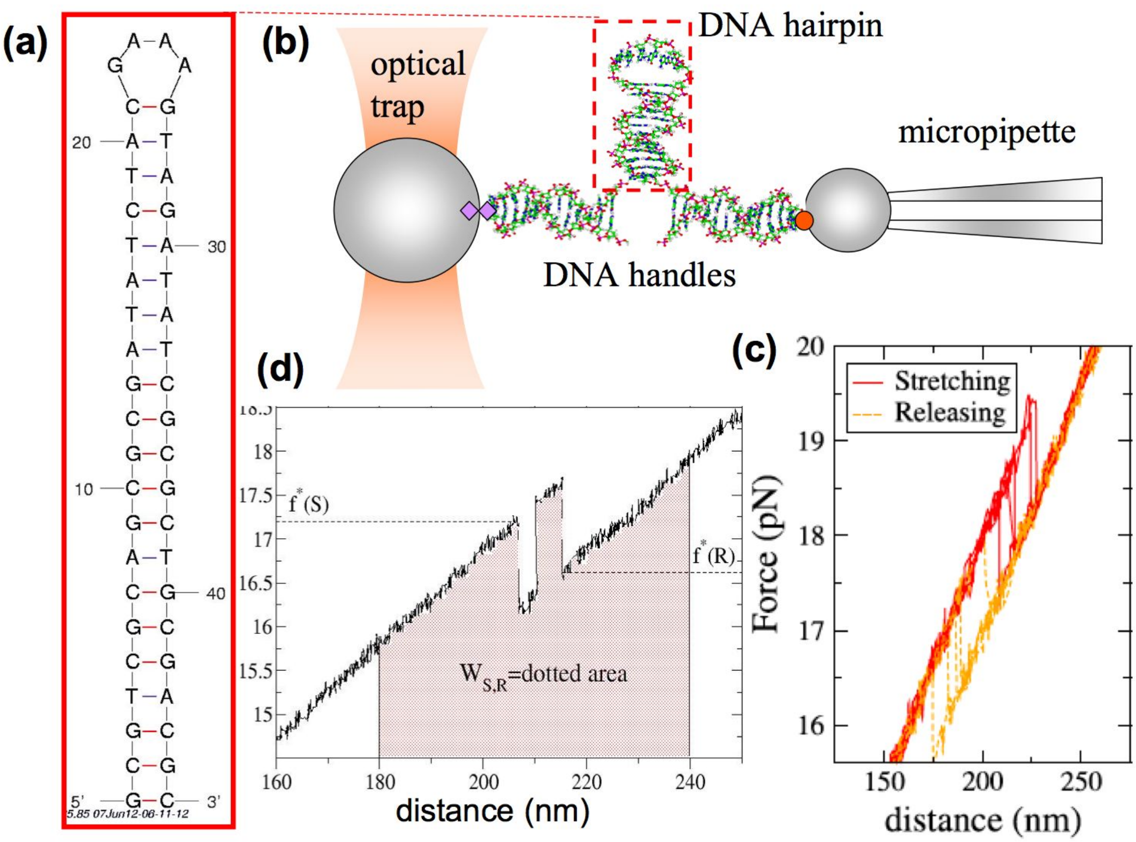

FIGURE 4. Mechanical folding/unfolding of DNA hairpins.(a) The sequence of a DNA hairpin with a 21bp stem ending in a tetraloop. (b) Experimental setup. A molecular construct made of the hairpin shown in (a) flanked by two dsDNA handles (29bp each) is tethered between two micron-sized beads. In the experiments the trap is moved relative to the pipette at speeds ranging from 10 to 1000nm/s. (c) Different force cycles recorded at 300nm/s. The red curves indicate the stretching parts of the cycle whereas the orange curves indicate the releasing parts of the cycle. Note that the forces of unfolding and refolding are random due to the stochastic nature of the thermally activated unfolding/folding process. The marked hysteresis is a signature of an irreversible process. (d) Measurement of work for a single trajectory. It is given by the area below the force-distance curve integrated between two trap positions. Trap distances are relative. Note that there might be more than one unfolding or refolding event along each trajectory. $f^*(S)(f^*(R))$ defines the first rupture force in the unfolding (refolding) process. Figure taken from [21].

$U(x,\lambda) = U_m(x) + (k/2)(\lambda - x)^2$ where $U_m(x)$ is the energy of the molecular system. From Eq.(3) and using $\lambda = x + y$ we get $F = ky = k(\lambda - x)$. From Eq.(2) we then conclude that the mechanical work that satisfies the CFR is the accumulated work W rather than the transferred work W'. We remark a few relevant facts,

1. **The transferred work W' does not satisfy the CFR and is dependent on the bandwidth of the measurement.** The FDC and FEC are sensitive to the bandwidth or data acquisition rate of the measurement (Figure 6b). Whereas W is insensitive to the bandwidth W' is not (see Figure 7a). This difference is very important because it implies that the bandwidth dependence implicit in the boundary term in Eq.(9)

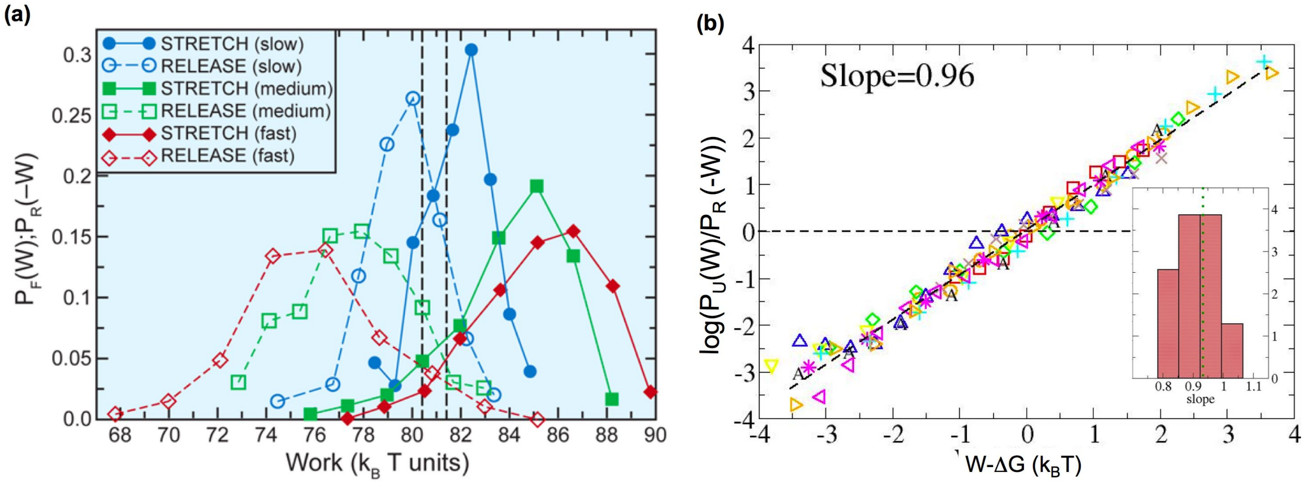

FIGURE 5. The Crooks fluctuation relation.(a) Work distributions for the hairpin shown in Figure 4 measured at three different loading rates: 50 nm/s (blue), 100 nm/s (green) and 300 nm/s (red). Unfolding or forward (continuous lines) and refolding or reverse work distributions (dashed lines) cross each other at a a value $\simeq 81k_BT$ independent of the loading rate.(b) Experimental test of the CFR for 10 different molecules pulled at different speeds. The log of the ratio between the unfolding and refolding work distributions is equal to $(W-\Delta G)$ in k_BT units. The inset shows the distribution of slopes for the different molecules which are clustered around an average value of 0.96. Figure taken from [21].

(the power spectrum of the force depends on the bandwidth if this is smaller than the corner frequency of the bead) is fully contained in W'. Operationally it is much easier to use W rather than W'. As shown in Figure 7b, W satisfies the CFR whereas W' does not. The logarithm of the ratio $\log(P_F(W')/P_R(-W'))$ plotted versus W'/k_BT is strongly bandwidth dependent and exhibits a slope 30 times smaller than 1 (i.e. the slope expected for W from the CFR) [27].

2. **How big is the error committed in recovering free energy differences by using W' rather than W?** Despite that W and W' only differ by a boundary term (cf. Eq.9) one can show that, for the case of the mechanical folding/unfolding of the hairpin, the error in recovering free energy differences using the Jarzynski equality can be as large as 100% [27]. The error or discrepancy increases with the bandwidth. Interestingly enough, for small enough bandwidths (but always larger than the coexistence kinetic rates between the folded and unfolded states, otherwise the folding/unfolding transitions are smeared out) fluctuations in the boundary term in Eq.(9) are negligible and both W and W' are equally good. This explains why previous experimental tests of the CFR that used W' instead of W produced satisfactory results (e.g. [20]).
3. **Inequivalence between moving the trap and the pipette or chamber.** The non-invariance of the CFR under Galilean transformations suggests that moving the optical trap inside the fluidic chamber should not be necessarily equivalent to moving the pipette glued to the fluidic chamber. We have to distinguish two cases depending on whether the fluid inside the chamber is dragged (*stick* conditions) or not (*slip* conditions) by the moving chamber. The two scenarios are physically

different because in the former case the bead in the trap is subject to an additional Stoke force due to the motion of the fluid. If the fluid is not dragged by the moving chamber (*slip* conditions) then y is the right configurational variable. In this case, $U(y,\lambda) = U_m(\lambda - y) + (k/2)(y)^2$ and the generalized force is equal to $F = U'_m(\lambda - y)$. Note that this F is not equal to the instantaneous force measured by the optical trap but the instantaneous force acting on the molecule. Even in case of mechanical equilibrium the difference between the two instantaneous forces, $U'_m(\lambda - y)$ and ky, produces a net non-negligible difference term. If the fluid does move with the chamber (*stick* conditions) then x is again the right configurational variable and we recover the main results of this section. Interestingly, all experiments done until now that use motorized stages to move chambers operate in *stick* conditions so we do not expect experimental discrepancies for the definition of the work.

4. **Other cases where the work definition matters.** As we showed in Figure 7 the CFR and the right definition of work W are both amenable to experimental test. Another interesting example where the boundary term is relevant is when the force f (rather than the trap position) is controlled. As we saw in Section the work in that case is given by $W_{X_0} = -\int_{f_i}^{f_f} X df$ where $X = y + x + X_0$ is the absolute trap-pipette distance. Because X_0 stands for an arbitrary origin, the work W_{X_0} is also a quantity that depends on X_0. This may seem unphysical but it is not [5]. The CFR is invariant respect to the value of X_0 as it can be easily checked by writing, $W_{X_0} = W_{X_0=0} - X_0(f_f - f_i)$, and using Eq.(8) gives $\Delta G_{X_0} = \Delta G_{X_0=0} - fX_0$. If the force f is controlled, then other work related quantities such as $W' = \int_{x_i}^{x_f} f dx$ or $W'' = \int_{X_i}^{X_f} f dX$ differ from W by finite boundary terms. Again these terms make the CFR not to be satisfied for W' and W''. These predictions are amenable to experimental test in magnetic tweezers (where the force is naturally controlled) or in optical tweezers operating in the force clamp mode with infinite bandwidth [28] (and possibly in a force feedback mode with finite bandwidth as well).

A GENERALIZED FLUCTUATION RELATION

The CFR can be generalized to cases where the system is initially in partial, rather than global, equilibrium both in the forward and the reverse protocol [29]. Suppose we take a system at fixed control parameter λ in thermal equilibrium with a bath at temperature T. The probability distribution over configurational variables x is Gibbsian over the whole phase space S meaning that: $P_\lambda^{\text{eq}}(x) = \exp(-E_\lambda(x)/k_BT)/Z_\lambda$ with Z_λ the partition function $Z_\lambda = \sum_{x\in S} \exp(-E_\lambda(x)/k_BT)$, where $E_\lambda(x)$ is the energy function of the system for a given pair λ, x. We refer to this condition as global thermodynamic equilibrium. However we might consider a case where the initial state is Gibbsian but restricted over a subset of configurations $S' \subseteq S$. We refer to this case as partial thermodynamic equilibrium. Partially equilibrated states satisfy $P_{\lambda,S'}^{\text{eq}}(x) = P_\lambda^{\text{eq}}(x)\chi_{S'}(x)Z_\lambda/Z_{\lambda,S'}$, where $\chi_{S'}$ is the characteristic function defined over the subset $S' \subseteq S$ [$\chi_{S'} = 1$ if $x \in S'$ and zero otherwise], and $Z_{\lambda,S'}$ is the partition function restricted to the subset S', i.e. $Z_{\lambda,S'} = \sum_{x\in S'} \exp(-E_\lambda(x)/k_BT)$. The partial free energy is then given by $G_{\lambda,S'} = -k_BT \log Z_{\lambda,S'}$.

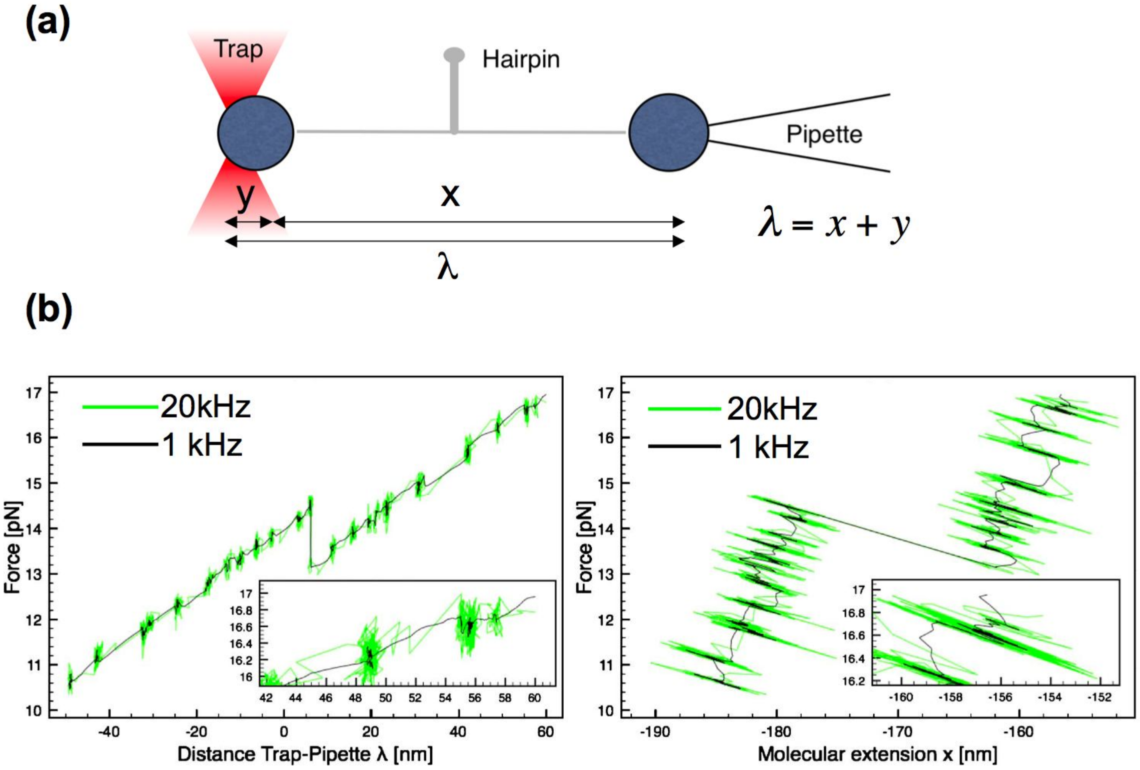

FIGURE 6. FDC versus FEC. (a) Experimental setup and different variables. (b) The FDC and FEC are defined as the curves obtained by plotting the force versus the trap position or the molecular extension respectively. Although force fluctuations in both types of curves show a dependence with the bandwidth of the measurement (black, 1kHz; green 20 kHz) only in the FEC the measurement of the work is very sensitive to such fluctuations. Figure taken from [27].

Let us suppose again the scenario depicted in Figure 3. Along the forward process the system is initially in partial equilibrium in S_0 at λ_0. Along the reverse process the system is initially in partial equilibrium in S_1 at λ_1. The generalized CFR reads,

$$\frac{p_{\mathrm{F}}^{S_0\to S_1}}{p_{\mathrm{R}}^{S_0\leftarrow S_1}}\frac{P^{S_0\to S_1}(W)}{P^{S_0\leftarrow S_1}(-W)}=\exp\left[\frac{W-\Delta G_{S_0,\lambda_0}^{S_1,\lambda_1}}{k_BT}\right], \tag{10}$$

where the direction of the arrow distinguishes forward from reverse, $p_{\mathrm{F}}^{S_0\to S_1}$ ($p_{\mathrm{R}}^{S_0\leftarrow S_1}$) stands for the probability to be in S_1 (S_0) at the end of the forward (reverse) process, and $\Delta G_{S_0,\lambda_0}^{S_1,\lambda_1}=G_{S_1}(\lambda_1)-G_{S_0}(\lambda_0)$ is the free energy difference between the partially equilibrated states S_0 and S_1.

Partially equilibrated states appear in many cases, from thermodynamic branches to intermediate and misfolded molecular states . The usefulness of the generalized CFR relies on our possibility to experimentally distinguish the substates visited along any trajectory and that these substates be visited frequently enough. For example, a molecule pulled by stretching forces can be in partial equilibrium when it stays either in the folded or unfolded state until it transits to the other state. If S_0 stands for the folded state and S_1

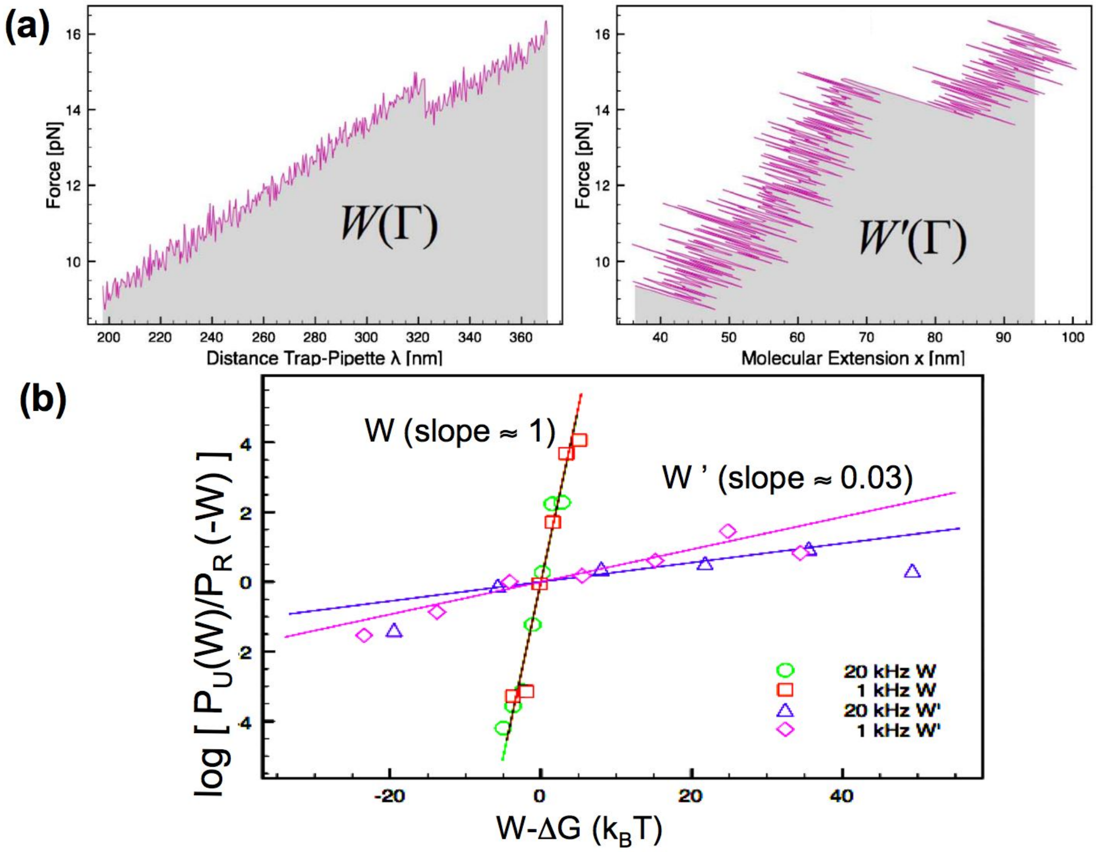

FIGURE 7. Accumulated (W) versus transferred (W') work. (a) The two work quantities for a given experimental trajectory. Note that the effect of bandwidth dependent force fluctuations is much larger for W' as compared to W, showing the importance of the boundary term Eq.9. (b) Experimental test of the CFR. When using W the CFR is satisfied at all bandwidths. However when we use W' the CFR is strongly violated and dependent on the measurement bandwidth. Figure taken from [27].

for the unfolded state, the generalized CFR makes possible to extract the free energies $G_{S'}(\lambda)$ of the folded and unfolded states $S' = S_0, S_1$ along the λ-axis, i.e. the folded and unfolded branches. Figure 8 shows an experimental verification of this result for a DNA hairpin that folds/unfolds in a two-states manner.

CONCLUSION

The possibility to experimentally measure the inverted motions remarked by Schrödinger more than half a century ago has boosted the study of energy fluctuations in very small objects under nonequilibrium conditions. The possibility to measure work fluctuations in single molecules that are mechanically unfolded has provided the testing ground for some of the most recent theoretical developments in nonequilibrium statistical physics. Fluctuation relations and fluctuation theorems (e.g. the Gallavotti-Cohen theorem for steady state systems [30]) are examples of new results that quantify

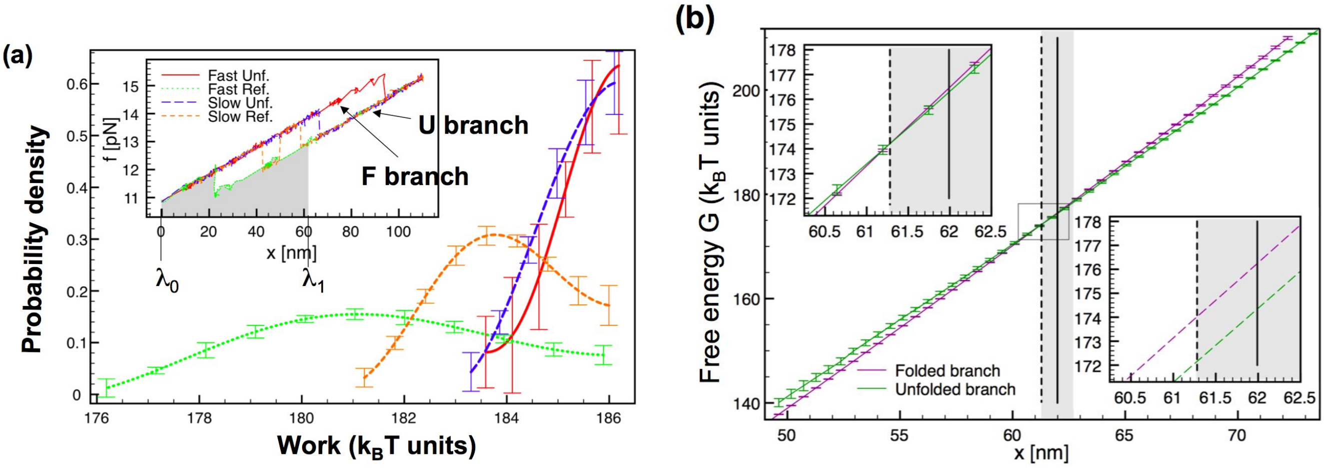

FIGURE 8. The generalized Crooks fluctuation relation. (a) Constrained work distributions measured in a 20bp hairpin at two different pulling speeds: 300nm/s (red, unfolding; green, refolding) and 40nm/s (blue, unfolding; orange, refolding). (a,Inset) The forward trajectories we consider are those where the hairpin starts partially equilibrated in the folded (F) state at λ_0 and ends in the unfolded (U) state (partially equilibrated or not) at λ_1.Note that, due to the correction term $p_{\mathrm{F}}^{F\to U}/p_{\mathrm{R}}^{F\leftarrow U}$ appearing in Eq.(10), restricted unfolding and refolding work distributions should not cross each other at a work value that is independent of the pulling speed. (b) Reconstruction of the folded (cyan color) and unfolded (green) free energy branches by applying the generalized CFR, Eq.(10), as shown in (a) and by varying the parameter $x \equiv \lambda_1$. The two branches cross each other around $x_c \simeq 82nm$ corresponding to the coexistence transition. For $x < x_c$ ($x > x_c$) the F (U) state is the minimum free energy state. The upper left inset shows an enlarged view of the crossing region. The lower left inset shows the importance of the correction term $p_{\mathrm{F}}^{F\to U}/p_{\mathrm{R}}^{F\leftarrow U}$ appearing in Eq.(10). If that term was not included in Eq.(10) the coexistence transition disappears. Figure taken from [29].

inverted motions in nonequilibrium states. Measuring *inverted motions* has also practical applications: the Crooks fluctuation relation (CFR), Eq.(8), and its generalization to partial (rather than full) equilibrium conditions, Eq.(10), allows us to extract free energy differences between native or non-native states and free energies of thermodynamic branches. Future studies will also show the reliability of these methodologies to extract free energies of misfolded and intermediate states in RNAs or proteins, and base-pair free energies in nucleic acids unzipped under irreversible conditions. We also stressed how important is the correct definition of mechanical work to ensure the validity of the CFR. In this regard serious inconsistencies are encountered using other definitions of mechanical work but such inconsistencies are nowadays amenable to experimental test. Related to this, it is also important to underline the general non-invariance of fluctuation relations and theorems under Galilean transformations [31], an aspect that has not been stressed enough and that can also be tested in experiments. Finally, all the studies covered in this note address energy fluctuations of small classical systems under Gaussian noise conditions. It would be highly desirable to have experiments done in systems in the regime of non-Gaussian noise (maybe at submicroseconds timescales), or in quantum systems where the concept of classical trajectory looses its usual meaning [32].

ACKNOWLEDGMENTS

A. A. and M. R. acknowledge financial support from the Spanish MEC-MICINN through the FPU fellowship program, grant no. AP2007-00995 and Human Frontier Science Program (HFSP) (RGP55-2008) respectively. F. R acknowledges financial support from Grants FIS2007-3454. Human Frontier Science Program (HFSP) (RGP55-2008) and Icrea Academia prize 2008.

REFERENCES

1. E. Schrödinger, *What is life?*, Cambridge University Press, Cambridge, 1944.
2. F. Ritort , *J. Phys. Condens. Mat.* **18**, R531-R583.(2006).
3. C. Bustamante, J. Liphardt , and F. Ritort, *Physics Today* **58**, 43 (2005).
4. F. Ritort, *Adv. Chem. Phys.* **137**, 31 (2008).
5. L. Peliti, *J. Stat. Mech.* P05002 (2008), and references therein.
6. G. M. Wang, E. M. Sevick, E. Mittag, D. J. Searles, and D. J. Evans, *Phys. Rev. Lett.* **89**, 050601 (2002).
7. O. Mazonka, and C. Jarzynski, e-print cond-mat/991212.
8. R. Van Zon, and E. G. D. Cohen, *Phys. Rev. Lett.* **91**, 110601 (2003).
9. S. Garnier, and S. Ciliberto, *Phys. Rev. E* **71**, 060101R (2005).
10. D. J. Evans, and D. J. Searles, *Phys. Rev. E* **50**, 1645 (1994).
11. G. E. Crooks, *Phys. Rev. E* **60**, 2721 (1999).
12. C. Jarzynski, *Phys. Rev. Lett.* **78**, 2690 (1997).
13. G. Hummer, and A. Szabo, *Proc. Nat. Acad. Sci. U.S.A.* **98**, 3658 (2001).
14. J. Liphardt, S. Dumont, S. B. Smith, I. Tinoco Jr., and C. Bustamante, *Science* **296**, 1832 (2002).
15. D. Zuckerman, and T. Woolf, *Chem. Phys. Lett.* **351**, 445 (2002); *Phys. Rev. Lett.* **89**, 180602 (2002).
16. F. Ritort, C. Bustamante, and I. Tinoco Jr., *Proc. Nat. Acad. Sci. U.S.A.* **99**, 13544 (2002).
17. C. H. Bennett, *J. Comp. Phys.* **22**, 245 (1976).
18. M. R. Shirts, E. Bair, G. Hooker, and V. S. Pande, *Phys. Rev. Lett.* **91**, 140201 (2003).
19. D. D. L. Minh, and A. B. Adib, *Phys. Rev. Lett.* **100**, 180602 (2008).
20. D. Collin, F. Ritort, C. Jarzynski, S. B. Smith, I. Tinoco Jr., and C. Bustamante, *Nature* **437**, 231 (2005).
21. A. Mossa, M. Manosas, N. Forns, J. M. Huguet, and F. Ritort, *J. Stat. Mech.* P02060 (2009).
22. M. Manosas, A. Mossa, N. Forns, J. M. Huguet, and F. Ritort, *J. Stat. Mech.* P02061 (2009).
23. J. M. Huguet, C. V. Bizarro, N. Forns, S. B. Smith, C. Bustamante, and F. Ritort, *Proc. Nat. Acad. Sci. U.S.A.* **107**, 15431 (2010).
24. M. T. Woodside, W. M. Behnke-Parks, K. Larizadeh, K. Travers, D. Herschlag, and S. M. Block, *Proc. Nat. Acad. Sci. U.S.A.* **103**, 6190 (2006).
25. N. Forns, S. De Lorenzo, M. Manosas, J. M. Huguet, and F. Ritort, submitted for publication.
26. J. M. Schurr, and B. S. Fujimoto, *J. Phys. Chem. B* **107**, 14007 (2003).
27. A. Mossa, S. De Lorenzo, J. M. Huguet, and F. Ritort, *J. Chem. Phys.* **130**, 234116 (2009).
28. W. J. Greenleaf, M. T. Woodside, E. A. Abbondanzieri, and S. M. Block, *Phys. Rev. Lett.* **95**, 208102 (2005).
29. I. Junier, A. Mossa, M. Manosas, and F. Ritort, *Phys. Rev. Lett.* **102**, 070602 (2009).
30. G. Gallavotti, and E. G. D. Cohen, *Phys. Rev. Lett.* **74**, 2694 (1995).
31. T. Speck, J. Mehl, and U. Seifert, *Phys. Rev. Lett.* **100**, 178302 (2008).
32. F. Ritort, *Physics* **2**, 43 (2009).

Universality in equilibrium and away from it: A personal perspective

Miguel A. Muñoz

Departamento de Electromagnetismo y Física de la Materia and Instituto de Física Teórica y Computacional Carlos I, Facultad de Ciencias, Campus Fuentenueva. Universidad de Granada, 18071 Granada, Spain.

Abstract. In this talk/paper I discuss the concept of universality in phase transitions and the question of whether universality classes are more robust in equilibrium than away from it. In both of these situations, the main ingredients determining universality are symmetries, conservation laws, the dimension of the space and of the order-parameter and the presence of long-range interactions or quenched disorder. The existence of detailed-balance and fluctuation-dissipation theorems imposes severe constraints on equilibrium systems, allowing to define universality classes in a very robust way; instead, non-equilibrium allows for more variability. Still, quite robust non-equilibrium universality classes have been identified in the last decades. Here, I discuss some examples in which (i) non-equilibrium phase transitions are simply controlled by equilibrium critical points, i.e. non-equilibrium ingredients turn out to be irrelevant in the renormalization group sense and (ii) non-equilibrium situations in which equilibrium seems to come out of the blue, generating an adequate effective description of intrinsically non-equilibrium problems. Afterwards, I shall describe different genuinely non-equilibrium phase transitions in which introducing small, apparently innocuous changes (namely: presence or absence of an underlying lattice, parity conservation in the overall number of particles, existence of an un-accessible vacuum state, deterministic versus stochastic microscopic rules, presence or absence of a Fermionic constraint), the critical behavior is altered, making the case for lack of robustness. However, it will be argued that in all these examples, there is an underlying good reason (in terms of general principles) for universality to be altered. The final conclusions are that: (i) robust universality classes exist both in equilibrium and non-equilibrium; (ii) symmetry and conservation principles are crucial in both, (iii) non-equilibrium allows for more variability (i.e. it is less constrained).

Keywords: Phase transitions, Universality, Renormalization group
PACS: 05.70.Fh, 64.60.ae, 64.60.fd, 64.60.Ht

UNIVERSALITY IN EQUILIBRIUM (STATICS AND DYNAMICS)

The concept of universality is very well established in equilibrium phase transitions [1]. The main ingredients determining universality classes are symmetries, conservation laws, the dimensions of the physical space and the order-parameter, quenched disorder and long-range. They all have a very general character and can be easily identified. Moreover, the presence of detailed-balance and fluctuation-dissipation relations impose severe constraints on equilibrium systems, and allows to define universality classes in a very robust way. Instead, in non-equilibrium, the lack of these constraints leaves more freedom and it is usually read in the literature that non-equilibrium universality classes are more fragile than their equilibrium counterparts (see the next section for some specific example of this [2]). Is this really true? If yes, to what extent? Can robustness be quantified?

Aimed at shedding some light into these and related questions, I present here a brief discussion of the concept of universality both in equilibrium and away from it.

Even if exact solutions of some equilibrium models exist [3, 4], universality is best understood in the framework of the renormalization group [5], as follows. Given a microscopic model, a coarse-grained continuous description is first constructed either in an exact way or by using some approximation or phenomenological description (for instance, the ϕ^4 Ginzburg-Landau Hamiltonian is the continuous representation of the Ising model) [1]. In this way, the problem can be parametrized and different microscopic models can be compared within a common language. Then, renormalization group transformations are applied and non-trivial fixed points in parameter space are identified. At such fixed points, many parameters vanish, i.e. their contribution becomes "irrelevant". Universality is then a straightforward consequence of the stability of fixed points under renormalization group transformations [1]. Robustness in universality classes is to be expected.

By extending these ideas to dynamics (i.e. including in the approach not only the stationary state, but also the relaxation towards it), Hohenberg and Halperin proposed in a seminal work [6] a classification of universality classes in terms of Langevin equations [7]. In particular, the (non-conserved) dynamical Ising model corresponds to the, so called, Model A, defined in terms of the following Langevin equation for the magnetization field $\phi(x,t)$:

$$\begin{aligned}\frac{\partial \phi(x,t)}{\partial t} &= -\frac{\delta H_{GL}[\phi]}{\delta \phi(x,t)} + \sigma \eta(x,t),\\ H_{GL}[\phi] &= \frac{a}{2}\phi^2 + \frac{b}{4}\phi^4 + \frac{D}{2}(\nabla \phi)^2, \end{aligned} \tag{1}$$

where $\eta(x,t)$ is a Gaussian white noise with variance $2\sigma^2 = K_B T$ (T is the temperature and K_B the Boltzmann constant), and the Ginzburg-Landau Hamiltonian H_{GL} is the minimal Hamiltonian exhibiting a paramagnetic and a ferromagnetic phase and allowing for the Z_2, up-down, symmetry to be spontaneously broken [1] (observe that some (x,t) dependences have been omitted, and will be omitted along the text, to unburden the notation). The associated stationary probability distribution is the equilibrium one, $P_{stat}[\phi] \propto \exp(-\frac{H_{GL}[\phi]}{KT})$. Another example is Model B, very similar to Model A but with the extra constraint of the magnetization field being conserved [6].

From any Langevin equation (as the one above), one can also construct an associated generating functional (by using the well-know Martin-Siggia-Rose or de-Dominicis-Peliti formalisms[8]) in terms of which to develop a renormalization program fully analogous to the one delineated above for equilibrium Hamiltonians [1]. Actually, the main advantage of having a dynamical formulation is that it allows for a simple extension to non-equilibrium problems (which are usually defined from their dynamics, given that a Hamiltonian and does not exist).

In what follows I shall identify any given universality class with a unique continuous theory (be it a Langevin equation or a generating functional) capturing in the most parsimonious way the main relevant ingredients and hence its critical behavior.

UNIVERSALITY IN NON-EQUILIBRIUM

Let me start this section by presenting a specific example supporting the belief that universality away from equilibrium is more fragile than it is in equilibrium.

Driven diffusive systems are variations of the Ising model or, better, its equivalent, the lattice-gas model [2], in which an external driving field induces an overall particle current (and hence anisotropy), preventing the system from being Hamiltonian [2, 10]. The prototypical example is the Katz-Lebowitz-Spohn, driven lattice gas (DLG) [9]. Below the critical point the DLG segregates forming characteristic stripes (as those shown in Figure 1) along the direction of the external field. The Langevin equation for this case (which is a variation of Model B including an external driving field, and hence an anisotropic direction) as well as a review of the properties of this and related universality classes can be found in [2, 10]. A Langevin theory alternative to the standard one was proposed in [11].

Leaving aside the subtle question of which of these is the proper Langevin equation for this universality class, and following Marro and collaborators, let me present a recently introduced off-lattice version of the DLG. It consists of a gas of hard-core particles interacting through (truncated) Lenard-Jones potentials [12]. In the absence of an external field, and in full analogy with the (un-directed) lattice gas, the model exhibits an Ising-like phase transition as could have been anticipated by relying on symmetry considerations. Instead, once an external field (dragging particles in a preferred direction) is switched on, the off-lattice model forms stripes similar to those characteristic of the DLG (see Figure 1). A priori, one would expect the external field to shift criticality from Ising-like to DLG-like. Instead, curiously enough, such an off-lattice non-equilibrium driven model exhibits critical exponents differing significantly from those of its microscopic counterpart [12]. To add further perplexity, even if anisotropic stripes appear, the exponents have been reported to be compatible with Ising (i.e. equilibrium and isotropic) values(!) [12]. Why does the off-lattice version differ from the lattice one away from thermodynamic equilibrium, even if in equilibrium they share the same universality class? Or in other words, why is the effect of the driving field irrelevant in the off-lattice version but not in the reticular one? The underlying reason for this remains a mystery.

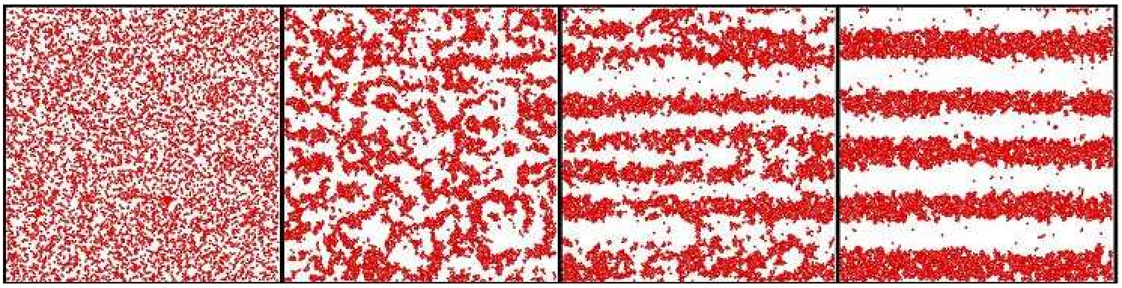

FIGURE 1. Stripped configurations appearing, as the temperature is lowered, in the ordered phase of the driven off-lattice gas of Lenard-Jones interacting particles.

Examples similar to this one have often appeared in the literature and it has been claimed that “universality is much more fragile in non-equilibrium than in equilibrium” [2]. Still, contrarily to initial expectations (in the 70*s* and early 80*s*), rather robust non-equilibrium universality classes have been identified in the last decades. Some of the best known ones can be classified in the following groups (let me caution the reader that this does not pretend to be, by any means, an exhaustive list):

- *Driven diffusive systems* (see the discussion above).
- *Rough interfaces*. Universality classes as the Kardar-Parisi-Zhang, the molecular-beam-epitaxy model, etc. are quite robust and ubiquitous, including a vast number of representatives. See the review articles in [13] for details and extensive reference lists.
- *Systems with absorbing states*. As first conjectured by Janssen and Grassberger [16], a huge number of models (including directed percolation [2, 14], the contact process [4], catalytic reactions on surfaces, branching annihilating random walks with odd parity, or damage spreading) exhibiting a transition into a unique absorbing phase (i.e. a fluctuation-less phase from which a system cannot escape) belong into the *directed percolation* (DP) universality class [14]. There is also (at last!) a nice experimental realization of this class [15]. The corresponding Langevin equation for the activity field $\rho(x,t)$ is [16]:

  $$\partial_t \rho(x,t) = a\rho(x,t) - b\rho^2 + D\nabla^2\rho + \sigma\sqrt{\rho}\,\eta(x,t). \tag{2}$$

  Observe the main differences with respect to Model A: (i) the field is positive definite, (ii) there is no up-down symmetry, and (iii) the amplitude of the noise is proportional to the square-root of the density, and hence noise vanishes in the absence of activity (i.e. the absorbing state is at work). This conjecture was extended to include multicomponent systems [17] as well as to systems with infinitely many absorbing states [18]. Finally, let me remark that two different interesting papers have made attempts to classify absorbing state universality classes (including DP and some others that will show up along this paper) by using a unifying framework [19].
- *Systems with multiplicative noise*. They are defined by a Langevin equation very similar to Eq.(2) but where the noise is linear in the order-parameter, i.e.

  $$\partial_t \rho(x,t) = a\rho(x,t) - b\rho^2 + D\nabla^2\rho + \sigma\rho(x,t)\,\eta(x,t). \tag{3}$$

  This equation describes transitions in models in theoretical ecology (where the noise describes environmental variability), synchronization transitions in spatially extended systems [20], or wetting under non-equilibrium conditions [21]. A detailed comparison between this class and DP can be found in [22]. For a review of this universality class see [23].

All these classes are robust in the sense that they are mostly insensitive to the modification of microscopic details as long as they do not alter general features as conservation laws, symmetries and so on. Indeed, for all of them there are plenty of distinct microscopic models lying in the same class. Furthermore, some of the discussed non-equilibrium Langevin equations, as for instance Eq.(2), can be renormalized along similar lines as their equilibrium counterparts (as Eq.(1)) leading to similar renormalization-group fixed points.

From this perspective, does it make any sense to assert that the (equilibrium) Ising universality is more robust than the (non-equilibrium) DP class? Probably not. It is clear that in the absence of a precise definition of what we mean by "robust" it is not meaningful to compare the robustness of different classes.

In the next two sections, aimed at giving a broader perspective on these problems, I shall present some examples illustrating that the borderline between equilibrium and non-equilibrium critical points is not as clearly outlined as one could think at first sight. Then, in the remaining section I shall explore some specific examples of non-equilibrium universality classes and discuss the effects that can be induced by changing apparently innocuous details.

NON-EQUILIBRIUM SYSTEMS WITH EQUILIBRIUM SCALING

In a seminal paper, Grinstein, Jayaprakash and He [24] showed that non-equilibrium systems (in which detailed-balance is explicitly violated) with up-down symmetry can still be described at sufficiently large scales by the equilibrium Ising class (i.e. by Model A above). While in systems relaxing to equilibrium we can write

$$\partial_t \phi(x,t) = -F_x[\phi] + \sigma \eta(x,t) \tag{4}$$

where the force F obeys the potentiality condition, and therefore can be written as the derivative of a Hamiltonian, in non-equilibrium cases with up-down symmetry (like some cellular automata [24]) the potentiality condition does not hold:

$$\frac{\delta F_x}{\delta \phi(y,t)} \neq \frac{\delta F_y}{\delta \phi(x,t)}, \tag{5}$$

and consequently, the dynamics cannot be derived from a potential. Furthermore, the noise variance, $2\sigma^2$, cannot be identified with the temperature (KT). However, expanding the force F in power-series

$$\partial_t \phi(x,t) = a\phi(x,t) - \sum_{x,y,z} b_{xyz} \phi(x,t)\phi(y,t)\phi(z,t) + \ldots + D\nabla^2\phi + \sigma\eta(x,t) \tag{6}$$

and similarly, for the noise amplitude

$$\sigma \to \sigma_0 + \sigma_2 \phi(x)\phi(x') + \ldots, \tag{7}$$

it is not difficult to see, after performing a Fourier transform, that the corresponding Langevin equation can be rewritten as a generalization of Model A but with k-dependent coefficients. Grinstein et al. showed that all the extra k-dependent terms are irrelevant in the renormalization group sense, leaving only the standard coefficients of Model A as the significant ones [24]. Hence, at criticality, this type of models become indistinguishable from their standard equilibrium counterparts; i.e. they exhibit equilibrium criticality.

There are many more similar examples of this type of situation in the literature; two of them are:

- the non-equilibrium randomly driven diffusive system, which turns out to be controlled by an equilibrium fixed point [10].

- The (strong disorder) critical behavior of the equilibrium disordered quantum Ising chain controls also the critical properties of non-equilibrium models in the directed-percolation with quenched disorder universality class [25].

EQUILIBRIUM SCALING COMING OUT OF THE BLUE

Just to give an illustration of how subtle the line separating equilibrium from non-equilibrium is, let me discuss a simple (highly irreversible and with no detailed-balance) non-equilibrium model, which at some mesoscopic scale happens to be describable by an effective equilibrium theory.

The “interacting Brownian bug” model, was introduced in [26] and further analyzed in [27]. It consists of branching-annihilating Brownian particles (bugs) which interact with any other within a finite distance, R [26]. Particles move off-lattice in a d-dimensional interval with periodic boundary conditions. They can:

- *diffuse* (at rate 1) performing Gaussian random jumps of variance $2D$,
- *disappear spontaneously* (at rate β_0),
- *branch*, creating an offspring at their same spatial coordinates with a density-dependent rate λ:
$$\lambda(j) = max\{0, \lambda_0 - N_R(j)/N_s\}, \tag{8}$$
where j is the particle label, λ_0 (reproduction rate in isolation) and N_s (a saturation constant) are fixed parameters, and $N_R(j)$ stands for the number of particles within a distance R from j.

The control parameter is $\mu = \lambda_0 - \beta_0$ and the function $max()$ enforces the transition rates positivity. For large values of μ there is a stationary finite density of bugs (active phase) while for small values the system falls ineluctably into the vacuum (absorbing phase). Separating these two regimes there is a critical point at some value μ_c, belonging to the directed percolation (DP) universality class [27]. In the active phase, owing to the local-density dependent dynamical rules particles group together forming clusters (see Figure 2). Such clusters have a well-defined typical diameter and a characteristic number of particles within, which depend on the parameters R, N_s, and μ [26, 27]. Well inside the active phase, when the clusters start filling the available space they *self-organize* in spatial structures with remarkable hexagonal order. The amount of ordering reached by such clusters is quite impressive (see Figure 2).

One could wonder whether the Mermin-Wagner theorem (establishing that, in equilibrium systems, fluctuations will destroy long range order in two-dimensional systems characterized by a continuous rotational symmetry [28]) applies also to this highly irreversible non-equilibrium model. In [27] a detailed analysis of the model was performed; the conclusion is, in a nutshell, that above the cluster scale, the system behaves as if it was a two-dimensional crystal in thermodynamic equilibrium. The ordering can be described in the very same terms as the equilibrium melting transition, mediated by defects and exhibiting a Kosterlitz-Thouless type of [29] transition.

In summary, even if there is no analytical way to map the Brownian bug model into an “effective Hamiltonian”, the striking patterns it produces resemble very much

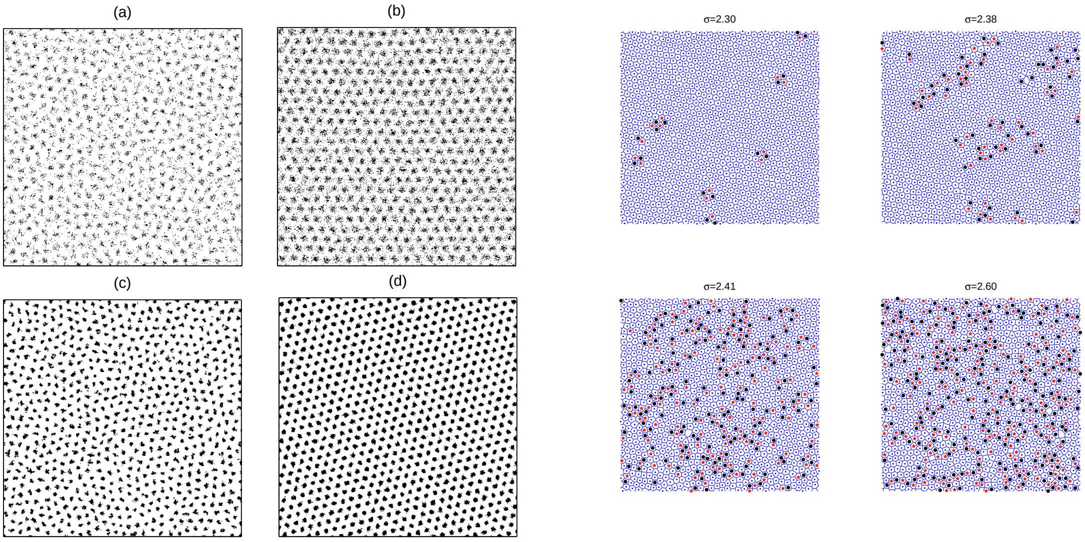

FIGURE 2. Snapshots of the Brownian bug model for different noise intensities and topological defect analysis. By constructing a Voronoi tessellation one observe the presence of topological defects (marked in red and white), which tend to group together forming dipoles and quadrupoles in the very same way as occurs in the melting of a two-dimensional solid. See [27] for more details.

the melting solid-liquid transition in two-dimensional equilibrium systems, suggesting that at some coarse-grained scale, the system behaves as an equilibrium one with some effective Hamiltonian.

INNOCUOUS DETAILS AFFECTING UNIVERSAL PROPERTIES?

It has been often asserted in the literature, as already illustrated above, that seemingly “innocuous details” can change the universality class in non-equilibrium problems. Actually, trying to shed some light onto such an assertion was the motivation for our discussion here. After expending some time scrutinizing the literature and looking for examples of this, we came to the conclusion that in (almost) all the cases we came across, the apparently “innocuous details” turned out to break-up some symmetry or conservation law, to restore some hidden symmetry, or to alter any of the general principles on the basis of which the concept of universality is built. Some of the examples discussed in detail the talk are enumerated here.

- Parity conserving class. This universality class puzzled researchers for quite a few years [31]. One-dimensional systems with absorbing states but in which the parity of the number of particles is conserved lie in a universality class, usually called parity-conserved, different from DP (see [14] for reviews and references). It is very surprising at first sight that a trait as the particle number parity can affect the system large-scale behavior. Actually, one could imagine that after some coarse-graining parity conservation should be lost. How could one write a Langevin equation encoding parity conservation?

After some struggling, a way out of this puzzle was given: parity-conservation was shown to be tantamount to the existence of two symmetric absorbing states: particles correspond two "kinks" separating the two symmetric absorbing states (see Figure 3). Once this observation has been made, it is not difficult to write down a Langevin equation analogous to Eq. (2) above but including 2 symmetric absorbing states:

$$\partial_t \phi = (a\phi - b\phi^3)(1-\phi^2) + D\nabla^2\phi + \sigma\sqrt{1-\phi^2}\,\eta \tag{9}$$

which in one-dimensional systems has been shown to capture the physics (i.e the critical behavior) of the parity conserving class [32]. As announced above, if universality is altered (with respect to DP) there is a good reason for it: in the present case an additional (Z_2) symmetry has been switched on.

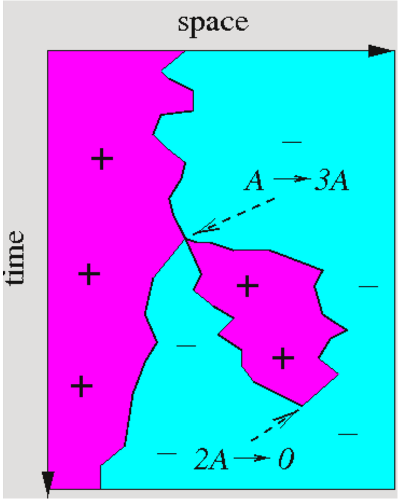

FIGURE 3. Schematic illustration of the equivalence between parity conserving branching processes and systems with two symmetric absorbing states. The parity conserving $2A \rightarrow 0$ and $A \rightarrow 3A$ processes correspond respectively to annihilation and creation of kinks separating two symmetric absorbing states.

Actually, depending on some parameter values, this equation can exhibit two separate phase transitions (one Ising like and one DP-like, corresponding respectively to the breaking of the up-down symmetry and the falling into an absorbing state, the one selected by the spontaneous breakdown of the symmetry) or instead a single one into the parity conserved class (corresponding to the coalescence of the two phenomena above). Hence, the Langevin equation above does include both equilibrium and intrinsically non-equilibrium critical points.

- A second example, also for systems with absorbing states, is the universality class of reaction diffusion models in which the vacuum (i.e. the absorbing state) is not reachable (i.e. there is always, at least, one remaining particle). An example of this is the reversible pair of reactions $A \leftrightarrow 2A$ (in which the state with just one particle cannot decay to the vacuum). It has been shown that other non-reversible sets of reactions lead to this same universality class [33]. It seems surprising that the non-accessibility of the absorbing state is relevant for the behavior of the system at large scales and, again, it is difficult to imagine how this property could survive to the coarse-graining process. However, it can be shown that owing to the unaccessibility of the vacuum, a detailed-balance property (missing in the DP class) is restored, and the system behaves quite differently from DP, and instead behaves as an equilibrium one [34, 33].

- Another example is provided by models of self-organized criticality [35]. Aimed at shedding some light on the origin of scale invariance in many contexts in Nature, different mechanisms for *self-organized criticality* (SOC) were proposed following the seminal work by P. Bak and collaborators [36, 37]. Sandpiles, ricepiles, and earthquake toy-models become paradigmatic examples capturing the essence of self-organization to scale-invariant (critical) behavior without apparently requiring the fine tuning of parameters [35, 38]. They are metaphors of real systems (as earthquakes, snow avalanches, stick-slip phenomena, etc.) in which some type of stress or energy is accumulated at some slow timescale and relaxed in a much faster way. In particular, sandpiles played a central role in the development of this field [36, 37]. Their dynamics can be summarized as follows: grains are slowly added to the pile until eventually they relax if locally an instability threshold is overcome. In such a case they are transmitted to neighboring sites which, on their turn, may become unstable and relax, generating avalanches of activity. Considering open boundaries (to allow for energy balance) a steady state with power-law distributed (i.e.critical) avalanches is eventually reached. Stochastic sandpiles have been argued to belong to a unique universality class characterized by an equation similar to Eq.(2) but (linearly) coupled to a second conserved and non-diffusive field [38]:

$$\begin{cases} \partial_t \rho(\vec{x},t) &= a\rho - b\rho^2 + \omega\rho E + D\nabla^2\rho + \sigma\sqrt{\rho}\,\eta(\vec{x},t) \\ \partial_t E(\vec{x},t) &= D_E \nabla^2 \rho(\vec{x},t). \end{cases} \tag{10}$$

  This universality class, sometimes called C-DP (by extension of the nomenclature introduced by Hohenberg and Halperin), or also Manna class, is quite robust and includes, apart from many variations of the original sandpile model with rather different microscopic rules, reaction diffusion and other types of models [39]. After some initial confusion, it became clear that the original Bak-Tang-Wiesenfeld (BTW) model, as well as some other similar sandpiles exhibit a type of scaling, not captured by Eq.(10), which instead describes very well many other sandpiles, ricepiles, etc. [40]. It was clarified that the difference between the BTW model and models in the C-DP class lies in the presence of *deterministic* toppling rules (vs. stochastic rules in the C-DP class). Even if this might seem to be an irrelevant trait, it is not; deterministic rules induce the existence of many "toppling invariants" or extra conservation laws, which would need to be implemented in the set of Langevin equations to achieve a proper coarse-grained description. Summing up, also in this subtle case, general principles (conservation laws) have been altered for universal features to be affected.

  To add further information (and make the overall picture even more intricate), let me stress that the C-DP class has been shown [41] to be fully equivalent to that of interfaces moving in the presence of quenched disorder (i.e. the Quenched Edwards Wilkinson class) [42]. The first one is intrinsically a non-equilibrium one with annealed disorder; the second one is an equilibrium class including quenched disorder; both of them share the same critical properties; they are simply two different descriptions of the same underlying phenomenon [41]. Once again, this illustrates the subtlety of the frontier separating equilibrium and non-equilibrium criticality.

- In particle systems, an important property is the presence of hard-core constraints. It seems that whether a spatial position can be occupied simultaneously by only one or more than one particles should influence decisively its critical properties. Instead, in systems with absorbing states it is customarily argued that in the neighborhood of the phase transition, as the density of particles becomes as small as wanted, this type of effect can be safely ignored. Actually, this is typically the case, and there is overwhelming evidence supporting such a conclusion. This justifies the generalized use of bosonic-type of Fock-space formalisms employed to derived field-theoretical actions or Langevin equations, in which analytic calculations or universality issues are more systematically analyzed [1].
  However, for a simple non-equilibrium particle model (in which particles react only at a particular point and diffuse without interacting elsewhere) it was claimed that Fermionic and bosonic versions of the model lead to different critical features [43]. However, in a subsequent work it was (numerically) shown that indeed, the Fermionic constraint is irrelevant and both versions of the model lie in the same universality class [44].

In summary, our main conclusion is that, as in equilibrium, general principles as symmetries, conservation laws, disorder, dimensionality... are the sole responsible for universal features. In (almost) all the cases under consideration in which universality is changed by apparently innocuous details, it has been shown that such details turn out to dramatically alter some general property. The reverse is also true; if general properties remain unchanged universality is preserved.

An exception to this general conclusion is the example of the off-lattice driven diffusive system, for which we do not have a satisfying explanation. Our bet, however, is that even if still un-covered a good reason (in terms of general principles) should also exist for the breakdown of universality in this case.

ACKNOWLEDGMENTS

I am in debt with all the colleagues who I had the pleasure to collaborate with on the topics discussed here; in particular, I want to express my gratitude to Pedro Garrido and Geoff Grinstein for introducing me to fascinating world of non-equilibrium phase transitions, and for honoring me with friendship. I acknowledge financial support from Projects FIS2009-08451 (FEDER) from the Spanish Ministry as well as from the Junta de Andalucía, Proyecto de Excelencia P09-FQM4682.

REFERENCES

1. D. J. Amit, *The Renormalization Group and Critical Phenomena*, World Scientific, Singapore, 1984; J. Zinn-Justin, *Quantum Field Theory and Critical Phenomena*, Oxford Science Publications, Ox-

ford, 1990; G. Parisi, *Statistical Field Theory*, Addsisson-Wesley, Reading MA, 1988; M. Le Bellac, *Quantum and Statistical Field theory*, Oxford Science Publications, Oxford, 1991; H. E. Stanley, *Introduction to Phase Transition and Critical Phenomena*, Oxford University Press, Oxford, 1971; J. Cardy, *Scaling and Renormalization in Statistical Physics*, Lecture Notes in Physics #5, Cambridge University Press, Cambridge, 1996; S.-K. Ma, *Modern Theory of Critical Phenomena*, Benjamin, Reading MA, 1976; L. P. Kadanoff, *Statistical Physics: statics, dynamics and Renormalization*, World Scientific, 2000; J. J. Binney, N. J. Dowrick, A. J. Fisher, and M. E. J. Newman, *The Theory of Critical Phenomena: An Introduction to the Renormalization Group*, Oxford Science Publications, Oxford, 1998; M. Kardar, *Statistical Mechanics of Fields*, Cambridge University Press, Cambridge, 2007.

2. J. Marro, and R. Dickman, *Non-equilibrium phase transitions in lattice models*, Cambridge University Press, Cambridge, 2005.
3. R. J. Baxter, *Exactly solvable model in Statistical Physics*, Academic Press, 1982.
4. T. M. Ligget, *Interacting Particle Systems*, Springer, Berlin, 1985.
5. K. G. Wilson, *Rev. Mod. Phys.* **47**, 773 (1975).
6. P. C. Hohenberg, and B. J. Halperin, *Rev. Mod. Phys.* **49**, 435, (1977).
7. Langevin equations are the simplest dynamical extension of equilibrium Hamiltonians; any Langevin equation can be also be written in terms of a generating functional (the reverse is not necessarily true), and hence and “action”, which plays a role formally similar to that of the Hamiltonian in the equilibrium formalism.
8. P. C. Martin, E. D. Siggia, and H. A. Rose, *Phys. Rev. A* **8**, 423, (1973); C. De Dominicis, and L. Peliti, *Phys. Rev. B* **18**, 353, (1978); R. Bausch, H. K. Janssen, and H. Wagner, *Z. Phys. B* **24**, 113, (1976).
9. S. Katz, J. L. Lebowitz, and H. Spohn, *Phys. Rev. B* **28**, 1655 (1983); *J. Stat. Phys.* **34**, 497 (1984).
10. B. Schmittmann, and R. K. P. Zia, *Statistical Mechanics of Driven Diffusive Systems*, in Phase Transitions and Critical Phenomena, edited by C. Domb and J. Lebowitz, Academic, London, 1995.
11. A. Achahbar, P. L. Garrido, J. Marro, and M. A. Muñoz, *Phys. Rev. Lett.* **87**, 195702 (2001), and references therein.
12. M. Díez-Minguito, J. Marro, and P. L. Garrido, *J. Phys. IV France 1*, (2007) (EDP Sciences) – Complex Systems: New Trends and Expectat; J. Marro, *Comp. Phys. Comm.* **179**, 144 (2008).
13. T. Halpin-Healy, and Y.-C. Zhang, *Phys. Rep.* **254**, 215 (1995); A. L. Barabási, and H. E. Stanley, *Fractal Concepts in Surface Growth*, Cambridge University Press, Cambridge, 1995 (and references therein); J. Krug, *Adv. Phys.* **46**, 139–282 (1997); For recent experimental realizations of the KPZ class see K. Takeuchi and M. Sano, *Phys. Rev. Lett.* **104** 230601 (2010).
14. H. Hinrichsen, *Adv. Phys.* **49**, 815 (2000); G. Ódor, *Rev. Mod. Phys.* **76**, 663 (2004); M. Henkel, H. Hinrichsen, and S. Lübeck, *Non-equilibrium Phase transitions*, Springer, Berlin, 2008. G. Ódor, *Universality In Nonequilibrium Lattice Systems: Theoretical Foundations*, World Scientific, Singapore, 2008; G. Grinstein, and M. A. Muñoz, “The Statistical Mechanics of Systems with Absorbing States”, in *Fourth Granada Lectures in Computational Physics*, edited by P. Garrido and J. Marro, Lecture Notes in Physics, Vol. 493 Springer, Berlin 1997, p. 223.
15. K. A. Takeuchi, M. Kuroda, H. Chate, and M. Sano, *Phys. Rev. Lett.* **99**, 234503 (2007).
16. H. K. Janssen, *Z. Phys. B* **42**, 151 (1981); P. Grassberger, *Z. Phys. B* **47**, 365 (1982).
17. G. Grinstein, Z.-W. Lai, and D. A. Browne, *Phys. Rev. A* **40**, 4820 (1989).
18. I. Jensen, and R. Dickman, *Phys. Rev. E* **48**, 1710 (1993); M. A. Muñoz, G. Grinstein, R. Dickman, and R. Livi, *Phys. Rev. Lett.* **76**, 451 (1996); íbid. *Physica D* **103**, 485 (1997). M. A. Muñoz, G. Grinstein, and R. Dickman, *J. Stat. Phys.* **91**, 541-569 (1998); C. López, and M. A. Muñoz, *Phys. Rev E.* **56**, 4864 (1997).
19. V. Elgart, and A. Kamenev, *Phys. Rev. E* **74**, 041101 (2006); J. Kockelkoren, and H. Chaté, cond-mat/0208497.
20. M. A. Muñoz, and R. Pastor-Satorras, *Phys. Rev. Lett.* **90**, 204101 (2003).
21. H. Hinrichsen, R. Livi, D. Mukamel, and A. Politi, *Phys. Rev. Lett.* **79**, 2710 (1997); F. de los Santos, M. M. Telo da Gama, and M. A. Muñoz, *Europhys. Lett.* **57**, 803 (2002); F. de los Santos, M. M. Telo da Gama, and M. A. Muñoz, *Phys. Rev. E.* **67**, 021607 (2003); A. C. Barato, *J. Stat. Phys.* **138**, 728 (2010); F. de los Santos and M. M. Telo da Gama, *Trends Stat. Phys.* **4**, 61 (2004).
22. M. A. Muñoz, *Phys. Rev. E.* **57**, 1377 (1998).

23. M. A. Muñoz, “Nonequilibrium Phase Transitions and Multiplicative Noise”, in *Advances in Condensed Matter and Statistical Mechanics*, edited by E. Korutcheva and R. Cuerno, Nova Science Publishers, 2004, p 34.
24. G. Grinstein, C. Jayaprakash, and Y. He, *Phys. Rev. Lett.* **55**, 2527 (1985).
25. J. Hooyberghs, F. Iglói, and C. Vanderzande, *Phys. Rev. Lett.* **90**, 100601 (2003).
26. E. Hernández-García, and C. López, *Phys. Rev. E* **70**, 016216 (2004).
27. F. Ramos, C. López, E. Hernández-García, and M. A. Muñoz, *Phys. Rev. E* **77** , 011116 (2008).
28. N. D. Mermin, and H. Wagner, *Phys. Rev. Lett.* **17**, 1133 (1966).
29. J. M. Kosterlitz, and D. J. Thouless, *J. Phys. C* **6**, 1181 (1973).
30. D. R. Nelson, *Defects and Geometry in Condensed Matter Physics*, Cambridge University Press, Boston, 2002; K. J. Strandburg, *Rev. Mod. Phys.* **60**, 161 (1988).
31. P. Grassberger et al., *J. Phys. A* **17**, L105 (1984); H. Takayasu, and A. Yu. Tretyakov, *Phys. Rev. Lett.* **68**, 3060 (1992). D. Zhong, and D. ben Avraham, *Phys. Lett. A* **209**, 333 (1995); N. Menyhárd, *J. Phys. A* **27**, 6139 (1994); N. Menyhárd, and G. Ódor, *Braz. J. Phys.* **30**, 113 (2000); M. H. Kim and H. Park, *Phys. Rev. Lett.* **73**, 2579 (1994); W. Hwang, et al. *Phys. Rev. E* **57**, 6438 (1998).
32. O. Al Hammal, H. Chaté, I. Dornic, and M. A. Muñoz, *Phys. Rev. Lett.* **94**, 230601 (2005); L. Canet, H. Chaté, B. Delamotte, I. Dornic, and M. A. Muñoz, *Phys. Rev. Lett.* **95**, 100601 (2005).
33. O. Al Hammal, J. A. Bonachela, and M. A. Muñoz, *J. Stat. Mech.* **12**, P12017 (2006).
34. R. Jack, P. Mayer, and P. Sollich, *J. Stat. Mech.* **12**, P03006 (2006).
35. G. Grinstein, *NATO Advanced Study Institute, Series B: Physics*, **344**, edited by A. McKane et al., Plenum, New York, 1995; H. J. Jensen, *Self Organized Criticality*, Cambridge University Press, 1998; D. Dhar, *Physica A* **369**, 29 (1999); M. Alava, in *Advances in Condensed Matter and Statistical Physics*, edited by E. Korutcheva and R. Cuerno, Nova Science, New York, 2004; D. L. Turcotte, *Rep. Prog. Phys.* **62**, 1377 (1999).
36. P. Bak, C. Tang, and K. Wiesenfeld, *Phys. Rev. Lett.* **59**, 381 (1987); *Phys. Rev. A* **38**, 364 (1988); see also D. Dhar, *Phys. Rev. Lett.* **64**, 1613 (1990); S. N. Majumdar, and D. Dhar, *Physica A* **185**, 129 (1992).
37. S. S. Manna, *J. Phys. A* **24**, L363 (1991); P. Grassberger, and S.S. Manna, *J. Phys. (France)* **51**, 1077 (1990); Y.-C. Zhang, *Phys. Rev. Lett.* **63**, 470 (1989); L.Pietronero, P. Tartaglia, and Y.-C. Zhang, *Physica A* **173**, 129 (1991); K. Christensen, A. Corral, V. Frette, J. Feder, and T. Jossang, *Phys. Rev. Lett.* **77**, 107 (1996).
38. R. Dickman, A. Vespignani, and S. Zapperi, *Phys. Rev. E* **57**, 5095 (1998); A. Vespignani, R. Dickman, M. A. Muñoz, and S. Zapperi, *Phys. Rev. Lett.* **81**, 5676 (1998); R. Dickman, M. A. Muñoz, A. Vespignani, and S. Zapperi *Braz. J. Phys.* **30**, 27 (2000); A. Vespignani, R. Dickman, M. A. Muñoz, and S. Zapperi, *Phys. Rev. E* **62**, 4564 (2000); J. A. Bonachela, J. J. Ramasco, H. Chaté, I. Dornic, and M. A. Muñoz, *Phys. Rev. E.* **74**, 050102(R) (2006); J. A. Bonachela, and M. A. Muñoz, *Phys. Rev. E* **78**, 041102 (2008).
39. R. Pastor-Satorras, and A. Vespignani, *Phys. Rev. E* **62**, R5875 (2000); R. Pastor-Satorras and A. Vespignani, *Eur. Phys. J. B* **19**, 583 (2001); S. Lübeck, *Int. J. Mod. Phys. B* **18**, 3977 (2004).
40. L. P. Kadanoff, S. R. Nagel, L. Wu, and S. Zhou, *Phys. Rev. A* **39**, 6524 (1989); C. Tebaldi, M. De Menech, and A. L. Stella , *Phys. Rev. Lett.* **83**, 3952 (1999); O. Biham, E. Milshtein, and O. Malcai, *Phys. Rev. E* **63**, 061309 (2001).
41. M. Alava, and M.A. Muñoz, *Phys. Rev. E* **65**, 026145 (2002); J. A. Bonachela, H. Chaté, I. Dornic, and M. A. Muñoz, *Phys. Rev. Lett.* **98**, 155702 (2007); J. A. Bonachela, M. Alava, and M. A. Muñoz, *Phys. Rev. E* **79**, R050106 (2009).
42. O. Narayan, and A. A. Middleton, *Phys. Rev. B* **49**, 244 (1994); M. Paczuski, S. Maslov, and P. Bak, *Phys. Rev. E* **53**, 414 (1996); M. Paczuski and S. Boettcher, *Phys. Rev. Lett.* **77**, 111 (1996); M. Alava, and K. B. Lauritsen, *Europhys. Lett.* **53**, 569 (2001); G. Pruessner, *Phys. Rev. E* **67**, 030301(R) (2003).
43. O. Delobrière, and F. van Wijland, *Phys, Rev. E* **65**, 046104 (2002).
44. A. C. Barato, J. A. Bonachela, C. E. Fiore, H. Hinrichsen, M. A. Muñoz, *Phys. Rev. E* **74**, 041130 (2009).
45. I. Dornic, H. Chaté, and M. A. Muñoz, *Phys. Rev. Lett.* **94**, 100601 (2005).

Fourier law, phase transitions, and the Stefan problem

Errico Presutti

Dipartimento di Matematica, Università di Roma Tor Vergata, Via della Ricerca Scientifica 1, 00133 Roma, Italy, presutti@mat.uniroma2.it

Abstract. When hydrodynamic or thermodynamic limits are performed in systems which are in the phase transitions regime we may observe perfectly smooth profiles develop singularities with the appearance of sharp interfaces. I will discuss the phenomenon in stationary non equilibrium states which carry non zero steady currents. The general context is the one where the Fourier law applies, but here it is complemented by a free boundary problem due to the presence of interfaces.

I will specifically consider an Ising system with Kac potentials which evolves under the stochastic Kawasaki dynamics. In a continuum limit the evolution is described by an integro-differential equation, as proved by Giacomin and Lebowitz in [2], see also [3]. I will then study its stationary solutions with a non zero current (produced by suitable boundary conditions) and derive, in the infinite volume limit, macroscopic profiles with an interface proving that the profiles satisfy a stationary Stefan problem and obey the Fourier law.

Keywords: Simple exclusion, Kac potentials, non local equations
PACS: 82, 35q

FOURIER'S LAW

We shall call conservative a dynamics where there is "an extensive quantity" conserved in the course of time, for instance energy, mass, or magnetization which are those considered in the following. If a quantity is conserved it means that it cannot be created nor destroyed, so it can only move and there is therefore a current which describes its motion. If $\rho(r,t) \in R_+$ is the density [of the conserved quantity] and $I(r,t) \in R^d$ the corresponding current the conservation law is expressed by the relation

$$\frac{\partial \rho}{\partial t} = -\nabla \cdot I \tag{1}$$

The Fourier's law holds if the current vector I is directed opposite to the gradient of ρ, more precisely

$$I = -D\nabla\rho \tag{2}$$

where $D > 0$ may be either a constant or a function of ρ. (1) and (2) together yield the conservation law

$$\frac{\partial \rho}{\partial t} = \nabla\Big(D\nabla\rho\Big) \tag{3}$$

More properly the Fourier's law refers to the case where the conserved quantity is the energy and the corresponding current is the heat current; when the conserved quantity is the mass (2) is called "the Fick's law", for brevity I will in the sequel refer to (2) as the Fourier's law no matter what is the conserved quantity. (3) is a diffusion equation with diffusion coefficient D, if D is a positive constant then (3) is the well known linear heat equation. When D depends on ρ (3) is the non linear heat equation. We shall see that if the fluid undergoes a phase transition then D may vanish and (3) becomes a free boundary problem. But this will come later after discussing the microscopic origin of the law.

THE SIMPLE EXCLUSION PROCESS

We shall eventually study the phase transition regime, but it is better to start from the simpler case of a lattice gas at infinite temperature (ideal gas). Lattice gas means that particles may only stay on the sites of the lattice Z^d (or of a finite subset Λ of Z^d) and that on each site there is at most one particle. Particles configurations are then functions $\eta(x)$, $x \in Z^d$, or $x \in \Lambda$, with values in $\{0,1\}$. In the ideal gas all allowed configurations are equally likely, therefore the stochastic evolution of the ideal gas is defined so that each particle independently of the others with same rate 1 "decides" to jump to one of its nearest neighbor sites: the jump then takes place if the chosen site is empty, otherwise the jump is suppressed. Rate 1 means that each possible jump has a clock which rings after an exponentially distributed time of mean 1, when the clock rings then the particle decides to jump; all clocks are independent of each other.

The expected current from x to $x+1$ is then

$$I = E\Big[\eta(x)\big(1-\eta(x+1)\big) - \eta(x+1)\big(1-\eta(x)\big)\Big] \tag{4}$$

Calling $\rho(x) = E[\eta(x)]$ we then have

$$I = -\Big(\rho(x+1) - \rho(x)\Big) =: -\nabla\rho \tag{5}$$

because the non linear terms on the right hand side of (4) cancel with each other (this is the big simplification of the process which for this reason is called the simple exclusion process, SEP).

Fourier's law thus holds already at the microscopic level and the "hydrodynamic equation" for the SEP is indeed the linear heat equation.

A MECHANISM FOR PHASE TRANSITIONS

In the late 80's Joel Lebowitz, inspired by some nice numerical simulations on phase separation by Rothman and Zaleski, proposed to modify the rules of the SEP in order to induce a phase transition. Referring for notational simplicity to $d = 1$, in Joel's proposal the rate to jump from say x to $x+1$ is modified into $\eta(x)\big(1-\eta(x+1)\big)\Big(1+B\Big)$, B the bias as with $B = 0$ this is the SEP. To have a bias toward higher densities we then set

$$B = \frac{c}{N^2}\sum_{\ell=1}^{N}\Big(\eta(x+\ell) - \eta(x-\ell)\Big) \tag{6}$$

FIGURE 1. $a_\beta(m)$ is flat in $[-m_\beta, m_\beta]$

Indeed if the are more particles to the right than to the left of x, B is positive while it is negative if there are more particles to the left than to the right. Writing (6) as

$$B = c\sum_{\ell=1}^{N} w(\ell;N)\Big(\frac{\eta(x+\ell)-\eta(x-\ell)}{2\ell}\Big), \quad w(\ell;N) := \frac{2\ell}{N^2}$$

we see B as a weighted average of discrete gradients, the weights converging to a probability distribution as $N \to \infty$.

If we repeat the computation in (4) for the expected current across the bond $(x, x+1)$ we then get

$$I \approx -\nabla\rho\Big(1 - 2c\rho(1-\rho)\Big) \tag{7}$$

The approximation comes from: • supposing the validity of a chaos property under which the measure factorizes; • identifying all the gradients $\dfrac{\rho(x+\ell)-\rho(x-\ell)}{2\ell}$ with a same $\nabla\rho$, we shall come back later on the validity of such approximations.

What happens to Fourier law if c is large ? The right hand side of (7) becomes negative if c is large and ρ is not too close to 0 or 1 and the current becomes directed as the gradient, contrary to Fourier's law. As we shall this is related to the occurrence of a phase transition.

THE STEFAN PROBLEM

Let us next see how the problem looks like at the macroscopic level and how it is solved. With in view applications to the Ising model it is convenient to have here the magnetization as order parameter. At phase transition the diagram of the free energy density $a_\beta(m)$ (β the inverse temperature, $\beta > \beta_c$, the critical value; m the magnetization density) has a flat segment $[-m_\beta, m_\beta]$ (we suppose $a_\beta(m)$ even) and it is strictly convex elsewhere, as in Fig. 1.

The non equilibrium free energy of a magnetization profile $m = m(r)$ is given (under a local equilibrium assumption) by the "barometric formula"

$$F_\beta(m) = \int_\Lambda a_\beta\big(m(x)\big)dx \tag{8}$$

By the second law of thermodynamics the free energy decreases (more precisely does not increase) in time. A natural way to implement such a property is to define the dynamics as a flow directed against the gradient. If we want a conservative dynamics we then set

$$\frac{\partial m}{\partial t} = -\nabla I, \quad I = -\chi \nabla \frac{\delta F(m)}{\delta m(x)} = -\chi a''_\beta(m) \nabla m \tag{9}$$

$\chi = \chi(m)$ a mobility coefficient suppose strictly positive and even; $D(m) := \chi a''_\beta(m)$ is the diffusion coefficient. Indeed if m_t is a solution of the equations of motion then

$$\frac{d}{dt} F(m_t) = -\int \chi |\nabla \frac{\delta F(m)}{\delta m(x)}|^2 \leq 0 \tag{10}$$

Also with the evolution (9) we find problems with the Fourier's law: suppose $m(x)$, $|x| \leq \ell$, is a one-dimensional stationary profile with $m(\pm\ell) = m_\pm$, $m_+ > m_\beta > -m_\beta > m_-$. The stationary current I is then spatially constant hence if m takes values in $[-m_\beta, m_\beta]$ (which is certainly the case if m is continuous) by (9) it must be $I = 0$. Thus the validity of the Fourier's law is strictly related to the appearance of singularities. Solutions of (9) are then defined in terms of a "free boundary problem".

The Stefan problem. Find $m = m(r,t)$, $r \in \Lambda$, $t \geq 0$, and $\Omega_t \subset \Lambda$ both smooth so that denoting by n the unit outward normal to $\partial\Omega$ and by $[f]$ the discontinuity of f across $\partial\Omega$ coming from inside Ω, ($[f] = f_+ - f_-$):

- $m(r,t) < -m_\beta$, $r \in \Omega_t \setminus \partial\Omega$, $m(r) \to -m_\beta$ as $r \to \partial\Omega$
- $m(r,t) > m_\beta$, $r \in \Omega^c \setminus \partial\Omega$, $m(r) \to m_\beta$ as $r \to \partial\Omega$
- $\dfrac{\partial m}{\partial t} = \nabla\Big(\chi a''_\beta(m) \nabla m\Big)$ in the interior of Ω_t and of Ω_t^c while the points on $\partial\Omega$ have velocity v such that

$$(2m_\beta)\mathrm{v} \cdot n = [I \cdot n], \quad r \in \partial\Omega \tag{11}$$

(11) follows from the conservation law. Indeed if Ω_t would not move then $(I_- \cdot n)d\Sigma$ and $-(I_+ \cdot n)d\Sigma$ would be the amounts of magnetization per unit time which leave Ω_t and respectively Ω_t^c through $d\Sigma$, thus $-[I \cdot n]d\Sigma$ is the magnetization change in Ω_t due to the current flux through $d\Sigma$. If on the other hand the magnetization was frozen while the interface $\partial\Omega$ moves with velocity vv, then, since $[m] = 2m_\beta$ at $\partial\Omega$, the contribution to the magnetization change in Ω_c is $-2m_\beta \mathrm{v} \cdot n d\Sigma$, hence (11).

The stationary case. In a time independent solution $\Omega_t = \Omega$ is constant, $\mathrm{v} = 0$ and therefore $I \cdot n$ is continuous across $\partial\Omega$. Supposing a planar symmetry, $I = I(x)$, $m = m(x)$, I is the same constant vector in Ω and Ω^c (as it is continuous across $\partial\Omega$); thus $I = -\chi \nabla m$ in $\Lambda \setminus \partial\Omega$ where ∇m is not defined. The Fourier's law is then valid at almost all points, i.e. away from the interface. We can however reformulate the Fourier's law so that it is valid at all points. Recall that the magnetic field h is the conjugate variable to m defined as $h := a'_\beta(m)$. The gradient flow dynamics is then

$$I = -\chi \nabla h \tag{12}$$

which shows that in the stationary case ∇h is continuous at the interface (recall that χ being even is continuous at the interface) so that in the form (12) the Fourier's law is valid everywhere. (12) is therefore a better formulation of the Fourier's law which is equivalent to the other away from phase transitions but which remains valid when they are present.

KAWASAKI DYNAMICS AND KAC POTENTIALS

As suggested by Herbert Spohn it is possible to interpret the Lebowitz rates in (6) in terms of Gibbs measures. As mentioned before it is now convenient to have spins rather than particles, so that instead of $\eta(x) \in \{0,1\}$ we have $\sigma(x) \in \{-1,1\}$. The hamiltonian is

$$H(\sigma) = -\frac{1}{2}\sum_{x\neq y} J_\gamma(x,y)\sigma(x)\sigma(y), \quad J_\gamma(x,y) = \gamma^d J(\gamma|y-x|) \tag{13}$$

where $\gamma > 0$ is "the Kac scaling parameter" and $J(|r|)$ a smooth, finite range, probability density. The range of the interaction scales as γ^{-1} so that a spin does interact with $\approx \gamma^{-d}$ other spins, hence the pre-factor γ^d in (13). The model for $\gamma > 0$ small does resemble mean field, yet for any $\gamma > 0$ it is a finite range interaction which is then likely to belong to the same universality class as the nearest neighbor Ising model. Dynamics is defined in the same spirit as the gradient flow dynamics in the macroscopic theory. In fact the rate at which the spins at two neighbor sites x and y exchange with each other is:

$$c(x,y;\sigma) = \exp\Big\{ -\frac{\beta}{2}\Big(H(\sigma^{(x,y)}) - H(\sigma)\Big)\Big\} \tag{14}$$

where $\sigma^{(x,y)}$ is obtained from σ by exchanging $\sigma(x)$ and $\sigma(y)$. One can easily check the detailed balance condition $\mu(\sigma)c(x,y;\sigma) = \mu(\sigma^{(x,y)})c(x,y;\sigma^{(x,y)})$, μ the Gibbs measure at inverse temperature β, which implies that μ is invariant under the evolution defined by the rates (14).

The difference $H(\sigma^{(x,y)}) - H(\sigma)$ is infinitesimal in γ as $\gamma \to 0$ and to leading order becomes equal to the Lebowitz rates in (6) for a suitable choice of J.

PHASE TRANSITIONS

The equilibrium theory for the Ising model with Kac potentials of (13) gives:

Theorem. 1 *In* $d \geq 2$ *for any* $\beta > 1$ *there is* $\gamma_\beta > 0$ *so that for all* $\gamma \leq \gamma_\beta$ *the thermodynamic free energy density* $a_{\beta,\gamma}(m)$ *is linear in the interval* $|m| \leq m_{\beta,\gamma}$ *and*

$$\lim_{\gamma\to 0} m_{\beta,\gamma} = m_\beta, \quad m_\beta = \tanh\{\beta m_\beta\} \tag{15}$$

A stronger version is proved in the literature, see for instance [5], Theorem 9.1.4.1, and references therein. The theorem shows that the phase transition is of mean field type and indeed $m_\beta = \tanh\{\beta m_\beta\}$ is the well known mean field equation for the magnetization. As already remarked this is not at all trivial as the statement holds for finite γ where the interaction has strictly finite range and indeed, in $d = 1$ there is no phase transition unlike in the mean field model where the analysis is dimension independent. We have thus reproduced at the microscopic level the setup we had in the macroscopic theory, let us now turn to dynamics.

HYDRODYNAMIC LIMITS

Hydrodynamic limits describe the behavior of the system on large space-time scales. Based on the analysis of many stochastic particle systems we conjecture that if $\sigma(x,t)$ denotes the spin at site x and time t under the evolution defined by the rates (14), then for any test function ϕ, in probability

$$\lim_{\varepsilon\to 0} \varepsilon^d \sum_x \phi(\varepsilon x)\sigma(x,\varepsilon^{-2}t) = \int \phi(r)m(r,t) \tag{16}$$

where m solves:

$$\frac{\partial m}{\partial t} = \nabla\Big(D\nabla m\Big) \tag{17}$$

As discussed in [3] we do not expect D to be as in the macroscopic theory, see below (12), but to have a more complex expression as given by the Green-Kubo formula.

The problem simplifies if we scale ε proportionally to γ, the Kac scaling parameter. This is not a hydrodynamic limit and it is referred to as “a mesoscopic” or “kinetic” limit. In this case it is indeed proved, see [2], that:

$$\lim_{\gamma\to 0} \gamma^d \sum_x \phi(\gamma x)\sigma(x,\gamma^{-2}t) \;=\; \int \phi(r)m(r,t) \tag{18}$$

where m solves the non local integro-differential equation

$$\frac{\partial m}{\partial t} = \nabla\Big(\nabla m - \beta(1-m^2)\nabla J * m\Big), \quad J*m(r) = \int J(|r-r'|)m(r') \tag{19}$$

which makes rigorous the heuristic argument presented in Section 3.

Our goal is to study the stationary profiles thus the correct limit is to take first $t \to \infty$ and then $\gamma \to 0$. We are not able to do that and we exchange the limits studying first the limit $\gamma \to 0$ and then the stationary solutions of (19) in the thermodynamic limit. The interchange of limits is not innocent, indeed in [4] it is proved that (16) holds if $\varepsilon = \gamma^b$, $b > 1$ (but “close to 1”) and when phase transitions are absent. The limit profile m satisfies (17) with $D = \chi a''_\beta(m)$, $\chi = (1-m^2)$, in agreement with the macroscopic theory, thus in the simultaneous limit when $\gamma \to 0$ together with the space-time scaling parameter ε we loose the time fluctuations contribution to the diffusion which is predicted by the Green-Kubo formula.

FREE ENERGY FUNCTIONALS AND LYAPUNOV FUNCTIONS

As discussed in Chapter 4, see Subsection 4.2.4, of [5] the equilibrium large deviations in the limits $\gamma \to 0$ are described by the functional

$$F(m) = \int \Big(-\frac{1}{2} mJ * m - \frac{S(m)}{\beta} \Big) \tag{20}$$
$$S(m) := -\frac{1-m}{2} \log \frac{1-m}{2} - \frac{1+m}{2} \log \frac{1+m}{2}$$

where $-\frac{1}{2} mJ * m$ is the continuum version of the hamiltonian (13) and $S(m)$ is the entropy of the product measure with magnetization m. Thus $F(m)$ has the familiar expression of energy minus T times the entropy.

$F(m)$ is the starting point of the mesoscopic equilibrium theory which goes back to the van der Waals works, as explained in Chapter 5 of [5]. Gradient flow dynamics can be defined starting from $F(m)$ just as we did in the macroscopic theory and (19) is equal to

$$\frac{\partial m}{\partial t} = -\nabla \Big(-\chi \nabla \frac{\delta F(m)}{\delta m(x)} \Big), \quad \chi = \beta(1-m^2) \tag{21}$$

which shows the close relation between the Kawasaki stochastic dynamics and the gradient flow dynamics in the limit $\gamma \to 0$. If m_t is a solution of (21) then

$$\frac{d}{dt} F(m_t) = -\int \chi |\nabla \frac{\delta F(m)}{\delta m(x)}|^2 \le 0 \tag{22}$$

which also shows that the free energy $F(m)$ does not increase with time and it is therefore a Lyapunov function for the evolution (19).

To have a better insight on the nature of (19), let us first rewrite $F(m)$ as

$$F(m) = \int f_\beta(m) + \frac{\beta}{4} \int \int J(|r-r'|) \Big(m(r) - m(r') \Big)^2 \tag{23}$$
$$f_\beta(m) := -\frac{m^2}{2} - \frac{S(m)}{\beta}$$

which is evidently a non local version of the well-known Ginzburg-Landau functional

$$F_{\mathrm{GL}}(m) = \int \Big(f_\beta(m) + c|\nabla m|^2 \Big) \tag{24}$$

The gradient flow dynamics for $F_{\mathrm{GL}}(m)$ (with $\chi = 1$) is the Cahn-Hilliard equation

$$\frac{\partial m}{\partial t} = -\Delta \Big(c\Delta m - f'_\beta(m) \Big) \tag{25}$$

We should therefore regard (21) as a non local version of the Cahn-Hilliard equation.

THE STATIONARY PROBLEM

We are finally ready to discuss the Fourier's law. We consider the stationary solution of the equation (19) defined in a cylinder of length 2ℓ and cross section a square of side $2R$, thus $\Lambda = \{(x,y,z) : |x| \le \ell, |y| \le R, |z| \le R\}$. We define the convolution $J * m$ by imposing periodic boundary conditions in the $y-z$ coordinates and Neumann conditions in the x-coordinates (namely the convolution sees a reflected m in the x coordinates while m is periodic in the $y-z$ coordinates). The problem is then well defined by specifying the values of m at $x = \pm\ell$: we impose that $m(\pm\ell) = m_\pm$ with $m_- < -m_\beta < m_\beta < m_+$. By looking for solutions with a planar symmetry, i.e. $m = m(x)$ we are then reduced to a one dimensional problem, in other words we may and will suppose that $d = 1$. Summarizing, we are looking for $m(x)$, $|x| \le \ell$, and a constant I so that

$$-\Big(\frac{dm}{dx} - \beta(1-m^2)\frac{d}{dx}\nabla J * m\Big) = I, \quad m(\pm\ell) = m_\pm \tag{26}$$

where $J * m$ is defined with Neumann conditions, in the sense explained above. In [1] it is proved that

Theorem. 2 *For all ℓ small enough there is a smooth increasing solution $m(x|\ell)$ of (26). Moreover there are $r_0 \in (-1,1)$ and a smooth increasing function $u(r)$, $r \ne r_0$, so that $|u(r)| > m_\beta$, $\lim_{\ell\to\infty} m(\ell r|\ell) = u(r)$ and*

$$\frac{d}{dr}\Big(\beta(1-u^2)\frac{d}{dr}a'_\beta(u)\Big) = 0, \quad u(\pm 1) = m_\pm,\ u(r_0^\pm) = \pm m_\beta \tag{27}$$

SELF CONSISTENT FIELDS

As discussed after (12) it is convenient to reformulate the problem in terms of magnetic fields. Following the thermodynamic prescription that the magnetic field is the derivative of the free energy with respect to the magnetization density we set

$$h(x) := \frac{\delta F(m)}{\delta m(x)} = \frac{1}{2\beta}\log\frac{1+m}{1-m} - J * m \tag{28}$$

so that the stationary problem (26) becomes

$$-\chi\frac{dh(x)}{dx} = I, \quad m = \tanh\big\{\beta J * m + \beta h\big\} \tag{29}$$

(29) has a nice physical interpretation. In the presence of an external magnetic field $h(\cdot)$ there is an additional term $-\int hm$ to the energy so that the free energy functional becomes:

$$F_h(m) := F(m) - \int mh \tag{30}$$

The non conserved evolution equation is then

$$\frac{\partial m}{\partial t} = -\frac{\partial F_h(m)}{\partial m(x)} = -\frac{1}{\beta}\text{arctanh}(m) + J * m + h \tag{31}$$

If we use instead the Ginzburg-Landau functional we then get the Allen-Cahn equation

$$\frac{\partial m}{\partial t} = \Delta m - \Big(\frac{1}{\beta}\operatorname{arctanh}(m) - m - h\Big) \tag{32}$$

The stationary solution of (31) is $m = \tanh\{\beta J * m + \beta h\}$, i.e. the second relation in (29), it is the response of the system to the external field $h = h(\cdot)$. Physically each point x of the system is in contact with a reservoir which acts on x with a magnetic field $h(x)$. On x acts also the molecular field $J * m(x)$ (which is the sum of the action that all the other parts of the system exert on x). The reservoirs exchange also magnetization with the system, indeed if $\nabla \cdot I \neq 0$ and since $\dfrac{\partial m}{\partial t} = 0$ the conservation law is violated, which means that the reservoirs absorb the excess magnetization $-\nabla I = -\nabla(-\chi \frac{\delta F(m)}{\delta m(x)})$. A magnetization field h is called "self-consistent" if the reservoir do not exchange magnetization with the system and this means that (29) holds.

A FIXED POINT PROBLEM

As seen in the previous section the stationary problem (26) can be formulated in the following way: find smooth functions $m(x)$ and $h(x)$, $|x| \leq \ell$, so that (29) holds. As a preliminary step we shall study a slightly modified problem: for fixed $r_0 \in (-1,1)$ and $I < 0$, find smooth functions $m(x)$ and $h(x)$, $|x| \leq \ell$, so that

$$h(x) = -\frac{1}{\ell}\int_{r_0\ell}^{x} \frac{I}{\beta(1-m^2(y))} \tag{33}$$

$$m(x) = \tanh\Big\{\beta J * m(x) + \beta h(x)\Big\} \tag{34}$$

(33) can then be stated as a fixed point problem. Define a map $m \to m'$ in two steps: given m find h using (33) and then m' by solving (34) with the h found in the first step. If we have a smooth fixed point of this map we then have a solution of (29) and by varying r_0 and I it will then be possible to match the boundary conditions at $\pm\ell$. The existence of a fixed point is proved by showing that iterates of the map (starting from a suitable initial point) converge, the limit then defines the desired fixed point. Suppose we have proved that given h there is m which solves (34), then to control the iteration scheme we need estimates on how much m changes if we change h by a small quantity δh. To first order m changes by $\delta m =: \psi$ with ψ solution of the linearized map:

$$L\psi = \beta(1-m^2)\delta h, \quad L\psi = (A-1)\psi, \; A\psi = \beta(1-m^2)J * \psi \tag{35}$$

having used that $\cosh^{-2} = 1 - \tanh^2$. Since $m_\beta = \tanh\{\beta m_\beta\}$, $\beta(1-m_\beta^2) < 1$ (as it can be easily checked). Thus there is $m'_\beta < m_\beta$ so that for $|m| \geq m'_\beta$, $\beta(1-m^2) \leq \alpha < 1$. Thus if $|m(x)| \geq m'_\beta$ then $|A\psi(x)| \leq \alpha \|\psi\|_\infty$. However since $\beta > 1$ if $m(x) = 0$ then the contraction property fails. We thus find again what seen in the beginning of this presentation, namely that the problems arise in a neighborhood of $m = 0$, that is at the interface between the plus and the minus phases.

The optimal way to connect plus and minus phases is a very interesting problem in its own which goes back to van der Waals. The problem is to minimize the free energy functional $F(m)$ of (23) with the constraint that $\lim_{x\to\pm\infty} m(x) = \pm m_\beta$. It has been proved, see Section 8.1 in Chapter 8 of [5] and references therein, that the minimum is achieved uniquely (modulo translations), that the minimizer, $\bar{m}(x)$, is a strictly increasing, antisymmetric smooth function which converges exponentially fast to m_β as $x \to \infty$ and is a critical point of the functional, namely it solves the equation $m = \tanh\{\beta J * m\}$. The proof is not simple and it uses dynamics. Let m_0 be a smooth non decreasing antisymmetric function equal to m_β for $x > 1$. Let then m_t be the solution at time $t > 0$ of

$$\frac{dm_t}{dt} = -m_t + \tanh\{\beta J * m_t\} \tag{36}$$

(starting from m_0). It can be easily checked that m_t is antisymmetric and non decreasing. Moreover $F(m_t)$ is a non increasing function of t and $F(m_0) < \infty$. Then the argument in the Lyapunov theorem can be adapted to show that (by subsequences) m_t converges to a stationary solution m^* of (36) and that $F(m^*) \le F(m_0)$. Since m^* is non decreasing it has a limit C as $x \to \infty$. Since $F(m^*) < \infty$ $|C| = m_\beta$ and since m^* is antisymmetric, $C = m_\beta$ and $\lim_{x\to-\infty} \bar{m}(x) = -m_\beta$.

There is another important property of the "instanton" $\bar{m}$ namely that the operator $A := \beta(1-\bar{m}^2)J*$ has an eigenvalue 0 (with eigenvector $\bar{m}'$ as it can be easily checked), moreover 0 is a simple eigenvalue and there is a spectral gap with the rest of the spectrum away in the negative axis. This is proved using the Perron-Frobenius theorem, details can be found in Section 8.3 of Chapter 8 in [5].

The iteration scheme to find the fixed point works more easily if we suppose $r_0 = 0$ and work in the space of antisymmetric functions. In such a case the starting point m_0 of the iteration is equal to $\bar{m}(x)$ for $|x| \le c \log \ell$, with c suitably chosen. After $c \log \ell$ m_0 is the rescaled solution of the macroscopic equation. It turns out that at all steps of the iteration h and m are antisymmetric so that $\beta(1-m^2)\delta h$, see (35), is also antisymmetric. Antisymmetric functions do not have a component along the eigenvector $\bar{m}'$ (which is symmetric) hence they have good decay properties (for the operator linearized around $\bar{m}$). Using these properties it is possible to prove a contraction property for (35) and then, eventually, the convergence of the iteration. The non symmetric case is much more complex and one has at each step to suitably shift the functions to avoid the dangerous components along $\bar{m}'$, but this is too technical and I refer for the proof to the original paper, [1].

ACKNOWLEDGMENTS

This paper profits of several comments and remarks following my presentation of the subject at the Granada seminars, for which I am very indebted. I also acknowledge very kind hospitality at La Harradura.

REFERENCES

1. A. De Masi, E. Presutti, and D. Tsagkarogiannis, preprint 2009.
2. G. B. Giacomin, and J.L. Lebowitz, *J. Stat. Phys.* **87**, 37–61, (1997); *SIAM J. Appl. Math.* **58**, 1707–29, (1998).
3. G. B. Giacomin, J. L. Lebowitz, and R. Marra, *Nonlinearity* **13**, 2143–2162 (2000).
4. J. L. Lebowitz, E. Orlandi, and E. Presutti *J. Stat. Phys.* **63**, 933–974 (1991).
5. E. Presutti, *Theoretical and Mathematical Physics*, Springer, Berlin-Heidelberg, 2009.

Bringing thermodynamics to non-equilibrium microscopic processes

J. Miguel Rubí

Departament de Fisica Fonamental, Facultat de Fisica, Universitat de Barcelona, Diagonal 647, 08028 Barcelona, Spain

Abstract. We present recent developments that extend the applicability of thermodynamic concepts deep into mesoscopic and irreversible regimes. We show how a probabilistic interpretation of thermodynamics together with probability conservation laws can be used to obtain Fokker-Planck equations for the relevant degrees of freedom. This approach provides a systematic method to obtain the stochastic dynamics of a system directly from the knowledge of its equilibrium properties. A wide variety of situations can be studied in this way, including many that were thought to be out of reach of thermodynamic theories, such as non-linear transport in the presence of potential barriers, activated processes, slow relaxation phenomena, and basic processes in biomolecules, like translocation and stretching.

Keywords: Mesoscopic level, non-equilibrium thermodynamics, non-equilibrium systems
PACS: 05.70.-a, 05.40.-a

INTRODUCTION

Systems in conditions of equilibrium strictly follow the rules of thermodynamics [1]. In such cases, despite the intricate behaviour of large numbers of molecules, the system can be completely characterized by a few variables that describe global average properties. The extension of thermodynamics to non-equilibrium situations entails the revision of basic concepts such as entropy and its related thermodynamic potentials as well as temperature that are strictly defined in equilibrium.

Non-equilibrium thermodynamics proposes such an extension [2] for systems that are in local equilibrium. Despite its generality, this theory is applicable only to situations in which the system manifests a deterministic behaviour where fluctuations play no role. Moreover, non-equilibrium thermodynamics is formulated in the linear response domain in which the fluxes of the conserved local quantities (mass, energy, momentum, etc.) are proportional to the thermodynamic forces (gradients of density, temperature, velocity, etc.). While the linear approximation is valid for many transport processes, such as heat conduction and mass diffusion, even in the presence of large gradients, it is not appropriate for activated processes such as chemical and biochemical reactions in which the system immediately enters the non-linear domain or for small systems in which fluctuations may be relevant.

To circumvent these limitations, one has to perform a probabilistic description of the system, which in turn has to be compatible with thermodynamic principles. We have recently proposed such a description [3], [4] aimed at obtaining a simple and comprehensive description of the dynamics of non-equilibrium systems at the mesoscopic scale. The theory, mesoscopic non-equilibrium thermodynamics (MNET), has provided a deeper understanding of the concept of local equilibrium [5] and a framework, reminiscent of non-equilibrium thermodynamics, through which fluctuations in non-linear systems can be studied. The probabilistic interpretation of the density together with conservation laws in phase-space and positiveness of global entropy changes set the basis of a theory similar to non-equilibrium thermodynamics in the method but of a much broader range of applicability. In particular, the fact of its being based on probabilities instead of densities allows for the consideration of mesoscopic systems and their fluctuations. The situations that can be studied with this formalism include, among others, slow relaxation processes, barrier crossing dynamics, chemical reactions, entropic driving, non-linear transport, and anomalous diffusion, processes which are generally non-linear. From the methodological point of view, given the equilibrium properties of a system, this theory provides a systematic and straightforward way to obtain stochastic non-equilibrium dynamics in terms of Fokker-Planck equations.

To set the basis for the development of the theory, we discuss first the basic concepts of MNET and proceed afterwards with the application of the theory to two illustrative cases: Brownian motion in a fluid in a stationary state and activated processes. The use of the theory in the study of a chemical reaction shows categorically how an adequate formulation of the local equilibrium hypothesis performed at the mesoscale is able to reproduce the intrinsic non-linear dynamics of these processes.

THERMODYNAMICS AND STOCHASTIC DYNAMICS

Scaling-down the size of a system usually brings about an increase in the number of degrees of freedom which have not yet equilibrated and that therefore influence the dynamics of the system. The nonequilibrated degrees of freedom, denoted by γ, may for example represent the velocity of a particle, the orientation of a spin, the size or the monomers of a macromolecule or any coordinate or order parameter whose values define the state of the system in a phase space. The characterization at the mesoscopic level of the state of the system follows from $P(\gamma,t)$ the probability density of finding the system at the state γ at time t. The entropy of the system in terms of this probability can be expressed through the Gibbs entropy postulate

$$S = S_{eq} - k_B \int P(\gamma,t) ln \frac{P(\gamma,t)}{P_{eq}} d\gamma \tag{1}$$

where S_{eq} is the entropy of the system when the degrees of freedom are at equilibrium. The equilibrium probability density is given by

$$P_{eq} \approx exp\left(\frac{-\Delta W(\gamma)}{k_B T}\right) \tag{2}$$

Here $\Delta W(\gamma)$ is the minimum reversible work required to create that state [6], k_B is Boltzmann's constant, and T is the temperature of the heat bath. Variations of the minimum work for a thermodynamic system are expressed as

$$\Delta W = \Delta E + pdV - T\Delta S - \mu dM + y\Delta Y \tag{3}$$

Here E is the internal energy, T the temperature of the bath, p the pressure, V the volume, μ the chemical potential and M the mass. The term $y\Delta Y$ represents other types of work: electric, magnetic or surface work, performed on the system. The expressions for these works is always the product of an intensive parameter y and the variation of its conjugated extensive variable ΔY. The expression of the minimum reversible work reduces to the different thermodynamic potentials by imposing the corresponding constraints that define those potentials [7]. Any other definition of work is not connected with the free energy of the system and may lead to inconsistencies [8]. The statistical mechanics definition of the entropy is therefore the key to connect thermodynamics with both the mesoscopic description in terms of the probability distribution $P(\gamma,t)$ and the equilibrium behavior of the system.

The combination of the statistical definition of the entropy with the systematic methodology of nonequilibrium thermodynamics, results in a powerful framework to describe the kinetics of a wide class of systems. To describe the dynamics of the mesoscopic degrees of freedom, the starting point is the statistical mechanics definition of the entropy given through the Gibbs entropy postulate. Taking variations in Eq. (1), one obtains

$$\delta S = -k_B \int \delta P(\gamma,t) ln \frac{P(\gamma,t)}{P_{eq}} d\gamma \tag{4}$$

The evolution of the probability density in the γ-space is governed by the continuity equation

$$\frac{\partial P}{\partial t} = -\frac{\partial J}{\partial \gamma} \tag{5}$$

where $J(\gamma,t)$ is a current in γ-space which has to be specified. Its form can be obtained by taking the time derivative in equation (4) and by using the continuity equation (5) to eliminate the probability time derivative. After a partial integration, one then arrives at

$$\frac{dS}{dt} = \int d\gamma \frac{\partial J_s}{\partial \gamma} \tag{6}$$

where

$$J_s = k_B J ln \frac{P}{P_{eq}} \tag{7}$$

is the entropy flux, and

$$\sigma = -k_B \int J(\gamma,t) \frac{\partial}{\partial \gamma} \left(ln \frac{P(\gamma,t)}{P_{eq}(\gamma)} d\gamma \right) \tag{8}$$

is the entropy production.

In this scheme, the thermodynamic forces are identified as the gradients in the space of mesoscopic variables of the logarithm of the ratio of the probability density to its equilibrium value. We will now assume a linear dependence between fluxes and forces and establish a linear relationship between them

$$J(\gamma,t) = -k_B L(\gamma, P(\gamma)) \frac{\partial}{\partial \gamma} \left(ln \frac{P(\gamma,t)}{P_{eq}(\gamma)} \right) \tag{9}$$

where $L(\gamma, P(\gamma))$ is an Onsager coefficient, which in general depends on the state variable $P(\gamma)$ and on the mesoscopic coordinates γ. To derive this expression, locality in space has also been taken into account, for which only fluxes and forces with the same value of γ become coupled.

The resulting kinetic equation follows by substituting Eq. back into the continuity equation:

$$\frac{\partial P}{\partial t} = \frac{\partial}{\partial \gamma}\left(DP_{eq}\frac{\partial}{\partial \gamma}\frac{P}{P_{eq}}\right) \tag{10}$$

where the diffusion coefficient is defined as

$$D(\gamma) = k_B \frac{L(\gamma, P)}{P} \tag{11}$$

This equation, which in view of Eq. (9) can also be written as

$$\frac{\partial P}{\partial t} = \frac{\partial}{\partial \gamma}\left(D\frac{\partial P}{\partial \gamma} + \frac{D}{k_B T}\frac{\partial \Delta W}{\partial \gamma}P\right) \tag{12}$$

is the Fokker-Planck equation for the evolution of the probability density in γ-space. Notice that the diffusion coefficient appearing in this equation may, according to (11), depend on P. The Fokker-Planck equation obtained is in general non-linear in the probability distribution and describes in this case anomalous diffusion [9]. Up to first order, when the Onsager coefficient is linear in P, the diffusion coefficient may still depend on γ. The case in which that coefficient is a constant corresponds to normal diffusion.

Under the conditions for which the minimum work is given by the Gibbs free energy G , $\Delta W = \Delta G = \Delta H - T\Delta S$, where H is the enthalpy, this equation transforms into the Fokker-Planck equation for a system in the presence of a free energy barrier:

$$\frac{\partial P}{\partial t} = \frac{\partial}{\partial \gamma}\left(D\frac{\partial P}{\partial \gamma} + \frac{D}{k_B T}\frac{\partial \Delta G}{\partial \gamma}P\right) \tag{13}$$

Other cases of interest concern different thermodynamic potentials. For instance, a particularly interesting situation is the case of a purely entropic barrier, often encountered in soft-condensed matter and biophysics [10].

It is important to stress that MNET provides a simple and direct method to determine the dynamics of a system from its equilibrium properties. In particular, by knowing the equilibrium thermodynamic potential of a system in terms of its relevant variables, one could easily derive the general form of the kinetics. The method proposed thus offers a general formalism able to analyze the dynamics of systems away from equilibrium. In the following section we will illustrate its applicability by means of some examples.

The scheme presented can be put in closer connection with nonequilibrium thermodynamics concepts. The link can be established through the non-equilibrium chemical potential $\mu(\gamma, t)$. We may then assume that the evolution of these degrees of freedom is described by a diffusion process and formulate the corresponding Gibbs equation

$$\delta S = -\frac{1}{T}\int \mu(\gamma)\delta P(\gamma, t)d\gamma \tag{14}$$

which resembles the corresponding law proposed in nonequilibrium thermodynamics for a diffusion process in terms of the mass density of particles. In this expression, the chemical potential in γ-space is conjugated to the distribution function $P(\gamma,t)$ interpreted as a state variable in a thermodynamic context.

Comparison of the Gibbs equation (14) with Eq. (4), where the variations of the equilibrium entropy are given by

$$\delta S_{eq} = -\frac{1}{T}\int \mu_{eq}\delta P(\gamma,t)d\gamma \tag{15}$$

and μ_{eq} is the value of the chemical potential at equilibrium, yields the identification of the generalized chemical potential as

$$\mu(\gamma,t) = -k_B ln\frac{P(\gamma,t)}{P_{eq}}(\gamma) + \mu_{eq} \tag{16}$$

or alternatively, using Eq. (2),

$$\mu(\gamma,t) = -k_B lnP(\gamma,t) + \Delta W \tag{17}$$

In this reformulation, the "thermodynamic force" driving this general diffusion process is $T^{-1}\partial\mu/\partial\gamma$, and the entropy production is given by

$$\sigma = -\frac{1}{T}\int J\frac{\partial\mu}{\partial\gamma}d\gamma \tag{18}$$

By comparison of the previous equation with Eq. (6), it is clear that the evolution in time of the system mimics a generalized diffusion process over a potential landscape in the space of mesoscopic variables. This landscape is conformed by the values of the equilibrium energy associated to each configuration . The treatment of a diffusion process in the framework of nonequilibrium thermodynamics can then be extended to the case in which the relevant quantity is a probability density instead of a mass density.

BROWNIAN MOTION IN A STATIONARY STATE

The advantages of using MNET become especially manifest when irreversible processes of different nature take place simultaneously, as for instance, when the system is subjected to fluctuations and exchanges heat or mass with a nonequilibrium environment that has its own dynamics. In such cases, the Langevin and the Fokker-Planck equations are not a mere extension of those formulated for simpler situations and must be derived by means of a nonequilibrium statistical mechanics theory. MNET uses a systematic and simple method through which those equations can easily be obtained. The cases of the translocation of a biomolecule [11], of the stretching of a RNA molecule [12] and of active trasnport through a protein channel [13] are illustrative examples. In these cases, the Fokker-Planck equation contains two currents corresponding to the two relevant dynamic variables.

To illustrate explicitly the influence of a nonequilibrium environment in the dynamics of the system, we consider Brownian motion in a temperature gradient [14]. The effects of the gradient on the probability current of a Brownian particle can directly be inferred from the entropy production in the space of mesoscopic variables by taking into account its Onsager coupling to the heat current. The form of the probability current is

$$\vec{J}_u = -L_{uT}\nabla T/T^2 - k_B L_{uu}\frac{\partial}{\partial \vec{u}} ln(P/P_{l.eq.}) \tag{19}$$

where $\vec{u}$ is the velocity of the Brownian particle, the L terms are Onsager coefficients and $P_{l.eq.}$ is the local equilibrium distribution function. The presence of particles, in turn, modifies the heat current through the system. This effect can also be analyzed through the entropy production. The resulting heat current is

$$\vec{J}_q = -L_{TT}\nabla T/T^2 - k_B \int L_{Tu}\frac{\partial}{\partial \vec{u}} ln(P/P_{l.eq.}) d\vec{u} \tag{20}$$

where the Onsager coefficients obey the Onsager relation $L_{Tu} = -L_{uT}$. These equations clearly show the existence of a coupling between the two irreversible processes present in the system: probability diffusion and heat conduction. The resulting Fokker-Planck equation is

$$\frac{\partial P}{\partial t} = -\vec{u}.\nabla P + \beta \frac{\partial}{\partial \vec{u}}\left(P\vec{u} + k_B T \frac{\partial P}{\partial \vec{u}}\right) + \frac{\varepsilon}{T}\frac{\partial P}{\partial \vec{u}}.P\nabla T \tag{21}$$

with β being the friction coefficient of the particles and ε, a coefficient related to the Onsager coefficient L_{uT} , coincides with that obtained from kinetic theory [15]. The Fokker-Planck equation and the evolution equation for the temperature field provide a complete description of the heat exchange process in the system. This example illustrates the way in which MNET can systematically be used to analyze heat exchange processes between the system and its environment in the presence of fluctuations.

A similar analysis was performed for the Brownian motion in a velocity gradient [16] showing that for large shear rates the fluctuation dissipation heorem is not fulfilled. The origin of the violation of the theorem has been analyzed in [17].

ACTIVATED PROCESSES

Activated processes are those that need a finite energy to proceed and change the system from one state to another. They can be modeled by a Brownian particle crossing of a free energy barrier that separates two well-differentiated states that lie at the local minima at each side of the barrier. The system needs to acquire energy to surmount the barrier. Once the barrier is crossed, energy is released. Processes like thermal emission in semiconductors, chemical reactions, adsorption, nucleation, and active transport through biological membranes, share these features and, therefore, are generically referred to as activated processes.

It is important to emphasize the essential difference between activated processes and the linear processes described by nonequilibrium thermodynamics. The latter constitute the response to the application of an external force or gradient and may emerge even at very low values of the applied force, in the linear response regime. Contrarily, the regime in which activated processes may take place is basically nonlinear. In this context, we can contrast the linear Fourier, Fick, or Ohm laws, in which the corresponding currents are proportional to the conjugated thermodynamic forces or gradients, with the exponential laws appearing in activated processes.

Let us consider a general process for which a system passes from state 1 to state 2 via activation. Instances of this process can be a chemical reaction in which a substance transforms into another, an adsorption process in which the adsorbing particle goes from the physisorbed to the chemisorbed state, or a nucleation process in which the metastable liquid transforms into a crystal phase. Nonequilibrium thermodynamics describes the process only in terms of the initial and final positions and is valid only in the linear response regime [2]. If we consider the process at shorter time scales, the state of the system progressively transforms by passing through successive molecular configurations. These different configurations can be characterized by a "reaction coordinate" . In this situation, one may assume that this reaction coordinate undergoes a diffusion process through a potential barrier separating the initial from the final states. The local entropy production is

$$\sigma(\gamma) = -\frac{1}{T} J \frac{\partial \mu}{\partial \gamma} \tag{22}$$

from which we can infer the linear law

$$J = -\frac{L}{T}\frac{\partial \mu}{\partial \gamma} \tag{23}$$

where the chemical potential is, as in Eq. (17), given by

$$\mu(\gamma,t) = k_B T lnP(\gamma,t) + \Phi(\gamma) \tag{24}$$

with $\Phi(\gamma)$ being the potential in terms of the reaction coordinate. Following the previous approach, we can obtain the Fokker-Planck equation

$$\frac{\partial P}{\partial t} = \frac{\partial}{\partial \gamma}\left(b(\gamma)P(\gamma)\frac{\partial \mu(\gamma)}{\partial \gamma}\right) \tag{25}$$

where $b(\gamma)$ is a mobility in the γ -space. This equation describes the dynamics of the probability distribution for an arbitrary potential and at any value of the temperature.

It is often the case that at the time scales of interest the system is mostly found in the states 1 and 2, which correspond to the minima at γ_1 and γ_2 , respectively. The probability distribution is strongly peaked at these values and almost zero everywhere else. This happens when the energy barrier is much higher than the thermal energy and intra-well relaxation has already taken place. Using MNET, we will show that the Fokker-Planck description, under these conditions, leads to a kinetic equation in which the net reaction rate satisfies the mass action law.

The current given in (23) can be rewritten in terms of the local fugacity defined along the reaction coordinate $z(\gamma) = \exp \mu(\gamma)/k_B T$ as

$$J = -k_B L \frac{1}{z}\frac{\partial z}{\partial \gamma} \tag{26}$$

which can also be expressed as

$$J = -D\frac{\partial z}{\partial \gamma} \tag{27}$$

where $D = k_B L/z$ represents the diffusion coefficient. We now assume D constant and integrate from 1 to 2, obtaining

$$\langle J\rangle = \int_1^2 J d\gamma = -D(z_2 - z_1) = -D\left(exp\frac{\mu_2}{k_B T} - exp\frac{\mu_1}{k_B T}\right) \tag{28}$$

This equation can alternatively be expressed as

$$\langle J\rangle = J_0\left(1 - e^{A/k_B T}\right) \tag{29}$$

where $\langle J\rangle$ is the integrated rate, $J_0 = D\exp(\mu_1/k_B T)$ and $A = \mu_2 - \mu_1$ is the affinity, the driving force of the process. We have then shown that MNET leads to nonlinear kinetic laws. Remarkably, it is possible to move from a linear continuous to a nonlinear discrete system; that is to say, a Fokker-Planck equation, linear in probabilities and in the gradient of $\mu\left[\gamma, P(\gamma)\right]$, accounts for a non-linear dependence in the affinity. This scheme has been successfully applied to different classical activated processes, like chemical reactions [18], adsorption [19], thermal emission in semiconductors [20], or nucleation [21], to obtain the corresponding kinetic laws.

THE ACTUAL MEANING OF 'SMALL' AND OF BEING 'FAR FROM EQUILIBRIUM'

Many of the studies performed at present about non-equilibrium systems refer to 'small' systems 'far from equilibrium'. Examples are many bio-systems such as protein channels, DNA molecules or nanomotors whose performance precise of the intervention of unbalanced thermodynamic forces. But, are these systems small because of their reduced size, of about some tens of nanometers? or because they contain a finite number of particles? The criterion for which a system is small should be more precise. It has been shown that the heat capacity of some proteins is an extensive quantity [22]. Consequently, despite their reduced size the proteins behave thermodynamically. This result shows that the robust criterion is thermodynamic extensivity. But when scaling-down the size of the system even more the question arises: is there a lower limit for a thermodynamic description of the system? Recent simulations performed with argon atoms moving through a zeolite [23] have shown that due to the heterogeneity of the interactions between the particles at very small scales, smaller than the crystalline unit cell of the zeolite, the equipartition law breaks down. This fact makes no possible a consistent definition of the temperature and consequently impedes a thermodynamic treatment of the system.

The presence of the unbalanced thermodynamic forces drives the system away from equilibrium. How far can these forces move the system away from equilibrium, as discussed in the classic monograph [2], depends not only on the values of the force but also on the nature of the process. For transport processes in simple systems, such as heat conduction, mass diffusion and viscous phenomena, local equilibrium hold even when the system is subjected to large or even very large gradients [22]. These processes can be described by means of the Fourier, Fick and Stokes-Einstein laws which can be derived from non-equilibrium thermodynamics [2]. We have seen that the probability current also obeys a linear law: the Fokker-Planck equation is linear and describes situations that can be far from equilibrium. Linearity does not necessarily imply in those cases closeness to equilibrium.

On the contrary, for the wide class of activated processes, linearity breaks down at small values of the affinity, which seems to imply that local equilibrium is lost almost immediately. The results of the theory we have presented indicate that existence of local equilibrium depends on the set of variables used in the characterization. When an activated process is described not just in terms of the initial and final states but through its reaction coordinate, local equilibrium holds. Increasing the dimensionality of the space of thermodynamic variables, by including as many dimensions as nonequilibrated degrees of freedom, leads to local equilibrium in the enlarged space and allows the use of nonequilibrium thermodynamics at shorter time scales in which fluctuations are still present. We can thus conclude that many kinetic processes, such as nucleation, chemical reactions or active transport, which have been assumed to be far away from equilibrium because of their intrinsic nonlinear nature, take place at local equilibrium when a finer description is adopted.

To better illustrate how systems brought outside equilibrium may be considered at local equilibrium in an extended space, we will study the case of a bio-molecule in a solvent at constant temperature subjected to an external driving force F. In addition to the position of its center of mass x, the molecule is characterized by an additional fluctuating variable θ , which might represent, for instance, its size or its orientation. For small values of the force, local equilibrium in γ-space holds in such a way that we can formulate the Gibbs equation expressed now in differential form

$$Tds(x) = -\mu(x)d\rho(x) - Fd\Theta \tag{30}$$

where Θ is the average value of the θ variable defined as

$$\Theta(x) = \int \theta P(x,\theta)d\theta \tag{31}$$

with $P(x,\theta)$ being the probability distribution and $\mu(x,\theta)$, its conjugated chemical potential. Let us now assume that the driving force increases in such a way that the system is no longer in local equilibrium in x-space. The way to restore local equilibrium is to increase the dimensionality by considering the fluctuating variable θ as an independent variable and defining the Gibbs equation as

$$Tds(x,\theta) = -\mu(x,\theta)dP(x,\theta) \tag{32}$$

Proceeding as indicated previously, one would obtain from this equation the corresponding Fokker-Planck equation, which would describe the dynamics of the bio-molecule in the extended space.

CONCLUSIONS

The classical way to study nonequilibrium mesoscopic systems is to use microscopic theories and proceed with a coarse-graining procedure to eliminate the degrees of freedom that are not relevant to the mesoscopic scale. Such microscopic theories are fundamental to understand how the macroscopic and mesoscopic behavior arises from the microscopic dynamics. On the downside, they usually involve specialized mathematical methods that prevent them to be generally applicable to complex systems; and more importantly, they use much detailed information that is lost during the coarse-graining procedure and that is actually not needed to understand the general properties of the mesoscopic dynamics.

The mesoscopic thermodynamic theory we have presented here starts from the mesoscopic equilibrium behavior and adds all the dynamic details compatible with the second principle of thermodynamics and with the conservation laws and symmetries that are present in the system. Thus, given the equilibrium statistical thermodynamics of a system, it is straightforward to obtain Fokker-Planck equations for its dynamics. The dynamics is characterized by a few phenomenological coefficients, which can be obtained for the particular situation of interest from experiments or from microscopic theories, and describes not only the deterministic properties but also their fluctuations.

Mesoscopic non-equilibrium thermodynamics has been used in a broad variety of situations, including activated processes in the nonlinear regime, inertial effects in diffusion, and transport in the presence of entropic forces. In transport phenomena at short time and length scales MNET provides a method to obtain relaxation equations and transport coefficients. Spin transfer [24] Radiative heat transfer has also been studied using the MNET theory, obtaining a non-equilibrium Stefan-Boltzmann law [25] and an expression for the heat conductance at the nanoscale [26] that agrees with computer simulations results [27].

ACKNOWLEDGMENTS

I would like to thank Jose, M. Vilar, David Reguera and Agustín Pérez for many interesting discussions. This work has been supported by the Spanish MICINN through Grant NO. FIS2008-04386.

REFERENCES

1. H B. Callen, *Thermodynamics and an Introduction to Thermostatistics*, John Wiley and Sons, New York, 1985.
2. S. R. de Groot, and P. Mazur, *Non-Equilibrium Thermodynamics*, Dover, New York, 1984.
3. D. Reguera, J. M. Rubí, and J. M. G. Vilar, *J. Phys. Chem. B* **109**, 21502–21515 (2005).
4. J M. Rubí, *Sci. Am.* **299**, 62–67 (2008).
5. J. M. G. Vilar, and J. M. Rubí, *Proc. Natl. Acad. Sci. U.S.A.* **98**, 11081–11084 (2001).
6. T.L. Hill, *Thermodynamics of small systems*, Dover, New York, 1994.
7. L. D. Landau and E. M. Lifshitz, *Statistical Physics, Parts 1 and 2*, Pergamon Press, New York, 1980.
8. J. M. G. Vilar, and J. M. Rubí, *Phys. Rev. Lett.* **100**, 020601 (2008).

9. T. D. Frank, *Thermodynamics and an Introduction to Thermostatistics*, John Wiley and Sons, New York, 1985.
10. D.Reguera, and J. M. Rubí, *Phys. Rev. E* **64**, 061106 (2001).
11. R. Zandi, D. Reguera, J. Rudnick, W D. Gelbart, *Proc. Natl. Acad. Sci. U.S.A.* **100**, 8649–8653 (2003).
12. J. M. Rubí, D. Bedeaux, and S. Kjelstrup, *J.Phys.Chem.B* **111**, 9598–9602 (2007).
13. S. Kjelstrup, J. M. Rubí, and D. Bedeaux, *Phys. Chem. Chem. Phys* **7**, 4009–4018 (2005).
14. A. Pérez-Madrid, J. M. Rubí, and P. Mazur, *Physica A* **212**, 231-238 (1994).
15. D.N. Zubarev, and A.G. Bashkirov, *Physica A* **39**, 334 (1968).
16. I. Santamaria-Holek, D.Reguera, and J. M.Rubí, *Phys. Rev. E* **63**, 051106 (2001).
17. A. Pérez-Madrid, J. M. Rubí, and P. Mazur, *Physica A* **329**, 357–364 (2003).
18. I. Pagonabarraga, A. Pérez-Madrid, J. M. Rubí, and P. Mazur, *Physica A* **329**, 205–219 (2003).
19. I. Pagonabarraga, and J. M.Rubí, *Physica A* **188**, 553–567 (1992).
20. G. Gomila, A. Pérez-Madrid, and J. M.Rubí, *Physica A* **233**, 208–220 (1996).
21. D. Reguera, J. M.Rubí, and A. Pérez-Madrid, *J. Chem. Phys* **109**, 5987–5993 (1998).
22. A. Lervik, F. Bresme,S. Kjelstrup, D. Bedeaux, and J. M. Rubí, *Phys. Chem. Chem. Phys* **12**, 1610–1617 (2010).
23. J.-M. Simon, and J. M. Rubí, preprint.
24. J.E. Wegrowe, S.M. Santos, M.C. Ciornei, H.J. Drouhin, and J. M. Rubí, *Phys. Rev. B* **77**, 174408 (2008).
25. A. Pérez-Madrid, J. M. Rubí, and L. Lapas, *J. Non-Equilib. Thermodyn.*, in press.
26. A. Pérez-Madrid, J. M. Rubí, and L. Lapas, *Phys. Rev. Lett.* **103**, 048301 (2009).
27. G. Domingues, S. Voltz, K. Joulain, and J.J. Greffet, *Phys. Rev. Lett.* **94**, 085901 (2005).

Noise-induced transitions *vs.* noise-induced phase transitions

Raúl Toral

IFISC (Instituto de Física Interdisciplinar y Sistemas Complejos), CSIC-UIB, E-07122 Palma de Mallorca, Spain

Abstract. I will briefly review the field of noise-induced phase transitions, emphasizing the main differences with the phase-induced transitions and showing that they appear in different systems. I will show that a noise-induced transition can disappear after a suitable change of variables and I will also discuss the breaking of ergodicity and symmetry breaking that occur in noise-induced phase transitions in the thermodynamic limit, but not in noise-induced transitions.

Keywords: Non-equilibrium transitions, fluctuations, finite-size effects
PACS: 05.40.-a,74.40.Gh,05.10.Gg,64.60.Cn

BIFURCATIONS IN STOCHASTIC SYSTEMS

A bifurcation in a dynamical system is a change in the number of fixed points, or in their relative stability, that occurs when varying a control parameter, the so-called bifurcation parameter. The value of this parameter at which the change occurs is the bifurcation point [1]. The normal form of a bifurcation is the simplest mathematical model (usually involving polynomials of the lowest possible order) for which a particular change of behavior occurs. One of the simplest examples is that of the *transcritical* bifurcation for which the normal form is $dx(t)/dt = \mu x - x^2$, the Verhulst, or logistic, equation [2]. This equation can model, for instance, the growth of biological populations, or autocatalytic reactions, amongst other applications. For $\mu < 0$, there is only one (stable) fixed point at $x = 0$, whereas for $\mu > 0$ there are two fixed points: the one at $x = 0$ (which is now unstable) and another one at $x = \mu$ which is stable. Another simple example is that of the *supercritical pitchfork* bifurcation for which the normal form is $dx(t)/dt = \mu x - x^3$, the Landau equation used in the context of phase transitions in the mean-field approach. For $\mu < 0$, there is only one (stable) fixed point at $x = 0$, whereas for $\mu > 0$ there are three fixed points: the one at $x = 0$ (which is now unstable) and two more at $x = \pm\sqrt{\mu}$ which are stable. In both examples, the bifurcation point is, hence, $\mu = 0$. The importance of the stable fixed points is that, under some additional conditions, they determine the long-time dynamical behavior, as the dynamical evolution tends to one of the stable fixed points, and then it stops [3]. In the supercritical pitchfork, the value $x = +\sqrt{\mu}$ is reached if the initial condition is $x(t = 0) > 0$, whereas the fixed point at $x = -\sqrt{\mu}$ is reached whenever $x(t = 0) < 0$. The symmetry $x \to -x$ of the differential equation is broken by the initial condition in the case $\mu > 0$.

When there are stochastic, so-called noise, terms in the dynamics, usually there are no fixed points but the long-time dynamical behavior still has some preferred values. Consider, for example, the normal form for the supercritical bifurcation with an additional noise term

$$\frac{dx(t)}{dt} = \mu x - x^3 + \sqrt{2D}\xi(t), \tag{1}$$

being $\xi(t)$ a Gaussian process of zero mean and correlations $\langle \xi(t)\xi(t')\rangle = \delta(t-t')$, or *white noise* [3]. D is the noise intensity. This equation can be written in terms of relaxational dynamics [3] in a double-well potential $V(x)$:

$$\frac{dx(t)}{dt} = -\frac{\partial V(x)}{\partial x} + \sqrt{2D}\xi(t), \qquad V(x) = -\frac{\mu}{2}x^2 + \frac{1}{4}x^4. \tag{2}$$

It is possible to prove using the Fokker-Planck equation [4] (see later) that the stationary probability distribution for the x variable is $P_{\text{st}}(x) = \mathscr{Z}^{-1}\exp\left[-\frac{V(x)}{D}\right]$, being $\mathscr{Z} = \int_{-\infty}^{\infty} dx \exp\left[-\frac{V(x)}{D}\right]$ a normalization factor. The stationary probability has **maxima** at $x = 0$ for $\mu < 0$ and at $x = \pm\sqrt{\mu}$ for $\mu > 0$. So it is still true that, from a probabilistic point of view, the fixed points of the deterministic, i.e. $D = 0$, dynamics are the ones **preferred** by the stochastic trajectories, but the dynamics does not end in one of the fixed points. Another important difference with the deterministic dynamics is that, for $\mu > 0$, the trajectories are not confined to the neighborhood of one of the maxima. There are constant jumps between the two maxima of the probability distribution. A classical calculation by Kramers [5], shows that the frequency of the jumps between the two maxima is proportional to $\exp\left[-\frac{\Delta V}{D}\right]$, being ΔV the height of the potential barrier between the maxima, or $\Delta V = \mu^2/4$ in the double well potential. As there are many jumps between the maxima, the noise terms have restored the symmetry $x \to -x$ of the equation.

There are other more complicated examples. Consider, for example, the Verhulst equation with the addition of a noise term ξ which is coupled multiplicatively to the dynamical variable x:

$$\frac{dx(t)}{dt} = \mu x - x^2 + \sqrt{2D}x\xi(t). \tag{3}$$

This can be thought as originated from the fact that the parameter μ randomly fluctuates and can be replaced by $\mu \to \mu + \sqrt{2D}\xi(t)$. There are some mathematical subtleties to handle the presence of the singular function $\xi(t)$. After all, the correlation function of $\xi(t)$ is a delta function, a not too well defined mathematical object. The different possible interpretations of the integral $\int dt\, g(x(t))\xi(t)$, for an arbitrary function $g(x)$, lead to different results. We will limit our considerations to the so-called Stratonovich interpretation [6, 7]. In this example, $x = 0$ is a fixed point of the stochastic dynamics. Therefore starting from $x(t = 0) > 0$ as it is the case in the biological or chemical applications, the barrier $x = 0$ can never be crossed. For $\mu < 0$, the value $x = 0$ is an *attracting boundary* [6]: it will be reached in the asymptotic limit $t \to \infty$. As a consequence, the stationary probability distribution is $P_{\text{st}}(x) = \delta(x)$. As μ increases and crosses zero, the picture changes. The full analysis uses the Fokker-Planck equation for the time dependent probability density $P(x,t)$. The stationary distribution for $0 < \mu < D$ is no longer a delta function at $x = 0$ but still has a maximum at $x = 0$. However, when $\mu > D$, the maximum of $P_{\text{st}}(x)$ is no longer at $x = 0$ but it moves to $x = \mu - D$.

Alternatively, for fixed $\mu > 0$ one finds that the maximum of the stationary distribution switches from $x = \mu - D$ for $0 < D < \mu$ to $x = 0$ for $D > \mu$. Note that this is a somewhat counterintuitive result in the sense that a large value of the noise intensity leads to a state where the maximum of the distribution is located at a state, $x = 0$, in which the noise term $x\xi(t)$ vanishes.

Similar shifts of the maxima of the probability distribution as the noise intensity increases appear in a large class of stochastic differential equations. They have been named generically as *noise-induced transitions* [8]. In the general case of a stochastic differential equation of the form $dx(t)/dt = q(x) + \sqrt{2D}g(x)\xi(t)$, the Fokker-Planck equation reads:

$$\frac{\partial P(x,t)}{\partial t} = -\frac{\partial}{\partial x}\left[\left(q(x) - Dg(x)g'(x)\right)P(x,t)\right] + D\frac{\partial^2}{\partial x^2}\left[g(x)^2 P(x,t)\right] \tag{4}$$

and the steady-state solution $\left.\frac{\partial P(x,t)}{\partial t}\right|_{P=P_{\rm st}} = 0$ is:

$$P_{\rm st}(x) = \mathscr{Z}^{-1}\exp\left[\int^x dx'\,\frac{q(x') - Dg(x')g'(x')}{Dg^2(x')}\right]. \tag{5}$$

The maxima $\bar{x}$ of this distribution are given by

$$q(\bar{x}) - Dg(\bar{x})g'(\bar{x}) = 0. \tag{6}$$

And it is clear that $\bar{x}(D)$ depends on the noise intensity D. There are examples [8] in which equations that display the $x \to -x$ symmetry are such that for small noise intensity D the distribution is unimodal centered at $\bar{x} = 0$, and that increasing D the distribution becomes bimodal with maxima at $\pm\bar{x}(D) \neq 0$. This is the generic behavior whenever $q(x) = -x + o(x)$ and $g(x) = 1 + x^2 + o(x^2)$. A specific example is Hongler's model [9] $q(x) = -\tanh(x)$, $g(x) = \mathrm{sech}(x)$. The transition occurs at $D = D_c = 1$. The situation, in principle, could be considered the equivalent of the supercritical pitchfork bifurcation, in the sense that the most visited states are $x = 0$ for $D < 1$ and $\pm\bar{x}(D)$ for $D > 1$. However, the same remarks than in the case of the model of Eq.(1) apply: the bifurcation does not break the $x \to -x$ symmetry, as trajectories visit ergodically all possible values of x and, therefore, there are many jumps between the two preferred states. Furthermore, it is possible to show that the change in the number of maxima in the probability distribution is simply a matter of the variable used and that a simple change of variables can eliminate the bifurcation. This is explained in the next section.

NOISE-INDUCED TRANSITIONS AS A CHANGE OF VARIABLES

Let us consider the Gaussian distribution:

$$f_z(z) = \frac{1}{\sqrt{2D\pi}}e^{-z^2/2D}. \tag{7}$$

It is obviously single-peaked for all values of D, the noise intensity. Let us now introduce the new variable $x = \mathrm{argsh}(z)$ or $z = \sinh(x)$. The change of variables (i) does not depend on the noise intensity D and (ii) it is one-to-one, mapping the set of real numbers onto itself. The probability distribution for the new variable is

$$f_x(x) = f_z(z)\left|\frac{dz}{dx}\right| = f_z(z)\cosh(x), \tag{8}$$

or

$$f_x(x) = \frac{1}{\sqrt{2D\pi}} e^{-[\sinh(x)^2 - 2D\ln\cosh(x)]/2D} \equiv \frac{1}{\sqrt{2D\pi}} e^{-\frac{V_{\mathrm{eff}}(x)}{D}}, \tag{9}$$

with an effective potential

$$V_{\mathrm{eff}}(x) = \frac{1}{2}\sinh(x)^2 - D\ln\cosh(x), \tag{10}$$

which depends on the noise intensity. The potential is monostable for $D < D_c$ and bistable for $D > D_c$ with $D_c = 1$, as the expansion $V_{\mathrm{eff}}(x) = \frac{1-D}{2}x^2 + \frac{2+D}{12}x^4 + O(x^6)$ shows. The Horsthemke-Lefever mechanism for noise-induced transitions is an equivalent way of reproducing this result. Just take the Langevin equation:

$$\frac{dz}{dt} = -z + \sqrt{2D}\xi(t), \tag{11}$$

being $\xi(t)$ zero-mean white noise, $\langle\xi(t)\xi(t')\rangle = \delta(t-t')$. Its steady-state probability is

$$f_z(z) = \mathscr{Z}^{-1} e^{-\frac{V(z)}{D}}, \tag{12}$$

with a potential function $V(z) = \frac{z^2}{2}$, $\mathscr{Z}$ is a normalization constant.

We now perform the aforementioned change of variables $x = \mathrm{argsh}(z)$ to obtain (Stratonovich sense)

$$\frac{dx}{dt} = -\tanh(x) + \mathrm{sech}(x)\sqrt{2D}\xi(t), \tag{13}$$

which is Hongler's model, one of the typical examples of noise-induced transitions explained above.

This result is very general. The same (well-known) trick can be used to reduce any one-variable Langevin equation with multiplicative noise:

$$\frac{dx}{dt} = q(x) + g(x)\sqrt{2D}\xi(t), \tag{14}$$

to one with additive noise. Simply make the change of variables defined by $dz = dx/g(x)$ or $z = \int^x dx'/g(x')$ to obtain

$$\frac{dz}{dt} = F(z) + \sqrt{2D}\xi(t), \tag{15}$$

with

$$F(z) = q(x)/g(x), \tag{16}$$

expressed in terms of the variable z. The steady-state distribution of z can be written as

$$f_z(z) = \mathscr{Z}^{-1} e^{-\frac{V(z)}{D}}, \tag{17}$$

with a potential

$$V(z) = -\int^z dz' F(z'). \tag{18}$$

The steady-state probability distribution in terms of the variable x (assuming a one-to-one change of variables) is

$$f_x(x) = f_z(z)\left|\frac{dz}{dx}\right| = \frac{f_z(z)}{|g(x)|} = \frac{\mathscr{Z}^{-1}}{|g(x)|} e^{\frac{1}{D}\int^z dz' F(z')} = \frac{\mathscr{Z}^{-1}}{|g(x)|} e^{\frac{1}{D}\int^x \frac{dx'}{g(x')}\frac{q(x')}{g(x')}} = \frac{\mathscr{Z}^{-1}}{|g(x)|} e^{\frac{1}{D}\int^x dx' \frac{q(x')}{g(x')^2}}, \tag{19}$$

the same steady-state probability distribution coming from the multiplicative-noise Langevin equation (14) that was written in Eq.(5). In terms of an effective potential: $f_x(x) = \mathscr{Z}^{-1} e^{-\frac{V\mathrm{eff}(x)}{D}}$ we have

$$V_{\mathrm{eff}}(x) = -\int^x dx' \frac{q(x')}{g(x')^2} + D\ln|g(x)|. \tag{20}$$

A noise-induced transition will appear if the potential $V_{\mathrm{eff}}(x)$ changes from monostable to bistable as the noise intensity D increases.

Another widely used example of a noise-induced transition [8] is that of $q(x) = -x + \lambda x(1-x^2)$ and $g(x) = 1-x^2$. The change of variables $z = \int^x \frac{dx'}{1-x'^2} = \frac{1}{2}\log\left(\frac{1+x}{1-x}\right)$, or $x = \tanh(z)$ leads to the Langevin equation:

$$\frac{dz}{dt} = -\sinh(z)\cosh(z) + \lambda\tanh(z) + \sqrt{2D}\xi(t). \tag{21}$$

Note that $x \in (-1,1)$, a fact already implied in the original Langevin equation since $x = \pm 1$ are reflecting barriers. The steady-state probability distribution of this Langevin equation is $f_z(z) = \mathscr{Z}^{-1} e^{-\frac{V(z)}{D}}$ with a potential $V(z) = \frac{1}{2}\cosh(z)^2 - \lambda\log(\cosh(z))$. The Taylor expansion $V(z) = \frac{1}{2} + \frac{1-\lambda}{2}z^2 + \frac{2+\lambda}{12}z^4 + O(z^6)$, shows that $f_z(z)$ has a single minimum at $z = 0$ for $\lambda < 1$ and double minima for $\lambda > 1$. As far as the x variable is concerned, the effective potential as given by (20) is

$$V_{\mathrm{eff}}(x) = \frac{1}{2(1-x^2)} + \frac{\lambda+2D}{2}\log(1-x^2). \tag{22}$$

The Taylor expansion $V_{\mathrm{eff}}(x) = \frac{1}{2} + \frac{1-\lambda-2D}{2}x^2 + \frac{2-\lambda-2D}{4}x^4 + O[x^6]$ shows that the potential leads to a monostable distribution if $\lambda + 2D < 1$ and to a bistable one if $\lambda + 2D > 1$. Hence, a noise-induced transition occurs for $\lambda < 1$ since a bistable distribution for the x variable appears for $D > D_c = (1-\lambda)/2$. Note, however, that the distribution of the z variable is monostable for all values of D, so that the noise-induced transition is dependent on the variable considered. In the case $\lambda > 1$ the distribution is always bistable, both for the x and the z variables.

The change $x = \tanh(z)$ also induces a transition in the simpler case that the z variable follows the Gaussian distribution Eq.(7). The probability distribution function for the new variable is $q(x) = \frac{1+x^2}{\sqrt{2D\pi}} e^{-\mathrm{argth}(x)^2/2D} = \frac{1}{\sqrt{2D\pi}} \left[1 + \left(1 - \frac{1}{2D}\right) x^2 + O(x^4)\right]$ which indicates a phase transition at $D_c = 1/2$.

A remarkable example is the change $x = \frac{z}{1+|z|}$ which leads to a probability distribution $q(x) = \frac{1}{\sqrt{2D\pi}} \frac{e^{-\left(\frac{x}{1-|x|}\right)^2/2D}}{(1-|x|)^2}$ for $x \in (-1,1)$ which is bimodal for any $D > 0$, or $D_c = 0$.

NOISE-INDUCED PHASE TRANSITIONS

How can one obtain a true, symmetry breaking, bifurcation in a stochastic model? The answer lies in the coupling of many individual systems in order to obtain a bifurcation in the macroscopic variable. Let us explain this with a simple example: the standard Ginzburg-Landau model for phase transitions [10]. It consists of many coupled dynamical variables $x_i(t)$, $i = 1, \ldots, N$ which individually follow Eq.(1). The full model is:

$$\frac{dx_i(t)}{dt} = \mu x_i - x_i^3 + \frac{C}{N_i} \sum_{j \in \mathcal{N}_i} (x_j - x_i) + \sqrt{2D}\xi_i(t). \tag{23}$$

The noise variables are now independent Gaussian variables of zero mean and correlations $\langle \xi_i(t) \xi_j(t') \rangle = \delta_{ij} \delta(t - t')$. $\mathcal{N}_i$ refers to the set of N_i variables x_j which are coupled to x_i. Typical situations include an all-to-all coupling where $\mathcal{N}_i$ is the set of all units and $N_i = N$, or regular d-dimensional lattices where a unit x_i is connected to the set of $N_i = 2d$ nearest neighbors, although in more recent applications one also considers non-regular, random, small world, scale free or other types of lattices [11]. C is the coupling constant. If $C = 0$ each unit is independent of the other and displays the stochastic bifurcation at $\mu = 0$ explained before. For $C > 0$, a collective state can develop in which the global variable $m(t) = N^{-1} \sum_{i=1}^{N} x_i(t)$ follows, in the thermodynamic limit, a true bifurcation from a state in which the stationary distribution is $P_{\mathrm{st}}(x) = \delta(m)$, to another one in which it is either $P_{\mathrm{st}}(x) = \delta(m - m_0)$ or $P_{\mathrm{st}}(x) = \delta(m + m_0)$. This is nothing but a phase transition. Here, borrowing the language from the para-ferromagnetic transition [12], m_0 is called, in this context, the *spontaneous magnetization* and it is a function of noise intensity D, coupling constant C and the parameter μ. It is important to stress that a true symmetry-breaking transition, with non-ergodic behavior, occurs only in the thermodynamic limit $N \to \infty$. For finite N the stationary probability distribution $P_{\mathrm{st}}(m)$ is either a function peaked around $m = 0$ or displays two large maxima around $\pm m_0$. The height of these maxima increases with N and the width around them decreases with N until delta-functions are reached for $N \to \infty$. One can see evidence of this behavior in Fig.1 The price one has to pay to obtain this symmetry-breaking bifurcation is that, for fixed C and D, the bifurcation point is no longer at $\mu = 0$, but is is shifted to a positive value μ_c [13]. Alternatively, for fixed $\mu > 0$ there is a bifurcation induced by varying the noise intensity: when $D < D_c$ (the critical noise intensity), the distribution of m is a delta function located either at $m = \pm m_0$; for $D > D_c$, the distribution is again a delta function around $m = 0$. The bifurcation acts in the way noise is expected to influence the dynamics: for larger noise intensity the distribution is peaked around $m = 0$ (a situation in which roughly half of the x_i variables have a positive value and the other half negative, or disordered). When the noise intensity is small, $D < D_c$, the distribution is peaked around $+m_0$ or m_0 and, hence, variables x_i have a probability distribution peaked around this value, or ordered. As either $+m_0$ or $-m_0$ is selected (depending on initial conditions and realizations of the noise variables), the $x \to -x$ symmetry has been broken for $D < D_c$ and it is restored for $D > D_c$. It is not possible, in general, to obtain the probability distribution $p(x_i,t)$ for a single unit x_i, but an approximate result can be derived within the so-called Weiss effective-field theory [14, 12]. In a nutshell, it consists in replacing the detailed interaction with the neighbors with the global variable $m(t)$. This leads to a single equation for x_i:

$$\frac{dx_i(t)}{dt} = \mu x_i - x_i^3 + C(m(t) - x_i) + \sqrt{2D}\xi_i(t). \tag{24}$$

From here it is possible to write the Fokker-Planck equation for $p(x_i,t)$. The stationary solution depends on the value of $m(t)$ in the steady state, m_0,

$$p_{\text{st}}(x_i;m_0) = \mathscr{Z}^{-1} \exp\left[-v(x_i;m_0)/D\right], \qquad v(x;m) = -Cm_0 x - \frac{\mu - C}{2}x^2 + \frac{1}{4}x^4 \tag{25}$$

m_0 is obtained via the self-consistency relation $\langle x \rangle = \int dx\, p_{\text{st}}(x;m_0) = m_0$. This yields $m_0 = m_0(D,C,\mu)$ and it is such that, for a range of values of μ and $\mu > C$, there is a critical value D_c such that $m_0 = 0$ for $D > D_c$ and there are two solutions $\pm m_0$ with $m_0 > 0$ for $D < D_c$. Therefore, the one-unit dynamical system x_i experiences a stochastic bifurcation, in the sense that the maxima of the probability of $p_{\text{st}}(x_i)$ change location as D crosses D_c.

The idea naturally arises of whether is is possible to obtain a bifurcation for the global variable if we couple N units $(x_1,x_2,\dots,x_N)$, each one of which experiences a noise-induced transition from unimodal to bimodal as the noise intensity increases. In other words, if we consider the coupled system:

$$\frac{dx_i(t)}{dt} = q(x_i) + \frac{C}{N_i} \sum_{j \in \mathscr{N}_i} (x_j - x_i) + \sqrt{2D}g(x_i)\xi_i(t). \tag{26}$$

such that the uncoupled unit $\frac{dx_i(t)}{dt} = q(x_i) + \sqrt{2D}g(x_i)\xi_i(t)$ undergoes a noise-induced transition in the sense of Hormthenske and Lefever, will the global variable $m(t)$ undergo a bifurcation from *disorder* to *order* as the noise intensity increases? The answer turns out to be no[15, 16], one of the reasons being that, as we have already noted, the shift in the maxima of the probability distribution of $p_{\text{st}}(x_i)$ might disappear after a change of variables, whereas a true bifurcation remains after a one-to-one change of variables.

However, it was found quite surprisingly [15, 16] that it is possible to find functions $q(x)$ and $g(x)$ such that the global variable $m(t)$ experiences a bifurcation from $m_0 = 0$ to $\pm m_0$ with $m_0 > 0$ increasing the noise intensity D. The minimal model (normal form) is

$$\frac{dx_i(t)}{dt} = -x_i(1 + x_i^2)^2 + \frac{C}{N_i} \sum_{j \in \mathscr{N}_i} (x_j - x_i) + \sqrt{2D}(1 + x_i^2)\xi_i(t). \tag{27}$$

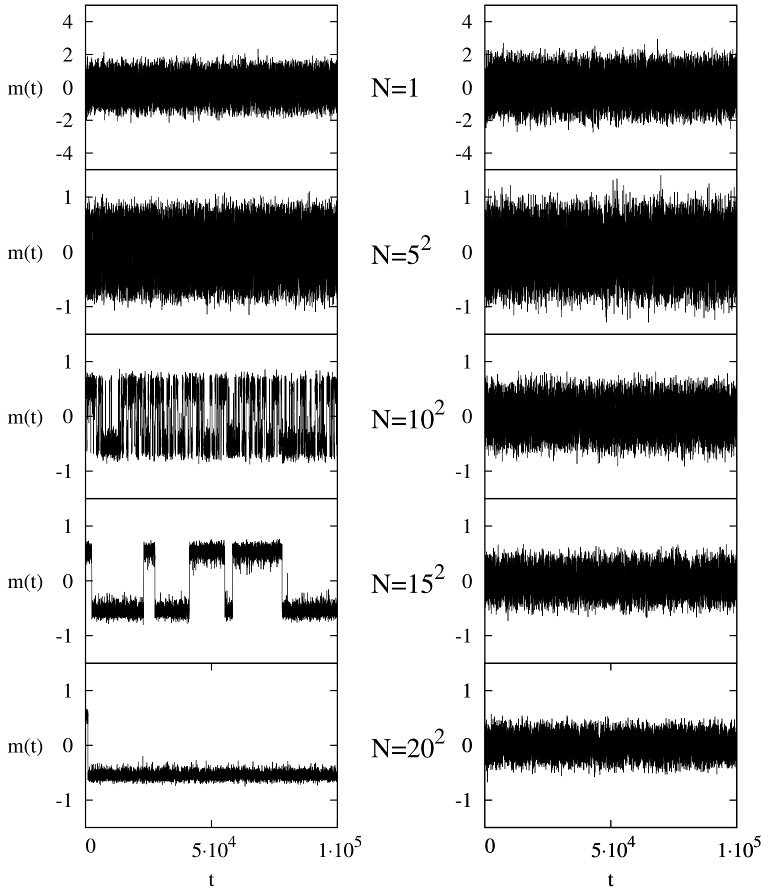

FIGURE 1. Time traces of the magnetization $m(t) = N^{-1}\sum_{i=1}^{N} x_i(t)$ for the Ginzburg-Landau model in a 2-d regular network with nearest-neighbors coupling. The right column corresponds to $D = 4$ (disordered state), and the left column to $D = 1.5$ (ordered stated). In both cases it is $\mu = 0.5$ and the coupling constant is $C = 20$. Note that the uncoupled system, $N = 1$ is always disordered as, in both cases, it has the maximum of the probability distribution located at $x = 0$. Note also that the width of the distributions decrease with N and tend to delta-functions in the limit $N \to \infty$.

It is remarkable, and counterintuitive, that a globally ordered situation arises as a result of an increase of the noise intensity. As it can be seen in Fig.2, the bifurcation is truly symmetry-breaking only for $N \to \infty$. If noise is increased even further, then a new bifurcation to the disordered state is obtained. However, as explained in detail in [15, 16] the explanation of this counterintuitive behavior has to do with the short-time dynamical instability of x_i rather than with the long-time steady distribution. We refer the interested reader to those papers and the excellent review in the book [17] for further details on this topic.

Let us now analyze this model using the results of the previous section with $q(x) = -x(1+x^2)^2$ and $g(x) = 1+x^2$. The change of variables in this case is $z = \int^x \frac{dx'}{1+x'^2} = \arctan(x)$ or $x = \tan(z)$. A one-to-one transformation is obtained if

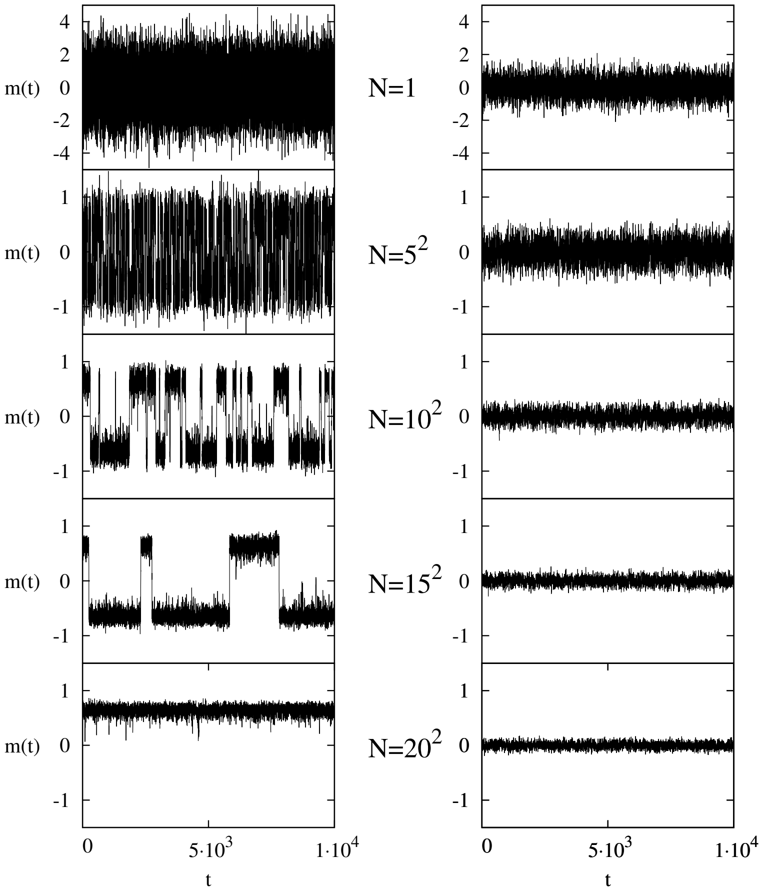

FIGURE 2. Time traces of the magnetization $m(t) = N^{-1}\sum_{i=1}^{N} x_i(t)$ for the canonical model displaying a noise-induced phase transition, Eq. (27) in a 2-*d* regular network with nearest-neighbors coupling. The right column corresponds to $D = 0.8$ (disorder state), and the left column to $D = 4$ (order induced by noise). The coupling constant is $C = 20$ in both cases. As in the previous figure, note that the uncoupled system, $N = 1$ is always disordered as, in both cases, it has the maximum of the probability distribution located at $x = 0$. Note also that the width of the distributions decrease with N and tend to delta-functions in the limit $N \to \infty$. Here and in Fig.1, the trajectories have been generated by a stochastic version of the Runge-Kutta algorithm, known as the Heun method [3] and using an efficient generator of Gaussian random numbers [18]

we limit $z \in (-\pi/2, \pi/2)$. The Langevin equation for the z variable is

$$\frac{dz}{dt} = -\frac{\sin(z)}{\cos(z)^3} + \sqrt{2D}\xi(t), \tag{28}$$

with a potential $V(z) = \frac{1}{2\cos(z)^2}$. The potential is monostable for $z \in (-\pi/2, \pi/2)$. The effective potential for the x variable is:

$$V_{\text{eff}}(x) = \frac{x^2}{2} + D\log(1 + x^2) \tag{29}$$

which, again, is always monostable. Therefore, in this case the change of variables does not induce any bistability.

In summary, we have revisited the concept of noise-induced transitions, defined as shifts in the maxima of the steady state probability distribution. They can not be considered "*bona fide*" bifurcations in the standard sense as (i) they can disappear through a one-to-one change of variables and (ii) there is no true symmetry breaking as all states can be visited independently of the initial condition. A noise-induced phase transition, on the other hand, can appear in the global variable of a coupled system. In the thermodynamic limit it displays symmetry breaking and lack of ergodicity. There are bifurcations from disorder to order when increasing the noise intensity (as in the Ginzburg-Landau model) but, more remarkably, there are cases in which an ordered state can appear as a result of an increase of the noise intensity. Generally, the transition is reentrant, in the sense that a large noise recovers the ordered state, but it is possible to find other situations in which reentrance does not occur [19].

ACKNOWLEDGMENTS

I thank N. Komin for help in plotting the figures. I acknowledge financial support by the MEC (Spain) and FEDER (EU) through project FIS2007-60327 (FISICOS).

REFERENCES

1. S. H. Strogatz, *Nonlinear dynamics and chaos*, Addison-Wesley, Reading, Mass., 1994, second edn.
2. A. Scott, editor, *Encyclopedia of Nonlinear Science*, Routledge, 2005.
3. M. S. Miguel, and R. Toral, “Stochastic effects in physical systems,” in *Instabilities and nonequilibrium structures VI*, edited by J. M. E. Tirapegui, and R. Tiemann, Kluwer academic publishers, 2000, pp. 35–120.
4. H. Risken, *The Fokker–Planck equation*, Springer–Verlag, Berlin, 1989, 2nd edn.
5. H. Kramers, *Physica (Ultrecht)* **7**, 284 (1940).
6. N. van Kampen, *Stochastic Processes in Physics and Chemistry*, North–Holland, Amsterdam, 1981, 1st edn.
7. C. Gardiner, *Handbook of Stochastic Methods for Physics, Chemistry and the Natural Sciences.*, Springer-Verlag, Berlin, 1983, first edn.
8. W. Horsthemke, and R. Lefever, *Noise-Induced Transitions: Theory and Applications in Physics, Chemistry, and Biology*, Springer, 1984.
9. M. Hongler, *Helv. Phys.Acta* **52**, 280 (1979).
10. D. J. Amit, and V. M. Mayor, *Field Theory, the Renormalization Group and Critical Phenomena*, World Scientific Publishing Co.Pte. Ltd., 2005, 3rd edn.
11. R. Albert, and A. Barabasi, *Rev. Mod. Phys.* **74**, 47 (2002).
12. H. Stanley, *Introduction to phase transitions and critical phenomena*, Oxford university press, 1971.
13. R. Toral, and A. Chakrabarti, *Phys. Rev. B* **42**, 2445 (1990).
14. C. Van den Broeck, J. Parrondo, J. Armero, and A. Hernández-Machado, *Phys. Rev. E* **49**, 2639–2643 (1994).
15. C. van den Broeck, J. M. R. Parrondo, and R. Toral, *Phys. Rev. Lett.* **73**, 3395 (1994).
16. C. van den Broeck, J. M. R. Parrondo, R. Toral, and K. Kawai, *Phys. Rev. E* **55**, 4084 (1997).
17. J. García-Ojalvo, and J. M. Sancho, *Noise in Spatially Extended Systems*, Springer–Verlag, New York, 1999.
18. R. Toral, and A. Chakrabarti, *Computer Physics Communications* **74**, 327 (1993).
19. M. Ibañes, J. García-Ojalvo, R. Toral, and J. M. Sancho, *Phys. Rev. Lett.* **87**, 20601 (2001).

On the approach to thermal equilibrium of macroscopic quantum systems

Sheldon Goldstein* and Roderich Tumulka†

*Departments of Mathematics and Physics, Rutgers University, Hill Center, 110 Frelinghuysen Road, Piscataway, NJ 08854-8019, USA E-mail: oldstein@math.rutgers.edu
†Department of Mathematics, Rutgers University, 110 Frelinghuysen Road, Piscataway, NJ 08854-8019, USA E-mail: tumulka@math.rutgers.edu

Abstract. In joint work with J. L. Lebowitz, C. Mastrodonato, and N. Zanghì [2, 3, 4], we considered an isolated, macroscopic quantum system. Let $\mathscr{H}$ be a micro-canonical "energy shell," i.e., a subspace of the system's Hilbert space spanned by the (finitely) many energy eigenstates with energies between E and $E+\delta E$. The thermal equilibrium macro-state at energy E corresponds to a subspace $\mathscr{H}_{eq}$ of $\mathscr{H}$ such that $\dim \mathscr{H}_{eq} / \dim \mathscr{H}$ is close to 1. We say that a system with state vector $\psi \in \mathscr{H}$ is in thermal equilibrium if ψ is "close" to $\mathscr{H}_{eq}$. We argue that for "typical" Hamiltonians, all initial state vectors ψ_0 evolve in such a way that ψ_t is in thermal equilibrium for most times t. This is closely related to von Neumann's quantum ergodic theorem of 1929.

Keywords: quantum statistical mechanics; approach to thermal equilibrium; thermalization of closed macroscopic quantum systems; micro-canonical energy shell; typical long-time behavior of quantum systems; typical Hamiltonian
PACS: 05.30.-d, 03.65.-w

INFORMAL STATEMENT OF RESULT

The result we wish to describe concerns a macroscopic quantum system, described by a wave function ψ evolving according to a Schrödinger dynamics ($\hbar = 1$):

$$i\frac{\partial \psi_t}{\partial t} = H\psi_t \,. \tag{1}$$

Here is the statement:

> For *every* initial state ψ_0 of a *typical* macroscopic quantum system (e.g., a gas in a box), the system will spend *most* of its time in *thermal equilibrium.*

We will need to explain what we mean by "typical" and "most," though you can probably guess. But first we must explain what we mean by "thermal equilibrium."

WHAT IS THERMAL EQUILIBRIUM?

There are, in fact, two basic views about what is meant by thermal equilibrium, corresponding to two different attitudes towards the foundations of statistical mechanics: the *individualist* view and the *ensemblist* view. According to the individualist *a system is in thermal equilibrium if it is in an appropriate pure state (given by a wave function or* *point in phase space).* According to the ensemblist *a system is in thermal equilibrium if it is in an appropriate statistical state (given by a density matrix or probability measure on phase space).* And depending upon what is intended by "appropriate" one obtains different individualist and ensemblist possibilities.

Individualist Equilibrium

In more detail, let's consider the meaning of equilibrium for an individualist for a classical macroscopic system. The state of the system is given by a point $X = (q_1,\dots,q_N,p_1,\dots,p_N)$ in its phase space, a point corresponding to the positions and velocities of its particles. The relevant part of the phase space is the energy surface $\Gamma = \{X : H(X) = E\}$, consisting of all phase points for which the energy H is the same value E. Then, depending on a choice of macro-variables, one may partition Γ into macro-states Γ_ν corresponding to different (small ranges of) values of the macro-variables, $\Gamma = \bigcup_\nu \Gamma_\nu$.

Here are two sketches of the partition into macro-states:

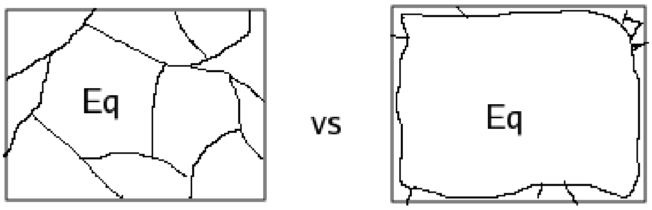

A crucial point is that the sketch on the left gives a completely distorted impression of the relative sizes of the macro-states. In particular, there will normally be one dominant macro-state, the equilibrium macro-state Γ_{eq}, that occupies almost the entire energy surface:

$$\frac{|\Gamma_{eq}|}{|\Gamma|} \approx 1$$

(using $|\cdot|$ for volume or area on the energy surface). With this is mind, we say that *a system is in equilibrium if its phase point is in the equilibrium macro-state, $X \in \Gamma_{eq}$.*

For a macroscopic quantum system the state of the system is given by its (normalized) wave function $\psi = \psi(q_1,\dots,q_N) \quad (\|\psi\| = 1)$. We shall assume that this belongs to the energy shell $\mathscr{H} = \operatorname{span}\{\phi_\alpha : E_\alpha \in [E, E+\delta E]\}$, spanned by the energy eigenstates ϕ_α whose eigenvalues E_α belong to the indicated range, i.e., $\psi = \sum_\alpha c_\alpha \phi_\alpha\,, \quad H\phi_\alpha = E_\alpha \phi_\alpha$. Then, instead of a partition into macro-states, we have an orthogonal decomposition into macro-spaces $\mathscr{H}_\nu$, corresponding more or less to different (small ranges of) values of the macro-variables (suitably "rounded" so that they commute),

$$\mathscr{H} = \bigoplus_\nu \mathscr{H}_\nu\,. \tag{2}$$

We assume that there is one dominant macro-space $\mathscr{H}_{eq}$:

$$\frac{\dim \mathscr{H}_{eq}}{\dim \mathscr{H}} \approx 1 .$$

We say that *the system is in equilibrium if its wave function* ψ *is near* $\mathscr{H}_{eq}$, meaning that the projection $P_{eq}\psi$ of ψ into $\mathscr{H}_{eq}$ is almost all of ψ, i.e., that

$$\langle \psi | P_{eq} | \psi \rangle \approx 1 . \tag{3}$$

Ensemblist Equilibrium

For an ensemblist a system is in equilibrium if its state X is random, or its quantum state is a mixture, with distribution or density matrix

$$\rho = \rho_{mc} \quad \text{or} \quad \rho = \rho_{can} = e^{-\beta H}/Z ,$$

where ρ_{mc} describes the microcanonical ensemble. This formulation has the defect that an individual system can't be in equilibrium and the virtue of being precise. It also has the virtue that it admits of a clean simple notion of approach to equilibrium.

Approach to Thermal Equilibrium

For an ensemblist a system approaches equilibrium of its time-evolving statistical state ρ_t has the obvious long-time limit:

$$\rho_t \longrightarrow \rho_{mc} \text{ (or } \rho_{can}) \text{ as } t \to \infty$$

in a suitable sense. This sort of *mixing* behavior, though rare and hard to prove for realistic deterministic dynamical systems, is a genuine mathematical possibility.

As a natural first attempt at an individualist formulation of approach to equilibrium, consider the condition that $X_t \in \Gamma_{eq}$ (or near Γ_{eq}) as $t \to \infty$, i.e., that $\langle \psi_t | P_{eq} | \psi_t \rangle \approx 1$ for $t \to \infty$. This is typically impossible, because of the phenomenon of Poincaré recurrence. It will typically not be the case that the system is in, or near, equilibrium for all sufficiently large times. Rather what is meant by *approach to equilibrium* for an individualist, and what we mean by it here, is that $X_t \in \Gamma_{eq}$ or, in the quantum case, with which we are concerned here,

$$\langle \psi_t | P_{eq} | \psi_t \rangle \approx 1$$

for *most* (sufficiently large) t (even when the system is initially not in equilibrium).

Equilibrium is Typical

It is important to recognize that with this (equation (3)) understanding of equilibrium, for *most* $\psi \in \mathscr{H}$ the system is indeed in equilibrium—just as in the classical case. Here the sense of "most" is given by the microcanonical distribution $\mu_{mc} = \mu$ on $\mathscr{H}$, i.e., the uniform distribution over the unit sphere in $\mathscr{H}$:

$$\langle\psi|P_{eq}|\psi\rangle \approx 1 \text{ for } \mu\text{-most } \psi s\,.$$

This is easily seen by computing the microcanonical average

$$\begin{aligned}\int \mu(d\psi)\langle\psi|P_{eq}|\psi\rangle &= \mathrm{Tr}\left[\left(\int \mu(d\psi)|\psi\rangle\langle\psi|\right)P_{eq}\right] \\ &= \mathrm{Tr}\left[\rho_{mc}P_{eq}\right] = \frac{\dim\mathscr{H}_{eq}}{\dim\mathscr{H}} \approx 1\,,\end{aligned}$$

where $\rho_{mc} = I/\dim\mathscr{H}$ (and $\mathrm{Tr}P_{eq} = \dim\mathscr{H}_{eq}$). Since $\langle\psi|P_{eq}|\psi\rangle$ can be no greater than 1, it follows that it must be near 1 for μ-most ψs.

That equilibrium is in this sense typical is crucial to the individualist understanding of the notion. However, it does have the consequence that the initial wave functions ψ_0 with which we are concerned for the issue of approach to equilibrium are atypical. We would like it to be the case that even for "most" non-equilibrium initial wave functions we have approach to equilibrium. The best that we could hope for in this regard is that we have approach to equilibrium for all such wave functions.

ABSOLUTE THERMALIZATION AND EIGENSTATE THERMALIZATION

When a system is such that we have approach to equilibrium for *all* initial wave functions ψ_0, we say that we have *absolute thermalization* (AT). Clearly, a necessary condition for AT is that

$$\langle\phi_\alpha|P_{eq}|\phi_\alpha\rangle \approx 1 \text{ for all } \alpha, \tag{4}$$

since the energy eigenstates ϕ_α, possible initial states, are stationary states. Equation (4) is a version of what Srednicki [8] has called *eigenstate thermalization* (ET).

It is also sufficient, as is easily seen by computing the time-average of $\langle\psi_t|P_{eq}|\psi_t\rangle$. Writing $\overline{f(t)}$ for the time average of f,

$$\overline{f(t)} = \lim_{T\to\infty}\frac{1}{T}\int_0^T dt\, f(t)\,,$$

we have that

$$\overline{\langle\psi_t|P_{eq}|\psi_t\rangle} = \mathrm{Tr}\left[\overline{|\psi_t\rangle\langle\psi_t|}P_{eq}\right]\,. \tag{5}$$

With

$$\psi_0 = \sum_{\alpha=1}^{D} c_\alpha|\phi_\alpha\rangle \quad (D = \dim\mathscr{H})$$

and hence

$$\psi_t = \sum_{\alpha=1}^{D} e^{-iE_\alpha t}c_\alpha|\phi_\alpha\rangle$$

we thus have that

$$\overline{|\psi_t\rangle\langle\psi_t|} = \sum_{\alpha,\beta} \underbrace{\overline{e^{-i(E_\alpha - E_\beta)t}}}_{\delta_{\alpha\beta}} c_\alpha c_\beta^* |\phi_\alpha\rangle\langle\phi_\beta| = \sum_\alpha |c_\alpha|^2 |\phi_\alpha\rangle\langle\phi_\alpha| \,.$$

Inserting this into (5), we find that

$$\overline{\langle\psi_t|P_{eq}|\psi_t\rangle} = \sum_\alpha |c_\alpha|^2 \langle\phi_\alpha|P_{eq}|\phi_\alpha\rangle \,. \tag{6}$$

Since $\langle\psi_t|P_{eq}|\psi_t\rangle$ can't be greater that 1, it follows from (6) and (4) that it must be near 1 for most times. Hence ET is indeed a sufficient condition for AT,

$$\mathrm{ET} \Rightarrow \mathrm{AT}\,.$$

Eigenstate Thermalization

Even though equilibrium is typical, since ET requires that *all* energy eigenstates in the microcanonical subspace $\mathscr{H}$, of which there are a great many, be in equilibrium, you might imagine that ET is a rather stringent condition. It can be shown [2], however, that ET in facts holds for a typical Hamiltonian H.

The meaning here of "typical" is in the sense of most Hs as provided by the uniform distribution on orthonormal bases of $\mathscr{H}$: Fix the energies $E_1, \dots, E_D$ (assumed nondegenerate). Let

$$H = \sum_\alpha E_\alpha |\phi_\alpha\rangle\langle\phi_\alpha|$$

with the orthonormal basis $\phi_\alpha, \alpha = 1, \dots D$, uniformly distributed. Equivalently, let

$$H = UH_0U^*, \quad H_0 = \sum_\alpha E_\alpha |\chi_\alpha\rangle\langle\chi_\alpha|$$

with χ_α any orthonormal basis of $\mathscr{H}$ and U a uniformly (Haar) distributed unitary on $\mathscr{H}$. By a typical Hamiltonian we refer to the distribution of such a random Hamiltonian H.

To appreciate why ET might be expected to hold for a typical Hamiltonian H, choose the basis $\{\chi_\alpha\}$ in such a way that the first $d_{eq} = \dim \mathscr{H}$ basis vectors lie in $\mathscr{H}_{eq}$. Then

$$\langle\phi_\alpha|P_{eq}|\phi_\alpha\rangle = \sum_{\beta=1}^{d_{eq}} |U_{\beta\alpha}|^2 \tag{7}$$

with

$$\phi_\alpha = \sum_{\beta=1}^{D} U_{\beta\alpha}\chi_\beta$$

where $U_{\beta\alpha}$ is uniformly distributed unitary $D \times D$ matrix. The distribution of (7) is independent of α, and the crucial estimate is that of the probability p that $\sum_{\beta=1}^{d_{eq}} |U_{\beta\alpha}|^2$ fails to be near 1.

For fixed α the $U_{\beta\alpha}$s are approximately independent complex Gaussian random variables with mean 0 and variance $1/D$. Suitably using large deviations estimates for independent Gaussians, p can be shown to be sufficiently small.

PRECISE STATEMENT OF RESULT

For the record, here is a precise statement of the main result:

For all $\eta, \delta, \delta' \in (0,1)$, *all integers* $D > D_0(\eta\delta', \delta)$ *and all integers* $d_{eq} > (1 - \eta\delta'/2)D$ *the following is true: Let* $\mathscr{H}$ *be a Hilbert space of dimension D; let* $\mathscr{H}_{eq}$ *be a subspace of dimension* d_{eq}*; let* P_{eq} *denote the projection to* $\mathscr{H}_{eq}$*; let* $E_1, \ldots, E_D$ *be pairwise distinct but otherwise arbitrary; choose a Hamiltonian at random with eigenvalues* E_α *and an eigenbasis* ϕ_α *that is uniformly distributed. Then, with probability at least* $1 - \delta$*, every initial quantum state will spend* $(1 - \delta')$*-most of the time in thermal equilibrium in the sense that*

$$\liminf_{T\to\infty} \frac{1}{T}\Big|\big\{0 < t < T : \langle\psi_t|P_{eq}|\psi_t\rangle > 1 - \eta\big\}\Big| \geq 1 - \delta', \qquad (8)$$

where $|M|$ *denotes the size (Lebesgue measure) of the set M.*

We don't want to go into many details here. But we do want to note that δ (≈ 0) makes precise what we have meant by most Hs, δ' (≈ 0) most times, and η (≈ 0) how near $\langle\psi_t|P_{eq}|\psi_t\rangle$ must be to 1.

VON NEUMANN'S QUANTUM ERGODIC THEOREM (1929) [10]

Here is an informal statement of von Neumann's quantum ergodic theorem:

> For *every* initial state ψ_0 of a *typical* macroscopic quantum system, the system will spend *most* of its time in *thermal equilibrium*.

This should seem rather similar to the earlier informal statement of the result I've been discussing up to this point. And, as a matter of fact, "every" and "most" mean here exactly what they meant there, and "typical" means almost the same thing. But the meaning here of "thermal equilibrium" is rather different.

In the orthogonal decomposition (2) of $\mathscr{H}$ into macro-spaces $\mathscr{H}_\nu$, let $d_\nu = \dim \mathscr{H}_\nu$ and let P_ν be the corresponding projections. For von Neumann a system with wave function ψ is in thermal equilibrium if, instead of (3), we have that

$$\langle\psi|P_\nu|\psi\rangle \approx d_\nu/D \qquad (9)$$

for all ν. And as a sufficient condition for absolute thermalization AT+ for this more stringent notion of equilibrium, von Neumann provides a strengthening ET++ of ET. ET++ is in fact a strengthening of a condition ET+, namely that for all ν

$$\langle\phi_\alpha|P_\nu|\phi_\alpha\rangle \approx d_\nu/D \qquad (10)$$

for all α, itself a strengthening of ET naturally suggested by comparing (3) and (9).

To better appreciate the significance of (9), observe that

$$\int \mu(d\psi)\langle\psi|P_\nu|\psi\rangle = \mathrm{Tr}\,[\rho_{mc}P_\nu] = d_\nu/D\,.$$

In particular, (9) is the same thing as

$$\langle\psi|P_\nu|\psi\rangle \approx \mathrm{Tr}\,[\rho_{mc}P_\nu]\,,$$

i.e., the requirement that the quantum averages of the macro-projections P_ν agree with their micro-canonical averages.

ET++ involves a certain non-resonance condition [10] (requiring non-degenerate energy gaps) together with the following:

$$\max_{\alpha\neq\beta}\left|\langle\phi_\alpha|P_\nu|\phi_\beta\rangle\right|^2 + \max_\alpha\left(\langle\phi_\alpha|P_\nu|\phi_\alpha\rangle - \frac{d_\nu}{D}\right)^2 \ll 1\,. \tag{11}$$

The second term on the left hand side of (11) corresponds to ET+, which implies that

$$\overline{\langle\psi_t|P_\nu|\psi_t\rangle} \approx \frac{d_\nu}{D}$$

in the same way that ET implies AT. But ET+ does not imply AT+, because $\langle\psi_t|P_\nu|\psi_t\rangle$ could have significant fluctuations above and below its mean. The first term is needed to control these fluctuations, via bounds on

$$\overline{\left(\langle\psi_t|P_\nu|\psi_t\rangle - \frac{d_\nu}{D}\right)^2}\,.$$

Von Neumann showed that ET++ indeed implies AT+. He also showed that ET++ is satisfied for a typical Hamiltonian. To do the latter is considerably more difficult than showing this for ET. (Because of certain assumptions on the dimensions of macro-spaces needed by von Neumann, the result in Section () is not a consequence of the quantum ergodic theorem.)

A Remark on Varieties of Individualism (Quantum Case)

Von Neumann's quantum ergodic theorem has both individualist and ensemblist aspects. It is individualist in that the relevant notion of equilibrium is for an individual pure state; it is ensemblist in that what it demands of that pure state is that it resemble the microcanonical ensemble. We're inclined to say that the quantum ergodic theorem is quasi-individualist—individualist by accident or necessity—and not pure individualist. This is true also for many of the related results—in which the individualism permits the extraction of thermal statistics without having to make any detailed a priori probabilistic assumptions—upon which we shall now touch.

RELATED RESULTS

Versions of eigenstate thermalization have been discussed by Schnirelman, see [1], and by M. Srednicki [8]. Results on equilibration and thermalization have been obtained by N. Linden, S. Popescu, A.J. Short, and A. Winter [5], by P. Reimann [6], by H. Tasaki [9], and by M. Rigol, V. Dunjko, and M. Olshanii [7].

Most of the equilibration and thermalization results say something in the vicinity of the following: *For physical initial states* ψ_0 *of suitable macroscopic quantum systems, the system will spend most of its time in thermal equilibrium.* Different results may involve different notions of "physical" and of "suitable." Here we wish only to mention that the various "thermal equilibrium" conditions involved are of the form

$$\langle \psi | A | \psi \rangle \approx \mathrm{Tr}\,[\rho_{mc} A]$$

for all $A \in \mathscr{A}$, with the different choices of a class $\mathscr{A}$ of observables corresponding to different notions of thermal equilibrium. For example, for von Neumann $\mathscr{A}$ consists of macroscopic observables, and for Linden et al. of observables for a small subsystem of a larger system.

REMARK ON TYPICALITY

We quote here from [3]:

> When employing the method of appeal to typicality, one usually uses the language of probability theory. But that does not imply that any of the objects considered is random in reality. Rather, it means that certain sets (of wave functions, of orthonormal bases, etc.) have certain sizes (e.g., close to 1) in terms of certain natural (normalized) measures of size. That is, one describes the behavior that is *typical* of wave functions, orthonormal bases, etc.. However, since the mathematics is equivalent to that of probability theory, it is convenient to adopt that language. For this reason, using a normalized measure μ does not mean making an "assumption of equal probability," even if one uses the word "probability." Rather, it means that, if a condition is true of most . . . , or most H, this fact may suggest that the condition is also true of a concrete given system, unless we have reasons to expect otherwise.
>
> Of course, a theorem saying that a condition is true of the vast majority of systems does not *prove* anything about a concrete given system; if we want to know for sure whether a given system is normal for every initial wave function, we need to check the relevant condition . . . . Nevertheless, a typicality theorem is, as we have suggested, illuminating; at the very least, it is certainly useful to know which behaviour is typical and which is exceptional. . . .
>
> The method of appeal to typicality belongs to a long tradition in physics, which includes also Wigner's work on random matrices of the 1950s. In the words of Wigner . . . :
>
>> One [. . .] deals with a specific system, with its proper (though in many cases unknown) Hamiltonian, yet pretends that one deals

> with a multitude of systems, all with their own Hamiltonians, and averages over the properties of these systems. Evidently, such a procedure can be meaningful only if it turns out that the properties in which one is interested are the same for the vast majority of the admissible Hamiltonians.

This method was used by Wigner to obtain specific new and surprising predictions about detailed properties of complex quantum systems in nuclear physics.

REFERENCES

1. Y. Colin de Verdière, *Commun. Math. Phys.* **102**, 497–502 (1985).
2. S. Goldstein, J. L. Lebowitz, C. Mastrodonato, R. Tumulka, and N. Zanghì, *Phys. Rev. E* **81**, 011109 (2010); `http://arxiv.org/abs/0911.1724`.
3. S. Goldstein, J. L. Lebowitz, C. Mastrodonato, R. Tumulka, and N. Zanghì, *Proc. R. Soc. Lond. A* **466**(2123), 3203–3224 (2010); `http://arxiv.org/abs/0907.0108`.
4. S. Goldstein, J. L. Lebowitz, R. Tumulka, and N. Zanghì, *Euro. Phys. J. H,* to appear; `http://arxiv.org/abs/1003.2129v1`
5. N. Linden, S. Popescu, A. J. Short, and A. Winter, *Phys. Rev. E* **79**, 061103 (2009); `http://arxiv.org/abs/0812.2385`.
6. P. Reimann, *Phys. Rev. Lett.* **101**, 190403 (2008); `http://arxiv.org/abs/0810.3092`
7. M. Rigol, V. Dunjko, and M. Olshanii, *Nature* **452**, 854–858 (2008); `http://arxiv.org/abs/0708.1324`.
8. M. Srednicki, *Phys. Rev. E* **50**, 888–901 (1994).
9. H. Tasaki, *Phys. Rev. Lett.* **80**, 1373–1376 (1998); `http://arxiv.org/abs/cond-mat/9707253`.
10. J. von Neumann, *Z. Phys.* **57**, 30–70 (1929).
11. E. P. Wigner, *SIAM Review* **9**, 1–23 (1967).

Temperature, entropy and second law beyond local equilibrium: An illustration

David Jou

Departament de Física, Universitat Autónoma de Barcelona, 08193 Bellaterra, Catalonia, Spain
Institut d'Estudis Catalans, Carme 47, 08001 Barcelona, Catalonia, Spain

Abstract. Local-equilibrium thermodynamics applies to local scale the concepts and methods of equilibrium thermodynamics concerning the meaning of entropy, temperature and equations of state. However, when going beyond local equilibrium, the basic problems avoided by local equilibrium hypothesis arise: how temperature and entropy are defined, how second law is formulated, how macroscopic theory is related to microscopic formulations. Here, we illustrate these topics with phonon hydrodynamics as a model for the description of heat transfer in nanosystems and its corresponding non-equilibrium thermodynamic potentials, and discuss the limits for the existence of non-equilibrium thermodynamic potentials in general situations.

Keywords: Non-equilibrium thermodynamics, temperature, entropy, heat transport in nanosystems
PACS: 05.70.Ln, 05.70.Ce, 05.60.Cd, 05.20.Jj

INTRODUCTION

One of the relevant conceptual questions in non-equilibrium thermodynamics is whether there exists the analogous of equilibrium thermodynamic potentials for non-equilibrium steady states, with such potentials depending on the currents through the system [1]. Non-equilibrium steady states share with equilibrium states the fact that the variables describing them do not depend on time, but they differ from them by the presence of non-vanishing fluxes of mass, energy, momentum, and some other relevant quantities. Thus, a natural generalization of equilibrium thermodynamics would be the thermodynamics of non-equilibrium steady states, including the non-zero currents as additional variables. In particular, we will provide an example of non-equilibrium thermodynamic potentials, and we will examine their form and their main physical contents. Thus, although such potentials are not expected to exist in general, they are useful in a number of relevant situations of much practical interest.

Usually, the approach towards the description of a system far from equilibrium is undertaken from a microscopic perspective, with emphasis on a kinetic equation describing the evolution of the distribution function, and with the obtention of such distribution function in special situations of interest. The microscopic information obtained in such a perspective is in fact considerably wider than that accessible through macroscopic and mesoscopic measurements. Therefore, it would be of interest to proceed in two complementary directions: the usual bottom-up approach of statistical mechanics, and the up-down approach of thermodynamics.

The second approach has been, up to now, less developed than the first one, because of the usual restriction of non-equilibrium thermodynamics to the local-equilibrium hypothesis [2], in which the thermodynamic potentials and equations of state keep locally the same form they have in equilibrium thermodynamics. From this point of view, non-equilibrium thermodynamics does not bring any approach towards a mesoscopic description, in which additional variables are needed besides the local-equilibrium ones. Then, a question arising in the up-down approach is which are the variables necessary for the description of the mesoscopic state. This question is related to the experimental capabilities and to the intrinsic nature and dynamics of the corresponding system and is also a topic of interest from the microscopic perspective, as one should identify them in terms of microscopic operators whose average could be calculated from the distribution function.

Among the observables there is the temperature, which deserves special mention because of its central relevance in thermodynamics, and because it exerts an influence on practically all the properties of the system. Thermometry in non-equilibrium states is not a trivial question, because there are many different ways to measure temperature, related to different variables. In equilibrium, measuring temperature in different ways yields the same value, but out of equilibrium the values of the different methods of measurement are different and, on the other side, they also depend not only on properties of the own system but also from the contact between the system and the thermometer. The question of temperature also appears in microscopic theories, asking for microscopic definitions of temperature, which may be different ones. A second group of questions refers to the entropy and second law. This question is especially delicate, because entropy is defined only for equilibrium states. Can an entropy be also defined for non-equilibrium steady states? Is it univocal? How is the formulation of the second law related to this entropy? Although up to now no clear answers are known for all these questions, asking for them is useful because the frontiers of local-equilibrium thermodynamics become better understood. Furthermore, the dialog between the up-down approach with the bottom-up approach is fostered if one has more general expressions than the local-equilibrium ones, and is also more fruitful and challenging.

PHONON HYDRODYNAMICS AND HEAT TRANSPORT IN NANOSYSTEMS

We will specify our analysis to heat transport in nanosystems, which is not described by usual Fourier's law, but by more detailed equations accounting for the transition from diffusive to ballistic transport [3, 4, 5, 6, 7]. This is necessary, for instance, when the size of the system (for instance, the radius of a nanowire, the thickness of thin layer, the size of each layer in a multilayered system, and so on) becomes comparable to the mean-free path ℓ of the heat carriers.

From the practical point of view Fourier's law is generalized as

$$\frac{dQ}{dt} = -\lambda_{eff}\left(\frac{\ell}{R}\right) A \nabla T \tag{1}$$

where dQ/dt stands for the heat along a nanowire per unit time, A is the transverse area of the nanowire, R its radius, and $\lambda_{eff}(\ell/R)$ is the effective thermal conductivity, which tends to the bulk thermal conductivity when ℓ/R (a dimensionless ratio usually known as Knudsen number) tends to zero, and tends to 0 when ℓ/R is big. The decrease of the effective thermal conductivity of nanowires with decreasing radius is well known from the experimental point of view [4, 5], and is expected to be useful, for instance, in thermoelectrical conversion, where it is convenient to have low thermal conductivity and high electrical conductivity.

To describe this behavior, one may use for the local heat flux $\mathbf{q}$ a transport equation incorporating the mean free path of the carriers. Furthermore, if one is interested in describing also fast perturbations, one should incorporate the relaxation time t of the heat flux, related to the collision time of the heat carriers. As a concrete illustration we consider the Guyer-Krumhansl equation, of the form [6, 7, 8]

$$\tau \frac{d\mathbf{q}}{dt} = -\mathbf{q} - \lambda \nabla T + \ell^2 \nabla^2 \mathbf{q} \tag{2}$$

with λ the bulk thermal conductivity (dependent on the material and temperature but not on the size of the system). When the terms in τ and ℓ are negligible, this equation reduces to Fourier's law. In the steady state, and when ℓ/R is higher than 1, this equation yields $\lambda_{eff} = (\lambda/8)(R/\ell)^2$, which tends to 0 when R tends to zero [8]. However, it tends to zero too fast, as for small R it is experimentally observed that λ_{eff} behaves linearly with R rather than quadratically.

This feature may be taken into account if one incorporates constitutive equations for a slip heat flow $\mathbf{q}_w$ along the wall, in the so-called Knudsen layer, a layer near the wall of thickness of the order of ℓ. This is a relevant contribution when ℓ is of the order of R or higher than R. In this case, and in analogy with the theory of rarefied gases, we take [8, 9]

$$\mathbf{q}_w = C\ell \left(\frac{\partial \mathbf{q}}{\partial r} \right)_{r=R} - \alpha \ell^2 \left(\frac{\partial^2 \mathbf{q}}{\partial r^2} \right)_{r=R} \tag{3}$$

The coefficient C takes into account specular and diffusive phonon collisions against the wall, and the coefficient α has been proposed to describe phonon-backscattering, a phenomenon of special interest in rough-walled nanowires. When this is taken into account one finds [8]

$$\lambda = \frac{\lambda_0}{8} \frac{R^2}{\ell^2} \left[1 + 4C \frac{\ell}{R} - 4\alpha \frac{\ell^2}{R^2} \right] \tag{4}$$

Thus, below a small value of the radius it seems that backscattering effects may turn the nanowire into a heat insulator with vanishing effective thermal conductivity. Thus, expression (4) is not meant to give negative values for the thermal conductivity, but zero values for R smaller than the value making (4) to vanish. The coefficients C and α depend on temperature and on the roughness of the wall. When they are taken into account, they provide a reasonable description of the effective thermal conductivity of nanolayers [8]. Alternative versions based on a continued-fraction expansion of the effective thermal conductivity in terms of the Knudsen number have also been studied [6, 10].

NON-EQUILIBRIUM THERMODYNAMIC POTENTIALS FOR RELAXATIONAL HEAT TRANSFER

Since Fourier's law, directly relating the heat flux to the instantaneous and local temperature gradient, has been replaced by an evolution equation for the heat flux **q**, as in (2), it is clear that **q** becomes an independent variable of the theory. Then, it is logical to incorporate it into the entropy of the system. In particular, in extended thermodynamics [1, 6, 7, 11, 12], the entropy per unit mass is seen to have the form

$$s\left(u,\mathbf{q}\right)=s_{eq}(u)-\frac{\tau v}{2\lambda T^{2}}\mathbf{q}\cdot\mathbf{q} \tag{5}$$

where $s_{eq}(u)$ is the local equilibrium entropy. Furthermore, the entropy flux is [6]

$$\mathbf{J}=\frac{\mathbf{q}}{T}-\frac{\ell^{2}}{\lambda T^{2}}\left(\nabla\mathbf{q}\right)\cdot\mathbf{q} \tag{6}$$

Both the entropy (5) and the entropy flux (6) reduce to their respective classical expressions when the terms in t and ℓ are negligible. From (5) one may define a Gibbs free energy of the form

$$g\left(T,\mathbf{q}\right)=g_{eq}(T)-\frac{\tau v}{2\lambda T}\mathbf{q}\cdot\mathbf{q}+\frac{\tau v}{T}\left(\nabla T\right)\cdot\mathbf{q} \tag{7}$$

This free energy becomes minimum when $\mathbf{q}=-\lambda\nabla T$, i.e. when Fourier's law is locally satisfied.

Some outstanding properties of the non-equilibrium thermodynamic potentials (5) and (7) are:

1) *The entropy (5) is more satisfactory for the expression of the second law of thermodynamics than the local-equilibrium entropy*; indeed, the advantage of the extended non-equilibrium entropy (5) with respect to the local-equilibrium one is that the extended entropy production has the form [1, 6, 7]

$$\sigma^{s}=\mathbf{q}\cdot\left[\nabla T^{-1}-\frac{\tau}{\lambda T^{2}}\left(\frac{d\mathbf{q}}{dt}\right)\right]+\frac{\ell^{2}}{\lambda T^{2}}\left(\nabla\mathbf{q}\right):\left(\nabla\mathbf{q}\right) \tag{8}$$

For **q** satisfying equation (2), this entropy production is always positive. Instead, the local-equilibrium entropy production is simply $\sigma^{s}=\mathbf{q}\cdot\nabla T^{-1}$, which may be positive or negative if the heat flux follows equation (2) instead of Fourier's law. In particular, the integrated entropy in an insulated system evolving towards equilibrium through equation (2) is always increasing for the generalized entropy (5) but not for the integrated local-equilibrium entropy, in which case the entropy production may oscillate.

2) *The entropy (5) is closer to the Boltzmann entropy than the local-equilibrium entropy itself.* Indeed, up to the second order in the non-equilibrium corrections, Boltzmann expression for the entropy in terms of the velocity distribution function may be written as [6, 7]

$$s=s_{eq}(u)-\left(\frac{k_{B}}{2}\right)\int\Phi_{1}^{2}\left(\mathbf{C}\right)f_{eq}\left(\mathbf{C}\right)d\mathbf{C} \tag{9}$$

with $\mathbf{C}$ the particle velocity, $f_{eq}(\mathbf{C})$ the local-equilibrium distribution function, $s_{eq}(u)$ the local-equilibrium entropy corresponding to the Boltzmann entropy for the Maxwell-Boltzmann distribution function, and $\Phi_1(\mathbf{C})$ the non-equilibrium correction, namely $f(\mathbf{C}) = f_{eq}(\mathbf{C})[1+\Phi_1^2(\mathbf{C})]$, where $\Phi_1(\mathbf{C})$ depends on the heat flux or the temperature gradient. It is checked that when the non-equilibrium correction to the distribution function is introduced into (9) and the integral is carried out, the non-equilibrium term of the entropy (5) is obtained, either in Grad's moment expansion or in Chapman-Enskog gradient expansion or in maximum-entropy distribution functions for a system submitted to a heat flux. Thus, using entropy (5) one is closer to microscopic results than merely using the local-equilibrium entropy.

3) *The generalized entropy (5) contains information on the fluctuations of the fluxes around an equilibrium state*. Indeed, using Einstein formula for the probability of fluctuations around equilibrium one finds from (5) that the second moments of fluctuations of the heat flux are given by [1, 6, 7]

$$\langle \delta q_i \delta q_j \rangle = k_B \left(\frac{\lambda T^2}{\tau v} \right) \delta_{ij} \tag{10}$$

This is a particular expression of the Green-Kubo relations between transport coefficients and the time integral of the time correlation function of the fluctuations of the fluxes, for relaxational dynamics consistent with equation (2) around an equilibrium (homogeneous) state. For more general kinds of dynamics, more general forms of the entropy should be used instead of (5). Some particular cases are known, but not the general answer.

4) *The free energy (7) contains information on the fluctuations of the heat flux around its steady state average value*. In particular, the relation between probability and free energy (7) leads to the following expression for the ratio of the relative probabilities that the heat flux $\mathbf{q}$ has a value $+\mathbf{q}$ in the forward direction (i.e. in the direction of the average steady state value given by Fourier's law) or a value $\mathbf{q}$ (in the backwards direction) [14]

$$\frac{Pr(\mathbf{q})}{Pr(-\mathbf{q})} = \exp\left(\frac{-2\lambda \nabla T \cdot \mathbf{q}}{\left\langle (\delta q_i)^2 \right\rangle_{eq}} \right) \tag{11}$$

The relative probability of fluctuations of the fluxes around non-equilibrium steady states is currently a topic of much interest in statistical physics [15, 16].

Thus, in general terms, it is seen that in some situations, non-equilibrium thermodynamic potentials dependent on the currents may be defined, and generalize a number of properties of the equilibrium thermodynamic potentials. We will comment that this result is not expected to be completely general, but since a considerable number of situations of practical interest fall in this range, its theoretical and practical interest is remarkable.

TEMPERATURE IN NON-EQUILIBRIUM STEADY STATES

Since in equilibrium thermodynamics the reciprocal of absolute temperature is given by the partial derivative of the entropy with respect to internal energy at constant volume and composition, the question about the meaning of this derivative for a non-equilibrium entropy arises in an immediate way. Evidently, since the entropy (5) depends on heat flux, its derivative with respect to internal energy will also depend on the heat flux, thus being different than the local-equilibrium absolute temperature. This idea does not seem very intuitive, and deserves some attention [17, 18, 19, 20]. In equilibrium thermodynamics there are more than a dozen ways to relate temperature of the system to some of its physical properties, let they be entropy, thermal or caloric equations of state, second moments of fluctuations in equilibrium, transport coefficients, average kinetic energy, average energy of different microscopic degrees of freedom [17]. In equilibrium, all these definitions lead to the same value of temperature in a given state of the system, but out of equilibrium all the definitions are expected to lead to different values, in general.

Thus, out of equilibrium the zero principle must be reformulated in more detail than in equilibrium, namely, by referring to the concrete kind of interaction between the system and the thermometer. In our opinion, all the different definitions of temperature out of equilibrium are physically interesting, and one should try to be able to understand their mutual relation and predict the outcomes of the different temperatures for a given non-equilibrium steady state [17]. For instance, in non-equilibrium steady state, the average kinetic energy depends on the spatial direction, and therefore the corresponding directional temperatures that could be defined will be different [17, 18, 19, 20, 21]. In simple situations one may study, for instance, the relation between the several directional temperatures in terms of the heat flux crossing the system. The difference is small in usual situations, but it may be very relevant in shock waves [21]. It seems (although it is not clear how general this statement is) that the thermodynamic temperature obtained from the derivative of the entropy with respect to internal energy is related to the kinetic temperature in an axis perpendicular to the heat flux, and that it is lower than the average kinetic energy along the direction of the heat flux [17]. Similar analyses could be done if configurational temperatures related to the average intermolecular potential energy are used; in this case, one should be able to know the kinetic and the configurational temperatures, and to know how the several degrees of freedom (kinetic and potential, for instance) contribute to the heat transport and thermal conductivity.

PHYSICAL INTERPRETATION AND LIMITS OF VALIDITY OF THE NON-EQUILIBRIUM POTENTIALS

The generalized entropy (5) may be given a relatively simple and appealing interpretation. Assume a system in a non-equilibrium steady state; assume that a small volume of it is suddenly isolated and let to decay to equilibrium. The difference between the final entropy (the local-equilibrium entropy) and the initial entropy (the unknown non-equilibrium entropy) will be related to the entropy production as

$$s_{fin} = s_{in} + \int_0^\infty \sigma^s dt \tag{12}$$

If the expression $\sigma^s = \mathbf{q} \cdot \mathbf{q} / \lambda T^2$ is used and an exponential decay for the heat flux is assumed in (12), the entropy (5) is obtained [6]. However, this process will lead to a unique entropy provided that the dissipation does not depend on the way the isolated system decays to equilibrium. In principle, there could be many situations in which such decay could depend on the specific way of decaying, in such a way that a non-equilibrium entropy could not be defined, unless one was able to characterize in full detail the whole decay. Then, it is conceivable that energy dissipation is a more general concept than entropy itself, in the sense that one could have the dissipation per unit time well defined, but its time integral would depend on the process. In this case, relation (12) would take processes rather than states as the basic focus of attention [22].

CONCLUSIONS

In this text we have presented an explicit non-equilibrium thermodynamic potential dependent on the heat flux, namely entropy (5) or free energy (7). Such potentials have a number of interesting properties relating them to a definite positive production or to the properties of the fluctuations of the fluxes, which generalize the properties of the local-equilibrium potentials. In particular, the potential we have shown is related to generalized transport equations, going beyond Fourier's law and describing the transition from diffusive to ballistic heat transport. Thus, this equation is useful for the description of heat transport in nanosystems. This kind of potentials has also been studied for mass transport, electrical current, and flowing systems submitted to viscous effects [6, 7].

We have also warned that in general it should not be expected to find such generalized thermodynamic potentials, unless one would be able to characterize in detail the particular process of decay of a system to equilibrium after it has been suddenly isolated. This may be too complicated and cumbersome to be practically useful, in which case one could directly take the processes themselves as the protagonists of the non-equilibrium analysis.

Since we have referred to nanosystems, it is also worth of mention the role of the constitutive equations on the boundaries, for instance, for a slip heat flow along the wall, which may have much influence on the effective thermal conductivity along nanowires. Thus, as it is logical to expect, non-equilibrium small systems require a detailed consideration of wall effects.

ACKNOWLEDGMENTS

The financial support of the Dirección General de Investigación of the Spanish Ministry of Science and Innovation under grant FIS 2009-13370-C02-01, and of the Direcció General of the Generalitat of Catalonia under grant 2009SGR-00164 is gratefully acknowledged.

REFERENCES

1. G. Lebon, D. Jou, and J. Casas-Vázquez, *Understanding non-equilibrium thermodynamics*, Springer, Berlin, 2008.
2. S. R. de Groot and P. Mazur, *Non-equilibrium thermodynamics*, North Holland, Amsterdam, 1972.

3. D. Y. Tzou, *Macro-to-microscale heat transfer. The lagging behaviour*, Taylor and Francis, New York, 1997.
4. G. Chen, *Nanoscale energy transport and generation*, Oxford University Press, Oxford, 2005.
5. Z. Zhang, *Nano/microscale heat transfer*, McGraw Hill, New York, 2007.
6. D. Jou, G. Lebon, and J. Casas-Vázquez, *Extended irreversible thermodynamics*, Springer, Berlin, 2010.
7. D. Jou, J. Casas-Vázquez, and M. Criado-Sancho, *Thermodynamics of fluids under flow*, Springer, Berlin, 2000.
8. A. Sellitto, F. X. Álvarez, and D. Jou, *J. Appl. Phys.* **107**, 114312 (2010).
9. H. Struchtrup, *Macroscopic transport equations for rarefied gas flows: approximation methods in kinetic theory*, Berlin, Heidelberg, 2005.
10. F. X. Álvarez, and D. Jou, *Appl. Phys. Lett.* **90**, 083109 (2007).
11. I. Müller, and T. Ruggeri, *Rational extended thermodynamics*, Springer, New York, 1997.
12. V. Méndez, S. Fedotov, and W. Horsthemke, *Reaction-Transport Systems. Mesoscopic Foundations, Fronts, and Spatial Instabilities*, Springer Verlag, Berlin, 2010.
13. M. Criado-Sancho, J. Casas-Vázquez, and D. Jou, *Phys. Lett. A* **373**, 3301 (2009).
14. D. Jou, M Criado-Sancho, and J Casas-Vázquez, *J. Appl. Phys.* **107**, 084302 (2010).
15. D. J. Evans, and D. J. Searles, *Adv. Phys.* **51**, 1529 (2002).
16. E. Seitaridou, M. M. Inamdar, R. Phillips, K. Ghosh, and K. Dill, *J. Phys. Chem. B* **111**, 2288 (2007).
17. J. Casas-Vázquez, and D. Jou, *Rep. Prog. Phys.* **66**, 1937 (2003).
18. A. Crisanti, and F. Ritort, *J. Phys. A.: Math. Gen.* **36**, R181 (2003).
19. O. G. Jepps, and L. Rondoni, *J. Phys. A : Math. Gen.* **43**, 133001 (2010).
20. W. G. Hoover, and C. G. Hoover, *Phys. Rev. E* **77**, 041104 (2008).
21. W. G. Hoover, and C. G. Hoover, this volume.
22. G. Gallavotti, and E. G. D. Cohen, *Phys. Rev. E* **69**, 035104 (2004).

Griffiths phases in the contact process on complex networks

Géza Ódor*, Róbert Juhász†, Claudio Castellano** and Miguel A. Muñoz‡

*Res. Inst, for Techn. Physics and Materials Science, H-1525 Budapest, P.O.Box 49, Hungary
†Research Institute for Solid State Physics and Optics, H-1525 Budapest, P.O.Box 49, Hungary
**Istituto dei Sistemi Complessi (CNR-ISC) UOS Sapienza and
Dipartimento di Fisica, "Sapienza" Universitá di Roma, P.le Aldo Moro 2, I-00185 Roma, Italy
‡Institute Carlos I for Theoretical and Computational Physics. Universidad de Granada, 18071 Granada, Spain.

Abstract. Dynamical processes occurring on top of complex networks have become an exciting area of research. Quenched disorder plays a relevant role in general dynamical processes and phase transitions, but the effect of *topological quenched disorder* on the dynamics of complex networks has not been systematically studied so far. Here, we provide heuristic and numerical analyses of the contact process defined on some complex networks with topological disorder. We report on Griffiths phases and other rare region effects, leading rather generically to anomalously slow relaxation in generalized small-world networks. In particular, it is illustrated that Griffiths phases can emerge as the consequence of pure topological heterogeneity if the topological dimension of the network is finite.

Keywords: Griffiths phase,network,contact process
PACS: 89.75.Fb, 89.75.-k, 05.90.+m

INTRODUCTION

The study of complex networks has been flourishing since the introduction of a simple model describing the emergence of scaling in random networks [1]. Multidisciplinary applications involve, for example, the World Wide Web, various biological, sociological and technological networks. These are, in many cases, scale-free networks (for recent reviews see [2],[3]). Other families of complex network models are those composed of a d-dimensional regular lattice and additional long edges [4]. These arise e.g. in sociophysics [3], in the context of conductive properties of linear polymers with cross-links that connect remote monomers [5], in public traffic systems [6], in the case of nanowires [7], and in many other examples. In general, a pair of nodes separated by the distance l is connected by an edge with the asymptotic probability for large l:

$$P(l) = \beta l^{-s} . \tag{1}$$

In the special case $s = 0$, the edges exist with a length-independent probability, as in small world networks, therefore we call the nets with generic s generalized small world networks (GSW). If $s \geq 2$, they are characterized by a finite topological dimension D, i.e. $N(l) \sim l^D$, where $N(l)$ is the number of nodes within a distance l from a given node. (Note that "small-world" property means that the number of neighbors of a node increases exponentially with the distance from it, i.e. formally $D = \infty$).

Dynamical processes defined on networks are of recent interest, for example in the context of optimization dynamics of spreading or transport processes [8]. Different dynamical processes, defined on regular lattices, often exhibit scaling behavior, that can be classified into basic universality classes [9]. Instead, the existence of scaling universality classes on network architectures is not clearly established. In many cases, the presence of short average distances induces mean-field type of (fast) dynamics. It is also well known that structural heterogeneity may lead to more complex behavior; for example, on scale-free networks, characterized by a power-law degree distribution $P(k) \propto k^{-\gamma}$ [1], critical exponents may vary with the degree exponent γ [12, 2]. In related 'annealed networks', where the links change rapidly, γ-dependent critical exponents have also been reported [10, 11]. Real networks are, however, 'quenched' in many cases, i.e. the topology changes slowly with respect to the dynamical process evolving on them.

In the context of the statistical physics of models defined on Euclidean lattices, it is well known that quenched randomness can generate "rare-region effects" in the so called *Griffiths phase* (GP), where, in many cases, algebraic scaling is observed (as opposed to pure systems in which power-laws are observed only at critical points) with scaling exponents changing continuously with the control parameter [13, 14, 15, 16, 30]. Furthermore, at the phase transition the evolution becomes logarithmically slow, and it is controlled by 'activated scaling'. A nontrivial question can be posed: Under which conditions do rare-region effects and GPs occur in network systems? Can they emerge out of topological disorder alone (i.e. without disorder in the transition rates)? These problems have not been systematically studied so far. At first sight one might guess that in network models the dynamics should be very fast, due to the strong interconnectedness, i.e. information can propagate very efficiently throughout the system, resulting in mean-field like, exponential relaxation. Recently, however, generic slow dynamics has been reported to occur in various network models; its origin has been attributed to heterogeneity [17] or to local bursty activity patterns [18, 19]. To tackle this type of problems, here we present a study of the contact process (CP) [20] (i.e. the simplest possible model for epidemic spreading, or information flow) on different GSW networks, including regular networks and non-regular ones.

NUMERICAL ANALYSES

We study the CP on random networks composed of a d-dimensional lattice and a set of long edges with unbounded length. Any pair of nodes, separated by the distance l, is connected by an edge with some l-dependent probability, Eq.(1) [4, 24, 25]. An intriguing feature of these type of graphs for $d = 1$ is that in the marginal case ($s = 2$) intrinsic properties show power-law behavior and the corresponding exponents vary continuously with the prefactor β. Indeed, the topological dimension D of such networks has been conjectured to depend on β [24]. Instead, for larger values of s long-ranged links are irrelevant, and $D(\beta) = 1$, while for $s < 2$ the topological dimension diverges. It has been claimed in a recent paper [28] that if $D(\beta)$ is finite, Griffiths phases and similar rare-region effects can appear.

We have considered the CP [20], in which each infected (active) sites is healed at rate 1, whereas each of its nearest-neighbor sites is infected at rate λ/k (where k is the degree of the site) so that the total infection rate is λ. In numerical simulations we update active sites randomly and increment the time by $1/N_a$, where N_a is the number of active sites. In this way, all active sites are updated on average once every time unit. For a critical infection rate λ_c we find a phase transition from the active to an absorbing phase [21], with vanishing density of infected sites.

We have performed numerical simulations initiated either from a fully active state or from a single active seed. In the former case, the density $\rho(t)$ of active sites has been measured.

Non-regular random networks

The precise definition of the networks we consider is as follows[23, 24]. We start with N nodes, numbered as $1,2,\ldots,N$ and define the distance between node i and j as $l = \min(|i-j|, N-|i-j|)$. We connect any pair of sites separated by a distance $l = 1$ (i.e. neighboring sites on the ring) with probability 1, and pairs with $l > 1$ with a probability $P(l) = 1 - \exp(-\beta l^{-s})$. This implies $P(l) = \beta l^{-s}$ at large distances. In the case $s > 2$, long-range links do not change the topological dimension, which remains unity, and hence the critical behavior is expected to be similar to that of the one-dimensional CP with *disordered transition rates*. In the latter model, the critical dynamics is logarithmically slow, for instance, starting from a fully active state, the density decays asymptotically as $\rho \propto (\ln(t))^{-\tilde{\alpha}}$ with $\tilde{\alpha} = 0.38197$ [16]. For $s = 3$ (and $\beta = 2$) we have run extremely long ($t_{max} = 2^{28}$ MCs) simulations on networks with number of nodes $N = 10^5$. Besides observing a GP, we have found that data are compatible with the above form of logarithmic dependence on time, and have located the critical point at $\lambda_c = 2.783(1)$. As Fig. 1(a) shows the assumption on activated scaling with $\tilde{\alpha} = 0.38197$ is satisfactory, although only after an extremely long crossover time to be discussed later [29].

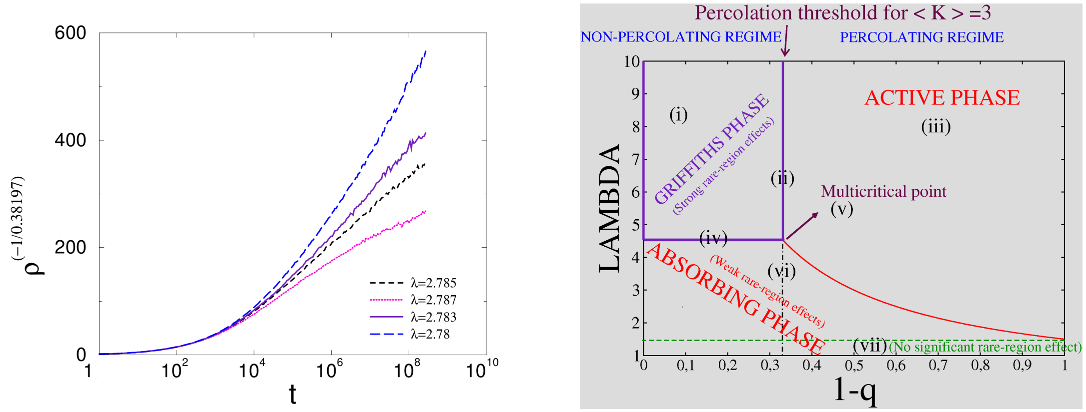

(a) **(b)**

FIGURE 1. Time-dependence of the density in the $s = 3$, $\beta = 2$ random network. Inset: local slopes of the same (lower curves), and local slopes of the survival probability in the 1d QCP simulations (dashed curves). Slow convergence of the effective exponents can be observed. (b) Phase diagram of QCP on the ER graph for $r = 0$.

For the marginal case $s = 2$, where the topological dimension is a continuous function of β, numerical simulations indicate qualitatively different scenarios of the phase transition for different values of β. If β is small enough, GP is observed and the scaling at the transition is of logarithmic form. However, when β is large enough, the GP seems to be lacking and the critical dynamics follows a power-law. The latter type of behavior is observed also for $s < 2$, where formally $D = \infty$.

An "annealed" counterpart of CP on the above random networks is the 1d CP with Lévy flight distributed activation probabilities $P(r) \propto r^{-d-\sigma}$. In this model the dynamical exponents are known to depend continuously on σ [27]. The estimated dynamical exponent of the CP on the above random networks in case of power-law critical behavior is found to be compatible with the dynamical exponent of the Lévy-flight CP with $d = 1$. For further details the reader is referred to [28, 29].

3-regular (or cubic) random networks

In the networks studied so far the degree of nodes was random. In the following we consider networks with a "weaker" topological disorder, in the sense that the degree of nodes is constant (3). Such random networks with nodes of degree 3 can be constructed in the following way [25]. A one-dimensional periodic lattice with N sites is given, where the degree of all sites is initially 2. Sites of degree 2 are called "free sites". Let us assume that N is even and k is a fixed positive integer. A pair of free sites is selected such that the number of free sites between them is $k-1$ (the number of non-free nodes can take any value) and this pair is then connected by a link. That means, for $k = 1$, neighboring free sites are connected, for $k = 2$ next-to-neighboring ones, etc. This step, which raises to 3 the degree of two free sites, is then iterated until $2(k-1)$ free sites are left. These are then paired in an arbitrary way, which does not affect the properties of the network in the limit $N \to \infty$. In the resulting network, all sites are of degree 3, and one can show that the probability of edges is given by Eq. (1) with $s = 2$. For certain networks of this type it has been demonstrated that the long-ranged connections result in a finite topological dimension which is less than one [25]. Furthermore, in the case of aperiodic networks, the critical exponents of the CP depend on the underlying aperiodic modulation [26]. In the following, we concentrate on random networks in which the pairs to be connected are selected randomly (with equal probability) in the above procedure for a fixed k. In this case, one can show that the prefactor in Eq. (1) is given by $\beta = k/2$.

We have performed numerical simulations for the CP on $k = 1$ random networks with $N = 10^7$ nodes. The averaging was done over 200 different network realizations for each λ value and the maximum time is $t_{max} \leq 2^{26}$. As Fig. 2(a) shows, power-law decay with continuously changing exponent emerges for a range of λ-s. By analyzing the effective decay exponents, defined as the local slopes of the density $\alpha_{\text{eff}}(t) = -(\ln\rho(t) - \ln\rho(t'))/(\ln(t) - \ln(t'))$, where $t/t' = 2$, the curves do not level-off for large times, instead one can observe a small drift. One can easily derive that the functional dependence of the effective exponent $\alpha_{\text{eff}}(t) = \alpha + x/\ln(1/t)$ is related to the scaling correction $\rho(t) = t^{-\alpha}\ln^x(1/t)$. By plotting $\alpha_{\text{eff}}(t)$ on logarithmic time scales (see inset of Fig. 2(a)) it turns out that the drift describes logarithmic corrections to power-laws and that α is a non-universal quantity which depends on λ. The possibility of logarithmic corrections has already been pointed out in the case of CP with quenched disorder [15].

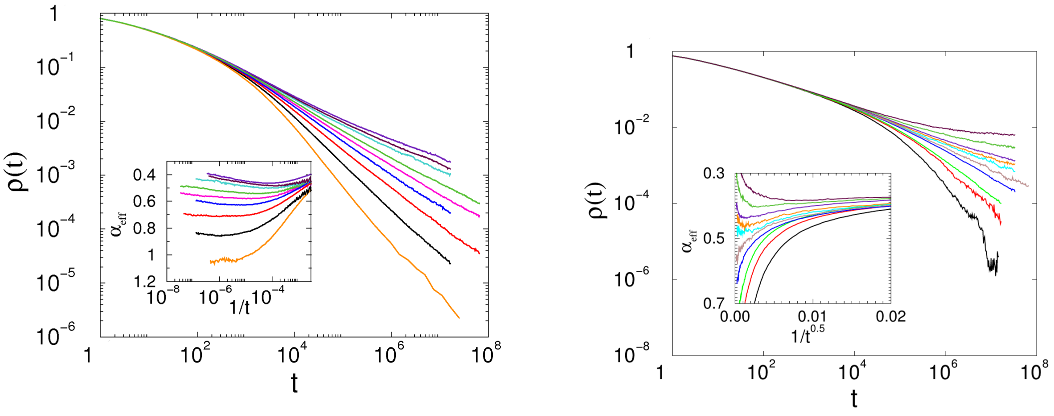

(a) **(b)**

FIGURE 2. Density decay in 3-regular, random networks. (a) GP in $k = 1$ between $\lambda = 2.535$ and $\lambda = 2.57$ (from bottom to top). (b) Critical point for $k = 2$ between $\lambda = 2.156$ and $\lambda = 2.1598$ (from bottom to top). The inset shows the corresponding local slopes.

In accordance with results on non-regular networks with $s = 2$, the phase transition is qualitatively different for $k = 2$ which corresponds to a higher value of β. Here, a standard phase transition seems to appear at $\lambda_c = 2.15835(5)$, with the density decay exponent $\alpha \simeq 0.51(5)$ (Fig. 2(b)). This value agrees again with that of the Lévy flight CP with $d = 1$ and $d + \sigma = 2$.

QCP ON ERDŐS-RÉNYI NETWORKS

Apart from studying the effect of heterogeneous (i.e. disordered) topologies on the dynamics of the contact process, we have also scrutinized the behavior of the disordered contact process on random networks. In particular, we have considered CP on ER graphs [22] with a quenched disordered infection rate: a fraction $1 - q$ of the nodes (type-I) take value λ and the remaining fraction q (type-II nodes) take a reduced value λr, with $0 \leq r < 1$. Pair mean-field approximations [28, 29] lead to the following critical threshold

$$\lambda_c(q) = \frac{\langle k\rangle}{\langle k\rangle - 1}\,\frac{1}{1-q}. \tag{2}$$

Type-I nodes experience a percolation transition, where the type I-to-type I average degree is 1, i.e. at $q_{perc} = 1 - \langle k\rangle^{-1}$. For $q > q_{perc}$ activity cannot be sustained: type-I clusters are finite and type-II ones do not propagate activity.

Numerical simulations and optimal fluctuation theory for $\langle k\rangle = 3$ ($q_{perc} = 2/3$) leads to the complex phase diagram shown on Fig. 1(b). In agreement with (2) one finds a critical active/absorbing phase transition, but below the percolation threshold the absorbing phase splits into parts. In particular, for $\lambda \gtrsim 4.5$ (iv) rare, percolating regions may occur, which cause power-law dynamics (i), i.e. a Griffiths phase, compared to the inactive phase of simple CP, which is purely exponential. Further details can be found in [28, 29].

CONCLUSIONS

We have illustrated that, besides quenched site disorder, topological disorder by itself can result in slow dynamics and non-universality, at least for the contact process. We expect these results to have a broad spectrum of implications for propagation phenomena and other dynamical process taking place on networks, and to be relevant for the analysis of both models and empirical data [17]. We have claimed in a different publication [28] that having finite topological dimension is a necessary condition for the occurrence of slow, GP type of evolution in complex networks, at least for CP type of dynamics. Investigation of other factors promises to be an interesting, open field of research.

ACKNOWLEDGMENTS

This work was supported by HPC-EUROPA2 pr.228398, HUNGRID and Hungarian OTKA (T77629,K75324), J. de Andalucía P09-FQM4682 and MICINN–FEDER project FIS2009–08451.

REFERENCES

1. A. -L. Barabási, and R. Albert, *Science* **286**, (1999) 509.
2. S. N. Dorogovtsev, A. V. Goltsev, and J. F. F. Mendes, *Rev. Mod. Phys.* **80**, 1275 (2008).
3. R. Albert, and A. -L. Barabási, *Rev. Mod. Phys.* **74**, 47–97 (2002).
4. J. M. Kleinberg, Nature **406**, 845 (2000).
5. D. Chowdhury, and B. Chakrabarti, *J. Phys. A: Math. Gen.* **18**, L377 (1985).
6. G. Li et al., *Phys. Rev. Lett.* **104**, 018701 (2010).
7. J. Hicks, A. Benham, and A. Ural, *Phys. Rev. E* **79**, 012102 (2009).
8. R. Pastor-Satorras, and A. Vespignani, *Evolution and Structure of the Internet: A Statistical Physics Approach*, Cambridge University Press, Cambridge, 2004.
9. G. Ódor, *Universality in Nonequilibrium Lattice Systems*, World Scientific, 2008; *Rev. Mod. Phys.* **76**, 663 (2004).
10. M. Boguna, C. Castellano, and R. Pastor-Satorras, *Phys. Rev. E* **79**, 026110 (2009).
11. S. H. Lee, et al., *Phys. Rev. E* **80**, 051127 (2009).
12. C. Castellano, and R. Pastor-Satorras, *Phys. Rev. Lett.* **96**, 038701 (2006).
13. R. B. Griffiths, *Phys. Rev. Lett.* **23**, 17 (1969).
14. A. J. Bray, *Phys. Rev. Lett.* **59**, 586 (1987); M. Thill, and D. Huse, *Physica A* **214**, 321 (1995); H. Rieger, and A. P.Young, *Phys. Rev. B* **54**, 3328 (1996); D. S. Fisher, *Phys. Rev. Lett.* **69**, 534 (1992).
15. A. J. Noest, *Phys. Rev. Lett.* **57**, 91 (1986).
16. T. Vojta, and M. Dickison, *Phys. Rev. E* **72**, 036126 (2005).
17. S. Johnson, J. J. Torres, and J. Marro, arXiv:1007.3122.
18. X. Castelló et al., *Europhys. Lett.* **79** 66006 (2007).
19. M. Karsai, et al. arXiv:1006.2125.
20. T. E. Harris, *Ann. Prob.* **2**, 969 (1974).
21. M. Henkel, H. Hinrichsen, and S. Lübeck, *Non-equilibrium Phase transitions*, Springer, Berlin, 2008.
22. P. Erdös, and A. Rényi, *Publicationes Mathematicae* **6**, 290 (1959).

23. M. Aizenman, and C. M. Newman, *Commun. Math. Phys.* **107**, 611 (1986).
24. I. Benjamini, and N. Berger, *Rand. Struct. Alg.* **19**, 102 (2001).
25. R. Juhász, *Phys. Rev. E* **78**, 066106 (2008).
26. R. Juhász, and G. Ódor, *Phys. Rev. E* **80**, 041123 (2009).
27. H. Hinrichsen, *J. Stat. Mech.: Theor. Exp.* P07066 (2007)
28. M. A. Muñoz, R. Juhász, C. Castellano, and G. Ódor, *Phys. Rev. Lett.* **105**, 128701 (2010).
29. C. Castellano, G. Ódor, R. Juhász, and M.A. Muñoz, preprint 2010.
30. A. Amir, Y. Oreg, and Y. Imry, *Phys. Rev. Lett.* **105**, 070601 (2010); *Phys. Rev. Lett.* **103**, 126403 (2009).

Stationary points approach to thermodynamic phase transitions

Michael Kastner

National Institute for Theoretical Physics (NITheP), Stellenbosch 7600, South Africa, and
Institute of Theoretical Physics, University of Stellenbosch, Stellenbosch 7600, South Africa

Abstract. Nonanalyticities of thermodynamic functions are studied by adopting an approach based on stationary points of the potential energy. For finite systems, each stationary point is found to cause a nonanalyticity in the microcanonical entropy, and the functional form of this nonanalytic term is derived explicitly. With increasing system size, the order of the nonanalytic term grows, leading to an increasing differentiability of the entropy. It is found that only "asymptotically flat" stationary points may cause a nonanalyticity that survives in the thermodynamic limit, and this property is used to derive an analytic criterion establishing the existence or absence of phase transitions. We sketch how this result can be employed to analytically compute transition energies of classical spin models.

Keywords: Phase transitions, stationary points, microcanonical entropy, transition energy
PACS: 05.70.Fh, 64.60.A-, 64.70.qd

A phase transition is an abrupt change of the macroscopic properties of a many-particle system under variation of a control parameter. An approach commonly used for the theoretical description of phase transitions is the investigation of the analyticity properties of thermodynamic functions like the canonical free energy of enthalpy. It is long known that nonanalytic behavior in a canonical or grandcanonical thermodynamic function can occur only in the thermodynamic limit in which the number of degrees of freedom N of the system goes to infinity [1]. Recently, however, it was observed that the microcanonical entropy, or Boltzmann entropy, s_N of a finite system is not necessarily real-analytic, i. e. not necessarily infinitely many times differentiable. More specifically, it was observed in [2] that stationary points of the potential energy function $V_N(q)$ of a classical many-body system with continuous variables $q = (q_1, \ldots, q_N)$ give rise to these nonanalyticities. Generically, with increasing N, the nonanalyticities appear in higher and higher derivatives of the microcanonical entropy s_N. Despite this "smoothening" of the entropy when approaching the thermodynamic limit, it was shown recently that a finite-system nonanalyticity of s_N can survive the thermodynamic limit if the Hessian determinant of V_N, evaluated along a suitable sequence of stationary points for different system sizes N, goes to zero in a suitable way. This observation was used in [3, 4] to derive an analytic criterion, local in microscopic configuration space, on the basis of which the existence of phase transitions can be analyzed and, in some cases, an exact analytical expression for the phase transition energy can be derived.

In this article, the functional form of the nonanalyticities of the finite-system entropy s_N is reviewed. Based on this result, we then sketch the criterion which relates the occurrence of a phase transition to the vanishing of the Hessian determinant evaluated along a sequence of stationary points. Finally, a simple strategy is discussed which

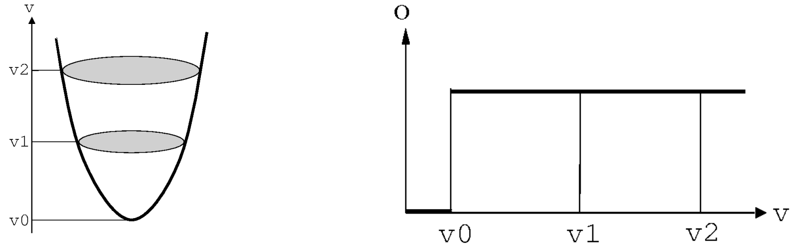

FIGURE 1. As a simple example, consider a two-dimensional configurational space R^2 on which a potential energy function $V_2(q_1,q_2) = q_1^2 + q_2^2$ is defined (left). The corresponding density of states as defined in (2) has a discontinuity at $v = v_0$ (right).

permits to construct sequences of stationary points for systems of arbitrary size N.

NONANALYTICITIES OF THE FINITE-SYSTEM ENTROPY

Canonical and grandcanonical ensembles are the ones most frequently used in statistical mechanics applications. The corresponding thermodynamic potentials, i.e. the free energy and the grandcanonical potential, are known to be analytic functions for all finite systems sizes, and many physicists have become so used to this property that they expected all finite-system thermodynamic functions to be smooth. It is, however, fairly easy to construct counterexamples to this false expectation. The thermodynamic function we consider here is the configurational microcanonical entropy[1]

$$s_N(v) = \ln \Omega_N(v)/N, \tag{1}$$

where

$$\Omega_N(v) = \int \mathrm{d}q\, \delta(V_N(q) - Nv) \tag{2}$$

is the configurational density of states. The integration in (2) is over configuration space, and v denotes the potential energy per degree of freedom. For a potential energy function $V_2(q_1,q_2) = q_1^2 + q_2^2$, the configurational density of states $\Omega_2(v)$ is easily shown to have a discontinuity at $v = v_0$ (see figure 1). For a slightly less trivial example of a potential with a proper saddle point, see figure 1 of [6].

In both examples, the nonanalyticities of $\Omega_N(v)$ occur precisely at the values of the potential energy per degree of freedom $v^{\mathrm{s}} = V_N(q^{\mathrm{s}})/N$ which correspond to stationary points of the potential, i.e. points q^{s} where $\mathrm{d}V_N(q^{\mathrm{s}}) = 0$. This observation remains valid in higher dimensional configuration spaces, and independent of whether the stationary point is a minimum, a maximum, or a saddle point. In the following, in order to obtain a general result characterizing the nonanalytic behavior of Ω_N induced by a stationary point, we require the potential V_N to be a Morse function, i.e. to have a non-vanishing determinant of the Hessian $\mathscr{H}_V$ at all stationary points of V_N. One may argue that this

---

[1] Nonanalyticities of the “usual” microcanonical entropy are related to nonanalyticities of its configurational counterpart in a rather straightforward way. See [5] for details.

is an insignificant restriction, since Morse functions form an open dense subset of the space of smooth functions [7] and are therefore generic. This means that, if the potential V_N we are interested in is not a Morse function, we can transform it into one by adding an arbitrarily small perturbation. An important consequence of the Morse property is that all stationary points of such a function are isolated which allows us to study the effect of a *single* stationary point on the configurational density of states (2). Such an asymptotic analysis has been reported in [8, 4]:

Theorem 1 *Let* $V_N : G \to \mathrm{R}$ *be a Morse function with a single stationary point* q^{s} *of index* k *in an open region* $G \subset \mathrm{R}^N$*. Without loss of generality, we assume* $V_N(q^{\mathrm{s}}) = 0$*. Then there exists a polynomial* P *of degree less than* $N/2$ *such that at* $v = 0$ *the configurational density of states* (2) *can be written in the form*

$$\Omega_N(v) = P(v) + \frac{h_{N,k}(v)}{\sqrt{|\det[\mathscr{H}_V(q^{\mathrm{s}})]|}} + o(v^{N/2-\varepsilon}) \tag{3}$$

for any $\varepsilon > 0$*. Here* Θ *is the Heaviside step function,* o *denotes Landau's little-o symbol for asymptotic negligibility, and*

$$h_{N,k}(v) = \begin{cases} (-1)^{k/2}\, v^{(N-2)/2}\Theta(v) & \text{for } k \text{ even,} \\ (-1)^{(k+1)/2}\, v^{(N-2)/2}\, \pi^{-1} \ln|v| & \text{for } N \text{ even, } k \text{ odd,} \\ (-1)^{(N-k)/2}(-v)^{(N-2)/2}\Theta(-v) & \text{for } N, k \text{ odd.} \end{cases} \tag{4}$$

For a proof of this result see [4]. In short, we see from theorem 1 that, at a nonanalyticity of $\Omega_N(v)$ induced by the presence of a stationary point of V_N, the configurational density of states is $\lfloor (N-3)/2 \rfloor$-times differentiable at the corresponding value v^{s} of the potential energy. Hence, when increasing the number N of degrees of freedom, the non-differentiability occurs in higher and higher derivatives of $\Omega_N(v)$ [or $s_N(v)$], and one might naively expect the nonanalyticity to disappear in the thermodynamic limit.

FLAT STATIONARY POINTS AND PHASE TRANSITIONS

The result of the previous section, and in particular the unbounded growth of the differentiability with increasing N, does not seem to suggest any connection between stationary points of the potential energy function and phase transitions in the thermodynamic limit $N \to \infty$. There is, however, a result by Franzosi and Pettini which indeed establishes such a relation. The following sloppy reformulation of the result will be sufficient for our purposes.

Sloppy theorem 1 *Let* V_N *be the potential of a system with* N *degrees of freedom and short-range interactions. If some interval* $[a, b]$ *of potential energies per degree of freedom remains, for any large enough* N*, free of stationary values of* V_N*, then the configurational entropy* $s(v) = \lim_{N\to\infty} s_N(v)$ *does not show a phase transition in this interval.*

Note that a precise formulation of this theorem requires further technical conditions on the potential V_N (see [9, 10] for details).

Indeed, the finite-system result of theorem 1 can be helpful towards an understanding of how nonanalyticities of the entropy s_N can give rise to a nonanalyticity in the thermodynamic limit: From equation (3), we observe that the nonanalytic term $h_{N,k}$ comes with a prefactor of $1/\sqrt{|\det[\mathscr{H}_V(q^{\mathrm{s}})]|}$. Although, with increasing N, the differentiability of $h_{N,k}$ grows unboundedly, this "smoothing" may be counterbalanced by a vanishing (with increasing N) Hessian determinant. This intuition has been made rigorous in [3, 4], but here we will give only a sloppy reformulation capturing the essence of this result.

Sloppy theorem 2 *The nonanalytic contributions of the stationary points of V_N to the configurational entropy cannot induce a phase transition at a potential energy per particle v_{t} if, in a neighborhood of v_{t},*

1. *the number of critical points is bounded by $\exp(CN)$ with some $C > 0$, and*
2. *the stationary points do not become "asymptotically flat" in the thermodynamic limit, i.e. $\lim_{N\to\infty}\left|\det\mathscr{H}_V(q^{\mathrm{s}})\right|^{1/N}$ is bounded away from zero for any sequence of stationary points q^{s} lying in the vicinity of v_{t}.*

For a precise formulation and a proof of this result see [4]. In short, this result classifies a subset of all stationary points of V_N as harmless as what regards phase transitions and leaves only the asymptotically flat ones as candidates capable of causing a phase transition.

SPECIAL SEQUENCES OF STATIONARY POINTS

Importantly for the application of sloppy theorem 2, knowledge of a suitably chosen subset of the stationary points of V_N may be sufficient: If one manages to find some sequence of stationary points such that, along this sequence,

$$\lim_{N\to\infty}\left|\det\mathscr{H}_V(q^{\mathrm{s}})\right|^{1/N} = 0, \tag{5}$$

the corresponding limiting value $v_{\mathrm{t}} = \lim_{N\to\infty} V_N\left(q^{\mathrm{s}}\right)/N$ is a good candidate for the exact value of the phase transition potential energy. This idea was first employed by Nardini and Casetti in [11], where suitably constructed sequences of stationary points were used to single out the phase transition of a model of gravitating masses and determine its critical energy.

To illustrate how special sequences of stationary points can be constructed, we consider a one-dimensional XY model with periodic boundary conditions, characterized by the potential energy function

$$V_N(q) = \sum_{i=1}^{N}\sum_{j=1}^{(N-1)/2}\frac{1-\cos(q_i - q_{i+j})}{j^{\alpha}} \tag{6}$$

where $q_i \in [-\pi,\pi)$ are angular variables, and α is some non-negative exponent. For $\alpha \in [1,2]$, this model is known to show a phase transition from a ferromagnetically ordered to a paramagnetic phase, but no exact thermodynamic solution is known.

FIGURE 2. Sketch of stationary points of V_N for $N=8$, where q_i is the angle between the arrow and the dashed axis. Left: Stationary points where all $q_i \in \{0,\pi\}$. Right: All differences $q_k - q_{k-1}$ between neighboring angles are equal, with differences chosen such that $q_0 = q_N$, in compliance with the periodic boundary conditions.

Stationary points of the potential energy (6) have to satisfy the set of equations

$$0 = \frac{\partial V_N(q)}{\partial q_k} = \sum_{j=1}^{(N-1)/2} \frac{\sin(q_k - q_{k+j}) + \sin(q_k - q_{k-j})}{j^\alpha} \tag{7}$$

for $k = 1,\dots,N$. To get rid of the trivial global rotational invariance of (6), we fix $q_N = 0$ and eliminate the equation with $k=N$ in (7). The thermodynamics of this reduced model is identical to that of the full one, as the contribution of one degree of freedom to the partition function is negligible in the thermodynamic limit.

There are two particularly simple classes of solutions of (7), similar in spirit to those constructed in [11] for a one-dimensional model of gravitating masses: First, any combination of $q_i \in \{0,\pi\}$ for $i = 1,\dots,N-1$ will make the sine functions in (7) vanish. A second class of solutions is given by $q_m^{(n)} = 2\pi mn/N$ for $m,n \in \{1,\dots,N\}$. These solutions have equal angles between neighboring spins. As a result, $\sin(q_k - q_{k+j}) = \sin(q_{k-j} - q_k)$, and therefore each of the summands in (7) vanishes separately. Both classes of solutions are sketched in figure 2. To employ these classes of stationary points along the lines of sloppy theorem 2, one needs to evaluate the Hessian determinant of (6) at the stationary points. This is work in progress and will be reported elsewhere.

ACKNOWLEDGMENTS

The author acknowledges financial support by the *Incentive Funding for Rated Researchers* program of the National Research Foundation of South Africa.

REFERENCES

1. R. B. Griffiths, in *Phase Transitions and Critical Phenomena*, edited by C. Domb, and M. S. Green, Academic Press, London, 1972, vol. 1.
2. L. Casetti, and M. Kastner, *Phys. Rev. Lett.* **97**, 100602 (2006).
3. M. Kastner, and O. Schnetz, *Phys. Rev. Lett.* **100**, 160601 (2008).
4. M. Kastner, O. Schnetz, and S. Schreiber, *J. Stat. Mech. Theory Exp.* **2008**, P04025 (2008).
5. L. Casetti, M. Kastner, and R. Nerattini, *J. Stat. Mech. Theory Exp.* **2009**, P07036 (2009).
6. M. Kastner, *J. Stat. Mech. Theory Exp.* **2009**, P02016 (2009).
7. M. Demazure, *Bifurcations and Catastrophes: Geometry of Solutions to Nonlinear Problems*, Springer, 2000.
8. M. Kastner, S. Schreiber, and O. Schnetz, *Phys. Rev. Lett.* **99**, 050601 (2007).
9. R. Franzosi, and M. Pettini, *Phys. Rev. Lett.* **92**, 060601 (2004).
10. R. Franzosi, M. Pettini, and L. Spinelli, *Nuclear Phys. B* **782**, 189–218 (2007).
11. C. Nardini, and L. Casetti, *Phys. Rev. E* **80**, 060103(R) (2009).

Energy bursts in vibrated shallow granular systems

N. Rivas*, D. Risso†, R. Soto* and P. Cordero*

*Departamento de Física, FCFM, Universidad de Chile, Santiago, Chile
†Departamento de Física, Universidad del BioBio, Concepción, Chile

Abstract. In a mixture of two species of inelastic spheres of equal size but different mass, placed in a vertically vibrated shallow box (large horizontal dimensions and height comparable to the grains' size), there is spontaneous segregation. Once the system is at least partly segregated energy bursts recurrently take place: the horizontal kinetic energy of the heavy particles, that normally is small, suddenly increases an order of magnitude. An explanation of these events is provided based on the existence of a fixed point for an isolated particle bouncing with only vertical motion between the top and bottom plates. Energy bursts occur when clusters of heavy particles start a chain reaction of collisions that transfer vertical energy to horizontal energy producing an expansion of the cluster.

Keywords: Statistical Physics, Granular Matter
PACS: 45.70.-n, 45.70.Mg

INTRODUCTION

Granular systems, like sand, are systems formed by hard macroscopic particles. They are intrinsically dissipative systems, since colliding grains transfer rotational and translational energy into their internal degrees of freedom. The temperature does not play a role in the dynamics of the system because the energy needed to considerably move a grain is much larger than the temperature energy scale $k_B T$. If no energy is injected into the system, the dissipative collisions will make all particles come to rest—as when we fill a sugar bowl. In this static state the top surface will most probably not be horizontal but rather the top layers will be forming a heap. But when energy is injected, the granular system may behave like a fluid, even though there are important differences with molecular fluids because of the energy dissipation at grain collisions [1]. In a wide variety of situations the presence of any interstitial fluid, such as air, can be neglected. When the system has two species of grains—that differ in their size, shape, density or inelasticity—segregation generically takes place. Depending on the forcing parameters, segregation can be partial or total with different driving mechanisms [2].

Granular systems found in nature normally are irregular in shape and with a diversity of sizes. However, it became evident that the main features of granular media are determined by their stiffness and the energy dissipation at collisions. For this reason and in order to make quantitative and reproducible predictions, the study of these systems are usually focused on systems consisting of *spherical particles* and quite often the systems are monodisperse or, perhaps, bidisperse. It is clear now that these systems present an immensely rich variety of behaviors.

The study of granular systems in a vibrated shallow box—a box with large horizontal dimensions and height comparable to the particle's diameter— allows both to study the collective behaviour of the system as well as that of individual particles [3, 4, 5, 6]. As it should be expected, the system variables behave quite anisotropically to the extent that, for example, the horizontal mean kinetic energy is quite different from the vertical one. Placing monodisperse inelastic spheres in a vertically vibrated shallow box of height comparable to the size of the particles, a particular phase separation takes place: regions appear with quite different densities and granular temperatures [3]. Namely, grains form solid-like regions surrounded by fluid-like regions. In this phase separation waves develop, driven by negative compressibility of the effective pressure [4].

In this article we study a mixture of two species of inelastic spheres of equal size but different mass, placed in a vertically vibrated shallow box when there is spontaneous segregation. Once the system is at least partly segregated energy bursts take place. An explanation of these events is provided based on the existence of a fixed point for an isolated particle bouncing with only vertical motion between the top and bottom plates.

SYSTEM CONFIGURATION

Two species of spheres of the same diameter σ but different mass are placed in a square shallow box as described below. The lighter/heavier particles will be called L and H respectively. In the simulations we use the so-called Inelastic Hard Sphere model, in which collisions are instantaneous and are characterized by restitution and friction coefficients (static and dynamic), which we take to be the same for the L's and H's in all their collisions. The spheres have translation and rotation degrees of freedom; their collision rules, including those with the walls, can be found in [7].

The shallow box, with horizontal periodic boundary conditions, oscillates with amplitude A and frequency ω. The simulations make use of an event driven algorithm [8] with the following parameters: mass ratio $m_H/m_L = 10$, box height $L_z/\sigma = 1.82$, normal and tangential restitution coefficients $r = 0.8$, static and dynamic friction coefficients $\mu_s = 0.3$ and $\mu_d = 0.15$, the angular frequency and amplitude of vibration are kept fixed at $\omega\sqrt{\sigma/g} = 7.0$ and $A/\sigma = 0.15$ so that the dimensionless acceleration is $\Gamma \equiv A\omega^2/g = 7.35$. Simulations are reported using two systems: (a) a small system $N_H = 500$, $N_L = 1000$ and $L_x/\sigma = L_y/\sigma = 40$ and (b) a large system $N_H = 2000$, $N_L = 4000$ and $L_x/\sigma = L_y/\sigma = 80$. Both simulations have the same area fraction $\rho = \pi\sigma^2(N_H + N_L)/(4L_xL_y) = 0.74$ and number ratio $N_H : N_L = 1 : 2$, and only differ in their size.

The appearance of the energy bursts is related to the existence of a fixed point in the dynamics of a single particle in the shallow box. The friction with the plates damps the horizontal and rotational motion, hence the fixed point is characterized by a vertical dynamics in which the particle collides alternatively with the bottom and top plates with the frequency ω of the box. For a wide range of the parameters this periodic trajectory is unique, and thus aligns all particles the vibrating box—in the form of a moving horizontal layer—even if there is no interaction between them.

For the parameters used in the simulation the fixed point is unique and stable. When the system is initialized, the particles approach the fixed point but the grain-grain collisions may prevent to reach it, with different results for the H and L particles. The H's reach the fixed point keeping a small horizontal energy due to the collisions with the L's while, due to the mass contrast, the L particles are continuously taken off the fixed point and, as a result, their average horizontal energy is significant

The mass difference produces segregation of the species but the underlying driving mechanism is not yet known. Such mechanism is not the focus of this article, but rather a phenomenon that takes place after segregation has occurred. Shortly after starting from an initial random configuration many small dense clusters of H's appear. Later on there is a slow dynamics in which the clusters coalesce. The clusters tend to have some L's in their bulk. Because of the fixed point, from a top view the H's appear as if they were standing still, while the L's outside the clusters show a significant horizontal agitation. The external pressure exerted by the light particles leads the heavy ones to form denser clusters. As the fixed point is unique, the clusters move in phase as practically one solid layer.

HE ENERGY BURSTS

As described in [9], once there is at least one cluster, the segregation process is repeatedly interrupted by sudden bursts of the horizontal kinetic energy of the H particles implying a fast expansion of the cluster. Figure 1 shows the evolution of the horizontal energy for the two simulated systems. Two regimes are clearly observed: the small system shows bursts that are irregular in intensity and time lags, while the bursts in the larger system are roughly periodically spaced with a rather well defined amplitude. Later we put forward an explanation of the observed periodicity.

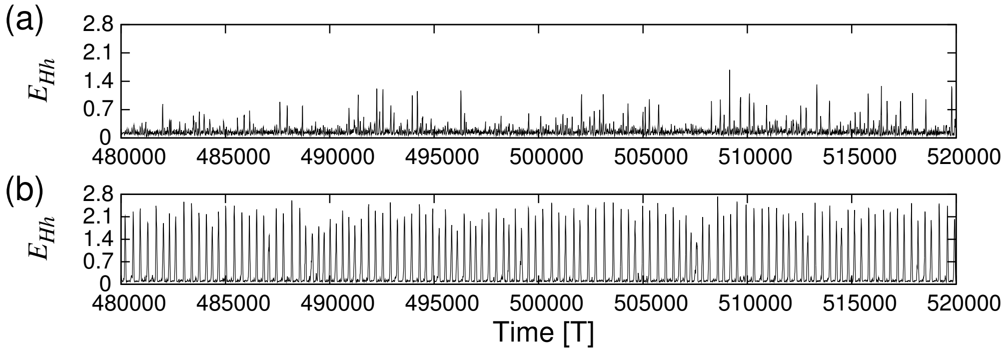

FIGURE 1. Horizontal kinetic energy of the H particles $E_{Hh}(t)$ obtained in the simulations for the (a) small and (b) large systems.

Each burst begins as an abrupt increase of the agitation of the H's in a small region in one of the clusters, implying a local expansion followed by a fast propagation of the horizontal agitation to a much larger zone. Next the L-H collisions slowly compress the cluster again, eventually recovering the original density. Two configuration sequences, one for each system size, are presented in Fig. 2. The main difference between the two systems is that in the large one the agitation always covers the complete cluster, while in the small one only part of the cluster is normally involved.

To analyze the bursts we show, in Fig. 3, the evolution of the average (per particle) horizontal and vertical kinetic energy of particles H, E_{Hh}, E_{Hv}. The standard deviation

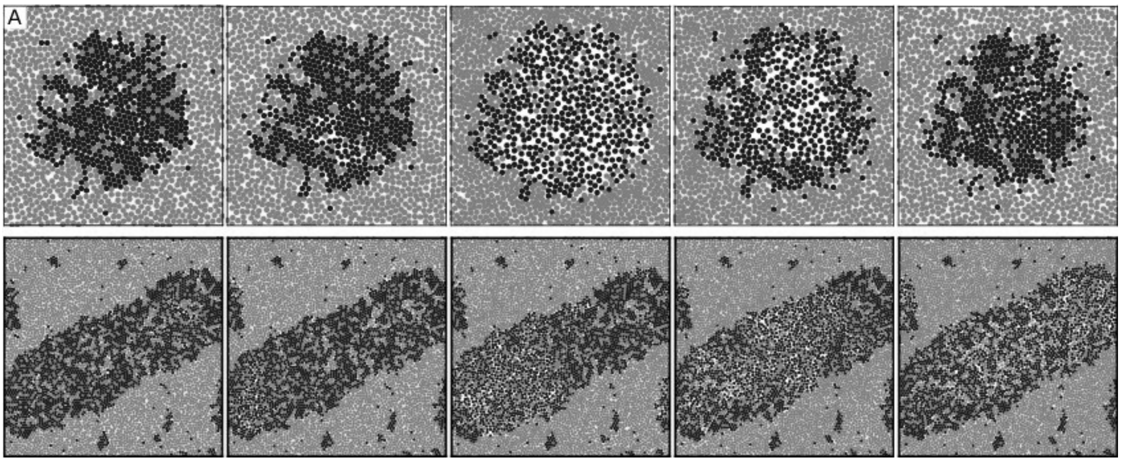

FIGURE 2. Sequence of top view configurations of the system showing an explosion for the small system (top) and the large system (bottom). The heavy particles are presented in black, while the light ones in gray.

σ_{Hz} of the stroboscopic height of the H's—when the box is at its lowest position—is also shown. Previous to the energy burst σ_{Hz} is small, showing that the H's move coherently in phase. It is seen that during the burst σ_{Hz} jumps an order of magnitude and it recovers its typical small value as soon as the burst has finished, namely the H's are again moving in phase. It is this coherent motion that is destroyed at every energy burst.

The picture at the particle level is that eventually two heavy particles, not exactly in phase, collide. This is a collision between two energetic particles which, as a result, all of a sudden, get a comparably large horizontal energy, triggering a chain reaction of collisions among neighboring H's rapidly propagating within the cluster. The chain reaction rapidly transforms the vertical kinetic energy E_{Hv} into horizontal energy E_{Hh}, phenomenon that is observed in Fig. 3.

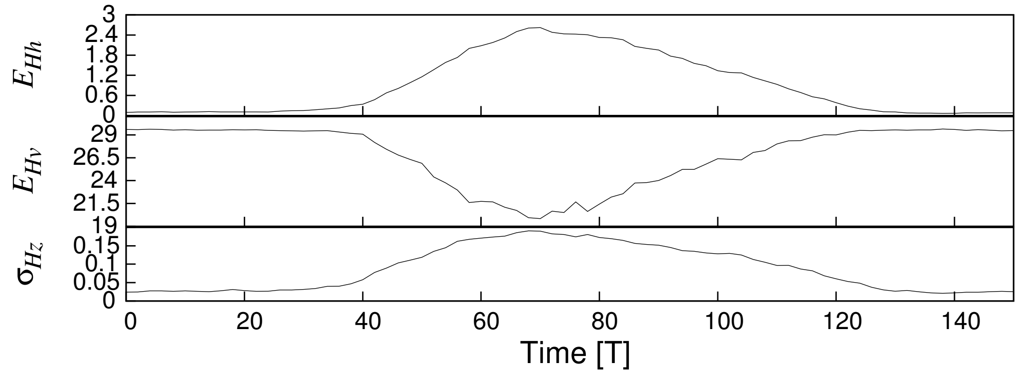

FIGURE 3. Evolution of a single energy burst. The average horizontal and vertical energies of the heavy particles E_{Hh}, E_{Hv}, and the standard deviation of the set of heights of particles H, σ_{Hz} taken stroboscopically when the box is at its lowest position.

THE REGULARITY OF THE EVENTS

The burst waiting times and intensities show different degrees of regularity and for the large system they even look almost as if they were periodic.

After observing many different realizations there appears to be an explanation for the different degrees of regularity. For bursts to take place, a high enough density of the cluster is needed. A burst produces an expansion and no other burst can take place in that region until the density increases again. This implies a necessary waiting time between bursts.

For the waiting times to be regular several conditions have to be met: (i) there must be a unique cluster; (ii) the cluster has to be sufficiently convex so that a burst does not destroy the connectivity of it; (iii) the concentration of L's inside the cluster must not be too large so that they do not block the burst propagating front allowing the existence of several alternative paths for the burst propagation.

If a burst does not propagate through all the cluster then the time of compression is highly variable as it depends on the amount of particles that were involved in it. Even more, other bursts can take place while the cluster is compressing in those parts of it that remain dense.

CONCLUSIONS

Numerical simulations of a granular mixture of two types of grains —in a vibrated shallow box— which only differ in their mass show energy bursts characterized by the rapid conversion of vertical energy into horizontal energy; these bursts are preceded by the segregation of the species. In the segregated state the massive grains approach a fixed point characterized by a vanishing horizontal energy and a vertical motion in phase with the box oscillations. The light grains cannot reach the fixed point because collisions with the heavy ones take them easily off, remaining with an important horizontal energy. The heavy grains trapped about the fixed point move in phase and collide most of the time with a tiny momentum transfer in the horizontal direction. As a result a densely packed cluster of the heavy grains develops. Eventually, however, a small dephasing between heavy grains or an energetic collision with a lighter one, allows a heavy grain to acquire significant horizontal momentum leaving the fixed point. The subsequent collisions with neighboring heavy grains transfer a high amount of energy to the horizontal agitation in the form of a chain reaction, generating an energy burst.

When there is a unique cluster different regimes may be reached depending on the relative number of light particles inside the cluster of the heavy ones. When there are too many light particles in the cluster the bursts are localized, and have a broad distribution of intensities and waiting times, otherwise the bursts propagate through all the cluster and show characteristic intensities and waiting times.

ACKNOWLEDGMENTS

We would like to thank Nicolás Mújica for many helpful discussions. This research is supported by Fondecyt Grants No. 1070958, No. 1100100 and Proyecto Anillo ACT 127.

REFERENCES

1. H. M. Jaeger, S. R. Nagel, and R. P. Behringer, *Rev. Mod. Phys.* **68**, 1259 (1996); L. P. Kadanoff, *Rev. Mod. Phys.* **71**, 435 (1999); P. G. de Gennes, *Rev. Mod. Phys.* **71**, 374 (1999); I. S. Aranson, and L. S. Tsimring, *Rev. Mod. Phys.* **78**, 641 (2006); J. Duran, *Sands, Powders, and Grains: An Introduction to the Physics of Granular Materials*, Springer-Verlag, New York, 1999.
2. A. Kudrolli, *Rep. Prog. Phys.* **67**, 209 (2004).
3. J. S. Olafsen, J. S. Urbach, *Phys. Rev. Lett.* **81**, 4369 (1998); A. Prevost, P. Melby, D. A. Egolf, and J. S. Urbach, *Phys. Rev. E*, **70** 050301(R) (2004); P. Melby, F. Vega Reyes, A. Prevost, R. Robertson, P. Kumar, D. A. Egolf, and J. S. Urbach, *J. Phys.: Condens. Matter* **17**, S2689-S2704 (2005).
4. M. G. Clerc, P. Cordero, J. Dunstan, K. Huff, N. Mújica, D. Risso and G. Varas, *Nature Phys.* **4**, 249 (2008).
5. T. Schnautz, R. Brito, C. A. Kruelle, and I. Rehberg, *Phys. Rev. Lett.* **95**, 028001 (2005).
6. F. F. Chung, S. S. Liaw, and C. Y. Ju, *Gran. Matter* **11**, 79 (2009).
7. D. Risso, R. Soto, S. Godoy, and P. Cordero, *Phys Rev E* **72**, 011305 (2005).
8. M. Marín, D. Risso, and P. Cordero, *J. Comput. Phys.* **109**, 306 (1993); P. Cordero, D. Risso, and M. Marín, *Chaos, Fractals and Solitons* **6**, 95 (1995); P. Cordero, and D, Risso, *Fourth Granada Lectures in Computational Physics*, edited by P. L. Garrido and J. Marro,, Springer-Verlag, 1997.
9. N. Rivas et al., *Phys. Rev. Lett.*, to appear.

Layering and wetting transitions for an interface model

Salvador Miracle Solé

Centre de Physique Théorique, CNRS, Marseille, France

Abstract. We study the solid-on-solid interface model above a horizontal wall in three dimensional space, with an attractive interaction when the interface is in contact with the wall, at low temperatures. The system presents a sequence of layering transitions, whose levels increase with the temperature, before the complete wetting above a certain value of this quantity.

Keywords: SOS model, wetting and layering transitions, interfaces, entropic repulsion.
PACS: 68.08.Bc, 05.50.+q, 60.30.Hn, 02.50.-r

Consider the square lattice $\mathbf{Z}^2$. To each site $x = (x_1, x_2)$ of the lattice, an integer variable $\phi_x \geq 0$ is associated which represents the height of the interface at this site. The system is first considered in a finite box $\Lambda \subset \mathbf{Z}^2$ with fixed values of the heights outside. Each interface configuration on Λ: $\{\phi_x\}$, $x \in \Lambda$, denoted ϕ_Λ, has an energy defined by the Hamiltonian

$$H_\Lambda(\phi_\Lambda \mid \bar{\phi}) = 2J \sum_{\langle x,x'\rangle \cap \Lambda \neq \emptyset} |\phi_x - \phi_{x'}| - 2(J-K) \sum_{x \in \Lambda} \delta(\phi_x) + 2J|\Lambda|, \tag{1}$$

where J and K are positive constants, the function δ equals 1, when $\phi_x = 0$, and 0, otherwise, and $|\Lambda|$ is the number of sites in Λ. The first sum is taken over all nearest neighbors pairs $\langle x, x'\rangle \subset \mathbf{Z}^2$, such that at least one of the sites belongs to Λ, and one takes $\phi_x = \bar{\phi}_x$ when $x \notin \Lambda$, the configuration $\bar{\phi}$ being the boundary condition, assumed to be uniformly bounded.

In the space $\mathbf{R}^3$, the region obtained as the union of all unit cubes centered at the sites of the lattice $\Lambda \times \mathbf{Z}$, that satisfy $x_3 \leq \phi(x_1, x_2)$, is supposed to be occupied by fluid $+$, while the complementary region above it, is occupied by fluid $-$. The common boundary between these regions is a surface in $\mathbf{R}^3$, the microscopic interface. The region $x_3 \leq -1/2$ is considered as the substrate, also called the wall W.

The considered system differs from the usual SOS model by the restriction to non-negative height variables and the introduction of the second sum in the Hamiltonian, the term describing the interaction with the substrate.

The probability of the configuration ϕ_Λ, at the inverse temperature $\beta = 1/kT$, is given by the finite volume Gibbs measure

$$\mu_\Lambda(\phi_\Lambda \mid \bar{\phi}) = Z(\Lambda, \bar{\phi})^{-1} \exp\big(-\beta H_\Lambda(\phi_\Lambda \mid \bar{\phi})\big), \tag{2}$$

where $Z(\Lambda, \bar{\phi})$ is the partition function

$$Z(\Lambda, \bar{\phi}) = \sum_{\phi_\Lambda} \exp\big(-\beta H_\Lambda(\phi_\Lambda \mid \bar{\phi})\big). \tag{3}$$

Local properties at equilibrium can be described by correlation functions between the heights on finite sets of sites, obtained as expectations with respect to the Gibbs measure.

We next briefly describe some general results, which are an adaptation to our case of analogous results established by Fröhlich and Pfister (ref. [1]) for the semi-infinite Ising model.

Let $\Lambda \subset \mathbf{Z}^2$ be a rectangular box of sides parallel to the axes. Consider the boundary condition $\bar{\phi}_x = 0$, for all $x \notin \Lambda$, and write $Z(\Lambda, 0)$ for the corresponding partition function. The associated free energy per site,

$$\tau^{W-} = -\lim_{\Lambda \to \infty} (1/\beta|\Lambda|) \ln Z(\Lambda, 0), \tag{4}$$

represents the surface tension between the medium $-$ and the substrate W.

This limit (4) exists and $0 \leq \tau^{W-} \leq 2J$. One can introduce the densities

$$\rho_z = \lim_{\Lambda \to \infty} \sum_{z'=0}^{z} \langle \delta(\phi_x - z') \rangle_\Lambda^{(0)}, \quad \rho_0 = \lim_{\Lambda \to \infty} \langle \delta(\phi_x) \rangle_\Lambda^{(0)}, \tag{5}$$

Their connection with the surface free energy is given by the formula

$$\tau^{W-}(\beta, K) = \tau^{W-}(\beta, 0) + 2\int_0^K \rho_0(\beta, K')dK'. \tag{6}$$

The surface tension τ^{W+} between the fluid $+$ and the substrate is $\tau^{W+} = 0$. In order to define the surface tension τ^{+-} associated to a horizontal interface between the fluids $+$ and $-$ we consider the ordinary SOS model, with boundary condition $\bar{\phi}_x = 0$. The corresponding free energy gives τ^{+-}. With the above definitions, we have

$$\tau^{W+}(\beta) + \tau^{+-}(\beta) \geq \tau^{W-}(\beta, K). \tag{7}$$

and the right hand side in (7) is a monotone increasing and concave (and hence continuous) function of the parameter K. This follows from relation (6) where the integrand is a positive decreasing function of K. Moreover, when $K \geq J$ equality is satisfied in (7).

In the thermodynamic description of wetting, the partial wetting situation is characterized by the strict inequality in equation (7), which can occur only if $K < J$, as assumed henceforth. We must have then $\rho_0 > 0$. The complete wetting situation is characterized by the equality in (7). If this occurs for some K, say $K' < J$, then equation (6) tells us that this condition is equivalent to $\rho_0 = 0$. Then, both conditions, the equality and $\rho_0 = 0$, hold for any value of K in the interval (K', J).

On the other hand, we know that $\rho_0 = 0$ implies also that $\rho_z = 0$, for any positive integer z. This indicates that, in the limit $\Lambda \to \infty$, we are in the $+$ phase of the system, although we have used the zero boundary condition, so that the medium $-$ cannot reach anymore the wall. This means also that the Gibbs state of the SOS model does not exist in this case.

That such a situation of complete wetting is present for some values of the parameters does not follow, however, from the above results. Actually this fact, as far as we know, remains an open problem for the semi-infinite Ising model in 3 dimensions. For the model we are considering an answer to this problem has been given by Chalker [2].

Chalker's result. We use the following notation:

$$u = 2\beta(J-K), \quad t = e^{-4\beta J}. \tag{8}$$

If $u < -\ln(1-t^2)$, then $\rho_0 = 0$.

Thus, for any given values of J and K, there is a temperature below which the interface is almost surely bound and another higher one, above which it is almost surely unbound and complete wetting occurs. At low temperature (i.e., if $u > \ln 16$), we have $\rho_0 > 0$.

The object of our study is to investigate the region not covered by this theorem when the temperature is low enough. As mentioned in the abstract, we shall prove that a sequence of layering transitions occurs before the system attains complete wetting. More precisely the main results can be summarized as follows.

Theorem 1. Let the integer $n \geq 0$ be given. For any $\varepsilon > 0$ there exists a value $t_0(n,\varepsilon) > 0$ such that, if the parameters t, u, satisfy $0 < t < t_0(n,\varepsilon)$ and

$$-\ln(1-t^2) + (2+\varepsilon)t^{n+3} < u < -\ln(1-t^2) + (2-\varepsilon)t^{n+2}, \tag{9}$$

then the following statements hold: (1) The free energy τ^{W-} is an analytic function of the parameters t, u. (2) There is a unique Gibbs state μ_n, a pure phase associated to the level n. (3) The density is $\rho_0 > 0$. The second inequality in (9) is not needed in the case $n = 0$.

An illustration for this theorem, in the plane (K, β^{-1}), is given in Figure 1. From it we can see, as mentioned in the abstract, that if the parameter K is kept fixed, that seems natural since it depends on the properties of the substrate, then the value n of the level increases when the temperature is increased.

Concerning this theorem, the following remarks can be made:

(1) The analyticity of the free energy comes from the existence of a convergent cluster expansion for this system. This implies the analyticity, in a direct way, of some correlation functions and, in particular, of the density ρ_0.

(2) The unicity of the Gibbs state means that the correlation functions converge, when $\Lambda \to \infty$, to a limit that does not depend on the chosen (uniformly bounded) boundary condition $\bar{\phi}_x$. Being unique and translation invariant this state represents a pure phase. It is associated to a level n in the sense that, for the typical configurations of the state, large portions of the interface are near to the level n.

(3) The condition $\rho_0 > 0$ means that the interface remains at a finite distance from the wall and hence, we have partial wetting. We can see that the region where this condition holds is, according to the Theorem, much larger, at low temperatures, than the region initially proved by Chalker. It comes very close to the line above which it is known that complete wetting occurs.

(4) We have, $t_0(n,\varepsilon) \to 0$ when $n \to \infty$ or $\varepsilon \to 0$.

The reason why $t_0(n,\varepsilon)$ depends on ε, satisfying remark 4, has an explanation. One may believe that the regions of uniqueness of the state extend in such a way that two neighboring regions, say those corresponding to the levels n and $n+1$, will have a common boundary where the two states μ_n and μ_{n+1} coexist.

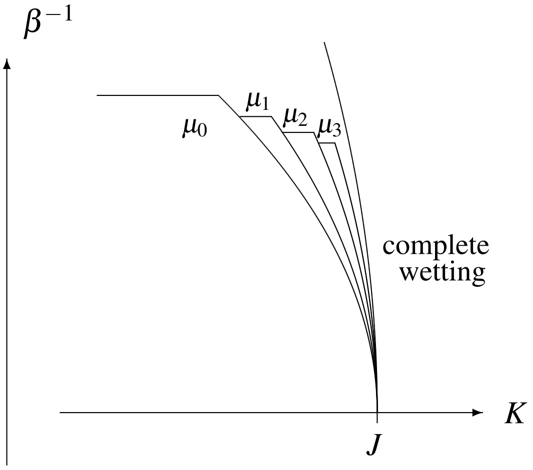

FIGURE 1. The analyticity regions of Theorem 1.

At this boundary there will be a first order phase transition, since the two Gibbs states are different. The curve of coexistence does not exactly coincide with the curve $u = -\ln(1-t^2) + 2t^{n+3}$. Theorem 1 says that it is however very near to it, if the temperature is sufficiently low.

Let us formulate in the following statement the kind of theorem that we expect. We think that such a statement could be proved using, as for Theorem 1, an extension of the Pirogov-Sinai theory.

Statement. For each given integer $n \geq 0$, there exists $t_0(n) > 0$ and a continuous function $u = \psi_{n+1}(t)$ on the interval $0 < t < t_0(n)$, such that the statements of Theorem 1 hold, for t in this interval, in the region where $\psi_{n+1}(t) < u < \psi_{n+2}(t)$ and for $n = 0$, in the region $\psi_1(t) < u$. When $u = \psi_{n+1}(t)$ the two Gibbs states, μ_n and μ_{n+1}, coexist.

The existence of a sequence of layering transitions has been proved for a related model, known as the SOS model with an external magnetic field. See the works by Dinaburg, Mazel [3], Cesi, Martinelli [4] and Lebowitz, Mazel [5]. This model has the same set of configurations as the model considered here, but a different energy: The second term in (1) has to be replaced by the term $+h\sum_{x\in\Lambda}\phi_x$ to obtain the Hamiltonian of the model with an external magnetic field. The method followed for the proof of the Theorem is essentially analogous to the method developed for the study of that model. The most important difference between the two systems concerns the restricted ensembles and the computation of the associated free energies.

Concerning the proof of Theorem 1 (paper in preparation) let us say that, for an interesting class of systems, among which our model is included, one needs some extension of the Pirogov-Sinai theory of phase transitions (see ref. [6]). In such an extension certain states, called the restricted ensembles, play the role of the ground states in the usual theory. They can be defined as a Gibbs probability measure on certain subsets of configurations. In the present case one considers, for each $n = 0, 1, 2, \ldots$, subsets of configurations which are in some sense near to the constant configurations $\phi_x = n$.

Namely, we consider the set $\mathscr{C}_k^{res}(\Lambda, n)$ of the microscopic interfaces, with boundary at height $\bar{\phi}_x = n$, and whose Dobrushin walls have, all of them, horizontal projections with diameter less than $3k+3$ (these walls are the maximally connected sets of vertical plaquettes of the interface). The Gibbs measure defined on the subset $\mathscr{C}_k^{res}(\Lambda, n)$ is the restricted ensemble corresponding to the level n. The associated free energies per unit area

$$f_k(n) = -\lim_{\Lambda\to\infty}(1/\beta|\Lambda|)\ln \sum_{\phi_\Lambda\in\mathscr{C}_k^{res}(\Lambda,n)} \exp(-\beta H(\phi_\Lambda|n)) \tag{10}$$

can be computed, with the help of cluster expansions (see, for instance, ref. [7]), as a convergent power series in the variable t. Then one is able to study the phase diagram of the restricted ensembles. The restricted ensemble at level n is said to be dominant, or stable, for some given values of the parameters u and t, if $f_k(n) = \min_{n'} f_k(n')$. We then have:

Proposition 1. Let the integer $n \geq 0$ be given and choose $k \geq 1$. Let $a, b \geq 0$ be two real numbers. Let $0 < t \leq t_1(k) = (3k+3)^{-4}$. If

$$-\ln(1-t^2) + (2+a)t^{n+3} \leq u \leq -\ln(1-t^2) + (2-b)t^{n+2}, \tag{11}$$

then, we have

$$f_k(n) \leq f_k(h) - at^{3n+3} + O(t^{3n+4}), \qquad \text{for any } h \geq n+1, \tag{12}$$

$$f_k(n) \leq f_k(h) - bt^{3n} + O(t^{3n+1}), \qquad \text{for any } 0 \leq h \leq n-1. \tag{13}$$

We notice that $k \geq n$ is the useful case in the proof of Theorem 1, and that the remainders in inequalities (12) and (13) can be bounded uniformly in h. Then the proof of Theorem 1 consists in showing that the phase diagram of the pure phases at low temperature is close to the phase diagram of the dominant restricted ensembles.

REFERENCES

1. J. Fröhlich, and C. E.Pfister, *Commun. Math. Phys.* **109**, 493–523 (1987); íbid. **112**, 51–74 (1987).
2. J. T. Chalker, *J. Phys. A: Math. Gen.* **15**, L481–L485 (1982).
3. E. I. Dinaburg, and A. E. Mazel, *J. Stat. Phys.* **74**, 533–563 (1996).
4. F. Cesi, and F. Martinelli, *J. Stat. Phys.* **82**, 823–913 (1996).
5. J. L. Lebowitz, and A. E. Mazel, *J. Stat. Phys.* **84**, 379–397 (1996).
6. Ya. G. Sinai, *Theory of Phase Transitions: Rigorous Results*, Pergamon Press, Oxford, 1982.
7. S. Miracle-Solé, *Physica A* **279**, 244–249 (2000).

On the role of Galilean invariance in KPZ

H. S. Wio*, J. A. Revelli†, C. Escudero**, R. R. Deza‡ and M. S. de La Lama§

*Instituto de Física de Cantabria (UC and CSIC), Spain
†FAMAF, Universidad Nacional de Cordoba, Argentina
**ICMAT, Dep. Matemáticas, Fac. Cs., Univ. Aut. de Madrid, Spain
‡IFIMAR (UNMdP and CONICET), Argentina
§Max-Planck-Institute, Göttingen, Germany

Abstract. Starting from a variational formulation of the Kardar-Parisi-Zhang (KPZ) equation, we point out some strong constraints and consistency tests, to be fulfilled by real-space discretization schemes. In the light of these findings, the mainstream opinion on the relevance of Galilean invariance and the fluctuation–dissipation theorem (peculiar of 1D) is challenged.

Keywords: KPZ, Variational Formulation, Galilean Invariance
PACS: 05.10.Gg, 64.60.Ht, 68.35.Ct, 68.35.Rh

The KPZ equation [1] that describes the growth of a rough interface, has become a paradigm of nonequilibrium growth processes [2, 3]. In a recent paper [4] it was shown that, despite the current negative belief, it is possible to write a Lyapunov or free energy-like functional for such an equation. Such a variational formulation has allowed us to analyze some discretization aspects, and to discuss the true role of the Galilean invariance (fulfilled by the continuous equation) in determining the universality class for the KPZ dynamics. We briefly discuss these points here.

We start from a general scalar reaction–diffusion equation with multiplicative noise

$$\partial_t \phi(x,t) = \nu \partial_x^2 \phi(x,t) + \gamma \phi(x,t) + \phi(x,t)\eta(x,t), \tag{1}$$

where $\eta(x,t)$ is a Gaussian white noise with zero mean and intensity σ. We may safely assume the physically grounded Stratonovich interpretation, since the parameter γ will absorb the divergences coming from noise interpretation by means of a renormalization argument.

Exploiting the Hopf–Cole transformation we can now define a new field $h(x,t) = \frac{2\nu}{\lambda} \ln \phi(x,t)$, which corresponds to an interface height and whose inverse is $\phi(x,t) = \exp[\frac{\lambda}{2\nu} h(x,t)]$. The transformed equation reads

$$\partial_t h(x,t) = \nu \partial_x^2 h + \frac{\lambda}{2} (\partial_x h)^2 + \frac{\lambda}{2\nu} \gamma + \xi(x,t), \tag{2}$$

which is the celebrated KPZ equation. The noise term, which had a multiplicative character in Eq. (1), becomes additive. The associated NEP is [4]

$$\mathscr{G}[h] = \int_\Omega e^{\frac{\lambda}{\nu} h(x,t)} \frac{\lambda}{2\nu} \left[-F + \frac{\lambda}{4} (\partial_x h(x,t))^2 \right] dx, \tag{3}$$

with $F = \frac{\lambda \gamma}{2\nu}$. It is easy to prove that this functional fulfills

$$\partial_t h(\mathbf{x},t) = -\Gamma[h] \frac{\delta \mathscr{G}[h]}{\delta h(x,t)} + \xi(x,t), \tag{4}$$

as well as the Lyapunov property $\frac{d}{dt}\mathscr{G}[h] \leq 0$, with $\Gamma[h] = \left(\frac{2\nu}{\lambda}\right)^2 \exp[-\frac{\lambda}{\nu} h(x,t)]$.

The KPZ equation in 1D has two main symmetries: Galilean invariance and the fluctuation–dissipation relation. On one hand, Galilean invariance has been traditionally linked to the exactness, in any spatial dimensionality, of the relation $\alpha + z = 2$ between the critical exponents [the roughness exponent α, characterizing the surface morphology in the stationary regime, and the dynamic exponent z, indicating the correlation length scaling as $\xi(t) \sim t^{1/z}$]. However, this interpretation has been criticized in this and other nonequilibrium models [5, 6]. On the other hand, the second symmetry essentially tells us that in 1D, the nonlinear (KPZ) term is not operative at long times.

Even recognizing the interesting analytical properties of the KPZ equation, it is clear that investigating the behavior of its solutions requires the (stochastic) numerical integration of a discrete version. Such an approach has been used e.g. to obtain the critical exponents in one and more spatial dimensions. Real-space discrete versions of the KPZ equation are still used for numerical simulations. One reason is their relative ease of implementation and of interpretation in the case of non-homogeneous substrates like, e.g. a quenched impurity distribution.

CONSISTENCY

We use the standard, nearest-neighbor discretization prescription [2, 3] as a benchmark to elucidate the constraints to be obeyed by any spatial discretization scheme, arising from the mapping between the KPZ equation and Eq. (1).

The standard spatially discrete version of Eq. (1) is

$$\dot{\phi}_j = \frac{\nu}{a^2}\left(\phi_{j+1} - 2\phi_j + \phi_{j-1}\right) + \frac{\lambda F}{2\nu}\phi_j + \frac{\lambda \varepsilon}{2\nu}\phi_j \xi_j, \tag{5}$$

where $1 \leq j \leq N \equiv 0$ (because periodic b.c. are usually assumed) and a is the lattice spacing. An important feature of the Hopf–Cole transformation is that it is *local*, i.e., it involves neither spatial nor temporal transformations. Then, using the discrete version of this transformation

$$\phi_j(t) = \exp\left[\frac{\lambda}{2\nu} h_j(t)\right],$$

we get

$$\dot{h}_j = \frac{2\nu^2}{\lambda a^2}\left(\mathrm{e}^{\delta_j^+ a} + \mathrm{e}^{\delta_j^- a} - 2\right) + \varepsilon\, \xi_j, \tag{6}$$

with $\delta_j^{\pm} \equiv \frac{\lambda}{2\nu a}(h_{j\pm1} - h_j)$ and $\gamma = 0 = F$. By expanding the exponentials up to terms of order a^2, and collecting equal powers of a (the zero-order contribution vanishes) yields

$$\dot{h}_j = \frac{\nu}{a^2}\left(h_{j+1} - 2h_j + h_{j-1}\right) + \frac{\lambda}{4a^2}\left[(h_{j+1} - h_j)^2 + (h_j - h_{j-1})^2\right] + \varepsilon\,\xi_j, \tag{7}$$

implying that the discrete form of the Laplacian is the same, regardless of whether it is applied to ϕ or h. Also, by virtue of the discrete Hopf–Cole transformation, the discrete form of the Laplacian in Eq. (6) constrains the discrete form of the nonlinear term in the transformed equation. In order to strengthen these observations we consider the discrete version of the KPZ functional indicated in Eq. (3)

$$\mathscr{G}[h] \approx \frac{\lambda^2}{8\nu} \sum_{j=1}^{N} e^{\frac{\lambda}{\nu} h_j(x,t)} \frac{1}{a}\left[(\phi_{j+1} - \phi_j)^2 + (\phi_j - \phi_{j-1})^2\right]. \tag{8}$$

The discrete analog of the variational procedure yields precisely Eq. (7), confirming that the discretizations of both terms are strictly related.

THE FLUCTUATION–DISSIPATION RELATION

This relation is a fundamental symmetry of the 1D KPZ equation. The stationary probability distribution for the KPZ problem in 1D is known to be [2, 3]

$$\mathscr{P}_{\text{stat}}[h] \sim \exp\left\{-\frac{\nu}{2\varepsilon}\int dx\,(\partial_x h)^2\right\}.$$

With the discretization scheme in Eq. (7), this is

$$\mathscr{P}_{\text{stat}}[h] \sim \exp\left\{-\frac{\nu}{2\varepsilon}\frac{1}{2a}\sum_j \left[(h_{j+1} - h_j)^2 + (h_j - h_{j-1})^2\right]\right\}. \tag{9}$$

Inserting this expression into the stationary Fokker–Planck equation, the only surviving term has the form $\frac{1}{2a^3}\sum_j \left[(h_{j+1} - h_j)^2 + (h_j - h_{j-1})^2\right] \times \left[h_{j+1} - 2h_j + h_{j-1}\right]$, whose continuum limit is $\int dx\,(\partial_x h)^2\,\partial_x^2 h$, that is identically zero [2, 3]. A numerical analysis of such discrete representation indicates that it is several orders of magnitude smaller than the value of the exponents' pdf [in Eq. (9)], and typically behaves as $\mathscr{O}(1/N)$, where N is the number of spatial points used in the discretization, with an even faster approach to zero if expressions with higher accuracy are used [7, 8]. This indicates that the problem with the fluctuation–dissipation theorem in 1+1, which is generically **not** fulfilled by discrete forms of the KPZ equation, can be circumvented by just using more accurate discretizations.

GALILEAN INVARIANCE

This invariance means that the transformation

$$x \to x - \lambda v t \quad , \quad h \to h + v x \quad , \quad F \to F - \frac{\lambda}{2} v^2, \tag{10}$$

where v is an arbitrary constant vector field, leaves the KPZ equation invariant. The equation obtained using the classical discretization

$$\partial_x h \to \frac{1}{2a}(h_{j+1} - h_{j-1}), \tag{11}$$

is invariant under the discrete Galilean transformation

$$ja \to ja - \lambda v t, \quad h_j \to h_j + v ja, \quad F \to F - \frac{\lambda}{2} v^2. \tag{12}$$

However, the associated equation is known to be numerically unstable [9], at least when a is not small enough. *No other discretization is known to be invariant under the discrete Galilean transformation*, and this assertion includes Eq. (7). In fact, the transformation $h \to h + v ja$ yields an excess term which is compatible with the gradient discretization in Eq. (11); however this discretization does not allow to recover the quadratic term in Eq. (7), indicating that this finite-difference scheme is not Galilean-invariant.

Since Eq. (5) is invariant under the discrete Galilean transformation, Eq. (12), the responsible for the loss of Galilean invariance is the (discrete, within the present context) nonlinear Hopf–Cole transformation. Note that these results are independent of whether we consider this discretization scheme or a more accurate one. It is clear that this symmetry is recovered when the continuum limit is taken in any reasonable discretization scheme.

As already argued, Galilean invariance has always been associated with the exactness of the one-dimensional KPZ exponents, and with the relation $\alpha + z = 2$, that holds even in higher dimensions [2, 3].

The fact that the numerical solution obtained from a non-Galilean invariant finite-difference scheme as Eq. (7), *yields the well known critical exponents*, strongly suggests it is not Galilean invariance what determines the KPZ universality class. The numerical results shown in [7, 8, 10] are a clear indication that this is the case.

CONCLUSIONS

The moral from the present analysis is clear: (i) a Lyapunov functional exists for KPZ; (ii) the problem with the fluctuation-dissipation theorem in 1D is tightly related to numerical accuracy; (iii) there is strong evidence that Galilean invariance does not play the relevant role previously assumed in defining the KPZ universality class.

ACKNOWLEDGMENTS

HSW acknowledges financial support from MEC (Spain) through Project CGL2007-64387/CLI, RRD from CONICET and UNMdP (Argentina), and CE from MICINN (Spain) through Project MTM2008-03754.

REFERENCES

1. M. Kardar, G. Parisi, and Y. -C. Zhang, *Phys. Rev. Lett.* **56**, 889 (1986)
2. A. -L. Barabási, and H. E. Stanley, *Fractal concepts in surface growth*, Cambridge University Press, Cambridge, 1995.
3. T. Halpin-Healy, and Y. -Ch. Zhang, *Phys. Rep.* **254**, 215 (1995)
4. H. S. Wio, *Int. J. Bif. Chaos* **19**, 2813 (2009)
5. M. Nicoli, R. Cuerno, and M. Castro, *Phys. Rev. Lett.* **102**, 256102 (2009)
6. A. Berera, and D. Hochberg, *Phys. Rev. Lett.* **99**, 254501 (2007); ibid., *Nucl. Phys. B* **814**, 522 (2009).
7. H. S.Wio, J. A.Revelli, R. R.Deza, C.Escudero, and M. S. de La Lama, *Europhys.Lett.* **89**, 40008 (2010).
8. H. S.Wio, J. A.Revelli, R. R.Deza, C.Escudero and M S. de La Lama, *Phys. Rev. E* **81**, 066706 (2010).
9. T. J. Newman, and A. J. Bray, *J. Phys. A: Math. Gen.* **29**, 7917 (1996).
10. H. S.Wio, J. A.Revelli, R. R.Deza, C. Escudero, and M. S. de La Lama, *Phil. Trans. Royal Soc. A* (in press).

Anomalous diffusion and basic theorems of statistical mechanics

Luciano C. Lapas[*], J. Miguel Rubí[†] and Fernando A. Oliveira[**]

[*] *Universidade Federal da Integração Latino-Americana, Av. Tancredo Neves 6731, 85867-970 Foz do Iguaçu, Brazil*
[†] *Departament de Física Fonamental, Facultat de Física, Universitat de Barcelona, Av. Diagonal 647, 08028 Barcelona, Spain*
[**] *Instituto de Física and International Center for Condensed Matter Physics, Universidade de Brasília, C. P. 04513, 70904-970 Brasília, Brazil*

Abstract. Recent works call attention that basic concepts in statistical mechanics are still under discussion. In particular, we have shown that some of those concepts can be discussed in a direct and analytical way in diffusion.

Keywords: Brownian motion; anomalous diffusion; irreversibility; ergodicity; fluctuation-dissipation theorem; Khinchin theorem
PACS: 05.40.-a; 05.70.-a; 05.40.Jc; 05.10.Gg

INTRODUCTION

Some of the basics theorems of statistical mechanics can be understood in the framework of diffusion. We shall discuss here the ergodic hypothesis (EH), the fluctuation-dissipation theorem (FDT), and the second law of thermodynamics[1]. The KT [2] is of great importance since it relates the ergodicity of a variable p to the irreversibility of its autocorrelation function $C_p(t)$ [2, 3, 4, 5, 6, 7, 8].

Most of the experimental situations in which the EH does not hold arise in complex nonlinear or far from equilibrium structures where detailed balance is not fulfilled. A few examples are found in supercooled liquids and glasses [9] and blinking nanocrystals [10]. The majority of those systems, however, apparently do not have an easy analytical solution. On the other hand, in this work we show that even anomalous diffusion treated with the Generalized Langevin Equation (GLE) can present closed solutions for the main expectation values, and can be used as a simple laboratory for the discussion of those properties. As we shall see, in this case, we can give a full description for the validity of the KT, even when the EH breakdowns.

The GLE for a single particle in the absence of a net external force can be written as

$$\frac{dp(t)}{dt} = -\int_0^t \Pi(t-t')p(t')dt' + \eta(t), \tag{1}$$

where $\Pi(t)$ is the memory function, and $\eta(t)$ is a random force of zero mean. Besides, the noise is uncorrelated with the initial-value $p(0)$, $\langle \eta(t)p(0)\rangle = 0$, and obeys the Kubo fluctuation-dissipation theorem (FDT):

$$\langle \eta(t)\eta(t')\rangle = \langle p^2\rangle_{eq}\Pi(t-t'), \tag{2}$$

where $\langle \ldots \rangle_{eq}$ is an average over an ensemble in thermal equilibrium. It is very useful to introduce the relaxation function $R(t) = C_p(t)/C_p(0)$, where the autocorrelation function of p is given by $C_p(t) = \langle p(t)p(0)\rangle - \langle p(t)\rangle\langle p(0)\rangle$, and $\langle \ldots \rangle$ stands for an ensemble average. Explicitly, the KT states that if

$$R(t \to \infty) = 0, \tag{3}$$

then p is ergodic [2]. We shall analyze that for diffusion.

DIFFUSION PHENOMENA

Diffusive dynamics is usually analyzed using the mean square displacement of the particles, which behaves in general as

$$\langle [x(t) - \langle x(t)\rangle]^2 \rangle \propto t^{\alpha},$$

where the exponent α classifies the different types of diffusion: subdiffusion for $0 < \alpha < 1$, normal diffusion for $\alpha = 1$, and superdiffusion for $1 < \alpha \leq 2$; for $\alpha = 2$ the process is called ballistic [5, 7, 11, 12, 13]. Morgado *et al.* [11] obtained a general relationship between the Laplace transform of the memory function $\tilde{\Pi}(z)$ and the diffusion exponent α, i.e. if $\lim_{z\to 0} \tilde{\Pi}(z) \propto z^{\nu}$, than

$$\alpha = \nu + 1. \tag{4}$$

To obtain the memory we define the noise $\eta(t)$ as

$$\eta(t) = \langle p^2(0)\rangle_{eq} \int \rho(\omega)\cos[\omega t + \phi(\omega)]d\omega, \tag{5}$$

where $\rho(\omega)$ is the noise density of states, and $\phi(\omega)$ is a set of random numbers $0 \leq \phi \leq 2\pi$. From the FDT

$$\Pi(t) = \int \rho(\omega)\cos(\omega t)d\omega. \tag{6}$$

A typical noise density has the form

$$\rho(\omega) = \begin{cases} a\omega^{\beta}, & for\ \ \omega \leq \omega_s \\ g(\omega), & otherwise. \end{cases} \tag{7}$$

Here, the function $g(\omega)$ is arbitrary as long as it is sufficiently well-behaved and that its integral in the memory function converges. If one is interested only in the long time behavior $t \gg 1/\omega_s$, it can be taken to be 0. With this noise density of states, it is possible to simulate many diffusive regimes. Noise of this form can be obtained either by formal methods or empirical data. Using this expression, Vainstein *et al.* [12] have shown that $\nu = \beta$ for $\beta \leq 1$ and $\nu = 1$ for $\beta \geq 1$ consequently $\nu \leq 1$, i.e. ballistic is the highest asymptotic limit for diffusion.

ENSEMBLE AVERAGE AND EQUILIBRIUM CONDITION

If a system is ergodic and there are no external forces, thermal equilibrium should be observed in a time $t \gg \tau$, where τ is a relaxation time. Then, the distribution function of p approaches the equilibrium distribution in the limit $t \to \infty$, and the mean energy converges to the equilibrium value, $\langle p^2(t \to \infty) \rangle = \langle p^2 \rangle_{eq}$.

For any initial distribution of values, $p(0)$, it is possible to obtain the temporal evolution of the moments $\langle p^n(t) \rangle$, with $n = 1, 2, \ldots$. The first moments are obtained directly by taking the ensemble average of Eq. (1):

$$\langle p(t) \rangle = \langle p(0) \rangle R(t), \tag{8}$$

$$\langle p^2(t) \rangle = \langle p^2 \rangle_{eq} + R^2(t) \left[\langle p^2(0) \rangle - \langle p^2 \rangle_{eq} \right]. \tag{9}$$

Consequently, we see that the knowledge of $R(t)$ allows one to describe completely these averages. Equations (8) and (9) are sufficient to show the condition of equilibrium for diffusion: if condition (3) holds, then the time evolution will produce the ensemble average with $\langle p(t \to \infty) \rangle = 0$ and $\langle p^2(t \to \infty) \rangle = \langle p^2 \rangle_{eq}$. This result also suggests that the EH holds, thus the KT holds. Now it is possible to show that $\lim_{t \to \infty} R(t) = \lim_{z \to 0} z\tilde{R}(z)$ which is null for all diffusive processes in the range $0 < \alpha < 2$. In fact, this occurs in equilibrium or near equilibrium states in which the validity of Linear Response Theory holds. On the other hand, this condition fails for ballistic motion, $\alpha = 2$, in which $R(t \to \infty) = \Lambda \neq 0$ and the autocorrelation function $C_p(t)$ will be non-null for long times[7]. In other words, if the ballistic system is not initially equilibrated, then it will never reach equilibrium and the final result of any measurement will depend on the initial conditions. In this situation, the EH will not be valid; however, once again the KT holds since the violation of the EH was due to the violation of the irreversibility condition, Eq. (3), as predicted by Khinchin. The main consequence of the violation of this condition is the presence of a residual current, Eq. (8). However, the effective current can be very small compared to $\langle p(0) \rangle$ and its value, as any other measurable property for ballistic diffusion, will depend on the value of Λ. In other words, the system decays to a metastable state and remains in it indefinitely, even in the absence of an external field.

CONCLUDING REMARKS

In this work, we have shown that the KT (proved by Khinchin for normal diffusion) holds for all kinds of diffusive processes, which are ergodic in the range of exponents $0 < \alpha < 2$. This result may have deep consequences in many areas [9, 10]. Moreover, it could be verified in and applied to experimental systems, such as the subdiffusive dynamics of the distance between an electron transfer donor and acceptor pair within a single protein molecule [14], which has been modeled by a GLE [15]. Such a model successfully explains the equilibrium fluctuations and its broad range of time scales, being in excellent agreement with experiments. As well a very important and growing research field is the transport in intracellular media[16, 17]. In principle, it is generally possible to derive a GLE for hamiltonian systems for example, the disordered spectra of the Heisenberg chain is incorporated in the memory kernel and in the colored noise [18]. In the analysis of those systems, the KT gives the EH a practical character, since it is expressed in terms of response functions: our results apply for real-valued relaxation functions $R(t)$; on the other hand, if the relaxation function assumes complex values, e.g. conductivity, the final value theorem may not be applied. For those systems, the KT fails, as proposed in Ref. [4]. Moreover many theorems, as the FDT, may fail [5].

ACKNOWLEDGMENTS

This work was supported by Brazilian Research Foundations: CAPES, CNPq, FINATEC, and FAPDF; and by the DGiCYT of the Spanish Government under Grant No. FIS2005-01299.

REFERENCES

1. J. M. Rubí, *Sci. Am.* **299**, 62 (2008).
2. A. I. Khinchin, *Mathematical Foundations of Statistical Mechanics*, Dover, New York (1949).
3. M. H. Lee, *Phys. Rev. Lett.* **87**, 250601 (2001).
4. M. H. Lee, *Phys. Rev. Lett.* **98**, 190601 (2007).
5. I. V. L. Costa et al., *Europhys. Lett.* **63**, 173 (2003).
6. L. C. Lapas et al., *Europhys. Lett.* **77**, 37004 (2007).
7. L. C. Lapas et al., *Phys. Rev. Lett.* **101**, 230602 (2008).
8. S. Borov et al., *Proc. Natl. Acad. Sci. USA* **107**, 13228 (2010).
9. M. D. Ediger et al., *J. Phys. Chem.* **100**, 13200 (1996).
10. G. Margolin et al., *Phys. Rev. Lett.* **94**, 080601 (2005).
11. R. Morgado et al., *Phys. Rev. Lett.* **89**, 100601 (2002).
12. M. H. Vainstein et al., *Europhys. Lett.* **73**, 726 (2006).
13. J. D. Bao et al., *Phys. Rev. E* **74**, 061111 (2006).
14. H. Yang et al., *Science* **302**, 262 (2003).
15. S. C. Kou et al., *Phys. Rev. Lett.* **93**, 180603 (2004)
16. I. Santamaria-Holek et al., *Physica A* **388**, 15133 (2009).
17. A. Caspi et al., *Phys. Rev. Lett.* **85**, 5655 (2000).
18. M. H. Vainstein et al., *Phys. Lett. A* **339**, 33 (2005).

Large deviations of the current in a two-dimensional diffusive system

C. Pérez-Espigares, J.J. del Pozo, P.L. Garrido and P.I. Hurtado

Departamento de Electromagnetismo y Física de la Materia, and Instituto Carlos I de Física Teórica y Computacional, Universidad de Granada, Granada 18071, Spain

Abstract. In this notes we study the large deviations of the time-averaged current in the two-dimensional (2D) Kipnis-Marchioro-Presutti model of energy transport when subject to a boundary gradient. We use the tools of hydrodynamic fluctuation theory, supplemented with an appropriate generalization of the additivity principle. As compared to its one-dimensional counterpart, which amounts to assume that the optimal profiles responsible of a given current fluctuation are time-independent, the 2D additivity conjecture requires an extra assumption, i.e. that the optimal, divergence-free current vector field associated to a given fluctuation of the time-averaged current is in fact constant across the system. Within this context we show that the current distribution exhibits in general non-Gaussian tails. The ensuing optimal density profile can be either monotone for small current fluctuations, or non-monotone with a single maximum for large enough current deviations. Furthermore, this optimal profile remains invariant under arbitrary rotations of the current vector, providing a detailed example of the recently introduced Isometric Fluctuation Relation.

Keywords: Current fluctuations, nonequilibrium physics, diffusive systems, fluctuation theorems
PACS: 05.40.-a, 02.50.-r, 05.70.Ln, 44.10.+i

INTRODUCTION

Large deviation functions measure the rate at which the empiric average of an observable converges toward its asymptotic value. Think for instance on the time-averaged current in a d-dimensional mesoscopic conductor of length L. As time increases, and provided that the system is ergodic, the time-averaged current $\mathbf{J} = \tau^{-1}\int_0^\tau \mathbf{j}(t)\,dt$ quickly converges toward its ensemble average $\langle \mathbf{J} \rangle$. For finite times, the measured $\mathbf{J}$ may fluctuate and the probability of a given output follows in general a large-deviation principle [1] for long times, $\mathrm{P}_L(\mathbf{J},\tau) \sim \exp[+\tau L^d G(\mathbf{J})]$. Here $G(\mathbf{J})$ is the current large deviation function (LDF), and measures the (exponential) rate at which $\mathbf{J} \to \langle \mathbf{J} \rangle$ as τ increases (notice that $G(\mathbf{J}) \le 0$, with $G(\langle \mathbf{J} \rangle) = 0$).

Large deviation functions akin to $G(\mathbf{J})$ play an important role in statistical physics [2]. For instance, the LDF of the density profile in equilibrium systems can be simply related with the free-energy functional, a central object in the theory [1, 2, 3]. In a similar way, we can use LDFs in systems far from equilibrium to define the nonequilibrium analog of the free-energy functional. This top-down approach is specially appealing in a nonequilibrium context, as we don't know in this case the statistical weight of microscopic configurations, equivalent to the equilibrium Boltzmann-Gibbs measure, from which to build up a nonequilibrium *partition function*. In any case, LDFs out of equilibrium may be non-local and/or non-convex [3, 4], reflecting in this way the pathologies associated to nonequilibrium behavior.

Computing LDFs from scratch, starting from microscopic dynamics, is in general an extraordinary difficult task which has been successfully accomplished only for a handfull of simple stochastic lattice gases. However, in a series of recent works [4], Bertini, De Sole, Gabrielli, Jona-Lasinio, and Landim have introduced a hydrodynamic fluctuation theory (HFT) which describes large dynamic fluctuations in diffusive systems and the associated LDFs starting from a macroscopic rescaled description of the system of interest, where the only inputs are the system transport coefficients. This is a very general approach which leads however to a hard variational problem whose solution remains challenging in most cases. However, if supplemented with a recently-introduced conjecture named additivity principle [5], HFT can be readily applied to obtain explicit predictions, opening the door to a systematic way of computing LDFs in nonequilibrium systems.

In this paper we apply this program to study the statistics of current fluctuations in a simple but very general model of diffusive energy transport in two dimensions, namely the 2D Kipnis-Marchioro-Presutti (KMP) model [6].

HFT FOR CURRENT FLUCTUATIONS

We start from a rescaled ($\mathbf{r} \to \mathbf{r}/L$, $t \to t/L^2$) continuity equation

$$\partial_t \rho(\mathbf{r},t) = -\boldsymbol{\nabla} \cdot \Big(\mathbf{Q}[\rho(\mathbf{r},t)] + \boldsymbol{\xi}(\mathbf{r},t) \Big) , \tag{1}$$

which describes a wide class of d-dimensional systems characterized by a single locally-conserved field $\rho(\mathbf{r},t)$, representing a density of e.g. energy, particles, momentum, charge, etc. Here $\mathbf{j}(\mathbf{r},t) \equiv -D[\rho]\boldsymbol{\nabla}[\rho(\mathbf{r},t)] + \boldsymbol{\xi}(\mathbf{r},t)$ is a fluctuating current, with local average $\mathbf{Q}[\rho(\mathbf{r},t)]$, and $\mathbf{r} \in \{0,1\}^d$. In particular, we focus in this paper on diffusive systems, for which the current obeys Fick's (or equivalently Fourier's) law, $\mathbf{Q}[\rho(\mathbf{r},t)] = -D[\rho]\boldsymbol{\nabla}\rho(\mathbf{r},t)$, where $D[\rho]$ is the diffusivity (a functional of the density profile in general). The (conserved) noise vector term $\boldsymbol{\xi}(\mathbf{r},t)$, which accounts for microscopic random fluctuations at the macroscopic level, is Gaussian and white with $\langle \boldsymbol{\xi}(\mathbf{r},t) \rangle = 0$ and $\langle \xi_\alpha(\mathbf{r},t)\xi_\beta(\mathbf{r}',t') \rangle = 2L^{-d}\sigma[\rho]\delta_{\alpha\beta}\delta(\mathbf{r}-\mathbf{r}')\delta(t-t')$, being $\sigma[\rho]$ the mobility functional and L the system linear size. This noise source represents the many fast microscopic degrees of freedom which are averaged out in the coarse-graining procedure resulting in eq. (1), and whose net effect on the macroscopic evolution amounts to a Gaussian random perturbation according to the central limit theorem. The above equation must be supplemented with appropriate boundary conditions, which in this work we choose to be gradient-like in the $\hat{x}$-direction, with fixed densities ρ_L and ρ_R at the left and right reservoirs, respectively, and periodic boundary conditions in all other directions.

We are interested in the probability $\mathrm{P}_L(\mathbf{J},\tau)$ of observing a space and time averaged current $\mathbf{J} = \tau^{-1}\int_0^\tau dt \int d\mathbf{r}\, \mathbf{j}(\mathbf{r},t)$. For long times [1, 2, 3, 4] $\mathrm{P}_L(\mathbf{J},\tau) \sim \exp[+\tau L^d G(\mathbf{J})]$, and we aim at computing the current LDF $G(\mathbf{J})$ starting from eq. (1) within a path integral formalism. In particular, the probability of observing a history $\{\rho(\mathbf{r},t),\mathbf{j}(\mathbf{r},t)\}_0^\tau$ of duration τ for the density and current fields, starting from a given initial state, can be written as a path integral over all possible noise realizations $\{\boldsymbol{\xi}(\mathbf{r},t)\}_0^\tau$

$$\mathrm{P}(\{\rho,\mathbf{j}\}_0^\tau) = \int \mathscr{D}\boldsymbol{\xi}\, \exp\left[-L^d \int_0^\tau dt \int d\mathbf{r} \frac{\boldsymbol{\xi}^2}{2\sigma[\rho]}\right] \prod_t \prod_{\mathbf{r}} \delta\Big[\boldsymbol{\xi} - (\mathbf{j} + D[\rho]\boldsymbol{\nabla}\rho)\Big], \quad (2)$$

with $\rho(\mathbf{r},t)$ and $\mathbf{j}(\mathbf{r},t)$ coupled via the continuity equation, $\partial_t\rho(\mathbf{r},t) + \boldsymbol{\nabla}\cdot\mathbf{j}(\mathbf{r},t) = 0$. Notice that this coupling does not determine univocally the relation between ρ and $\mathbf{j}$. For instance, the fields $\rho'(\mathbf{r},t) = \rho(\mathbf{r},t) + \chi(\mathbf{r})$ and $\mathbf{j}'(\mathbf{r},t) = \mathbf{j}(\mathbf{r},t) + \mathbf{g}(\mathbf{r},t)$, with $\chi(\mathbf{r})$ arbitrary and $\mathbf{g}(\mathbf{r},t)$ divergenceless, satisfy the same continuity equation. This freedom can be traced back to the loss of information during the coarse-graining from the microscale to the macroscale [4]. Eq. (2) naturally leads to $\mathrm{P}\left(\{\rho,\mathbf{j}\}_0^\tau\right) \sim \exp\left(+L^d I_\tau[\rho,\mathbf{j}]\right)$, with

$$I_\tau[\rho,\mathbf{j}] = -\int_0^\tau dt \int d\mathbf{r} \frac{(\mathbf{j}(\mathbf{r},t) + D[\rho]\boldsymbol{\nabla}\rho(\mathbf{r},t))^2}{2\sigma[\rho]}. \quad (3)$$

The probability $\mathrm{P}_L(\mathbf{J},\tau)$ of observing an averaged current $\mathbf{J}$ can be written now as

$$\mathrm{P}_L(\mathbf{J},\tau) \sim \int^* \mathscr{D}\rho\mathscr{D}\mathbf{j}\, \mathrm{P}(\{\rho,\mathbf{j}\}_0^\tau)\, \delta\left(\mathbf{J} - \tau^{-1}\int_0^\tau dt \int d\mathbf{r}\,\mathbf{j}(\mathbf{r},t)\right),$$

where the asterisk means that this path integral is restricted to histories $\{\rho,\mathbf{j}\}_0^\tau$ coupled via the continuity equation. As the exponent of $\mathrm{P}\left(\{\rho,\mathbf{j}\}_0^\tau\right)$ is extensive in both τ and L^d, see above, for long times and large system sizes the above path integral is dominated by the associated saddle point, resulting in the following current LDF

$$G(\mathbf{J}) = \tau^{-1} \max_{\rho,\mathbf{j}} I_\tau[\rho,\mathbf{j}], \quad (4)$$

with the constraints $\mathbf{J} = \tau^{-1}\int_0^\tau dt \int d\mathbf{r}\,\mathbf{j}(\mathbf{r},t)$ and $\partial_t\rho + \boldsymbol{\nabla}\cdot\mathbf{j} = 0$. The optimal density and current fields solution of this variational problem, denoted here as $\rho_{\mathbf{J}}(\mathbf{r},t)$ and $\mathbf{j}_{\mathbf{J}}(\mathbf{r},t)$, can be interpreted as the optimal path the system follows in order to sustain a long-time current fluctuation $\mathbf{J}$. It is worth emphasizing here that the existence of an optimal path rests on the presence of a selection principle at play, namely a long time, large size limit which selects, among all possible paths compatible with a given fluctuation, an optimal one via a saddle point mechanism.

The variational problem posed in eq. (4) is a complex spatiotemporal problem whose solution remains challenging in most cases. In order to proceed, we now make the following hypotheses:

1. We assume that the optimal profiles responsible of a given current fluctuation are time-independent, $\rho_{\mathbf{J}}(\mathbf{r})$ and $\mathbf{j}_{\mathbf{J}}(\mathbf{r})$. This, together with the continuity equation, implies that the optimal current vector field is divergence-free, $\boldsymbol{\nabla}\cdot\mathbf{j}_{\mathbf{J}}(\mathbf{r}) = 0$.
2. A further simplification consists in assuming that this optimal current field is in fact constant across space, so $\mathbf{j}_{\mathbf{J}}(\mathbf{r}) = \mathbf{J}$.

Provided that these hypotheses hold, the current LDF can be written as

$$G(\mathbf{J}) = -\min_{\rho(\mathbf{r})} \int \frac{(\mathbf{J} + D[\rho(\mathbf{r})]\boldsymbol{\nabla}\rho(\mathbf{r}))^2}{2\sigma[\rho(\mathbf{r})]} d\mathbf{r}, \quad (5)$$

which expresses the *locally*-Gaussian nature of fluctuations [3, 11]. In this way the probability $\mathrm{P}_L(\mathbf{J},\tau)$ is simply the Gaussian weight associated to the optimal density profile responsible of such fluctuation. Note however that the minimization procedure gives rise to a nonlinear problem which results in general in a current distribution with non-Gaussian tails [3, 4, 7]. As opposed to the general problem in eq. (4), its simplified version, eq. (5), can be readily used to obtain quantitative predictions for the current statistics in a large variety of nonequilibrium systems.

The minimization of the functional in eq. (5) leads to the following differential equation for the optimal profile $\rho_{\mathbf{J}}(\mathbf{r})$

$$D^2[\rho_{\mathbf{J}}]\big(\boldsymbol{\nabla}\rho_{\mathbf{J}}\big)^2 = \mathbf{J}^2\big\{1+2\sigma[\rho_{\mathbf{J}}]K(\mathbf{J}^2)\big\}\,, \tag{6}$$

where $K(\mathbf{J}^2)$ is a constant which guarantees the correct boundary conditions for $\rho_{\mathbf{J}}(\mathbf{r})$. Remarkably, the optimal profile solution of eq. (6) depends exclusively on the magnitude of the current vector, via $\mathbf{J}^2$, not on its orientation, i.e. $\rho_{\mathbf{J}}(\mathbf{r}) = \rho_{|\mathbf{J}|}(\mathbf{r})$, as demanded for time-reversible systems by the recently introduced Isometric Fluctuation Relation (IFR) [11].

The assumption of time-independent optimal profiles has been shown [4] to be equivalent to the additivity principle recently introduced by Bodineau and Derrida for one-dimensional (1D) diffusive systems [5]. Let $\mathrm{P}_L(J,\rho_L,\rho_R,\tau)$ be the probability of observing a time-averaged current J during a long time τ in a *one-dimensional* system of size L in contact with boundary reservoirs at densities ρ_L and ρ_R. The additivity principle relates this probability with the probabilities of sustaining the same current in subsystems of lengths $L-\ell$ and ℓ, i.e, $P_L(J,\rho_L,\rho_R,\tau) = \max_\rho[P_{L-\ell}(J,\rho_L,\rho,\tau)\times P_\ell(J,\rho,\rho_R,\tau)]$. The maximization over the contact density ρ can be rationalized by writing this probability as an integral over ρ of the product of probabilities for subsystems and noticing that these should obey also a large deviation principle. Hence a saddle-point calculation in the long-τ limit leads to the above expression. The additivity principle can be rewritten for the current LDF as $LG(J,\rho_L,\rho_R) = \max_\rho[(L-\ell)G(J,\rho_L,\rho)+\ell G(J,\rho,\rho_R)$. Slicing iteratively the 1D system of length N into smaller and smaller segments, and assuming locally-Gaussian current fluctuations, it is easy to show that in the continuum limit a variational form for $G(J,\rho_L,\rho_R)$ is obtained which is just the 1D counterpart of eq. (5). Interestingly, for 1D systems the conjecture of time-independent optimal profiles implies that the optimal current profile must be constant. This is no longer true in higher dimensions, as any divergence-free current field with spatial integral equal to $\mathbf{J}$ is compatible with the equations. This gives rise to a variational problem with respect to the (time-independent) density and current fields which still poses many technical difficulties. Therefore an additional assumption is needed, namely the constancy of the optimal current vector field across space. These two hypotheses are equivalent to the iterative procedure of the additivity principle in higher dimensions.

The validity of the additivity principle has been recently confirmed for a broad range of current fluctuations in extensive numerical simulations of the 1D Kipnis-Marchioro-Presutti model of energy transport. However, this conjecture is known to break down in some special cases for extreme current fluctuations, where time-dependent optimal profiles in the form of traveling waves propagating along the current direction may emerge. Even in these cases the additivity principle correctly predicts the current distribution in a very large current interval. As for higher-dimensional systems, the range of applicability of the generalized additivity hypothesis here proposed is an open issue [12].

In what follows we derive explicit predictions for the current LDF in the 2D KMP model of heat conduction based on the above generalization of the additivity principle.

RESULTS FOR THE 2D-KMP MODEL

The 2D-KMP model is a microscopic stochastic lattice model of energy transport in which Fourier's law holds. Each site on the lattice models an harmonic oscillator which is mechanically uncoupled from its nearest neighbors but interacts with them through a random process which redistributes energy locally. The system is coupled to boundary heat baths along the x-direction at *temperatures* ρ_L and ρ_R, whereas periodic boundary conditions hold in the y-direction. For $\rho_L \neq \rho_R$ the system reaches a nonequilibrium steady state with a nonzero rescaled average current $\langle \mathbf{J} \rangle = \hat{x}(\rho_L - \rho_R)/2$ and a stationary profile $\rho_{\text{st}}(\mathbf{r}) = \rho_L + x(\rho_R - \rho_L)$. At the macroscopic level the KMP model is characterized by a diffusivity $D[\rho] = \frac{1}{2}$, and a mobility $\sigma[\rho] = \rho^2$ which characterizes the variance of energy current fluctuations in equilibrium ($\rho_L = \rho_R$).

To study the statistics of the averaged current, first notice that the symmetry of the problem suggests that the optimal density profile associated to a given current fluctuation depends exclusively on x, with no structure in the y-direction, i.e. $\rho_{|\mathbf{J}|}(\mathbf{r}) = \rho_{|\mathbf{J}|}(x)$, compatible with the presence of an external gradient along the x-direction. Under these considerations, and denoting $J = |\mathbf{J}|$, eq. (6) becomes

$$\left(\frac{d\rho_J(x)}{dx}\right)^2 = 4J^2\left(1 + 2K(J)\rho_J^2(x)\right) \tag{7}$$

Here two different scenarios appear. On one hand, for large enough $K(J)$ the rhs of eq. (7) does not vanish $\forall x \in [0,1]$ and the resulting profile is monotone. In this case, and assuming $\rho_L > \rho_R$ henceforth without loss of generality,

$$\frac{d\rho_J(x)}{dx} = -2J\sqrt{1 + 2\rho_J^2(x)K(J)}\,. \tag{8}$$

On the other hand, for $K(J) < 0$ the rhs of eq. (7) may vanish at some points, resulting in a $\rho_J(x)$ that is non-monotone and takes an unique value $\rho_J^* \equiv \sqrt{-1/2K(J)}$ in the extrema. Notice that the rhs of eq. (7) may be written in this case as $4J^2[1 - (\rho_J(x)/\rho_J^*)^2]$. It is then clear that, if non-monotone, the profile $\rho_J(x)$ can only have a single maximum because: (i) $\rho_J(x) \leq \rho_J^*$ $\forall x \in [0,1]$ for the profile to be a real function, and (ii) several maxima are not possible because they should be separated by a minimum, which is not allowed because of (i). Hence for the non-monotone case (recall $\rho_L > \rho_R$)

$$\frac{d\rho_J(x)}{dx} = \begin{cases} +2J\sqrt{1-\left(\frac{\rho_J(x)}{\rho_J^*}\right)^2}\,, & x < x^* \\ -2J\sqrt{1-\left(\frac{\rho_J(x)}{\rho_J^*}\right)^2}\,, & x > x^* \end{cases} \tag{9}$$

where x^* locates the profile maximum. This leaves us with two separated regimes for current fluctuations, with the crossover happening for $J = \frac{\rho_L}{2}\left[\frac{\pi}{2} - \sin^{-1}\left(\frac{\rho_R}{\rho_L}\right)\right] \equiv J_c$. This crossover current can be obtained from eq. (15) below by letting $\rho_J^* \to \rho_L$

Region I: Monotonous Regime ($J < J_c$)

In this case, using eq. (8) to change variables in eq. (5) we have

$$G(\mathbf{J}) = \int_{\rho_L}^{\rho_R} d\rho_J \frac{1}{4J\rho_J^2\sqrt{1+2K(J)\rho_J^2}} \left[\left(J_x - J\sqrt{1+2K(J)\rho_J^2}\right)^2 + J_y^2\right], \tag{10}$$

with J_α the α component of vector $\mathbf{J}$. This results in

$$G(\mathbf{J}) = \frac{J_x}{2}\left(\frac{1}{\rho_R} - \frac{1}{\rho_L}\right) - J^2K(J) + \frac{J}{2}\left[\frac{\sqrt{1+2K(J)\rho_L^2}}{\rho_L} - \frac{\sqrt{1+2K(J)\rho_R^2}}{\rho_R}\right] \tag{11}$$

Notice that, for $\rho_J(x)$ to be monotone, $1+2K(J)\rho_J^2 > 0$. Thus, $K(J) > -(2\rho_L^2)^{-1}$. Integrating now eq. (8) we obtain the following implicit equation for $\rho_J(x)$ in this regime

$$2xJ = \begin{cases} \frac{1}{\sqrt{2K(J)}} \ln\left[\frac{\rho_L + \sqrt{\rho_L^2 + \frac{1}{2K(J)}}}{\rho_J(x) + \sqrt{\rho_J(x)^2 + \frac{1}{2K(J)}}}\right], & K(J) > 0 \\ \frac{\sin^{-1}\left[\rho_L\sqrt{-2K(J)}\right] - \sin^{-1}\left[\rho_J(x)\sqrt{-2K(J)}\right]}{\sqrt{-2K(J)}}, & -\frac{1}{2\rho_L^2} < K(J) < 0 \end{cases} \tag{12}$$

Making $x = 1$ and $\rho_J(x=1) = \rho_R$ in the previous equation, we obtain the implicit expression for the constant $K(J)$. To get a feeling on how it depends on J, note that in the limit $K(J) \to (-1/2\rho_L^2)$, the current $J \to J_c$, while for $K(J) \to \infty$ one gets $J \to 0$. In addition, from eq. (12) we see that for $K(J) \to 0$ we find $J = (\rho_L - \rho_R)/2 = \langle \mathbf{J} \rangle$.

Sometimes it is interesting to work with the Legendre transform of the current LDF [3, 4, 7], $\mu(\boldsymbol{\lambda}) = \max_{\mathbf{J}}[G(\mathbf{J}) + \boldsymbol{\lambda}\cdot\mathbf{J}]$, where $\boldsymbol{\lambda}$ is a vector parameter conjugate to the current. Using the previous results for $G(\mathbf{J})$ is is easy to show [7] that $\mu(\boldsymbol{\lambda}) = -K(\boldsymbol{\lambda})\mathbf{J}^*(\boldsymbol{\lambda})^2$, where $\mathbf{J}^*(\boldsymbol{\lambda})$ is the current associated to a given $\boldsymbol{\lambda}$, and the constant $K(\boldsymbol{\lambda}) = K(|\mathbf{J}^*(\boldsymbol{\lambda})|)$. The expression for $\mathbf{J}^*(\boldsymbol{\lambda})$ can be obtained from eq. (12) above in the limit $x \to 1$. Finally, the optimal profile for a given $\boldsymbol{\lambda}$ is just $\rho_{\boldsymbol{\lambda}}(x) = \rho_{|\mathbf{J}^*(\boldsymbol{\lambda})|}(x)$.

Region II: Non-Monotonous Regime ($J > J_c$)

In this case the optimal profile has a single maximum $\rho_J^* \equiv \rho_J(x = x^*)$ with $\rho_J^* = 1/\sqrt{-2K(J)}$ and $-1/2\rho_L^2 < K(J) < 0$. Splitting the integral in eq. (5) at x^*, and using now eq. (9) to change variables, we arrive at

$$\begin{aligned} G(\mathbf{J}) &= \frac{J_x}{2}\left(\frac{1}{\rho_R} - \frac{1}{\rho_L}\right) - \frac{J}{2}\left[\frac{1}{\rho_L}\sqrt{1-\left(\frac{\rho_L}{\rho_J^*}\right)^2} + \frac{1}{\rho_R}\sqrt{1-\left(\frac{\rho_R}{\rho_J^*}\right)^2}\right. \\ &- \left.\frac{1}{2\rho_J^*}\left(\pi - \sin^{-1}\left(\frac{\rho_L}{\rho_J^*}\right) - \sin^{-1}\left(\frac{\rho_R}{\rho_J^*}\right)\right)\right]. \end{aligned} \tag{13}$$

Integrating eq. (9) one gets an implicit equation for the non-monotone optimal profile

$$2xJ = \begin{cases} \rho_J^*\left[\sin^{-1}\left(\frac{\rho_J(x)}{\rho_J^*}\right) - \sin^{-1}\left(\frac{\rho_L}{\rho_J^*}\right)\right] & \text{for } 0 \le x < x^* \\ 2J + \rho_J^*\left[\sin^{-1}\left(\frac{\rho_R}{\rho_J^*}\right) - \sin^{-1}\left(\frac{\rho_J(x)}{\rho_J^*}\right)\right] & \text{for } x^* < x \le 1 \end{cases} \tag{14}$$

At $x = x^*$ both branches of the above equation must coincide, and this condition provides simple equations for both x^* and ρ_J^*

$$J = \frac{\rho_J^*}{2}\left[\pi - \sin^{-1}\left(\frac{\rho_L}{\rho_J^*}\right) - \sin^{-1}\left(\frac{\rho_R}{\rho_J^*}\right)\right] \;;\; x^* = \frac{\frac{\pi}{2} - \sin^{-1}\left(\frac{\rho_L}{\rho_J^*}\right)}{\pi - \sin^{-1}\left(\frac{\rho_L}{\rho_J^*}\right) - \sin^{-1}\left(\frac{\rho_R}{\rho_J^*}\right)}. \tag{15}$$

Finally, as in the monotone regime, we can compute the Legendre transform of the current LDF, obtaining as before $\mu(\boldsymbol{\lambda}) = -K(\boldsymbol{\lambda})\mathbf{J}^*(\boldsymbol{\lambda})^2$, where $\mathbf{J}^*(\boldsymbol{\lambda})$ and the constant $K(\boldsymbol{\lambda}) = K(|\mathbf{J}^*(\boldsymbol{\lambda})|)$ can be easily computed from the previous expressions [7]. Note that, in $\boldsymbol{\lambda}$-space, monotone profiles are expected for $|\boldsymbol{\lambda} + \boldsymbol{\varepsilon}| \le \frac{1}{2\rho_R}\sqrt{1-\left(\frac{\rho_R}{\rho_L}\right)^2}$, where $\boldsymbol{\varepsilon} = (\frac{1}{2}\left(\rho_L^{-1} - \rho_R^{-1}\right), 0)$ is a constant vector directly related with the rate of entropy production in the system, while non-monotone profiles appear for $\frac{1}{2\rho_R}\sqrt{1-\left(\frac{\rho_R}{\rho_L}\right)^2} \le |\boldsymbol{\lambda} + \boldsymbol{\varepsilon}| \le \frac{1}{2}\left(\frac{1}{\rho_L} + \frac{1}{\rho_R}\right)$.

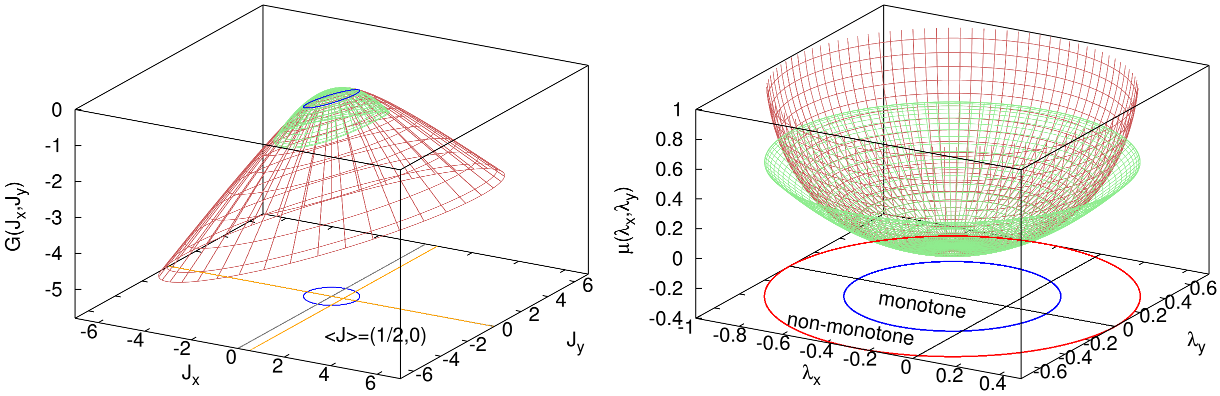

FIGURE 1. Left panel: $G(\mathbf{J})$ for the 2D-KMP model for $\rho_L = 2$ and $\rho_R = 1$. The blue circle signals the crossover from monotone ($J < J_c \equiv \pi/3$) to non-monotone ($J > \pi/3$) optimal profiles. The green surface corresponds to the Gaussian approximation for small current fluctuations. Right panel: Legendre transform of both $G(\mathbf{J})$ (brown) and $G(\mathbf{J} \to \langle \mathbf{J} \rangle)$ (green), together with the projection in $\boldsymbol{\lambda}$-space of the crossover between monotonous and non-monotonous regime.

Fig. 1 shows the predicted $G(\mathbf{J})$ (left panel) and its Legendre transform (right panel) for the 2D-KMP model. Notice that the LDF is zero for $\mathbf{J} = \langle \mathbf{J} \rangle = ((\rho_L - \rho_R)/2, 0)$ and negative elsewhere. For small current fluctuations, $\mathbf{J} \approx \langle \mathbf{J} \rangle$, $G(\mathbf{J})$ obeys the following quadratic form

$$G(\mathbf{J}) \approx -\frac{1}{2}\left(\frac{(J_x - (\rho_L - \rho_R)/2)^2}{\sigma_x^2} + \frac{J_y^2}{\sigma_y^2}\right), \tag{16}$$

with $\sigma_x^2 = (\rho_L^2 + \rho_L\rho_R + \rho_R^2)/3$ and $\sigma_y^2 = \rho_L\rho_R$, resulting in Gaussian statistics for currents near the average as expected from the central limit theorem. A similar expansion for the Legendre transform yields

$$\mu(\boldsymbol{\lambda}) \approx \frac{\lambda_x}{2}\left[(\rho_L - \rho_R) + \sigma_x^2 \lambda_x\right] + \frac{\sigma_y^2}{2}\lambda_y^2. \tag{17}$$

Notice that beyond this restricted Gaussian regime, current statistics is in general non-Gaussian. In particular, for large enough current deviations, $G(\mathbf{J})$ decays linearly, meaning that the probability of such fluctuations is *exponentially* small in J (rather than J^2). Fig. (2) shows the x-dependence of optimal density profiles for different values of J, including both the monotone and non-monotone regimes.

Despite the complex structure of $G(\mathbf{J})$ in both regime I and II above, it can be easily checked that for any pair of isometric current vectors $\mathbf{J}$ and $\mathbf{J}'$, such that $|\mathbf{J}| = |\mathbf{J}'|$, the current LDF obeys

$$G(\mathbf{J}) - G(\mathbf{J}') = \boldsymbol{\varepsilon} \cdot (\mathbf{J} - \mathbf{J}'), \tag{18}$$

where $\boldsymbol{\varepsilon} = (\frac{1}{2}\left(\rho_L^{-1} - \rho_R^{-1}\right), 0)$ is the constant vector defined above, linked to the rate of entropy production in the system. The above equation is known as Isometric Fluctuation

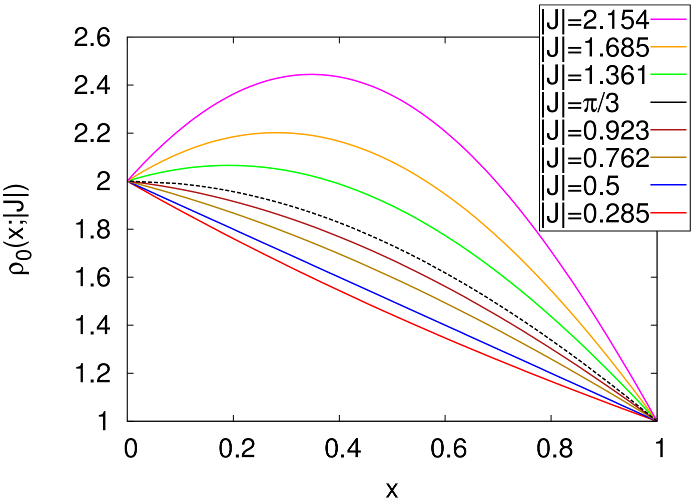

FIGURE 2. Optimal $\rho_J(x)$ for $\rho_L = 2$ and $\rho_R = 1$ and different J. The dash line ($J = J_c = \pi/3$) corresponds to the crossover between the monotone and non-monotone regimes.

Relation (IFR) [11], and is a general results for time-reversible systems described at the macroscopic level by a continuity equation similar to eq. (1), for which time-reversibility implies the invariance of optimal profiles under arbitrary rotations of the current vector. The IFR, which has been confirmed in extensive simulations [11], links in a strikingly simple manner the probability of any pair of isometric current fluctuations, and includes as a particular case the Gallavotti-Cohen Fluctuation Theorem in this context. However, the IFR adds a completely new perspective on the high level of symmetry imposed by time-reversibility on the statistics of nonequilibrium fluctuations.

CONCLUSIONS

We have derived explicit predictions for the statistics of current fluctuations in a simple but very general model of diffusive energy transport in two dimensions, the KMP model [6]. For that, we used the hydrodynamic fluctuation theory recently introduced by Bertini and coworkers [4], supplemented with a reasonable set of simplifying hypotheses, namely:

(i) The optimal profiles responsible of a given current fluctuation are time-independent.
(ii) The resulting divergence-free optimal current profile is in fact constant across space.
(iii) The ensuing optimal density profile has structure only along the gradient direction.

While assumption *(i)* is known to break down for extreme current fluctuations in some particular cases [4, 9, 10], it would be interesting to explore the range of validity of conjectures *(ii)-(iii)* in the time-independent regime. This could be achieved using a local stability analysis in the spirit of the results in [9]. Moreover, the emergence of time-dependent optimal profiles (probably traveling waves) in high-dimensional systems is an open and interesting problem which deserves further study.

Provided that hypotheses *(i)-(iii)* hold, we have obtained explicitly the current distribution for this model, which exhibits in general non-Gaussian tails. The optimal density profile which facilitates a given fluctuation can be either monotone for small current fluctuations, or non-monotone with a single maximum for large enough deviations. Furthermore, this optimal profile remains invariant under arbitrary rotations of the current vector, providing a detailed example of the recently introduced Isometric Fluctuation Relation [11].

ACKNOWLEDGMENTS

Financial support from Spanish MICINN project FIS2009-08451, University of Granada, and Junta de Andalucía is acknowledged.

REFERENCES

1. R.S. Ellis, *Entropy, Large Deviations and Statistical Mechanics*, Springer, New York, 1985.
2. H. Touchette, *Phys. Rep.* **478**, 1 (2009).
3. B. Derrida, *J. Stat. Mech.* P07023 (2007); T. Bodineau, and B. Derrida, *C. R. Physique* **8**, 540 (2007).
4. L. Bertini, A. De Sole, D. Gabrielli, G. Jona-Lasinio, and C. Landim, *Phys. Rev. Lett.* **87**, 040601 (2001); *Phys. Rev. Lett.* **94**, 030601 (2005); *J. Stat. Mech.* P07014 (2007); *J. Stat. Phys.* **135**, 857 (2009).
5. T. Bodineau, and B. Derrida, *Phys. Rev. Lett.* **92**, 180601 (2004).
6. C. Kipnis, C. Marchioro, and E. Presutti, *J. Stat. Phys.* **27**, 65 (1982).
7. P. I. Hurtado, and P. L. Garrido, *Phys. Rev. Lett.* **102**, 250601 (2009); *Phys. Rev. E* **81**, 041102 (2010).
8. P. I. Hurtado, and P. L. Garrido, *J. Stat. Mech.* (2009) P02032.
9. T. Bodineau and B. Derrida, *Phys. Rev. E* **72**, 066110 (2005).
10. P. I. Hurtado, and P. L. Garrido, to appear.
11. P. I. Hurtado, C. Pérez-Espigares, J. J. del Pozo, and P. L. Garrido, arXiv:1009.1243
12. C. Pérez-Espigares, P. L. Garrido, and P. I. Hurtado, to appear.

Stochastic resonance between propagating extended attractors

M. G. dell'Erba*, G. G. Izús*, R. R. Deza* and H. S. Wio†

*IFIMAR (UNMdP and CONICET), Deán Funes 3350, B7602AYL Mar del Plata, Argentina.
†IFCA (UC and CSIC), Avda. de los Castros, s/n, E-39005 Santander, Spain.

Abstract. The nonequilibrium Ising–Bloch (NIB) bifurcation of the FitzHugh–Nagumo (FHN) model with nondiffusing inhibitor provides a beautiful instance of an extended bistable system with counterpropagating fronts or Bloch walls (BW) as stable attractors. Moreover, these fronts are chiral and parity-related, and the barrier between them is the unstable stationary front or Ising wall (IW). Here we show by means of numerical simulation the presence of stochastic resonance in the transition between 1D BW of opposite chiralities when an additive noise is included. A scaling law of the signal-to-noise ratio (SNR) with the distance to the critical point is numerically observed and theoretically characterized in terms of an effective nonequilibrium potential.

Keywords: Fluctuation phenomena in statistical physics, nonlinear dynamics
PACS: 05.40.-a,05.45.-a,

Stochastic resonance (SR) is a well-studied phenomenon in concentrated (0D) systems [1]. Regarding nonlinear *media*, much of the analytical work in SR has been done on transitions between stable *static* patterns in reaction–diffusion systems [2] exploiting the nonequilibrium analog of a free energy, the *nonequilibrium potential* (NEP) [3]. Our concern here is with SR in the transitions between counterpropagating stable *traveling fronts* [4, 5]. In particular we consider systems undergoing a NIB front bifurcation [6]—a pitchfork bifurcation where an IW exchanges stability with a pair of counterpropagating and opposite-chirality BW—an important pattern-forming mechanism. A well-studied instance (besides optical ones [7, 8]) is the FHN model with nondiffusing inhibitor [9, 10, 11]:

$$\frac{\partial u}{\partial t} = \nabla^2 u + [u + S(t)](1-u^2) - v + \xi(x,t), \qquad \frac{\partial v}{\partial t} = \varepsilon\,[u - a v],$$

where independent additive Gaussian white-noise sources $\xi(x,t)$ with strength γ and a *multiplicative* signal $S(t) = \delta \sin \omega t$ that adiabatically forces the uniform unstable fixed point have been included. BW are stable for $\varepsilon < \varepsilon_c = a^{-2}$ and propagate at velocities $c = \pm\sqrt{\frac{5}{2u_+^2}(\varepsilon_c - \varepsilon)}$, with $u_+ = \sqrt{1 - a^{-1}}$. Their leading-order form for $|c| \ll 1$ is $u(x,t) = u_0(x - ct)$, $v(x,t) = a^{-1}\,u_0(x - ct + ca)$, with $u_0(x) = -u_+ \tanh(u_+ x/\sqrt{2})$.

In an appropriate γ range under external forcing, coherent noise-assisted jumps are numerically observed between counterpropagating BW. The SNR averaged over 20 realizations presents the characteristic SR shape as a function of γ [Fig. 1(a)]. Moreover, the γ level needed to induce jumps decreases as $\varepsilon \to \varepsilon_c$. Figure 1(b) shows log(SNR) (averaged over 24 realizations) *vs* $(\varepsilon_c - \varepsilon)^2$ for fixed γ, indicating a scale law. After reducing to the central manifold, this effect can be described in terms of a canonical NEP

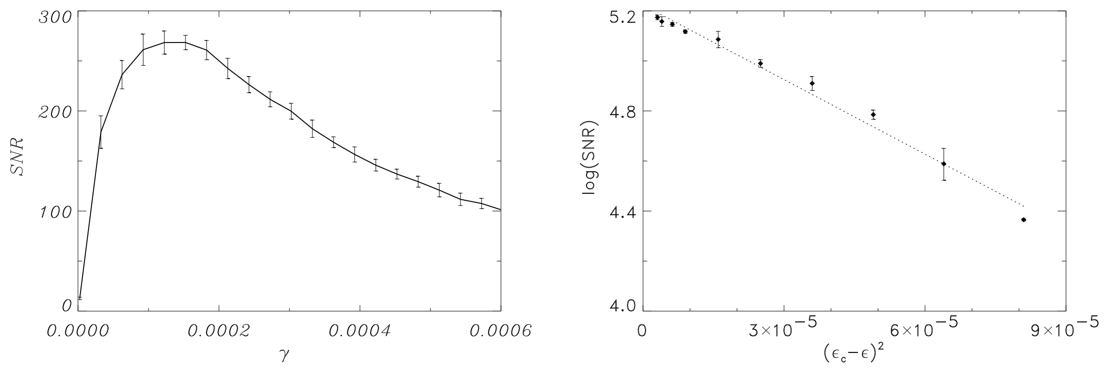

FIGURE 1. a) SNR *vs* γ, for $\varepsilon_c - \varepsilon = .01$ (average over 20 realizations); b) log(SNR) *vs* $(\varepsilon_c - \varepsilon)^2$ for $\gamma = 1.8 \times 10^{-4}$ (average over 24 realizations).

for the normal form $\frac{d\eta_{\mathrm{op}}}{dt} = (\varepsilon_c - \varepsilon)\,\eta_{\mathrm{op}} - \eta_{\mathrm{op}}^3$ of a pitchfork bifurcation. The transitions between attractors are then governed by the NEP $\Phi = -(\varepsilon - \varepsilon_c)\,\eta_{\mathrm{op}}^2 + \frac{\eta_{\mathrm{op}}^4}{4}$. The maximum of Φ ($\eta_{\mathrm{op}} = 0$) corresponds to an IW, and its symmetric minima to the BW. Hence the NEP difference between the saddle (IW) and the local attractors (BW) is proportional to $(\varepsilon_c - \varepsilon)^2$, which yields a linear dependence of log(SNR) with $(\varepsilon_c - \varepsilon)^2$, at least in a neighborhood of the NIB bifurcation [12].

In conclusion, we have presented numerical evidence of SR in the transition between traveling chiral fronts in the the symmetric FHN model with nondiffusing inhibitor, as a nontrivial example of SR between dynamic attractors in extended systems. In particular, we have extended early work on reaction–diffusion systems that exploited the NEP concept to analyze transitions between *static* patterns. The SNR was found to scale with the distance to the critical point, in agreement with an analysis in terms of the NEP for the pitchfork normal form.

Financial support from MEC (Project CGL 2007-64387/CLI) and AECID (Projects A/013666/07 and A/018685/08) of Spain, and CONICET and UNMdP of Argentina, is acknowledged.

REFERENCES

1. L. Gammaitoni, P. Hänggi, P. Jung, and F. Marchesoni, *Rev. Mod. Phys.* **70**, 223–287 (1998).
2. H. S. Wio, and R. R. Deza, *Eur. Phys. J.–Special Topics* **146**, 111–126 (2007).
3. R. Graham, and T. Tél, *Phys. Rev. A* **33**, 1322–1337 (1986).
4. H. S. Wio et al., *Eur. Phys. J. B* **69**, 71–80 (2009).
5. M. G. dell'Erba, G. G. Izús, R. R. Deza, and H. S. Wio, *Eur. Phys. J. D* in press.
6. P. Coullet, J. Lega, B. Houchmanzadeh, and J. Lajzerowicz, *Phys. Rev. Lett.* **65**, 1352–1355 (1990).
7. G. Izús, M. San Miguel, and M. Santagiustina, *Opt. Lett.* **25**, 1454–1456 (2000).
8. G. Izús, M. San Miguel, and M. Santagiustina, *Phys. Rev. E* **64**, 056231 (2001).
9. A. Hagberg, and E. Meron, *Nonlinearity* **7**, 805–835 (1994).
10. D. Pazó, R. R. Deza, and V. Pérez-Muñuzuri, *Phys. Lett. A* **340**, 132–138 (2005).
11. G. Izús, D. Pazó, R. R. Deza, and V. Pérez-Muñuzuri, *Phys. Rev. E* **72**, 045205(R) (2005).
12. H. S. Wio, S. Bouzat, and B. von Haeften, *Physica A* **306**, 140–156 (2002).

Heat and chaotic velocity in special relativity

A. L. García-Perciante

Depto. Matemáticas Aplicadas y Sistemas, Universidad Autónoma Metropolitana, México D. F.

Abstract. The nature of the heat flux in special relativistic kinetic theory is discussed to some detail emphasizing the need to explicitly include the chaotic velocity in order to correctly define dissipative fluxes while retaining both their physical meaning and the Lorentz covariance of the theory.

Keywords: Relativistic kinetic theory, heat flux
PACS: 05.70.Ln, 51.10.+y, 03.30.+p

Special relativity is based on two postulates: the relativity principle, which states that the physics laws are the same for all inertial observers, and the invariance of the speed of light in vacuum. These two requirements are satisfied when covariant formalisms are used such that physical quantities are given by tensors which undergo Lorentz transformations within a Minkowski space-time. On the other hand, kinetic theory is a formalism in which the macroscopic properties of a gas can be deduced from averages of the dynamics variables of molecules. The Boltzmann equation gives the time evolution of the single particle distribution function. When the temperature of the gas is high enough, the speed of the molecules can become close to the speed of light and thus, relativistic effects must be taken into account. In this scenario is where special relativistic kinetic theory is on call.

The relativistic Boltzmann equation has been established as well as the local equilibrium distribution function [1]. However, when referring to the non-equilibrium situation, many questions remain unanswered. Most formalisms express macroscopic quantities in terms of a decomposition with respect to the direction of the hydrodynamic velocity. The equations are thus written for an arbitrary observer. However, such formulation has two drawbacks. Firstly, the nature of the dissipative fluxes is lost since the concept of chaotic velocity is absent in the theory. Secondly, some fine points remain unclear for example the fact that the local equilibrium assumption, needed in order to specify an entropy production, is assumed to be satisfied within a parcel of the fluid. However, observers do not agree on distances and thus, the size of the region where local equilibrium is assumed to be valid is not an invariant. Also, different observers do not agree on simultaneity such that assumptions regarding time, for instance the distribution function not changing significantly over a mean collision time, turn out to be also ambiguous if one does not specify the state of motion of the observer measuring that time.

In special relativity all inertial frames are equivalent. However, for any given event in space-time, some quantities are defined as the ones measured by a comoving observer. In the case of relativistic kinetic theory, when we talk about a comoving frame, it is in an averaged sense. To understand this, consider an arbitrary observer O in a reference frame S which averages the velocity of molecules in a fluid element and concludes that the hydrodynamic four-velocity in that region is U^{ν}. With that information, the observer can set up a reference frame S' that moves with velocity U^{ν} with respect to himself such that an observer O' in that system measures zero average velocity. For observer O' the molecules are at rest in average *but each one moves with its chaotic velocity*. By repeating the procedure for every parcel in the fluid, one ends up with a collection of reference frames S', one for each volume where local equilibrium can be assumed. These reference frames are what we call local comoving frames. The transformation law for tensor quantities between S and each S' is given by a Lorentz transformation between two frames that move with a relative velocity given by U^{ν}. Since U^{ν}, as measured by an arbitrary observer is in general not constant, this transformation depends on space-time and thus can be thought of as a point dependent transformation. Notice that this concept is also used in the non-relativistic case without giving too much thought into it. The idea here proposed, which was originally formulated by Sandoval-Villalbazo and García-Colín [2], is completely analogous to the decomposition introduced in the non-relativistic case when one writes the molecular velocity as the vector sum of the chaotic and the hydrodynamic velocities. This amounts to setting local reference frames by Galilean transformations.

In Ref. [3] the ideas discussed above, are developed and the results analyzed. The different contributions to the stress-energy tensor $T^{\mu\nu}$ are clearly identified by separating the parts arising from the systematic and the chaotic components of the velocity, a procedure analog to the one preformed in the non-relativistic case. As a consequence, the heat flux is defined as the total energy flux measured in S'. As a part of $T^{\mu\nu}$, the energy flux associated with heat dissipation is given by the Lorentz transformation of the corresponding terms in $T^{\mu\nu}$ as calculated in S'

Thus, in this framework $T^{\mu\nu}$ is calculated in the local comoving frame where there is no ambiguity on how to measure distances and time intervals. Also, Boltzmann's equation is solved in S' to obtain constitutive equations [4]. Once all this information is gathered, the Lorentz transformation is used in order to express $T^{\mu\nu}$ in an arbitrary frame. It is important to point out that, as shown in Ref. [3], the constitutive equation for the heat flux obtained in this framework is consistent with the one obtained following the standard method [1]. However, the formalism here described is conceptually different. The introduction of chaotic velocities in relativistic kinetic theory leads to definitions for the dissipative fluxes that are direct generalizations of the non-relativistic ones. In this way the concept of heat arising from the chaotic motion of particles, as firstly introduced by Kroenig, Clausius and Maxwell [5], is also present in the relativistic formalism.

The author wishes to thank A. Sandoval-Villalbazo and L. S. García-Colín for their valuable comments.

REFERENCES

1. C. Cercignani, and G. Medeiros Kremer, *The Relativistic Boltzmann Equation: Theory and Applications*, Cambridge University Press 3rd Ed., Cambridge, 1991, and references therein.
2. A. Sandoval-Villalbazo, and L. S. García-Colín, *Physica A* **278**, 428 (2000).
3. A. L. García-Perciante, A. Sandoval-Villalbazo, and L. S. García-Colín; arxiv.1007.2815.
4. A. Méndez, A. L. García-Perciante, to appear in *Proceedings of the IV Mexican Meeting in Mathematical and Experimental Physics*, AIP Conf. Proc. 2010. See also arxiv.1009.6220.
5. S. Brush, *The Kind of the Motion we Call Heat*, North Holland Pub., Amsterdam, 1967.

Computing free energy differences using conditioned diffusions

Carsten Hartmann and Juan Latorre

Institut für Mathematik, Freie Universität Berlin, D-14195 Berlin, Germany

Abstract. We derive a Crooks-Jarzynski-type identity for computing free energy differences between metastable states that is based on nonequilibrium diffusion processes. Furthermore we outline a brief derivation of an infinite-dimensional stochastic partial differential equation that can be used to efficiently generate the ensemble of trajectories connecting the metastable states.

Keywords: Conditional free energy, fluctuation theorem, rare events, diffusion bridge
PACS: 02.50.Ga, 05.10.Gg, 05.70.Ln, 65.40.gh

INTRODUCTION

Given a system assuming states $x \in \mathscr{X} \subseteq \mathbb{R}^d$ with the energy $V(x)$, the free energy at temperature $\varepsilon > 0$ as a function of a scalar reaction coordinate $\Phi(x)$ is defined as

$$F(\xi) = -\varepsilon \ln \int_{\mathscr{X}} \exp(-\varepsilon^{-1} V(x)) \delta(\Phi(x) - \xi) dx . \tag{1}$$

Given that $x \in \mathscr{X}$ follows the Boltzmann distribution $\rho \propto \exp(-\varepsilon^{-1} V)$, the free energy is just the marginal distribution in $\Phi(x)$. However estimating the marginal numerically from samples of ρ may be prohibitively expensive, e.g., when V has large barriers in the direction of Φ. Therefore we dismiss this option and propose a different scheme that employs realizations of the overdamped Langevin equation

$$dX_\tau = f(X_\tau, \tau) d\tau + \sqrt{2\varepsilon} dW_\tau , \quad \tau \in [0, T] \tag{2}$$

subject to the boundary conditions (see Fig. 1)

$$\Phi(X_0) = \xi_A \quad \text{and} \quad \Phi(X_T) = \xi_B . \tag{3}$$

The vector field $f(x, \tau) = -\nabla V(x) + g(x, \tau)$ is assumed to be smooth with the time-dependent part g being such that the process hits the level set $\{\Phi(x) = \xi_B\}$ at time T; without loss of generality we set $T = 1$.

As we will demonstrate below, the free energy difference $\Delta F = F(\xi_B) - F(\xi_A)$ can be computed as the weighted average (cf. [1, 2, 3])

$$\Delta F = -\varepsilon \ln \mathbf{E} \left[\exp \left(-\varepsilon^{-1} \int_0^1 g(X_\tau, \tau) \circ dX_\tau \right) \right] \tag{4}$$

where "$\circ$" means integration in the sense of Stratonovich and $\mathbf{E}[\cdot]$ denotes the expectation over all (bridge) paths that solve the conditioned Langevin equation (2)–(3).

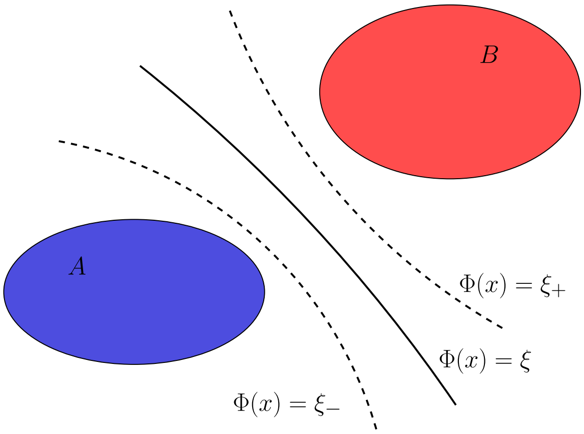

FIGURE 1. Boundaries of metastable states A and B as level sets of the reaction coordinate Φ.

DERIVATION: EULER'S METHOD

Our derivation of (4) is based on the discrete Euler-Maruyama approximation of (2),

$$X_{k+1} = X_k + \Delta\tau f(X_k, \tau_k) + \sqrt{2\varepsilon\Delta\tau}\,\eta_{k+1}\,, \quad k = 0, \dots, n-1\,. \tag{5}$$

Here $\Delta\tau = 1/n$ and $\eta_k \sim \mathcal{N}(0, I)$ are i.i.d. distributed Gaussian random variables.

We call $\mathbf{P}_n(x) = \text{Prob}\,[X_0 = x_0, X_1 = x_1, \dots, X_n = x_n]$ the joint distribution of the path $x = \{x_0, x_1, \dots, x_n\} \subset \mathscr{X}$. Assuming that the x_0 follow the Boltzmann distribution ρ conditional on $\Phi(x_0) = \xi_A$, the distribution of the paths is readily shown to be

$$\mathbf{P}_n(x) \propto \rho(x_0|\xi_A)\exp\left(-\frac{\Delta\tau}{4\varepsilon}\sum_{k=0}^{n-1}\left|\frac{x_{k+1}-x_k}{\Delta\tau} - f(x_k,\tau_k)\right|^2\right)\delta(\Phi(x_n) - \xi_B)\,.$$

We are interested in the likelihood ratio of forward and backward paths. To this end we introduce $\tilde{\mathbf{P}}_n(x) = \mathbf{P}_n(\tilde{x})$ as the distribution of the reversed paths $\tilde{x} = \{x_n, x_{n-1}, \dots, x_0\} \subset \mathscr{X}$ with $x_n \sim \rho(\cdot|\xi_B)$. By the smoothness of f, the forward measure $\mathbf{P}_n$ has a density with respect to $\tilde{\mathbf{P}}_n$ that is is given in terms of their Radon-Nikodym derivative,

$$\psi_n(x) = \exp\left(\varepsilon^{-1}(\Delta V + W_n(x))\right)\exp\left(-\varepsilon^{-1}\Delta F\right)\,. \tag{6}$$

Here $\Delta V = V(x_n) - V(x_0)$ and

$$W_n(x) = \frac{1}{2}\sum_{k=0}^{n-1}(x_{k+1} - x_k)\cdot(f(x_k,\tau_k) + f(x_{k+1},\tau_{k+1})) + \mathscr{O}(|\Delta\tau|)$$

is the Stratonovich approximation of the stochastic work integral, i.e.,

$$\lim_{n\to\infty} W_n(x) = -\Delta V + \int_0^1 g(X_\tau,\tau)\circ dX_\tau \quad (\Delta\tau \to 0,\, n\Delta\tau = 1)\,.$$

The free energy difference in (6) pops up as a boundary term, $\exp(-\varepsilon^{-1}\Delta F) = Z_B/Z_A$, with Z_A and Z_B normalizing the conditional distributions for forward and backward paths. Upon noting that both $\mathbf{P}_n$ and $\tilde{\mathbf{P}}_n$ are probability measures, (6) entails (4) as $n \to \infty$.

AN INFINITE-DIMENSIONAL LANGEVIN SAMPLER

Now comes our main result: To evaluate the expectation in (4) we have to generate the ensemble of bridge paths. For this purpose we introduce the auxiliary potential

$$\varphi = \Delta\tau^{-1} V(x_0) + \frac{1}{4}\sum_{k=0}^{n-1}\left|\frac{x_{k+1}-x_k}{\Delta\tau} + f(x_k,\tau_k)\right|^2 + \Delta\tau^{-1}\varepsilon\left(\ln|\nabla\Phi(x_0)| + \ln|\nabla\Phi(x_n)|\right),$$

so that $\exp(-\varepsilon^{-1}\Delta\tau\varphi)$ is the density of $\mathbf{P}_n$ with respect to the surface element on the image space $\Sigma = \{x \in \mathscr{X}^{n+1} \colon \Phi(x_0) = \xi_A,\, \Phi(x_n) = \xi_B\} \subset \mathscr{X}^{n+1}$ of admissible paths. Conversely, $\exp(-\varepsilon^{-1}\Delta\tau\varphi)$ is the stationary distribution of the Langevin equation [4]

$$dQ_s = -\left(\nabla\varphi(Q_s) + \nabla\sigma(Q_s)\lambda^T\right)ds + \sqrt{2\varepsilon\Delta\tau^{-1}}\,dW_s\,, \quad \sigma(Q_s) = 0 \tag{7}$$

where $Q_s = (q_0(s), \ldots, q_n(s))$ and $\lambda = (\lambda_1, \lambda_2)$ labels the Lagrange multipliers determined by the constraint $\sigma = 0$, the latter being shorthand for $\Phi(q_0) = \xi_A$ and $\Phi(q_n) = \xi_B$.

Using formal arguments (that can be made rigorous using Girsanov's theorem), we can take the limit $n \to \infty$ which turns the Langevin sampler (7) into a stochastic partial differential equation (SPDE) for bridge paths [5]. If we denote the continuous path by $\gamma = \gamma(\tau, s)$ with $\tau \in [0,1]$ now being the "spatial" variable, our SPDE reads

$$\begin{aligned}
\frac{\partial\gamma}{\partial s} = \frac{1}{2}\frac{\partial^2\gamma}{\partial\tau^2} - \frac{1}{2}\left(\nabla f f + \varepsilon\nabla(\nabla\cdot f)\right)(\gamma) + \sqrt{2\varepsilon}\,\frac{\partial W}{\partial s} \quad & \forall(\tau,s)\in[0,1]\times(0,\infty)\\
\Phi(\gamma) = \xi_A\,,\ \left(\frac{\partial\gamma}{\partial s}\right)^{\|} = \left(2\varepsilon Sn(\gamma) - f(\gamma)\right)^{\|} \quad & \forall(\tau,t)\in\{0\}\times(0,\infty)\\
\Phi(\gamma) = \xi_B\,,\ \left(\frac{\partial\gamma}{\partial s}\right)^{\|} = \left(f(\gamma) - 2\varepsilon Sn(\gamma)\right)^{\|} \quad & \forall(\tau,t)\in\{1\}\times(0,\infty)\\
\gamma = \gamma_0 \quad & \forall(\tau,s)\in[0,1]\times\{0\}
\end{aligned} \tag{8}$$

where $\partial W/\partial s$ is space-time white noise and we have introduced the various shorthands: $n = \nabla\Phi/|\nabla\Phi|$ for the unit normal to the level sets $\{\Phi(x) = \xi\}$, $f^{\|} = (I - n\otimes n)f$ for the vector field f tangent to the level sets, and $S = \nabla^2\Phi/|\nabla\Phi|$ for the shape operator (second fundamental form) of $\{\Phi(x) = \xi\}$ understood as a submanifold of $\mathscr{X}$.

Note that although γ lives in $\mathscr{X} \subseteq \mathbb{R}^d$, which may be high-dimensional, its two arguments are scalar variables (namely, arc length τ and time s). Methods for numerically solving SPDEs such as (8) are discussed in, e.g., [6].

REFERENCES

1. C. Jarzynski, *Phys. Rev. Lett.* **78**, 2690–2693 (1996).
2. G. Crooks, *J. Stat. Phys.* **90**, 1481–1487 (1998).
3. J.C. Latorre, C. Hartmann, and Ch. Schütte, *Procedia Computer Science* **1**, 1591–1600 (2010).
4. G. Ciccotti, T. Lelièvre, and E. Vanden-Eijnden, *Commun. Pure Appl. Math.* **61**, 371–408 (2008).
5. A. M. Stuart, J. Voss, and P. Wiberg, *Commun. Math. Sci.* **2**, 685–697 (2004).
6. A. Beskos, G. O. Roberts, A.M. Stuart, and J. Voss, *Stochastics and Dynamics* **8**, 319–350 (2008).

Dynamical behavior of heat conduction in solid Argon

Hideo Kaburaki*, Ju Li†, Sidney Yip** and Hajime Kimizuka‡

*Center for Computational Science and e-Systems, Japan Atomic Energy Agency, Tokai,Ibaraki,319-1195,Japan
†Department of Materials Science and Engineering, University of Pennsylvania, Philadelphia, Pennsylvania 19104,USA
**Department of Nuclear Science and Engineering, Department of Materials Science and Engineering, Massachusetts Institute of Technology, Cambridge,Massachusetts,02139,USA
‡Graduate School of Engineering Science, Osaka University, Toyonaka,Osaka,560-8531,Japan

Abstract. Equilibrium molecular dynamics is performed to obtain the thermal conductivity of crystalline argon using the Green-Kubo formalism, which permits the study of dynamical details of the transport process. A large system run to longer times is used to derive the heat flux autocorrelation functions from the low temperature solid to the liquid state. The power spectrum of an autocorrelation function reveals the change in the nature of the underlying atomic motions across the temperature range.

Keywords: heat conduction, molecular dynamics method, Geen-Kubo method, solid Argon
PACS: 02.70.Ns, 66.70.-f

The theory of thermal conduction in electronically insulating crystals is based on the phonon concept in which the individual (rapid) atomic motions are averaged out. Molecular dynamics method enables us to look into both fast and slow atomic motions, at the cost of computational efforts. Crystalline argon is a good benchmark target because the interatomic potential is well described by the Lennard-Jones potential and experimental data are available. The temperature dependence of thermal conductivity has been studied using the equilibrium molecular dynamics method with the Green-Kubo formalism and the results compared with experiment. We have previously performed a simulation [1] for a system of 864 particles with 10^7 time steps, and the resulting thermal conduc-

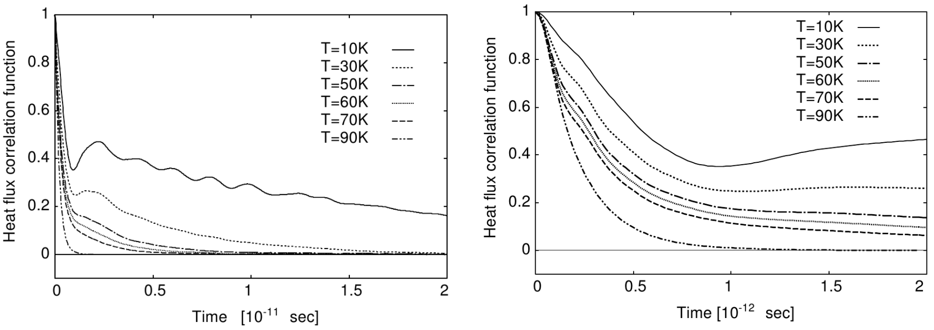

FIGURE 1. Heat flux autocorrelation function for the long (left) and short (right) time range

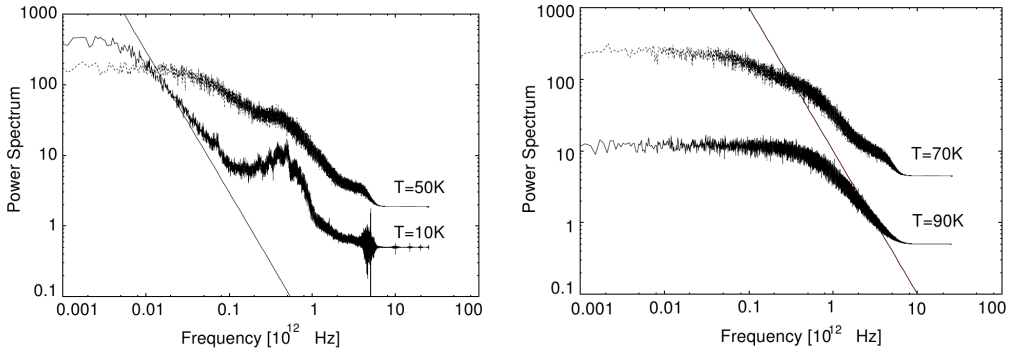

FIGURE 2. Power spectra at $10K, 50K$(left) and $70K, 90K$(right). The data of $50K$ and $70K$ are shifted upward for easy comparison. The linear line in the figure shows a guide to $(frequency)^{-2}$ relation.

tivity was found to be in good agreement with experiment. However, we did not obtain the power spectrum with adequate accuracy due to insufficient sampling. Here, a larger system of 4000 atoms with total time steps of 10^8 is employed to obtain a good power spectrum.

Figure 1 shows the results of the heat flux autocorrelation function at various temperatures. The form of the heat flux autocorrelation function for $N = 4000$ is almost the same with the previous $N = 864$ case, so the values of thermal conductivity are mostly the same. However, a slight reduction of the autocorrelation is observed in the lower temperatures with increasing the system size, suggesting that longer-wavelength phonons, now allowed to exist in the supercell, enhances scattering. A more quantitative analysis should be made on the N-dependence of thermal conductivity. We see clearly in Fig.1 (left) the two-stage relaxation process, except in the liquid case($90K$), where the first (fast) relaxation is ascribed to single-particle like motions and the second relaxation to collective atomic motions (phonons) [1, 2]. Single particle motions, which are observed in the diffusion of atoms in the liquid state, can be expected to become more prominent in the solid state during the continuous transition from high-temperature solid to the liquid. At the lower temperatures, the autocorrelation is oscillatory at the beginning of the second stage[2, 1], corresponding to the resonant peak in the power spectrum(Fig.2 (left)). Also, a slight shoulder, likely a damped shear mode in a solid, is observed in the first stage[1]. A wide range of power spectra has been obtained by taking Fourier-transform of the heat flux correlation functions (see Fig.2) which show from low frequency collective motions to high frequency atomic motions. Oscillatory modes are seen as characterized by the resonant peak at 0.5 THz and the step at 4 THz. These features appear to persist even below the melting point. Because the highest phonon frequency in Ar is 1.9 THz, the step at 4 THz appears to be due to frequency cutoff of second harmonic generation.

Both H.K. acknowledge support by the Grand-in-Aid for Scientific Research (C).

REFERENCES

1. H. Kaburaki, J. Li, S. Yip, and H. Kimizuka, *J. Appl. Phys.* **102**, 043514 (2007).
2. A. J. C. Ladd, B. Moran, and W. G. Hoover, *Phys. Rev. B* **34**, 5058–5064 (1986).

Fast transients in mesoscopic systems

A. Kalvová*, V. Špička* and B. Velický†

*Institute of Physics, Academy of Sciences of the Czech Republic, Na Slovance 2, 182 21 Praha 8, Czech Republic
†Center for Theoretical Study at Charles University and the ASCR, Jilská 1, 110 00 Praha 1, Czech Republic

Abstract. We study fast transient dynamics of an open quantum system at the initial stage of its equilibration starting far from equilibrium from correlated initial conditions reflecting entanglement with the environment. These correlations rapidly decay and the process enters the non-equilibrium quasi-particle mode controlled by a generalized master equation. As a model system, the nanoscopic molecular bridge between two leads is considered. The coupling to the leads is assumed to be intermittent. Properties of the resulting transients are demonstrated and analyzed.

Keywords: Molecular bridge, Initial conditions, Decay of correlations, Non-equilibrium Green's Functions
PACS: 05.30.-d,05.60.Gg,72.10.Bg,73.23.-b,73.63-b

1. MOLECULAR BRIDGE IN TRANSIENT REGIME

We study electronic transients in the well-known model of molecular bridge [1] :

LEFT LEAD	J_L	BRIDGE ISLAND	J_R	RIGHT LEAD

The central island is represented by a single molecular level, while the leads are metallic and serve as both particle and energy reservoirs. They are floating at their externally imposed potentials kept at a finite bias. The connectivity in the system is controlled by the two tunneling junctions J_L and J_R. In the paper [2], we have introduced a formalism for calculating the transient response of the electrons to sudden changes of the connectivity, modeled by switching on or off each of the two junctions independently. We use the technique of time-partitioning for non-equilibrium Green's functions (NGF)whose general framework is described in [3]. For a parallel development based on NGF and the time-dependent density functional, the most recent reference is [4].

Here, we present and discuss first results of calculation of these transients, using the model of independent electrons and looking at the time dependence of the occupancy of the central island. The initial transient reflects the details of the tunneling through the junctions and depends sensitively on the initial conditions at the time of the sudden change of the connectivity. These may be simple, dependent on the one-particle distribution only, called uncorrelated (UIC), or they may be "correlated" that is incorporate higher order initial correlations (CIC). The initial transient typically dies out within a decay time $\tau^\star \cong \max\{\tau_Q, \tau_c\}$ (Q ... quasi-particle formation, c ... decay of correlations). The generic quasi-particle (QP) stage ensues characterized by a relaxation time $\tau \gg \tau^\star$.

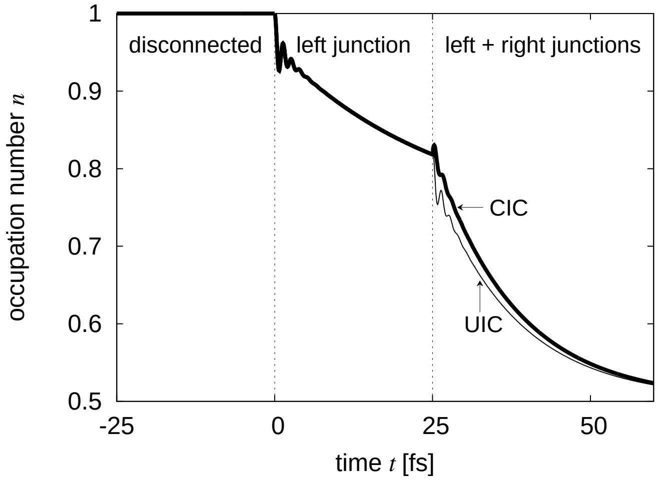

FIGURE 1. sland occupation number. For $-25 < t < 0$ (“disconnected”) J_L, J_R are off. For $0 < t < 25$ (“left junction”) J_L is on, J_R is off ... UIC transient. For $25 < t$ (“left+right junction”) both J_L, J_R are on ... CIC transient. An artificial UIC transient is show for comparison, see curve labels.

2. FORMAL TREATMENT AND RESULTS

The central island occupancy for $t > t_{\mathrm{I}}$, where the initial time t_{I} coincides with the switching time of a junction, has the following NGF form:

$$n(t) = G^R(t,t_{\mathrm{I}})n(t_{\mathrm{I}})G^A(t_{\mathrm{I}},t) - \mathrm{i}\int_{t_{\mathrm{I}}}^{t}\mathrm{d}v\int_{t_{\mathrm{I}}}^{t}\mathrm{d}u\; G^R(t,v)(\Sigma^<(v,u) + \{\text{CIC terms}\})G^A(u,t) \tag{1}$$

It has the first, coherent transient, term and the integral "transport term", persisting in time. The time range of the $\Sigma^<$ self-energy is τ_c. These two terms together reflect the UIC. The additional CIC terms have kernels acting within a $\sim\tau_c$ vicinity of t_{I}. They express the initial correlations in terms of their gradual build-up during the bridge history prior to t_{I}. Propagators $G^{R,A}$ have a QP formation period $\sim\tau_Q$ followed by the standard QP regime.

The results in Fig.1 are for a semirealistic model with leads of heavily doped semiconductor at nitrogen temperature. The island starts as disconnected, with the level occupancy $n = 1$. First, at $t_{\mathrm{I}} = 0\,\mathrm{fs}$, J_L is switched on. We see the UIC controlled transient given mostly by the QP formation. A saturation tending to $n \sim 0.78$ follows. This is interrupted by connecting also J_R at $t_{\mathrm{I}} = 25\,\mathrm{fs}$. The transient starts now from a correlated initial state. To show the effect of CIC, we also plot the transient with correlations neglected, largely repeating the J_L behavior before. Again, the gradual saturation, now to $n = 0.51$ follows. The initial correlations decay quickly, but their cumulative effect is propagated by $G^{R,A}$ with the damping time equal to the QP relaxation time.

ACKNOWLEDGMENTS

This research was partially supported by the Grant Agency of the Czech Republic within the grant project 202/08/0361. The research was carried out by A.K. within the Institutional Research Plan AV0Z10100520, by V.S. within the AVOZ10100521, both financed by the Academy of Sciences of the Czech Republic and by B.V. within MSM0021620845 financed by the Ministry of Education.

REFERENCES

1. A. P. Jauho, N. S. Wingreen, and Y. Meir, *Phys. Rev. B* **50**, 5528 – 5544 (1994).
2. B. Velický, A. Kalvová, and V. Špička, *Physica E* **42**, 539 – 549 (2010).
3. B. Velický, A. Kalvová, and V. Špička, *Phys. Rev. B* **81**, 235116(1) – 235116(12) (2010).
4. P. Myöhänen, A. Stan, G. Stefanucci, and R. van Leeuwen, *Phys.Rev. B* **80**, 115107(2009).

Dynamical aspect of group chase and escape

Shigenori Matsumoto*, Tomoaki Nogawa*, Atsushi Kamimura†, Nobuyasu Ito* and Toru Ohira**

*Department of Applied Physics, School of Engineering, The University of Tokyo, 7-3-1 Hongo, Bunkyo, Tokyo 113-8656, JAPAN
†Institute of Industrial Science, The University of Tokyo, 4-6-1 Komaba, Meguro-ku, Tokyo 153-8505, JAPAN
**Sony Computer Science Laboratories, Inc., 3-14-13, Higashi-gotanda, Shinagawa-ku, Tokyo 141-0022, JAPAN

Abstract. Recently, a new concept is proposed for chasing and evading in crowds, called "group chase and escape" through a simple model. In this model, two kinds of players, chasers and escapees, play tag on a two-dimensional square lattice. Each chaser approaches its nearest escapee. On the other hand, each escapee steps away from its nearest chaser. Although there are no communications within each group, players appear to cooperate among themselves to chase or escape. We found relation between this cooperative behavior and group formations depend on the density of chasers and targets.

Keywords: Chase and Escape, Pursuit and Evasion, Diffusion, Computer simulations
PACS: 05.10.-a

Recently, group chase and escape is proposed [1] as an extended concept of "Chase and Escape" or "Pursuit and Evasion", which is a traditional mathematical problem [2, 3]. This new problem indicates that chasers or targets (escapees) segregate spontaneously without attractive interactions in order to prey or survive more efficiently. However, it has not been clarified how this group formation affects the efficiency of chase or escape behavior under various conditions. In this article, we characterize it by lifetime of target and estimate the effect of the group formation.

The model is the same as the one in Ref. [1]. The field is a two-dimensional square lattice $L_x \times L_y$ with periodic boundary conditions. Initially, chasers and targets are randomly distributed over the lattice. Each player hops to one of the nearest neighboring sites at each step. The next site is chosen to approach or distance oneself from the nearest opponent. Here, if there are multiple nearest chasers (targets), the target (chasers) chooses one of them randomly. On the square lattice, there are two types of hopping situations. When a chaser and its nearest target are aligned, the chaser moves in one direction toward the opponent, but the target randomly chooses one of three neighboring sites to increase the distance. In the other case, both chasers and targets decide one of two possible nearest sites with an equal probability in order to get closer to, or get away from their opponents. When a target resides in the nearest neighboring sites of a chaser, the chaser catches the target by hopping to the site, and then the target is removed from the system. After the catch, the chaser pursues remaining targets in the same manner. We run the simulations until all targets are caught by chasers.

It was pointed out, by observing the time $\mathscr{T}$ for catching all targets, that there are two qualitatively different regimes of chasing process [1]. However, the group behavior

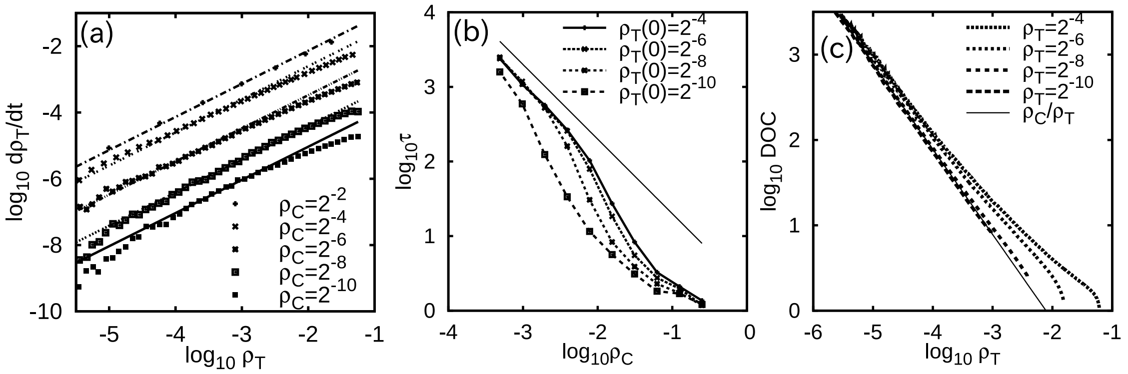

FIGURE 1. (a) Three types of decay regimes for several ρ_C with $\rho_T(0) = 2^{-4}$. (b) The lifetime of target τ vs. the density of chaser ρ_C and (c) the degree of convergence vs. that of target $\rho_T(t)$ for $\rho_C = 2^{-7}$ with the different $\rho_T(0)$. Solid line is guide to the eye for ρ_C^{-1} in (b). The lattice size is set to $L_x = L_y = 2^{11}$.

was not identified in detail since the parameter $\mathscr{T}$ includes dependence on an initial configuration and a finite-size effect. To characterize the players' behavior, we analyze a lifetime of targets estimated from time evolution of the density of targets, $\rho_T(t)$.

Figure 1(a) plots the decay rate of ρ_T, $d\rho_T(t)/dt$, with respect to ρ_T, which shows three types of decay regimes. The first stage is the initial relaxation, in which some targets have short lifetimes because they happen to be near chasers initially. In the final stage, a group of chasers locks on to one final target for a long time, leading to the eventual catch. In the middle of these stages, ρ_T shows exponential decay. Thus, the lifetime of target $\tau(\rho_C, \rho_T(0))$ is estimated from $d\rho_T(t)/dt = -\rho_T(t)/\tau(\rho_C, \rho_T(0))$, where $\tau(\rho_C, \rho_T(0))$ depends on the density of chaser, ρ_C, and $\rho_T(0)$. Figure 1(b) shows a plot of τ against ρ_C for different $\rho_T(0)$.

Around $\rho_C = 1$, $\tau \sim 1$. In the region $\rho_C < \rho_T$, τ decreases proportionally to ρ_C^{-1}. In the middle region, however, τ decreases more rapidly as ρ_C increases. Therefore, in this region increasing the number of chasers enhances effectiveness of catching.

While τ increases with the initial density of target, the group formation influences these increments. To parametrize the group formation effect, we calculate the degree of convergence (DOC) in Fig. 1(c) defined as number of chasers divided by that of chased targets. If the targets are randomly distributed, this value is close to ρ_C/ρ_T,

as in the case of $\rho_T(0) = 2^{-10}$. The DOC increases, however, with $\rho_T(0)$ at the same ρ_T, indicating existence of targets which are not chased due to group formation. Here, while chasers catch some targets in the initial stage, others escape and form groups away from chasers.

This work was partly supported by Award No. KUK-I1-005-04 made by King Abdullah University of Science and Technology (KAUST).

REFERENCES

1. A. Kamimura, and T. Ohira, *New J. Phys.* **12**, 053013 (2010).
2. R. Isaacs, *Differential games*, John Wiley & Sons, New York, 1965.
3. P. J. Nahin, *Chases and Escapes: The Mathematics of Pursuit and Evasion*, Princeton University Press, Princeton, 2007.

Onset of thermal rectification in graded mass systems: Analysis of the classic and quantum self-consistent harmonic chain of oscillators

Emmanuel Pereira*, Humberto C. F. Lemos† and Ricardo R. Ávila*

**Departamento de Física–ICEx, UFMG, CP 702, 30.161-970 Belo Horizonte MG, Brazil*
†Campus Alto Paraopeba, UFSJ, 36420-000, Ouro Branco, MG, Brazil

Abstract. To investigate the onset of thermal rectification in graded mass systems, we study the classic and quantum self-consistent harmonic chain of oscillators. We show that rectification is absent in the classic, but present in the quantum chain. We note the ingredient of rectification, and its existence in this simple model indicates that rectification may be an ubiquitous phenomenon.

Keywords: heat flow; classic and quantum microscopic models; thermal rectification
PACS: 05.70.Ln; 05.40.-a; 44.10.+i

The derivation of the macroscopic laws of thermodynamic transport from the underlying microscopic Hamiltonian models is still a challenge: in particular, our knowledge about the mechanism of heat flow is quite incomplete. Anyway, by performing numerical simulations or analytical investigations in simplified models, interesting properties have been discovered and their use proposed: e.g., the possibility to control the heat flow by using devices such as thermal diodes, transistors, gates, memories, etc. The main object here, the thermal diode or rectifier, is a device in which heat flows preferably in one direction. Recently, Chang et al. [1] built a diode in a experimental work by using graded materials, i.e., nanotubes inhomogeneously mass-loaded with heavy molecules.

In these notes, we address the onset of thermal rectification in these experimental reliable class of diodes: the graded mass materials. Our crystal model is given by a chain of oscillators with harmonic interparticle and on-site potentials, and with a reservoir connected to each site, but with the "self-consistent condition", that means absence of heat flow between each inner reservoir and its site in the steady state.

We examine the classic and quantum versions of this graded chain of oscillators, and note that thermal rectification is absent in the classic, but present in the quantum chain.

Our microscopic classical model is a chain of N oscillators with the Hamiltonian

$$H(q,p) = \frac{1}{2}\sum \frac{p_j^2}{m_j} + \frac{1}{2}\sum q_j^2 + \frac{1}{2}\sum q_l J_{lj} q_j, \tag{1}$$

where we assume graded masses: $m_1 > \ldots m_j > \ldots m_N$; J_{ij} is the interparticle (nearest neighbor) interaction. The dynamics is given by the differential equations

$$dq_j = (p_j/m_j)dt, \;\; dp_j = -(\partial H/\partial q_j)dt - \zeta_j p_j dt + \gamma_j^{1/2} dB_j, \tag{2}$$

where $\eta_j = dB_j/dt$ are white noises; ζ_j is the dissipative constant; $\gamma_j = 2m_j\zeta_j T_j$; T_j is the temperature of $j-th$ bath, chosen to lead to the self-consistent condition.

To study the heat flow, we write the energy H_j of the site j, where $H = \sum_j H_j$. Then, we study $\langle dH_j(t)/dt \rangle$ and identify the heat flow coming from the inner reservoir (that we vanish in the steady state) and the heat current in the chain.

Let us list the main results for the heat current in the classic model. For the simpler case of a homogeneous chain, i.e. $m_1 = \ldots = m_N$, an exact solution for the heat flow is well known [2]: Fourier's law holds, and, an important physical feature, the thermal conductivity depends on the particle mass, but not on temperature. For the graded mass chain ($m_1 > \ldots > m_N$), the computation of the conductivity is very difficult, but the absence of thermal rectification is shown[3].

Now we turn to the quantum self-consistent harmonic model. We use a Ford-Kac-Mazur approach, as presented in ref.[4], to describe the quantum system and its evolution to the steady state. Here, all the baths are modeled as mechanical harmonic systems, with initial coordinates and momenta determined by some statistical distribution. Then, we solve the quantum dynamics given by Heisenberg equations, take the stochastic distribution for the initial coordinates of the baths, as well as the limit $t \to \infty$, and obtain the expression for the heat flow in the steady state.

The expression obtained for the heat flow from the l-th reservoir to the chain is

$$\mathscr{F}_l = \sum_{m=1}^{N} \zeta^2 \int_{-\infty}^{+\infty} \mathrm{d}\omega\, \omega^2 \left| \left[G_W^+(\omega) \right]_{l,m} \right|^2 \frac{\hbar\omega}{\pi} \left[f(\omega, T_l) - f(\omega, T_m) \right], \tag{3}$$

with $G_W^+(\omega) = \left[-\omega^2 M_W + \Phi_W - i\zeta\omega \right]^{-1}$, where M_W is the matrix for the particle masses, Φ_W gives the interparticle interaction, and $f(\omega, T_l) = [\exp(\hbar\omega/k_B T_l) - 1]^{-1}$ is the phonon distribution for the l-th bath (details in ref.[4]).

We list the main results for the heat flow in the quantum self-consistent chain. For the simpler homogeneous chain, it is shown [4] that the Fourier's law holds, and, the main physical feature, now the thermal conductivity depends on the particle masses and also on their temperatures. For the graded mass chain, it is shown the absence of rectification in the linear response regime [5] (small gradient of temperature). But, beyond linear approximation, we note the existence of rectification [6] (for few particles: a proof for a system with any number of particles is in preparation [7]).

The ingredient behind rectification is the combination of particle masses and temperatures in the thermal conductivity for the quantum model (the classic conductivity does not involve temperature). As we invert the chain, the temperature profile and the mass distributions change in a different way. This difference gives the rectification.

Work supported by CNPq and Fapemig (Brazil).

REFERENCES

1. C. W. Chang et al., *Science* **314**, 1121 (2006).
2. F. Bonetto, J. L. Lebowitz, and J. Lukkarinen, *J. Stat. Phys.* **134**, 1097 (2004).
3. E. Pereira, and H .C. F. Lemos, *Phys. Rev. E* **78**, 031108 (2008); D. Segal, ibid. **79**, 012103 (2009).
4. A. Dhar, and D. Roy, *J. Stat. Phys.* **125**, 801 (2006).
5. E. Pereira, and H. C. F. Lemos, *J. Phys. A* **42**, 225006 (2009).
6. E. Pereira, *Phys. Lett. A* **374**, 1933 (2010).
7. E. Pereira, H. C. F. Lemos, and R. R. Ávila, to appear.

Covariant Lyapunov vectors and local exponents

Harald A. Posch and Hadrien Bosetti

Faculty of Physics, University of Vienna, Boltzmanngasse 5, A-1090 Wien, Austria

Abstract. Using a doubly-thermostated heat-conducting oscillator as an example, we demonstrate how time-reversal invariance affects the perturbation vectors in tangent space and the associated local Lyapunov exponents. We also find that the local covariant exponents vary discontinuously along directions transverse to the phase flow.

Keywords: Lyapunov exponents, tangent-space perturbations, time-reversal invariance
PACS: 05.45.–a, 05.10.–a, 02.70.–c

For classical chaotic systems, the set of Lyapunov exponents, $\{\lambda_\ell\}, \ell = 1, \ldots, D$, measures the exponential growth, or decay, of small (infinitesimal) perturbations of the phase-space trajectory. Here, D is the dimension of the phase space. The standard algorithms for the computation of the exponents (see Ref. [1] for a review) probe the tangent-space dynamics by a set of orthonormal Gram-Schmidt (GS) vectors $\{\mathbf{g}_\ell\}$. Since their orthonormality is not preserved, it must be periodically restored by a GS procedure, or continuously kept up by Lagrange-multiplier constraints. These schemes are all based on the volume changes of d-dimensional volume elements in phase space, $d \leq D$, but they simultaneously destroy any information concerning the angles between the perturbation vectors. Thus, symmetries concerning phase-space volumes generate symmetries of the associated local GS Lyapunov exponents[1], whereas time-reversal symmetry does not. For example, for a phase-space conserving *symplectic system* the equalities ${}^{(+)}\Lambda_\ell^{\mathrm{GS}}(t) = -{}^{(+)}\Lambda_{D+1-\ell}^{\mathrm{GS}}(t)$ and ${}^{(-)}\Lambda_\ell^{\mathrm{GS}}(t) = -{}^{(-)}\Lambda_{D+1-\ell}^{\mathrm{GS}}(t)$ hold, if the trajectory is followed forward or backward in time as indicated by the upper indices ${}^{(+)}$ and ${}^{(-)}$, respectively. However, time reversal invariance of the motion equations is not reflected by the GS local exponents: ${}^{(-)}\Lambda_\ell^{\mathrm{GS}}(t) \neq -{}^{(+)}\Lambda_{D+1-\ell}^{\mathrm{GS}}(t)$.

The multiplicative ergodic theorem of Oseledec [2, 3] asserts that there exists another spanning set of normalized vectors $\mathbf{v}^\ell(\Gamma(0))$ in tangent space. These vectors evolve (co-rotate) with the natural tangent flow, $\mathbf{v}^\ell(\Gamma(t)) = D\phi^t|_{\Gamma(0)}\, \mathbf{v}^\ell(\Gamma(0))$, (where $D\phi^t|_{\Gamma(0)}$ is the propagator), and directly generate the Lyapunov exponents, $\pm\lambda_\ell = \lim_{t\to\pm\infty}(1/|t|)\ln\left\| D\phi^t|_{\Gamma(0)}\, \mathbf{v}^\ell(\Gamma(0))\right\|$, $\ell \in \{1, \cdots, D\}$, along the way. They are referred to as covariant vectors. Generally, they are not pairwise orthogonal and span invariant manifolds, for which the local expansion (contraction) rates are given by the local covariant Lyapunov exponents ${}^{(\pm)}\Lambda_\ell^{\mathrm{cov}}$. In contrast to the GS exponents, they respect

---

[1] Local Lyapunov exponents give the local (time-dependent) exponential rate of growth (shrinkage) of the norm for GS or covariant vectors at a phase point $\Gamma(t)$ along the trajectory. The global exponents are time averages of the local exponents.

the time-reversal invariance of the motion equations, such that

$$^{(-)}\Lambda_{\ell}^{\text{cov}}(\Gamma(t)) = -^{(+)}\Lambda_{D+1-\ell}^{\text{cov}}(\Gamma(t))\ ; \quad \ell = 1,\cdots,D. \tag{1}$$

Local expansion forward in time implies local contraction backward in time and *vice versa*. However, they do not reflect (possible) phase-volume conservation.

Recently, reasonably efficient algorithms for the computation of covariant vectors have become available [4, 5], which were applied to a variety of systems [1, 6, 7]. In the panel on the left of the figure we demonstrate the time-reversal symmetry displayed by the local covariant exponents for a one-dimensional harmonic oscillator coupled to a position-dependent temperature $T(q) = 1 + \varepsilon \tanh(q)$ with a two-stage Nosé-Hoover thermostat, which makes use of two thermostat variables [1]. The equations of motion are time reversible and not symplectic, and $D = 4$. The control parameter ε denotes the temperature gradient at the oscillator position $q = 0$. As the figure shows, the time-reversal symmetry of Eq. (1) is clearly obeyed for the maximum ($\ell = 1$) and minimum ($\ell = 4$) covariant exponents. Since, by construction, $^{(+)}\Lambda_1^{\text{GS}} \equiv ^{(+)}\Lambda_1^{\text{cov}}$ [1], one observes that no analogous relation holds for the GS exponents.

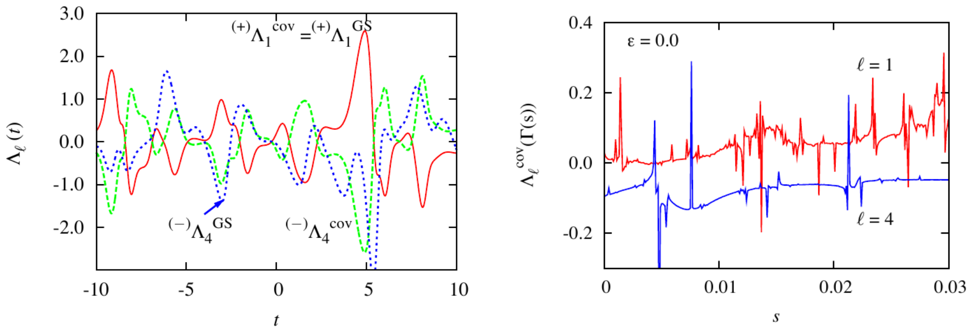

FIGURE 1. Panel on the left: Time-dependent local Lyapunov exponents $\Lambda(t)$ (as identified by the labels) for the doubly-thermostated oscillator in a nonequilibrium stationary state ($\varepsilon = 0.25$). Panel on the right: Fractal behavior of the local covariant exponents $^{(+)}\Lambda_i^{\text{cov}}$ for $\ell \in \{1,4\}$ along a parametric straight line transverse to the phase flow. The parameter s specifies the location $\Gamma(s)$ in phase space. The data are for the doubly-thermostated oscillator in thermal equilibrium ($\varepsilon = 0$).

In the panel on the right of the figure it is demonstrated that the local covariant exponents show a fractal-like structure along a straight line transverse to the phase-space flow [1]. This is to be expected in view of the different past (and future) histories for trajectories passing through adjacent phase-space points transverse to the flow.

REFERENCES

1. H. Bosetti, H. A. Posch, C. Dellago, and Wm. G. Hoover, *Phys. Rev. E*, in press (2010).
2. V. I. Oseledec, *Trudy Moskow. Mat. Obshch.* **19**, 179 (1968) [Trans. Mosc. Math. Soc. **19**, 197 (1968)].
3. D. Ruelle, *Publications Mathématiques de l'IHÉS* **50**, 27 (1979).
4. F. Ginelli, P. Poggi, A. Turchi, H. Chaté, R. Livi, and A. Politi, *Phys. Rev. Lett.* **99**, 130601 (2007).
5. C. L. Wolfe, and R. M. Samelson, *Tellus* **59**A, 355 (2007).
6. H. Bosetti, and H. A. Posch, *Chem. Phys.* **375**, 296 (2010).
7. M. Romero-Bastida, D. Pazó, J. M. López, and M. A. Rodríguez, *Phys. Rev. E* **82**, 036205 (2010).

Statics and dynamics of a harmonic oscillator coupled to a one-dimensional Ising system

A. Prados*, L. L. Bonilla† and A. Carpio**

*Física Teórica, Univ. de Sevilla, Apartado de Correos 1065, 41080 Sevilla, Spain
†G. Millán Institute for Fluid Dynamics, Nanoscience and Industrial Mathematics, Univ. Carlos III de Madrid, 28911 Leganés, Spain
**Departamento de Matemática Aplicada, Univ. Complutense de Madrid, 28040 Madrid, Spain

Abstract. We investigate an oscillator linearly coupled with a one-dimensional Ising system. The coupling gives rise to drastic changes both in the oscillator statics and dynamics. Firstly, there appears a second order phase transition, with the oscillator stable rest position as its order parameter. Secondly, for fast spins, the oscillator dynamics is described by an effective equation with a nonlinear friction term that drives the oscillator towards the stable equilibrium state.

Keywords: phase transitions, harmonic oscillator, Glauber dynamics, nonlinear friction
PACS: 64.60.Cn,02.50.Ey,05.45.Xt

We analyze the behaviour of a classical harmonic oscillator (mass m, frequency ω_0, position x and momentum p) linearly coupled to a one dimensional Ising system (N spin variables $\sigma_i = \pm 1$) in contact with a heat bath at temperature T. After a suitable nondimensionalization of the variables, the system energy per spin site is [1]

$$\mathscr{H}(x,p,\boldsymbol{\sigma}) = \frac{p^2+x^2}{2} - \frac{x}{N}\sum_{i=1}^{N} \sigma_i \sigma_{i+1}\,, \tag{1}$$

The oscillator dynamics follows from Hamilton's equations, $\ddot{x}+x = (1/N)\sum_{i=1}^{N}\sigma_i\sigma_{i+1}$, while the spins dynamics is governed by a master equation with Glauber single-flip transition rates [2]. Then, the rate at which the i-th spin flips in configuration $\boldsymbol{\sigma}$ is $W_i(\boldsymbol{\sigma}|x,p) = \delta\left[1-\gamma\sigma_i(\sigma_{i-1}+\sigma_{i+1})/2\right]/2$, with $\gamma = \tanh(2x/\theta)$. In these rates, δ gives the (dimensionless) characteristic attempt rate for the spin flips and θ is the dimensionless temperature [1]. The equilibrium properties of the system are obtained from the canonical distribution $\mathscr{P}_{eq}(x,p,\boldsymbol{\sigma}) \propto \exp\left[-N\mathscr{H}(x,p,\boldsymbol{\sigma})/\theta\right]$. By summing over the spin variables, we calculate the marginal probability for the oscillator variables,

$$\mathscr{P}_{eq}(x,p) \propto \exp\left[-N\left(\frac{p^2}{2}+\mathscr{V}_{eff}(x)\right)/\theta\right], \quad \mathscr{V}_{eff}(x) = \frac{x^2}{2} - \theta\left[\ln\cosh\left(\frac{x}{\theta}\right)+\ln 2\right] \tag{2}$$

in which the spins produce a non-harmonic additional contribution to the effective potential of the oscillator, $\mathscr{V}_{eff}(x)$. The equilibrium stable rest points $\widetilde{x}_{eq}$ of the oscillator are the minima of $\mathscr{V}_{eff}$, so that they verify the bifurcation equation $\widetilde{x}_{eq} - \tanh(\widetilde{x}_{eq}/\theta) = 0$. Thus, there is a second order phase transition at $\theta = 1$, with $\widetilde{x}_{eq}$ as its order parameter.

In the limit of fast spins, a perturbative analysis in powers of $\delta^{-1} \ll 1$ yields an approximate nonlinear equation for the macroscopic (completely neglecting the fluctua-

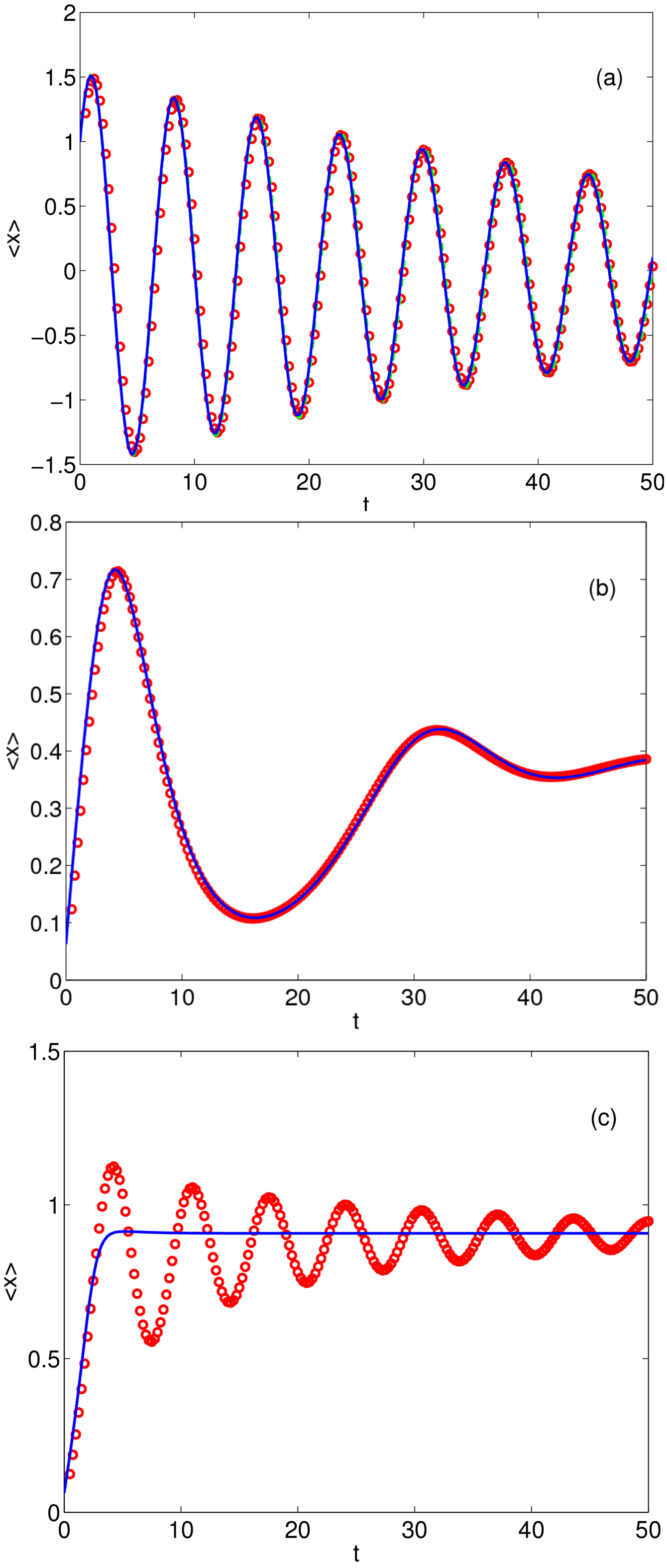

FIGURE 1. Averaged stochastic trajectories $\langle x(t)\rangle = \widetilde{x}(t)$ (circles) versus nonlinear (solid blue line) predictions for (a) $\theta = 4$, (b) $\theta = 0.95$, and (c) $\theta = 0.6$.

tions) value of the oscillator position $\widetilde{x}$

$$\frac{d^2\widetilde{x}}{dt^2} = -\mathscr{V}'_{eff}(\widetilde{x}) - \delta^{-1}\frac{1}{2\theta}R(\widetilde{x})\frac{d\widetilde{x}}{dt}, \qquad R(\widetilde{x}) = \frac{1+\tanh^2(\frac{\widetilde{x}}{\theta})}{1-\tanh^2(\frac{\widetilde{x}}{\theta})}. \tag{3}$$

The spins are so fast that they relax, almost instantaneously, to the equilibrium state corresponding to $\widetilde{x}(t)$. But, since $\widetilde{x}(t)$ is slowly varying, there is a small separation from equilibrium proportional to $d\widetilde{x}/dt$, which gives rise to the friction term.

In the figure, the theoretical result (3) (its numerical integration) is compared to the simulation of the stochastic model, for a random initial configuration of the spins and suitable initial conditions for the oscillator [1]. For high temperatures, case (a), and for a temperature below (but close to) the critical value $\theta = 1$, case (b), the agreement between simulation and theory is excellent. On the other hand, for a further lower value of the temperature, case (c), the theory breaks down. This was to be expected, since for very low temperatures the spins relaxation time diverge and they are actually slow as compared with the oscillator. Hence, another approach is needed, in which the fast vibrations of the oscillator are averaged using the method of multiple scales [3].

ACKNOWLEDGMENTS

This research has been supported by the Spanish Ministerio de Ciencia e Innovación (MICINN) through Grants No. FIS2008-01339 (AP), FIS2008-04921-C02-01 (LLB), and FIS2008-04921-C02-02 (AC). We would like also to thank the Spanish National Network Physics of Out-of-Equilibrium Systems (MICINN Grant FIS2008-04403-E).

REFERENCES

1. A. Prados, L. L. Bonilla, and A. Carpio, *J. Stat. Mech* P06016 (2010).
2. R. J. Glauber, *J. Math. Phys.* **4**, 294 (1963).
3. L. L. Bonilla, A. Prados, and A. Carpio, *J. Stat. Mech* P09019 (2010).

Strong ratchet effects for heterogeneous granular particles in the Brownian limit

Pascal Viot, Alexis Burdeau and Julian Talbot

Laboratoire de Physique Théorique de la Matière Condensée
Université Pierre et Marie Curie, Paris, CNRS UMR 7600, France.

Abstract. We investigate the dynamics of a heterogeneous granular chiral rotor immersed in a bath of thermalized particles. We use a mechanical approach, which is consistent with the Boltzmann-Lorentz equation, to obtain the efficiency of the motor in the Brownian limit.

Keywords: Granular motor, Boltzmann-Lorentz equation
PACS: 05.20.Dd,45.70.-n

Brownian ratchets, which are devices that extract work from a thermal bath, have a long history. A ratchet effect is possible whenever there is a breakdown of detailed balance and a lack of spatial symmetry[1]. The time reversal symmetry is obviously broken in collisions of inelastic particles and, as a result, several models have been proposed for granular ratchets[2, 3, 4]. Here we examine a granular chiral rotor composed of two materials with different coefficients of restitution[5]: See Fig. 1a. When the rotor collides with a bath particle of mass m and velocity v, the post-collisional velocities are given by:

$$\begin{pmatrix} \Omega' \\ v' \end{pmatrix} = \begin{pmatrix} \Omega \\ v \end{pmatrix} + \frac{1+\alpha}{I+mx^2}(v-\Omega x)\begin{pmatrix} mx \\ -I \end{pmatrix} \tag{1}$$

where Ω is the angular velocity, I is the moment of inertia and $-L/2 \leq x \leq L/2$ is the algebraic distance of impact from the center. The granular temperature of the rotor is given by $T_g = I < (\Omega - <\Omega>)^2 >$. Given a bath characterized by a velocity distribution $\phi(v)$ (which is assumed to be invariant) the problem is to determine the angular velocity distribution of the rotor, $F(\Omega)$. An approximate theoretical approach was proposed by Costantini et al.[4] for the case of an asymmetric piston and, subsequently, we proposed a force-based approach that gives the exact drift velocity in the Brownian limit [5], Here we illustrate the approach for the chiral rotor.

For a given angular velocity, the net torque acting on the rotor is given by

$$\Gamma(\Omega) = 2m\rho \int_0^{L/2} dx \int_0^{\infty} dy \frac{xy^2}{1+\frac{mx^2}{I}}((1+\alpha_+)\phi(x\Omega+y) - (1+\alpha_-)\phi(x\Omega-y)) \tag{2}$$

where ρ is the bath particle density. We obtain the mean angular velocity, Ω^*, in the Brownian limit, $mL^2/I \to 0$, by setting the torque equal to zero: $\Gamma(\Omega^*) = 0$. A major interest of heterogeneous granular particles is that they have a non-zero mean velocity in the Brownian limit, contrary to homogeneous asymmetric granular particles where the mean velocity vanishes as $m/M \to 0$. To confirm this strong ratchet effect, we now consider the mechanical work that can be extracted from this motor by coupling it to a work source. By imposing a constant external torque Γ_{ext} a mechanical power $\Gamma_{ext} < \Omega >$ is obtained. Collisions between bath particles and chiral rotor are dissipative. One then defines the efficiency of the heterogeneous rotor as the ratio of the power to the dissipation rate. In the Brownian limit, we obtain the following exact expression

$$\frac{\eta}{2\Omega} = \frac{\int_0^{L/2} dx \int_0^{\infty} dy\, x y^2 ((1+\alpha_+)\phi(x\Omega+y) - (1+\alpha_-)\phi(x\Omega-y))}{\int_0^{L/2} dx \int_0^{\infty} dy\, y^3 ((1-\alpha_+^2)\phi(x\Omega+y) + (1-\alpha_-^2)\phi(x\Omega-y))} \qquad (3)$$

Figure 1b shows the efficiency versus external torque for different values of M/m for a Gaussian bath distribution. The maximum efficiency is 4.32% and occurs for $\Omega \approx \Omega^*/2$. Conversely, the efficiency vanishes when $\Omega = \Omega^*$ and $\Omega = 0$. In the later case, Eq.1 provides an upper bound of external torque, $\Gamma_{ext}^{max} = \rho L^2(\alpha_- - \alpha_+)T/8$ for an arbitrary bath distribution characterized by a temperature T.

If the solid friction about the axis is smaller than Γ_{ext}^{max}, the chiral rotor should be a good candidate for experimental realization. Indeed, a recent study demonstrated a motor effect using a similar device [6].

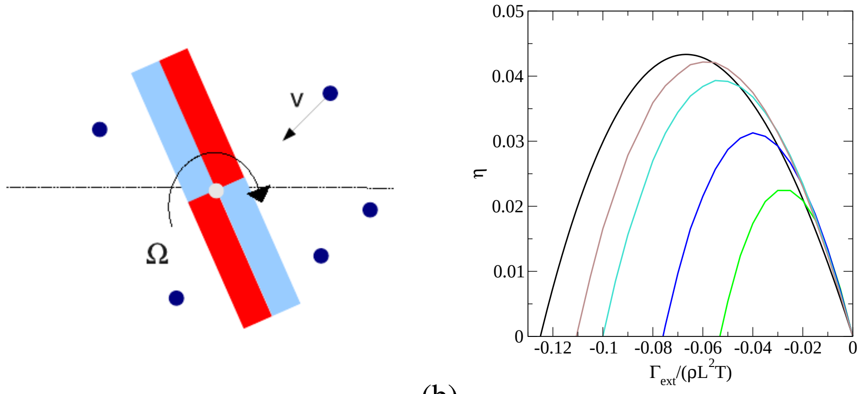

(a) (b)

FIGURE 1. (a) The chiral rotor, made with two different materials is immersed in a bath of thermalized particles. The red and blue materials have coefficients of restitution α_+ and α_-, respectively. (b) efficiency η versus external torque $\Gamma_{ext}/(\rho L^2 T)$ for $M/m = 1, 2, 5, 10$ and $\alpha_+ - \alpha_- = 1$. The upper curve corresponds to the Brownian Limit, Eq.3.

REFERENCES

1. P. Reimann, *Phys. Rep.* **361**, 57–265 (2002).
2. G. Costantini, U. M. B. Marconi, and A. Puglisi, *Phys. Rev. E* **75**, 061124 (2007).
3. B. Cleuren, and R. Eichhorn, *J. Stat. Mech.* p. P10011 (2008).
4. G. Costantini, U. Marini Bettolo Marconi, and A. Puglisi, *Europhys. Lett.* **82**, 50008 (2008).
5. J. Talbot, A. Burdeau, and P. Viot, *Phys. Rev. E* **82**, 011135 (2010).
6. P. Eshuis, K. van der Weele, D. Lohse, and D. van der Meer, *Phys. Rev. Lett.* **104**, 248001 (2010).

Stochastic protein production and time-dependent current fluctuations

Mieke Gorissen and Carlo Vanderzande

Faculty of Sciences, Hasselt University, 3590 Diepenbeek, Belgium

Abstract. Translation is the cellular process in which ribosomes make proteins from information encoded on messenger RNA. We model this process using driven lattice gases and take into account the finite lifetime of mRNA. The stochastic properties of the translation process can then be determined from the time-dependent current fluctuations of the lattice gas model. We illustrate our ideas with a totally asymmetric exclusion process with extended objects.

Keywords: Stochastic protein production, current fluctuations, driven lattice gases
PACS: 05.70.Ln, 87.10.Mn, 87.18.Tt

The production of proteins from genes occurs in two steps. In the first one, called *transcription*, information encoded on the genes is used to synthesize messenger RNA (mRNA). In the second step of *translation*, a ribosome uses the information stored on the codons of mRNA to make a new protein.

Cellular processes are noisy because of the small number of molecules involved and because they occur in a crowded environment [1]. In this contribution, we study the stochastic aspects of the translation process. In the standard model (Fig.1, left-side), proteins are produced with rate k while the mRNA decays with a rate λ. The number of proteins produced by one mRNA then follows a geometric distribution with average k/λ [2]. This approach does not take into account that at a particular moment several ribosomes are attached to a single mRNA which can lead to delays due to jamming and is an extra source of stochasticity [3]. A simple model that describes these effects [4] is the totally asymmetric exclusion process (TASEP) with extended objects [4, 5]. In the TASEP, mRNA is modelled as a one-dimensional lattice of N sites, each site corresponding with one codon. Ribosomes are large in comparison with a codon and are therefore represented as an extended 'particle' that covers l lattice sites. Following [5], we will take $l = 12$. Each site can be occupied by at most one ribosome. The dynamics of the TASEP is that of a Markov process: a ribosome can move forward one codon with rate 1, translation is initiated with rate α and terminates with rate β. The total number of proteins produced up to time t therefore equals the time integral $J(t)$ of the particle current $j(t)$ through the last site: $J(t) = \int_0^t j(t')dt'$. To take into account the finite lifetime of mRNA, we add an extra empty state $\emptyset$ to the configuration space of the process. This absorbing state can be reached from any other state with rate λ describing the decay of mRNA and the end of the translation process. Our model is summarized on the right side of Fig. 1.

We are interested in the probability $P(Q)$ that Q proteins are produced by one mRNA. This quantity can easily be obtained from simulations of our model. It is however also possible to gain some further insight in this distribution from a link with known

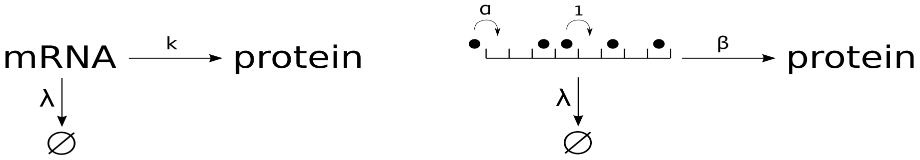

FIGURE 1. Standard model (left) and our model (right) for translation.

properties of current fluctuations.

Using a simple argument starting from the master equation, one can derive a relation between the generating function of Q, $Z(s) = \langle e^{sQ} \rangle$ and that of $J(t)$, $W(s,t) = \langle e^{sJ(t)} \rangle$, where $\langle \cdot \rangle$ is the average over the realizations of the process. This relation reads

$$Z(s) = \lambda \int_0^\infty W(s,t) e^{-\lambda t} dt \tag{1}$$

Using (1), we can relate the moments of Q to those of the current distribution.

We recently showed that the cumulants of the time dependent current in the TASEP have an interesting scaling form [6]. From that, one can then derive scaling forms for the N-dependence of the cumulants of Q. We find for example

$$\langle Q \rangle = J^\star/\lambda + \sqrt{N} H(\lambda N^{3/2}) \tag{2}$$

where H is a scaling function and $J^\star$ is the steady-state current of the TASEP in the thermodynamic limit. In a mean-field approximation, it was found that $J^\star = 1/(1+\sqrt{l})^2$ in the maximal current phase of the TASEP [5]. The first term in (2) equals the one found in the standard model if we identify $J^\star = k$. The second term in (2) determines deviations from the standard theory which are due to the finite size of mRNA and which can become important for small proteins. Similar expressions can be obtained for the variance of Q.

Our results indicate that mRNA-length may be an important quantity, which so far has been overlooked, in problems of stochastic gene expression.

REFERENCES

1. N. Maheshri, and E. K. O'Shea, *Annu. Rev. Biophys. Biomol. Struct.* **36**, 413-434 (2007).
2. O. Berg, *J. Theor. Biol.* **71**, 587-603 (1978).
3. M. Dobrzyński, and F. Bruggeman, *Proc. Natl. Acad. Sci. U.S.A.* **106**, 2583-2588 (2009).
4. C. MacDonald, J. Gibbs, and A. Pipkin, *Biopolymers* **6**, 1-25 (1968).
5. L. B. Shaw, R. K. P. Zia, and K. H. Lee, *Phys. Rev. E* **6**8, 021910 (1-17) (2003).
6. M. Gorissen, and C. Vanderzande, preprint, `arXiv:1010.5139`

Creating the conditions of anomalous self-diffusion in a liquid with molecular dynamics

J. Ryckebusch, S. Standaert, and L. De Cruz

Department of Physics and Astronomy, Ghent University, Belgium

Abstract. We propose a computational method to simulate non-Gaussian self-diffusion in a simple liquid. The method is based on nonequilibrium molecular dynamics (NEMD).

Keywords: Nonequilibrium molecular dynamics, anomalous diffusion
PACS: 05.70.Ln, 05.10.-a

INTRODUCTION

A simple liquid is the prime example of a system of interacting units that possesses Gaussian self-diffusion properties. This implies that the mean square displacements are proportional with time $\Delta r^2(t) \sim t$. This is for example reflected in the Gaussian character of the single time step (defined by Δt) displacement distributions $P_{\Delta t}\left(\frac{\Delta x}{\sigma(t)}\right)$ with $\Delta x_i = x_i(t+\Delta t) - x_i(t), i = 1, \ldots, N$. The distribution $P_{\Delta t}\left(\frac{\Delta x}{\sigma(t)}\right)$ is one of the quantities that can be determined in a molecular-dynamics (MD) simulation of a system of N molecules. Under equilibrium conditions, the width σ of the distribution can be connected to the diffusion coefficient and depends on the temperature, on the intermolecular interaction, and on the density. We propose a simulation technique to create conditions of anomalous self-diffusion in a simple liquid. More in particular, we are seeking to simulate systems with a (non-Gaussian) fat-tailed $P_{\Delta t}\left(\frac{\Delta x}{\sigma(t)}\right)$. This implies that the Δx's are no longer confined to a certain scale (determined by the quantity σ) and that every so often molecules perform steps Δx that are much larger than average.

COMPUTATIONAL METHOD AND RESULTS

Events of "all" sizes are encountered in systems which display self-organized criticality (SOC) and reside in a steady-state nonequilibrium state [1]. To summarize the major ideas of SOC: the system gets very slowly driven, which allows it to relax according to the rules of its internal dynamics. During the relaxation stage one typically observes events of all sizes.

We have translated the above-mentioned SOC ideas to a liquid as it is simulated in MD. We drive the simulation system by injecting potential energy at various locations in the simulation system at intermittent times. Clearly, this creates a temporal nonequilibrium situation with a highly non-uniform potential energy density. Subsequently, we let the system evolve according to Newton's energy-conserving laws. The dissipation of the locally injected potential energy under conditions of constant total energy which characterizes the dynamics of the system, results in a small amount of very fast molecules. The anomalous feature of the self-diffusion properties of the system is reflected in non-Gaussian single time step displacement distributions $P_{\Delta t}\left(\frac{\Delta x}{\sigma(t)}\right)$ during the nonequilibrium time periods of the simulation. One can discriminate between the equilibrium and nonequilibrium time periods of the simulation system by monitoring the average kinetic energy $< T >$. During nonequilibrium time periods, the $< T >$ is an increasing function of time.

In comparison to the equilibrium situation, we observe that under nonequilibrium conditions, small Δx's become more abundant, medium Δx's less probable, and that really large Δx's can be observed. In other words, the distribution $P_{\Delta t}\left(\frac{\Delta x}{\sigma(t)}\right)$ has fat tails, which is equivalent to saying that displacements Δx of all sizes occur or that the self-diffusion properties are anomalous.

In the simulation we use an interaction potential $U_{SC}(r_{12})$ with a soft-core repulsion at short inter-particles distances r_{12} and an attractive part at medium r_{12}. Hard-core potentials are observed to drive the simulation system out of control under nonequilibrium conditions. The driving, or injection of potential energy, is achieved by subjecting the system to changes in the system's length scale at intermittent times. The rescaling modifies the intermolecular interaction according to $U_{SC}(r) \longrightarrow U_{SC}(\lambda(t)r)\,(\lambda(t) < 1)$. The λ gets modified in a stepwise fashion: $\lambda(t) = \lambda_0^{\lfloor(\frac{t}{\tau})\rfloor}$, where $\lfloor(\frac{t}{\tau})\rfloor$ rounds $\left(\frac{t}{\tau}\right)$ towards positive integer values. The parameter τ determines the time interval between two subsequent rescalings of λ. From the above it becomes clear that for a given temperature, density and interaction, the nonequilibrium features of the simulation are controlled by (λ_0, τ). The parameter τ is expressed in units of simulation steps. In line with typical SOC conditions [1], it is required that the driving is done in a sufficiently slow fashion. For a broad range of the two parameters λ_0 and τ, we observe that our NEMD simulation technique generates conditions of anomalous self-diffusion. This proves the robustness of the proposed simulation method and hints at the fact that the anomalous self-diffusion is an emergent feature of the nonequilibrium simulation system. The "anomalous" character of $P_{\Delta t}\left(\frac{\Delta x}{\sigma(t)}\right)$ can be quantified by means of a non-vanishing fourth moment (or, kurtosis) of the distribution.

Summarizing, we have created a rather simple and robust simulation method to achieve conditions of anomalous self-diffusion in an interacting system. This emergence of global behaviour that cannot be determined from local properties is also a property of SOC, to which our simulation system bears similarities.

REFERENCES

1. Kim Christensen and Nicholas R. Moloney, *Complexity and Criticality*, Imperial College Press, London, 2005.
2. S. Standaert, J. Ryckebusch, L. De Cruz, *J. Stat. Mech.* P04004 (2010).

Cluster size distribution in Gaussian glasses

S.V. Novikov

A.N. Frumkin Institute of Physical Chemistry and Electrochemistry, Leninsky prosp. 31,
Moscow 119991, Russia

Abstract. A simple method for the estimation of the asymptotics of the cluster numbers in Gaussian glasses is described. Validity of the method was tested by the comparison with the exact analytic result for the non-correlated field and simulation data for the distribution of random energies in strongly spatially correlated dipolar glass model.

Keywords: organic glasses, correlations, clusters
PACS: 02.50.-r, 05.10.-a, 05.40.-a

A common feature of any random medium is the formation of clusters. In this report we consider the cluster distribution on size n_s (here s is the number of sites in a cluster) for a random Gaussian field. In many cases the random Gaussian field is a good model for the description of physical properties of amorphous materials. Assuming a zero average, the only relevant characteristic of the Gaussian field is the binary correlation function $C(\vec{r})$. In some cases spatial correlations are extremely strong; for example, for the distribution of random energies $U(\vec{r})$ in polar organic materials (dipolar glasses) $C(\vec{r}) \approx A\sigma^2 a/r$ for $r \gg a$ (here $A \approx 0.76$ for a simple cubic lattice, a is a lattice scale, and $\sigma^2 = \langle U^2 \rangle$) [1]. In terms of random energy $U(\vec{r})$ a cluster is defined as a set of connected sites, where all of them have site energy greater than some boundary energy U_0. Correlated nature of the dipolar glass directly dictates the main features of charge carrier transport and injection in polar organic materials [1].

Cluster distribution on size is one of the simplest yet basic characteristics of the random media. Typically, it is very difficult to calculate, and the reason is obvious: a difficulty to take into account a vast variety of possible shapes of clusters. At the moment, our knowledge of n_s is mostly limited to the case of non-correlated Gaussian field in the vicinity of the percolation threshold [2].

There is another parameter which is much more easy to calculate, namely the distribution $P_V(U_0)$ of the spatial average $U_0 = \frac{1}{V}\int_V d\vec{r}U(\vec{r})$ of the random energy $U(\vec{r})$ in a finite domain having volume V [3]. For the Gaussian field an exact result is

$$P_V(U_0) = \frac{V}{\sqrt{2\pi K}}\exp\left(-\frac{U_0^2 V^2}{2K}\right), \quad K = \int_V d\vec{r}d\vec{r}_1 C(\vec{r}-\vec{r}_1). \tag{1}$$

Naturally, parameter K depends on the shape of the domain, apart from the case of non-correlated field. We may expect that Eq. (1) gives a reasonable estimation for the number n_s of the true clusters, i.e. domains, where $U(\vec{r}) > U_0$ everywhere (assuming $V = a^3 s$), at least for the leading term of the asymptotic dependence of n_s on s. This hypothesis seems to be plausible at least for the case of very correlated fields (for example, the dipolar glass), where the deep clusters should have a compact structure. For the same reason we performed all calculations for spherical (most compact) domains.

The hypothesis was tested for the random energies in the dipolar glass and non-correlated Gaussian field. Surprisingly enough, it was true even in the latter case, where there is no reason for the compact structure of the cluster. The asymptotics for the non-correlated field according to (1) is

$$\ln n_s = -\frac{U_0^2}{2\sigma^2} s + o(s), \tag{2}$$

and agrees with the well-known exact result [4]. For the 3D dipolar glass (1) gives

$$\ln n_s = -B\frac{U_0^2}{\sigma^2} s^{1/3} + o(s^{1/3}), \quad B = \frac{5}{4A(36\pi)^{1/3}} \approx 0.34, \tag{3}$$

and agrees well with the result of the computer simulation [3]. It is worth to emphasize that not only the functional form of the dependence of n_s on s is well captured by the extremely simple calculation, but the numeric coefficients in (2) and (3) are valid, too (at least, the discrepancy between the calculated value of B in (3) and corresponding coefficient for the simulation data is no worse than 10% [3]).

Results (2) and (3) can be immediately generalized to any power-law correlation function $C(\vec{r}) \propto 1/r^n$ in d-dimensional space. Indeed, the direct estimation of the integral in (1) gives $K \propto V$ for $n > d$, while $K \propto V^{2-n/d}$ for $n < d$. This means that for $s \gg 1$

$$\ln n_s \propto -\frac{U_0^2}{\sigma^2} s^{n/d}, \quad n < d, \tag{4}$$

$$\ln n_s \propto -\frac{U_0^2}{\sigma^2} s, \quad n > d. \tag{5}$$

Interesting example of a spatially non-uniform disorder is the distribution of random energies in the dipolar glass near the electrode [5, 6]. How to use the suggested method to estimate n_s for the spatially non-uniform disorder is an open question and promising direction of future development. The major problem here is a difficulty to choose a proper shape of the domain (clusters near the electrode do not have a spherical symmetry and are elongated in the direction, perpendicular to the electrode).

ACKNOWLEDGMENTS

This study has been supported by the ISTC grant 3718 and RFBR grant 08-03-00125-a.

REFERENCES

1. S. V. Novikov, *J. Polymer Sci. B* **41**, 2584–2593 (2003).
2. D. Stauffer, and A. Aharony, *Introduction to Percolation Theory*, Taylor and Francis, London, 1992.
3. S. V. Novikov, and M. Van der Awerauer, *Phys. Rev. E* **79**, 041139 (2009).
4. G. Parisi, and N. Sourlas, *Phys. Rev. Lett.* **46**, 871–872 (1981).
5. S. V. Novikov, and G. G. Malliaras, *Phys. Rev. B* **73**, 033308 (2006).
6. S .V. Novikov, *Annalen der Physik* **18**, 949–954 (2009).

A non-equilibrium potential function to study competition in neural systems

Jorge F. Mejías

Department of Physics and Centre for Neural Dynamics,
University of Ottawa, K1N 6N5 Ottawa, Ontario, Canada

Abstract. In this work, I overview some novel results concerning the theoretical calculation of a non-equilibrium potential function for a biologically motivated model of a neural network. Such model displays competition between different populations of excitatory and inhibitory neurons, which is known to originate synchronous dynamics, fast activity oscillations, and other nontrivial behavior in more sophisticated models of neural media.

Keywords: Nonequilibrium potential, neural dynamics, stochastic resonance
PACS: 87.19.lj; 87.19.lc; 05.70.ln

INTRODUCTION AND MODEL

The development of a complete framework to characterize the behavior of non-equilibrium systems constitutes, up to date, one of the main challenges in Physics, with strong implications for other disciplines such as Chemistry, Biology, or Economics. One of the most remarkable attempts to build such a framework is the so called *non-equilibrium potential* (NEP), developed some decades ago [1, 2]. In the particular field of Theoretical Neuroscience, this framework has been proven to be of much interest for simple neuron models (see, for instance, [3, 4]). However, the calculation of a NEP for more realistic neural systems, such as large populations of neurons interconnected in a recurrent manner, is hardly achievable with this method in a straightforward manner.

In this work I briefly present an alternative approach to this problem. By assuming a highly simplified model of a neural population (which captures, however, some interesting features of more sophisticated models), I compute an approximated expression of the NEP for a network of interconnected excitatory and inhibitory neurons. The resulting NEP can be used to explore some characteristics of the model which may prevail for actual neural networks.

Lets assume that the dynamics of the electrical activity of a neural network is described by the following equations,

$$\dot{\nu}_e(t) = -\nu_e(t) + h\, S[J_{ee}\nu_e(t) + J_{ei}\nu_i(t) + \mu] + \sigma_{11}\xi_1(t) + \sigma_{12}\xi_2(t), \qquad (1)$$

$$\dot{\nu}_i(t) = -\nu_i(t) + h\, S[J_{ie}\nu_e(t) + J_{ii}\nu_i(t)] + \sigma_{21}\xi_1(t) + \sigma_{22}\xi_2(t), \qquad (2)$$

where ν_e, ν_i are the activity level of the excitatory and inhibitory neural populations, respectively. The parameter μ represents a constant external input, $S[x] = \frac{1}{2}(1 + x - x^3/3)$ is the transduction function which gives the effect of input currents on the activity level of each population, h is a constant factor, and J_{mn} is the mean strength of the synaptic connections which go from neurons of population n to the ones of population m. A certain level of stochasticity and correlation is introduced by random Gaussian noise sources ξ_k of variance η, with σ_{kl} being noise amplitudes.

RESULTS

Following [1, 3], we define the NEP as $\Phi(\nu_e,\nu_i) \equiv -\lim_{\eta\to 0}\eta \log P_{stat}(\nu_e,\nu_i)$, with $P_{stat}(x,y)$ being the stationary probability density distribution. Here, we will restrict to the case $J_{ei}=0$ for simplicity (details of the calculation and more general situations will be considered elsewhere). Using standard procedures (see [3, 5, 6]) one arrives at

$$\Phi(\nu_e,\nu_i) = \frac{\nu_e^2}{\lambda_1}\left(1-\frac{hJ_{ee}}{2}+\frac{\lambda hJ_{ie}}{\lambda_2}\right)+\frac{\nu_i^2}{\lambda_2}\left(1-\frac{hJ_{ii}}{2}\right)+\frac{h\nu_e}{\lambda_1}\left(\frac{2\lambda}{\lambda_2}-\mu-1\right)-\frac{h\nu_i}{\lambda_2}(1+J_{ie}\nu_e)$$
$$+\frac{h}{12\lambda_2 J_{ii}}(J_{ie}\nu_e+J_{ii}\nu_i)^4+\frac{h}{12\lambda_1 J_{ee}}(J_{ee}\nu_e+\mu)^4-\frac{h\lambda}{6\lambda_1\lambda_2 J_{ie}}(J_{ie}^4\nu_e^4+J_{ii}^4\nu_i^4) \tag{3}$$

where $\lambda_1 \equiv \sigma_{11}^2+\sigma_{12}^2$, $\lambda_2 \equiv \sigma_{21}^2+\sigma_{22}^2$ and $\lambda \equiv \sigma_{11}\sigma_{21}+\sigma_{12}\sigma_{22}$. The above equation constitutes the NEP for our neural population, and it properly describes the dynamics of equations (1, 2) as long as the integrability conditions $J_{ii}=2/(1-h)$ and $J_{ie}=2\lambda/(h-1)$, which emerge in the calculations, are satisfied by the particular values of the model parameters.

The strategy presented in this work also suggests to consider other realistic biophysical mechanisms (such as dynamic synapses [7, 8, 9]) and extract the NEP of the corresponding model. An extension of the present study will be published elsewhere.

ACKNOWLEDGMENTS

This work was supported by NSERC Canada. I would like to thank Joaquín J. Torres, Horacio Wio, Roberto Deza, and Raúl Toral for their advice, and for useful comments and discussions.

REFERENCES

1. R. Graham, and H. Haken, *Zeitschrift für Physik* **243 (3)**, 289–302 (1971).
2. R. Graham, and T. Tel, *Europhys. Lett.* **13 (8)**, 715–720 (1990).
3. G. G. Izus, R. R. Deza, and H. S. Wio, *Phys. Rev. E* **58 (1)**, 93–98 (1998).
4. G. G. Izus, R. R. Deza, and H. S. Wio, *Comput. Phys. Comm.* **406**, 121–122 (1999).
5. H. S. Wio, and R. R. Deza, *Eur. Phys. J. Special Topics* **146**, 111–126 (2007).
6. M. S. Miguel, and R. Toral, *Stochastic effects in physical systems*, in Instabilities and Nonequilibrium Structures VI, Kluwer Academic Publishers, 2000.
7. J. F. Mejías, and J. J. Torres, *Neurocomput.* **70**, 2026–2029 (2007).
8. J. F. Mejías, and J. J. Torres, *J. Comput. Neurosci.* **24**, 222–234 (2008).
9. J. F. Mejías, and J. J. Torres, *Neural Comput.* **21**, 851–871 (2009).

Quasi-stationary states and a classification of the range of pair interactions

A. Gabrielli*, M. Joyce† and B. Marcos**

*Istituto dei Sistemi Complessi (ISC), CNR, Via dei Taurini 19, Rome, Italy
†Laboratoire de Physique Nucléaire et Hautes Énergies, Université Pierre et Marie Curie, France
**Laboratoire J.- A. Dieudonné, Université de Nice – Sophia Antipolis, France

Abstract. Systems of long-range interacting particles present typically "quasi-stationary" states (QSS). Investigating their lifetime for a generic pair interaction $V(r \to \infty) \sim 1/r^{\gamma}$ we give a classification of the range of the interactions according to the dynamical properties of the system.

Keywords: Statistical mechanics, long-range interactions, thermal relaxation
PACS: 05.70.-y, 05.45.-a, 04.40.-b

When we consider a system of interacting particles, it is natural to make a classification between *"short range"* and *"long range"* interactions. The range of interactions is usually defined as a function of the additivity of the potential energy of an uniform system. If it is additive (like in many common gases, liquids, etc.), then the system is said to be "*short range*". Otherwise, it is said to be "*long range*". Typical examples of such systems are astrophysical objects interacting by gravity, vortices or non-neutral plasmas [1]. This classification corresponds mathematically to the integrability of the associated pair potential: a pair interaction $V(r \to \infty) \sim 1/r^{\gamma}$ is *short range* if $\gamma > d$ in d space dimensions and *long range* otherwise. A consequence of the additivity of the energy are the properties of the thermal equilibrium of the system (if it exists). When the interaction is long range, peculiar properties (compared to short range systems) appear [1, 2]: different ensembles are not equivalent, the specific heat can be negative, etc.

On the other hand, observations of real systems (such as galaxies) and numerical simulations have shown that thermal equilibrium is attained on a timescale much longer than the one in which the system evolves macroscopically, the "mean field" (Vlasov) timescale τ_{mf}. After a process called "violent-relaxation", there is typically the formation of a "quasi-stationary" state (QSS) which evolves, on a much longer timescale (diverging with the number of particles N) to thermal equilibrium [1, 2]. Therefore, in the mean field (Vlasov) limit (where $N \to \infty$), QSS are stable. However, we have seen that interactions are usually classified according to their thermal equilibrium properties, but equilibrium *may never* be attained in the Vlasov limit for long-range systems. It is therefore interesting to consider whether a purely dynamical classification of interactions can be given, which will depend on the existence of QSS in the Vlasov limit.

In this proceedings, we will describe briefly the work presented in [3]. The approach is the following: *(i)* we assume that a QSS exists, *(ii)* we estimate the relaxation rate Γ_{relax} associated with *soft* two-body scattering (assumed to be the leading process for thermal relaxation), and *(iii)* we study the existence of the QSS independently of the short range properties of the potential.

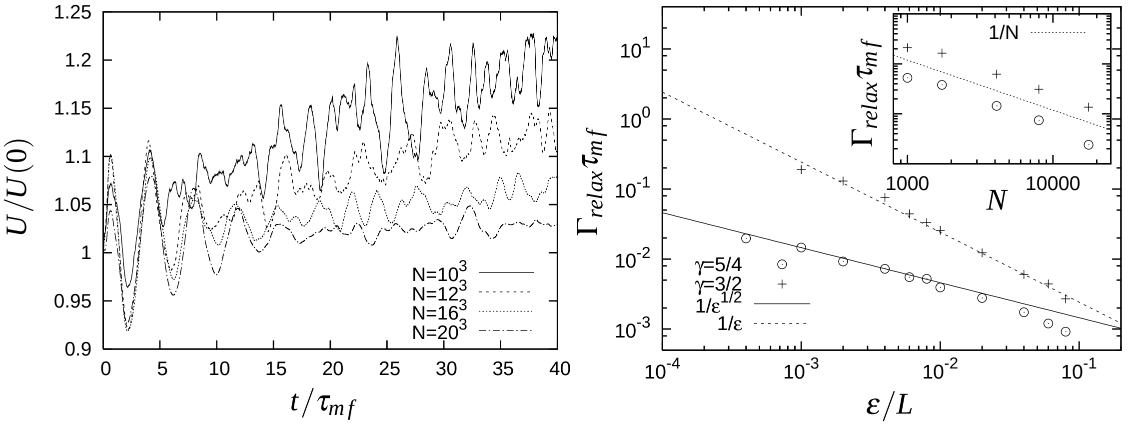

FIGURE 1. Left: evolution of the potential energy for $\gamma = 5/4$ and different N. The relaxation rate is estimated measuring the slope of these curves. Right: relaxation rate as a function of the small scale softening ε in $V(r)$ for $N = 8000$ and system size L. The straight lines are the theoretical prediction (1) with $b_{min} = \varepsilon$. In inset same quantity in function of N for $\gamma = 5/4$. For more details see [3].

Generalizing a work by Chandrasekhar, we assume the existence of a spatially homogeneous spherical QSS, and we consider a test particle with velocity v which suffer a two-body collision with impact factor b. Integrating over all the possible collisions, we estimate δv^2, the *square velocity change of a particle per crossing*. (i.e. in a time of order τ_{mf}). A particle has relaxed when $\delta v^2/v^2 \simeq 1$. It is possible to show [3]:

$$\Gamma_{relax}\,\tau_{mf} \sim \begin{cases} N^{-1} & \text{if}\,\gamma < (d-1)/2 \\ N^{-1}\left(\frac{R}{b_{min}}\right)^{2\gamma-d+1} & \text{if}\,\gamma > (d-1)/2, \end{cases} \qquad (1)$$

where R is the size of the system and b_{min} the minimal impact factor. The latter parameter can be controlled "by hand" using a softening ε at small scales in the potential $V(r)$. Using the condition for soft collisions and the mean field scaling of N, it is possible to estimate $b_{min} \sim RN^{-1/\gamma}$. We obtain then, for $\gamma > (d-1)/2$, $\Gamma_{relax}\tau_{mf} \sim N^{-(d-1-\gamma)/\gamma}$.

This result leads to a "dynamical" classification of the interactions as follows: *(i)* for $\gamma < d-1$, $\lim_{N\to\infty}\Gamma_{relax}\tau_{mf} = 0$ and we call the interaction "*dynamically* long range", and *(ii)* for $\gamma > d-1$, $\lim_{N\to\infty}\Gamma_{relax}\tau_{mf} \to \infty$ and we call the interaction "*dynamically* short range". In the latter case, a QSS may however exist if a sufficiently large and sufficiently soft core is introduced in the potential [3]. A different formalization of this classification is given in terms of the behavior of the probability distribution function of the force in the infinite system limit in [4].

All these results have been checked with molecular dynamics simulations, see Fig. 1.

REFERENCES

1. A. Campa, T. Dauxois and S. Ruffo, *Phys. Rep.* **480**, 57 (2009).
2. J. Binney and S. Tremaine, *Galactic Dynamics* Princeton University Press, 1994.
3. A. Gabrielli, M. Joyce and B. Marcos, *Phys. Rev. Lett.* (2010), to appear.
4. A. Gabrielli, M. Joyce, B. Marcos and F. Sicard, *J. Stat. Phys.* (2010), to appear.

Fluctuation relations and fluctuation-response relations for molecular motors

G. Verley and D. Lacoste

Laboratoire de Physico-Chimie Thorique – UMR CNRS Gulliver 7083, ESPCI, 10 rue Vauquelin, F–75231 Paris Cedex 05, France

Abstract. Fluctuation relations are a set of remarkable relations obeyed by a large class of systems and arbitrarily far from equilibrium. It is interesting to discuss the implications of these relations for molecular motors, which are chemically driven enzymes. These enzymes operate stochastically at the molecular level and for these reasons undergo large thermal fluctuations. Using simple ratchet models of molecular motors, the various forms of fluctuation relations can be illustrated in a simple way. In the linear regime, finite time fluctuation relations imply specific modified fluctuation-dissipation relations.

Keywords: fluctuation relations, fluctuation–dissipation
PACS: 05.40.-a, 05.70.Ln, 87.16.Nn

INTRODUCTION

In recent years, a renewed interest has arisen in ratchet models in the context of non-equilibrium statistical physics. There is large family of ratchet models, but only the isothermal models are relevant for molecular motors. In these models, the coupling of the ratchet to some external agent (e.g., a chemical reaction) continuously drives the system out of equilibrium, and this allows work to be extracted under certain conditions. There is no contradiction with thermodynamics here: the system is far from equilibrium and the ratchet plays the role of a transducer between the energy put in by the agent (e.g., chemical energy) and the mechanical work extracted. The analysis of the energetics of such devices far from equilibrium requires concepts that go beyond the classical laws of thermodynamics. The fluctuation relations, is one of such concepts. These relations, which hold arbitrarily far from equilibrium, can be seen as macroscopic consequences of the invariance under time reversal of the dynamics at the microscopic scale. It is interesting to apply these concepts to small systems such as molecular motors, which operate naturally far from equilibrium and undergo large thermal fluctuations.

As shown in [1], models of molecular motors can provide a particularly clear and pedagogical illustration of fluctuation relations, such as the Gallovotti-Cohen symmetry relation, which is known to hold generally for systems obeying markovian dynamics. This study has been carried out for both the discrete and for the continuous version of the model, called the flashing ratchet [2]. Interestingly, one finds that the Gallavotti-Cohen symmetry is no longer guaranteed if the system is not described by sufficiently variables to properly account for the reversibility of the microscopic dynamics. However, the symmetry can be restored in these models, when variables are added so as to render the dynamics markovian.

LINEAR RESPONSE NEAR A NON-EQUILIBRIUM STEADY-STATE

Within the linear response regime and for slightly perturbed non-equilibrium steady states (Ness), finite time fluctuation relations, can be used to obtain modified fluctuation-response relations for systems obeying markovian dynamics [3, 4, 5]. These fluctuation-response relations qualify as extensions of the well-known fluctuation-dissipation theorem (FDT), because they hold in the vicinity of a non-equilibrium steady-state rather than near an equilibrium state as in the classic FDT.

Let us consider a system initially in non-equilibrium steady state, characterized by a (set of) control parameters denoted by λ. For a given value of λ, we assume that there exists a steady state with stationary probability distribution $P_{stat}(c,\lambda) = \exp(-\phi(c,\lambda))$. A time-dependent perturbation of the dynamics around the fixed value λ_0 will be described by $\lambda(s) = \lambda_0 + \delta\lambda(s)$ for $t > s$. The response $R(t,s) = \delta\langle A(c(t),\lambda_0)\rangle_{\mathrm{path}}/\delta\lambda(s)$ of the dynamic observable A that depends on the microscopic configuration $c(t)$ at time t is given by the nonequilibrium FDT [3, 4]:

$$R(t,s) = -\frac{d}{ds}\left\langle \frac{\partial\phi(c(s),\lambda_0)}{\partial\lambda} A(c(t),\lambda_0) \right\rangle_0, \tag{1}$$

where $\langle..\rangle_0$ denotes the average in the stationary state with the control parameter λ_0. For thermal equilibrium, we have $\phi(c,\lambda) = \beta(H(c) - \lambda O(c) - F(\lambda))$, where H is the unperturbed hamiltonian, O is a perturbation, F is the free energy; and the usual form of the fluctuation-dissipation theorem is recovered from Eq. 1.

In Ref. [5], we have given a compact derivation of Eq. 1 and provided two applications: In the first application introduced in Ref. [6], a particle obeying overdamped Langevin dynamics is subjected to a periodic potential and a non-conservative force. In the second application, a discrete two-states ratchet model of a molecular motor is considered. In this case, the modified FDT takes the form of Green-Kubo relations characterizing the response of the motor near a NESS. We have observed that the modified FDT relation requires a knowledge of the relevant degrees of freedom in order to be able to distinguish an equilibrium state from a non-equilibrium steady state, just as it does for the existence of a Gallavotti-Cohen symmetry [2].

REFERENCES

1. D. Lacoste, and K. Mallick, *Fluctuation relations for molecular motors*, vol. 60 of *Progress in Mathematical Physics*, BirkhÃd'user, 2010, http://arxiv.org/abs/0912.0391.
2. D. Lacoste, and K. Mallick, *Phys. Rev. E* **80**, 021923 (2009).
3. R. Chetrite, G. Falkovich, and K. Gawedzki, *J. Stat. Mech.* p. P08005 (2008).
4. U. Seifert, and T. Speck, *Eur. Phys. Lett.* **89**, 10007 (2010).
5. G. Verley, K. Mallick, and D. Lacoste (2010), http://arxiv.org/abs/1009.4123.
6. T. Speck, and U. Seifert, *Europhys. Lett.* **74**, 391 (2006).

Why are so many networks disassortative?

Samuel Johnson, Joaquín J. Torres, J. Marro, and Miguel A. Muñoz

Dpto. de Electromagnetismo y Física de la Materia, and Institute Carlos I for Theoretical and Computational Physics, Universidad de Granada, 18071 Granada, Spain.

Abstract. A wide range of empirical networks –whether biological, technological, information-related or linguistic – generically exhibit important degree-degree anticorrelations (i.e., they are *disassortative*), the only exceptions being social ones, which tend to be positively correlated (*assortative*). Using an information-theory approach, we show that the equilibrium state of highly heterogeneous (scale-free) random networks is disassortative. This not only gives a parsimonious explanation to a long-standing question, but also provides a neutral model against which to compare experimental data and ascertain whether a given system is being driven from equilibrium by correlating mechanisms.

Keywords: Random graphs, correlated networks, assortativity, Shannon entropy
PACS: 89.75.Fb, 89.75.Hc, 05.90.+m

One of the great scientific challenges we face today is to understand complex systems: sets of many elements –genes, people, routers, neurons, airports, species...– interacting in such a way that non-trivial collective phenomena emerge. In other words, those for which the whole is more than the sum of the parts. Often, many essential characteristics of these systems are captured by representing them as networks, in which elements are nodes and edges play the part of interactions (genetic activation, sexual intercourse, telephone lines, synapses, flights, predation...). Over the past dozen years or so *complex networks* have been the focus of intense study. One of the objectives in this field is to determine universal properties of networks and to understand how these come about [1].

An intriguing feature of most real networks is the existence of degree-degree correlations: the degree (number of neighbours) of a given node is correlated with that of its neighbours, either positively or negatively. The network is then called *assortative* or *disassortative*, respectively. This can be measured, for instance, computing Pearson's coefficient, r, over all edges. It turns out that a high proportion of empirical networks – whether biological, technological, information-related or linguistic – are disassortatively arranged (high-degree nodes, or hubs, are preferentially linked to low-degree neighbours, and viceversa) while social networks are usually assortative. Such degree-degree correlations have important consequences for network characteristics. For instance, assortative networks have lower percolation thresholds and are more resilient to targeted attacks [2], while disassortative ones make for more stable ecosystems and are more synchronizable [3]. Assortativity has also been shown to increase the robustness to noise of attractor neural networks [4].

We have recently shown how the ensemble of networks compatible with given macroscopic constraints can be partitioned, conceptually, into subsets such that each contains all networks with a given correlation profile [5]. We computed the Shannon entropy (which coincides with the thermodynamic entropy for intensive constraints [6]) of scale-

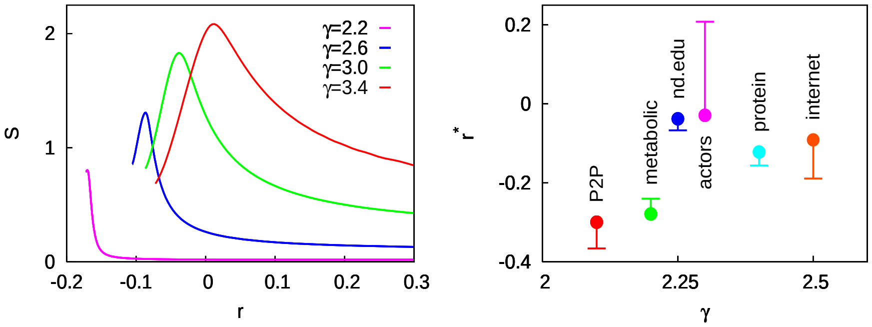

FIGURE 1. (Color online) **Left:** Entropy of scale-free networks in the correlation ensemble against Pearson's coefficient r for various values of γ (increasing from bottom to top). $\langle k \rangle = 10$, $N = 10^4$. **Right:** Level of assortativity that maximizes the entropy, r^*, for various real-world, scale-free networks, as predicted theoretically against exponent γ. Bar ends show the empirical values.

free networks, and found that it exhibits a non-monotonic curve when plotted against assortativity (see Fig. 1, left). Maximum entropy corresponds to the macrostate compatible with the largest number of microstates, and should thus be seen as the most likely kind of configuration in the absence of further information regarding how a particular network was formed. In general, this maximum occurs for a certain level of disassortativity (negative degree-degree correlations), which provides a simple explanation for the ubiquity of such networks. Indeed, some real networks display correlations very close to those predicted by entropic considerations (in the right panel of Fig. 1, the metabolic, Web page and protein interaction networks). However, others turn out not to be so near their equilibrium point, displaying either a negative bias (like the Internet and P2P network of Fig. 1, probably due to node hierarchy), or a positive one (like the actor graph, since well-known actors tend to work together). The extent to which these systems are driven from equilibrium by correlating mechanisms can be estimated from the entropy reduction.

ACKNOWLEDGMENTS

This work was supported by Junta de Andalucía projects FQM-01505 and P09-FQM4682, and by Spanish MEC-FEDER project FIS2009-08451. Many thanks to Ginestra Bianconi, Sebastiano de Franciscis, Jorge Mejías, Pablo Sartori and Miguel Ibáñez de Berganza for stimulating conversations.

REFERENCES

1. M. E. J. Newman, *SIAM Reviews* **45**, 167 (2003).
2. M. E. J. Newman, *Phys. Rev. Lett.* **89**, 208701 (2002); *Phys. Rev. E* **67**, 026126 (2003).
3. M. Brede, and S. Sinha, arXiv:cond-mat/0507710
4. S. de Franciscis, S. Johnson, and J. J. Torres, submitted.
5. S. Johnson, J. J. Torres, J. Marro, and M. A. Muñoz, *Phys. Rev. Lett.* **104**, 108702 (2010).
6. K. Anand, and G. Bianconi, *Phys. Rev. E* **80**, 045102(R) (2009).

Analytical study of hysteresis in the $T = 0$ random field Ising model

T P Handford*, F-J Perez-Reche* and S N Taraskin*,†

*Department of Chemistry, University of Cambridge, UK
†St. Catharine's College, University of Cambridge, UK

Keywords: Hysteresis, Disordered Systems, Critical Phenomena
PACS: 75.10.Nr, 75.60.Ej, 05.70.Jk

Although thermal fluctuations are believed to be essential to many first-order phase transitions, there are multiple examples in which such fluctuations do not play a prominent role. These include magnetisation reversal (Barkhausen noise [1, 2]), martensitic transformations [3] and vapour condensation in porous media [4]. A prototype model for systems exhibiting athermal first order phase transitions is the random field Ising model at zero temperature [5].

This model consists of a set of classical spins, each in one of two states $s_i = \pm 1$, placed on the sites of a lattice. The system is described by the following Hamiltonian:

$$\mathscr{H} = -J \sum_{\langle ij \rangle} s_i s_j - H_{\text{ext}} \sum_i s_i - \sum_i h_i s_i \ . \qquad (1)$$

Here, J is the strength of ferromagnetic interactions between nearest-neighbour spins and H_{ext} is an external magnetic field. The local fields, h_i, are independent identically distributed random variables characterised by normal probability density functions with standard deviation Δh. The system obeys synchronous Glauber dynamics at $T = 0$ [6].

The state of such a system can be characterised by the total magnetisation of the lattice ($m = N^{-1} \sum_i s_i$), which displays hysteresis when the external magnetic field is varied (see Fig. 1). The properties of the hysteresis loop have previously been studied analytically in the mean-field approximation [6] and on Bethe lattices [7], and numerically on hyper-cubic lattices [8].

It has been found that the hysteresis loop consists of many small discontinuities, associated with microscopic avalanches. In addition, in certain topologies, the system undergoes a single infinite avalanche at a particular value of H_{ext}, provided the disorder, Δh, is below a critical value, Δh_{c}. This infinite avalanche manifests itself as a macroscopic discontinuity in the magnetisation (see the dashed line in Fig. 1(a)). As the degree of disorder increases, the size of the discontinuity approaches zero continuously at the critical disorder Δh_{c} and external field H_{c}. Above the critical disorder ($\Delta h > \Delta h_{\text{c}}$), no infinite avalanche is observed (solid line in Fig. 1(a)). Topologies known to display this transition include the mean-field system, Bethe lattices with coordination number $q > 3$ and hyper-cubic lattices with $d \geq 3$.

We have introduced a new method which extends the range of lattices in which the magnetisation is analytically solvable as a function of external field. This procedure is

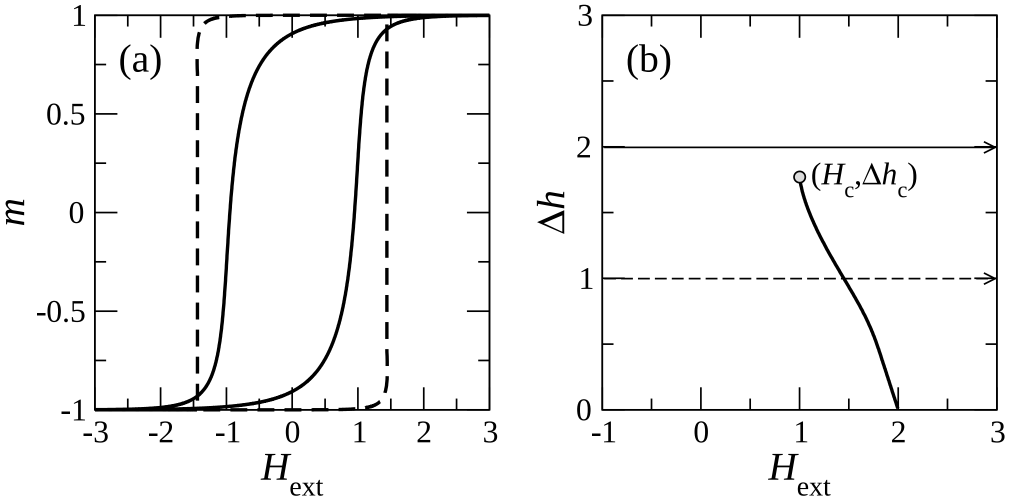

FIGURE 1. (a) Hysteresis loops for magnetisation as a function of the external field (which is swept cyclically between $-\infty$ and $+\infty$) for Bethe lattice with $q = 4$. The solid and dashed lines correspond to $\Delta h = 2$ and $\Delta h = 1$, respectively. (b) Phase diagram in the $(H_{\text{ext}}, \Delta h)$ space. The solid line shows the field at which the infinite avalanche occurs for increasing external field. The critical point $(H_c, \Delta h_c)$ is marked. Solid and dashed lines correspond to paths taken by systems in panel (a).

iterative and modifies the existing approach used to solve the problem for the Bethe lattice with arbitrary q [7]. The main advantage of our method is that certain systems containing both large and small lattice loops, such as the ladder (two regularly linked 1D chains), can be systematically analysed. Using this method, we have shown, by analytically evaluating the spin-spin correlation function, that the correlation length diverges as a power law at $(H_c, \Delta h_c)$ for a Bethe lattice with $q > 3$ (Fig. 1(b)). In contrast, although a discontinuity in magnetisation is observed in a 1D system and $q = 3$ Bethe lattice at $\Delta h = 0$, we have shown that the divergence in correlation length is exponential rather than a power law. This confirms the absence of a critical point.

TPH thanks the UK EPSRC for funding. FJP and SNT acknowledge funding from BBSRC (Grant No. BB/E017312/1).

REFERENCES

1. G. Durin, and S. Zapperi, *The science of hysteresis*, Elsevier, Amsterdam, 2006, chap. The Barkhausen effect.
2. J. P. Sethna, K. A. Dahmen, and C. R. Myers, *Nature (London)* **410**, 242–250 (2001).
3. F. J. Pérez-Reche, E. Vives, L. Mañosa, and A. Planes, *Phys. Rev. Lett.* **87**, 195701–1 – 195701–4 (2001).
4. E. Kierlik, P. A. Monson, M. L. Rosinberg, L. Sarkisov, and G. Tarjus, *Phys. Rev. Lett.* **87**, 055701–1 – 055701–4 (2001).
5. J. P. Sethna, K. A. Dahmen, and O. Perković, "Random-Field Ising Models of Hysteresis," in *The science of hysteresis II*, edited by G. Bertotti, and I. D. Mayergoyz, Academic Press, New York, 2006.
6. J. P. Sethna, K. A. Dahmen, S. Kartha, J. Krumhansl, B. Roberts, and J. Shore, *Phys. Rev. Lett.* **70**, 3347 – 3350 (1993).
7. D. Dhar, P. Shukla, and J. P. Sethna, *J. Phys. A: Math. Gen.* **30**, 5259–5267 (1997).
8. O. Perković, K. A. Dahmen, and J. P. Sethna, *Phys. Rev. Lett.* **75**, 4528 – 4531 (1995).

Queues on narrow roads and in airplanes

Vidar Frette* and Per C. Hemmer†

* *Department of Engineering, Stord/Haugesund College, Bjørnsons gt 45, N-5528 Haugesund, Norway. e-mail: vidar.frette@hsh.no*
† *Department of Physics, Norwegian University of Science and Technology, N-7491 Trondheim, Norway. e-mail: per.hemmer@ntnu.no*

Abstract. We consider N particles with unidirectional motion in one dimension. The particles never pass each other, and they are distinguishable (labelled). We have studied two types of particle interactions, both of which lead to queue formation due to bottlenecks. There are variations in queue structure from particle scale up to system size. We are interested in quantities obtained after averaging over all $N!$ permutations of particles.

Keywords: particle system, one dimension, bottlenecks, scaling
PACS: 02.50.-r, 05.40.-a

QUEUES ON NARROW ROADS

In a first contribution, we study the queues formed when each particle has a preferred velocity and all these preferred (initial) velocities differ. As a result, clustering occurs behind slow particles, as initially faster particles must reduce their velocities to comply. This is similar to cars on a narrow road that does not allow overtaking.

Consider, as an example, particles (cars) with *preferred* velocities

$$0.67 \quad 0.97 \quad 0.04 \quad 0.12 \quad 0.71 \quad 0.22$$

all moving to the right. After clustering, the *actual* velocities in this case are

$$0.04\,0.04\,0.04 \qquad 0.12 \qquad 0.22\,0.22$$

in three queues as indicated.

From preferred velocities to actual velocities high values are typically replaced by low ones. Thus, one ends up with a systematically increased probability for low actual velocities, as compared to the preferred velocities. The actual velocities increase along the direction of motion. The lower a preferred velocity is, the larger the number of particles (cars) it tends to influence. Furthermore, with increasing system size N, more particles will in general be influenced by a low preferred velocity. From observations like these, one may infer that the average particle velocity $\langle v \rangle$ (obtained after averaging all actual velocities over all permutations of preferred velocities) will decrease with N. However, the functional form of $\langle v(N) \rangle$ is not obvious.

We have found exact expressions for the average particle velocity (after clustering) and for the average number of clusters with given size and velocity [1, 2, 3]. The expression for the average velocity applies for a uniform distribution of initial velocities on $[0, V_{\max}]$, and is

$$\langle v \rangle = \frac{V_{max}}{N} \cdot \sum_{i=1}^{N} \frac{1}{i+1} \simeq V_{\max} \frac{\ln N}{N} ,$$

which is much smaller than the average over initial velocities $V_{\max}/2$.

As outlined above, the average velocity is a result of a redistribution (lowering) of velocities from the preferred ones to the actual ones. Thus, $\langle v \rangle$ will be sensitive to the probability distribution of the preferred velocities. We have explored this issue through increasing and decreasing power-law distributions, for which we have found asymptotic (large-N) expressions for the average velocity [3]. Of particular interest is the decaying power law, with several $\langle v(N) \rangle$ asymptotics depending on the exponent value. There is even a regime where $\langle v \rangle$ *increases* with N.

QUEUES IN AIRPLANES

In a second contribution, we study queues that result from mismatch between the queue ordering and the ordering of sinks on a substrate, as when some airplane passengers must wait in line before they reach their reserved seats. Due to different degrees of mismatch, the total time to settle all particles varies significantly between queue configurations.

A simple example is shown below. Here, the first line represents the numbered seats in an airplane, here with only one seat in each row (underlined). The next three lines show three stages (time steps) during passenger boarding. Each passenger is labelled by the number of the seat for which s/he has a reservation.

$$\begin{array}{ccccccccc}
 & & & \underline{1} & \underline{2} & \underline{3} & \underline{4} & \underline{5} & \underline{6} \\
4 & 6 & 1 & 2 & 5 & 3 & & & \\
 & 4 & 6 & 1 & 2 & & & 5 & \\
 & & & & & & 4 & & 6
\end{array}$$

In the first time step, passenger 3 has reached her/his seat and is busy with hand luggage, etc, while all the others are waiting. After 3 is seated, 1, 2, and 5 are able to rush to their seats, while 4 and 6 are waiting and are able to get seated only in the third time step. Thus, the boarding time T for this particular case is $T = 3$.

The average time (averaging over all permutations of passengers), to first order, is $\langle T \rangle = (N+1)/2$ [4]. This result is obtained based on structuring of the passenger queue that occurs during boarding. However, complete enumeration shows that the average boarding time is significantly lower, current estimates give $\langle T \rangle \propto N^{\alpha}$, with $\alpha = 0.7$. This is due to a hierarchy of correlations between queue ordering and substrate ordering. Thus, the number of correlations increases with N at least as fast as $N!$ [4].

REFERENCES

1. P. C. Hemmer, *Fra fysikkens verden* **53**, 51 (1991); *ibid* 72.
2. V. Frette, *Eur. J. Phys.* **30**, 497–514 (2009).
3. V. Frette, and P. C. Hemmer, *Phys. Rev. E* **80**, 051115 (2009).
4. V. Frette, and P. C. Hemmer, in preparation.

Fluctuations out of equilibrium

V.V. Belyi

IZMIRAN, Russian Academy of Sciences, Troitsk, Moscow region, 142190, Russia and and Service de Physique Statistique et des Plasmas, CP 231, ULB, 1050 Bruxelles, Belgium

Abstract. A generalization of the fluctuation-dissipation formula for systems with slowly varying parameters is given using the Langevin approach and momentum method. It is shown that spectral function of the fluctuations in these systems is determined not only by the dissipation but also by the derivations of the dispersion. The non Joule dispersion contribution is characterized by a new nonlocal effect originating from an additional phase shift between the force and response of the system. That phase shift results from the parametric control to the system.

Keywords: Fluctuation-dissipation theorem; Non-Marcovian processes
PACS: 05.40.Hp; 05.40.-a; 05.10.Gg; 07.50.Hp

Fluctuations play an important role in the formation of the dissipative structures [1], find applications in diagnostic procedures. Moreover fluctuations determine the sensitivity of the devices. Any oscillating system is characterized by two main parameters: the proper frequency and the quality factor Q. The latter is inversely proportional to the width of the spectral line of the parameter fluctuations. The higher Q factor, the more sensitive the system is. In thermodynamic equilibrium, fluctuations are determined by the system temperature and the dissipation. The fluctuation-dissipation relation was extended by Callen and Welton [2] to a general class of dissipative thermodynamic equilibrium systems. In the classical case the spectral function of the fluctuations of the variable x has the form:

$$\left(x^2\right)_\omega = \frac{2T}{\omega} Im\alpha(\omega) \tag{1}$$

where α - is the response function, and T - is the temperature in energy units. However, it is not evident that the systems parameters can be kept constant in both space and time. Inhomogeneities in space and time of these quantities will certainly also contribute to the fluctuations. For generalization of fluctuation-dissipation theorem to a general class system with slowly varying parameters, we use the so-called momentum method, which is alternative to the Langevin method. This method is based on the equation for two-time correlation function [3]. Let us consider an arbitrary system whose evolution is described by the following equation:

$$\left(\frac{\partial}{\partial t} + \underline{\underline{L}}\right) \bullet \underline{\underline{G}}(t,t') = 0, t > t' \tag{2}$$

where L - is generally a non self-conjugate, linear operator in the Hilbert space. This operator varies slowly in time. The term "slowly" means that the control parameter undergoes only a small change during the period of the system motion. The slow scale is much larger than the characteristic fluctuation time. We can therefore introduce a small parameter μ, which allows us to describe fluctuations on the basis of a multiple time scale analysis. Obviously, fluctuations vary on both ”fast” and ”slow” time scales. At first order with respect to μ the expression for the spectral function of the fluctuations in the classical limit takes the form [4]:

$$(\delta A \delta B)_{\omega} = \frac{2T}{\omega}[Im\alpha_{AB}(\omega) + \frac{d^2}{d\mu t d\omega} Re\alpha_{AB}(\omega)] \tag{3}$$

When expanding the Green’s function of Eq. (2) in terms of the small parameter μ, there appears an additional term at first order. It is important to note that the imaginary part of the response function is now replaced by the real part. If the quality factor of the system is of the order of one, (it can be a broadband system or a process near the zero frequency), the real and imaginary parts of the response function are of the same order and the correction is negligibly small. However, in the case of systems with a high quality factor, for which the real part of the response function is greater than the imaginary part, the second small parameter appears to be inversely proportional to the quality factor. An example of such system with a high quality factor could be plasma fluctuations near the Langmuir frequency when the quality factor is inversely proportional to the small plasma parameter [5]. When this small parameter is comparable with μ, the second term in Eqs. (3) may have an effect comparable to the first term. At the second order in the expansion in μ , the corrections appear only in the imaginary part of the response function, and they can reasonably be neglected. It is therefore sufficient to retain the first order corrections to solve the problem. As an example, we consider the electrical oscillation circuit, which can be used to model many oscillation processes in nature and it is demonstrated that the dispersive contribution may strongly affect the quality factor.

Conclusion

We have generalized the Callen-Welton formula to systems with slowly varying parameters. The spectral function of the fluctuations is determined not only by the dissipation but also by the derivatives of the dispersion. The non-Joule dispersion contribution is characterized by a new nonlocal effect originating from an additional phase shift between the force and the response of the system. That phase shift results from the parametric control to the system. Referring to the example of an electrical oscillation circuit it is demonstrated that the dispersive contribution may strongly affect the quality factor.

REFERENCES

1. I. Prigogine, *Science* **201**, 777 (1978); R. Lefever, *Fluctuations, Instabilities and Phase Transitions*, Plenum, New York, 1975.
2. H. B. Callen, and T. A. Welton, *Phys. Rev.* **83**, 34 (1951).
3. R. Balescu, *Equilibrium and Nonequlibrium Statistical Mechanics*, Wiley, New York, 1975.
4. V. V. Belyi, *Phys. Rev. E* **69**, 017104 (2004).
5. V. V. Belyi, *Phys. Rev. Lett.* **88**, 255001 (2002).

Long-range interacting systems and dynamical phase transitions

Fulvio Baldovin*, Enzo Orlandini* and Pierre-Henri Chavanis†

Dipartimento di Fisica, Sezione INFN, CNISM, and Università di Padova, Via Marzolo 8, I-35131 Padova, Italy
† *Laboratoire de Physique Théorique (IRSAMC), CNRS and UPS, Université Paul Sabatier, F-31062 Toulouse, France*

Abstract. We briefly review the derivation of the Vlasov equation, which is a convenient approximation for the description of the transport properties of long-range interacting systems. We then point out that the presence of an external source of noise, like for instance a heat bath, induces dynamical phase transitions from ordered non-equilibrium Vlasov-stable states to disordered ones.

Keywords: Nonequilibrium statistical mechanics; Long-range systems; Dynamical phase transitions
PACS: 05.20.-y; 05.40.-a; 05.70.Ln

A rigorous, standard, derivation of the kinetic equations describing the transport properties of a Hamiltonian system is the Born-Bogoliubov-Green-Kirkwood-Yvon (BBGKY) hierarchy, which amounts to a set of exact, interlaced equations for the many-particle distribution functions, obtained starting from the Liouville equation. In order to be useful, the equations of the hierarchy must be closed by some appropriate approximation. Thinking, for the sake of simplicity, in terms of a one-dimensional Hamiltonian of the form $H = \sum_{i=1}^{N} \frac{m\, v_i^2}{2} + \sum_{i<j}^{N} V\left(x_i - x_j\right)$, and separating in the two-particle distribution function f_2 the correlated part g_2, due to the effects of the "collisions", from the independent one: $f_2 \equiv f\, f + g_2$ [here, $f(x,v,t) \equiv f_1(x,v,t)$ is the one-particle distribution function], the first BBGKY equation reads

$$\frac{\partial f}{\partial t} + v\frac{\partial f}{\partial x} - \frac{1}{m}\frac{\partial \Phi}{\partial x}\frac{\partial f}{\partial v} = \left(\frac{\partial f}{\partial t}\right)_{coll}, \tag{1}$$

where

$$\Phi(x,t) \equiv \int_{-\infty}^{+\infty} dx'\, V\left(x - x'\right) \int_{-\infty}^{+\infty} dv\, f(x',v,t). \tag{2}$$

One-dimensional long-range systems are those for which $V(x)$ decays at large $|x|$ slower than $1/|x|$. Among other fields, examples are present in plasma physics, astrophysics and wave-matter interacting systems (e.g., the Free Electron Laser). In these cases $\left(\frac{\partial f}{\partial t}\right)_{coll} \sim 1/N$ and, in the thermodynamic limit obtained by rescaling the interaction strength by $1/N$ (Kaĉ prescription), the first BBGKY equation becomes the Vlasov equation

$$\frac{\partial f}{\partial t} + v\frac{\partial f}{\partial x} - \frac{1}{m}\frac{\partial \Phi}{\partial x}\frac{\partial f}{\partial v} = 0. \tag{3}$$

Those cases in which a long-range system is in contact with external noise sources, like for instance a heat bath, are conveniently described by adding at the r.h.s. of the Vlasov equation a diffusive and a damping term:

$$\frac{\partial f}{\partial t}+v\frac{\partial f}{\partial x}-\frac{1}{m}\frac{\partial \Phi}{\partial x}\frac{\partial f}{\partial v}=\frac{\partial}{\partial v}\left(D\frac{\partial f}{\partial v}+\gamma f v\right), \tag{4}$$

where D and γ are the diffusion and the damping coefficients, respectively. Typically, the fluctuation-dissipation relation imposes $D=\gamma k_B T/m$, but one can also conceive more general external noise sources.

Here we are interested in Hamiltonians such that there exists a critical temperature T_c, which separates a high-temperature equilibrium homogeneous phase characterized by a zero order parameter φ from a low-temperature inhomogeneous one in which $\varphi \neq 0$. Considering a spatially homogeneous nonequilibrium initial condition $f(x,v,0)=f_0(v)$ [$\varphi(0)=0$], we have $\frac{\partial \Phi}{\partial x}=0$, and, as long as the spatially homogeneous distribution remains dynamically stable, the previous equation simplifies into

$$\frac{\partial f}{\partial t}=\frac{\partial}{\partial v}\left(D\frac{\partial f}{\partial v}+\gamma f v\right). \tag{5}$$

By performing a Landau stability analysis it is possible to identify the critical time t_c at which the dynamical stability is lost and, as a consequence, $\varphi(t_c)\neq 0$. It is the minimum time t for which equation

$$1-\frac{\widetilde{V}(k)}{m}\int dv\,\frac{f'(v,t)}{v}=0 \tag{6}$$

admits a solution for at least a $k\in\mathbb{R}$, $k\neq 0$ ($\widetilde{V}$ is the Fourier transform of V). Taking advantage of the fact that the propagator of Eq. (5) is simply a Gaussian Green function, it is possible to prove that t_c is equivalently identified by the first zero of the function

$$I(t,k)\equiv 1+\frac{m\,\widetilde{V}(k)}{2}\int_{-\infty}^{+\infty} dw\,|w|\,\widetilde{f_0}\,(a(t)\,w)\;e^{-\sigma^2(t)\,w^2/2}, \tag{7}$$

for some $k\neq 0$, where $a(t)\equiv e^{-\gamma t}$, $\sigma^2(t)\equiv k_B T\left(1-e^{-2\gamma t}\right)$, and $\widetilde{f_0}(w)$ is the Fourier transform of $f_0(v)$. This is a general result valid for any one-dimensional long-range system with a symmetric potential and for spatially homogeneous distribution functions with a single maximum at $v=0$. It shows that external noise sources can induce dynamical phase transitions to long-range systems, which correspond to restore the full ergodic occupation of phase space. In particular, it predicts that a peak ("pulse") in the time evolution of $\varphi(t)$ can be used as a signature of the existence of Vlasov-stable out-of-equilibrium states in experiments with long-range systems. Extensions to more general situations are also possible.

REFERENCES

1. See P. H. Chavanis, F. Baldovin, and E. Orlandini, to be published (2010) [arXiv:1009.5603] and references therein.

Irreversibility of the renormalization group flow and information theory

S. M. Apenko

I E Tamm Theory Department, P N Lebedev Physical Institute, Moscow, 119991, Russia

Abstract. Here we discuss the problem of irreversibility of the renormalization group (RG) flow from the point of view of the information theory. The main idea is to look at the RG transformation as a signal transmission and to focus on the mutual information of the fast and slow variables.

Keywords: renormalization, irreversibility, mutual information
PACS: 05.10.Cc, 11.10.Hi, 89.70.Cf

Wilsonian renormalization group (RG) starts from dividing all the variables of a given statistical or field-theoretic system into two parts: fast and slow ones, with subsequent elimination of the fast ones [1]. This means that initially we have some system in equilibrium with variables ϕ and probability distribution $p(\phi)$. Now, to define the renormalization procedure we divide ϕ's into fast variables x and slow ones, y, and in the simplest case introduce the following transformation of probability measures

$$p(\phi) \to p(y) = \sum_x p(x,y), \tag{1}$$

If the marginal coarse-grained probability $p(y)$ has the same functional dependence on the fields as the initial one $p(\phi)$, with only some parameters g_i (coupling constants) changed, then the RG transformation may be written as $g_i \to g_i'$ and its successive application results in a flow in the space of parameters g_i.

In general, the nonlinear mapping $g_i \to g_i'$ may be very complicated. While normally one is interested in fixed points of this transformation (they define the critical behavior at phase transitions [1]) more general questions may be asked, e.g. could the RG flow be chaotic as many nonlinear mappings are? What kind of attractors may appear, are limit cycles or strange attractors possible? Or this flow is strictly irreversible due to obvious information loss related to elimination of fast variables? Irreversibility here means that the flow in the space of couplings resembles that of a purely dissipative system with a given trajectory never returning back to its starting point.

Certainly, the RG transformation does not have the inverse, so the irreversibility here is not something unexpected, but to prove it rigorously is nevertheless not an easy task. In 2D field theory this was done first by Zamolodchikov [2], who constructed a "c-function" (a kind of Lyapunov function) which monotonically decreases along the flow. Many later attempts to generalize this c-theorem to other situations are not so widely known and in general pay no attention to informational aspects (see, however, [3]).

If, however, we start from the information theory, then the most natural way is to view the RG transformation as a signal transmission through a noisy channel. Namely, we may view x variables as an input signal, which is not directly available, and y as an output, which we receive. Then the average information loss under a single step of Wilsonian RG is given by a *conditional entropy* [4] of the fast variables, conditioned by slow ones. Its positivity results in the monotonic decrease of the informational entropy $H(X,Y) = -\sum_{x,y} p(x,y)\ln p(x,y)$ under renormalization, i.e. $H(X,Y) \geq H(Y) = -\sum_y p(y)\ln p(y)$. This, however, does not necessarily imply the irreversibility of the RG flow, because the entropy explicitly depends on the total number of variables, which is reduced, and thus H cannot be a proper Lyapunov function. Probably only some part of information losses is relevant to the irreversibility problem [5], but this point is not clear.

One possible way out is to focus on the information which is transferred through the "channel". This is given by the *mutual information* [4] of the fast and slow variables

$$I(X,Y) = \sum_{x,y} p(x,y)\ln\frac{p(x,y)}{p(x)p(y)} = H(X) + H(Y) - H(X,Y) \geq 0. \tag{2}$$

The positivity of $I(X,Y)$ may itself provide some restrictions on the RG flow. For example, for some *decimation* real-space RG transformations [1], when "fast" and "slow" spins are located on two complementary sublattices and exactly half of spin variables are summed away, one can easily prove that the entropy per lattice site always increases [5]. Thus, such decimation RG flows are irreversible and resembles, in many aspects, an approach to equilibrium.

Mutual information of this kind may appear useful in some other problems as well. For example, simple diffusion evolution of the probability distribution function

$$p(y,t) = \frac{1}{\sqrt{4\pi Dt}}\int dx\,\exp\left[-\frac{(y-x)^2}{4Dt}\right]p(x,0) \tag{3}$$

may also be viewed as a renormalization. Equation (3) is in fact just a generalization of Eq. (1) and corresponds to Kadanoff block-spin transformation [1] (though with conserved number of variables). Here we actually have a kind of coarse-graining with x being the "fast" variable while y in $p(y,t)$ is a "slow" one, and t plays the role of a scale parameter. Evaluating the mutual information between the initial coordinate of the diffusing particle and its final position results in

$$I(X,Y) \geq 0 \qquad \longrightarrow \qquad h(t) \geq \ln(\sqrt{4\pi \mathrm{e} Dt}), \tag{4}$$

where $h(t) = -\int dx\, p(x,t)\ln p(x,t)$. Surely, for diffusion we already know that the entropy increases with time, but the analogy between a time evolution and some RG transformation (coarse-graining) may probably be of some use in less trivial cases, and irreversibility of the RG flow could possibly be related somehow to irreversibility in statistical physics.

REFERENCES

1. K. G. Wilson, and J. Kogut, *Phys. Rep.* **12**, 75 (1974); K. G. Wilson, *Rev. Mod. Phys.* **47**, 773 (1975)
2. A. B. Zamolodchikov, *Pis'ma Zh. Eksp. Teor. Fiz.* **43**, 565 (1986) [*JETP Lett.* **43**, 730 (1986)].
3. J. Gaite, and D. O'Connor, *Phys. Rev. D* **54**, 5163 (1996); J. Gaite, *Phys. Rev. Lett.* **81**, 3587 (1998)
4. T. M. Cover, and J. A. Thomas, *Elements of Information Theory*, 2nd ed., Wiley, Hoboken, 2006.
5. S. M. Apenko, *preprint ITEP-TH-48/09*, arXiv: 0910.2097.

Classical systems: moments, continued fractions, long-time approximations and irreversibility

R. F. Álvarez-Estrada

Departamento de Física Teórica I, Facultad de Ciencias Físicas, Universidad Complutense, 28040, Madrid, Spain. E-mail: rfa@fis.ucm.es

Keywords: hierarchy for Liouville equation; initial non-equilibrium distribution; long-time approximation; relaxation towards thermal equilibrium
PACS: 0.5.20.Gg, 05.20.Jj, 05.40.Jc

Let a classical particle, with mass m, position x and momentum p, be subject to a real potential $V = V(x)$, in the presence of a "Heat bath" at equilibrium, at temperature T. The classical Hamiltonian of the particle is: $H = p^2/(2m) + V$. Its probability distribution function is: $W = W(x,p;t)(> 0)$ at time t. The equilibrium distribution is: $W = W_{eq} = \exp[-\beta(p^2/(2m) + V)]$. Let $H_n(q)$ be the standard n-th Hermite polynomial. We introduce the moments $W_n = W_n(x;t)$ $(n = 0,1,2,...)$ of W [1, 2]:

$$W_n = \int dp \frac{H_n(p/q)}{(\pi^{1/2}2^n n!)^{1/2}} W(x,p;t),\ q = (2m/\beta)^{1/2} \tag{1}$$

($\beta = (K_B T)^{-1}$, $K_B =$ Boltzmann's constant). If $W = W_{eq}$, then $W_{eq,0}$ is proportional to $\exp[-\beta V]$ and $W_{eq,n} = 0$, $n = 1,2,....$ Let W_{in} be an initial off-equilibrium distribution, at $t = 0$. The corresponding initial moments, using (1), are $W_{in,n}$. The irreversible Kramers equation (with a friction constant $\sigma > 0$ on the particle due to the "Heat bath") [1] provides one temporal evolution: $(\partial W/\partial t) + (p/m)(\partial W/\partial x) - (\partial V/\partial x)(\partial W/\partial p) = (1/\sigma)(\partial/\partial p)[p + (m/\beta)(\partial/\partial p)]W$. The latter and (1) yield the infinite irreversible three-term linear hierarchy for W_n's ($n = 0,1,2,...$, $W_{-1} = 0$) [1]:

$$\frac{\partial W_n}{\partial t} = -M'_{n,n+1}W_{n+1} - M'_{n,n-1}W_{n-1} - \frac{n}{\sigma}W_n \tag{2}$$

$M'_{n,n\pm1}$ being linear operators. From (2), W_n relax the quicker the larger n. W_0 (fulfilling the Smoluchowski equation) dominates the approach towards equilibrium for $t \to +\infty$.

As a source of insight, we shall treat an idealization (in presence of the "Heat bath" but without friction effects): $(\partial W/\partial t) + (p/m)(\partial W/\partial x) - (\partial V/\partial x)(\partial W/\partial p) = 0$ (the reversible Liouville equation, $\sigma^{-1} = 0$). The infinite reversible three-term linear hierarchy for W_n's ($n = 0,1,2,...$, $W_{-1} = 0$) is the same as in (2), with $\sigma^{-1} = 0$. Let us consider the Laplace transforms $\tilde{W}_n(s) \equiv \int_0^{+\infty} dt W_n \exp(-st)$ and introduce: $g_n = W_{eq,0}^{-1/2}\tilde{W}_n$. This and (2) with $\sigma^{-1} = 0$ yield the symmetric reversible three-term hierarchy for g_n:

$$sg_n = W_{eq,0}^{-1/2}W_{in,n} - M_{n,n+1}g_{n+1} - M_{n,n-1}g_{n-1} \tag{3}$$

$$M_{n,n\pm1}g_{n\pm1} \equiv [\frac{(n + (1/2)(1 \pm 1))K_B T}{m}]^{1/2}[\frac{\partial g_{n\pm1}}{\partial x} - \frac{(\pm1)g_{n\pm1}}{2K_B T}\frac{dV}{dx}] \tag{4}$$

The hierarchy (3) for g_n can be solved formally, in terms of the linear operators:

$$D[n;s] = [s - M_{n,n+1} D[n+1;s] M_{n+1,n}]^{-1} \tag{5}$$

By iteration, $D[n;s]$ becomes an infinite continued fractions of products of linear operators. $D[n;s]$ has been evaluated for $V = 0$ and for a harmonic oscillator [2]. We choose $n_0 (\geq 1)$ and fix $s = \varepsilon \geq 0$ in any $D[n;s]$ (ε suitably small). The $D[n;\varepsilon]$'s are Hermitian, and all their eigenvalues are non-negative (if all eigenvalues of $D[n+1;\varepsilon]$ are ≥ 0, the same holds for $D[n;\varepsilon]$). The long-time approximation for $n \geq n_0$ reads as follows. One replaces any $D[n';s]$ yielding $\tilde{W}_n(s)$, $n' \geq n \geq n_0$, by $D[n';\varepsilon]$: this approximation is not done for $n < n_0$ and is the better, the larger n_0. We regard $D[n_0;\varepsilon]$ as a fixed (s-independent) operator. For a simpler hierarchy, neglect all $W_{in,n'}$'s for $n' \geq n_0$. Then, for small s: $g_{n_0}(s) \simeq -D[n_0;\varepsilon] M_{n_0,n_0-1} g_{n_0-1}(s)$. The resulting hierarchy for g_n's ($n = 0,1,.,n_0-1$), through inverse Laplace transform, yields a closed approximate irreversible hierarchy for W_n, $n = 0,1,.,n_0-1$. The solutions of the last closed hierarchy for W_n relax irreversibly, for large t and reasonable W_{in}, towards $W_{eq,0} \neq 0$ and $W_{eq,n} = 0$, $n = 0,1,.,n_0-1$ (thermal equilibrium). As an example, let $n_0 = 1$ and regard the linear operator $D[1;\varepsilon]$ as a real constant (> 0), playing a role similar to $\frac{\sigma}{m}$ (for Kramers equation). One finds the irreversible Smoluchowski equation for the $n = 0$ moment: $\partial W_0/\partial t = (D[1;\varepsilon]/\beta_{eq})(\partial/\partial x)[(\partial/\partial x) + \beta(\partial V/\partial x)]W_0$, with initial condition $W_{in,0}$.

Finally, we treat a closed large system of many ($N \gg 1$) classical particles, in 3 spatial dimensions. Neither a "Heat bath" nor external friction mechanisms are assumed. The interaction potential is: $V = \Sigma_{i,j=1,i<j}^{N} V_{i,j}(\mid \mathbf{x}_i - \mathbf{x}_j \mid)$. The classical distribution function is: $W([\mathbf{x}],[\mathbf{p}];t)$. The initial distribution W_{in} at $t = 0$ describes thermal equilibrium with homogeneous temperature T for large distances and nonequilibrium for intermediate distances (with spatial inhomogeneities). The reversible Liouville equation is:

$$\frac{\partial W}{\partial t} = \Sigma_{i=1}^{N}[(\nabla_{\mathbf{x}_i} V)(\nabla_{\mathbf{p}_i} W) - \frac{\mathbf{p}_i}{m}(\nabla_{\mathbf{x}_i} W)]\,. \tag{6}$$

We introduce moments $W_{[n]}$ of W (using products of Hermite polynomials, by generalizing (1)) and $g_{[n]}$. One gets an infinite reversible three-term linear recurrence for $g_{[n]}$'s, generalizing (3), which is formally solved in terms of continued-fraction operators $D[[n];s]$ for the actual $N (\gg 1)$. One also gets a generalized Hermitian operator $D[[n];\varepsilon]$ with non-negative eigenvalues. All that leads to formulate a similar long-time approximation and to a closed approximate hierarchy, which yields an irreversible evolution towards thermal equilibrium (consistently, approximately, with Fluid Dynamics).

Project FIS2008-01323 (Ministerio de Ciencia e Innovación, Spain) supports us.

REFERENCES

1. H. C. Brinkman, *Physica* **22**, 29 (1956). H. Risken, *The Fokker-Planck Equation*, 2nd ed., Springer, Berlin, 1989. W. T. Coffey et al., *The Langevin Equation*, 2nd ed., World Sci., Singapore, 2004.
2. R. F. Álvarez-Estrada, *Ann. der Physik* (Leipzig) **11**, 357 (2002); **15**, 379 (2006); *Eur. Phys. J. A* **31**, 761 (2007); *J. Comput. Appl. Math.* **233**, 1453 (2010).

ABSTRACTS OF SELECTED CONTRIBUTIONS

Reentrant behavior of effective attraction between like-charged macroions immersed in electrolyte solution

Ryo Akiyama, Ryo Sakata, and Yuji Ide

Department of Chemistry, Graduate School of Sciences, Kyushu Univ.
(rakiyama@chem.kyushu-univ.jp)

Strong effective attraction between like-charged macroions appears in electrolyte solution. The attraction between the monomers in DNA is experimentally measured[1,2]. The attraction depends on the concentration of electrolyte. When the electrolyte concentration is low, the effective interaction between like-charged macroions is repulsive. Addition of salt inverts the sign of the effective interaction. The dimer of macroions is strongly stabilized when the charges of the macroions are enough large and the electrolyte concentration is $\sim$ 1 mM. However the strong attraction disappears, when the electrolyte concentration becomes higher than 0.1M. We studied this reentrant behavior on the basis of the HNC-OZ theory with a simple model. The attraction is caused by the overlap of ionic clouds which surround the macroions. This ionic "covalent" bond, namely shared-ion-bond, is similar to the molecular covalent bond consists of electronic cloud. (See Fig. 1.) Moreover, the result s indicates that the role of co-ions is important in disappearing the attraction. We will discuss the detail of our results and a model of molecular motor driven by the growth of actin filament in neutrophil (a kind of white blood cells) in our presentation.

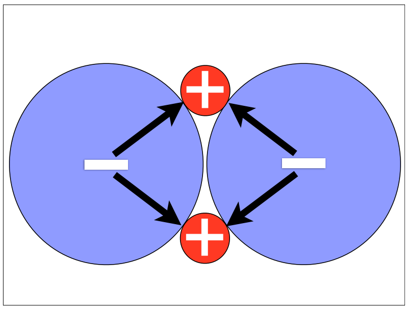

FIGURE 1. Ionic "covalent" bond.

[1] Y. Murayama et al. *Phys. Rev. Lett.* **90**, 018102 (2003).
[2] K. Besteman et al., *Nature Phys.* **3**, 641 (2007).

Nonlinear Boltzmann equation for the homogeneous isotropic case: Some improvements to deterministic methods and applications to relaxation towards local equilibrium

P. Asinari

Department of Energetics, Politecnico di Torino, Corso Duca degli Abruzzi 24, Torino, Italy
Email: pietro.asinari@polito.it
URL: http://staff.polito.it/pietro.asinari

Boltzmann equation is one the most powerful paradigms for explaining transport phenomena in fluids. Since early fifties, it received a lot of attention due to aerodynamic requirements for high altitude vehicles, vacuum technology requirements and nowadays, micro-electro-mechanical systems (MEMs).

Because of the intrinsic mathematical complexity of the problem, Boltzmann himself started his work by considering first the case when the distribution function does not depend on space (*homogeneous* case), but only on time and the magnitude of the molecular velocity (*isotropic* collisional integral).

The interest with regards to the homogeneous isotropic Boltzmann equation goes beyond simple dilute gases. In the so-called *econophysics*, a Boltzmann type model is sometimes introduced for studying the distribution of wealth in a simple market. Another recent application of the homogeneous isotropic Boltzmann equation is given by opinion formation modeling in quantitative sociology, also called socio-dynamics or *sociophysics*.

The present work [1] aims to improve the deterministic method for solving homogenous isotropic Boltzmann equation proposed by Aristov [2] by two ideas: (a) the homogeneous isotropic problem is reformulated first in terms of particle kinetic energy (this allows one to ensure exact particle number and energy conservation during microscopic collisions) and (b) a DVM-like correction (where DVM stands for Discrete Velocity Model) is adopted for improving the relaxation rates (this allows one to satisfy exactly the conservation laws at macroscopic level, which is particularly important for describing the late dynamics in the relaxation towards the equilibrium).

[1] P. Asinari, accepted for publication in *Comp. Phys. Comm.*, arXiv:1004.3491v1 [physics.comp-ph], 2010.

[2] V.V. Aristov, *Direct Methods for Solving the Boltzmann Equation and Study of Nonequilibrium Flows*, Kluwer Academic Publishers, 2001.

Effective dimension in flocking mechanisms

Gabriel Baglietto and Ezequiel V. Albano

Instituto de Investigaciones Fisicoquímicas Teóricas y Aplicadas (INIFTA),
UNLP, CCT La Plata, CONICET, Casilla de Correo 16, Sucursal 4, (1900) La Plata, Argentina.

Even in its minimal representation (Vicsek Model, VM [T. Vicsek, A. Czirok, E. Ben-Jacob, I. Cohen and O. Shochet. Phys. Rev. Lett. 75, 1226 (1995).]), the widespread phenomenon of flocking raises intriguing questions to the statistical physicists. While the VM is very close to the better understood XY Model because they share many symmetry properties, a major difference arises by the fact that the former can sustain long-range order in two dimensions, while the latter can not. Aiming to contribute to the understanding of this feature, by means of extensive numerical simulations of the VM, we study the network structure of clusters showing that they can also sustain purely orientational, mean-field-like, long-range order. We identify the reason of this capability with the key concept of "effective dimension." In fact, by analyzing the behavior of the average path length and the mean degree, we show that this dimension is very close to four, which coincides with the upper critical dimension of the XY Model, where orientational order is also of a mean-field nature. We expect that this methodology could be generalized to other types of dynamical systems.

The Liouville equation and BBGKY hierarchy for a stochastic particle system

M. Baryło

Faculty of Mathematics, Informatics and Mechanics, University of Warsaw, Banacha 2, 02-097 Warsaw, mbarylo@mimuw.edu.pl

We consider the dynamics of stochastic system of particles moving according to Newton's Laws of Motion, with additional stochastic perturbations of position (q_i) and momentum (p_i) of each particle. We assume that particles are interacting through smooth repulsive potential Φ, not admitting any collisions between different particles. The system under consideration can be described by a system of equations ($i = 1, \ldots, N$):

$$\begin{cases} dq_i = \frac{p_i}{m}\,dt + \eta_i\,dw_i, \\ dp_i = -\sum_{j \neq i} \nabla\Phi(q_i - q_j)\,dt + \xi_i\,d\widetilde{w}_i, \end{cases}$$

where w_i and $\widetilde{w}_i$ are independent standard Wiener processes in $\mathbf{R}^3$, η_i and ξ_i – constant real diagonal matrices of dimension 3.

We establish a stochastic Liouville equation (the evolution equation for a density function of position the system in the phase space) and a stochastic BBGKY hierarchy (the system of equations describing the time evolution of density functions for arbitrary subsystems of particles) for this system.

To model kinetic description

V.V. Belyi

Department of Theoretical Physics, IZMIRAN, Russian Academy of Sciences, Troitsk, 142190, Russia.

A new form of the collision operator for a Boltzmann gas of hard spheres and Coulomb plasma is proposed [1]. One-component and many-component systems are considered. The proposed collision operator properly takes into account the relaxation of the first 13 hydrodynamic moments. Besides this, it accounts for the non-diagonal component contribution in the quadratic approximation in the expansion of the linearized collision operator with respect to the complete system of Hermite polynomials. It is shown that for a system of charged particles with the Coulomb interaction potential, these contributions are essential and lead to Spitzer corrections to the transport coefficients. An expression for the intensity of the Langevin source in the kinetic equation is obtained in the same approximation. A new form of the model collision operator for a Boltzmann gas of hard spheres is proposed. For a many-component system we have reconstructed a non-linear model collision integral by using the linearized collision integral found. Unlike previous ones, it does not contain complicated exponential dependence and avoids the coefficients ambiguity in the many-component collision integral.

[1] V.V. Belyi, *J. Stat. Mech: Theor. Exp.*, **6**, P06001 (2009).

Experimental densities of binary mixtures: Acetic acid with benzene at several temperatures

Georgiana Bolat, Daniel Sutiman, and Gabriela Lisa

"Gheorghe Asachi" Technical University of Iasi, Faculty of Chemical Engineering and Environmental Protection, Mangeron Blvd., no. 71, Iasi, Romania, 700050

Hydrocarbons are the most commonly used chemicals in the hydrocarbon processing industries. The knowledge of thermodynamic properties of various binary organic or inorganic mixtures is essential in many practical aspects concerning the mass transport and fluid flow. Such properties are important from the fundamental point of view to understand their mixing behaviour (molecular interactions), as well for practical applications (e.g. in the petrochemical industry). The density of acetic acid-benzene mixtures at several temperatures (T = 296.15, 302.15, 308.15, 314.15 and 319.15 K) were measured over the whole composition range and atmospheric pressure, along with the physical-chemical properties of the pure components (e.g. density, viscosity, refractive index at 298.15 K). The excess molar volumes at the above-mentioned temperatures were calculated from experimental data and fitted by using a new polynomial equation comparing the results with the known equation of Redlich-Kister. The excess volumes for acetic acid with benzene were positive and increase with the temperature. Results were analyzed in terms of molecular interactions. This research was financed by the postdoc grant PERFORM-ERA-ID 57649.

Enhanced memory performance thanks to neural network assortativity

S. de Franciscis, S. Johnson, and J.J. Torres

Departamento de Electromagnetismo y Física de la Materia, and
Institute Carlos I for Theoretical and Computational Physics,
Facultad de Ciencias, University of Granada, 18071 Granada, Spain

The behaviour of many complex dynamical systems has been found to depend crucially on the structure of the underlying networks of interactions. An intriguing feature of empirical networks is their assortativity – i.e., the extent to which the degrees of neighbouring nodes are correlated. However, until very recently it was difficult to take this property into account analytically, most work being exclusively numerical. We get round this problem by considering ensembles of equally correlated graphs [1] and apply this novel technique to the case of attractor neural networks. Assortativity turns out to be a key feature for memory performance in these systems – so much so that for sufficiently correlated topologies the critical temperature diverges. We predict that artificial and biological neural systems could significantly enhance their robustness to noise by developing positive correlations [2].

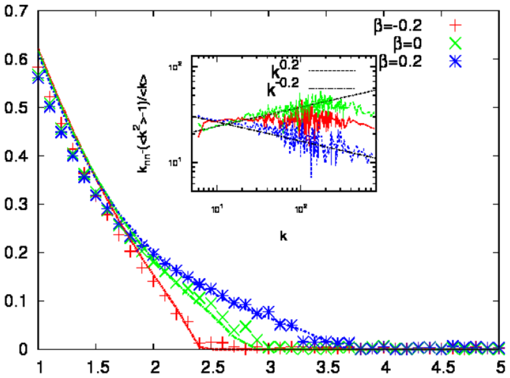

[1] S. Johnson, J.J. Torres, J. Marro, and M.A. Muñoz, *Phys. Rev. Lett.* **104**, 108702 (2010).
[2] S. de Franciscis, S. Johnson, and J.J. Torres, in preparation.

New insights in a 2-D hard disk system under a temperature gradient

J.J. del Pozo, C. Pérez-Espigares, P.I. Hurtado, and P.L. Garrido

Departamento de Electromagnetismo y Física de la Materia, and
Institute Carlos I for Theoretical and Computational Physics,
Facultad de Ciencias, University of Granada, 18071 Granada, Spain

Hard Disks system is a paradicmatic model well suited, numericaly, to test new approaches to nonequilibrium fenomena, being also easy and fast to simulate due to efficient event driven algorithms present in the literature. In this poster we study several properties of the model under a temperature gradient on the stationary regime. In this situation the sistem has well defined gradients in temperatures and densities allowing us to calculate experimentaly the thermal conductivity. We found this result compatible with the Enskog expresion even for large gradients. We also check that Henderson's state equation, although is an expresion derived under equilibrium conditions, is valid in our system for a wide range of temperatures gradients. We explain this fact showing that the system reach a local thermal equilibrium. Finaly we focus on the role of fluctuations of the energy current finding good agreement with the, recently introduced, Isometric Fluctuation Relation (IFR). We conclude that IFR also stands in our system, although it was formulated from a much simpler case.

Automatic optimization of experiments with coupled stochastic resonators

Mauro F. Calabria and Roberto R. Deza

Electronics Dept., School of Eng., National U. of Mar del Plata (UNMdP),
J.B. Justo 4302, B7608FDQ Mar del Plata, Argentina.
IFIMAR (UNMdP and CONICET), Deán Funes 3350, B7602AYL Mar del Plata, Argentina

As a step in our experimental study of the noise-enhanced propagation of a low-frequency periodic signal through a chain of one-way coupled bistable oscillators—a mock-up of synaptic transmission between neurons [1]—and exploiting an acquisition and control system recently developed by us [2], we automatically optimize the units' input parameters with the goal of achieving maximal coherence between the last oscillator's response and the input signal. The optimization is carried out by means of a genetic algorithm, using as measures of input–output coherence either the Hamming distance or the mutual information, and as input parameters the signal-to-noise ratio α_i and the switching threshold β_i of each oscillator. The figure shows that in the uniform case ($\alpha_i = \alpha$, $\beta_i = \beta$, $\forall i$) the optimal setup is basically the same, regardless of which coherence measure is employed.

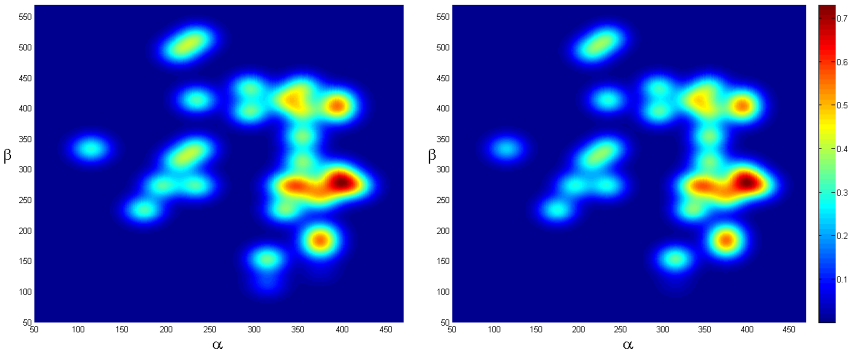

Comparison between coherence measures for 2 bistable units.

[1] R. Perazzo, L. Romanelli, and R. R. Deza, *Phys. Rev. E* **61**, R3287–R3290 (2000).
[2] M. F. Calabria, and R. R. Deza, *Rev. Sci. Instr.* **81**, in press (2010).

Velocity-velocity correlation function for anomalous diffusion

Rogelma M.S. Ferreira[1,2] and Fernando A. Oliveira[1]

(1) Instituto de Física and International Center for Condensed Matter Physics, Universidade de Brasília
(2) Departamento de Física, Universidade Federal do Ceará, Caixa Postal 6030, 60455-900 Fortaleza, Ceará, Brazil

In this work we used a previous theory [1,2,3] to explain and resolve a problem of diffusion studied by Srokowski [4]. In order to do that, we have used a generalized formalism of Langevin equation to develop a computational algorithm and treat the problem numerically. To confirm the result of the method, an analytical alternative asymptotic method for long times was derived, and both results were compared through the introduction of a time scaling factor. After all, it was presented a final characterization to the anomalous diffusion through the calculation of some functions and parameters such as correlation function, diffusion coefficient and mean square displacement. We show that for long times the diffusion coefficient behaves as

$$\lim_{t\to\infty} D(t) = \frac{1}{K+\ln(t)}$$

Where K is a constant determined by the theory. The good agreement between theory and numerical results, in the asymptotic limit is a prime result of our theory. Those results open the possibility of applications in more complex systems such as dynamics of disordered spin systems [5] and anomalous transport in cells [6]. As well the asymptotic method alow us to validate results for ergodicity [1,7,8], and fluctuation dissipation theorem where the detail balance fails [9].

This work was supported by Brazilian Research Foundations: CAPES, CNPq, FINATEC, and FAPDF.

[1] L. C. Lapas et al. *Phys. Rev. Lett.* **101**, 230602 (2008).
[2] R. Morgado et al., *Phys. Rev. Lett.* **89**, 100601 (2002).
[3] L. C. Lapas et al., *Europhys. Lett.* **77**, 37004 (2007).
[4] T. E. Srokowski, *Phys. Rev. Lett.* **85**, 2232 (2000).
[5] M. H. Vainstein et al., *Phys. Lett. A* **339**, 33 (2005).
[6] I. Santamaria-Holek et al., *Physica A* **388**, 15133 (2009).
[7] M. H. Lee, *Phys. Rev. Lett.* **87**, 250601 (2001).
[8] M. H. Lee, *Phys. Rev. Lett.* **98**, 190601 (2007).
[9] I. V. L. Costa et al., *Europhys. Lett.* **63**, 173 (2003).

Excess of low frequency vibrational modes, glass transition and inherent structures

Hugo M. Flores-Ruiz and Gerardo G. Naumis

Instituto de Física, Universidad Nacional Atutónoma de México (UNAM), Distrito Federal, México.
E-mail: hugomarcelofr@gmail.com
E-mail: naumis@fisica.unam.mx

Using a repulsive soft potential, molecular dynamics (MD) at constant pressure in a monodispersive glass and MD in a binary glass at constant volume, we are able to study the relationship between the excess of low frequency vibrational modes (known as the boson peak), square mean displacement (SMD) and glass transition temperature T_g. It is observed that the SMD is enhanced by such modes as predicted using a harmonic Hamiltonian for metastable states. As a result, glasses lose mechanical stability at lower temperatures than the corresponding crystal. We found that the average force is reduced in the glass due to such excess of modes. For the binary binary glass, we are able to study the SMD in the inherent structures (IE) over several temperatures below and around T_g. In this way, we can make the statistics of SMD over diferent IE.

[1] G. G. Naumis, and H. M. Flores-Ruiz, *Phys. Rev. B* **78**, 094203 (2008).
[2] H. M. Flores-Ruiz, and G. G. Naumis, *J. Chem. Phys.* **131**, 154501 (2009).

Analysis of ship maneuvering data from simulators

V. Frette[1], G. Kleppe[1], and K. Christensen[2]

(1) Department of Engineering, Stord/Haugesund College,
Bjørnsons gt 45, N-5528 Haugesund, Norway
vidar.frette@hsh.no; gisle.kleppe@hsh.no
(2) Institute for Mathematical Sciences, Imperial College London,
53 Prince's Gate, Exhibition Road, London SW7 2PG, United Kingdom.
k.christensen@imperial.ac.uk

We analyze complex manuevering histories of ships obtained from training sessions on bridge simulators.

Advanced ships are used in fields like offshore oil exploration: dive support vessels, supply vessels, anchor handling vessels, tugs, cable layers, and multi-purpose vessels. Due to high demands from the operations carried out, these ships need to have very high maneuverability. This is achieved through a propulsion system with several thrusters, water jets, and rudders in addition to standard propellers. For some operations, like subsea maintenance, it is crucial that the ship accurately keeps a fixed position. Therefore, bridge systems usually incorporate equipment for Dynamic Positioning (DP).

DP is a method to keep ships and semi submersible rigs in a fixed position using the propulsion systems instead of anchors. It may also be used for sailing a vessel from one position to another along a predefined route. Like an autopilot on an airplane, DP may operate without human involvement. The method relies on accurate determination of position from external reference systems like GPS, as well as a continuously adjusted mathematical model of the ship and external forces from wind, waves and currents.

In a specific simulator exercise for offshore crews, a ship is to be taken up to an installation consisting of three nearby oil platforms connected by bridges (Frigg field, North Sea), where a subsea inspection is to be carried out. Due to the many degrees of freedom during maneuvering, including partly or full use of DP, the chosen routes vary significantly. In this poster we report preliminary results on representations of the complex maneuvering histories; representations that allow comparison between crew groups, and, possibly, sorting of the different strategic choices behind.

Unfying approach for fluctuation theorems from joint probability distributions

Reinaldo García-García[1], D. Domínguez[1], Vivien Lecomte[2,3], and A.B. Kolton[1]

(1) Centro Atómico Bariloche, 8400 S. C. de Bariloche, Argentina
(2)Laboratoire de Probabilités et Modèles Aléatoires (CNRS UMR 7599), Université Pierre et Marie Curie - Paris VI - Université Paris-Diderot - Paris VII, 2 Place Jussieu, 75005 Paris, France
(3)DPMC-MaNEP, Université de Genève, 24 Quai Ernest-Ansermet, 1211 Geneva 4, Switzerland

Any decomposition of the total trajectory entropy production for markovian systems have a joint probability distribution satisfying a generalized detailed fluctuation theorem, without relying in dual probability distributions, when all the contributing terms are odd with respect to time reversal. We show that several fluctuation theorems for perturbed non-equilibrium steady states are unified and arise as simple particular cases of this general result. In particular, we show that the joint probability distribution of the system and reservoir trajectory entropies satisfy a detailed fluctuation theorem valid for all times although each contribution does not do it separately

[1] C. Bustamante, J.Liphardt, and F. Ritort, *Physics Today*, **58** 43 (2005).
[2] F. Ritort, *Adv. Chem. Phys.* **137**, 31 (2008); arXiv:0705.0455v1.
[3] D. J. Evans, E.G.D. Cohen, and G. P. Morriss, *Phys. Rev. Lett.* **71**, 2401 (1993).
[4] G. Gallavotti and E.G.D. Cohen, *Phys. Rev. Lett.* **74**, 2694 (1995).
[5] J. Kurchan, *J. Phys. A: Math. Gen.* **31**, 3719 (1998).
[6] J.L. Lebowitz and H. Spohn, *J. Stat. Phys.* **95**, 333 (1999).
[7] C. Jarzynski, *Phys. Rev. Lett.* **78**, 2690 (1997); C. Jarzynski, *Phys. Rev. E* **56**, 5018 (1997).
[8] G. E. Crooks, *J. Stat. Phys.* **90**, 1481 (1998); G. E. Crooks, *Phys. Rev. E* **61**, 2361 (2000).
[9] T, Hatano and Shin-ichi Sasa, *Phys. Rev. Lett.* **86**, 3463 (2001).
[10] S. Yukawa, *J. Phys. Soc. Japan*, **69**, 2370 (2000); S. Mukamel, *Phys. Rev. Lett.* **90**, 170604 (2003); C. Jarzynski and D. K. Wojcik, *Phys. Rev. Lett.* **92**, 230602 (2004).
[11] Y. Oono and M. Paniconi, *Prog. Theor. Phys. Suppl.* **130**, 29 (1998).
[12] T. Speck and U. Seifert, *J. Phys. A: Math. Gen.* **38**, 581 (2005).
[13] V. Y. Chernyak, M. Chertkov, and C. Jarzynski, preprint cond-mat/0605471 (2006).
[14] M. Esposito and Ch. Van den Broeck, preprint cond-mat/09112666.
[15] U. Seifert, *Phys. Rev. Lett.* **95**, 040602 (2005).
[16] J. Prost, J.-F. Joanny, and J.M.R. Parrondo, *Phys. Rev. Lett.* **103**, 090601 (2009).

Thermally activated escape far from equilibrium: A unified path-integral approach

S. Getfert and P. Reimann

Universität Bielefeld, Fakultät für Physik, 33615 Bielefeld, Germany

Thermally activated escape over potential barriers is addressed for systems driven out of equilibrium by time-dependent forces, temperatures, or dissipation coefficients of rather general type. Particular examples are periodic perturbations, single pulses, and the initial convergence towards Kramers rate in a time-independent set up. The general problem is treated within one common, unifying path-integral approach in the simplest case of an overdamped, one-dimensional model dynamics [1]. As an application, the following quite astonishing effect is demonstrated: For a suitably chosen, but still quite simple static potential landscape, the net escape rate may be substantially *reduced* by temporally *increasing* the temperature above its unperturbed, constant level [2].

[1] S. Getfert and P. Reimann, *Chem. Phys.*, in press.
[2] S. Getfert and P. Reimann, *Phys. Rev. E* **80**, 030101(R) (2009).

The crystal nucleation theory revisited: The case of 2D colloidal crystals

A.E. González[1] and L. Ixtlilco-Cortés[2,1]

(1) Instituto de Ciencias Físicas, UNAM, Cuernavaca, Morelos 62210, México.
(2) Centro de Investigación en Ingeniería y Ciencias Aplicadas, Cuernavaca, Morelos 62209, México.

Most of the theories and studies of crystallization and crystal nucleation consider the boundaries between the crystallites and the fluid as smooth. The crystallites are the small clusters of atoms, molecules and/or particles with the symmetry of the crystal lattice that, with a slight chance of success, would grow to form the crystal grains. In fact, in the classical nucleation theory, the crystallites are assumed to have a spherical shape (circular in 2D). As far are we are aware, there is only one experimental work [1] on colloidal crystals that founds rough surfaces for the crystallites and for the crystal grains.

Motivated by this work, we performed large Kinetic Monte Carlo simulations in 2D, that would follow the eventual growing of a few crystallites to form the crystal grains. The used potential has, besides the impenetrable hard core, a soft core followed by a potential well. We found that indeed the crystallites have a fractal boundary, whose value we were able to obtain. See the figure below of a typical isolated crystallite. We were also able to obtain the critical crystallite size, measured by its number of particles, N_c, and not by any critical radius. The boundaries of the crystals above N_c also have a fractal structure but of a lower value, closer to one. Finally, we also obtained the line tension between the crystallites and the surrounding fluid, as function of temperature and particle diameter, as well as the chemical potential difference between these two phases.

In the URL: www.fis.unam.mx/∼agus/ there are posted two movies that can be downloaded: (1) 2D_crystal_nucleation.mp4, and (2) 2D_crystal_growth.mp4, that illustrate the crystal nucleation and its further growth.

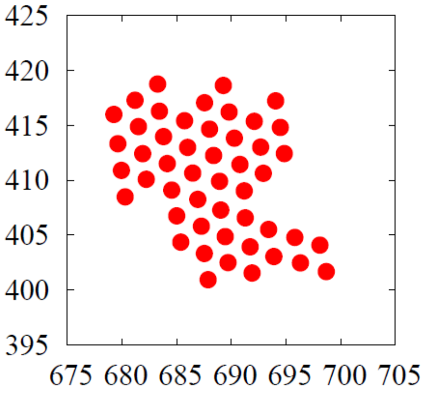

[1] U. Gasser et al., *Science* **292**, 258 (2001).

Space-time phase transitions in the totally asymmetric simple exclusion process

M. Gorissen[1] and C. Vanderzande[1,2]

(1) Faculteit Wetenschappen, Universiteit Hasselt, 3590 Diepenbeek, België
(2) Instituut Theoretische Fysica, Katholieke Universiteit Leuven, 3001 Heverlee, België

One can drive a system away from equilibrium by brining it in contact with reservoirs at a different temperature or chemical potential; as a result, heat or particle currents will develop. Recently, the interest in the fluctuations of these currents has increased considerably, both from a theoretical and an experimental point of view.

We studied current fluctuations in the Totally Asymmetric Simple Exclusion Process (TASEP), which consists of a one-dimensional lattice in which each site is either empty or occupied by at most one particle. The particles enter the lattice with rate α, move to the right in the bulk of the lattice with rate 1, and exit the lattice with rate β, provided these moves are allowed by the exclusion statistics. In our work, the current is then taken to be equal to the total number of particles that has passed through all bonds up to a certain time.

Using a powerful numerically exact technique called the Density Matrix Renormalization Group (DMRG), we were able to obtain results for the first three cumulants of the current and their time dependence in the various phases of the TASEP (determined by the values of α and β). Furthermore, by studying ensenbles of histories weighted by an exponential function of the current, we found that the TASEP displays a space-time phase transition.

Modeling of early stages of island growth during pulsed deposition: Role of closed compact islands

M. Kotrla and M. Masin

Institute of Physics, Academy of Sciences of the Czech Republic,
Na Slovance 2, 182 21, Praha 8, Czech Republic
(E-mail: kotrla@fzu.cz)

After a brief review of recent modeling of growth during Pulsed Laser Deposition (PLD), we present the study of a role of adatom interactions on growth of surface islands during PLD in submonolayer regime. We employ kinetic Monte Carlo simulation with *reversible* growth, see e.g. [1]. Attachment of monomers to islands is irreversible at low temperatures while it becomes reversible at higher temperatures, small islands become unstable with growing temperature. In the case of real system we have to take into account not only diffusion of monomers but also diffusivity of dimers and larger clusters and theirs stability.

Our new code allows us to study processes which proceed on different time scales which are typical in PLD experiments: fast deposition (on scale order of 10^{-5} s) during individual pulses, and relaxation of a system between pulses (on scale order of 0.1 s). We calculate and compare the temperature dependence of island density for two modes pulsed deposition and continuous Molecular Beam Epitaxy (MBE) growth. The island densities in PLD mode are substantially higher than in MBE mode, provided the temperature is sufficiently high. In the case of PLD, we observe anomalous temperature dependence of the island density in a certain temperature interval. It is due to the interplay between a cluster decay time and an interval between pulses. The cluster decay time depends not only on temperature but also on clusters size and shape. The anomalous behavior is caused by the temperature limited stability of the *closed–compact* clusters.

This scenario was revealed for the simplified model with only nearest–neighbor interaction. Now, it is elucidated further and we also include interaction to second and third neighbors. We analyze role of the *closed–compact* surface island in kinetics of both growth modes. Furthermore, by varying interactions energies, diffusion barrier and parameters of deposition, we compare results of simulations with the PLD experiment for Fe/Mo system [2].

[1] M. Kotrla, *Comp. Phys. Comm.* **97**, 82-100 (1996).
[2] P. O. Jubert, O. Fruchart, and C. Mayer, *Surf. Sci.* **522**, 8 (2003).

Fluctuations of the dissipated energy in a granular system

Antonio Lasanta[1,2]*, Pablo I. Hurtado[2], Pedro L. Garrido[2] and J. Javier Brey[1]

(1)Física Teórica, Universidad de Sevilla, Apartado de Correos 1065, E-41080 Sevilla, Spain
(2) Departamento de Electromangnetismo y Física de la Materia, Universidad de Granada, Granada 18071, Spain
**E-mail:alasanta@us.es*

Large fluctuations, play an important role in many fields of science as they crucially determine the fate of a system. The statistics of these fluctuations encodes essential information on the physics of the system at hand. This is particularly important in systems far from equilibrium, where no general theory exists up to date capable of predicting macroscopic and fluctuating behavior in terms of microscopic physics.The study of fluctuations far from equilibrium may open the door to such general theory. In this work we follow this path by studying the fluctuations of the dissipated energy in an oversimplified model of a granular system. The model, first proposed and solved by Levanony and Levine [1], is a simple one dimensional diffusive lattice system which includes energy dissipation as a main ingredient. When subject to boundary heat baths, the system reaches an steady state characterized by a highly nonlinear temperature profile and a nonzero average energy dissipation. For long but finite times, the time-averaged dissipated energy fluctuates, obeying a large deviation principle. We study the large deviation function (LDF) of the dissipated energy by means of advanced Monte Carlo techniques [2], arriving to the following results: (i) the LDF of the dissipated energy has only a positive branch, meaning that for long times only positive dissipation is expected, (ii) as a result of microscopic time-irreversibility, the LDF does not obeys the Gallavotti-Cohen fluctuation theorem, (iii) the LDF is Gaussian around the average dissipation, but non-Gaussian, asymmetric tails quickly develop away from the average, and (iv) the granular system adopts a precise optimal profile in order to facilitate a given dissipation fluctuation, different from the steady profile. We compare our numerical results with predictions based on hydrodynamic fluctuation theory [3], finding good agreement.

[1] D. Levanony and D. Levine, *Phys. Rev. E* **73** , 055102 (2006).
[2] C. Giardina, J. Kurchan, and L. Peliti, *Phys. Rev. Lett.* **96**, 120603 (2006).
[3] T. Bodineau and M. Lagouge. *J. Stat. Phys.* **139** , 201 (2010).

Study of the dynamic behavior of quantum cellular automata in graphane nanoclusters

A. León[1] and M. Pacheco[2]

(1) Facultad de Ingeniería, Universidad Diego Portales, Ejército 441 Santiago, Chile
(2) Departamento de Física, Universidad Técnica F. Santa María, Casilla 110 V, Valparaíso, Chile.

The possible creation of architectures of quantum cellular automata formed by simple molecules opens a very promising and interesting area of research due to the possibility of going beyond the current limits of miniaturization and integration of devices. In this research we theoretically study the electronic properties of a quan- tum dot array in graphene nanoribbons and in an array of molecules with graphane structures. The role of quantum dots in the ribbons and in the mole- cules is played by oxide reduction centers that can trap or release electrons. With the knowledge about these properties we design cellular automata archi- tectures with nanoribbons and molecular arrays, with this it will be feasible to store and process logic information at room temperature. The stability of the proposed graphene structures are studied using quan- tum methods of geometric optimization [1]. The electronic properties of the nanoribbons are obtained from first-principle calculations based on pseudo- potentials by using the generalized gradient approximation (GGA) of Perdew- Burke-Ernzerhof [2-3]. With the parameters obtained from the study of the electronic properties of the cells that make up the automata, we can make a simulation of the dynamical response of the system. To do this, we use a set of accelerated algorithms for discrete systems [4] based on the Glauber dynamic [5]. Our results show that the studied system can be scaled so that the propagation of digital information throughout the automata is possible at room temperature.

[1] P. Csaszar and P. Pulay, *J. Mol. Struct.:THEOCHEM* **114**, 31 (1984).
[2] J. P. Perdew, K. Burke, and M. Ernzerhof, *Phys. Rev. Lett.* **77**, 3865 (1996).
[3] http://www.openmx-square.org
[4] W. Krauth, *Statistical Mechanics: Algorithms and Computations*, Oxford University Press, New York, 2006.
[5] R. J. Glauber, *J. Math. Phys. (Cambridge, Mass.)* **4**, 294 (1963).

Breeding gravitational lenses

J. Liesenborgs[1], S. De Rijcke[2], H. Dejonghe[2], and P. Bekaert[1]

(1) Expertisecentrum voor Digitale Media, Universiteit Hasselt, Wetenschapspark 2, B-3590, Diepenbeek, Belgium
`jori.liesenborgs@uhasselt.be`
(2) Sterrenkundig Observatorium, Universiteit Gent, Krijgslaan 281, S9, B-9000, Gent, Belgium

Gravitational lenses are a spectacular astrophysical phenomenon, a cosmic mirage caused by the gravitational deflection of light in which multiple images of a same background object can be seen. Their beauty is only exceeded by their usefulness, as the gravitational lens effect is a direct probe of the total mass of the deflecting object. Furthermore, since the image configuration arising from the gravitational lens effect depends on the exact gravitational potential of the deflector, it even holds the promise of learning about the distribution of the mass. In this presentation, a method for extracting the information encoded in the images and reconstructing the mass distribution is presented. Being a non-parametric method, it avoids making a priori assumptions about the shape of the mass distribution. At the core of the procedure lies a genetic algorithm, an optimization strategy inspired by Darwin's principle of "survival of the fittest". One only needs to specify a criterion to decide if one particular trial solution is deemed better than another, and the genetic algorithm will "breed" appropriate solutions to the problem. In a similar way, one can create a multi-objective genetic algorithm, capable of optimizing several fitness criteria at the same time. This provides a very flexible way to incorporate all the available information in the gravitational lens system: not only the positions and shapes of the multiple images are used, but also the so-called "null space", i.e. the area in which no such images can be seen. The effectiveness of this approach is illustrated using simulated data, which allows one to compare the reconstruction to the true mass distribution.

Improved macroscopic traffic flow model for aggresive drivers

A.R. Méndez[1] and R.M. Velasco[2]

(1) Departamento de Matemáticas Aplicadas y Sistemas, Universidad Autónoma Metropolitana-Cuajimalpa, 11950, México. (2) Departamento de Física, Universidad Autónoma Metropolitana-Iztapalapa, 09340, México.

As has been done for the treatment of diluted gases, kinetic methods are formulated for the study of unidirectional freeway traffic. Fluid dynamic models obtained from kinetic equations have inherent restrictions, the principal one is the restriction to the low density regime. Macroscopic models obtained from kinetic equations tends to selfrestrict to this regime [1] and makes impossible to observe the medium density region. In this work, we present some results heading to improve this model and extend the observable region. Now, we are presenting a fluid dynamic model for aggressive drivers [2] obtained from kinetic assumptions to extend the model to the medium density region in order to study synchronization phenomena which is a very interesting transition phase between free flow and traffic jams. We are changing the constant variance prefactor condition imposed before [1] by a variance prefactor density dependent, the numerical solution of the model is presented, analyzed and contrasted with the previous one. We are also comparing our results with heuristic macroscopic models [3] and real traffic observations.

[1] R. M. Velasco and W. Marques, Jr., *Phys. Rev. E* **72**, 046102 (2005).
[2] A. R. Méndez and R. M. Velasco, *J. Non-Newtonian Fluid. Mech.*, (2010) (accepted).
[3] D. Helbing, *Phys. Rev E* **51**, 3164-3169 (1995).

A formula on the pressure for a set of generic points

A.M. Meson and F. Vericat

Instituto de Física de Líquidos y Sistemas Biológicos (IFLYSIB) CONICET–UNLP
Grupo de Aplicaciones Matemáticas y Estadísticas de la Facultad de Ingeniería (GAMEFI) UNLP, La Plata, Argentina
meson@iflysib.unlp.edu.ar

Let (X,f) be a dynamical system, with X a compact metric space and $f:X\to X$ a continuous map. For any $x\in X$, let us consider the empirical measures $E_n(x)=\frac{1}{n}\sum_{i=0}^{n-1}\delta_{f^i(x)}\subset M(X)$, where δ is the Dirac point mass measure. The limit set of the sequence $\{E_n(x)\}$ will be denoted by $V(x)$. A particularly interesting case is when $V(x)=\{\mu\}$, i.e. the points for which the time-average along their orbits of any continuous potential ψ agrees with the average of ψ with respect to μ. This kind of points are called *generic* for the measure μ and let us denote $G_\mu=\{x:V(x)=\{\mu\}\}$. A measure μ is called a *physical measure* if there is a Lebesgue measure m such that $m(G_\mu)>0$. In the case of considering C^2 -maps $f:M\to M$ with a negative Lyapunov exponent, where M is a compact Riemannian manifold, the *Sinai-Ruelle-Bowen* measures (*SRB-measures*) are physical measures. In the context of Lattice Statistical Mechanics the scheme is the following: the phase space X is a subset of the space $\left\{x:x=(x_i)_{i\in Z^d},x_i\in\Omega=\{1,2,\cdots,k\}\right\}$, i.e. a space of configurations with spin Ω and sites in the lattice $L=\mathbf{Z}^d$, the dynamics are given by the shift $\sigma(x)_i=x_{i+d}$, for any $i\in\mathbf{Z}^d$ and the measures (states) are $E_n(x)=\frac{1}{\Delta_n}\sum_{i=0}^{n-1}\delta_{f^i(x)}$, where Δ_n is the volume of the lattice $[-n,n]^d$. The goal is to find an expression for $P_{G_\mu}(\psi)$, the topological pressure for the set G_μ of the potential ψ. Our analysis is more general, in the sense that we obtain a variational expression for sets $G_K=\{x:V(x)=K\}$, with K a compact set of measures in X instead of working just in G_μ The condition imposed on the dynamical system is the so called almost property product, which is weaker than specification. Equilibrium case is when the dynamics have the properties of expansiveness and specification. This work generalizes previous results obtained for $\psi\equiv 0$, i.e. for the topological entropy, (C.E. Pfister and W.G. Sullivan, *Ergod. Th. and Dynam. Sys.* **27**, 929-956 (2007)) and for the pressure of potentials ψ,but with specification (D. Thompson, *J. London Math. Soc.* **80**, 585-602 (2009)).

Statistical thermodynamics of a relativistic gas

Afshin Montakhab and Malihe Ghodrat

Department of Physics, Shiraz University, Shiraz 71454, Iran.

Classical statistical thermodynamics is one of the oldest, most well-established physical theories and its basis and results have not been challenged within its domain since the time of Boltzmann. Special relativity, however, introduces some constraints as well as ambiguities into such a theory. For example, the cornerstone of classical statistical mechanics, the Maxwell-Boltzmann (MB) distribution does not respect the maximal velocity of light, the cornerstone of special relativity. Additionally, the Lorentz transformation of temperature, i.e. how a moving body's temperature compares to its rest frame value, has long caused controversies. Special relativity also introduces a new concept of *proper* time, which could potentially affect fundamental concepts of ergodicity and time-averaging in thermodynamics.

In this work, we propose a model of a relativistic hard-sphere gas, and via molecular dynamics simulations, investigate all the above issues. In particular we show that the so-called Jüttner distribution is the correct relativistic generalization of the MB distribution. Introducing proper time averaging simply rescales such distribution by similar energy factor γ. We also show that temperature is best understood as an invariant quantity, i.e. temperature does not change under the motion of inertial frames, and is not affected by time reparametrization. Additionally, we have studied this model under a temperature gradient and have shown that the model satisfies the minimal ingredients to study nonequilibrium transport properties, i.e. the existence of a non-equilibrium steady state and local thermal equilibrium. This will allow us to study generalizations of transport properties to relativistic regimes.

[1] A. Montakhab, M. Ghodrat, and M. Barati, *Phys. Rev. E* **79**, 031124 (2009).
[2] M. Ghodrat and A. Montakhab, *Phys. Rev. E* **82**, 011110 (2010).

Noninteracting classical spins in a rotating magnetic field: Exact results

Suhk Kun Oh[1,2] and Seong-Cho Yu[1]

(1) Department of Physics, Chungbuk National University, Cheongju, Korea
(2) skoh@chungbuk.ac.kr

A model of noninteracting classical spins in a time-dependent rotating magnetic field, described by the Hamiltonian of the form

$$\begin{aligned} H &= -\overrightarrow{h}(t)\cdot\sum_{i=1}^{N}\overrightarrow{s}_i \\ &= -h_z\sum_{i=1}^{N}s_i^z - h_0\sum_{i=1}^{N}(s_i^x\cos\omega t - s_i^y\sin\omega t) \end{aligned}$$

is investigated. The nonequilibrium magnetization, equal-time total spin correlation functions, time-displaced total spin correlation functions, and the energy are exactly calculated to see their dependence on the magnitude of a transverse rotating magnetic field and a rotating angular frequency. The time-displaced correlation function shows nonstationarity as expected. Even for very small rotating fields, compared to a static field along the z-axis, all the nonequilibrium quantities show remarkable increases in the oscillation amplitudes at the resonance frequency. However, due to competition between the static field and the rotating field, the oscillation amplitude increases monotonically for large rotating fields as we increase the angular frequency beyond the resonance angular frequency.

Optimal mutation rates in dynamic environments: The eigen model

Mark Ancliff and Jeong-Man Park

Department of Physics, The Catholic University of Korea, Bucheon, Gyeonggi-do 420-743, Korea
(email: jmanpark@catholic.ac.kr)

We consider the Eigen quasispecies model with a dynamic environment. For an environment with sharp-peak fitness in which the most-fit sequence moves by k spin-flips each period T we find an asymptotic stationary state in which the quasispecies population changes regularly according to the regular environmental change. From this stationary state we estimate the maximum and the minimum mutation rates for a quasispecies to survive under the changing environment and calculate the optimum mutation rate that maximizes the population growth. Interestingly we find that the optimum mutation rate in the Eigen model is lower than that in the Crow-Kimura model, and at their optimum mutation rates the corresponding mean fitness in the Eigen model is lower than that in the Crow-Kimura model, suggesting that the mutation process which occurs in parallel to the replication process as in the Crow-Kimura model gives an adaptive advantage under changing environment.

[1] M. Ancliff and J.-M. Park, *Phys. Rev. E* **80**, 061910 (2009).

Current fluctuations in a two dimensional model of heat conduction

Carlos Pérez-Espigares, Pedro L. Garrido, and Pablo I. Hurtado

Instituto Carlos I de Física Teórica y Computacional, Universidad de Granada, Spain

In this work we study numerically and analytically current fluctuations in the two-dimensional Kipnis-Marchioro-Presutti (KMP) model of heat conduction. For that purpose, we use a recently introduced algorithm which allows the direct evaluation of large deviations functions. We compare our results with predictions based on the Hydrodynamic Fluctuation Theory (HFT) of Bertini and coworkers, finding very good agreement in a wide interval of current fluctuations. We also verify the existence of a well-defined temperature profile associated to a given current fluctuation which depends exclusively on the magnitude of the current vector, not on its orientation. This confirms the recently introduced Isometric Fluctuation Relation (IFR), which results from the time-reversibility of the dynamics, and includes as a particular instance the Gallavotti-Cohen fluctuation theorem in this context but adds a completely new perspective on the high level of symmetry imposed by timereversibility on the statistics of nonequilibrium fluctuations.

Quasistatic heat processes in mesoscopic non-equilibrium systems

J. Pešek[1,2] and K. Netočný[2]

(1) Faculty of Mathematics and Physics, Charles University, Prague
(2) Institute of Physics AS CR, Prague
(pesek@fzu.cz, http://www.fzu.cz/∼netocny)

A basic difficulty in measuring and computing the energy exchange between a system, its thermal environment, and time-dependent external fields is the divergence of energy flows in the quasistatic limit. This problem is overcome by properly constructing their finite or 'excess' parts [1,2]. It has been recently proposed that for weakly equilibrium processes the excess heat (approximately) satisfies thermodynamic relations extending those for equilibrium processes, with a generalized entropy function [2].

In order to systematically analyze these propositions, we first derive nonperturbative formulas for quasistatic excess path quantities in markovian systems, and we propose a method how to possibly access them experimentally. By extending the method of [3], we perturbatively construct the excess work and heat for both over- and under-damped diffusions driven by small nongradient forces. It is shown that the excess heat always satisfies the (generalized) Clausius relation up to the first order in nonequilibrium driving, whereas this is no longer true in general when beyond the leading order [4]. In the latter case, the excess path quantities do not derive from (generalized) thermodynamic potentials but they require new nonpotential corrections, as demonstrated numerically. We also discuss the possible meaning of those new corrections.

[1] D. Ruelle, *Proc. Nat. Acad. Sci. USA* **18**, 3054 (2003).
[2] T. S. Komatsu, N. Nakagawa, S. Sasa, and H. Tasaki, *Phys. Rev. Lett.* **100**, 230602 (2008).
[3] C. Maes and K. Netočný, *J. Math. Phys.* **51**, 015219 (2010).
[4] J. Pešek and K. Netočný, in preparation.

Violation of fluctuation-dissipation theorem in the off-equilibrium dynamics of a system with non additive interactions

O.A. Pinto[1], F. Romá [1], A.J. Ramirez-Pastor[1], and F. Nieto [1]

(1) Dpto. de Física, Universidad Nacional de San Luis, INFAP, CONICET, Chacabuco 917, D5700BWS
San Luis, Argentina.
oapinto@unsl.edu.ar

In this work we study the critical equilibrium properties and the off-equilibrium dynamics of an Ising system with non additive interactions. The traditional assumption of additivity is modified for one more general, where the energy of exchange J between two spins depends on their neighbourhood. First, for several non additive situations, we calculated the critical temperature T_c by using paralell tempering Monte Carlo in the canonical assemble and standard finite-size scaling techniques. Then, we carry out a quench from infinite temperature to a low temperature below T_c (off-equilibrium dynamics protocol) and we compute two-time correlation and response functions. We find a violation of fluctuation-dissipation theorem like coarsening systems. All this was done for several waiting time and several non additive situations. Finally, we analyze the scaling of correlation and response functions for a critical quench from infinite temperature.

Geometric aspects of Schnakenberg's network theory of macroscopic nonequilibrium observables

M. Polettini

University of Bologna

Schnakenberg's network theory deals with macroscopic thermodynamical observables (forces, currents and entropy production) associated to the steady states of diffusions on generic graphs. Using results from graph theory and from the theory of discrete differential forms we recast Schnakenberg's treatment in the form of a simple discrete gauge theory, which allows to interpret macroscopic forces as the Wilson loops of a real connection. We discuss the geometric properties of transient states, showing that heat fluxes allow for a notion of duality of macroscopic observables which interchanges the role of the environment and that of the system. We discuss possible generalizations to less trivial gauge groups and the relevance for nonequilibrium fluctuation theorems.

Based on work in collaboration with professor A. Maritan, University of Padua, to be published.

[1] J. Schnakenberg, *Rev. Mod. Phys.* **48**, 571 (1976).
[2] D. Andrieux and P. Gaspard, *J. Stat. Phys.* **127**, 107 (2007).

Nonequilibrium thermodynamics of single DNA hairpins in a dual-trap optical tweezers setup

M. Ribezzi Crivellari[1], J.M. Huguet[1], and F. Ritort[1,2]

(1) Departament de Fisica Fonamental, Universitat de Barcelona
Martí i Franques 1, 08028 Barcelona.
(2) Ciber de Bioingeniería, Biomateriales y Nanomedicina,
Instituto de Sanidad Carlos III, Madrid

We use two counter propagating laser beams to create a dual trap optical tweezers setup which is free from cross interference between the beams and provides great instrumental stability. This setup works by direct measurement of light momentum, separately for each trap, and is based on the Minitweezers design [1]. The dual trap setup has many applications: it can be used to study the force-dependent unfolding kinetics of single molecules and to address fundamental problems in nonequilibrium thermodynamics of small systems [2]. Recent progress in statistical physics has shown the importance of considering large energy deviations in the beahvior of systems that are driven out-of-equilibrium by time-dependent forces. Prominent examples are nonequilibrium work relations (e.g. the Jarzynski equality [3]) and fluctuation theorems. By repeated measurement of the irreversible work the Jarzynski equality allows us to recover the free energy difference between two thermodynamic states, ΔF, by taking exponential averages of the work W done by the external agent on the system, $e^{-\beta\Delta F} = \left\langle e^{-\beta W} \right\rangle$, where the average in the rhs is taken over an infinite number of experiments. A crucial aspect of nonequilibrium work relations and fluctuation theorems in general is their non-invariance under Galilean transformations. This implies that mechanical work must be measured in the proper reference that is solidary with the thermal bath for these relations to hold. We have carried out repeated mechanical unfolding/folding cycles on short (20 bp) DNA hairpins and measured work distributions in the dual-trap setup along this process. Our aim is to check under which experimental conditions we can discern the non-invariance property of fluctuation relations thereby establishing the correct operative definition of the work in our setting. This study may help to identify and quantify potential violations of the fluctuation relations.

[1] C. Bustamante, S.B. Smith, 2006 US PATENT, 7, 133, 132, B2.
[2] F. Ritort, *Adv. Chem. Phys.* **137**, 31 (2008).
[3] C. Jarzynski, *Phys. Rev. Lett.* **78**, 2690 (1997).

Quantum revivals and Zitterwebegung in monolayer graphene

Elvira Romera[1,2] and Francisco de los Santos[1,3]

(1) Instituto Carlos I de Física Teórica y Computacional, Universidad de Granada, E18072, Spain
(2) Departamento de Física Atómica Molecular y Nuclear, Universidad de Granada, E18072, Spain
(3) Departamento de Física de Electromagnetismo y Física de la Materia, Universidad de Granada, E18072, Spain

We have studied the dynamics of electron currents in graphene subject to a magnetic field. Several types of periodicity must be distinguished if the wave packets representing the electrons are sufficiently localized around some large enough central quantum number n_0. In this case, currents initially evolve quasiclassically and oscillate with a period T_{Cl}, but at later times the wave packet eventually spreads, leading to the collapse of the classical oscillations. At times that are multiple of T_{R}, or rational fractions of T_{R}, the wave packet (almost) regains its initial form, and the electron current its initial amplitude. For this to occur, the presence of a quantizing magnetic field is necessary, for if $B = 0$ the spectrum is continuous which rules out the possibility of revivals. Associated with the revival of the wave packet the quasiclassical oscillatory motion of the currents resumes. Additionally, when both positive and negative Landau levels are populated, permanent ZB oscillations are observed, in agreement with previous results. We relate the temporal scales of these three effects and discuss to what extent these results hold for real graphene samples.

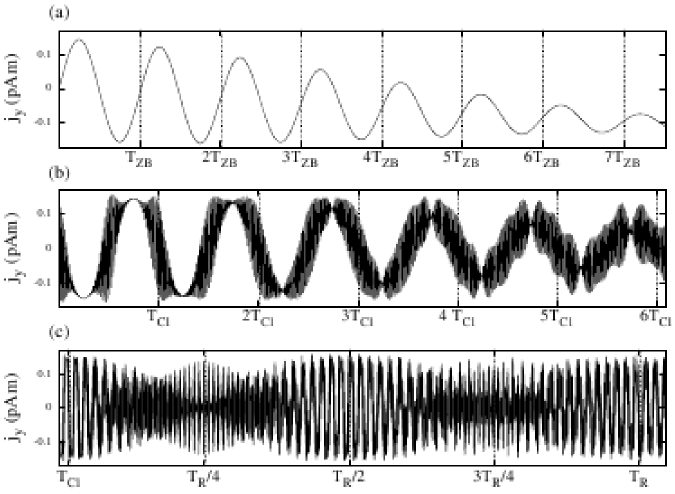

[1] E. Romera and F. de los Santos, *Phys. Rev. A* **78**, 013837 (2008).

The non-equilibrium and energetic cost of sensory adaptation

G. Lan, Pablo Sartori, and Y. Tu

IBM T.J. Watson Research Center, Physics Department

Biological sensory systems respond to external signals in short time and adapt to permanent environmental changes over a longer timescale to maintain high sensitivity in widely varying environments. In this work we have shown how all adaptation dynamics are intrinsically non-equilibrium and free energy is dissipated. We show that the dissipated energy is utilized to maintain adaptation accuracy. A universal relation between the energy dissipation and the optimum adaptation accuracy is established by both a general continuum model and a discrete model i n the specific case of the well-known E. coli chemosensory adaptation. Our study suggests that cellular level adaptations are fueled by hydrolysis of high energy biomolecules, such as ATP.

The relevance of this work lies on linking the functionality of a biological system (sensory adaptation) with a concept rooted in statistical physics (energy dissipation), by a mathematical law. This has been made possible by identifying a general sensory system with a non-equilibrium steady state (a stationary state in which the probability current is not zero, but its divergence is, see figure), and then numerically and analytically solving the Fokker-Planck and Master Equations which describe the sensory adaptive system. The application of our general results to the case of E. Coli has shed light on why this system uses the high energy SAM molecule to perform adaptation, since using the more common ATP would not suffice to obtain the required adaptation accuracy.

[1] D.E. Koshland, A. Goldbeter, and J.B. Stock, *Science* **217**, 220 (1982).
[2] Y. Tu, *Proc. Natl. Acad. Sci. U.S.A.* **105**, 11737 (2008).
[3] Y. Tu, T.S. Shimizu, and H.C. Berg, *Proc. Natl. Acad. Sci. U.S.A.* **105**, 14855 (2008).

Negative specific heat in the canonical statistical ensemble

F. Staniscia[1,2], A. Turchi[3], D. Fanelli[4], P.H. Chavanis[5,6], and G. De Ninno[7,2]

(1) Dipartimento di Fisica, Università di Trieste, 34127 Trieste, Italy
(2) Sincrotrone Trieste, S.S. 14 km 163.5, Basovizza, 34149 Trieste, Italy
(3) Dipartimento di Sistemi e Informatica, Universitià di Firenze and INFN, via S. Marta 3, 50139 Firenze, Italy
(4) Dipartimento di Energetica "Sergio Stecco" and CSDC, Università di Firenze, and INFN, via Santa Marta, 3, 50139 Firenze, Italy
(5) Université de Toulouse, UPS, Laboratoire de Physique Théorique (IR- SAMC), F-31062 Toulouse, France
(6) CNRS, Laboratoire de Physique Théorique (IRSAMC), F-31062 Toulouse, France
(7) Physics Department, Nova Gorica University, 5001 Nova Gorica, Slovenia

According to thermodynamics, the specific heat of Boltzmannian short-range interacting systems is a positive quantity. Less intuitive properties are in- stead displayed by systems characterized by long-range interactions. In that case, the sign of specific heat depends on the considered statistical ensemble: negative specific heat can be found in isolated systems, which are studied in the framework of the microcanonical ensemble; on the other hand, it is generally recognized that a positive specific heat should always be measured in systems in contact with a thermal bath, for which the canonical ensemble is the appropriate one. We demonstrate that the latter assumption is not generally true: one can in principle measure negative specific heat also in the canonical ensemble if the system under scrutiny is non-Boltzmannian and/or our-of-equilibrium

Dynamical systems approach to the study of a sociophysics agent-based model

André M. Timpanaro[1*] and Carmen P.C. Prado[1**]

(1) Instituto de Física da Universidade de São Paulo, São Paulo, Brazil
*timpa@if.usp.br, **prado@if.usp.br

The Sznajd model is a Potts-like model that has been studied in the context of sociophysics [1,2] (where spins are interpreted as opinions). In a recent work [3], we generalized the Sznajd model to include assymetric interactions between the spins (interpreted as biases towards opinions) and used dynamical systems techniques to tackle its mean-field version, given by the flow:

$$\dot{\eta}_\sigma = \sum_{\sigma'=1}^{M} \eta_\sigma \eta_{\sigma'} (\eta_\sigma p_{\sigma' \to \sigma} - \eta_{\sigma'} p_{\sigma \to \sigma'}).$$

Where η_σ is the proportion of agents with opinion (spin) σ, M is the number of opinions and $p_{\sigma \to \sigma'}$ is the probability weight for an agent with opinion σ being convinced by another agent with opinion σ'.

We made Monte Carlo simulations of the model in a complex network (using Barabási-Albert networks [4]) and they displayed the same attractors than the mean-field. Using linear stability analysis, we were able to determine the mean-field attractor structure analytically and to show that it has connections with well known graph theory problems (maximal independent sets and positive fluxes in directed graphs).

Our dynamical systems approach is quite simple and can be used also in other models, like the voter model.

[1] K. Sznajd-Weron and J. Sznajd, *Int. J. Mod. Phys. C*, **11(6)**, 1157-1165 (2000).
[2] A. T. Bernardes, D. Stauffer, and J. Kertész, *Eur. Phys. J. B*, **25**, 123-127 (2002).
[3] A. M. Timpanaro and C. P. C. Prado, *Phys. Rev. E*, **80(2)**, 021119 (2009).
[4] A. L. Barabási and R. Albert, *Science* **286(5439)**, 509-512 (1999).

Conversion process of chemical reaction into mechanical work through solvation change

Ken Tokunaga[1], Takuya Furumi[2], and Ryo Akiyama[2]

(1) General Education Department, Faculty of Engineering, Kogakuin Univ.
(2) Department of Chemistry, Graduate School of Sciences, Kyushu Univ.

Many systems in which the hydrolysis of ATP is finally converted into the mechanical work are known (e.g. actin-myosin motor protein system). It seems that there are various types of the conversion mechanism. In this work, we examined a possibility of conversion from chemical reaction into mechanical work due to solvation change around the reaction site by using the molecular dynamics simulation (MD) with explicit solvent model.

In our model, solvent molecules, S, and a motor (colloidal particle), M, are treated as Lennard-Jones (LJ) particles. Effect of chemical reaction is taken in the system as the change of LJ potential parameter ε between S and M, however the reaction site is restricted on the M. The parameter ε is switched to ε'=1000 ε during the reaction (Δt), Fig. (a).

Averaged displacement of the motor M is shown in Fig. (b). The motor M is driven by this reaction model, however the direction and efficiency are dependent on the reaction time Δt and the thermodynamic state of the solvent.

(a)

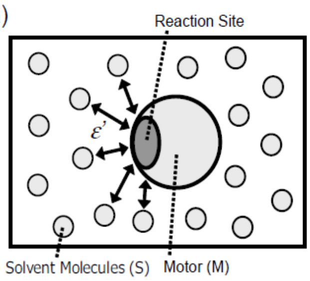

(b)

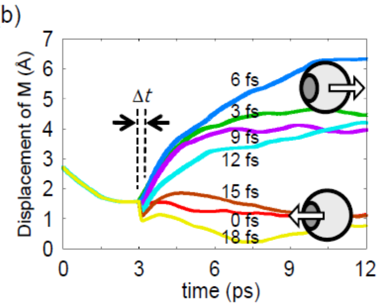

LIST OF PARTICIPANTS

Akiyama, Ryo	Japan
Álvarez-Estrada, R.	Spain
Apenko, Sergey	Russia
Araujo, Aderaldo I.	Brazil
Asinari, Pietro	Italy
Ávila, Ricardo	Brazil
Baglietto, G.	Argentina
Baldovin, Fulvio	Italy
Barylo, Mariusz	Poland
Belyi, Viatcheslav	Russia
Bolat, Georgiana	Romania
Borromeo, M.	Italy
Chialvo, Dante	USA
Ciccotti, Giovanni	Italy
Cordero, Patricio	Chile
Cortés, Jesús	Spain
de Franciscis, S.	Italy
de los Santos, F.	Spain
del Pozo, Jesús	Spain
Deza, Roberto	Argentina
Domínguez, V.	Spain
Fernández, Julio	Spain
Ferreira, Rogelma	Brazil
Flores Ruiz, Hugo	Mexico
Frette, Vidar	Norway
Gallavotti, G.	Italy
García, Reinaldo	Argentina
Gª-Perciante, A. L.	Mexico
Garcia, Odd Erik	Norway
Garrido, Pedro	Spain
Genovese, G.	Italy
Getfert, Sebastian	Germany
Goldstein, Sheldon	USA
González-Flores, A.	Mexico
Gorissen, Mieke	Belgium
Gudowska-Now., E.	Poland
Handford, Thomas	UK
Hartmann, C.	Germany
Hidalgo, Jorge	Spain
Hoover, William G.	USA
Hoover, Carol	USA
Hurtado, Pablo	Spain
Johnson, Samuel	Spain
Jou, David	Spain
Kaburaki, Hideo	Japan
Kalvova, Andela	Czech R.
Kastner, Michael	S. Africa
Kleppe, Gisle	Norway
Koga, Kenichiro	Japan
Kotrla, Miroslav	Czech R.
Lacoste, David	France
Lasanta, Antonio	Spain
Latorre, J.C.	Germany
Lebowitz, Joel	USA
Lecomte, Vivien	France
Lemos, Humberto	Brazil
Letizia, Viviana	Italy
León, Alejandro	Chile
Liesenborgs, Jori	Belgium
Livi, Roberto	Italy
Lorenzo, Antonio	Spain
Marcos, Bruno	France
Marro, Joaquín	Spain
Martin, Cristina H.	USA
Martín, José M.	Spain
Mehdi, Si Khaled	Algeria
Mejías, Jorge	Canada
Méndez, Alma	Mexico
Meson, A.	Argentina
Miracle-Solé, S.	France

Montakhab, Afshin	Iran
Muñoz, Miguel A.	Spain
Netocny, Karel	Czech R.
Novikov, Sergey	Russia
Nowak, Maciej	Poland
Odor, Geza	Hungary
Oh, Suhk Kun	S. Korea
Ohira, Toru	Japan
Ojeda García, Juan	Spain
Oliveira, Fernando	Brazil
Orlandini, Enzo	Italy
Ortiz de Zárate, JM.	Spain
Park, J.M.	S. Korea
Paskauskas, R.	Lithuania
Pereira, Emmanuel	Brazil
Pérez-Espigares, C.	Spain
Pérez-Reche, F.	UK
Pesek, Jiri	Czech R.
Pinto, Alejandro	Argentina
Polettini, Matteo	Italy
Popescu, Sandu	UK
Posch, Harald	Austria
Prados, Antonio	Spain
Presutti, Errico	Italy
Ribezzi, Marco	Italy
Ritort, Félix	Spain
Romera, Elvira	Spain
Rubí, Miguel	Spain
Ruiz, Jean Franc.	France
Ryckebusch, Jan	Belgium
Rypdal, Kristoffer	Norway
Sartori, Pablo	Germany
Seifert, Udo	Germany
Shchur, Lev	Russia
Simonella, Sergio	Italy
Spicka, Vaclav	Czech R.
Staniscia, Fabio	Italy
Stankievich, Yolan.	Poland
Thomas, Simi	Belgium
Timpanaro, André	Brazil
Tokunaga, Ken	Japan
Toral, Raúl	Spain
Torres, Joaquín J.	Spain
Vanderzande, C.	Belgium
Verley, Gatien	France
Viot, Pascal	France
Wio, Horacio	Argentina
Worrakitpoonpo, T.	Thailand

AUTHOR INDEX

A

Akiyama, Ryo 261, 295
Albano, Ezequiel V. 263
Alemany, A. 94
Álvarez-Estrada, R. F. 259
Ancliff, Mark 285
Apenko, S. M. 257
Asinari, P. 262
Ávila, Ricardo R. 226

B

Baglietto, Gabriel 263
Baldovin, Fulvio 255
Baryło, M. 264
Bekaert, P. 280
Belyi, V. V. 253, 265
Bolat, Georgiana 266
Bonilla, L. L. 230
Bosetti, Hadrien 228
Brey, J. J. 278
Burdeau, Alexis 233

C

Calabria, Mauro F. 269
Carpio, A. 230
Castellano, Claudio 170
Chavanis, P.H. 255, 293
Christensen, K. 272
Ciccotti, Giovanni 75
Cordero, P. 182
Crivellari, M. R. 290

D

De Cruz, L. 237
de Franciscis, S. 267
de La Lama, M. S. 193
de los Santos, Francisco 1, 291
De Ninno, G. 293
De Rijcke, S. 280
Dejonghe, H. 280
del Pozo, J. J. 202, 268
dell'Erba, M. G. 212
Deza, R. R. 193, 212, 269
Domínguez, D. 273

E

Escudero, C. 193

F

Fanelli, D. 293
Ferreira, Rogelma M. 270
Flores-Ruiz, Hugo M. 271
Frette, Vidar 251, 272
Furumi, Takuya 295

G

Gabrielli, A. 243
García-García, Reinaldo 273
Garcia-Perciante, A. L. 214
Garrido, P.L. 1, 202, 268, 278, 286
Getfert, S. 274
Ghodrat, Malihe 283
Goldstein, Sheldon 153
González, A.E. 275
Gorissen, M. 235, 276

H

Handford, T. P. 249
Hartmann, Carsten 216
Hemmer, Per C. 251
Hoover, Carol G. 21
Hoover, Wm. G. 21
Huguet, J. M. 290
Hurtado, P.I. 202, 268, 278, 286

I

Ide, Yuji 261
Ito, Nobuyasu 224
Ixtlilco-Cortés, L. 275
Izús, G. G. 212

J

Johnson, S. 247, 267
Jou, David 162
Joyce, M. 243
Juhász, Róbert 170

K

Kaburaki, Hideo 219
Kalvová, A. 221
Kamimura, Atsushi 224
Kastner, Michael 177
Kimizuka, Hajime 219
Kleppe, G. 272
Kolton, A.B. 273
Kotrla, M. 277

L

Lacoste, D. 245
Lan, G. 292
Lapas, Luciano C. 198
Lasanta, Antonio 278
Latorre, Juan 216
León, A. 279
Lebowitz, Joel L. 1
Lecomte, Vivien 273
Lemos, Humberto C. 226
Li, Ju 219
Liesenborgs, J. 280
Lisa, Gabriela 266

M

Méndez, A. R. 281
Marcos, B. 243
Marro, J. 1, 247
Masin, M. 277
Matsumoto, Shigenori 224
Mejías, Jorge F. 241
Meloni, Simone 75
Meson, A.M. 282
Montakhab, Afshin 283
Muñoz, Miguel A. 109, 170, 247

N

Naumis, Gerardo G. 271
Netočný, K. 287
Nieto, F. 288
Nogawa, Tomoaki 224
Novikov, S.V. 239

O

Ódor, Géza 170
Oh, Suhk K. 284
Ohira, Toru 224
Oliveira, Fernando A. 198, 270
Orlandini, Enzo 255
Orlandini, Sergio 75

P

Pérez-Espigares, C.   202, 268, 286
Pacheco, M.   279
Park, Jeong-Man   285
Pešek, J.   287
Pereira, Emmanuel   226
Perez-Reche, F-J   249
Pinto, O. A.   288
Polettini, M.   289
Posch, Harald A.   228
Prado, Carmen P.   294
Prados, A.   230
Presutti, Errico   121

R

Ramirez-Pastor, A.J.   288
Reimann, P.   274
Revelli, J. A.   193
Ribezzi, M.   94
Risso, D.   182
Ritort, F.   94, 290
Rivas, N.   182
Romá, F.   288
Romera, Elvira   291
Rubí, J. M.   132, 198
Ryckebusch, J.   237

S

Sakata, Ryo   261
Sartori, Pablo   292
Seifert, Udo   54
Solé, Salvador M.   188
Soto, R.   182
Špička, V.   221
Standaert, S.   237
Staniscia, F.   293
Sutiman, Daniel   266

T

Talbot, Julian   233
Taraskin, S N   249
Timpanaro, Andrá M.   294
Tokunaga, Ken   295
Toral, Raúl   143
Torres, J. J.   247, 267
Tu, Y.   292
Tumulka, Roderich   153
Turchi, A.   293

V

Vanderzande, C.   235, 276
Velasco, R. M.   281
Velický, B.   221
Vericat, F.   282
Verley, G.   245
Viot, Pascal   233

W

Wio, H. S.   193, 212

Y

Yip, Sidney   219
Yu, Seong-Cho   284